Childhood growth in the Neolithic: a detailed case study of Çatalhöyük

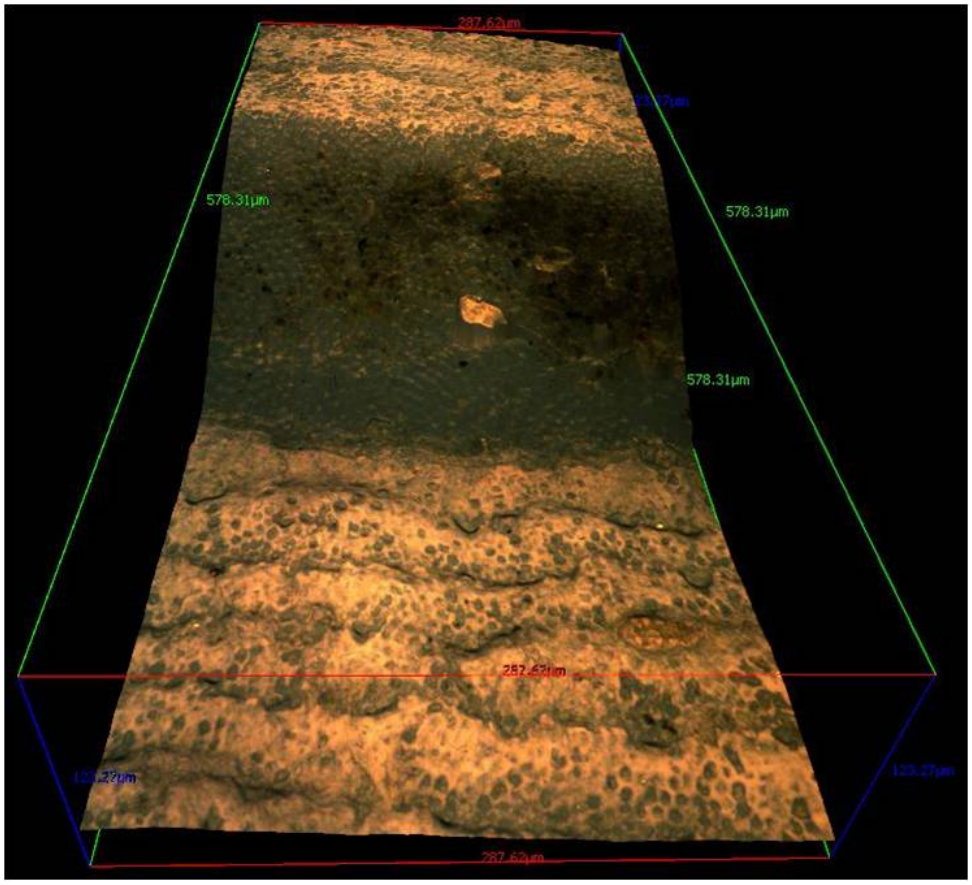

Emmy Bocaege
Institute of Archaeology
University College London

2015

Thesis submitted for the degree of Doctor of Philosophy

Disclaimer

I, Emmy Bocaege, confirm that the work presented in this thesis is my own. Where information has been derived from other sources, I confirm that this has been indicated in the thesis.

Emmy Bocaege

Abstract

The main aim of this project is to provide an insight into childhood experiences in the Neolithic Near East and to investigate the variation in skeletal and dental growth patterns within the context of the profound social and environmental changes taking place during this time period. Detailed archaeological information is available for the Neolithic site of Çatalhöyük, Turkey (7400-7100 BC to 6200-5900 BC) as well as a considerable sample of immature human remains, which is unique for this time period and area of the world.

In order to better understand the lives of the Çatalhöyük children, a two-fold methodology based on osteological and dental analysis of growth and development is utilised and results are interpreted using archaeological evidence. Tooth enamel does not remodel during life and teeth are well recovered from archaeological sites, making tooth crowns an important archive of an individual's development. Using a newly developed 3D technique, a detailed investigation into the variation in the expression of dental growth disturbances (furrow-form enamel hypoplasia) is carried out. The relationship between dental development and skeletal growth is analysed by comparing the enamel hypoplasia dataset to skeletal growth patterns which are considered to be more influenced by environmental factors than dental development. In order to capture differences in growth occurring throughout the child's life, skeletal growth trajectories are explored by quantitative assessments of skeletal variables representing different functional regions (cranium, mandible and postcranial bones) which grow at different rates. Together, the data outline a life history for each child, and are used to reveal the pattern of growth disruptions experienced by children buried in different houses and in different time periods. Results show that growth disruptions affect skeletal and dental growth in different ways, suggesting that interpretations based solely on enamel hypoplasia or skeletal growth patterns might obscure the level of disruption experienced by children in past populations. This study also indicates that there are no consistent differences in the level of growth disruptions affecting the dental and skeletal development of children buried in different houses. In contrast, there are consistent differences in skeletal growth patterns between children buried in different time periods, with individuals buried in the later occupation phase displaying smaller skeletal sizes for their ages than individuals buried in the earlier occupation phase. As this later phase is also the time in which the population size declined at Çatalhöyük, it is suggested that smaller support groups provided less buffering against growth disruptions during this later period.

Table of Contents

Table of Contents

List of Figures

List of Figures

List of Figures

List of Figures

List of tables

List of tables

Acknowledgements

Firstly, I would like to thank Simon Hillson, Louise Humphrey and Anna Clement for supervising this research, for the helpful discussions and for their continuous support.

Secondly, I am very grateful to the Çatalhöyük Research Project for providing access to the material used in this research and in particular Shahina Farid, Lori Hager and Basak Boz for their support.

During my Undergraduate and Postgraduate degrees, I have undertaken study, research and voluntary work at University College London, the Natural History Museum and the Royal College of Surgeons of England and many people at these institutions have helped me develop into the scholar I am today.

At the Natural History Museum, I am grateful for the use of the imaging suite; Silvia Bello and Jonathan Krieger are acknowledged for their assistance during my first steps on the microscope, Robert Kruszyinski for initial access to collections and Isabelle de Groote for her support.

At University College London, I would particularly like to thank Sandra Bond and Kevin Reeves for technical support, Clive Orton and Andy Bevan and Eugenio Bertolini for statistical advice, Karen Wright, Louise Martin and Liz Henton for helpful discussions on the archaeology of Çatalhöyük and the Near East, Stuart Robson for initial discussions on 3D imaging, Lisa Daniel for administrative help and Cyprian Broodbank for his support as graduate tutor, my colleagues from the EUROEVOL project for the opportunity to broaden my knowledge of Neolithic archaeology and Nancy Tang, Brenna Hassett and Carolyn Rando for their advice.

A big thank you also goes to my friends Nick, Helen, Rob, Jo and Andy who spent time proofreading various parts of this thesis.

At the Royal College of Surgeons of England, I would like to thank Sam Alberti, Martyn Cooke, John Carr, Amalia Lemprière, Kritanand Poonyth and Carina Phillips for their continuous support and for allowing me the flexibility I needed to complete this project.

I would also like to thank my friends and family for providing much needed distractions and a special mention goes to my parents, Luc and Dominique, for their enormous help and support throughout this project. This thesis is dedicated to them.

Chapter 1. Introduction

1.1. Framework of research

As a discipline, bioarchaeology uses the physical body as a source of information on past lifeways. Teeth and bones in particular are often used as variables for measuring health. For example, in comparisons of skeletal series, a high prevalence of skeletal and pathological conditions and changes in skeletal and dental growth patterns, including stature reduction and increasing evidence of dental growth disruptions (enamel hypoplasia), are commonly seen as adaptive transformations in response to a deteriorating health status (Larsen 1995).

Most of the bioarchaeological studies focusing on the Neolithic period are comparative. For example, Angel has studied the impact of changing lifestyles on health by comparing samples from the Palaeolithic, Neolithic and Bronze Age in the Eastern Mediterranean (Angel 1984). Based upon the decrease in stature and the increase in frequency of enamel hypoplastic defects, he argued that health deteriorated from 10000 to 5000 BC in this region (Angel 1984). Similarly, Smith and Horwitz (2007) used the frequency of enamel hypoplastic defects as evidence for the decline in health during the Neolithic in the Southern Levant.

Many assemblages are very small and lack detailed contextual information, it is often hard to undertake in depth palaeopathological studies within specific Neolithic populations in the Near East (Smith and Horwitz 2007). In addition to this, Angel stressed the importance of local site variability and argued that before any site comparisons are undertaken, "*the causal network of disease-health-culture-environment must be untangled at the local level* (Angel 1984, 68)".

Children are one of the best indicators for the well being of a living community, because their rate of growth is strongly affected by their health, nutrition and socio-economic conditions (Cardoso 2005; Eveleth and Tanner 1990). Childhood growth, for example, is used by the World Health Organization as a sensitive measure of the need for aid. Sciulli (2007) and Cardoso (2005) suggested that the distribution of plant and animal species, the size, structure and spatial distribution of settlements and the interactions between

neighbouring populations are amongst a multiplicity of factors affecting the nutritional status and associated disease load of populations and that these effects are likely to be manifested most markedly in infants and children.

Due to small sample sizes, preservation and recovery issues, most of the previously mentioned comparative analyses of human remains do not include children. In contrast to previous comparative studies of various assemblages from Near Eastern Neolithic sites, the goal of this research project is to undertake an in-depth case study of one Neolithic site. This study will examine childhood experience in the Neolithic Near East using a detailed case study of childhood growth at Çatalhöyük, a Neolithic settlement located in the Konya plain, Turkey, dated between 7400-7100 BC to 6200-5900 BC (Hodder 2005a). The site has a very detailed archaeological record and a large number of excavated human remains (N=388), of which about two thirds are children, providing a solid basis for an in-depth study of human dental and skeletal development.

The first issue addressed in this research project concerns the methodology for the identification of furrow-form enamel defects. In previous studies, enamel defects were visually identified, either macroscopically, with a hand-held magnifying glass or using a binocular microscope, which introduced a high degree of subjectivity and made inter-site comparisons problematic. In addition, traditional methods used the distance between defects and the cement-enamel junction in order to time enamel defects, assuming a constant rate of development (Goodman and Armelagos 1985b).

Recent advances in dental anthropology have demonstrated that the rate of crown formation gradually decreases, highlighting the inaccuracy of previous methods used to time enamel defects (Hillson and Bond 1997; Reid and Dean 2000). Microscopic studies have made it possible to establish detailed chronologies of dental development by examining microscopic growth lines inside teeth. The surface expressions of these dental microstructures are called perikymata and these provide an archive of an individual's development, similar to the growth rings of trees. Anomalies in the spacing pattern of perikymata can be used to identify and time dental growth disturbances, which can be linked to episodes of systemic perturbances (Guatelli-Steinberg *et al.* 2004; Hassett 2011; Hillson and Bond 1997; King *et al*. 2002, 2005; Temple *et al.* 2012).

Although there is reasonable consensus on the timing of defects using a microscopic approach, identification methods have not yet been standardised. This research project

is the first application of a new method for identifying enamel defects, which will not only be applicable to other modern human assemblages, but may also be applied to fossil specimens. It is based on three-dimensional models of crown surfaces constructed from a stack of images, preserving x, y and z coordinates for any point within the resolution of the scan, providing a detailed micrographic record (dental growth profile) of the incremental structures on the surface of teeth.

The new methodology is used to gain a greater understanding of childhood health at Çatalhöyük by focusing directly on the important social issue of health by creating aged chronologies of development for children who were alive when profound societal changes were taking place. The detailed archaeological evidence of settlement, lifestyle, diet, and living conditions at Çatalhöyük provides an excellent contextual framework for this study.

Hodder (2012, 152) wrote that at Çatalhöyük, "*House, human and society were all materially entangled together*". Therefore, in order to study how children experienced living in this past society, one needs to consider the house in detail. As such, in this study, the subadult remains are analysed with the specific characteristics of the Çatalhöyük buildings in mind, including multiple rebuilding over time and the existence of "history houses". In this way, variation in human growth patterns within the site will be assessed in terms of spatial and temporal differences. Spatial differences are explored in terms of "households" and "house societies" and temporal comparisons are based on archaeological information on diachronic change within the sample.

1.2. Outline of study

Using a new method for a detailed 3D study of furrow-form enamel hypoplasia, a large dataset of skeletal growth measurements and the integration of artefactual, ecofactual and architectural information, four main research questions are proposed, of which two are related to methodological issues and a further two are related to the interpretation of health at Çatalhöyük.

1.3. Key research questions

1. Can enamel defects be assessed objectively?

Recent advances in dental anthropology have made it possible to establish detailed chronologies of dental development. This project uses a newly developed technique to

identify and quantify human dental growth patterns by examining the surface expressions of microscopic growth lines inside teeth. Based upon the assessment of these surface expressions (perikymata), the project aims to standardise the detection of anomalies in dental growth patterns (furrow-form enamel hypoplasia).

2. Is there a correlation between delayed skeletal growth and patterns of furrow-form enamel hypoplasia?

As skeletal growth patterns are considered to be more strongly influenced by environmental factors than dental development, the relationship between dental developmental disturbances and skeletal growth is assessed by comparing the dental growth profiles generated by the newly developed microscopic method with a large dataset of skeletal growth measurements.

3. Did human growth patterns vary in terms of place of residence at Çatalhöyük and if so, can differences in skeletal and dental growth patterns be detected by looking at burial context?

In other words, is there a consistent difference in patterns of furrow-form enamel hypoplasia and skeletal growth between children buried in special contexts as opposed to children buried in other contexts?

4. Did changes in community size and density affect human growth at Çatalhöyük?

In other words, can a diachronic change in skeletal and dental growth patterns be detected at the site?

Chapter 2 provides an overview of the theoretical framework of the thesis and the biocultural context of the site, followed by an anatomical introduction of skeletal and dental growth (Chapter 3). Chapter 4 reviews past and current methods used in the study of furrow-form enamel hypoplasia and skeletal growth patterns, critically assessing the advantages and disadvantages of each approach. The quantitative methods used in the analysis of skeletal growth and the recording, timing and interpretation of furrow-form hypoplasia are presented in Chapter 5, followed by a description of the sample under study (Chapter 6). Results are presented in Chapter 7, followed by the discussion of the main issues arising from these analyses (Chapter 8). Chapter 9 provides a summary of the main conclusions from this study as well as suggestions for future research.

Chapter 2. Archaeological context

This thesis explores the interrelationship between childhood growth, culture and environment at Çatalhöyük through the examination of two bioarchaeological datasets: enamel and skeletal growth patterns. This chapter examines the archaeological and anthropological background to the research questions: the first part explains the rationale behind the use of the cultural parameters (dwellings) in this study; the second part outlines the archaeological evidence for climate, architecture, food consumption, health and socio-economic organisation at this site, and a detailed definition of the research questions is given in the third and final part.

2.1. Theoretical framework

Over the last two decades, specialisation and diversification within anthropological subdisciplines have deepened the differences between biological and cultural anthropologists (Goodman and Leatherman 1998; Holden 1993; Stephens and Herring 2011). Goodman and Leatherman (1998) argued that developments within biological anthropology have nearly entirely been methodological and aimed at measuring human biologies rather than developing models and theories. Similarly, Parker Pearson (2003) suggested that osteological analyses of malnutrition have taken an evolutionary, processual approach, focusing on levels of “stress” and “health” as abstract markers of the biological fitness of human societies in prehistory and minimising any cultural dimensions of malnutrition.

Goodman and Leatherman (1998) proposed that in order to surpass the current bio-cultural split, researchers need to bring together perspectives from human adaptability, human ecology and political-economic anthropology. Because human biologies are affected by and also influence the control, production and distribution of material resources, ideology and power, a political-economic perspective is a necessary complement to biological anthropology (Goodman and Leatherman 1998). In relation to this political-economic perspective, they outlined five interrelated issues which should be emphasised in a bio-cultural synthesis.

Firstly, the examination of biological variation in terms of social relations should be included in any synthesis, as it is through these that individuals gain access to basic

resources and labour and these determine what an individual eats and his or her exposure to pathogens. Secondly, it is important to assess the links between the local and the global. In other words, to take into account how regional (macro) processes influence local (micro) conditions. The third major point is the integration of an understanding of the local history and potential diachronic changes. Fourthly, as humans are influenced by their environment and involved in creating their own environment, it is important to integrate the idea of humans as active agents in any interpretations of biological adaptation. Finally, ideology is a key issue in understanding humans as active agents (Goodman and Leatherman 1998).

In order to deal with some of the issues set out by Goodman and Leatherman (1998), this study refers to the classic social anthropological themes of social interaction and agency in order to situate the concept of "growth" within the complex social networks operating at an archaeological site. As such, site-specific "local biologies" will be created and used as a tool to assess to what extent social and physical circumstances become incorporated biologically (Littleton 2007).

Lock and Kaufert (2001) created the concept of "local biologies" to account for differences in the reporting of biomedical findings. This widely used concept does not refer to measurable biological differences across populations, but to "*the way in which biological and social processes are inseparably entangled over time, resulting in biological differences* (Lock and Nguyen 2010, 90)". The concept of local biology deconstructs the modernist assumption of a universal material body and considers the human body (in terms of its anatomy and pathology) as an artifact, a snapshot in time of an ever-changing differentiation, reflecting changes over the course of evolutionary time and during historical change.

Local biologies result from interactions among human genes, the lived-in environment, social and economic arrangements, diets and behavioural styles and can vary greatly in different populations (Lock and Nguyen 2010). Therefore, in contrast to previous comparative studies assessing the differences between Neolithic sites in the Near East, this study uses an integrated approach to assess the interactions of biological and social processes across time and space at one archaeological site, Çatalhöyük.

A key theme in this study is the investigation of childhood growth patterns as products of individual lived experiences through the association of bioanthropological data with

interpretations from material culture. In the current bioarchaeological study, results are interpreted in terms of the built environment at the site, with a similar view to Düring who wrote that *"buildings are not simply tools that we design and use, they partly constitute the fabric of society* (Düring 2001, 3)*"*.

Based on the lack of other symbolic meeting places and the careful orientation, continuity and wall decorations in houses, Bloch (2010, also see Hodder 2007a) likened the Çatalhöyük social organisation to a wider category of ethnographically described "house societies", a concept proposed by Lévi-Strauss (1979).

Using the term "house societies", Hodder and Pels (2010) considered the house as the basis of a society's social organisation (Hodder and Pels 2010). Whereas Lévi-Strauss (1979) described this social organisation mainly as a type of kinship organisation, Bourdieu (1979) and Carsten and Hugh-Jones (1995), focusing on the processual aspect of houses, considered both kinship relations and material culture as aspects of the house's identity (Hodder 1990; 1998; Hodder and Pels 2010). Similarly, Düring (2007), based on a multi-scalar framework proposed by Flannery (1976), argued that instead of interpreting Çatalhöyük in terms of a town or city, it is more useful to focus on how the built environment structures social interactions.

To summarise, this thesis uses a site-specific approach in the interpretation of two scientific datasets (patterns of dental and skeletal growth). The theoretical framework in which the project is situated makes use of the concept of a dwelling as a way of ordering social relationships and maintaining social memory. It is through this approach that spatial differences within the site are explored.

2.2. The case study site: Çatalhöyük

Çatalhöyük ("fork mound") is located in the Konya plain, Central Anatolia (Turkey) and consists of two tells: a Neolithic mud-brick settlement (7400-7100 BC to 6200-5900 BC) located on the eastern side of the Carşamba river, known as Çatalhöyük East, and Çatalhöyük West (Fig. 2.1), which shows evidence of a Chalcolithic occupation (Hodder 2005a; 2007b). The site was discovered in the late 1950s and excavations of the East mound were undertaken by James Mellaart in the 1960s and from 1993 onwards by an international team of researchers led by Ian Hodder. Whereas Mellaart was interested in

exposing the various levels of occupation over a wide area (160 buildings in the southwest area), the more recent excavations were much more detailed, with a focus on individual houses and community organisation in different areas within the site (South, North, BACH, 4040) as well as the excavation of an off-site area (KOPAL). A single-context recording system was used based upon a hierarchy of *units (*the basic recording element, also referred to as context in British archaeology*), features, spaces, buildings, area and mound* and chronological groupings related to phases and levels (Cessford 2005; Farid 2004; Farid 2007a; Hodder 2005a; Hodder 2007a).

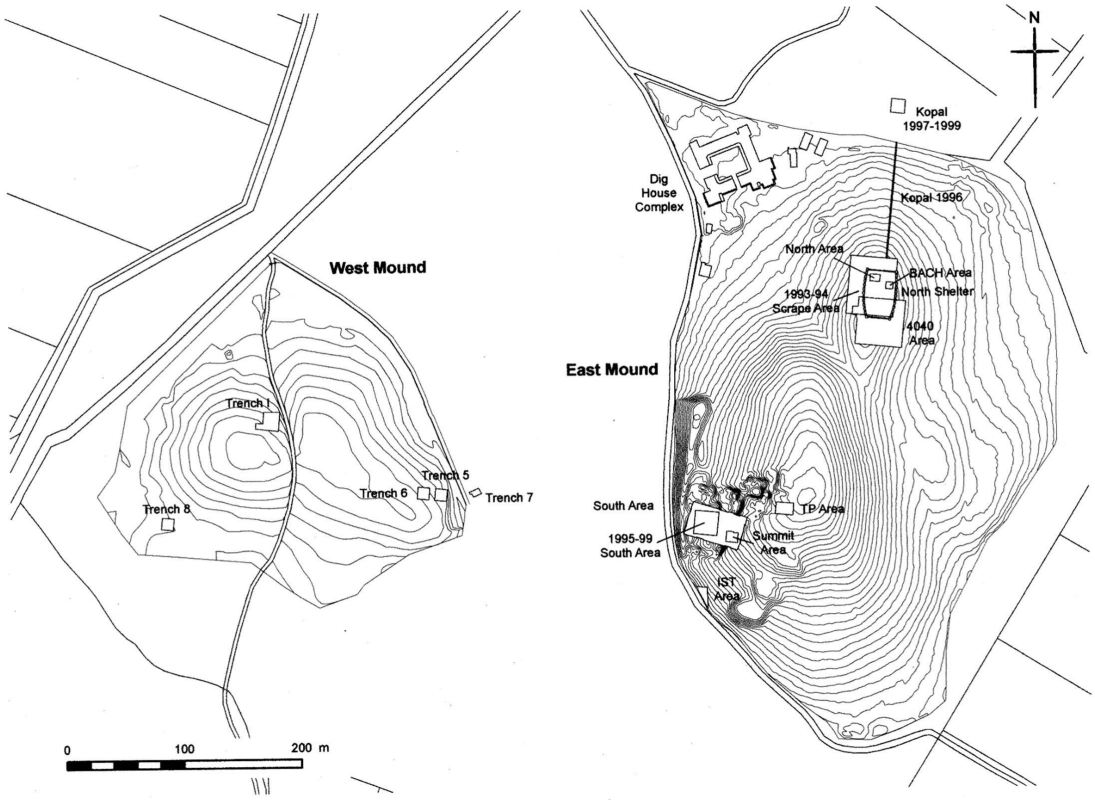

Figure 2.1: Çatalhöyük: East and West mound excavation areas (including South, North, Bach, KOPAL and 4040, TP = Team Poznan Area) (from Wright 2014, 3)

Information from a regional survey shows that there were very few contemporary sites on the Carşamba river alluvial fan (Baird 2002; Hodder 2005a). However Çatalhöyük is one of around thirty Neolithic settlements excavated in Turkey and stands out because of its size: Çatalhöyük East is around 13 hectares, whereas most Neolithic sites in this area range between approximately 1 or 2 hectares (Baird 2002; Cessford 2005). Together with Abu Hureyra 2 (11.5-16ha), 'Ain Ghazal (12-13ha) and Basta (14ha), Çatalhöyük (13.6ha) is one of the largest Neolithic sites in the Near East (Cessford 2005; Düring 2007).

Although Çatalhöyük is located within central Anatolia, the site has often been compared to Levantine “mega-sites”, as many cultural practises identified at the site overlap with Near Eastern sites, such as a social focus on memory construction through the re-building of houses directly over earlier ones and a symbolic focus on wild animals (Hodder 2007b). Çatalhöyük has therefore often been viewed within the context of a Levantine cultural chronology rather than an Anatolian one.

The Levantine Neolithic cultural sequence is divided into Pre-Pottery and Pottery Neolithic (early Ceramic) periods. Figure 2.2 shows the further subdivision of the cultural phases in the Pre-Pottery Neolithic period, which include the Pre-Pottery Neolithic A (PPNA), Pre-Pottery Neolithic B (PPNB) and Pre-Pottery Neolithic C (PPNC). The Pre-Pottery Neolithic B is characterised by the emergence of plant and sheep-goat domesticaton, whereas during the Pre-Pottery Neolithic C, the Levantine “mega-sites” started to appear (Wright 2014).

As Anatolia did not possess a strong tradition of Epipalaeolithic and Pre-Pottery Neolithic A habitation, Asouti (1995) argued that Anatolian sites should not be considered as integrated in the “nuclear zone” where the socio-economic changes leading to the emergence of the first agricultural settlements in the Near East took place (Asouti 1995). Instead, Asouti proposed to situate Çatalhöyük within the period of the later PPNB expansion and consolidation of the control over “new” territories, a time where communities experienced drastic changes, drew upon shared cultural traditions and in which group identity and social relations were actively negotiated (Asouti 1995). However, this has been contested by Wright (2014) and Baird (2005), who suggested that due to its large size and apparent isolation within the region, Çatalhöyük is unique and should not be considered as representative of the PPNB or PPNC.

Asouti (1995) argued that the earliest local evidence for an archaeological sequence building up to the emergence and growth of Çatalhöyük comes from the hunter-gatherer site of Pınarbaşı A (9500 BC) as well as several survey sites in the Konya plain (also see Baird 2005a; Fig. 2.3). The earliest Neolithic settlement in the Konya plain, where Çatalhöyük is located, is Boncuklu hoyuk (9000-8500 BC) 9km away, where architectural practices such as the continual reconstruction of buildings, show clear similarities to those apparent at Çatalhöyük (Baird 2006; Baird 2008).

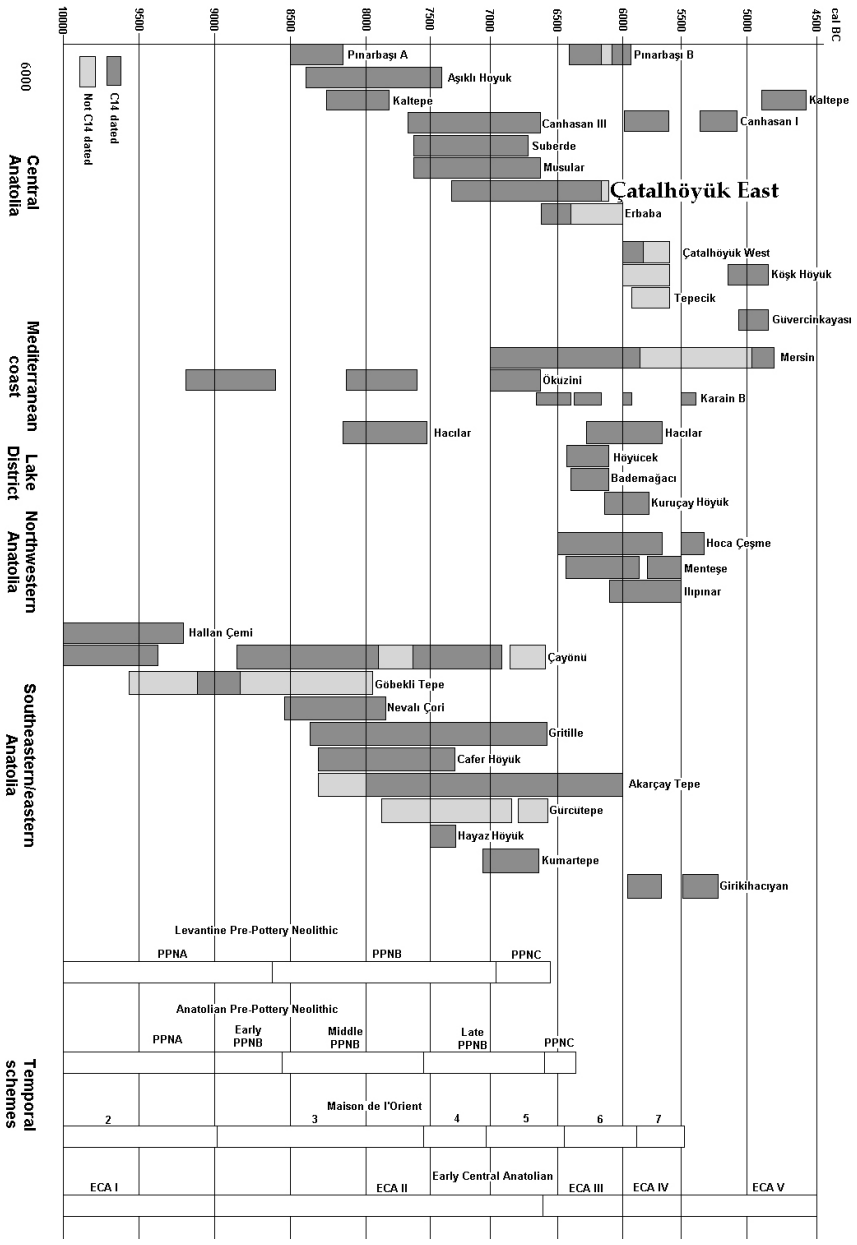

Figure 2.2: The dating of Çatalhöyük in relation to other sites in Anatolia and the Middle East (based on Cessford *et al.* 2005, reproduced in Hodder 2010, 4. For further discussion on chronology see Bayliss *et al*. in press)

From around 8400 BC, there are signs of obsidian exploitation in Anatolia, with quarries detected in Central Anatolia (the site of Kaletepe in the Cappadocia region), and, contemporary to this exploitation, the emergence of the earliest known permanent settlement in the region, Aşıklı höyük (Asouti 1995; Hodder and Cessford 2004; Hodder 2010). Around 7600 BC, before the abandonment of Aşıklı höyük, the non-domestic site of Musular appeared and was broadly contemporary with Canhasan III in the Eastern Konya plain (Asouti 1995; Fig. 2.2).

Asouti (1995) wrote that the emergence of Çatalhöyük, around 7400 BC (in Levantine terms: the later part of the PPNB) in the western Konya plain, can be understood in terms of the circulation of obsidian between Konya and Cappadocia, as evidenced by lithic finds in the early phases of the settlement, which appear to have links to Canhasan III, Aşıklı, Musular, Suberde, southeastern Anatolia and the Levant. In contrast, Baird (2010) argued that there is little evidence to suggest that Çatalhöyük had a substantial role in terms of the distribution of chipped stone. In any case, the site formed part of a network of small aceramic sites exploiting the wetlands in the Carsamba delta, which came to an end during the maximum growth period of Çatalhöyük (Asouti 1995).

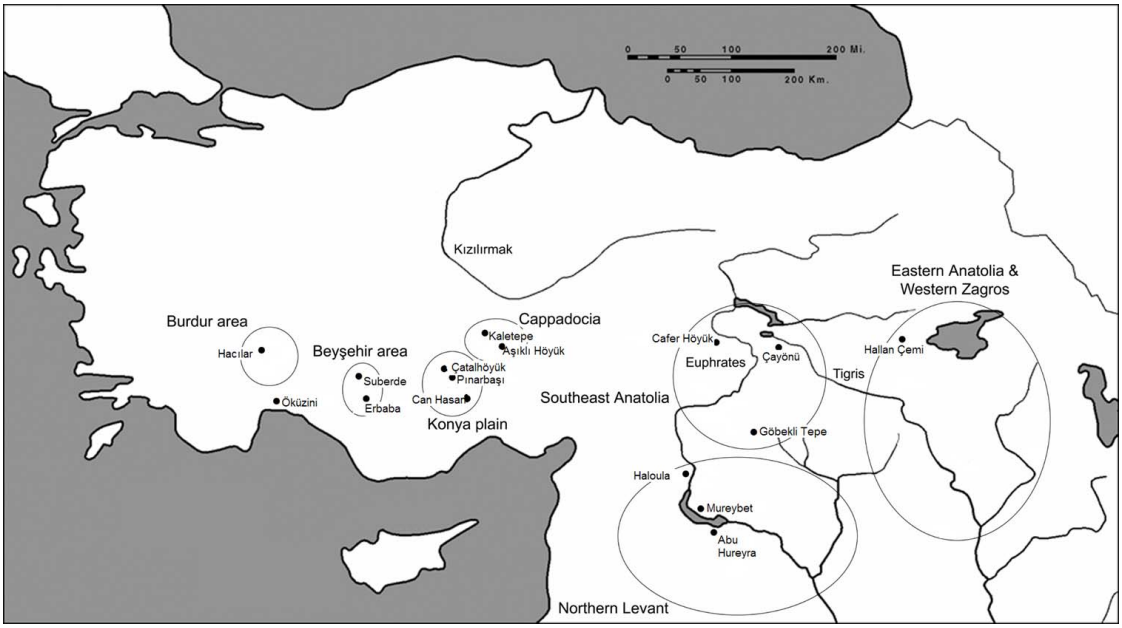

Figure 2.3: Location of Çatalhöyük and neighbouring sites (from Asouti 1995, 78)

2.2.1. Chronology

The East mound of Çatalhöyük has an estimated height of 21m, which Mellaart divided into 14 levels, labelled from 0 to XII with a subdivision of level VI (Farid 2007a; Hodder 2005a, 2007a). The Hodder excavations have added to this sequence, dividing the site into 18 stratigraphic levels (Hodder 2007a). Since 2008, a re-assessment of the existing dating from the East mound has been under way, integrating the stratigraphic sequence for the Hodder and Mellaart excavations based on published stratigraphic sequences from the Mellaart buildings, re-interpreting the taphonomic deviations of the dated samples and re-assessing the technical procedures used to obtain measurements (Bayliss and Farid 2008, 2010, 2012).

Levels from the current excavations and information from Mellaart's and Hodder's stratigraphic sequences can be divided into categories based upon the analysis of the number and density of buildings (Cessford *et al*. 2005; Düring 2006; Matthews 1996). Three broad temporal categories have been identified, organised around a "Peak" period in which density and community size were at a maximum: the Early ('Pre-Peak') period, including Mellaart levels pre-VII and Hodder levels South H, South J, South K, South L; the Middle ('Peak') period, including Mellaart levels VII-VI and Hodder levels North G, BACH.G, 4040.G, South M, and the Late ('Post-Peak') period, including Mellaart levels post-VI and Hodder levels 4040 H, South O, South P, South Q, South R, South S, South T (Table 2.1).

Table 2.1: Summary of Mellaart and Hodder levels

*Chronology based on Cessford *et al*. 2005; Stratigraphy based on Hodder 2011 (for detailed comparison with Levantine chronology and Central Anatolian periodisation, see Wright 2014)

(For further discussion on chronology see Bayliss *et al.* in press)

Mellaart level	**Hodder level: South**	**Hodder level: 4040**	**Cal BC***
pre-XII	SOUTH G		7560-6940 BC
XII	SOUTH H		
XI	SOUTH I		
X	SOUTH J		
IX	SOUTH K		
VIII	SOUTH L	4040F	
VII	SOUTH M	4040F	
VII	SOUTH N	4040G	
VI	SOUTH O	4040G	
VI	SOUTH P	4040H	
IV	SOUTH Q	4040H	
III	SOUTH R	4040J	
III	SOUTH S	4040J	
I	SOUTH T		
	TP (team Poznan)		
	IST (Istanbul)		
	Çatalhöyük West		
	Çatalhöyük West		5480-4340 BC

2.2.2. Neolithic climate and landscape in Central Anatolia

During the Neolithic, the Central Anatolian climate was semi-arid, but with a greater level of precipitation than today (Charles *et al*. 2014; Fairbairn 2005; Roberts *et al.* 2001). The environmental history of the Konya plain has been studied during two research programmes, the Konya Basin Palaeoenvironmental Research Programme (KOPAL,

see Roberts *et al.* 1999, Roberts *et al.* 2007) and the current Landscape and Coring programme (Doherty *et al*. 2007; Doherty 2008).

Research based on information from the KOPAL trench, located at the northern edge of the site, indicates that the alluvial basin in which Çatalhöyük is located was formerly a Pleistocene lake, which subsequently dried up, leaving a marl plain during the Neolithic period (Boyer *et al*. 2006; Love 2012; Roberts *et al.* 1996; Roberts and Rosen 2009; Roberts *et al.* 2007). A number of rivers flow on this marl plain, depositing alluvial sediments and forming alluvial landforms, such as the Çarşamba alluvial fan, which today covers around 474km^2 (Asouti and Hather 2001; Boyer *et al*. 2006; Roberts *et al*. 1996).

As such, Çatalhöyük is located within an undulating landscape of marshy flood basins and natural marl hummocks (Roberts and Rosen 2009). A recent analysis of phytoliths derived from midden deposits found a substantial presence of large-sized C3 reed and sedge conjoined phytoliths, supporting the hypothesis of a local wetland environment (Shillito *et al*. 2011a). Similarly, the consistent presence of amphibians within the Çatalhöyük microfaunal assemblage suggests the site's wetland surroundings and the bird bones found on site also suggest the exploitation of a wetland habitat (Jenkins 2009; Russell and McGowan 2005).

Roberts and Rosen (2009) argued that during regularly occurring flood periods, Çatalhöyük resembled an island within an inundated landscape (also see Boyer *et al*. 2006; Roberts *et al.* 1996; Roberts *et al*. 2007). However, evidence of non-swamp mudbricks at the site indicates the existence of drier silty deposits near the site (Doherty *et al*. 2007). Results of the recent coring programme (Doherty *et al.* 2007; Doherty 2008) indicated some level of seasonality, but that rather than an inundated landscape, a combination of wet and dry micro-environments with seasonally joined ponds is more likely. This is also supported by the presence of C3 and C4 phytoliths at the site (Shillito *et al.* 2011a).

2.2.3. Population

The population at Çatalhöyük has previously been estimated based upon the number of buildings within the site as well as ethnographic comparisons (Cessford 2005; Düring 2007). Another approach was to take into account the building density and estimated

population size by multiplying building number by assumed household size, i.e. a modal household size of five (Düring 2007). Assessments based on both approaches provide an estimated range of 5000 to 10 000 people (Table 2.2).

Table 2.2: Maximum population estimates for Çatalhöyük (from Düring 2007, 158)		
Author	**Publication**	**Estimate**
Mellaart	1965: 202	8000 - 10 000
Mellaart	1975: 99	5000 - 6000
Cohen	1970: 122-123	5000+
Angel	1971: 82-83	5000 - 6000
Matthews	1996: 86	5060 - 6748
Cessford	2005: 326	3500 - 8000
Düring	2006: 234	5362 - 8044

Cessford (2005) argued that estimating the population size of Çatalhöyük is extremely difficult using building numbers and burials, but that it is evident that the population size at this site was substantial. He also proposed that this high number of inhabitants was likely to produce problems in terms of resource procurement and stress related to this agglomeration.

As described above (p. 24), based upon the analysis of the number and density of houses at the site, a diachronic change in population density and community size can be distinguished at Çatalhöyük, dividing the periods before (‘Pre-Peak’) and after (‘Post-Peak’) the time during which population size was at a maximum (‘Peak’).

2.2.4. Architecture

The East mound (höyük) of Çatalhöyük consists of densely packed flat-roofed mudbrick buildings which were repeatedly plastered with white clay and could be accessed via ladders through openings in the roofs (Düring 2001; Farid 2007a; Hodder 2007a; Matthews 2005a; Matthews 2005b). A range of activities appear to have taken place on the roofs, such as food processing and craftwork (Cutting 2005; Düring 2007). Matthews (2005a) also suggested that cooking might have taken place on the roof, as evidenced by areas of scorching and an oven base on a segment of collapsed roofing on Building three. Düring (2007) wrote that domestic buildings were clustered in neighbourhoods, with the site consisting of between 27 and 53 such clusters. Similarly, Matthews (2005b) argued that refuse areas were surrounded by clusters of around 20 to 30 buildings.

Various researchers have stressed the degree of continuity in the Çatalhöyük structures, with buildings constructed on top of older ones and with the same orientation over

hundreds of years (Baird 2006; Cutting 2005; Düring 2007; Hodder 2007a; Hodder 2007b; Fig. 2.4). Radiocarbon dates and plaster analyses estimate the use-life of buildings at around sixty years (Cessford 2005; Düring 2007; Matthews 2005b). The foundation opening and building closure followed a constant pattern throughout the occupation (Farid 2007a). Buildings were usually cleaned on abandonment, floors scoured, walls dismantled and houses filled with processed building material and other infill to make a solid foundation for the next building (Farid 2007a; Hodder 2007a; Shillito *et al*. 2011a; Twiss *et al.* 2008).

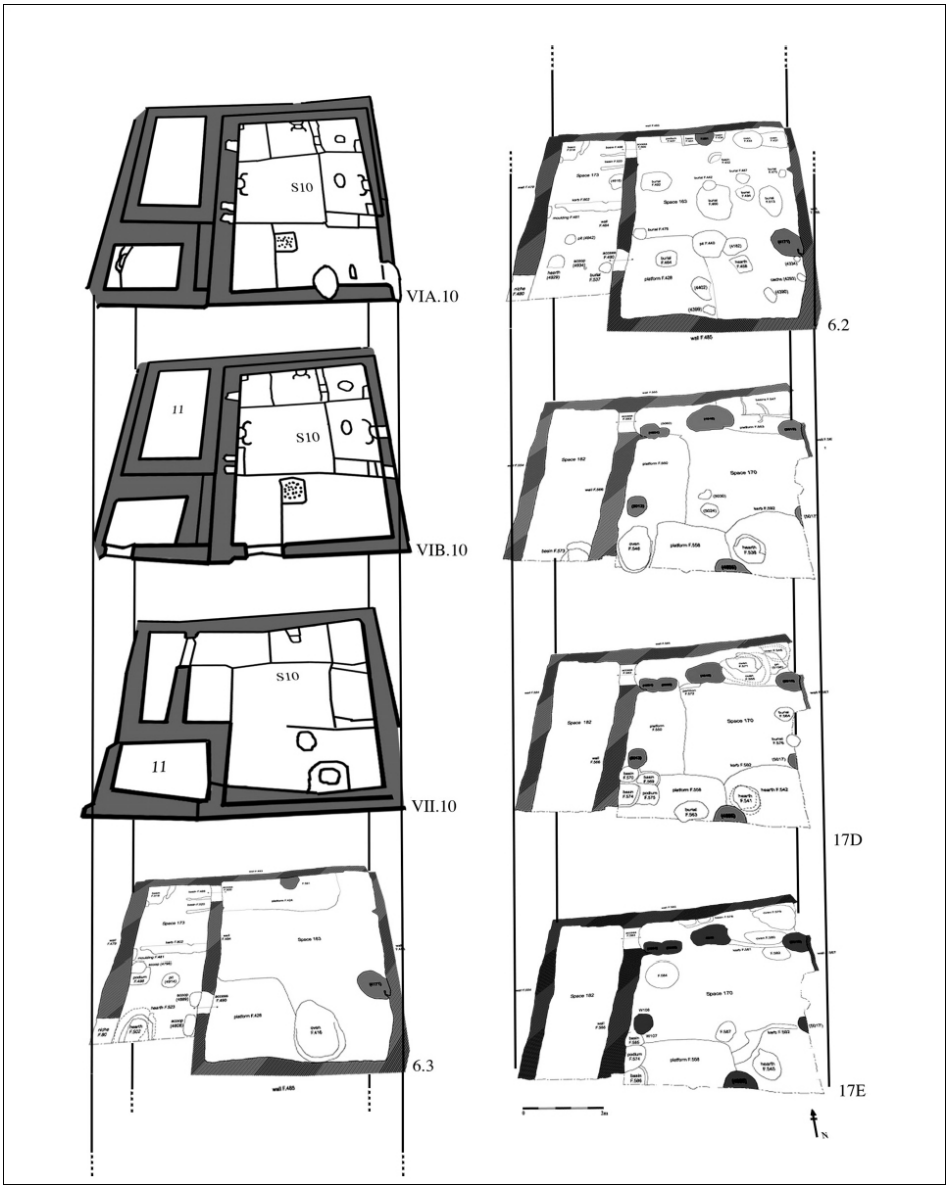

Figure 2.4: Schematic overview illustrating the continuity of buildings in one location over time, from Building 17 phase E (bottom right), through the phases of Building 6 and into Mellaart's shrines 10 in his Levels VII, VIB and VIA (upper left) (from King in Hodder and Pels 2010, 170)

Buildings generally had their own set of outer walls and average building size was about 27m^2 (Düring 2007). Inside houses, space was divided in rooms with subsidiary smaller storage spaces (Farid 2007a; Twiss *et al.* 2008; Fig. 2.5). Larger rooms were further subdivided by shallow features and ledges (Farid 2007a). Düring (2007) identified two room types within the buildings, "living rooms", often containing storage bins, with an average size of 21m^2 and "ante-rooms", with an average size of 5m^2.

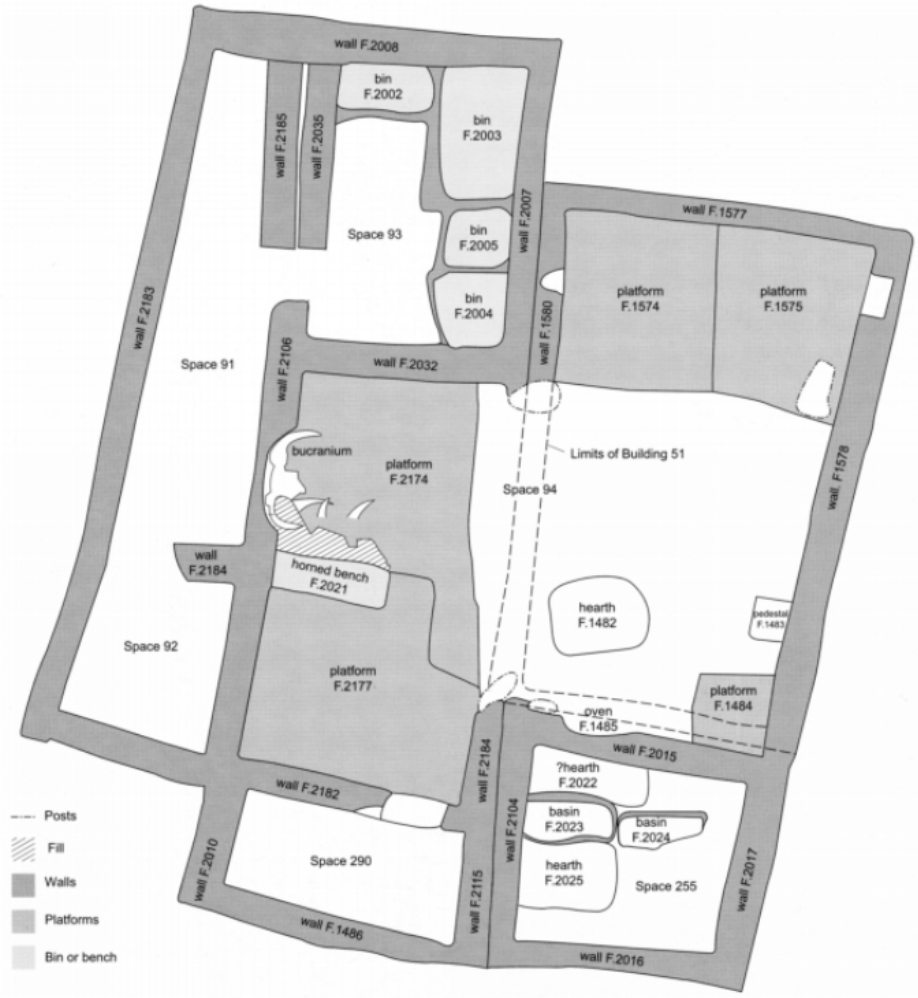

Figure 2.5: Plan of Building 52, 4040 area, Hodder level 4040G. North on top (drawing by Wilkins A, in Twiss *et al.* 2008, 45)

The southern end of the living rooms usually consisted of fire installations, an entrance ladder, storage features and a "dirty area" with evidence of cooking and craft practices (Düring 2001, Farid 2007a; Hodder 2007a). Two types of fire installations within buildings can be identified, ovens, which appear as large, oval, dome-shaped structures built against walls or posts and smaller free-standing hearths (Cutting 2005; Farid 2007a).

Platforms were also located in the main rooms and generally placed along the east and north walls (Düring 2001). As well as evidence for everyday activities carried out on these platforms, such as sitting, eating and sleeping, these structures also contained sub-floor burials (Düring 2001). A large assemblage of art (wall paintings, moulded features) and animal parts (making up installations) were incorporated in the architecture of the site (Düring 2007; Last 2005).

Russell and colleagues (Russell and Meece 2005; Russell *et al.* 2009) argued that various types of special deposits occur in the majority of houses throughout the site.Some of these special deposits tended to be concealed in the fill of a building's foundations, within walls or below floors and have been found to contain feasting remains or scapulae and horn of cattle and other taxa (Russell and Meece 2005). Others have been identified as "ritual trash deposits", which were deposited outside (in middens, for example) and within abandonment deposits and include remains of feasts, dismantled installations and dumps of raw material stores (Russell et al. 2009). In contrast to these deposits which were kept out of view (Fig. 2.6), installations are deliberately placed to be visible within the building and include horns, mandibles and skulls mounted on walls, benches and pillars (Russell and Meece 2005, Russell *et al*. 2009, Last 2005). Russel and colleagues (2009, 108) wrote that these special structures "*incorporate the memory of ceremonial events into the physical fabric of the house."*

In terms of diachronic changes in the construction and demolition of buildings, a pattern of extensive house burning has been noted from level VI, in the South, North, Istanbul and 4040 areas (Twiss *et al*. 2008; Fig. 2.7). In contrast, no evidence of burning has been found pre-level-VI during the recent excavations in the South area.

Whereas Mellaart (1998) considered fires as accidents destroying neighbourhoods, Cessford and Near (2005) interpreted the burning of buildings as a deliberate act by the site's inhabitants, linked to the abandonment of buildings. Hodder (2009) wrote that the fires at the end of level VI (Buildings 79 and 80) seem to be associated with a shift in the pattern of occupation.

Figure 2.6: Commemorative deposit: Cluster of stone and bone objects and some obsidian (F14009) placed in a circular pattern under a bench on the east side of Building 65, South area, Hodder level South. Q (Photography by Quinlan J, Çatalhöyük research project)

Hodder and Pels (2010) argued that the increased pattern of burning events is associated with a decrease in building size and a break in the exact replication of the structure of the house. Similarly, Düring (2005; 2007) proposed a difference in building practices between the earlier levels (Mellaart levels XII-VI, early Ceramic Neolithic 7000-6000 BC) and the later levels (V-I, late Ceramic Neolithic 6600-6200 BC), as the density of houses changes from clustered neighbourhoods in Mellaart levels XII to VI, to more open areas in later levels (Düring 2007; Fairbairn *et al.* 2005).

In terms of building construction, Doherty (2007; Charles *et al*. 2014) also noticed a change in materials, from mudbrick composed of dark-grey brown “backswamp clay” in the earlier levels to a reddish-brown “mineral based” composition. This is interpreted as “better performance material” from the transition between the Pre-Peak and Peak periods (Mellaart levels VII-VIII/Hodder levels L and M; also see Love 2012). In addition, the latest (Post-Peak) levels seem to show that the mudbrick was composed of recycled midden material (Charles *et al*. 2014; Hodder 2007a).

Figure 2.7: Fire-related discolouration to main floor platform, Building 52, 4040 area, Hodder level 4040G (From Harrison 2009, 278)

Similarly, Düring (2007) and Hodder (2010, Hodder and Meskell 2011) argued that the symbolism used at Çatalhöyük also changed over time, from a predominating focus on elaborate animal installations in houses in the earlier (pre–level V) buildings, to fleshy figurines with removable heads in later (level V and above) levels. In addition, Last (2005) suggested that there may be temporal changes in the nature and subject matter of wall paintings in the houses. Düring (2007) expanded on this, noting an increasing level of complexity in the wall paintings. He argued that in levels VI and earlier, walls were occasionally painted red or with simple red-and-black geometric patterns. Whilst this style continued in the upper levels, there is more evidence of figurative paintings, such as the bull-leopard in Level IX and vultures in VIII and VII, or the hunting scenes of Level V onwards.

2.2.5. Food consumption

The archaeological evidence suggests that the inhabitants of Çatalhöyük practised a combination of crop agriculture and caprine herding, supplemented by hunting and intensive gathering (Twiss *et al*. 2008). The following is an overview of the evidence for the consumption, storage and processing of plants, meat, fish and fuel.

Plant consumption

In most houses, one or two types of pulses were found, with pea being the most common (Bogaard *et al*. in press; Roberts and Rosen 2009). A range of cereals has also been found within buildings, including einkorn wheat, emmer wheat, naked barley and free-threshing wheat (Fairbairn 2005; Fairbairn *et al.* 2007). In an initial analysis of two samples of human dental calculus, van de Locht and Hardy (2009) also found evidence of starch.

In addition to the abundant remains of cultivated crops found at Çatalhöyük, a wide range of wild plants has been recovered from the buildings, including remains of wild crucifers, bulbs of sedges, wild mustard, hackberries, almonds and acorns (Bogaard *et al*. 2009; Fairbairn 2005; Fairbairn *et al.* 2007). These were found consistently throughout the site, indicating that wild seed exploitation was a regular subsistence practice and that an extensive range of crops was consumed (Bogaard *et al*. 2009; Fairbairn *et al*. 2007).

Wild plants, commonly found in the arable fields in the Çatalhöyük area today, could potentially have provided a buffer against food shortages in an unstable and unreliable natural environment (Fairbairn 2005; Fairbairn *et al*. 2007; Roberts and Rosen 2009). Spatial analysis of wild and domestic plant and animal remains in one of the houses (Building 52) found no clear-cut differences in the distribution of wild versus domestic resources and their placement seems thus to be related to their consumability rather than their wild or domestic status (Bogaard *et al.* 2011; Twiss *et al*. 2009).

Additional evidence of wild plant resources supplementing the human diet at Çatalhöyük is provided by coprolites. Wild pistachios, acorn and almond shells were found in a coprolite recovered from the South area (Atalay and Hastorf 2006). Charred seeds and tubers of sea club-rush, a starch-rich wild plant typical of saline environments, have also been recovered in comparatively large quantities from the site (Wollstonecroft and Erkal 1999).

In an experimental study on the harvesting and processing of sea club-rush, Wollstonecroft and Erkal (1999) found that the tubers are edible as a raw vegetable and as flour. Based on ethnographic comparisons, they found that a composite sedge/wheat flour can be used to make bread, gruel, dumplings or as a thickening agent for mixing into soups. As this plant would have been available all year round in the surrounding

wetlands, they argued that sea club-rush might have provided a critical source of carbohydrate in times of crop failure or as a complement to diminishing wheat stores (Wollstonecroft and Erkal 1999).

Plant storage

There is extensive evidence for plant storage at the site, ranging from perishable containers, as indicated by phytolith traces and plant impressions, and built storage features (clay bins) to big concentrations of grain in burnt buildings (Atalay and Hastorf 2006; Bogaard *et al.* 2009). As some of the Çatalhöyük buildings were burnt upon abandonment, they provide an excellent in-situ record of storage practices. For example, Building 52 in the 4040 area has evidence of four storage bins along two (the eastern and northern) walls of a medium-sized space (Twiss *et al.* 2008; Fig. 2.5). Spatial analysis of the botanical and faunal remains found in this building demonstrates an exclusive concentration of food and raw material in this space (space 93, north of the main central room of the building, Fig. 2.8), both confirming the regimented nature of the Neolithic house and indicating that storage practices were confined to specific areas of the house (Twiss *et al.* 2008, 2009).

Some of the bins in space 93 were heavily damaged by fire, but in one of the bins (feature 2005), over 30 litres of seeds of small-seeded crucifers has been discovered (Twiss *et al*. 2008, 2009). These seeds were probably used for oil or as a spicy flavouring (Fairbairn *et al.* 2007; Twiss *et al*. 2009). Another, more damaged bin (feature 2004) contained a dense concentration of faunal (wild boar mandible, red deer antler tinet and worked cattle-sized rib fragment), lithic (a fine projectile point) and botanical (crucifer seeds, cereal remains and several literes of peas) remains (Twiss *et al.* 2008, 2009). Twiss (2012) calculated that average bin capacities amounted to around 1200 litres ($1.2m^2$). Notwithstanding the storage space in perishable containers such as bags or baskets and the possibility of off-site storage space, which cannot be accounted for, regionally appropriate ethnographic parallels suggest that the stores were supporting residents of each house rather than larger groups (Twiss 2012).

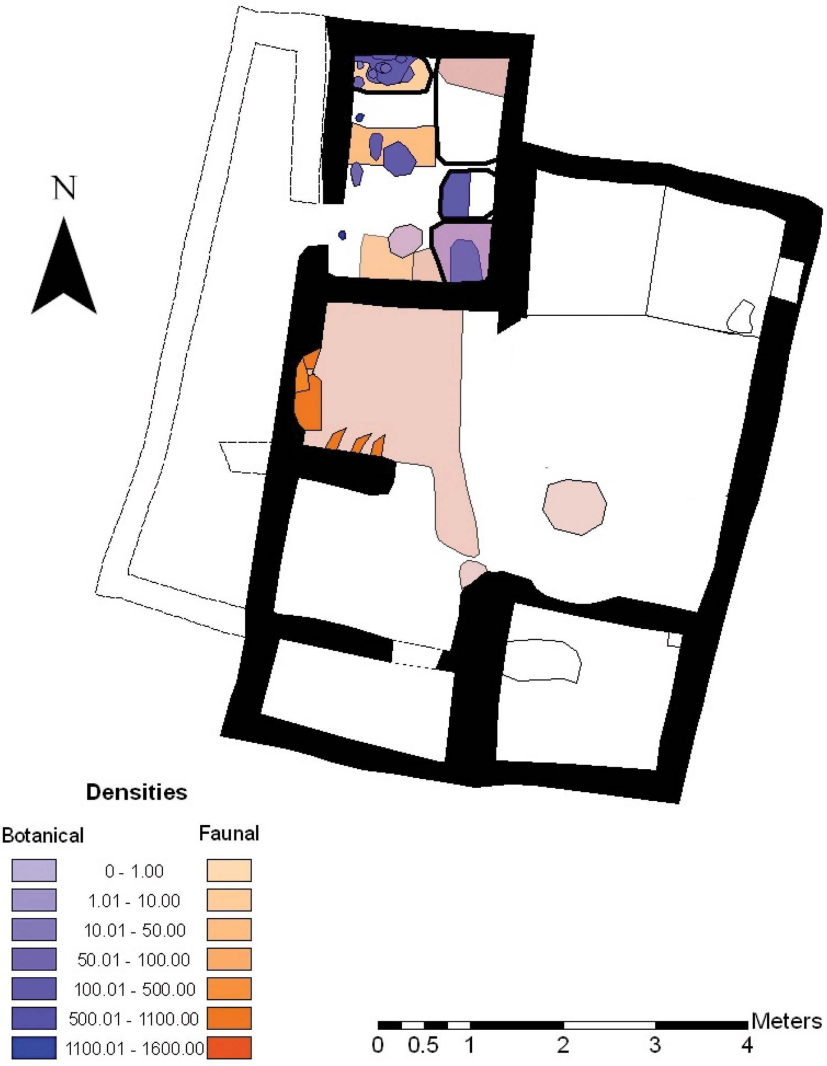

Figure 2.8: Macrobotanical and macrofaunal distributions within Building 52 (From Twiss *et al.* 2008, 891)

In addition to built features and in-situ concentrations, microfaunal analysis also provides (indirect) evidence for storage practices. For example, findings of charred mouse pellets and burnt mouse bones indicate that the storage area in Building 52 was infected by rodents (Twiss *et al.* 2008, 2009). Jenkins (2009) also noted a consistent number of house mice at Çatalhöyük, possibly from Pre-Level XII.B (Hodder level G, Pre-Peak period), but certainly from Level X (Hodder level J, Pre-Peak period). Jenkins (2009; 2012) suggested that small carnivores (possibly weasels) were encouraged to enter the site as some form of pest control. Based on the large concentrations of microfauna with signs of digestion, gnawing and puncture marks recovered from three burials, including one burial excavated by Mellaart (Building VIII.31) and two burials uncovered in 1999 (burials 460 and burial 513 found in space 163, Building 6, South area), Jenkins (2009,

2012) argued that scats of small carnivores were deliberately placed within human burials, possibly as grave goods for the people (one young adult male and two adult females) who monitored these pest control activities.

Meat consumption

In terms of animal consumption, the main source of meat (and fat) at Çatalhöyük was sheep. Faunal analyses of cull patterns suggest that sheep and goat were mainly kept for meat consumption, with mostly subadults and young adults being killed (Evershed *et al*. 2008; Russell and Martin 2005). Similarly, preliminary results from the stable isotope analysis indicate that the adult diet consisted of a mixture of animal and plant proteins and that goat and sheep were most frequently consumed (Richards *et al.* 2003; Richards and Pearson 2005).

Early analysis of the faunal remains at Çatalhöyük suggested that the diet mainly consisted of cattle consumption (Perkins 1969), but later analyses by Russell and colleagues (2005, 2009) revealed that this assumption was based on an over-representation of cattle remains due to the lack of screening and systematic collection during the Mellaart excavations. In addition, stable isotope analysis found that cattle were not the main source of dietary protein for all the occupants at Çatalhöyük (Richards *et al*. 2003).

In terms of the domestication of cattle, Russell and colleagues' (in press) recent analysis of faunal remains from the later levels of the East mound and the (Chalcolithic) West mound has found evidence of smaller cattle sizes, a new male horn shape and younger male cull patterns, all of which points towards the presence of morphologically domestic cattle in the Post-Peak period (Hodder levels South N and O). In contrast, Russell and colleagues' (2009) morphological study on cattle bones in the earlier levels confirmed the results of previous studies (Ducos 1988; Grigson 1989) that they fall within the wild range and their mortality profiles represent a hunted assemblage (Russell and Martin 2005; Russell *et al.* 2005, 2009).

Russell and Meece (2005) argued that cattle bones are over-represented in special deposits and that males form two-thirds of these deposits, suggesting a symbolic significance of cattle, especially bulls, rather than dietary importance (Russell *et al*. 2009). The disproportionally high representation of horn and scapulae, unlikely to be

selected for their nutritional value, also points towards the symbolic rather than nutritional value of cattle at Çatalhöyük (Russell and Martin 2005).

In addition to sheep/goat and a limited amount of cattle being consumed at the site, small mammal species, including foxes, hares and badgers, also show butchery marks consistent with consumption (Atalay and Hastorf 2006; Russell and Martin 2005). The mortality profile of foxes indicates that these were probably trapped rather than selectively hunted (Russell and Martin 2005).

Compared to other prehistoric assemblages, there is a large amount of bird remains at Çatalhöyük, with about 387 specimens identified by Russell and McGowan (2003, 2005). This included large numbers of waterfowl, in particular ducks and geese but also grebes and coots, and various types of raptors were also well represented within the sample. The authors argued that birds formed part of both the dietary and symbolic sphere at Çatalhöyük (Bogaard *et al.* 2011; Russell and McGowan 2000, 2005). Additionally, over a thousand samples of egg shell from at least three species (goose, duck and an as yet unidentified species) have been recovered from the North, South and KOPAL areas of the site (Sidell and Scudder 2005). The majority of the shells examined come from unhatched eggs, indicating that either birds were bred for eggs on site or that eggs were collected from the wild (Sidell and Scudder 2005).

In terms of diachronic change, recent zooarchaeological work by Russell and colleagues (in press) showed an increased reliance on cattle in the Pre-Peak period, from South G (6.2%) to South H (21.9%), which sharply decreased again between the Peak period (South M; 19%) and the Post-Peak period (South Q; 7.7%). Interestingly, this drop in the proportion of cattle in the overall faunal assemblage coincides with the apparent adoption of cattle herding (see above, p. 37). There is no indication of temporal change in bird habitats exploited by the Çatalhöyük residents (Russell and McGowan 2005).

Indications for domestic meat storage practices are limited, as faunal material found inside storage bins probably represents raw material storage for bone and antler working rather than the storage of food supplies (Twiss 2012). However, Atalay and Hastorf (2006) mentioned the possibility of some meat preservation based on salting, as concentrations of salt deposits (pale yellow salts) have been found in food preparation areas (Mellaart area: area A-E in South) and in oven rake-outs such as one found in the Northeast platform (space 170) of Building 17 (Matthews 1996, 2005a).

Fish and seafood

Most fish bones and scales have been recovered through the flotation process and are included in heavy residue samples (Jenkins 2000). The entirety of the fish bone assemblage appears to be from very small fish and fish samples are found in a wide variety of contexts at Çatalhöyük (Frame *et al.* 1999). It is possible that fish (mainly Cyprinidae, anchovy-sized fish) were also consumed at the site (Bogaard *et al.* 2011; Popkin in press; Twiss 2012). For example, In Building 1 (North area), findings of small fish vertebrae recovered adjacent to a small hearth suggest that the platform was used for processing or depositing small fish (Hodder 1996; Matthews 1996). Similarly, in the central platform (F1656) of Building 49 (4040 area), the semi-articulated fish bones found together with a small ashy deposit (13698) and evidence of knapping activity can be interpreted as evidence of food waste, possibly deliberately swept into the corner of the platform (Eddisford 2006).

In addition to fish, the majority of shells recovered at the site have been identified as freshwater shells (mainly *Unio*), which would have been available locally (from the nearby Çarşamba river), and were probably used as food source in addition to their use as raw material for ornaments and containers for pigment (Reese 2005).

Food processing

Various studies have provided insights in food processing practices at the site, including pottery analysis, object analyses (based on clay balls and baskets) and faunal analysis (burning patterns and cutmarks on bones).

Due to the porous nature of unglazed pottery vessels, evidence of food processing (cooking – lipids) is absorbed in the vessels' walls (Copley *et al*. 2005). In a preliminary analysis of pottery sherds (N=28, from North and South areas and from Mellaart levels IX to V), Copley and colleagues (2005) found that 18% of their sample contained lipid residues, with the majority (80%) of the fatty acids indicative of ruminant adipose fat and none containing dairy fat. They also proposed that the ruminant fat is probably derived from sheep/goats (Copley *et al.* 2005). Similarly, Evershed and colleagues (2008) undertook a major analysis of organic (lipid) residues preserved in pottery from archaeological sites in southeast Europe, Anatolia and the Levant and found that in contrast to other Neolithic sites in (northwest) Anatolia such as Toptepe, Hoca Çesme and Pendik, milk was being utilised on a small, nearly invisible scale at Çatalhöyük.

Atalay and Hastorf (2006) argued that foods were either boiled, by placing oven-heated clay balls in baskets or skins and/or roasted directly in the oven. However, preliminary lipid analysis of clay balls (N=9 from Mellaart levels VII, IX, VIII, IX, South area) suggested that these items were not in contact with liquefied lipid-rich organic materials during their use, which does not support the use of clay balls in pot boiling (Copley *et al.* 2005). Wendrich (2005) suggested that baskets could have been used as an alternative type of food preparation. Çatalhöyük basketry was made of fine bundles, ranging in size from 3-8mm, and small winders and the plant material used for this type of material (possibly grass leaves) was able to expand through the absorption of moisture, so could have been used for holding fluids and for cooking (Wendrich 2005).

In relation to preparation of meat, Russell and Martin (2012) wrote that burning patterns on animal bones are mainly post-depositional, which suggests that meat was stewed or baked rather than burnt. Cut marks are rare on animal bones (0.2% of the faunal remains bear cut marks of which 20% are filleting marks). One explanation for this is that the particular type of chipped stone tool thought to have been used in food preparation at Çatalhöyük was obsidian, which leaves few traces on bones. However, when cutmarks are found on bones, they appear not to be related to dismemberment but to cutting the meat off the bones (they have been found mostly ribs and some long bones) after cooking (Russell and Martin 2012; Twiss 2012). As stewed meat requires less cutting, this also suggests that food was baked rather than stewed (Russell and Martin 2012). In addition, fragmentation patterns of animal bones at the site suggest that most long bones were broken for marrow or grease (Russell and Martin 2012; Twiss 2012). Body part distribution patterns indicate that whole caprines were consumed by single households.

In addition to evidence for the preparation of daily domestic mails, there is also evidence of feasting at Çatalhöyük. Twiss (2008, 2012) argued that the consumption of symbolically important foods is one of four main correlates of feasting deposits. The symbolic status of wild cattle is indicated by its iconographical presence at Çatalhöyük, which includes representations in the zoomorphic figurine assemblage, wall paintings and its incorporation into installations and special deposits (Russell and Martin 2005, 2012; Twiss 2012). Twiss (2012) wrote that aurochsen, which are notably difficult and dangerous animals to hunt, would have provided hundreds of kilos of meat per animal. Therefore, Russell and colleagues (2009; Twiss 2012) linked the feasting deposits with large-scale consumption, which probably included various households.

Fuel consumption

Atalay and Hastorf (2006) wrote that the majority of cooking activities occurred around ovens and/or hearths. The proximity of ovens near ladder impressions in wall plaster indicates that ovens were generally placed below the roof entrance, to allow smoke to disappear, although soot evidence in wall plaster indicates that smoke did not entirely dissipate (Atalay and Hastorf 2006; Düring 2001; Farid 2007a; Matthews 2005a).

In terms of fuel consumption, Shillito and colleagues (2011b) studied thin sections of ash layers from middens at the site and found evidence of calcite plants (reed and grass phytoliths), amorphous forms of wood as well as occasional animal dung spherulites, suggesting the presence of dung fuel (also see Bogaard and Charles 2007; Cessford and Near 2005; Matthews 2005a; Twiss *et al*. 2008). Cessford and Near (2005) argued that both wood and slower-burning dung fuel may have been employed as a result of seasonal differences in availability and functional preferences. Various experiments have been conducted in order to reconstruct oven firing, with some also using dung fuel (Eddisford *et al*. 2009; Harrison 2009). Most of these experiments resulted in excessive smoke, leading to the suggestion that external fires might have been used, as evidenced by fire spots in open midden areas in the South area (Eddisford *et al.* 2009).

Some diachronic changes have been detected in the types of wood exploitation and fuel consumption (Fairbairn *et al*. 2005). For example, Fairbairn and colleagues (2005) found that dung fuel was more predominant than riparian tree charcoals in the earlier occupation of Çatalhöyük whereas, in later levels, dung persists but oak and juniper charcoal becomes more frequent.

2.2.6. Human remains

Burial

The human remains at Çatalhöyük were deposited in various ways. A total of 1903 depositions have been found, ranging from single fragments of bones or teeth to complete, articulated skeletons (Hager and Boz in press). Most interments were primary (complete or nearly complete skeletons) or primary disturbed single events, but secondary (partial or complete re-deposited skeletons) and tertiary (scattered,

disarticulated bone found in non-internment contexts) depositions have also been recorded(Hager and Boz in press). The more complete skeletons have generally been found in a flexed position (Fig. 2.9) and there are no indications that burials were left open, as no slumping of burial cuts is apparent (Farid 2007b).

Figure 2.9: Young adult female skeleton 18457 found in a flexed position under northeast platform in Building 76, Hodder level South O (Photo: human remains team)

Evidence from phytoliths indicates that material from plant remains (cloth) could have been used for wrapping or binding the body (Hager and Boz in press; Fig. 2.10). Neonates and young infant remains are frequently found in baskets. More specifically, in a detailed phytolith study of baskets found in the North area, Wendrich (2005) discovered that some of these funerary baskets showed more patterns of wear than others, indicating that they might have been used previously.

Figure 2.10: Humerus of juvenile skeleton 17939 (feature 4028, Building 49, area 4040, Hodder level 4040G) showing thick layers of phytoliths wrapped around bone (Photo: human remains team)

There is substantial evidence that some graves contained pigments, mainly red and yellow ochre, but also some blue, green and grey pigments and brown residues, the latter possibly indicating the remains of leather pouches (Hager and Boz in press). Some skulls, for example, EVI 20 from the Mellaart excavations and an adult male from Building 42, were found with evidence of paint (cinnabar) or plaster and red ochre (Molleson *et al*. 1999). Other occasional grave goods, such as animal bones, shells and stones are present throughout the site (Hager and Boz in press). However, these are relatively rare; which led Hamilton (2005) to argue that they cannot be considered to give any indication of individual identity.

Primary burials have mainly been found under house floors, especially in the northern and eastern platforms and the central floor of the houses. Graves were closed and covered with layers of plaster and were often re-opened for new interments. During these

occasions, previously interred remains were often pushed aside (Hager and Boz in press). Selected elements were sometimes removed, to be put in different locations or included in the grave fill. A small number of isolated skulls (N=24) as well as other isolated skeletal elements (such as femora) have also been found in secondary deposits, in platforms, under floors, in middens, infills, between walls and in one particular example (Building 17), at the base of a supporting house post (Hager and Boz in press; Molleson *et al.* 2005). Two headless individuals also showed evidence of cutmarks on the hyoid (1466, adult male, Building 1, North area) and on the first cervical vertebra (4593, adult male, Building 6), indicating the intentional removal of body parts (Molleson *et al*. 2005; Fig. 2.11).

Figure 2.11: Burial with headless skeleton 4593, adult male from Building 6, Hodder level South. L (photography from Farid 1999)

Health

In terms of oral health, Boz (2005), based on sample of 63 individuals (corresponding to 829 teeth) argued that the degree of dental calculus (33% slight, 11.3% moderate and 2.1% heavy) and the rate of caries (6.6% by tooth count) was high compared to other Neolithic sites such as Çayönü and Aşıklı höyük. In a more recent study using a larger sample, Boz and colleagues (2013) confirmed this high caries prevalence and suggested a carbohydrate rich diet was consumed at the site. In this later study, differences were not found between males and females could be detected, suggesting equality in access to various foods between the sexes.

Reporting the results of a macroscopic study on enamel defects, Boz (2005) argued that the frequency of furrow-form enamel hypoplasia (12.8%) at Çatalhöyük is high compared to other Neolithic sites such as Çayönü and Aşıklı höyük (Table 2.3). Similarly, Angel (1971) also reported a frequency of linear enamel hypoplasia of 13% at Çatalhöyük.

Table 2.3: Frequency of linear enamel hypoplasia at Çatalhöyük (based upon Boz 2005)

Tooth type	N	N hypoplasia	% hypoplasia
LI1	36	5	13.8
LI2	32	3	9.3
UI1	39	11	28.2
UI2	32	3	9.3
Total (all tooth types)	490	63	12.8

In their analysis of the skeletal and dental assemblage at Çatalhöyük, Molleson and colleagues (2005; Molleson 2007) emphasised the high number of immature individuals within this sample, arguing that this might be evidence of high levels of stress affecting the young. Molleson and colleagues (2005; Molleson 2007) also found that the Çatalhöyük children (N=62) were small for their dental age in comparison to modern reference samples, and interpreted this as an indication that they were brought up in an environment which was detrimental to their health.

In terms of adult stature, based on a sample of 24 individuals (13 females and 11 males), Molleson (2007) estimated an average height of 154.4 (+/- 1.32) cm for females and 162.8 (+/- 7.45) cm for males. This suggests that individuals from the community at Çatalhöyük were short in stature and showed evidence of low sexual dimorphism. Similarly, Ruff and colleagues (2006a) calculated body mass (from femoral head size) and stature (femoral length) from the adult assemblage of human remains at Çatalhöyük

and found that both were relatively low (59.6kg and 162cm for males and 54.9kg and 156cm for females). Both studies associate this relatively short adult stature to insufficient nourishment during growth. However, Molleson also noted that the estimated stature is similar to the ranges found in the region today, indicating that non-nutritional factors might also be involved (Molleson 2007).

Another indicator of unfavourable living conditions comes from residues found on some of the human ribs. Rib fragments from various individuals (burial 513 found in space 163, Building 6, South area/ unit 2119, North area and units 1378 and 1424 from Building 1) were covered with a black carbon-like residue (Molleson 2007). A detailed analysis of the residue from the ribs of two adults (1378 and 1424 Building 1, North area) suggested that these residues might have been the result of smoke pollutants caused by cooking (Birch 2005).

A small amount of evidence for intestinal parasites has also been found at Çatalhöyük, including a fossilised example of *Echinococcus Granulosus* (Fig. 2.12), found in the stomach cavity (where the liver would be) of a young female (Skeleton 15960, Foundation trench 23 area 4040) (Lomas 2008).

Figure 2.12: Intestinal parasite (*Echinococcus Granulosus*) found in the stomach cavity of Skeleton 15960, adult female, around 18-25 years old from Foundation trench 23, area 4040 (Photo: Lomas 2008)

In a sample of 216 adults and 72 subadults excavated by Mellaart in the 1960s, Angel (1971) noted high levels of porotic hyperostosis, as indicated by porosity and/or thinning of the outer table of the cranial vault, linked to the expansion of the marrow space of the skull.

Angel (1966, 1971) argued that this condition was the result of iron-deficiency anaemia caused by *falciparum* malaria. The view that porotic hyperostosis is caused by chronic iron-deficiency anemia has been widespread since the 1950s, but recently, this hypothesis has been questioned based on hematological research, which indicates that the human response to iron-deficiency anaemia is to restrict rather than increase red blood cell production and as such, the marrow expansion that produces porotic hyperostosis cannot be explained in this way (Walker *et al*. 2009).

Despite mentioning the potential impact from malaria, on the health status of the people living in Çatalhöyük, Angel (1971) also wrote that stand out because of their good diet, adequate growth and “excellent teeth”. More recently, with the advancement of analytical techniques and continued excavations, increasing the size of the sample under study, the view of the Çatalhöyük community as a stressed population has also been challenged. For example, Ruff and colleagues (Garofalo *et al.* 2011; Ruff *et al*. 2013) examined growth through stature, body mass and cortical area, derived from femoral length (for stature), femoral head breadth (for body mass) and femoral mid-shaft measurements (for percentage cortical area) for a subset from the entire Çatalhöyük sample (N=32 for stature, N=28 for body mass). They compared these parameters with proto-historic (Arikira) and modern 20th century (US Denver growth study) populations and found that the ontogenetic patterns of the Çatalhöyük population do not support the view of a negative impact on health at this site.

Biomechanical analysis of skeletal morphology can also inform us about levels of activity, workload and mobility. Larsen and colleagues (2012, Charles *et al.* 2014) carried out a detailed study of bone strength at Çatalhöyük, as inferred from measurements of the femoral midshaft (50% section, Zp, polar section modulus, standardised for body size). Using a sample of 61 adults (30 males and 31 females), they found differences in bone strength between males and females. When comparing the antero-posterior and medio-lateral bending strength of the sample to other (Upper Palaeolithic, Mesolithic, Neolithic and Bronze Age) series, Çatalhöyük females and males seem to be most comparable with other Neolithic (sedentary) assemblages. From their data, Larsen and

colleagues (2012; Charles *et al.* 2014) also inferred an active, sedentary environment with adequate nutrition.

Skeletal trauma

The bioarchaeological analysis of skeletal trauma in archaeological populations can give an insight in the conditions experienced by individuals in the past, including day-to-day situations and potential episodes of violent conflict. At Çatalhöyük, patterns of injury include (healed and unhealed) fractures of the cranial vault (depressed fractures), ulna ("parry" fractures) and other anatomical regions.

Sadvari and Larsen (in press) noted that there is minimal evidence of injury caused by interpersonal violence at Çatalhöyük and that cranial depressed fractures are more likely to be caused by falls of ladders than by fights. Similarly, Molleson (2007) interpreted the unhealed fractures on the ribs, shoulder, arm and hand bones of a young male (3368) as the result of a fall.

The few cases of healed traumatic lesions, such as the multiple episodes of trauma (displaced hip and broken ribs) on an adult female aged 40-45 years (8115 from Building 3, BACH area), suggest some level of post-traumatic care (Sadvari and Larsen in press). Similarly, Molleson (2007) suggested that the traces of red or black pigment and ochre found on the bones of some individuals with signs of chronic pathology buried in Buildings 6, 17 and 23 (Mellaart levels VIII and IX) could have been used as a poultice treatment based on the fact that a similar bright red pigment (cinnabar) is widely used as a medical treatment in the Middle East.

In terms of diachronic changes, apart from an increase in adult mobility from Peak (Mellaart pre-level V) to the Post-Peak period (Mellaart post-level VI) detected by Larsen and colleagues (2012; Charles *et al*. 2014), no clear indications of temporal changes have been found in the human remains analyses at the site.

2.2.7. Socio-economic organisation

The following section is an exploration of the social and economic organisation at Çatalhöyük, providing summaries of previous research on craft activities, cultivation and herding practices and on the interactions between households.

Craft activities

There is evidence for a wide range of craft activities at Çatalhöyük, including grease processing, bead manufacture, obsidian knapping and bone working (Hodder 2007a; Matthews 2005b). However, there is no indication of intensive craft activities indicative of households who obtained their livelihood from full-time craft production (Düring 2007).

In terms of obsidian knapping, Cessford and Carter (2005) argued that knapping events took place in each building and more than once in a building's lifetime. Similarly, Connolly (1999) suggested that most craft activities at the site were household-based, as indicated by the presence of domestically produced flake tools.

In addition to lithic evidence of small scale production activities, a detailed cross-disciplinary analysis of burnt Building 52, located in the 4040 area, has also revealed evidence of bone working. In a medium-sized room north of the main central room (space 93), a cluster of bones (mainly caprine metapodials) was found, which was possibly stored in a perishable container. Associated with the cluster was an obsidian blade, which could have been used for shaping bone points (Twiss *et al.* 2008). Two antler pieces showing signs of working have been found within this context (Twiss 2012). Inside one of the bins, multiple fragmentary animal bones in various stages of processing were found (Twiss 2012).

Russell (2001) analysed a total of 385 bone tools and found the majority to be utilitarian tools, mainly points (made largely of sheep/goat metapodials) and ornaments (most commonly rings made from sheep/goat femora). There is evidence for manufacture of these rings, including Building 18 (South area), where four separate deposits have one or more unfinished bone beads representing different bead types and manufacturing techniques (Russell 2001).

Russell (2001) found evidence for the repair and re-use of both utilitarian tools and ornaments, including the resharpening of bone points and the repair of shell pendants, beads and bone pendants. However, she also found that bone points (and ornaments) were often discarded while still in a usable state. She (2001) argued that the short-use lives of these objects might indicate that such tools were associated with certain tasks and/or individuals and therefore considered as appropriate offerings to place in middens along with ceremonial remains.

Cultivation

In terms of plant cultivation, Bogaard and colleagues (2009) compared the storage capacity at Çatalhöyük with modern farmers, who produce surplus for sale as well as for their own use. Based on this comparison, they suggested that the restricted storage capacity at the site reflects the relative small-scale size of manual plant cultivation. The presence of sickle blades made from non-local obsidian and shaped on-site also supports this small scale productivity, as it suggests that the occupants of each building made their own tools for cutting plants (Carter 2011; Cessford and Carter 2005; Fairbairn 2005).

Based on densely distributed silicified awns, spines, hairs and glume beaks (results of winnowing and threshing) in the KOPAL trench, Atalay and Hastorf (2006) argued that initial crop processing at the site was carried out at the edge of the settlement. In addition, Twiss (2012) wrote that restricted amounts of plants were processed in the house yard and in side-rooms of the house. For example, *in-situ* charred lenses found in Building 65 (space 314, South area) have yielded pea pot fragments, a byproduct of the cleaning of peas by hand and evidence has also been found for the hand-cleaning of glume wheat grains (space 314, Building 65, South area) and crop fine-sieving (Bogaard and Charles 2007; Longford 2010; Twiss 2012).

Small nutshell-rich deposits havebeen found within middens (Space 181) from the early levels (Mellaart pre level XII) of the site, suggestingconcentrated shelling of nuts (Twiss 2012). In addition, grinding and abrading tools have been found in the same contexts as plant remains such as cereals, acorns, lentils, tubers and hackberries, but Baysal and Wright (2005) argued that these tools were likely to be unspecialised and multifunctional.

Wright (2014), in her recent analysis of 2429 ground stone artefacts from 20 buildings and external yards, found that most houses had evidence of small, hand-held quern fragments in their bins. As the largest querns seemed to appear during the Peak and Post-Peak periods of the site (South Q and 4040G), Wright (2014) proposed an increasing intensification of post-harvest activities from the Peak period onwards.

Charles and colleagues (2014) argued that the Neolithic landscape in Konya, where Çatalhöyük is situated, accommodated long-lived cultivation plots suitable for the production of rain-fed crops (in excess of 300mm per year) and the exploitation of dry and

wet, grassy and wooded areas for sheep herding as well as providing diverse foraging options.

Robert and Rosen (2009) argued that the cultivation plots were located on the nearest upland zone to the site which was free from spring flooding in the alluvial plain (limestone terraces). However, the results of an initial stable isotope (87Sr/86Sr) study based a subset of plant taxa (naked barley, peas, wild mustard seeds, almonds and clubrush) from the burned Building 52 show that the barley, clubrush and almonds grew either on the alluvial plain or in the Taurus mountains, which has a similar Sr signature to the plain (Bogaard *et al.* 2013; Charles *et al.* 2014). In contrast, the wild mustard and peas appear to come from a different, more radiogenic location which is as yet not possible to identify (Bogaard *et al.* 2013; Charles *et al.* 2014).

Herding

As the zooarchaeological assemblages at Çatalhöyük are dominated by caprines (sheep/goat) (Russell and Martin 2005), herding practices at the site have been studied in detail (Bogaard *et al.* 2013; Charles *et al.* 2014; Henton 2010, 2012; Henton *et al.* 2010; Matthews 2005a).

The pathology rate (0.3% of sheep/goat elements) in caprines is low, indicating a healthy population associated with good herding practices (Russell and Martin 2005). Similarly, a pilot study examining the histology and ultrastructural chemistry of sheep tibia indicates good husbandry practices (Pawłowska 2007).

There is some evidence of on-site penning (in space 181, 4715, 4710), possibly located at the edge of the settlement (Atalay and Hastorf 2006; Russell and Martin 2005). Matthews (2005a) identified penning deposits based on the micromorphological detection of compressed dung, which resembled ethnoarchaeological samples of roofed winter pens for large and medium sized ungulates, probably sheep and goats. Dung spherulites, associated primarily with sheep faeces (Canti 1999) have also been identified in the heavily compacted layers found in these spaces (Matthews 2005a).

The presence of deciduous teeth and perinatal bones within the faunal assemblages provide addition evidence of such penning and lambing practices (Russell and Martin 2005). Oxygen isotope analysis of sheep teeth at Çatalhöyük showed that 59% (27 out of

46) of lambs were born in late spring/early summer and 17% (8 of 46) of the lambs were born earlier, possibly in March (Charles *et al.* 2014; Henton 2012). Henton and colleagues (Charles *et al.* 2014; Henton 2012) argued that the differences in lambing timings indicate that birth manipulation was probably not important to the herding schedule.

Archaeobotanical evidence (seeds of wild taxa found in dung pellets) of sheep diet indicated that some animals were grazing near arable land towards freshwater marsh or along streams, whereas others were grazing on pasture off the alluvial plain nearby dry-steppe vegetations (Charles *et al.* 2014). The isotopic and dental microwear evidence suggests that herds were kept within a day of the settlement, within the plain and/or terraces (Bogaard *et al.* 2013; Charles *et al.* 2014; Henton 2012). However, the alluvial plain is large and it is possible that sheep could have travelled over considerable distances to graze in pistachio or almond parklands on the terraces, necessitating the possible seasonal separation of herder from the settlement (Charles *et al.* 2014).

In terms of diachronic changes in herding practices, dental microwear analyses of sheep teeth from different levels in the South area indicate an increasing reliance on dry grass-rich nutrition before slaughter from Hodder levels K, L (Pre-Peak period) and M (Peak Period) onwards, which becomes more marked during Hodder levels Q and R (Post-Peak period). Carbon isotopes in bones also point towards an increase in C4 plants in the sheep's diet (Charles *et al.* 2014; Pearson *et al.* 2007; Richards *et al.* 2003). Charles and colleagues (2014) suggested that this gradual change in feeding practices might point towards a widening exploitation of grassland, either for pasture or fodder into the plain, further away from the freshwater alluvium. Added to this, by level South P (Post-Peak period), there is a marked increase in the size of herds and domestic cattle herds were introduced (Charles *et al.* 2014). As such, this change in diet can be explained by the reservation of pasture on the alluvium for cattle herds and the more extensive pasturing or supplementary foddering of sheep herds (Charles *et al.* 2014). However, samples for these analyses are small and as such, these inferences should be considered as tentative (Charles *et al.* 2014).

Interactions between households

Twiss (2012) argued that the material culture at Çatalhöyük points towards a careful balance between a communal identity and the autonomy of individual households. An example of this is the apparent dichotomy of hidden, day-to-day food items which were

kept out sight (in side-room stores) and highly visible bucrania and horned pillars and benches (Bogaard *et al.* 2009, 2011; Twiss 2012). Bogaard and colleagues (2009) stated that similar concealed household storage practices have also been noted in other contemporary sites within Southwest Asia, which has been interpreted as an indicator of "household economic autonomy". However, they also stated that at Çatalhöyük this process was balanced by the highly visual installations of animal parts, which Bogaard and colleagues (2009; Twiss 2012) argued were deliberately placed to show visitors the house's involvement in communal feasts. The unequal distribution of cattle remains and the bias towards taurine crania in Buildings 52, 44 and 3 fit in well with ethnographic information on inter-household feasting (Bogaard *et al.* 2011; Demirergi *et al.* 2008).

Twiss (2012) argued that bucrania, rather than abstract symbolisations, should be seen as concrete memoralisations of specific feasts. Adams (2005), drawing on ethnographic parallels, mentioned similar traditional displays in Indonesia (West Sumba and Tana Toraja) and western Papua New Guinea (Akha). He wrote that within these societies, feasting is considered "*the glue that holds the lineage and kindred corporate groups together* (Adams 2005, 186)". In a reply to Adams, Hodder (2005b) wrote that at Çatalhöyük, the burial of the dead underneath houses, as well as the circulation of human skulls, through the digging up, plastering, painting and reburial of heads of certain individuals, were also a way of linking individuals to house-based social units.

The number of burials within each house points towards the social importance of the broader community. At Çatalhöyük, there is considerable variation in burial numbers between buildings (Andrews *et al.* 2005; Düring 2007), and in Building 1 the number of burials beneath floors (N=62) exceeds that expected from house occupants alone (Düring 2005; Hodder 2010). Based upon the variation in burial numbers, Düring (2007) suggested that some buildings might have acted as burial sites for multiple houses and that these houses might have been organised in "house-groups". He argued that this concept fits well with ethnographic information on house-groups in agricultural societies, where household groups of this size cooperate economically (Plog 1990).

History houses

In relation to the interaction between the household and the broader community (or supra-household), Conolly (1999) referred to the possibility of socio-economic organisation based on kin-groups. He mentions that although most production activities seem to be household-based, findings of prismatic blades and concentrations of blade

and blade cores in more elaborated houses also provides evidence for the existence of a localised lithic production system at the kin-group level (Conolly 1999).

It has been argued that Çatalhöyük's "corporate kin groups" would have been maintained by social memory, which was created by the repeated building of houses and burials of important kin-group members underneath house floors (Carleton *et al.* 2013; Hodder 2006, 2010; Hodder and Cessford 2004; Hodder and Pels 2010; Fig. 2.4). In other words, the house can be seen as an important mechanism for creating social rules and constructing social memory (Hodder and Cessford 2004). As household continuity reveals ancestry and houses are the architectural and spatial manifestations of households, the latter may reflect ancestral sequences (Twiss *et al.* 2008).

During the 1960s excavations, Mellaart already introduced the concept of "shrines" to account for differences in elaboration and burial numbers between houses (Fig. 2.13). The most richly elaborated houses, which showed evidence of plaster reliefs, heads of animals with great horns, benches and pillars with horns and rich burials were interpreted as serving a cult and referred to as shrines (Mellaart 1998).

Similarly to Mellaart (1998), Hodder (2005b; 2006) also wrote that symbolic manifestations, including wild bull horns and wall paintings have also been found in these "special houses" (Hodder 2005b, 2006). He argued that certain houses were preferred burial locations and that the building sequences of these houses spanned over a longer period of time than other houses. However, Hodder (2010) argued against the idea of "religious" versus "mundane" houses or between religious and everyday life, mentioning that no such distinction between domestic and ritual (either in between or within houses) can be made in the context of Çatalhöyük. Instead, he suggested that both spheres are interlinked and considers these previously called "shrines" or "special" buildings as "history houses" and defines these as "guardians of memories" and stresses their importance in the regulation of daily activities (Hodder 2006, 2010; Hodder and Pels 2010). These houses are believed to be buildings in which the inhabitants of Çatalhöyük accumulated more "transcendent knowledge and symbolic capital" than in others (Hodder and Pels 2010).

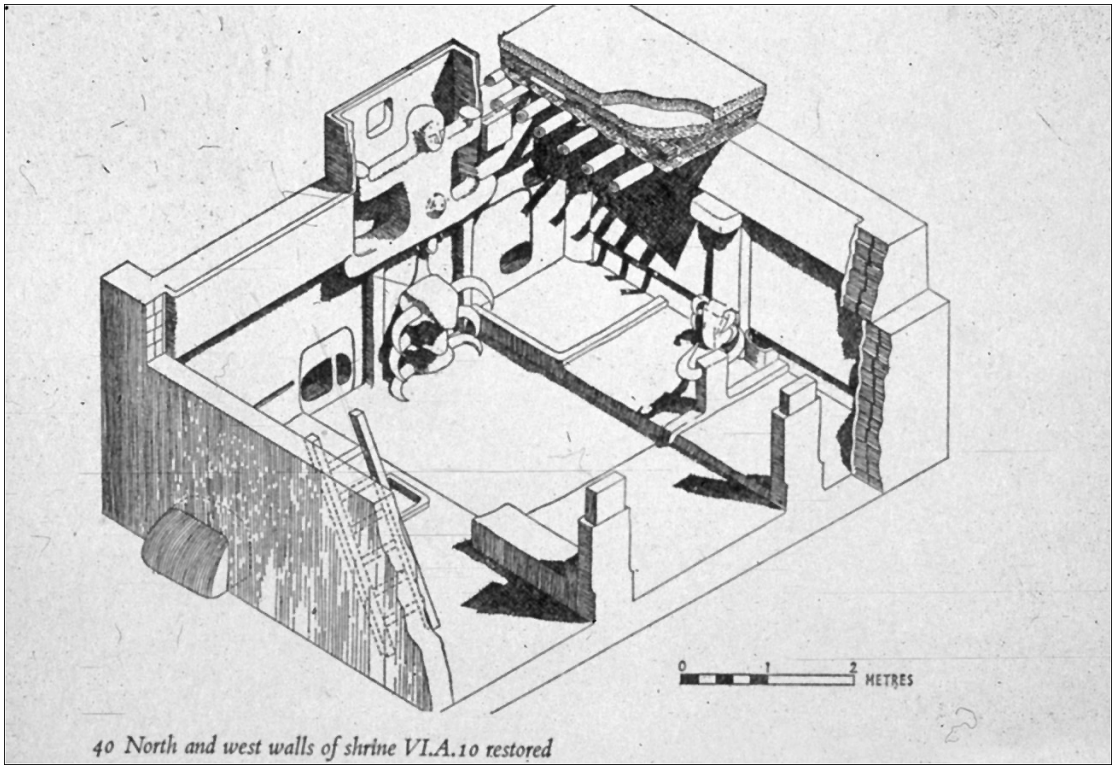

Figure 2.13: Reconstruction of Mellaart "shrine" 10 from Mellaart level VIB (excavated by Mellaart, from Mellaart in Hodder 2010, 6)

Hodder (2006) emphasised the importance of reiterative practices, which are most often focused on the house and are clearly seen in Mellaart Levels XII–V (Hodder levels H to P corresponding to the Pre-Peak to Post-Peak periods). Similarly, Hodder and Meskell (2011) stressed the concept of history houses as enabling the building of memories, arguing that they demonstrate the passing down of male cattle horns, resulting from feasts and other events in which dangerous wild animals were involved. They also argued that the manipulation of the human body was an important part of history making (as seen in the removal and circulation of human heads).

Ritchey (1996) assessed Mellaart's concept of shrines versus non-shrines based on a ranked sequence of variation in architectural complexity and argued that this cannot be substantiated by architectural features alone and that there is a need for a fine-scaled analysis comparing architectural features with artifacts. In a more recent attempt to refine the concept of history houses, Hodder and Pels (2010) calculated an "elaboration index" based on sums for any phases of a building in terms of number of floor segments, basins, benches, installations, pillars and paintings in the main rooms. Based upon this index, they found that buildings with more than 12 burials tend to be more elaborate, confirming

previous results on “special houses” by Düring (Hodder and Pels 2010). They also found a (albeit weak) correlation between building size and elaboration. In terms of storage space, they argued that, within building sequences, as burials increase and buildings become more elaborate, storage space remains relatively similar or decreases (Hodder and Pels 2010).

There are various problems with the quantification, identification and analysis of history houses. Firstly, in terms of the identification of history houses, it is often hard to define “main rooms”; partition walls may or may not have been full height and not all floors are fully excavated, making it difficult to establish the contemporaneity of elaborate features (Hodder and Pels 2010). Additionally, recent excavations distinguished many phases within each level of the site’s occupation, whereas Mellaart combined all phases into levels. Mellaart’s drawings are therefore difficult to compare with the current data on building elaboration, as they probably contain more features than there probably were within one phase (Hodder and Pels 2010).

Secondly, in terms of the analysis of history houses, the concept of “kin groups” in terms of “biological kin” might not necessarily apply to the social organisation on the site. Using dental data, Pilloud (2009; Pilloud and Larsen 2011) carried out a biological distance analysis, which is a statistical approach to compare phenotypic to genotypic similarities. The results from this analysis did not support the hypothesis that people buried in history houses are biologically related, indicating that membership of these house groups did not rely on biological definitions, but was rather defined by social or cultural factors (Pilloud 2009; Pilloud and Larsen 2011). Pilloud (2009) suggested that instead of Bourdieu’s (1979) notion of “biological kin”, it might be more useful to focus on the concept of “practical kin”. Such groups would be united based on utilitarian reasons such as animal husbandry (herding of sheep) and land use (planting and harvesting crops).

Neighbourhoods

Düring (2007) suggested that at Çatalhöyük, house groups were organised in neighbourhoods. Similarly, Hodder (2006, 2012; Hodder and Pels 2010) referred to these as sectors, large groups of houses (10-30) bounded by refuse areas or alleyways (Hodder and Pels 2010). An example of this is the “street” identified in area 4040, separating Buildings 52, 48 and 49 from Buildings 64, 55 (Matthews 1996; Yeomans 2008). Similarly, Pilloud (2009), based on dental metrics and morphology, argued that there seemed to be two distinct descent groups or moieties at the site, which were located

in two distinct areas of the mound (north and south). However, she suggested that these distinctions, in terms of non-metric dental traits, are not vastly different and that membership of such moieties might have been fluid and not completely based on relatedness (Pilloud 2009).

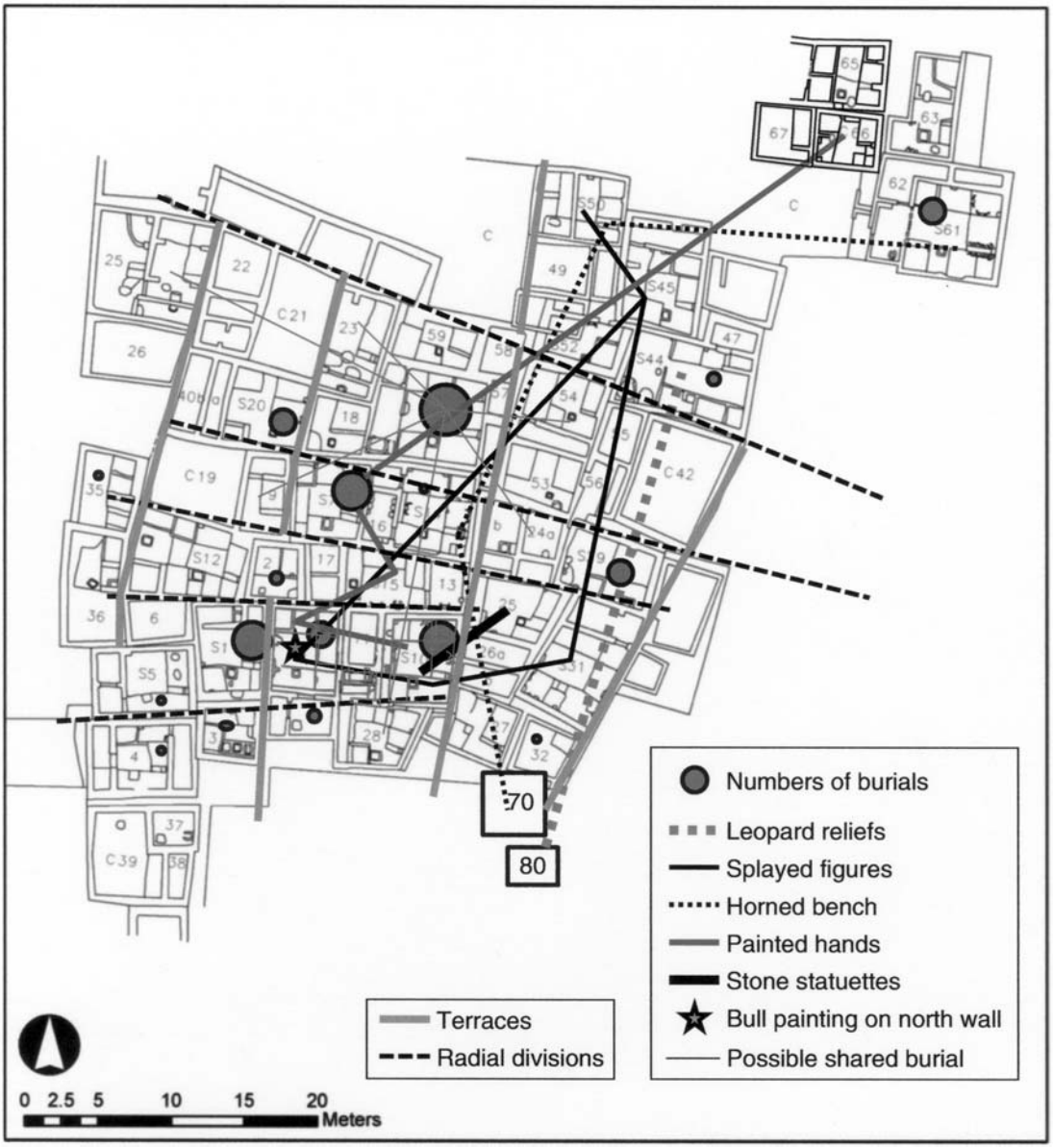

Figure 2.14: Spatial distribution of radial zones in Level VIB at Çatalhöyük. Lines are drawn between houses that have distinctive cultural attributes such as leopard reliefs and painted hands on walls (From Hodder 2012, 187)

Hodder (2012) stated that within the larger sectors, some radial zones existed in which the inhabitants mutually supported each other in times of difficulty (Fig. 2.14). Similarly,

Düring (2007) argued that this specific type of spatial organisation was yet another way to reinforce social cohesion, this time in terms of the neighbourhood community. Additionally, Düring (2007) suggested that the corporate identity of this community was based on face-to-face interactions, which probably occurred on a daily basis through rooftop interactions. The concept of corporate communities has been used in archaeology to describe autonomous local communities which lacked evidence for institutionalised elites and which in some cases held land in a variety of communal forms (Düring 2007).

2.2.8. Diachronic change

Site size and house construction

Çatalhöyük is an optimal site for the study of diachronic change due to its long-lasting habitation sequence, which spans over 1400 years (Hodder 2007a, b). Previous archaeological research at Çatalhöyük has revealed an increase in size and occupation density of the site (ca 6500 BC) followed by a marked reduction in house number and density (Düring 2007).

As mentioned above (p. 30), the changing building and deconstruction practices at Çatalhöyük include an increase in density of houses from clustered neighbourhoods in Mellaart levels XII to VI to more open areas in later levels; the appearance of house burning from level VI, in the South, North, Istanbul and 4040 areas (Table 2.4) and changes in construction materials from mudbrick composed of dark-gray brown “backswamp clay” in the earlier levels to a reddish-brown “mineral based” composition in the later levels.

In terms of the symbolism present at the site, a shift from a focus on elaborate animal installations in houses in the earlier buildings to figurines with removable heads in later levels can be detected as well as an increasing level of complexity in the wall paintings with hunting scenes of Level V onwards (Table 2.4).

Consumption and animal husbandry

With regards to consumption practices, there was an increased reliance on cattle in the Pre-Peak period which sharply decreased between the Peak and the Post-Peak period.

In contrast, there is no indication of diachronic change in the bird habitats exploited by the Çatalhöyük residents.

With regards to herding practices, the increasing reliance on dry grass-rich nutrition before slaughter of sheep, already noted from the Pre-Peak period onwards, becomes more marked during the Post-Peak period. Possibly associated to this, there is a marked increase in the size of herds in the Post-Peak period, at around the time when domestic cattle herds were introduced.

Population

There is an increase in adult mobility from the Peak to the Post-Peak periods, but no other clear indications of temporal changes in terms of human health have been found (p. 46).

Craft activities

Carter (2011) noted that a there is a change through time in terms of lithic traditions at Çatalhöyük, with unipolar shapes completely replacing the bipolar form from Mellaart level VIb (i.e. during the Post-Peak period) onwards (Table 2.4). During this time, a change in procurement of lithics also occurred, replacing material from the Kaletepe workshop with stone artefacts from another quarry-based workshop (Carter 2011). In terms of ground stone tools, the largest querns of the Çatalhöyük assemblage appear in the Peak and Post-Peak periods of the site (South Q and 4040G), which could indicate an increasing post-harvest intensification from the Peak period onwards (p. 48, Table 2.4).

Diachronic changes have also been detected in the bead sample. Hamilton (2005) wrote that the occurrence of Dentalium shell beads is limited to levels VI and V. The most common types of beads (types 1 and 21 –slices with straight edges, mainly in stone) occur in all levels of the site. However, deer teeth (incisors of adult male red deer) are mainly found in the early levels of the site, particularly in levels VIII and VII. After that, real deer teeth become rare, but bone imitations become more common (Hamilton 2005; Table 2.4).

Table 2.4: Overview of diachronic changes at Çatalhöyük (based on Henton 2010, 119-121; Wright 2014)

	Pre-XIIE-A (G)	XII (H)	XI (I)	X (J)	IX (K)	VIII (L)	VII (M/N)	VI (N/O)	V (P)	IV (Q)	III (R)	II (S)	I (T)
Settlement	No buildings	Rising population				Max. pop.			Declining population				
Neighbourhood		Tightly packed buildings							More space				
Buidings		Party walls				Separate walls							
Walls		Thinner mudbrick walls, timber uprights							Walls thicker			Brick pillars	
Bricks		Dark silty clays				Buff silty material							
Timbers		Riperian	Oaks and junipers										
Roofs		No change											
Floors		Plaster or mud								Gravel added to floor			
Plaster		Buff coloured				White							
Ovens		No change											
Bins		No change											
Hearths		Round near oven								Rectangular, nearer clean area			
Platforms		No change											
Installations		No change											
Paintings		Plain red, geometric			Figurative, black pigment				Hunting scenes				
Burials Graves		No change											
Special deposits		No change											
Caches		No change											
Ornamentation-Stone beads	Less diverse				More diverse materials								
Ornamentation Natural beads	Real deer teeth							Dentalium VI/V, imitation teeth, complex bone					
Ornamentation Rings	Common							Rare					
Stamp seals	Absent						Present						
Figurines Anthropomorphic	No change												
Figurines Zoomorphic	No change												
Figurines Abbreviated	No change												
Chipped stone Obsidian	Micros, local	Bipolar blades. Local & Kaltepe cores						Unipolar blades new source					
Chipped stone Flints													
Bone tools	Less woodworking				More woodwork, soft hammers			More groove splitting, pressure flakers, burnishers					
Ground-stone	Smaller querns									Larger querns			
Clay balls	Local, shapes	Mineral rich sediment					Rapid disappearance						
Pottery	Aceramic	Mainly local clay, organic tempered						Mineral rich, more burnishing, form, decoration					
Baskets/mats	Reeds, rushes, grasses									Barley straw introduced			

2.3. Definition of the archaeological research questions

2.3.1. Did human growth patterns vary in terms of place of residence at Çatalhöyük and if so, can differences in skeletal and dental growth patterns be detected according to burial context?

In Çatalhöyük, some houses were preferred locations for burial and there is evidence that they were rebuilt over more generations than other houses. In addition, symbolic manifestations such as wild bull horns, relief sculptures and wall paintings have been found in these "special houses" (Hodder 2005a, b, 2006). Hodder (2006, 144) considered these structures as "history houses" and defines these as *"dominant houses, guardians of archive of memories alongside particular investment in the regulation of daily activities"*.

Hodder and Pels (2010, 180), in a recent analysis of the concept of history houses at Çatalhöyük, asked *"What are the conditions that allowed some buildings to amass histories while others did not?"* This question will be explored in terms of growth. If children buried in the *"dominant history houses"* were advantaged in comparison to children buried in other houses, it is expected that the "history house" individuals will show less evidence of growth disruptions in childhood, evidenced by a lower proportion of enamel affected by growth disturbances and an earlier achievement of skeletal growth states than "non-history house" individuals.

2.3.2. Did changes in community size and density affect human growth at Çatalhöyük?

By comparing the skeletal and dental growth patterns of subadults between three broad temporal categories, early ("Pre-Peak"), middle ("Peak") and late ("Post-Peak"), consistent differences in skeletal and dental growth patterns are expected. More specifically, it is anticipated that the increase in community size and density, from the early and middle periods will be associated with increased growth disruptions, evidenced by a higher proportion of enamel affected by growth disturbances and late attainment of skeletal growth stages in Peak period individuals compared to Pre-Peak individuals. It is also expected that the decline in population size occurring between middle and late periods will be associated with increased growth disruptions in Post-Peak individuals compared to Peak individuals.

Chapter 3. Introducing the concept of growth

Scheuer and Black (2000a, 4) referred to growth as "*a general term applied to the progressive incremental changes in size and morphology that occur throughout the development of an individual*". Similarly, according to Eveleth and Tanner (1976, 198) "*growth is a movement through time and progress may be fast or slow.*" Growth can be seen as consisting of two components, increase in size (in terms of height and weight) and in maturity, with individuals reaching developmental milestones at different chronological ages (Eveleth and Tanner 1976; Garcin *et al*. 2010; Scheuer and Black 2000a). Modern humans are considered unique among primates for having a particularly slow pattern of growth and development (Krovitz *et al*. 2003; Šešelj 2013).

Variation constitutes a persistent aspect of growth studies, in terms of the normal and the abnormal and in terms of differences in size, rate of growth and timing of maturational stages (Himes 2004). Such variation has been studied across and within populations (Himes 2004; Sutphen 1985; Waterlow 1988). The analysis of human growth is a traditional area of study within physical anthropology and growth variation has been studied both in terms of evolutionary selection and environmental adaptation (Bogin 1999; Himes 2004; Krovitz *et al.* 2003).

Some of the variation in human growth patterns arises from the developmental sensitivity to fluctuations in nutritional status and disease loads and based upon this, growth has often been used as an indicator of health (Himes 2004; Lewis 2007). It is within this context that this study is situated. The aim of this introductory chapter is to provide a general background on teeth, bones and their development and to introduce some of the terminology and developmental processes that will be referred to throughout this project. The first part gives an overview of the anatomy and growth of the permanent dentition, whereas the second part focuses on skeletal anatomy and development. Both sections finish with a summary of archaeological applications, which are further discussed in detail in the next chapter (Chapter 4).

3.1. Dental development and anatomy

3.1.1. Physical structure and properties of teeth and their supporting tissues

Enamel hypoplasia is closely related to the development and characteristics of dental structures and it is therefore important to provide an overview of these features and the complex processes related to them. This chapter introduces some of the terminology and developmental processes that will be referred to throughout this project.

A tooth's function is primarily mastication, the cutting and grinding of food (Berkovitz *et al*. 2009). To this purpose, the tooth crown is covered by enamel, the hardest biological tissue in the human body and thus relatively wear-resistant, durable and hard enough to damage food stuff (Berkovitz *et al*. 2009; Boyde 1989; Owen 1840-1845). The study of teeth and especially enamel is particularly useful for bioarchaeologists, as unlike bone, enamel does not remodel during life (Hillson 1996). Teeth are also often recovered from archaeological sites (Hillson 1996).

The human dentition is divided into four quadrants, based upon the median sagittal plane (the midline of the skull). This line passes between the two upper first incisors and the two lower first incisors, dividing the dentition into upper left, upper right, lower left and lower right quadrants, with each quadrant of the permanent dentition containing different tooth types, incisors (two), canines (one), premolars (two) and molars (three). Any surface of those teeth that faces the median sagittal plane is defined as mesial, whereas surfaces away from the median sagittal plane are considered distal (Fig. 3.1).

Each tooth consists of two main structural parts, a crown and a root. The root is embedded in the jaw and holds the tooth in place (Hillson 2005). The crown provides the biting surface of the tooth and projects into the mouth, with its different surfaces facing either the lips (labially), the cheeks (buccally) or the tongue (lingually). The cervix is the location where the root and the crown meet (Hillson 1996). The base of the crown is referred to as the cervical part of the crown, as opposed to the occlusal part of the crown, which is nearer to the biting surface of the tooth (Hillson 1996).

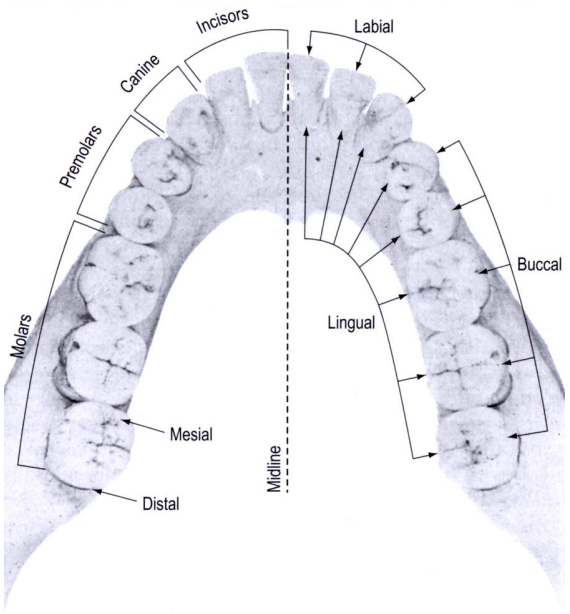

Figure 3.1: Mandible with permanent teeth demonstrating siding terminology (Based on Standring 2008, 509)

Teeth acquire their final form and shape early in human development and once established, their size and shape does not change during life. The human dentition is characterised by the successive eruption of two sets of teeth. The size of the first dentition, the deciduous dentition (primary or milk teeth) is constrained by the size of the fetal jaws, but as the jaws grow and space for teeth increases, the larger, permanent teeth start to erupt (Dean and Cole 2013).

Dental eruption is a three-dimensional process by which teeth migrate through bone and soft tissue and emerge into the mouth (Dean and Cole 2013; Marks and Schroeder 1996). In a pre-eruptive stage, teeth develop in the alveolar bone and before the tooth root is completed, the developing tooth emerges through the gingival tissues into the oral cavity and continues to erupt until it reaches its functioning position (Dean and Cole 2013; Marks and Schroeder 1996). Opposing pairs of teeth emerge successively during development, increasing occlusal stability, food processing capacity and potential energy intake (Dean and Cole 2013).

There is considerable variation in the timing of tooth eruption between individuals, but a general eruption timeline goes through three stages, a period of deciduous dentition, mixed dentition and the final stage in which all deciduous teeth have been replaced by their permanent successors (Hillson 1996). The first, deciduous set of teeth starts forming

before birth and is fully erupted into the mouth during the two or three years after birth. The deciduous eruption sequence normally starts with the incisors and finishes with the fourth premolars (Liversidge and Molleson 2004). From around six years, this deciduous dentition is gradually replaced by a larger set of more teeth, the secondary or permanent dentition (Fig. 3.2). The eruption sequence of the permanent teeth generally begins with the first molars and the incisors, between five and eight years. Next to emergence are the canines, premolars and second molars between the ages of nine and thirteen (Hillson 1996). The last tooth to form is the third molar, which erupts later in life, usually around the early twenties (AlQahtani 2008; Schour and Massler 1941; Smith 1991; Ubelaker 1978).

Figure 3.2: Mixed permanent and deciduous upper and lower dentition (specimen RCSOM/A 18.4 from Royal College of Surgeons of England, Photo: Carr J)

Teeth are composed of three types of mineralised tissues, cement, dentine and enamel (Berkovitz *et al*. 2009). Nutritive support is provided through the dental pulp, a connective tissue which is held within the pulp cavity inside the tooth (Berkovitz *et al*. 2009; Hillson 2005). The pulp chamber is the centre of the tooth, containing its nervous and blood supply. The core of the tooth consists of dentine, which surrounds the pulp chamber. The dentine of the tooth root is coated with a thin mineralised layer called cement, which provides an attachment for the periodontal ligament. The dentine of the tooth crown is covered by enamel (Fig. 3.3). The locations where the different tissues meet are the enamel-dentine junction (EDJ), the cement-dentine junction (CDJ) and the cement-enamel junction (CEJ).

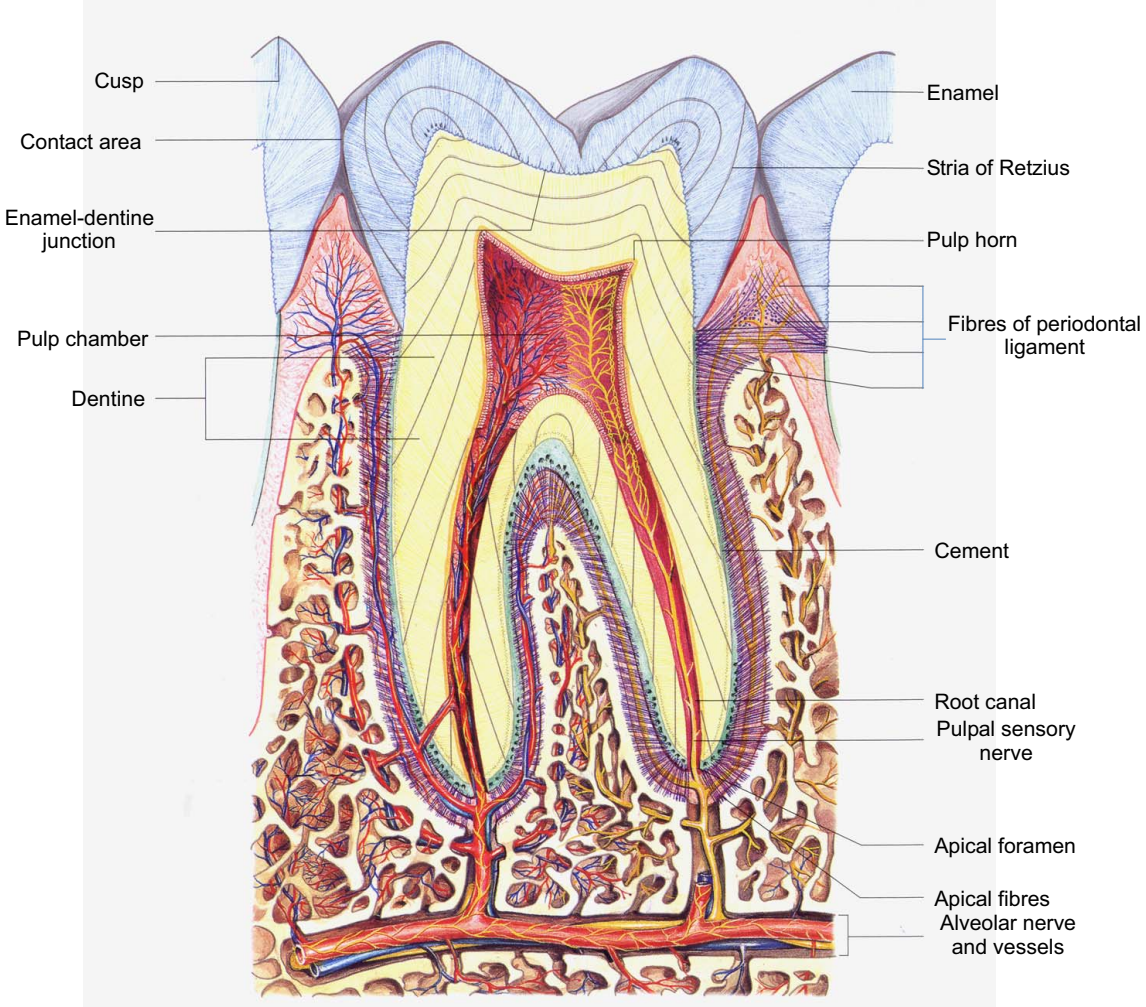

Figure 3.3: Drawing demonstrating the principal parts of a tooth: root and crown with pulp chamber, enamel, cement and dentine (Based on Standring 2008, 513)

3.1.2. Organic and inorganic composition of mineralised tissues

Enamel

Dental enamel is relatively translucent and its colour ranges between yellow and greyish white. The enamel layer varies in thickness according to tooth type and its location on the crown. In modern humans, enamel thickness varies from 1mm or less in deciduous teeth to 2.3mm in the cusps of the cheek teeth (Boyde 1989). The enamel coating is thickest at the level of the biting edges of the crown and thinnest at the cervix (Boyde 1989).

Mature enamel is an almost entirely mineral structure composed of calcium hydroxyapatite (88-90% of tissue by volume or around 95-96% of tissue by weight). Within the enamel matrix, there are also small traces of water (2% by weight or 5-10% by volume) and organic material (1-2% by weight), which mainly consists of enamel proteins and a small proportion of (less studied) lipid material (Berkovitz *et al*. 2009). The protein constituents of enamel (amelogenins) make up a higher proportion during development (especially during mineralisation) than in mature enamel (Berkovitz *et al*. 2009).

The main component of mature enamel, hydroxyapatite, appears in the form of crystallites which are hexagonal in cross-section (Berkovitz *et al*. 2009). Several million of these hexagonal shapes combine to form enamel prisms or rods, the basic structural unit of enamel (Berkovitz *et al*. 2009; Boyde 1989; Eisenmann 1994; Risnes 1998). The total number of prisms, each sized between 4 and 8μm in diameter and running from the enamel-dentine junction (EDJ; Fig. 3.3) to the surface, amounts to around 12 million in a single tooth (Berkovitz *et al*. 2009; Goodman and Rose 1990).

Amongst mammals, differences are found in enamel structure and prism patterns. The most common form exhibited by humans is a key-hole structure in which each prism has a certain amount of inter-prismatic enamel (also called prism-free space or inter-rod space) attached at its cervical side, lying between the two prisms in the row directly below. In this key-hole prism structure, the prisms can be seen as heads and the inter-prismatic enamel as tails (Boyde 1989; Hillson 1996; Risnes 1998). Enamel is the most highly mineralised structure in the vertebrate body and due to this complex structure of rods and inter-rods, enamel is adapted to absorb abrasive (wear) and mechanical (mastication) strains and the rigidity of this enamel material also limits fractures (Berkovitz *et al*. 2009; Fincham *et al*. 1999; Tomes 1882).

Dentine

In contrast to enamel, dentine is yellow in colour and has a lower mineral content. Mature dentine is composed of 70% (by weight, 40% by volume) inorganic material, mostly hydroxyapatite. It is formed by odontoblasts and the odontoblast processes are contained in dental tubules (Hillson 1996). During adult life, these tubules persist and start forming secondary dentine, which ensures the continued protection of the pulp chamber and root canal (Hillson 1996).

Cement

Cement (or cementum) is light yellow in colour and like dentine, cement contains a higher amount of water and organic components than enamel. Both tissues are also softer than enamel. Cement is formed by cementoblasts and consists of 65% (by weight, 45% by volume) inorganic material (Berkovitz *et al*. 2009). The organic content of cement is mostly made up of collagen fibres (Hillson 1996).

3.1.3. Tooth germ development

The development of teeth (also called odontogenesis) starts with the appearance and growth of embryonic cells and finishes with the eruption of the teeth into the mouth. Most of the permanent teeth start forming after birth, with the exception of the of the first molars, which starts forming *in utero*, just before normal full-term birth (Hillson 1996, 2014).

Tooth germ development involves a series of interactions between two tissues, the epithelium and the underlying ectomesenchyme (Fig. 3.4). Both layers will eventually develop into the many tissues constituting the jaw and face, including bone and cartilage (Hillson 1996; Simmer *et al*. 2010; Ten Cate 1994).

The first stage of tooth germ development, the bud stage, is the transition from an arch-shaped proliferation of epithelial cells to a primary epithelial band. This band subsequently divides into two lobes, the vestibular and dental laminae (Berkovitz *et al*. 2009; Hillson 2005; Ten Cate 1994). During the bud stage, a series of small epithelial swellings develop around the dental lamina and these are called tooth germs (Hillson 1996, 2014). The deciduous tooth germs appear by 8 weeks gestational age and the permanent molar germs appear around 14 weeks gestational age (Hillson 2014).

During the second stage, the cap stage, the epithelial swellings develop various indentations (hence appear cap-shaped), which continue to grow (Hillson 2005). During the third stage, the bell stage, the indentations in the epithelial swellings deepen, leading to the formation of the enamel organ, the dental papilla, which is filled with mesenchyme cells, and a surrounding mesenchyme forming the dental follicle (Fig. 3.4). The dental follicle will lead to cement formation, the dental papilla will eventually form dentine and the inside layer of the enamel organ, the internal enamel epithelium, will be responsible for the formation of the enamel matrix (Berkovitz *et al*. 2009; Hillson 2005, 2014; Ten Cate 1994).

During the bell stage, the internal enamel epithelium grows by division and will cause the enamel organ to eventually fold into is future crown shape (Hillson 1996, 2014). When all the cells have stopped dividing, the internal enamel epithelium corresponds roughly to the shape of the future enamel-dentine junction (Fig. 3.3) and the cells begin to differentiate into ameloblasts cells. This causes the dental papilla cells to differentiate into odontoblasts (Berkovitz *et al*. 2009; Fitzgerald and Rose 2000; Hillson 2005, 2014; Ten Cate 1994).

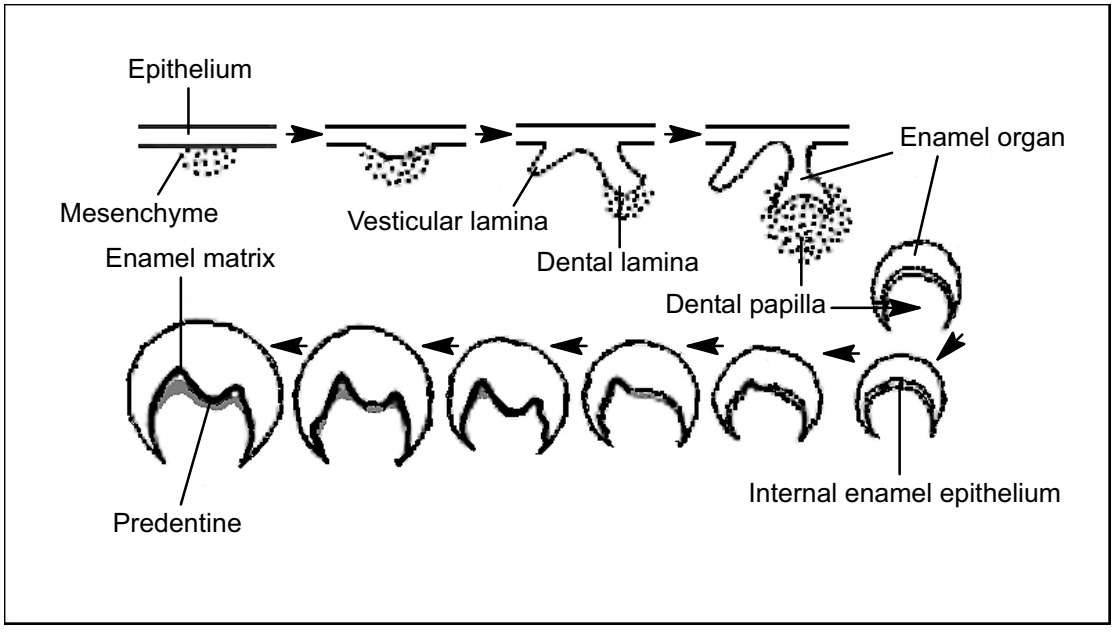

Figure 3.4: Diagram illustrating the process of tooth germ development (after Hillson 1996, adapted from Ten Cate 1994)

3.1.4. Crown formation

The crown formation process (or amelogenesis) starts with the enamel initiation of the first deciduous incisor, around 14 to 16 weeks after fertilisation or an average of 166 days before birth (Hillson 1996; Mahoney 2012). Amelogenesis or enamel formation can be divided into five main stages, ranging from an initial presecretory phase to a final postmaturation phase (Berkovitz *et al*. 2009). During the first, presecretory phase, ameloblast and odontoblast cells are differentiated at the level of the future enamel-dentine junction, as descibed above (p. 67).

During the second, secretory phase, the ameloblast cells are responsible for the production of an enamel matrix on top of the dentine matrix secreted by the odontoblasts (Hillson 2014). Whereas the dentine matrix is entirely organic when first secreted by odontoblasts, the enamel matrix is composed of mineral (one third), protein (one third) and water (one third) when first secreted by ameloblasts (Hillson 2014).

After the initial production of a thin structureless enamel layer (prism-free or aprismatic enamel), the ameloblast cells develop secretory specialisations, Tomes' processes, on their distal, secretory ends (Berkovitz *et al*. 2009; Boyde 1989; Eisenmann 1994; Risnes 1998). This roughly conical protuberance is present during most of the enamel matrix secretion and each process occupies a pit in the surface of the developing enamel (Boyde 1989; Risnes 1998).

The surface of the Tomes' processes secretes crystallites which are organised into enamel prisms (Eisenmann 1994; Fitzgerald and Rose 2000; Hillson 2005; Risnes 1998). The enamel prisms run from the enamel-dentine junction to the crown surface, each reflecting the trajectory of an ameloblast cell during development (Hillson 1996). However, this trajectory is not linear and the angle between the path of the prisms and the crown surface changes between the occlusal and cervical parts of the crown (Hillson 1996). The prism path also undulates, a phenomenon called decussation (Boyde 1989; Hillson 1996). When viewed as a ground section under a polarising microscope, this phenomenon can be identified by the presence of bright and dark bands (Hunter-Schreger bands) which are produced as the result of the sectioning of prisms at different locations of their wave-like path (Hillson 1996).

In a third transitional phase, the secretion of the organic matrix, which initially has a high content of water and protein in addition to mineral, ceases once the full thickness of the

enamel matrix has been deposited (Berkovitz *et al*. 2009; Eisenmann 1994). During this development stage, the ameloblast cells change in both function and shape. It is the point at which the Tomes' processes retract so that the ameloblasts' distal end becomes flattened and the cells change from a secretory to a maturation form (Berkovitz *et al*. 2009).

The fourth stage or maturation phase marks the change of the enamel matrix into a mineralised form (Hillson 1996). This development involves the removal of protein and water as well as the increase in width and thickness of the crystallites, leading to their fully developed, mature form (Hillson 2005). During the final or postmaturation stage, the enamel coverings are fully established (Berkovitz *et al*. 2009).

3.1.5. Incremental structures

"*Growth layers exist in the structural parts of many biological systems and usually reflect a rhythmic metabolism which is synchronised with the environment* (Dean 1987a, 157)".

During the development of the permanent tooth crown, ameloblast cells move away from the enamel-dentine junction, depositing enamel as series of layers. Dome-like layers are laid down on the top (occlusal part) of the crown (the cusps or mamelons) and sleeve-like layers are deposited towards the cervix of the crown (Hillson 1996). The area of dome-like growth is generally referred to as appositional or cuspal enamel, whereas the sleeve-like lateral enamel is called imbricational or lateral enamel (Hillson 1996; Fig. 3.5).

The different incremental lines visible internally and externally are a representation of this layered growth. In contrast to bone, which undergoes remodeling (the replacement of osseous tissue with new tissue) throughout an individual's life, enamel does not undergo any post-mineralisation remodeling and therefore, these incremental markings represent a permanent record of the secretory activity of ameloblasts specifically and the physiological activity of the individual in general (Dean 1989). Slower forming tissues, such as cement, leave a record as widely spaced increments of growth, whereas dentine and enamel are formed more rapidly and record rhythms with shorter periodicities (Dean 1989).

This section focuses on the incremental growth markings in enamel, but Dean (1995, 2006; Dean and Scandrett 1996) and Smith (2008; Smith and Tafforeau 2008) have given

an extensive overview of incremental growth in both enamel and dentine. With regard to cement, Hillson (1996) and Renz and Radlanski (2006) provided a critical overview of cement layers and the issues related to the analysis of these layers.

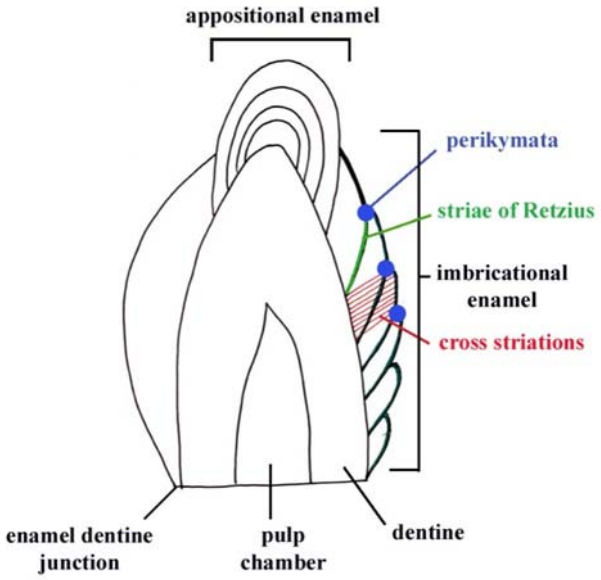

Figure 3.5: Schematic representation of tooth with appositional and imbricational enamel, striae of Retzius and perikymata

Enamel - Internal Structures

During human development, two main types of internal incremental features are recorded, prism cross-striations (or short-period lines, Fig. 3.6) and brown striae of Retzius (or long-period lines). Prism cross-striations are regular microscopic structures (light and dark bands) which have been observed on fractured enamel and ground sections of teeth using transmitted, polarised, reflected light, phase-contrast and scanning electron microscopy (Antoine *et al*. 2009a; Boyde 1989; Retzius 1837). They can also be stained in partially demineralised ground sections (Antoine 2000; Berkovitz *et al*. 2009). Radial sections, cut through the tooth longitudinally, parallel to the main axis of the tooth, through the cusps or central mamelon of the incisors, with a thickness of 100 to 120μm are recommended because they provide the most complete and clear record of these incremental features (Antoine 2000). The striations cross the long axis of enamel prisms at perpendicular angles, dividing the prisms into segments, at intervals between 3 and 6μm (Hillson 2014). They are more closely spaced near the cement-enamel junction and are further apart in the cuspal region (Berkovitz *et al*. 2009).

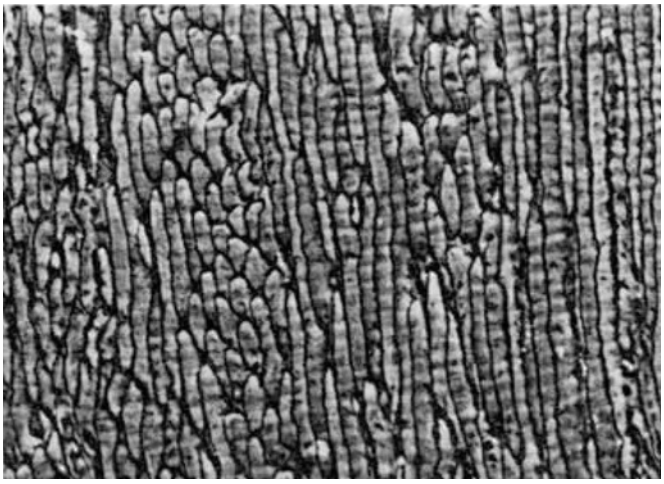

Figure 3.6: Back-scattered electron image of section of enamel surface showing cross striations. Width of field = 200μm (From Boyde 1979, 983)

Boyde (1979) suggested that changes in ameloblast metabolic activity may lead to local variations in CO_2, with a higher carbonate content of hydroxyapatite occurring during the faster growth phases. This higher carbonate concentration enhances the refractive index at the cross-striations, which makes them visible under light microscopy in polished sections (Antoine 2000; Boyde 1979). Cross-striations are also visible in micro-radiography and synchotron radiation micro-CT, which indicates the variation in mineral composition of these features (Hillson 2014).

Striae of Retzius or Brown striae of Retzius are a second type of incremental structure (Fig. 3.7). These features are regularly spaced parallel lines which appear microscopically as light brown and orange-brown to black in colour when using transmitted light microscopy and have a blueish-white colour if using reflected light microscopy. This brown colour seen using conventional light microscopy is due to a light scattering effect (Antoine 2000; Hillson 2014). On longitudinal sections (with a recommended thickness of around 100μm), these lines can be seen running obliquely across the enamel prisms (Antoine 2000; Asper 1916; Berkovitz *et al*. 2009; Dean 1989; Fitzgerald and Rose 2000; Hillson 2014; Retzius 1837; Risnes 1990; Risnes 1998; Soggnaes 1949). On transverse sections, the striae of Retzius appear as rings encircling the tooth (Fitzgerald and Rose 2000). The expression of striae is variable within a tooth, with these incremental lines being more discernible in the outer enamel (the crown surface) and in the cervical enamel (Antoine 2000; Fitzgerald and Rose 2000; Hillson 2014).

The spacing of the striae of Retzius varies according to their position relative to the cemento-enamel junction, with a spacing from around 22μm near the cusp to 5-20μm near the cervix (Berkovitz *et al*. 2009; Hillson 2014). The number of striae of Retzius within a tooth crown varies according to tooth type (Hillson 1996). The average permanent human incisor possesses around 150 brown striae, whereas the striae counts in molars ranges between 120 and 150 and the permanent canines have a total of 180 or more of these incremental lines (Hillson 1996).

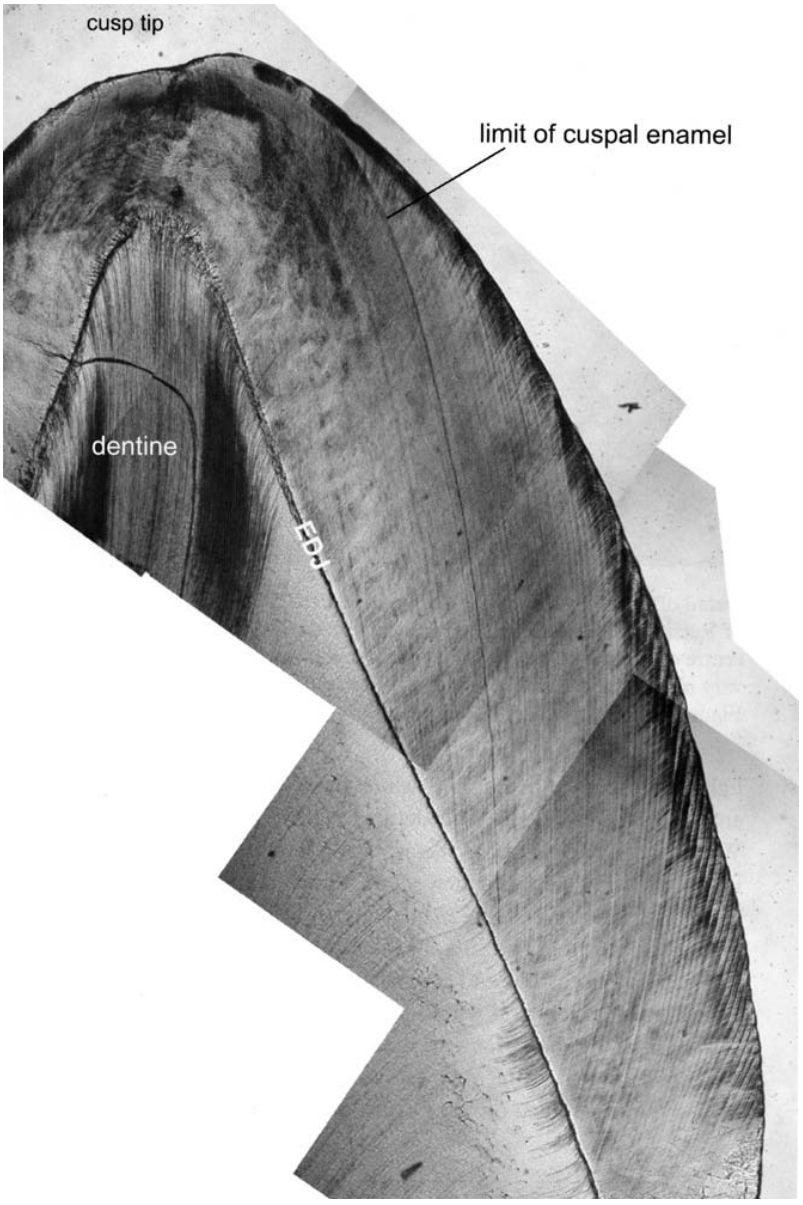

Figure 3.7: Crown section of a lower third premolar showing the buccal cusp tip and side of the crown. Striae of Retzius are seen as dark lines (adapted from Hillson 2014, 91)

Schour and colleagues studied the periodicity of the incremental structures in enamel and dentine through experimental work (Massler and Schour 1946a, b; Schour and Hoffmann 1939a; Schour and Massler 1937; Schour and Poncher 1937). Schour and Hoffmann (1939a) used a range of injection techniques at known intervals, creating a line in dentine and enamel which was visible on decalcified sections of 17 species, ranging from fish to humans. Between this marker line, incremental structures could be counted and tissue formation rate measured. Based upon this technique, Schour and colleagues (Massler and Schour 1946; Schour and Hoffmann 1939b) detected a regular occurrence of cross-striations which they later interpreted as the possible result of a diurnal and nocturnal rhythm in the formation and calcification of enamel and they identified an enamel matrix secretion rate for permanent teeth (maxillary and mandibular molars) of around 4.5μm per day.

The growth rhythm proposed by Schour and colleagues fits in well with an earlier proposed circadian (approximately 24-hour) enamel growth rhythm based on cross-striation counts on sections of permanent teeth (upper canines and upper premolars) of non-injected subjects (Asper 1916; Gysi 1931). More recent experimental work with fluorochrome markers on laboratory macaques (Bromage 1991; Smith 2006) and anthropological work on known age primate and human teeth have also shown that cross-striations reflect daily (circadian) changes in ameloblast activity (Antoine *et al*. 1999; Antoine 2000; Antoine *et al*. 2009a; Boyde 1979; Dean 1987a; Dean 1987b; Fitzgerald 1998; Fitzgerald and Rose 2000; Hillson 1996; Risnes 1998; Shellis 1998).

Based upon the comparison of counts of prism cross-striations between several neighbouring striae of Retzius, the latter are thought to appear with a regular periodicity (Boyde 1979; Bullion 1987; Dean 1987a; Dean 1989; Fitzgerald 1998; Fitzgerald and Rose 2000; Hillson 1996; Newman and Poole 1974; Reid and Dean 2006; Reid and Ferrell 2006; Shellis 1998). Fitzgerald (1998), using a sample of 158 anterior teeth from three modern populations (contemporary South African, Medieval British and Native American), provided the first statistical evidence that the number of cross-striations between adjacent striae of Retzius is uniform within a tooth and between teeth from a single individual. The actual number of cross-striations between striae varies between 7 and 10, referred to as circaseptan (near weekly) intervals representing a long period rhythm in dental growth than the circadian rhythm of the prism cross-striations (Fitzgerald 1998).

The physiological cause underlying the periodicity of striae of Retzius is currently unknown (Dean 1987a; Dean 1989; Witzel *et al.* 2008), but it is possible that the characteristic morphology of striae of Retzius is due to periodic structural changes of enamel. This could be a similar process to the one leading to the appearance of cross-striations, involving the rhythmic expansion and reduction of enamel prisms and inter-prism growth regions (Risnes 1990; Risnes 1998). Striae of Retzius may be the record of an "interference beat", the result of the interaction between two or more biorhythms (Dean 1987a; Newman and Poole 1974; Reid and Ferrell 2006; Simmer *et al*. 2010).

The periodicity of these long-period lines (i.e. the cross-striation count between neighbouring striae of Retzius) differs between individuals and taxa (Dean 1989; Newman and Poole 1974; Reid and Ferrell 2006; Risnes 1998; Smith *et al*. 2003). Reid and Dean (2006) using a sample of 326 molars and 352 anterior teeth from South Africa, Northern Europe, Medieval Denmark and North America, found a modal periodicity of 8 in the combined (South African, Northern European and Medieval Danish) posterior tooth sample and a modal value of 9 for the combined anterior tooth sample. More recently, Smith and colleagues (2010) used synchrotron phase contrast imaging to study a larger sample of 464 modern human teeth from more than 300 individuals and confirmed that the periodicity ranges between 6-12 days (Table 3.1).

Table 3.1: Retzius line periodicity (in days) for Homo (based on Reid and Ferrell 2006, 197 and Smith *et al*. 2007a, 182)

Sample	Nr of individuals	Mean	Mode	Range
South African	121	8.6	8	6-12
Medieval Danish	84	8.5	8	6-12
Northern England	83	8.1	8	6-11
North America	100	7.9	8	7-9

Enamel - Crown surface

Early in the developmental sequence of each tooth, striae of Retzius constitute dome-shaped layers around the tip of the dentine (the cusps and incisal edges) which do not reach the crown surface (Fig. 3.5). Later in the developmental sequence, the striae are sleeve-like, reaching the surface of the lateral enamel in a series of grooves running circumferentially around the crown (Berkovitz *et al*. 2009; Dean 1989; Fitzgerald 1998; Goodman and Rose 1990; Hillson and Bond 1997; Risnes 1998; Wilson and Shroff 1970). The amount of dome-shaped incremental layers (cuspal or appositional enamel)

represents a significant part of crown formation time, amounting to 15 to 20% of the incremental growth in anterior teeth (Hillson and Bond 1997). So, as a theoretical example, in a modern human permanent lower central incisor, where a total of 105 striae could be identified histologically in the cuspal and imbricational enamel, only 85 striae will reach the crown surface.

These surface manifestations of the striae of Retzius are called perikyma grooves and are separated by perikyma ridges (Fitzgerald and Rose 2000; Goodman and Rose 1990; Hillson 2005). The pattern of grooves and ridges is often referred to as perikymata (Hilllson 1996, 2014). Perikymata are long-period lines which have the same periodicity as brown striae of Retzius.

Perikymata on permanent teeth have a different appearance and spacing according to their location on the crown. Occlusally, they appear as broad and wave-like features spaced at a distance of 100μm or more. Mid-crown perikymata also appear wave-like but their grooves are much more pronounced and have a closer spacing of around 70μm. The cervical perikymata are more tile-like, with even sharper grooves and with an average spacing of around 50μm (Hillson and Bond 1997). The wider spacing in the occlusal/cuspal part of the crown is caused by the shallow angle (around 15°) of brown striae of Retzius with the surface, whereas the closer spacing towards the cervix is caused by the gradual sharpening of the angles of brown striae with the crown surface at the mid-crown (30°-40°) and cervical (60°) parts of the tooth (Hillson and Bond 1997).

Prenatal enamel does not normally contain striae of Retzius and their related surface expressions (Mahoney 2011). Therefore, in deciduous dentitions, perikymata can only be identified on the postnatal enamel. The amount of enamel formed at birth varies according to gestation length, but first incisor crowns are largely complete by birth (a small cervical part might still be developing in some cases). In contrast, perikymata could be observable on the cervical enamel of the second incisors and third premolars and on most of the lateral enamel of the canines and fourth premolars (Hillson 2014). However, perikymata are never as prominent in deciduous teeth as on permanent teeth, possibly due to the specific characteristics of the deciduous enamel, which is very smooth (Hillson 2014).

Based on histological techniques, using the number of cross-striations as markers of cuspal formation times, Reid and Dean (2000, 2006) have provided estimates for the

timing of the appearance of the first perikymata in each tooth type. For the permanent teeth, the earliest forming perikymata appear on the lower central and lateral incisors, at around 1 year of age, followed by the upper central incisor, for which the first grooves appear at about 1.1 years (Reid and Dean 2000). At a later stage, perikymata start to appear on the lower and upper canines (1.5 and 1.7 years respectively) and the upper lateral incisor (1.8 years). Cuspal formation times in posterior teeth are much longer, resulting in a smaller number of striae of Retzius reaching the crown surface (Reid and Dean 2006). As such, anterior teeth form visible increments over 4-5 years, first permanent molars only show perikymata over a period of 2 years or less (Reid and Dean 2000).

3.1.6. Growth disturbances

Disturbances in the tooth formation process lead to defects in the dental hard tissues (Pindborg 1970). Changes may be visible only in enamel, dentine or cementum or they can affect all of these tissues (Pindborg 1970). Microscopically, zones of interglobular dentine (unmineralised dentine matrix) are considered as indicators of disruptions to root development, whereas Wilson bands are considered indicators of disturbances during enamel formation (Hillson 2014). This section focuses on enamel defects, but an overview of defects in dentine is provided by Molnar and colleagues (Molnar and Ward 1975; Molnar *et al*. 1981).

Wilson bands are sometimes also referred to as “pathological” bands (Fitzgerald and Saunders 2005; Gustafson 1959; Gustafson and Gustafson 1967; Hillson 1996; Risnes 1998; Rose 1977; Wilson and Shrof 1970). Morphologically, they appear as accentuated lines and can be identified under a light microscope by their dark and broad appearance and by the irregular structure of the prisms (abnormal prism bending and the absence or distortion of prism structure) within this dark band (Rose *et al*. 1978; Hillson 2014). Apart from being longer and broader, these markings are very similar to the regularly spaced striae of Retzius and according to Fitzgerald and Saunders (2005, 278), “*the only difference between regular striae of Retzius and Wilson bands is the nature of the systemic trigger that produced them*.” These accentuated lines vary in appearance and prominence, but all of these are visible along more of their length than regular striae of Retzius (Fitzgerald and Rose 2000; Fitzgerald and Saunders 2005; Fitzgerald *et al*. 2006; Goodman and Rose 1990; Rose 1977, 1979; Rose *et al*. 1978; Wilson and Shrof 1970; Witzel *et al*. 2006, 2008).

At the time of birth, a specific type of accentuated line can be observed in the enamel of all deciduous teeth and most (but not all) mesiobuccal cusps of first permanent molars, the neonatal line (Fig. 3.8). This line varies in prominence between individuals, possibly reflecting specific (disruptive) circumstances at birth (Antoine *et al.* 1999; Eli *et al*. 1986; Hillson 1996; Massler *et al*. 1941; Rushton 1933; Sabel *et al*. 2008; Schour 1936; Schour and Kronfeld 1938; Schour and Massler 1937; Weber and Eisenmann 1971; Whittaker and Richards 1978). The line occupies a characteristic position within the tooth crowns for children born full-term. In a histological study of 173 deciduous teeth (21 males and 23 females) of children who were born significantly post or pre-term, Skinner and Dupras (1993) found that the neonatal line was located further occlusally in children born prematurely in comparison to children born full-term. In contrast, the position of the neonatal line in children born post-term was located closer to the cervix in comparison to children born full-term. This variation in the position of the neonatal line provides the strongest proof of its timing (Hillson 2014).

The neonatal line marks a separation between the prenatal enamel and the “normal” postnatal enamel structure (Antoine *et al*. 2009a). As prenatal enamel does not show the clear incremental structures (striae of Retzius) visible in postnatal enamel, it has been suggested that the neonatal line may be a marker of the start of the newborn’s child own independent biorhythm, as opposed to the earlier, less intense, metabolic rhythm it shared with its mother (Ferrell 2006; Fitzgerald and Saunders 2005). The neonatal line is a broad band which appears dark in thick sections under conventional light microscopy. On thinner sections, the neonatal line is a particularly prominent mark between cross-striations (Hillson 2014). This neonatal line is the basis of many chronological inferences based on internal incremental structures, as it forms a reference point for both cross-striation and striae of Retzius counts on first permanent molars (Antoine *et al*. 2009a; Fitzgerald and Saunders 2005).

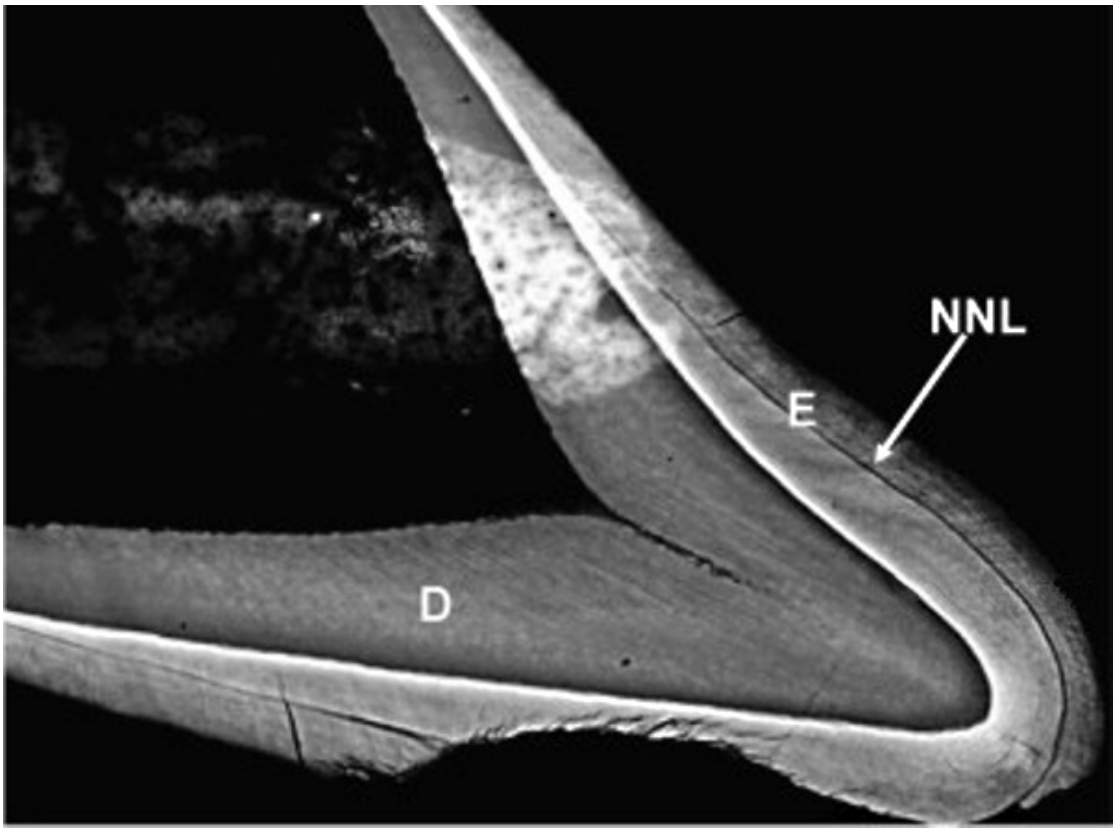

Figure 3.8: Microradiograph of a primary incisor from a 2 month old individual (5×). E = enamel, D = dentine, NNL = neonatal line (adapted from Sabel *et al.* 2008, 957)

Other accentuated lines have also been used to infer patterns of developmental disturbances in animal and human populations (Goodman and Rose 1990; Rose 1977; Schwartz *et al.* 2006). Individual accentuated lines can be matched across different teeth in one dentition, suggesting they correspond to the same metabolic disturbance (Fitzgerald and Saunders 2005; Fitzgerald *et al*. 2006). It is generally agreed that accentuated lines are caused by non-specific systemic disturbances, but some occurrences have been linked to specific conditions including neonatal asphyxia, hypocalcaemia and maternal diabetes (Fitzgerald and Saunders 2005).

A unique study comparing life history details with dental developmental sequences carried out by Schwartz and colleagues (2006) supports the association of accentuated lines with specific disruptive factors such as injuries and other traumatic events. Schwartz and colleagues (2006) studied ground sections (with a thickness of 180-200μm) of 14 permanent anterior and posterior teeth of a captive female western gorilla and compared the identified accentuated lines with detailed life history data recorded by zoo personnel. They found that each recorded stress episode (birth, injury, hospital visits) could be

matched with an accentuated line visible in the cuspal or imbricational enamel of all of the permanent teeth developing at the time of the stress episode (Schwartz *et al.* 2006). Interestingly, these accentuated lines were associated with both major physiological disturbances (birth, injuries) and psychological traumas such as hospital visits and enclosure transfers (Fig. 3.9).

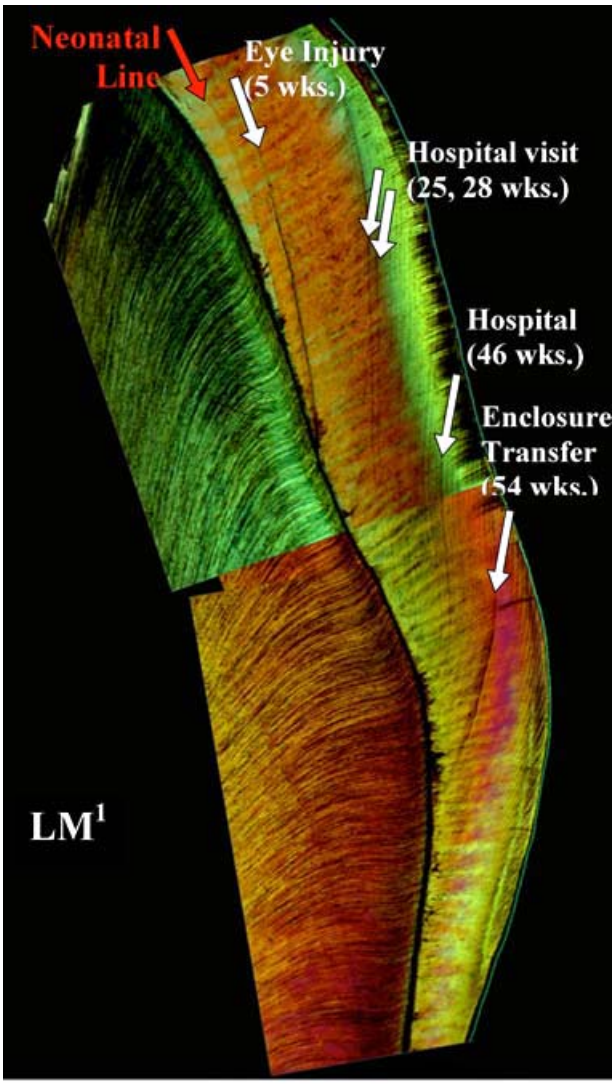

Figure 3.9: Polarised light montage of a section (90–110μm) of the crown of the first molar (lingual cusp) illustrating the position of the accentuated lines associated with the major life events in a gorilla specimen (from Schwartz *et al.* 2006, 1210)

Various authors have tried to study the link between accentuated lines and another condition caused by a non-specific growth disruption known as **enamel hypoplasia** (Fitzgerald and Saunders 2005; Goodman and Rose 1990; Kreshover 1940; Kronfeld and Schour 1939; Rose 1977; Witzel *et al*. 2008). Enamel hypoplasia is a condition where

enamel defects are visible at the surface of the crown. The condition is defined by Goodman and Rose (1990, 59) as a "*deficiency in enamel thickness resulting from physiological perturbations during the secretory phase of amelogenesis*". Similar to accentuated lines, enamel defects can be matched on teeth across an individual's dentition, which is also an indication of its systemic origin (Hillson 1996). The concept of enamel hypoplasia, its identification and interpretation will be reviewed in the next chapter.

Even though the internal accentuated lines and the external enamel hypoplasia have both been linked to (non-specific) disruptions in ameloblast activity, the link between the defects is not entirely clear, as internal defects are not always associated with external (enamel hypoplasia) defects (Goodman and Rose 1990; Hillson 1996). There is no clear consensus concerning the relationship between defects in the enamel microstructure and various manifestations of enamel hypoplasia (Goodman and Rose 1990; Hillson *et al*. 1999; Kierdorf and Kierdorf 1997; Witzel *et al*. 2008; Wright 1990). For example, Condon (1981 cited in Goodman and Rose 1990), in his study of 30 canines and premolars, found all identified accentuated lines to correspond with enamel hypoplasia. In contrast, Macho and colleagues (1996), in their study of East African fossil specimens (*Theropithecus oswaldi*, from Koobi Fora and Olorgesaili), found many accentuated lines but no corresponding external manifestations of dental disturbances. Similarly, Ferrell (2006) found a very infrequent correspondence between enamel defects and accentuated lines.

Interestingly, Witzel and colleagues (2008) found evidence of enamel hypoplasia without the presence of accentuated lines as well as evidence of accentuated lines without enamel hypoplasia. They have also shown that the presence of accentuated lines in the absence of an associated enamel hypoplastic defect can occur both in the appositional and imbricational enamel (Witzel *et al*. 2008).

Some researchers argued that the lack of clear relationship between accentuated lines and enamel hypoplasia can be explained by the hypothesis that the phenomena are the result of different stressors (Ferrell 2006; Simpson 1999). Others have put forward a threshold model in which enamel hypoplasia represents a more severe disruption to ameloblast activity than an accentuated line (Goodman and Rose 1990; Kreshover 1940; Rose *et al*. 1985; Wright 1990). However, evidence of external enamel hypoplastic defects in the imbricational enamel without the presence of internal accentuated lines

contradicts this. In this case, the presence of enamel hypoplasia would indicate that the threshold for accentuated lines would necessary have been passed, as arguably this is the result of a more intense stress episode (for a more detailed discussion on this subject, also see Witzel *et al*. 2008).

An alternative explanation is the effect of crown geometry on the appearance of both accentuated lines and enamel hypoplasia. Fitzgerald and Saunders (2005) argued that disruptions to ameloblast activity can manifest themselves in different ways depending on both the time of occurrence and the intensity of the irregularity. For example, when a disruption occurs during the maximum depression in the circaseptan cycle, an accentuated line will always occur. Whether or not the associated external enamel defect will appear depends on the time of development (imbricational or appositional stages of development). In contrast, when a disturbance does not occur within this maximum depression, an accentuated line may or may not form depending on the length and severity of the disruption, as the perturbation would have to be sufficiently strong to produce a markedly different structure than the regular brown striae of Retzius (Fitzgerald and Saunders 2005).

3.1.7. Applications

As counts of total numbers of cross-striations from the enamel-dentine junction to the crown surface correspond well crown formation times, these have been extensively used as a tool for examining characteristics of enamel formation in humans, primates and fossils (Beynon *et al*. 1998; Bromage and Dean 1985; Dean *et al*. 2001; Dirks 1998; Kelley and Schwartz 2010; Macchiarelli *et al*. 2006; Reid *et al*. 1998; Smith *et al*. 2003). Similarly, in teeth which cannot be sectioned (for example fossil teeth), perikymata have also been used to gather information concerning enamel formation patterns within and between species (Dean and Reid 2001; Dean *et al*. 1986; Guatelli-Steinberg *et al*. 2005; Guatelli-Steinberg *et al*. 2007a; Guatelli-Steinberg *et al*. 2007b; Ramirez Rozzi and Bermudez de Castro 2004; Ramirez Rozzi and Sardi 2007; Smith *et al*. 2010).

Dental development is widely used to estimate age in sub-adult human remains. Dental development diagrams, based on tooth formation and eruption patterns are routinely used as a basis for the ageing of the remains of children (AlQahtani 2008; Gustafson and Koch 1974; Schour and Massler 1941). For individuals up to 6 years of age, however, a

more precise alternative is the use of incremental structures, such as cross-striations, striae of Retzius and perikymata to reconstruct an individual's age at death (Antoine *et al*. 2009a; Antoine *et al*. 2009b; Bacon 1989; Boyde 1963; Boyde 1990; Bullion 1987; Dean and Beynon 1991; Hillson 2005; Hillson and Bond 1997; Huda and Bowman 1995; Smith *et al*. 2007b).

Chronologies of growth established through the incremental structures of teeth also allow the identification of disturbances that occur during growth and their timing. This in turn is a useful tool when analysing patterns of developmental disturbances in human populations and non-human primates (Antoine *et al*. 2005; Bullion 1987; Fitzgerald and Saunders 2005; Fitzgerald *et al*. 2006; Guatelli-Steinberg 2003; Guatelli-Steinberg *et al*. 2004; Hassett 2011; Hillson 1992; Hillson and Bond 1997; King *et al*. 2002; King *et al*. 2005; Reid and Dean 2000; Rose 1977; Rose *et al.* 1978; Rudney 1983; Skinner and Pruetz 2012; Skinner *et al*. 2012; Temple 2010; Temple *et al*. 2012; Wright 1990). The definition, etiology, recording and interpretation of enamel defects are further described in Chapter 4.

3.2. Skeletal growth

The main function of the vertebrate skeleton is to support the weight and movement of soft tissues and to protect internal organs (White and Folkens 2005). Through the attachment of muscles by strong and flexible tendons, the skeletal system also enables movement of the body (Wigley 2008). In addition, bone provides the basic reservoir for the storage of calcium in the body (Johnston and Zimmer 1989; Wigley 2008). Calcium, in turn, ensures the rigidity of the musculoskeletal system and enables the transmission of nerve impulses (Johnston and Zimmer 1989).

In order to deal effectively with mechanical stresses, bone undergoes modelling and remodelling throughout life, with most of the modelling occurring during growth (Pfeiffer *et al.* 2006; White and Folkens 2005). The fetal precursor tissue of many bones is cartilage and its replacement by bone is a complex process. In terms of human skeletal growth, three phases of development can be identified: the appearance of ossification centres; the morphological development of the ossification centres, including the increase in size, length and width; and the fusion of two or more ossification centres (Scheuer and Black 2000a). This project focuses on morphological changes in the ossification centres, so only a brief review of the fusion of ossification centres will be provided.

3.2.1. Physical structure and properties of bone

A section of any bone is composed of two main structural components, an exteriorly located, dense tissue (compact or cortical bone) and a cancellous or honeycombed tissue (spongy or trabecular bone), which is located interiorly (Boskey 2007; White and Folkens 2005; Wigley 2008). The molecular and cellular composition of these structures are identical, they only differ in the degree of porosity (Boyde and Jones 1998). The relative quantities of these two tissues differ according to the type of bone (its position and function within the skeleton) and is related to bone strength (Wigley 2008). Long bones consist of thick compact bone with a few trabeculae on the inner surface, enclosing a large marrow cavity. In flat bones (such as ribs) the interior is mostly cancellous (Boskey 2007; Wigley 2008).

The external surface of bone is covered by a fibrocollagenous membrane, the periosteum, and is attached to the bone by collagen fibres (Sharpey's fibres), which penetrate into the cortical bone tissue (Boyde and Jones 1998). The periosteum plays a major role in the repair of fractures. The internal cavities of bone are lined by a thinner layer, the endosteum (Clarke 2008). This lining is thought to be important in calcium homeostasis, i.e. maintaining adequate calcium levels (Wigley 2008).

Histologically, bone matrix displays two different types of organisation, woven and lamellar bone. Young fetal bones are characterised by a large amount of woven bone, in which bone crystals and collagen fibers are irregularly arranged (Boyde and Jones 1998; Wigley 2008). Lamellar bone tissue (Fig. 3.10) makes up most of the adult osseous skeleton, but the arrangement of lamellae depends on their location (Boyde and Jones 1998). They form continuous circumferential layers at the periosteal and endosteal surfaces, but the greatest proportion of lamellae form concentric cylinders around neurovascular channels called Haversian canals and as such, the lamellae and Haversian canals form the basic unit of bone tissue, called the osteon (Boyde and Jones 1998; Clarke 2008; Currey 2002; Parfitt 1994). There are approximately 21 million osteons in the adult skeleton, which vary in diameter between 100 to 400μm and a medium-sized osteon contains about 30 lamellae, each around 3μm thick (Wigley 2008).

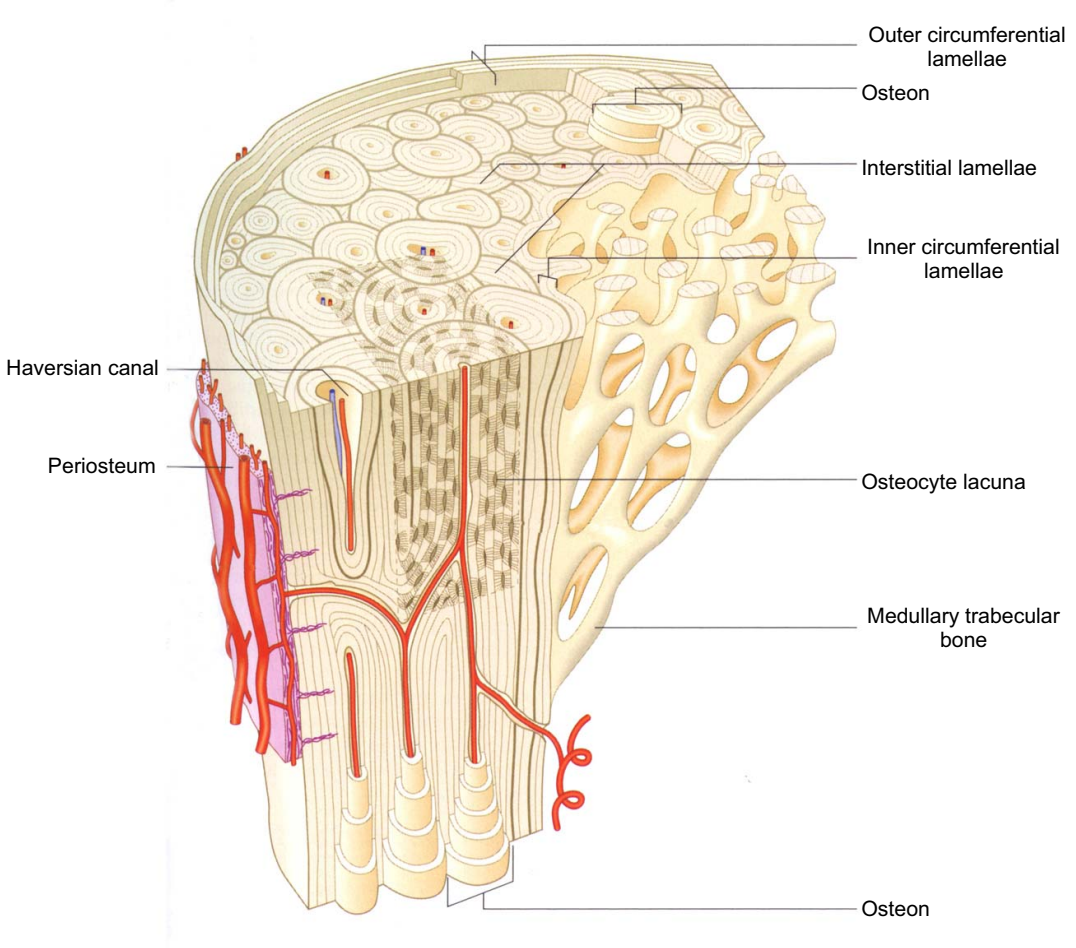

Figure 3.10: Main features of the microstructure of bone (Adapted from Standring 2008, 89)

3.2.2. Organic and inorganic composition of mineralised tissues

Bone tissue is composed of osteocytes encased within a mineralised matrix (Boskey 2007; Young 2003). The bone matrix is largely mineral (70-90%) and this mineral portion is mainly composed of hydroxyapatite, a form of calcium phosphate which creates the hardness and rigidity of bone (Boskey 1989; Clarke 2008; Wigley 2008). Approximately 30% of bone (by dry weight) is made up of collagen, a fibrous protein providing mechanical strength and flexibility (Boyde and Jones 1998; Wigley 2008). Attached to these collagen fibres and surrounding bone crystals are small amounts of non-collagenous proteins, including osteocalcin and fibronectin (Boskey 1989; Franz-Odendaal *et al.* 2006; Young 2003). The proportions of these bone matrix components vary with age, bone type and metabolic status (Boskey 2007; Wigley 2008).

Bone growth or remodelling involves the resorption and deposition of bone due to the activity of osteoclasts and osteoblasts, which are a series of specialised cells surrounded

by bone matrix (Franz-Odendaal *et al.* 2006; Wigley 2008). Osteoblasts are mononuclear cells with features typical of protein-secreting cells and are responsible for the synthesis, deposition and mineralisation of the bone matrix (Boskey 2007; Franz-Odendaal *et al.* 2006; Wigley 2008). Once embedded in the matrix, they become osteocytes, which are long-lived cells and constitute the main type of cell in mature bone. Osteocytes do not secrete new matrix, but actively maintain the bone matrix and their death leads to the resorption of the matrix through osteoclast activity (Boskey 2007; Wigley 2008). Osteoclasts are large polymorphic cells responsible for the local removal (or resorption) of bone tissue during bone growth and the subsequent remodelling of osteons (Boskey 2007; Franz-Odendaal *et al.* 2006; Wigley 2008).

3.2.3. Appearance of ossification centres

Vertebrate bone growth results from the deposition of bone on a pre-existing surface (White and Folkens 2005). Long bones (bones of the arm, legs and back) are pre-formed in cartilage (endochondral ossification), while flat bones (bones of the cranial vault) are formed through the transformation of mesenchymal tissue (intramembranous ossification) (Enlow 1990; Lewis 2007; Scheuer and Black 2000a). The section directly below focuses on endochondral ossification, intramembranous ossification is further explained on p. 90.

Endochondral ossification is a process in which the initial shape and position of bones are defined by cartilage models (miniature templates of the bone), followed by a gradual replacement of the cartilage by bone (Scheuer and Black 2000a; Tanner 1989; White and Folkens 2005, Wigley 2008). Initial sites of ossification are called primary centres and most of these appear in the embryonic and fetal period (Tanner 1989; Scheuer and Black 2000a). All long bones have only one primary centre of ossification, which is the precursor of the long bone shaft (diaphysis). More irregular postcranial elements such as the os coxae (ilium, ischium and pubis), clavicle (medial and lateral) and vertebrae have multiple primary centres of ossification (Black and Scheuer 1996).

Primary centres continue to grow in length and diameter for many months or years, depending on the type of bone, but eventually, one or more secondary centres of ossification start to appear in the cartilaginous extremities (Tanner 1989; Wigley 2008). Most of these secondary centres continue to enlarge during the postnatal and adolescent

years (Tanner 1989; Wigley 2008; Fig. 3.11). In long bones, these secondary centres develop into epiphyses, consisting either of large areas of bone (distal femur) or having a flake-like appearance (rib tubercles).

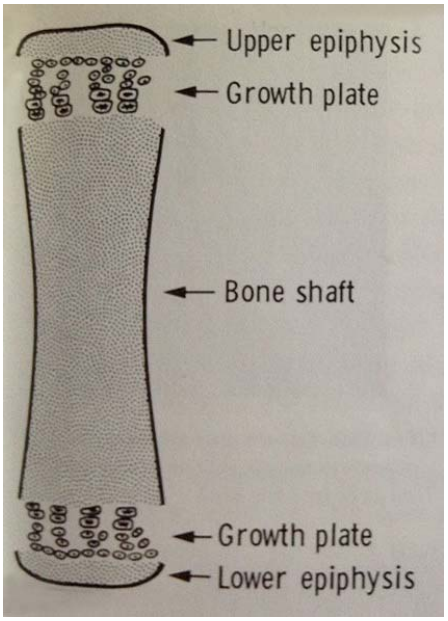

Figure 3.11: Epiphysis, diaphysis (bone shaft) and metaphysis/growth plate (From Tanner 1989, 32)

The order of appearance of ossification centres is highly variable (Francis and Werle 1939). Garn and Rohmann (1960) studied the appearance of 28 ossification centres in the hand and wrist using 2880 serial longitudinal radiographs of 154 healthy Ohio-born children. Based on deviations from the median order of development, they found a high variability in the appearance of these centres, both within and between sexes. Large deviations from the expected order of development could be associated with illness episodes (even in clinically healthy children), but health history records indicated that there was no clear cut evidence that atypical ossification appearances were related to ill health (Garn and Rohmann 1960). In a later study, Garn and colleagues (1966) found significant differences in timings of the appearance of ossification centres in the elbow and knee, with boys often showing an inverse pattern to girls. For example, in boys, the appearance of the capitulum of the radius was followed by the appearance of the medial epicondyle of the humerus, whereas the medial epicondyle appeared before the capitulum of the radius in girls. The appearance of the epiphysis of the proximal fibula preceded the appearance of the patella in boys as opposed to a patella-proximal fibula sequence in girls (Garn *et al.* 1966). Similarly, in a larger study on 852 individuals (429

boys and 423 girls) from the Samaritan's children hospital in Stockholm, Sweden, Elgenmark (1946) made a total of 1190 observations of 68 different centres of ossification (on hand, foot, knee, hip, elbow and shoulder) and found that independent of sex, individual centres appeared at highly variable ages.

Garn and colleagues (1966) referred to this developmental variation as ossification sequence polymorphism and argued that this might be explained genetically, as their studies have shown familial syndromes of atypical ossification of hand and wrist bones, such as the early appearance of the triquetral over two generations. However, they also suggested that the type of methodology (serial radiographs) used may account for some of the observed variation. It is easier, for example, to detect sequences in slower-growing children, where a greater number of radiographs can be taken. Similarly, Scheuer and Black (2000a) also noted that the detection of ossification varies according to the technique of observation. For example, alizarin staining and radiological investigations have a different sensitivity for the detection of bone. The timing of the appearance of prenatal ossification centres is extremely difficult to define, as age itself is difficult to establish in the prenatal period (Scheuer and Black 2000a).

3.2.4. Morphological development of ossification centres

The morphological appearance of the ossification centres changes during life. They increase in size and length from birth to skeletal maturity (around 18 years for long bones) and in width (bone diameter and thickness) from birth to around 30 years (Duren *et al.* 2013). The increase in length of the bone shaft generally occurs through endochondral ossification. The cartilage in the junction between the epiphysis and the metaphysis of the shaft, which appears translucent in radiographs, is called the growth plate. The part of the growth plate immediately below the epiphysis contains a layer of chondrocytes or stem cells (previously called chondroblasts). These cells differentiate, divide and eventually become absorbed into the diaphysis, thus enlarging the bone shaft (Tanner 1989; Rauch 2005).

The increase in width occurs through appositional growth. This involves osteoblast activity, adding mineralised tissue on the outer (periosteal) bone surface (Augustin *et al.* 2007; Black and Scheuer 1996; Rauch 2005). Periosteal resorption also takes place, as can be noticed on X-rays of the knees of growing children, where the growth plates of the

distal femur are much wider than the diaphyses (Fig. 3.12). As most of the tissue produced at the growth plate will eventually be absorbed into the diaphyseal bone, this indicates some level of periosteal resorption occurring at the metaphyses (Rauch 2005). In children, this process involving the “sculpting of a developing bone” is continuous, whereas in adults, periostal bone may undergo the cyclical resorption and formation patterns characteristic of the re-modelling process (Parfitt *et al*. 2000; Rauch 2005; Scheuer and Black 2004).

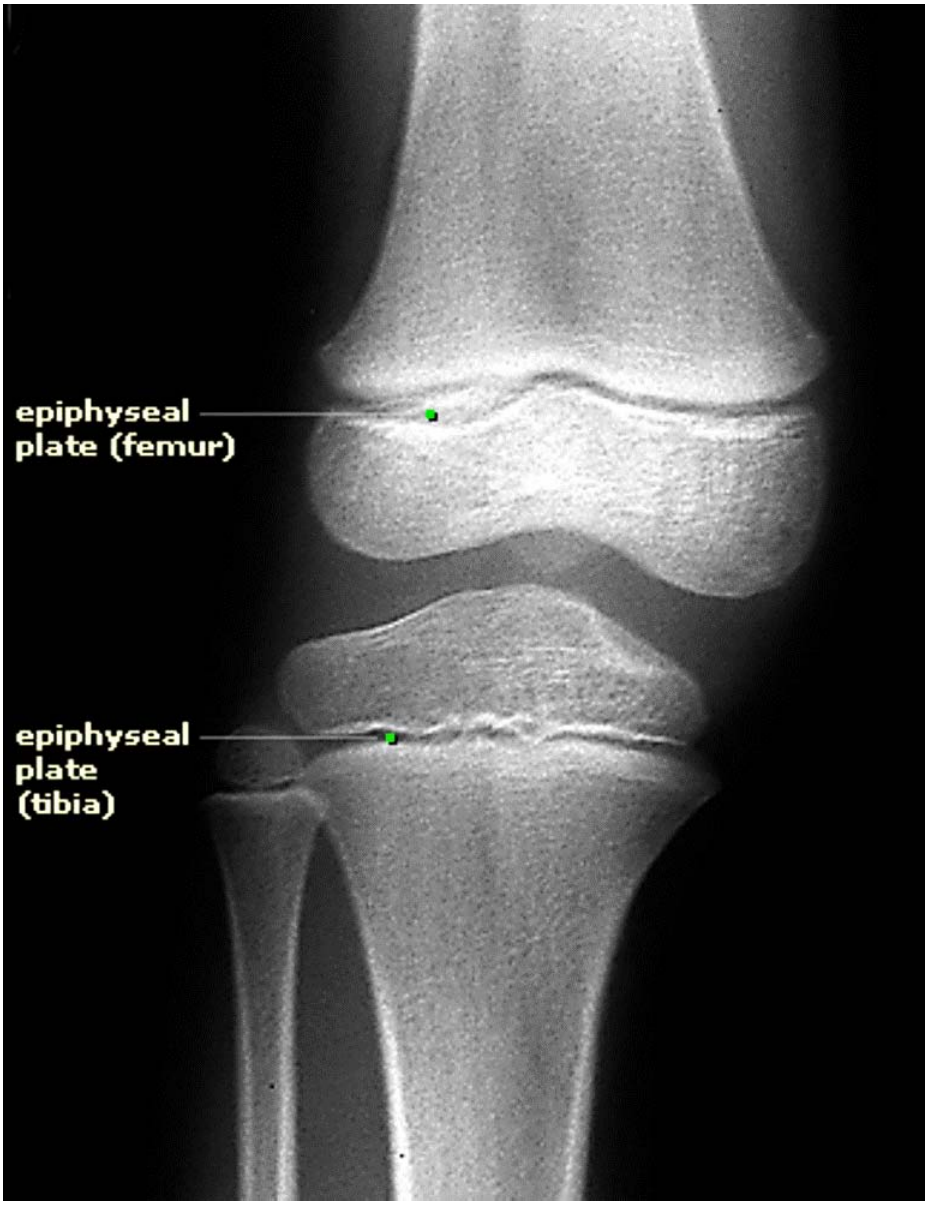

Figure 3.12: X-ray (anterior view) of a developing knee (From O’Rahilly *et al.* 2004)

The morphological development of the centres of ossification has been demonstrated by Ogden and colleagues (McCarty and Ogden 1982a; McCarty and Ogden 1982b; Ogden 1984a; Ogden 1984b; Ogden and McCarthy 1983; Ogden and Phillips 1983; Ogden *et al.* 1978; Ogden *et al.* 1986), who carried out detailed studies on developing skeletal elements based on dissections, radiography and histology (Fig. 3.13). In their study of 23 pairs of proximal humeri ranging from full-term stillborns to 14 year olds (12 males and 11 females), they reported morphological changes including a thickening of the metaphyseal cortices which took place around 7 months, the enlargement of primary and secondary ossification centres, and the epiphyses and metaphyses taking their typical conical contour at three years (Ogden *et al.* 1978).

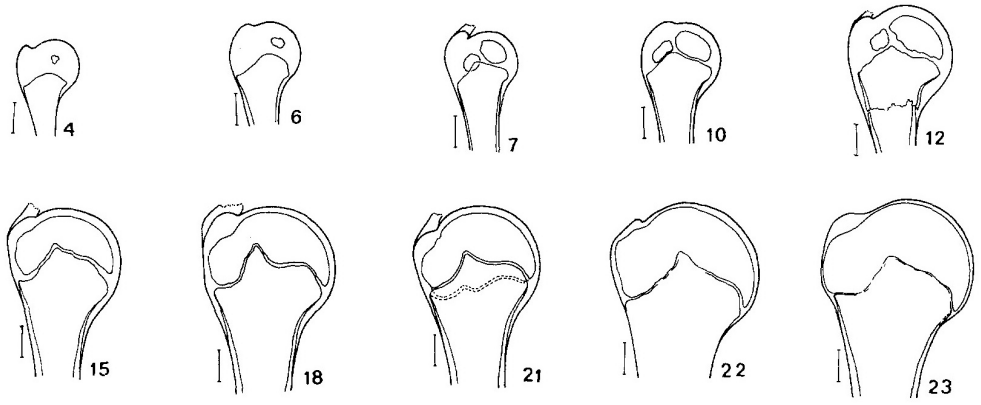

Figure 3.13: Schematic representation of the development of the epiphysis and metaphysis of the proximal humerus (From Ogden *et al.* 1978, 154)

3.2.5. Fusion of ossification centres

Fusion of primary centres of ossification occurs early in life, with fusion times of different parts of the sphenoid documented from 5 fetal months to the fusion of the ossiculum terminale of the dens (filling its apical cleft) of the axis from 11 years (Schaefer *et al*. 2009). Epiphyseal fusion starts later in life, after the eruption of the second molar, from around the age of twelve, and concludes with the fusion of the sternal end of the clavicle to its body, at around 21 years of age. Complete bone fusion is the end result of a gradual development in which the metaphyseal and epiphyseal ossification processes gradually encroach upon one another and eventually meet when the bony fusion of the epiphysis occurs (Scheuer and Black 2000a; Wigley 2008).

3.2.6. Skull growth

The skull has two major functional and anatomical components, the neurocranium and the viscerocranium. The skeletal components of the neurocranium (the skull vault and base) protect the brain and the special sense organs of olfaction, vision, hearing and balance (Fazekas and Kósa 1978; Scheuer and Black 2000a; Standring 2008). The face and palate, which are the skeletal components of the viscerocranium, are related to functions such as feeding, breathing and facial expression (Standring 2008).

The skull is a unique skeletal structure and its development is characterised by a combination of intramembranous and endochondrial ossification. The flat bones of the cranial vault (frontals and parietals) and the facial bones develop through the transformation of mesenchymal tissue (intramembranous ossification). Intramembranous ossification involves the formation of bone structures through the direct ossification (by osteoblasts) within a thick connective tissue membrane, so without the appearance of a cartilaginous precursor (Lewis 2007; Standring 2008). In contrast to the frontals, parietals and facial bones, bones of the cranial base develop through endochondral ossification (described on p. 85). The mandible, temporal, occipital and sphenoid bones undergo a combination of the two types of ossification (Lewis 2007; Scheuer and Black 2000a; Standring 2008).

At birth, the ossification of the skull is incomplete and many elements of individual bones are still separate, including the two halves of the frontal bone, the mandible, and the squamous, lateral and basilar parts of the occipital bone (Standring 2008). Once these elements are fused, the individual bones are held together by large fibrous joints (sutures: metopic, coronal, sagittal, lambdoid, squamosal, etc.) and contain large cartilaginous areas (fontanelles) which allow the head to compress and pass through the birth canal (Standring 2008). Later, these flexible sutures also allow for postnatal expansion for brain growth (Standring 2008).

Postnatally, the growth of the skull is determined by the changing proportions of its components as the skull vault, facial skeleton and cranial base grow at different rates (Standring 2008). The vault is largely influenced by cerebral maturation, but also by other neural structures such as the eyes and the spinal cord (Enlow 1976; Humphrey 1998; Standring 2008). This region grows rapidly during the first year of life, starting with an

increase in frontal breadth, and continues at slower rate until the age of seven, when most of its adult dimensions have been reached (Standring 2008).

The facial skeleton grows over a longer period of time than the skull vault (Standring 2008). The facial bones grow in response to the development of teeth and muscles of mastication but their development is also influenced by functional requirements such as respiration, chewing, swallowing and speech (Humphrey 1998; Standring 2008). Growth in this region continues until puberty and is linked to the growth spurt and hormonal influences of secondary sexual alteration (Standring 2008).

The growth and remodelling of the basicranium is markedly more complex than the facial skeleton and skull vault. Its size and shape is adapted to the dimensions of the brain, but it is also the platform upon which the midface is constructed (Enlow 1976). Similarly to the skull vault, the basicranium has sutures, but this region of the skull also has synchondroses (a type of cartilagenous joint) and three synchondroses exist in the cranium, the spheno-ethmoid, the intersphenoid and the spheno-occipital (Cendekiawan *et al*. 2010). Morphologically, they can be regarded as similar to long bone growth plates, except that in synchondroses, there are two growth plates which are positioned back to back, sharing a common zone of chondrocytes, which play a crucial role in endochondral bone formation (Cendekiawan *et al*. 2010; Enlow 1976; Standring 2008).

The complexity of the development of the cranial base is largely due to the fact that various endocranial fossae (such as the anterior, middle, posterior fossae and the sella turcica) as well as the passageway of major vessels and nerves need to be accommodated during growth (Enlow 1976). At around the age of six years, the fusion of the four parts of the occipital bone means that the foramen magnum is fully enclosed by bone, but the cranial base continues to grow at the spheno-occipital synchondrosis, until around 18 years of age (Humphrey 1998; Standring 2008).However, there is some evidence that growth ceases around the age of 15 years, following the eruption of the second molar (Standring 2008). In any case, most cranial dimensions reach adult size earlier than postcranial elements (Humphrey 1998; Lewis 2007; Ruff *et al*. 2013).

3.2.7. Developmental disturbances

Epidemiological studies of living people have shown that one of the best indicators for the well being of a community is its children, as their rate of growth is strongly affected by their

health, overall nutrition and socio-economic conditions (de Onis *et al*. 2006a; de Onis *et al*. 2006b; Eveleth and Tanner 1976; Johnston and Zimmer 1989; Susanne 1980). Eveleth and Tanner (1976) suggested that many environmental factors affect the rate of growth and that bodily adaptations for survival include a smaller body size of children who receive insults during growth as opposed to better-off children. Anthropologists, human biologists and economic historians therefore considered adult stature and stature-for age as sensitive indicators of quality of life (Bogin *et al.* 2002).

Growth rates can be assessed in terms of body size and shape. In osteological analyses, attainment of size refers to single parameters such as the length of limbs or measurements of limb morphology or body proportions. It is especially the relationship between size and life history parameters such as nutritional status that is of interest to childhood health researchers, as body shape is less affected by environmental factors (Eveleth and Tanner 1990).

Different aspects of skeletal development may vary in environmental sensitivity. For example, skeletal maturation (in terms of the fusion of epiphyses) is generally less retarded than growth in height during periods of poor nutrition (Frisancho *et al*. 1970; Martorell *et al.* 1979). This is because elements of the environment which adversely affect growth have the greatest effect in early childhood years, during which most of the (rapid) linear growth takes place, as opposed to adolescence, which is a relatively slower period of skeletal maturation (Eckhardt *et al.* 2005a; Hoppa 1992; Schroeder *et al.* 1995).

Whilst it may be possible to identify a cause for a small size for age in individual cases, it is very difficult to identify a specific cause at a population level, as growth stunting is a non-specific response to a number of specific noxious influences (Keller 1988). Nevertheless the most commonly recognised and documented factors affecting childhood growth are malnutrition and repeated infections, especially of the gastrointestinal tract (Keller 1988).

Environmental factors

"*A universal observation in vertebrate biology is that of a low plane of nutrition in early life slows the rate of growth and, if it persists may result in small stature at maturity (*Fraser 1988, 127*)."*

In growing human beings, the multiplication of cells or their enlargement in size, leading to normal rates of bone growth, depends on an adequate supply of energy, amino acids,

water, lipids, vitamins and minerals (Alvear *et al*. 1986; Bogin 1999, Duren *et al*. 2013; Wigley 2008). Small body size for age is often used as an anthropometric diagnosis of **malnutrition** in humans (Sutphen 1985; Waterlow 1988).

In order to assess the link between bone apposition and protein deficiency, Glick and Rowe (1981) conducted an experimental study on rats (N=275), in which 172 young (29 days old) rats were put on a protein-deficient diet. They found that in relation to the control group, the protein-deficient rats showed radiographic and histological features of an abnormal pattern of endochondral bone formation (Glick and Rowe 1981). In addition, they reported a significantly decreased rate of appositional growth in the protein-deficient rats, as measured by the percentage of endosteal surfaces undergoing active bone formation. However, chemical analysis revealed no significant differences in the mineral content of the bones of the nutritionally deficient rats in comparison with the control group. Fraser (1988) reported similar results from experimental studies on growing rats, puppies and kittens, where severe calcium deficiency induced skeletal retardation.

In contrast to animal studies, little attention has been paid to micronutrients in the investigation of human growth faltering. Golden (1988) put forward two types of micronutrients: when a deficiency occurs for type 1 nutrients, such as iodine, copper, iron or calcium, body stores can be depleted and a decrease in tissue concentration can be detected, but growth is rarely affected; in contrast, a lack of type 2 nutrients, which includes zinc, potassium and magnesium, for which there is no body store to rely on as these nutrients are involved in essential physiological functions, can result in growth retardation. However, in most cases, it is not possible to clarify if one or more nutrients has been responsible for the growth disturbance (Golden 1988).

Van Lerberghe (1989) suggested that growth disturbances can also be caused by **infection** through the reduction in dietary energy intake concomitant with a sustained or increased level of energy expenditure. However, the results of growth studies analysing the association between illness and physical growth did not provide clear-cut evidence for this hypothesis. For example, McGregor and colleagues (1961) measured the weight and height of children in Keneba, a village in rural Gambia and argued that infections such as malaria, measles, whooping cough and gastroenteritis were the main factors affecting growth in this sample. In contrast, a longitudinal study of 276 children in Morelos (Mexico) who were regularly measured in terms of length, weight, thickness of triceps skinfold and head, chest and arm circumference, found no correlation between illness history and any of the growth variables (Johnston *et al.* 1980).

A review of longitudinal growth studies in which individual illness histories were gathered, revealed that most of the studies in developed countries report no associations between illness and physical growth, whereas in studies from developing nations, childhood ailments and in particular diarrheal diseases are strongly associated with poor physical growth. It is not clear if these differences are related to methodological factors or the increased vulnerability of malnourished children in developing countries (Martorell 1980).

Some differences in growth patterns between populations might also be related to differences in altitude (Frisancho and Baker 1970). Stature, weight, sitting height, chest width and depth of Quechua children from Puno in the southern highlands of Peru were measured in order to assess the influence of hypoxic conditions on growth. Cross-sectional (N=1202) and semi-longitudinal (N=300) samples were divided into low altitude (4000m) and high altitude (4500m) groups. Children in the high altitude group were slightly smaller for their age than those in the low altitude group. Both groups of children were consistently smaller for their age than US and Peruvian children who lived at sea level or moderate altitudes (Frisancho and Baker 1970). These differences may be due to the hypoxic effect of high altitudes or genetic adaptations (Frisancho and Baker 1970).

The impact of **socio-economic conditions** on growth was tested by Bogin and colleagues (2002) who compared the height and sitting height of children aged between 5 and 12 years from Mayan families in Guatemala (N=1347) and from Mayan families who immigrated to the United States (N=4631). They found that the children from the US have significantly longer legs in relation to their head and trunk than the children in Guatemala. Bogin and colleagues (2002) interpreted this difference as reflecting improvements in the quality of life for the migrant Mayans, which include safe drinking water, health care and nutritional supplementation. Similarly, Susanne (1980) gave an overview of studies where increasing trends in height were correlated with annual income or educational level, but suggested that most of the factors influencing socioeconomic differences, including income, educational level, transport, health care, nutrition, number of children per family etc., are interrelated, making it difficult to isolate one particular factor.

Based on a cross-sectional study of 22 small-scale societies, Walker and colleagues (2006) questioned the assumption that poor environmental conditions lead to slower growth. They highlighted the example of the Hiwi, Negritos and Pygmies, where relatively fast development of females can be interpreted as an adaptation to high-mortality

regimes. Walker and colleagues (2006) argued that ontogenetic trajectories not only depend on energetic constraints (influences of malnutrition and disease), but are also influenced by other demands, particularly in terms of fertility (current versus future reproduction).

Genetic factors

All processes of skeletal growth are affected by genetic constraints (Eveleth and Tanner 1990; Duren *et al*. 2013; Sutphen 1985). Duren and colleagues (2013) suggested that both environmental (diet, physical activity etc.) and genetic influences change during life. One well-known example of this change is osteoporosis, where the same genetic code is present throughout life, but its effect on the bone phenotype generally only appears during late adulthood (Duren *et al*. 2013).

To assess genetic and environmental constraints on human growth and identify periods of increased sensitivity to those influences, Duren and colleagues (2013) analysed a large sample of 1761 individuals (from 235 nuclear or extended families from the Fels longitudinal study) between 1.5 and 93 years of age. Using quantitative measures (length, diameter and cortical thickness of the left 2nd metacarpal) and quantitative genetic methods (narrow sense heritability using all familial information for parameter estimation) they found statistically significant differences between sexes for all studied bone traits as well as differences in heritability between these traits. Phenotypic sex differences in bone diameter, cortical index, cortical thickness and metacarpal length occurred at distinctly different ages, from early childhood (2 years of age) for bone diameter and from puberty for cortical thickness and metacarpal length (Duren *et al.* 2013).

Duren and colleagues (2013) reported that the genetic contribution to bone length was very high at 2 years of age and that this trend continued during early childhood and young adulthood, with an average heritability of 0.92 from 7 to 29 years of age. Similarly, the heritability of bone robusticity (measured as bone diameter) was also high during childhood. In contrast, the genetic influences on cortical thickness and the cortical index fluctuated with age but were much lower on average than the average heritability of bone length and diameter (Duren *et al*. 2013).

In their study of parents and children aged three to nine, Eveleth and Tanner (1990) found that correlation coefficients of height between parents and offspring are slightly less than

0.5, indicating a substantial family-line control over height. Although there was less information about other anthropological measurements, the authors argued that this family-line control is similar with regards to lengths of limbs and the trunk, but lower in relation to skeletal breadths, muscle and fat (Eveleth and Tanner 1990).

3.2.8. Applications

Immature remains are often assigned age at death estimates based on the developmental stage of their skeletal elements (Desbat *et al*. 2012; Schaefer *et al*. 2009; Scheuer and Black 2000a). In archaeological assemblages, secondary ossification centres are often absent or isolated finds and therefore of limited use when estimating the age of skeletal assemblages. They can, however, be used during the examination of mummified remains or in specific forensic situations where they are likely to be recovered and identified (Scheuer and Black 2000a). In contrast, changes in size and morphology of primary ossification centres are often used as age estimators in both archaeological and forensic assemblages (Scheuer and Black 2000a).

Based upon the ages obtained by these methods, individual ages or age groups can be assigned to skeletal remains. Individual age estimates are often employed in forensic situations, when dealing with single burials or small numbers of individuals (Cattaneo 2007; Duarte *et al*. 1999). Age groups are used to summarize age at death estimates for larger assemblages. As such, relative frequencies of the immature individuals are compared to numbers of adults and based upon these comparisons, inferences about the demography of past populations can be made (Bocquet-Appel 2002; Jackes and Meiklejohn 2008; Scheuer and Black 2000a).

Since human growth and development are strongly influenced by environmental and genetic variables, ontogenetic studies can reveal information about health and environmental factors (Krovitz *et al.* 2003). Following the theoretical proposition that slowing or cessation of growth is an expected response by an organism to increased levels of physiological disturbances, the growth of a child reflects his or her health and nutritional status (Bogin 1999; Eveleth and Tanner 1990; Hoppa 1992; Saunders *et al*. 1993). As a consequence, skeletal indicators, including postcranial and cranial measurements and analyses of epipyseal fusion patterns, can be used as an indicator of growth disruptions in children (Hoppa and Fitzgerald 1999; Humphrey 2000a; Johnston 1968; Mays 1999).

Differences in long bone growth have been documented: between past populations and modern samples (Hoppa 1992; Lovejoy *et al.* 1990; Saunders *et al.* 1993); populations from different geographical regions (Hummert and Van Gerven 1983; Lewis 2002; Mays *et al*. 2008; Pinhasi *et al*. 2005); different time periods (Jantz and Owsley 1984; Hoppa 1992), and within individual populations (Armelagos *et al.* 1972; Hummert and Van Gerven 1983; for an overview see Humphrey 2000a). Studies include examinations of variation in skeletal growth between males and females (Menninger 2008) and in relation to social status (Mays *et al.* 2009), migration (Saunders *et al.* 1993), mortality or morbidity (Pinhasi *et al.* 2006, Harrington and Pfeiffer 2008) and chronological horizon (Cardoso and Garcia 2009; Okazaki 2004). Analyses of growth have also helped to address phylogenetic issues in the palaeontological record (Bastir *et al.* 2007; Coqueugniot 1999; Coqueugniot 2005; Coqueugniot and Minugh-Purvis 2003; Coqueugniot *et al.* 2004; Enlow 1990; Gunz *et al.* 2012; Jeffery and Spoor 2004; Krovitz *et al*. 2003; Lieberman 2000; Ponce de Leon and Zollikofer 2001). The types of skeletal measurements, assessments of skeletal maturity in bioarchaeological studies and the rationale and details behind the interpretation of skeletal growth are further described in Chapter 4.

Chapter 4. Literature review

4.1. Furrow-form enamel hypoplasia

4.1.1. Early definitions

The earliest reference to dental defects dates back to the sixteenth century. Urbain Hémard (1582), a French dentist, often referenced by Fauchard (1746), described dental defects as "*érosions*", establishing this term in the French tradition. Bunon (1743) further defined this condition as "*teeth with grooved, pitted, rimpled or disagreeably coloured enamel or completely lacking enamel* [page 62, my translation]". Similarly, Magitot (1881) distinguished five types of *érosions*, including: "indentations" within the enamel, roughened enamel, single or multiple grooves, patches with congenital absence of enamel and complete absence of the crown of certain teeth [page 130, my translation].

In England, Hutchinson (1861) was one of the first scholars to diagnose enamel defects, referring to them as "honeycombed teeth". Similarly, Tomes described the appearance of pronounced grooves or pits "*which are pathological, and are marks of checks in development* (Tomes 1882, 43-44)". Later, Black (1908) used the term *atrophy* or *dystrophy* for enamel defects.

It was Zsygmondi (1893, 63) who, at the World Dental Congress in Columbia (USA) coined the current term, *hypoplastische emaildefekte* or "hypoplasia" to this condition. Without going into the causes of enamel defects, he differentiated between various forms of enamel hypoplasia, including single or rows of more or less deep *Grübchen* or little pits to furrows visible around the circumference of the tooth crown (Zsygmondi 1893, 49).

Today, the term "hypoplasia" refers to an underdevelopment or incomplete development (from Greek – *hypo* refers to "under" and *plastikos* to "mould") and as a MeSH (Medical Subject Headings) term, it is used to indicate congenital defects producing morphological anomalies in tissues or organs. Examples of hypoplasia or underdevelopment of skeletal elements include anencephaly (malformation of cranial vault), cleft palate and lip and

spina bifida. Similarly, in the nineteenth century, Zsygmondi suggested that enamel hypoplasia is "*an interruption in the process of development that leaves indelible traces upon the teeth*" (Zsygmondi 1893, 50).

4.1.2. Hypoplasia and crown development

The relationship between enamel defects and (disturbances to) the formation of the tooth crown was established very early on. Bunon (1743, 62), for example, mentioned that once teeth have erupted, no disease can leave such an "*erosive*" impression on teeth. He also referred to the developmental schedule of teeth, mentioning that when "*erosions*" appear on the deciduous teeth, only these teeth will be affected and not the later developing permanent teeth (Bunon 1743, 66). Similarly, both Fauchard (1746) and Magitot (1881) compared enamel defects with "*des érosions de l'ongle*", grooves or lesions on the finger or toenails, with the difference being that due to the rapid development (or turnover rate) of nails, nail lesions disappear quickly, whereas they remain permanent in teeth.

Magitot (1881) called enamel defects "*the permanent and indelible indication of a disturbance to the formation of the tooth crown, occurring during the intra-folliculary period and of which the pathological cause is related to the period of development during the time of the alteration of the tooth crown* [page 129, my translation]". He was also aware of the different developmental schedule of tooth types, as he mentioned a case study of a 23 year old male who had a "condition" when aged between two months and two years and hence showed honeycombed teeth on the permanent incisors, canines and first molars. In contrast, there were no apparent lesions on the 2nd molar (Magitot 1881). Similarly, Black (1908) argued that enamel defects resulted from an arrest (or partial arrest) of enamel (and dentine) growth in the part of enamel or dentine being developed at that particular time.

4.1.3. Hypoplasia and cell structure

The link between enamel defects and cell structure was also discovered very early on in the history of dentistry. In 1893, Zsygmondi already referred to the "decay of ameloblasts" and Berten (1895, cited in Gottlieb 1920) mentioned that "*the rods above the line of*

Retzius connected with the defect showed very frequently a deviation from their normal course". Similarly, Pickerill (1914, 97) argued that hypoplasia was caused by a "gross arrest of the function of the enamel organ" and that these "gross arrests" will result in "gross imbrications and striations".

Suckling (1989) provided a detailed overview of historical perspectives on the pathogenesis of dental defects. She considered the re-conceptualisation of amelogenesis in the 1940s as a turning point, as advances in the understanding of secretory and maturation phases required the rethinking of the process of enamel defect formation. Prior to the 1940s, it was generally agreed that amelogenesis consisted of the deposition of mineral matter (matrix formation), directly followed by calcification, also considered as the deposition of inorganic "calcium salts" within the formed matrix (Suckling 1989).

Based upon the idea of two depositional stages, some scholars regarded enamel hypoplasia to be caused by the defective deposition of "salts", referred to as earth salts, calcium salts or lime salts (Gottlieb 1920; Marshall 1939; Walkhoff 1894). Later, various researchers attributed the cause of enamel defects more specifically to the injury done to cells during growth (Kreshover 1940; Sarnat and Schour 1941). Kreshover (1940) carried out a rigorous study of enamel hypoplasia, based upon five cases with clinical history and a control group of six individuals. He argued that the abnormal formation or secretion of enamel substance represents a manifestation of injured ameloblasts. He suggested that ameloblasts may be injured to varying degrees and that some injuries may be reversible (Kreshover 1940, 1098).

In 1940, a new theory regarding enamel development, also involving two main developmental stages, emerged (Suckling 1989; Weinmann *et al.* 1945). According to this idea, the first stage was represented by ameloblasts depositing the complete organic matrix, which included mineral matter. This stage was then followed by a second, maturation stage, which involved the withdrawal of organic matter starting from the surface of the cuspal enamel and proceeding cervically (Suckling 1989; Weinmann *et al.* 1945; Fig. 4.1). Further work has subdivided this two-staged concept of amelogenesis into additional phases and confirmed that hypoplastic lesions are formed as a result of an impairment during the secretory phases of amelogenesis (Suckling 1989, 90; Witzel *et al.* 2008).

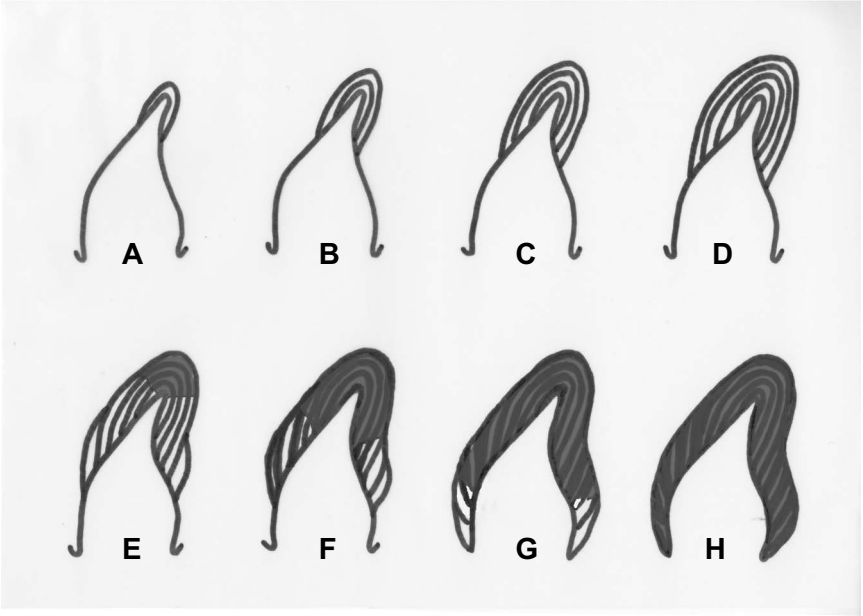

Figure 4.1: Diagrammatic representation of amelogenesis according to Weinmann *et al.* 1945, 415

4.1.4. Types of enamel hypoplasia

Enamel hypoplasia is commonly categorised under the term “dental enamel defect” a collective term relating to any condition with abnormal enamel formation (Pindborg 1970, 1982; Poulsen *et al.* 2008). Broadly speaking, dental enamel defects can be divided into two types, quantitative and qualitative defects, resulting from disturbances during different stages of enamel formation (Sarnat and Moss 1985).

Whereas Weinmann and colleagues (1945) defined quantitative defects as resulting from disturbances in the formation of the enamel matrix leading to a reduced amount of enamel, they considered qualitative defects as caused by disturbances in enamel maturation resulting in a normal amount of enamel, but of a different (lesser) quality (soft or chalky). Qualitative defects include enamel opacities (hypocalcified enamel), discolourations (deposits of pigment or staining) and hypomaturation (Hillson 1996; Sarnat and Moss 1985).

Enamel hypoplasia is considered a quantitative enamel defect, as it refers to a deficiency in enamel thickness and, as mentioned previously, results from a disturbance in the deposition of enamel matrix (Hillson 1996; Suckling 1989). In her experimental work on dental structures of dogs and other mammals, Mellanby (1930) highlighted both micro-

and macroscopic differences in enamel and dentine structure between “normal” and “hypoplastic” teeth (Table 4.1). Using her study based on more than 1000 deciduous and around 226 permanent human teeth, she argued that various grades of hypoplasia exist between these extremes, ranging from slight to severe hypoplasia (Mellanby 1929).

Table 4.1: Definition of normal versus hypoplastic teeth (based on Mellanby 1930, 70)

Normal	**Hypoplastic**
White, smooth, shiny enamel	Rough, discoloured enamel
Microscopically well formed enamel, little pigmentation	Calcified area comparatively thin, pigmented enamel
No interglobular spaces in dentine	Many interglobular spaces in dentine
Difficult or impossible to see Brown striae of Retzius	Brown striae of Retzius clearly defined

Lady Mellanby differentiated furrow-like defects (M-hypoplasia) from “gross defects” or G-hypoplasia, the latter involving pitting and large areas of deficient thickness (Hillson 1992; Mellanby 1929). Various other classification schemes have been put forward (Pindborg 1982; Sarnat and Moss 1985). Berten (1895) described three main types of defects and this description has become the basis of the current system used for the classification of hypoplastic defects. Berten differentiated between enamel defects appearing as *Grübchen* or pits, *Fürchen* or furrows and *flächenformig* or plane-form defects (Berten 1895; Hillson 1996; Hillson and Bond 1997; Fig. 4.2).

Figure 4.2: Types of enamel hypoplasia, including furrow-type defects (for example, first from left; top and bottom row), pit-form defects (for example, third from left; top row) and plane-form defects (for example, fourth from left; bottom row) (Specimen RCSOM/D 35.1 from Royal College of Surgeons of England. Photo: Carr J)

Linear enamel hypoplasia (LEH) or furrow-type defects are the most commonly occurring form of enamel hypoplasia and consist of one or more clearly defined horizontal bands around the circumference of the imbricational zone of the crown (Hillson 1996; Hillson and Bond 1997). As the term linear enamel hypoplasia has often been used to describe defects on deciduous teeth and might be linked to a specific perinatal aetiology (Infante and Gillespie 1974, 1977), Hillson (2014) suggested referring to the horizontal bands on permanent teeth as **furrow-form** enamel defects.

Microscopically, furrow-type defects can be recognised by an exaggeration of one or multiple adjacent perikymata in the occlusal wall of the defect, with perikyma grooves further apart than usual for that particular area of the crown (Hillson 1996; Hillson and Bond 1997; Witzel *et al.* 2008; Fig. 4.3). This type of defect is produced by the premature cessation of matrix secretion of a larger than usual band of ameloblasts (Hillson 1996).

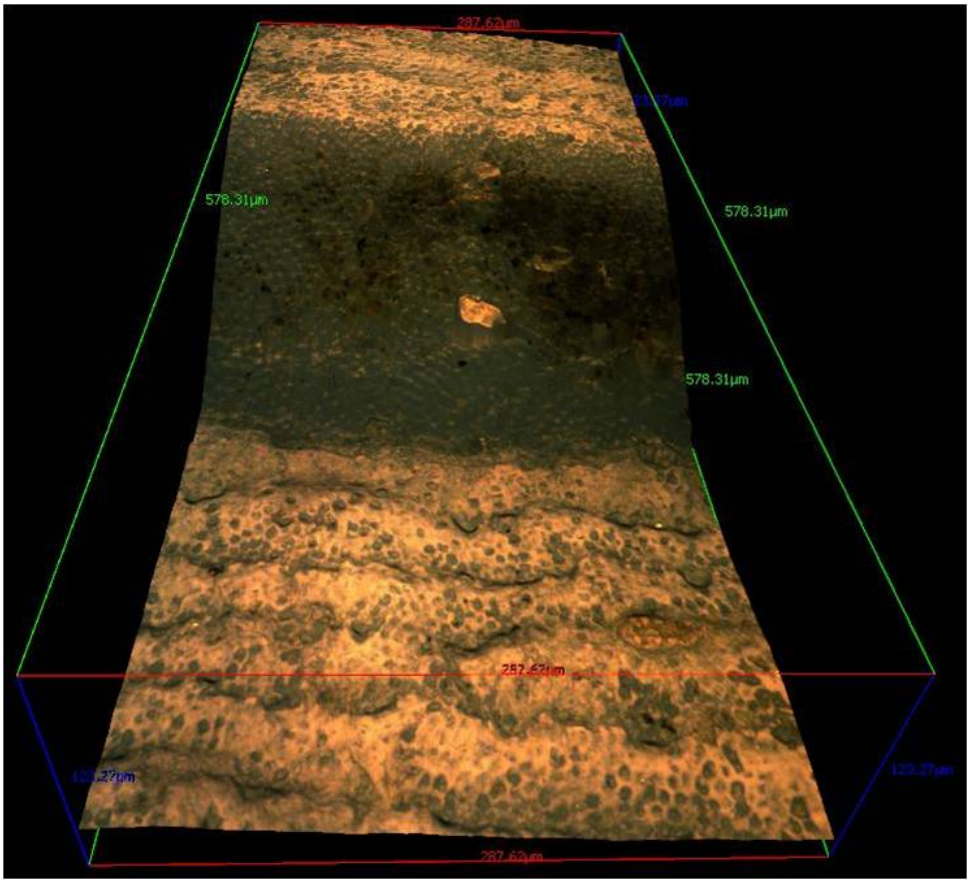

Figure 4.3: 3D image showing perikymata within a furrow-form defect

Pit-type defects vary in size and number, involve single pits or a spread of pits, which are sometimes arranged in bands, and often follow furrow-type defects (Hillson 1996). The

diameter of these pits varies, ranging from around 500μm to 10μm in the pit floor (Hillson and Bond 1997). Whereas furrow-type defects result from entire bands of ameloblasts prematurely stopping matrix secretion, pit-type defects are caused by the early cessation of enamel secretion by clusters (ranging from tens to hundreds) of ameloblasts (Hillson and Bond 1997).

Plane-type defects are extended areas of thinner than normal enamel (Witzel *et al*. 2006, 2008). They are often wedge-shaped and expose large areas of brown striae planes (Hillson 1996). It has been argued that plane-type hypoplastic defects represent more severe disruptions to ameloblast activity than furrow-type defects, but more research is needed to confirm this (Hillson 1996; Witzel *et al.* 2008).

4.1.5. Etiology

More than 100 factors have been linked to enamel hypoplastic defects, both environmental and genetic, and including prenatal, neonatal, or postnatal influences on development (Brook *et al.* 1997, 213; Hall 1989; Kreshover 1960; Suckling *et al.* 1983; Suckling 1989). Pindborg (1982) divided enamel defect aetiology into two categories, namely local and systemic. Similarly, Weinmann and colleagues (1945) and Orban (1957) suggested hereditary, local and systemic causes as the basic aetiological factors related to the appearance of enamel hypoplasia (Dobney 1991; Goodman and Rose 1990; Upex 2009).

Genetic disorders

Some inherited disorders only affect enamel, but other syndromes also affect other parts of the body (Goodman and Rose 1990; Hillson 1996; Pindborg 1982; Witkop 1989). Inherited enamel defects are often grouped under the broader term amelogenesis imperfecta (AI), which includes enamel hypoplasia but also other enamel defects, such as hypocalcification and hypomaturation (Weinmann *et al.* 1945; Witkop 1989). Amelogenesis imperfecta can affect both primary and secondary dentitions (Hillson 1996). Witkop stated that there are more than 70 conditions in which such enamel defects occur (Witkop 1989). Inherited defects are very rare; Witkop (1989) estimated a minimal prevalence of all types of amelogenesis imperfecta (and thus not only limited to hypoplastic defects) of one in 14 000 of 96 471 children examined in different counties in Michigan. Other epidemiological studies have shown similar prevalences of inherited

enamel defects, with hypoplastic defects being the most frequently encountered type of amelogenesis imperfecta (Bäckman and Holm 1986; Sundel and Valentin 1986).

Localised trauma

Disruption to enamel formation can also be caused by a localised impact, in which case only one or possibly two teeth will be affected (Dobney 1991; Goodman and Rose 1990; Hillson 1996). Examples of such local disturbances include trauma, such as a fall or a gunshot wound, electrical or other burns, radiation or localised osteitis (Hillson 1996; Pindborg 1982).

Turner (1912) described a clinical case study in which a child's permanent canine showed evidence of localised enamel hypoplasia as a result of an abscess on the preceding deciduous tooth, a condition subsequently referred to as "Turner's hypoplasia" (Rajendran 2009; Skinner and Hung 1989). Andreasen and Ravn (1973) argued that dental trauma in children under two years of age usually results in a hypoplastic defect on the permanent dentition, whereas in older children (over three years of age), opacities are more commonly found on permanent teeth.

Clinical studies have shown that the appearance of trauma-induced defects is related to the phase of activity of ameloblasts at the time of the injury. For example, Andreasen and colleagues (1971) carried out a detailed study on permanent teeth which had been traumatised during injuries to the primary teeth and found that 24 out of 207 teeth were affected by discolorations and linear enamel hypoplasia. In a follow-up study, they found that the appearance of defects was related to the age of the patient at the time of the injury as well as the type of injury sustained in the primary dentition (Andreasen and Ravn 1971). Similarly, Skinner and Hung (1989) carried out a histological study of deciduous teeth from kindergarten-aged children in Vancouver and found that 2.4% of 1350 children examined were affected by localised hypoplasia on deciduous teeth. They noted that the common age at occurrence of this defect on deciduous canines was around 6 months, indicating that it is likely to be caused by minor oral trauma among infants learning to handle and mouth objects. This pattern has also been confirmed by experimental studies on animals. Suckling and Cutress (1977) carried out an experimental study, damaging the developing permanent left central incisor of 18 sheep with a sharp instrument after surgical exposure and found that 14 out of 18 left teeth showed a dental defect, as opposed to the 18 normal permanent right central incisors. In a more detailed follow-up study, Suckling and Purdell-Lewis (1982) found that the severity of the injury also affected the appearance of the lesions.

Systemic disturbances

Metabolic growth disturbances resulting from diseases, malnutrition and toxicity, can be differentiated from local trauma using developmental schedules of teeth. Whereas trauma only affects isolated teeth, metabolic disturbances stand out because of their symmetry: they are apparent in all teeth which are developing at the time these disturbances occur (Hillson 1992; Hillson 1996).

Disease

Congenital syphilis has often been linked to the appearance of enamel defects, as the latter are often considered as classical stigmata of this condition (Hillson 1996; Hillson *et al.* 1998; Hutchinson 1861; Zsygmondi 1893). Distinctive changes in tooth morphology related to this condition include defects on permanent upper central incisors (Hutchinson's incisors) and first permanent molars, also called Moon's molars and Mulberry molars (Hillson 1996; Jacobi *et al.* 1992). Hutchinson's incisors, which can be recognised by their short and narrow morphology and a distinctive deep vertical notch resulting from the undeveloped middle mamelon, are found in 10-60% of syphilis patients (Hillson 1996; Hutchinson 1861; Jacobi *et al.* 1992). Molars are affected in up to 60% of congenital syphilis cases and include Mulberry molars (Fig. 4.4), with plane-formed defects around the cusps and Moon's molars, which are irregularly shaped and narrower, shorter and more dome-shaped than other molars (Hillson 1996; Hillson *et al.* 1998; Jacobi *et al.* 1992). The relationship between these classical stigmata of congenital syphilis and the wider range of enamel hypoplasia is still debated, but Hillson and colleagues (1998) suggested that, in contrast to Mulberry molars, which show characteristics overlapping with other plane-formed hypoplastic defects, Hutchinson's incisors and Moon's molars show defects very unlike other hypoplastic defects and should therefore be considered pathognomonic of congenital syphilis.

Figure 4.4: Four molars, from individual with congenital syphilis. Known as mulberry molars for the distinctive appearance of the deformity, including large nodule-like structures (specimen RCSOM/D 33.633 from Royal College of Surgeons of England, Photo: Carr J. For a detailed description of this specimen see Hillson *et al.* 1998)

Early reports on enamel hypoplasia suggested a link between enamel defects and certain other diseases such as rickets, tetanus, syphilis, smallpox, anemia, typhoid, pneumonia, tuberculosis, measles, whooping cough, chickenpox, scarlet fever, eclampsia and diphtheria (Black 1908; Bunon 1743; Fauchard 1746; Gottlieb 1920; Kassowitz 1924; Magitot 1881; Marshall 1936). Other types of metabolic disturbances influencing the occurrence of furrow-form enamel hypoplasia include childhood fever and low birth weight and brain injuries at birth (Boyde 1970; Jackson 1961; Willson and Cleaton-Jones 1978).

Some researchers consider low birth weight and brain injuries at birth as especially related to defects on deciduous teeth (Brook *et al.* 1997; Fearne *et al.* 1994; Hall 1989; Lewis and Roberts 1997; Seow 1992). However, published reports do not show a strong correlation between low birth weight and linear enamel hypoplasia. For example, Sweeney and colleagues (1969) studied the deciduous maxillary incisors of children aged two to three years old from Guatemala together with their medical history from birth. In comparison to the children without lesions, the 31 children with enamel defects showed no statistically significant difference in birth weight. They were, however, significantly more affected by infectious diseases (such as diarrhoea, thrush and stomatitis) during the first 35 days of life than the children without linear enamel hypoplasia (Sweeney *et al.* 1969).

Sarnat and Schour (1941, 1942), cross-matching enamel defects with the medical history of sixty patients, found possible correlations between the occurrence of enamel hypoplasia and some episodes of convulsions, chicken pox, measles, pneumonia and whooping cough. However, they also found that other instances were questionable or could not be supported. This might be related to the methodology used in terms of age estimation (for a discussion of this, see p. 127) as well as the non-specific nature of enamel hypoplasia. Similarly, as far back as the mid-eighteenth century, Bunon (1743, 58) stated that enamel hypoplasia cannot be linked to specific diseases, but that instead, it is merely one of the possible outcomes of these conditions.

Malnutrition

Despite little being known of the relative sensitivity of hard tissues to changes in nutritional status, the causal link between poor nutrition and enamel hypoplasia has been thoroughly explored, both by lab experiments and clinical and epidemiological studies (May *et al.* 1993).

Animal experiments carried out by Mellanby (1930, 1941) have linked enamel hypoplasia with the diets eaten by animals (mainly beagle dogs and rats) during their development. Specifically, Mellanby (1941) found a correlation between vitamin D deficiencies and the occurrence of enamel hypoplasia. Calorie, protein and mineral deficiencies have also been studied in relation to enamel hypoplasia, with varying results (May *et al*. 1993; Pindborg 1970). For example, Glick and Rowe (1981) studied 276 rat incisors with induced protein deficiency and found no macro-or microscopic evidence of enamel hypoplasia. Similarly, Paynter and Grainger (1956) found no significant differences in the macroscopic appearance of enamel hypoplasia on the upper first molars of weanling rats whose mothers were fed a vitamin A deficient diet as opposed to other, sufficiently fed rats.

Similarly, epidemiological studies, mainly carried out in developing countries, have produced contrasting results. Nikiforuk and Fraser (1981) conducted a 25 year study of the effect of calcium and phosphate deficiencies on the primary dentitions of children (N=56) using clinical, radiographic and histological information. They found a clear correlation between the clinical diagnosis of hypocalcaemia (low serum calcium levels in the blood) and linear enamel hypoplasia, but not between enamel defects and plasma phosphate concentrations. In addition, Zhou and Corruccini (1998) analysed the effect of the Great Chinese famine (1959-1961) and found significantly higher levels of enamel hypoplasia in teeth developed under famine stress compared to teeth from individuals with a better nutritional status. In contrast, in their 1969 study, Sweeney and colleagues found no statistically significant correlation between enamel hypoplasia and vitamin A levels from the umbilical cord cold-blood serum.

Goodman and colleagues (1987), in their study on enamel hypoplasia prevalence in rural Mexico, linked the high prevalence (46.7%) of this condition in the permanent and deciduous dentition to the poor nutritional status of their subjects. In a further Mexican study, analysing enamel hypoplasia prevalences in adolescents who were given daily nutritional supplements since birth (N=42) and non-supplemented individuals (N=42), they found that non-supplemented individuals were twice as likely to exhibit furrow-form defects on permanent teeth as supplemented ones (Goodman *et al*. 1989). Similar results were found in a later nutritional supplementation study in rural Guatemala (May *et al.* 1993). Goodman and colleagues (1989) argued that enamel hypoplasia seemed to be sensitive to variations in nutrient intake from around 1200kJ per day. In contrast, Infante and Gillespie (1974), in their study of 429 Guatemalan children aged three to 83 months, did not find any correlation between the availability of protein supplements to mothers and

children and the prevalence of enamel hypoplasia on the deciduous dentition. However, they argued that this is not necessarily evidence against the association between enamel defects and malnutrition, as it is possible that the protein supplement was used as a substitute rather than a supplement.

Parasitic infections have also been suggested to have a causal link with enamel hypoplasia. Suckling and colleagues (1983, 1986) have carried out various experimental studies, inducing intestinal parasites on sheep. They infected 34 sheep with nematode parasites during the formation of the central incisors and found hypoplastic lesions corresponding to this time of development, indicating the infection's interference with ameloblast activity (Suckling *et al.* 1983).

Toxicity

A number of researchers have suggested that concentrations of fluorine from and above 1ppm may interact with the cellular processes during the secretion of enamel matrix (Fejerskov *et al.* 1977; Hillson 1996; Suckling and Thurley 1984). The exact mechanisms of this interaction are still not well understood, but some researchers have argued that the amount of smaller-sized fluorapatite unit cells in relation to the larger-sized hydroxyapatite cells might have an effect on crystal growth during the secretion and maturation stages of enamel formation (Fejerskov *et al.* 1977; Kierdorf *et al.* 2004).

The effect of high concentrations of fluoride on enamel maturation is often referred to as "mottled enamel", an enamel defect which shows a spectrum of pathological changes and thus varies in appearance, ranging from discoloration ("spotted enamel" and opaque areas), pitting and brownish staining between pits to a corroded appearance, with an extensive loss of surface enamel (Dean 1934; Fejerskov *et al.* 1977; Rajendran 2009; Suckling and Thurley 1984). Black and McKay (1916), in their histological study of teeth from the Rocky Mountains region, argued that "mottled enamel", also referred to as "endemic white enamel", can be identified histologically by "browning" in the spaces between the enamel rods and the "absence of cementing substance" between these rods. According to Hillson (2014), mottled enamel is not enamel hypoplasia, even though the appearance of mottled enamel may be similar to a hypoplastic defect.

Socio-economic status

Sweeney and colleagues (1971) argued that enamel hypoplasia is very closely related to socio-economic status, as it is most often found in the lower socio-economic classes. In

their epidemiological study of 2015 Nigerian schoolchildren aged 4-16 years old, Orenuga and Odukoya (2010) found a prevalence of 11.22% in enamel defects, of which enamel hypoplasia was the most frequently encountered condition. They link this condition with poor socio-economic status. Similarly, in a cross-sectional study carried out over a period of 2 years, studying dentitions of 872 Nigerian schoolchildren aged zero to seven years, Enwonu (1973) also linked the appearance of enamel hypoplasia on deciduous teeth with low socio-economic status.

Dobney (1991), in his study on 2082 children from middle schools in the Bradford area, found no correlation between socio-economic status and the frequency of enamel hypoplasia (based on the index proposed by the Fédération Dentaire Internationale, described below p. 117). Interestingly he identified significant differences in the pattern of furrow-form enamel hypoplasia between ethnic groups, with white schoolchildren showing significantly higher frequencies than Asian children (Dobney 1991). These results indicate the difficulties in interpretation related to hypoplasia studies in terms of determining socio-economic status, as the latter can interact with other social factors such as ethnicity and sex (Braveman *et al.* 2005).

The main problem related to linking socio-economic status to enamel hypoplasia is the fact that socio-economic status or social class is a multidimensional variable and as such, it can operate at different levels, including individual, household or neighbourhood levels (Braveman *et al*. 2005). Goodman and colleagues (1992) studied the association between socio-economic status and linear enamel hypoplasias in five to 15 year olds from various villages in the Solis valley, in the Mexican Highlands at the household level. They measured socio-economic status using household characteristics such as type of walls, flooring and roof and number of rooms, as well as signs of material wealth in terms of ownership of chickens and other animals (Goodman *et al.* 1992). They found consistently lower socio-economic means in those individuals with furrow-form enamel hypoplasia, but it is possible that by using different variables, such as total house size, this decrease might be less consistent (Braveman *et al*. 2005).

4.1.6. Enamel hypoplasia and “noise”

The inherent problems related to the lack of independent variables to measure socio-economic status can be seen as a general problem related to the etiology of enamel

hypoplasia as well. Firstly, it is important to note that many enamel hypoplasia studies are derived from individual case histories rather than large longitudinal samples, which makes it difficult to make generalised conclusions. However, even in the case of longitudinal studies, attributing the appearance of enamel defects to a specific cause, is very difficult, as the nature and extent of the defects are affected by factors such as the severity and duration of the insult, the developmental stage of the tooth and the individual-specific response to the injury, including the vulnerability of the individual (Brook *et al.* 1997; Neiburger 1990).

Living populations consist of an unknown mixture of individuals who vary in their susceptibility to disease and death (Wood *et al.* 1992). This variation has been noted early on in the study of enamel hypoplasia: Magitot (1881) warned that "*certain differences* [in the manifestation of defects] *exist between the examined subjects, their disposition and the type of disease they have been affected with* [page 130 my translation]. The individuality of response, both in terms of biological and social variation, is an important factor when growth disturbances are interpreted in terms of health of a community as a whole (Bush 1991). For example, some individuals might appear to have a prolonged and good health, but at the same time experience physical, financial and emotional deprivation, while others succumb to repeated illness despite living in what would seem to be extremely favourable circumstances.

The age of the individual also has an influence on the type and extent of the response to growth disruptions. For example, Sarnat and Schour (1941) and Pindborg (1970) argued that a peak in furrow-form defects on permanent first molars, incisors (except the upper lateral incisors) and canines is most likely to occur in early infancy, during the first year of life. This early infancy peak might be related to neonatal complications or congenital problems (Goodman 1988). Goodman (1988), in his study of the Hamann-Todd skeletal collection, found that in this industrial population from the greater Cleveland area, with individuals born between 1855 and 1913, the peak in enamel defects occurred slightly later, after 1.5 years. He linked this peak to an increased vulnerability, with weaning as one of a series of potential nutritional, immunological and socio-economic factors influencing the health of children between these particular ages (Goodman 1988). This issue of susceptibility and age is problematic, as estimations of the timing of furrow-form enamel hypoplasia and the related defect peaks are confounded by the use of different approaches to ageing based on dental development. These are further described below (p. 127).

In addition to individual susceptibility to diseases, sex differences may also influence responses to diseases or other growth disruptions. More specifically, some researchers have argued that there may be a sexually dependent response to growth disturbances as females may be better buffered against environmental influences (Gawlikowska-Sroka *et al.* 2013). Guatelli-Steinberg and Lucaks (1999) have carried out an extensive review of the potential etiological factors contributing to possible sex differences in the expression of enamel hypoplasia. They found no consistent evidence in favour of female buffering or male vulnerability in human, skeletal and non-human primate samples and argued that a more complex set of interacting factors affects the population distribution of enamel defects, including cultural (such as biases in child rearing practices) influences (Guatelli-Steinberg and Lucaks 1999).

It is also possible that not only one single, but multiple etiological factors may influence the expression of enamel hypoplasia (Seow 1997). For example, Sweeney and colleagues (1969, 1971) highlighted the interrelationship of low socio-economic status, protein-calorie malnutrition and infections as blurring the potential of a clear etiology of furrow-form enamel hypoplasia.

To conclude, as Zhou and Corruccini (1998, 724) wrote, "*the information content of hypoplasias as pathologies is mixed with variable amounts of ''background noise'' in given populations.*" Although the specific etiology of identified patterns of enamel hypoplasia is likely to remain obscure and caution is clearly appropriate in any interpretation of patterns of enamel hypoplasia, the study of these patterns and can still give us an indication of growth disturbances in past and present populations and has often been used in bioarchaeology (also see Goodman 1991; Ogilvie and Trinkaus 1990).

4.1.7. Enamel hypoplasia and bioarchaeology

Case studies

The earliest archaeological applications of studies of furrow-form enamel hypoplasia were individual case studies, used to support or illustrate medical reports. For example, Magitot (1881) made use of archaeological material to demonstrate his identification of *les érosions dentaires*. In his article, next to a wealth of case studies reported by various dentists, and including the name, sex, clinical history and morphology and severity of the

érosions on the teeth of living patients, he included a Gallo-Roman merovingian jaw found at the Breny cemetery in Aisne and teeth found at the dolmen by Lozère (Magitot 1881).

Other early archaeological studies of enamel hypoplasia were generally carried out in relation to caries (Brothwell 1959). For example, Bodecker (1930, 313) wrote about "*flaws in the protective covering of teeth*" from American Pueblo Indians (1100 AD, New Mexico) to try and disprove that these defects are of modern origin and have an effect on caries prevalence. Hartweg (1945) undertook a large-scale study of teeth from different regions and time periods (Massif Central, Bassin Parisien, Western, Southwestern, Eastern and Mediterranean) in France, in which he mainly focused on caries, but briefly mentioned "rare instances" of furrow-form enamel hypoplasia.

Soggnaes (1955, 1956) was one of the first researchers to carry out a large histological and macroscopic bioarchaeological study looking at enamel defects. More specifically, he compared postmortem changes, developmental disturbances and post-formative defects on teeth from the Palaeolithic to recent times from archaeological sites in Mount Carmel (Palaeolithic sites of Skhul and Tabun), Medieval Norway, Iceland, Central America, Predynastic Egyptian (Keneh) and Prehistoric Greece. In relation to the surface structure, he differentiated between full-fledged gross hypoplasia and minor grooves and pits. For a limited sample (Prehistoric Greece), he compared the number of defects, calculated by dividing the number of teeth with defects by the total number of teeth, between the different time periods. More specific archaeological analyses of enamel hypoplasia followed, including Falin's (1961) histological study of Neolithic, Mesolithic and Bronze Age dentitions from Dniepropetrovsk, Ukraine.

Enamel hypoplasia and past human and animal populations

In terms of types of hypoplasia studied in an archaeological context, only one case study of hereditary enamel hypoplasia has been reported. Cook (1980) noted pitting, wrinkling and exposed dentine in the deciduous and permanent dentition of a six-year old child found at the Schild cemetery in Illinois, 1100 AD. Localised trauma has also been identified in archaeological populations: Goodman and Rose (1990) mentioned one example of "severe" enamel hypoplasia on a permanent upper central incisor which could not be matched with other teeth within the same dentition. Skinner (1986) gives examples of localised enamel hypoplasia on deciduous teeth from a range of Palaeolithic and Neolithic sites, including Krapina, Bruniquel and She Gabi. Apart from these limited

archaeological examples of hereditary enamel hypoplasia and localised trauma, most bioarchaeological studies have focused on the causal relationship between metabolic and dental disturbances.

Swärdstedt (1966) was one of the first researchers to link dental growth disturbances in past populations to ancient standards of health. He suggested that "*the occurrence of hypoplasias can be taken as a kind of criterion of the standard of living (the more hypoplasias, the poorer the standard)*" (Swärdstedt 1966, 11). He studied dentitions from a Medieval Swedish population both macroscopically and histologically in order to compare social groups.

In the 1980s, there was an increase in research on the adaptive response by the human organism as evidenced by dental and skeletal features, commonly referred to as "*indicators of stress*" in biological anthropology and bioarchaeology (Bush 1991; Goodman *et al.* 1988). The Selyean definition of stress as a non-specific response to stimuli was seen as a good basis to model stress and general biological and social adaptations in prehistoric populations. Studies of enamel defects, which were previously limited to clinical studies, fitted well within this framework of bioarchaeological research, as enamel hypoplasia was considered a good indicator of a variety of factors which might disrupt growth, including generalised nutritional deficiency (Bush 1991; Goodman *et al.* 1988; Huss-Ashmore *et al.* 1982; Rose *et al.* 1985). In addition, teeth preserve well archaeologically and are easily recovered (Cook 1981; Goodman *et al.* 1988).

The first analyses of enamel defects conducted within this bioarchaeological framework focused on the frequency, chronological distribution and histological characteristics of enamel hypoplasia on individuals from the prehistoric site of Dickson and Pete Klunk mounds in Illinois; Middle Mississipian cemeteries; prehistoric Native American California, and ancient Nubia and Egypt (Black 1979; Cook 1981; Goodman *et al*. 1980; Goodman *et al*. 1984a, b; Goodman and Armelagos 1985a, b; Rose 1977; Rose *et al*. 1978; Rudney 1983; Schultz and McHenry 1975) and were soon followed by studies worldwide.

Some studies have been carried out on deciduous teeth (Duray 1990; Sciulli 1977; Oyamada *et al.* 2008), but the majority of research papers have looked at the appearance of enamel hypoplasia on permanent teeth. They include anthropological investigations into differences in expression of enamel defects between: males and females

(Berbesque and Doran 2008; Guatelli-Steinberg and Lukacs 1999; King *et al.* 2005; Oyamada *et al.* 2012; Palubeckaité *et al*. 2002; Saunders and Keenleyside 1999) and the differences between early hominins, including australopithecines, early *Homo*, Neanderthals and anatomically modern humans (Lacruz *et al.* 2005; Guatelli-Steinberg 2003; Guatelli-Steinberg *et al*. 2004; Guatelli-Steinberg *et al*. 2011; Ogilvie *et al*. 1989).

Other bioarchaeological studies of enamel defects have been undertaken to examine the relationship between patterns of enamel hypoplasia and mortality (Ferrell 2006; Goodman and Armelagos 1988; Jennings 2010; Mittler *et al.* 1992; Palubeckaité *et al.* 2002; Steckel 2005) and to identify cultural differences in health between individuals within a population, specifically in relation to weaning (Blakey *et al*. 1994; Corruccini *et al*. 1985; Goodman and Rose 1990; Lanphear 1990; Moggi-Cecchi *et al*. 1994) and social status (Craig and Buckberry 2010; Mayes and Barber 2008; Miszkiewicz 2012; Palubeckaité *et al*. 2002; Robb *et al.* 2001). Hypoplasia patterns have also been compared between different populations within one region (Dabbs 2011; King *et al*. 2005; Mitchell 2006), in different geographical regions (Garcín *et al.* 2010; Oyamada *et al*. 2010; Temple 2008, 2010) and different time periods (Cucina 2002; Goodman *et al.* 1984a, b; Skinner 1996; Šlaus 2008; Tomczyk *et al*. 2012).

A recurrent theme in bioarchaeological studies of enamel hypoplasia is the focus on cultural transitions, especially the transition from a hunter-gatherer subsistence to agriculture in areas such as Ecuador (Ubelaker 1984), the Near East (Larsen 1995; Smith *et al*. 1984), Nubia (Starling and Stock 2007) and Europe (Formicola 1987; Lillie 1996; Meiklejohn and Zvelebil 1991), as well as increased levels of (maize) cultivation in the US (Goodman *et al.* 1980) and the influence of the arrival of Europeans in the New World (Hutchinson and Larsen 1988; Wright 1990).

A large number of studies have looked at enamel hypoplasia patterns in great apes and monkeys, mainly to analyse: differences between species (Hannibal and Guatelli-Steinberg 2005; Guatelli-Steinberg 2001; Guatelli-Steinberg and Skinner 2000; Newell *et al*. 2006; Skinner 1986); the appearance of enamel hypoplasia in fossil teeth (cattarhines – Lukacs 2001); the influence of seasonality (Guatelli-Steinberg and Skinner 2000; Kelley and Bulicek 2000; Macho 2008; Skinner 1986, 2000; Skinner *et al.* 1995; Skinner and Hopwood 2004; Skinner and Pruetz 2012; Skinner *et al*. 2012); weaning (Dirks 1998), and environmental factors such as differences between habitat (Chollet and Teaford 2008) and regular and irregular provisioning in captive monkeys (Guatelli-Steinberg and Benderlioglu 2006).

In comparison to humans and other primates, a smaller number of studies have been carried out on other animal teeth (Colyer 1936, 1947), including studies on fossils such as Miocene rhinoceros (Mead 1999) and Pliocene giraffids (Franz-Odendaal *et al*. 2003, 2004). Patterns of enamel hypoplasia have also been compared between wild and captive species, including giraffes (Franz-Odendaal 2004) and bison (Byerly 2007; Niven *et al.* 2004). Dobney and colleagues have looked at differences between patterns of hypoplasia between domesticated and wild *Sus scrofa* (pig and boar) populations in Neolithic Turkey, central and northern Europe, south-west Asia, China and Japan and found enamel hypoplasia frequencies in archaeological domestic pigs generally higher than in their recent wild counterparts (Dobney *et al.* 2004; Dobney *et al.* 2007; Ervynck *et al.* 2001). Other studies have identified the effect of different husbandry practices based on enamel hypoplasia studies in pigs and sheep (Bertini 2011; Ervynck and Dobney 1999; Upex 2009).

4.1.8. Recording furrow-form enamel hypoplasia

Despite furrow-form enamel hypoplasia being defined as a quantitative defect, as opposed to qualitative defects such as a change in colour or opacity of enamel (Goodman and Rose 1990), its identification is most often based on a qualitative, visual identification. Various attempts have been made to provide a rational method of classifying and measuring levels of enamel defects, including macroscopic and microscopic approaches and these are outlined below.

Macroscopic identification

The most commonly used method for the recording of enamel hypoplasia is the index produced by the *Fédération Dentaire Internationale* in 1982, which was slightly modified in 1992 (DDE index). In this index, hypoplasia is classified as a defect, along with opacity and discoloration, and listed as occurring in the form of pits, grooves (horizontal or vertical) or missing enamel. The index also recommends the recording of the number (single or multiple) and location (gingival one half, incisal one half, occlusal or cuspal) of enamel defects. Hypoplasia is defined as "*a quantitative defect of enamel visually and morphologically identified as involving the surface of the enamel (an external defect) and associated with a reduced thickness of enamel* (FDI Commission on Oral Health 1982, 160). It is indicated that this defect may occur as:

a. shallow or deep pits or rows of pits arranged horizontally in a linear fashion across the tooth surface or generally distributed over the whole or part of the enamel surface

b. small/large, wide/narrow grooves

c. partial/complete absence of enamel over small/considerable areas of dentine

The index provides a chart to aid the recording of the defects, where the teeth involved, the type, number and location can be recorded. In terms of methods for recording the defects, both photography and direct visual examination (cleaned surfaces, under natural or artificial light and using a probe) are recommended. The DDE index is also widely used in anthropology (Griffin and Donlon 2009; Keenleyside 2008; Kozak and Krenz-Niedbała 2002; Littleton and Townsend 2005; Lovell and Dawson 2003; Malville 1997; Starling and Stock 2007).

Goodman and Rose (1990) argued that the method has various shortcomings, including limitations in assessing pit-formed enamel hypoplasia (it does not distinguish between single and multiple pits and between a linear and random arrangement), the lack of a standardised way of assessing the size, depth and width of defects, as well as the lack of a minimum criterion for defects. For those reasons, some researchers have slightly modified this index (Clarkson and O'Mullane 1989; Dobney 1991). For example, in his study of enamel defect presence within dentitions of Bradford schoolchildren, Dobney (1991) applied a slightly modified DDE recording method, specifying the number of defects rather than ticking "multiple" occurrences and the crown surface and also dividing the crown surface into thirds in order to establish the location of defects rather than just using gingival and incisal halves. Dobney (1991) divided the grades of severity into four categories: slight, mild (clearly visible, affecting <10% of zone 1, 2 or 3), severe (affecting >10% but <30% of zone 1, 2 or 3) and gross (affecting >30% of zone 1, 2 or 3).

Similarly to Dobney (1991), the Institute of Field Archaeologists/British Association for Biological Anthropology and Osteology guidelines (Roberts and Connell 2004) and London's Osteology Method Statement (Kausmally 2008), also recommended a division of the crown into three zones (cusp, middle and lower), but, in contrast to Dobney (1991), both guidelines mentioned only three divisions of severity (1 = just discernible line, 2 = clear groove, 3 = gross defects). Three divisions of severity were also used in the data collection codebook for the Global history of health project (Steckel *et al*. 2006). However,

Steckel and colleagues (2006) proposed different degrees of severity, with the first division referring to “no hypoplastic lines”, the second to “one hypoplastic line (felt with fingernail) and the third to “two or more hypoplastic lines”.

The different approaches to the recording of the “severity of defects” represent varying ideas about the minimum threshold of defect identification. Danforth and colleagues (1993) studied inter and intra-observer differences in the scoring of furrow-form linear hypoplasia and found great differences in the identification of defects. In their study, they compared observations on 59 teeth (canines and incisors) carried out by three individuals. In about 25% of the comparisons, one observer scored a tooth as hypoplasia free, whereas the other observer scored the same tooth as having hypoplasia episodes present. As most of the hypoplasia episodes were very slight, Danforth and colleagues (1993) stressed the need to put forward a minimum threshold of enamel hypoplasia determination.

In terms of this minimum threshold, Goodman and Rose (1990) suggested that defects which are only visible under high magnification are too small to be reliably recorded and should therefore not be interpreted as “true hypoplasia”. Similarly, Pindborg (1970, 88) defined enamel hypoplasia as “*any disturbance in tooth formation associated with* ***macroscopic*** *defects in the surface of enamel*”. However, Hillson and Bond (1997) argued that, as enamel hypoplasia is related to disturbances at the level of cells forming the enamel matrix, this type of enamel defect can only be understood clearly in relation to the layered growth structures of each tooth on which a defect appears. In addition, they noted that, for anthropologists, the main aim in most hypoplasia studies is to estimate the time and duration of these enamel growth disturbances and microscopy therefore provides a way to analyse enamel defects against the highly detailed background of the layered crown growth (Hillson and Bond 1997).

Microscopic identification

Pickerill (1913) developed various techniques to analyse microscopic structures on the crown surface. One method was to rub the crown’s surface with fine graphite and to examine the result by microscope and reflected light. Using this method, perikymata can be visualised as “*fine black bands running round the surface of all teeth*” as depressions on the crown surface retain graphite and the elevations remain white (Mellanby 1927, 740; Pickerill 1913).

Another method proposed by Pickerill, was the so-called “Odontograph”, defined as “*a needle on a lever, the point of which impinges upon the surface of the tooth to be examined*.” (Pickerill 1914, 82). The elevations and depressions on the enamel surface cause the needle to rise or fall and as such these oscillations are recorded on paper and the instruments records “imbrications lines” (Pickerill 1914, 83). Pickerill applied this method to various dentitions from *Fijians, Australian aborigines, Maoris, Morioris, Rarotongans, inhabitants of New Guinea and New Hebrides, Chinese, Mexicans, Anglo-Saxons* and others and found that all the studied specimens showed these “imbricational lines” on the enamel surface. Similarly, Eisenberg (1938, 222) studied the surface of enamel microscopically with a binocular microscope at 30x to 750x magnification and described perikymata as “ripple marks”. He defined these as “a wave which reaches a more or less sharp crest with the crest break directed toward the neck of the tooth, the distance between these crests ranging between 30-50 micrometers and at a depth of 5-10 micrometers.

With the exception of Pickerill (1914) and Eisenberg (1938), little was written about the properties of the microstructure of the external enamel surface until the advance of replication techniques in the 1940s, which circumvented imaging problems related to the reflectivity of the enamel (Beynon 1987; Hillson 1992; Scott and Wyckopf 1946, 1949; Scott 1952). In the 1940s, Scott and Wyckopf (1949) used optical and electron microscopy to study metal-shadowed collodion (nitrocellulose) replicas of enamel surfaces and were able to observe both normal patterns of perikymata and bands of irregularly shaped depressions. They also found that the loss of surface structure was greater on labial, buccal and lingual surfaces as opposed to proximal surfaces and that the enamel loss was more advanced in incisors in contrast to molars (Scott and Wyckopf 1949).

Since the introduction of replication techniques, various microscopic methods have been applied to the visualisation of perikymata and the identification of furrow-form enamel hypoplasia, including the use of a low-powered stereomicroscope (Bullion 1987), phase-contrast microscope (Grimbert and Pigeat 1961), a scannning electron microscope (Antoine *et al.* 2009a; Beynon 1987; Dean 2010; Guatelli-Steinberg *et al*. 2004; Hassett 2011; King *et al.* 2002, 2005; Newman and Poole 1974; Risnes 1998; Witzel *et al.* 2008), optical profilometry (Elhechmi 2010; Elhechmi *et al.* 2013; Hillson and Jones 1989; Hillson 1992; King *et al*. 2002, 2005; Temple *et al*. 2012, 2013) and confocal scanning microscopy (Bromage *et al*. 2007).

Hillson and Jones (1989) developed two methods to construct crown surface profiles, a stylus and an application with a measuring microscope. The stylus worked in a similar way to Pickerill's odontograph: a replica of a tooth crown is mounted on a stage and the profiler instrument on which a stylus is fitted, runs over the crown surface as the stage is moved and logs coordinates for each part of the crown's profile. By applying a filter to reduce mechanical noise, the main features of the crown profile can be reproduced, including minor dips (perikymata) and major troughs (hypoplastic defects).

A second method developed by Hillson and Jones (1989) is the use of a measuring microscope, in which a mechanical stage allows the measurement along the horizontal plane and a mechanical depth gauge fitted to the microscope's focusing mechanism measures along the vertical plane (Hillson and Jones 1989). When the transects cuts the deepest point in the perikyma groove, a push-button operated switch allows a reading to be taken and the position coordinates of each point down the surface of the crown can be used to construct a crown surface profile (Hillson and Jones 1989; Hillson 1992).

Using a measuring microscope, depressions in the enamel surface can also be matched with wider perikyma spacings on perikyma spacing profiles, as the coordinates of recorded points can be converted into distances between perikymata, providing a linear measurement (in microns or mm) between two perikyma grooves (Hillson 1992; King *et al.* 2002, 2005; Temple *et al.* 2012, 2013). A similar method is the combined use of an SEM and measuring software (such as ImageJ) providing "digital callipers" (Guatelli-Steinberg 2003; Newell *et al.* 2006). More recently, the use of 3D imaging has added to the body of research related to dental growth studies by providing high-resolution images which can be analysed in much more detail than previous studies (Bocaege *et al*. 2010; Colombo *et al*. 2013; Elhechmi 2010; Elhechmi *et al*. 2013; Smith and Tafforeau 2008).

By comparing the perikyma groove spacing to the underlying trend along the crown surface, irregularities in perikymata spacing can be detected and a wider than expected spacing between consecutive pairs of perikymata can be used as a threshold to identify the occurrence of furrow-form enamel hypoplasia, if this spacing anomaly can be cross-matched between teeth with overlapping developmental schedules (Guatelli-Steinberg 2004; Hassett 2011; Hillson and Bond 1997; King *et al*. 2002, 2005; Newell *et al*. 2006; Temple *et al*. 2012, 2013; Witzel *et al*. 2008).

4.1.9. Interpreting furrow-form enamel hypoplasia

The following section discusses the problems and issues surrounding the interpretation of furrow-form enamel hypoplasia. Three of these (missing teeth, different levels of recording and ageing) relate to practical issues, whereas others describe and assess the theoretical discussions related to the study of enamel growth disturbances in bioarchaeology, including the deduction of health from bioarchaeogical analyses and the concept of stress.

Different levels of recording

One particular complication related to the interpretation of furrow-form enamel hypoplasia relates to the difficulty in comparing the occurrence of enamel defects between archaeological sites, as there is a lack of consistency in the recording and interpretation of defects.

Hassett (2011) argued that the scale of observation (macroscopic or microscopic) is an important source of variation in enamel hypoplasia studies. For example, she suggested that macroscopic identification (with the naked eye or low-powered microscopy), which is the standard method of observation of enamel defects (Buikstra and Ubelaker 1994; Kausmally 2008; Roberts and Connell 2004; Steckel *et al.* 2006), is likely to result in the under-recording of defects in the cervical region of the tooth crown (Hassett 2011).

In addition to the differences in identification techniques, different techniques are also employed to interpret the identified defects. For example, some reports record the presence of furrow-form enamel hypoplasia at a specific site either per individual or dentition (PPNB site of Tell Ain el-Kerkh: see Hudson *et al.* 2003; PPNB site of Yiftahel: see Hershkovitz *et al.* 1986), per tooth (Romano-British Poundbury: see Brook and Smith 2006; PPNB site of Wadi Shuieib: see Al-abassi and Sarie 1997) or per tooth type (Neolithic Çatalhöyük: see Boz 2005). Comparing prevalence per tooth with prevalence per tooth type is difficult, as the identification of defects on single teeth may include unmatched defects, which have a different etiology (localised trauma) than matched defects on two or more teeth (metabolic disturbances). In addition, comparing rates per tooth type with rates per dentition are also difficult, as the number of defects per dentition is likely to be higher, with more teeth available for analysis and matching.

Limiting studies to the presence or absence of defects is likely to underestimate defect frequency, as the entire dentition might be affected by more than one defect. Another way of interpreting enamel defects is to calculate the number of defects. For example, Brothwell (1963) reported on the frequency of hypoplastic defects in Upper Palaeolithic and Mesolithic assemblages and calculated the number of none, slight, medium and marked defects per individual as a percentage of the total number of individuals under study. In contrast, Berbesque and Doran (2008) limited their calculation to defect counts per individual and did not distinguish between defect characteristics (slight, medium or marked). Other frequency calculations divided the number of teeth with at least one defect by the total number of observed teeth or take the number of individuals with at least one defect present as a percentage of the total number of individuals with teeth available for analysis (Temple 2010). It is doubtful that the comparison of these differently calculated frequencies can provide meaningful insights into the health of past populations.

Potential comparisons may also be biased by limiting the reporting of furrow-form enamel hypoplasia to the number of matched defects, as some individuals might display a high frequency of short duration defects and others a low frequency of long duration defects (King *et al*. 2005; Temple *et al*. 2013). Additional variables have also been included in some hypoplasia studies, such as the duration of defects, the interval between defects and the percentage of growth affected by defects (Ensor and Irish 1995; Guatelli-Steinberg *et al.* 2004; Hubbard *et al.* 2008; King *et al.* 2002, 2005; Temple *et al*. 2012, 2013).

Missing teeth and tooth types as a source of variation

Missing teeth

The problem of lost teeth and abrasion of tooth crowns in relation to the interpretation of enamel hypoplasia frequencies was noted very early on in the history of this subject (Swärdstedt 1966). The resulting decreased sample size can bias the inference of systemic disturbances, as missing teeth (due to ante or postmortem tooth loss) within a dentition might prevent the identification and matching of defects (King *et al.* 2005).

In order to deal with this bias, the DDE 1982 index recommended that unerupted, missing, heavily restored, badly decayed or fractured teeth or teeth that could not be classified were coded to allow them to be excluded from statistical analyses. However,

Hillson (2001) argued that in the past, bioarchaeological approaches to the recording of dental status have generally lacked consistency. Similarly, Jackes (2011, 138) stated that "*Dental pathology is still reported as crude rates without reference to the age structure of the sample or differential preservation of tooth types*."

Tooth types

Theoretically, all teeth for which enamel is forming at the time of a growth disturbance should show a corresponding enamel defect (Bunon 1743; Condon and Rose 1992; Hillson and Bond 1997; Magitot 1881; Sarnat and Schour 1941). However, various researchers have pointed out that there is a different level of susceptibility to enamel defects in different tooth types, within teeth and across taxa (Black 1979; El-Najjar *et al.* 1978; Goodman *et al*. 1980; Goodman and Armelagos 1985a, b; Goodman and Rose 1990; Guatelli-Steinberg 2000, 2001; Hubbard *et al*. 2008; Lovell and Dawson 2003).

Potential differences in levels of susceptibility can have substantial implications of the analysis of furrow-form enamel hypoplasia within and between populations, as differential preservation of tooth types and especially the lack of reporting of such differential preservation can bias comparative studies, as some assemblages might include more or fewer examples of different tooth types (Goodman and Armelagos 1985a).

In terms of the variation in susceptibility between tooth types, Goodman and Rose (1990) stated that the highest number of defects occur on upper central incisors and lower canines in comparison with other teeth. Similarly, other scholars have argued that anterior teeth (incisors and canines) are generally more affected by furrow-form enamel hypoplasia than posterior teeth (premolars and molars), both in human and non-human primates (Black 1979; El-Najjar *et al*. 1978; Goodman and Rose 1990; King *et al*. 2005; Moggi-Cecchi and Crovella 1991; Saunders and Keenleyside 1999; Skinner 1986). Other suggested differences in the number of defects include higher hypoplasia frequencies on upper versus lower teeth and on the most polar teeth as opposed to teeth further from the midline (Goodman and Rose 1990). This difference in susceptibility has been linked to differences related to plasticity, crown height, enamel secretion rates and enamel thickness (Goodman and Armelagos 1985a; Hillson and Bond 1997).

In terms of differences in **plasticity**, it has been suggested that teeth which are more developmentally stable, such those with the highest heritability scores (so-called "polar

teeth": upper central incisors, lower lateral incisors, first molars and first premolars) are in fact more susceptible to disruptions (Goodman and Armelagos 1985a; Goodman and Rose 1990). Goodman and Armelagos (1985a), in their study of 14 permanent teeth (upper and lower teeth, first incisors to second molars) from 30 individuals from the prehistoric Dickson mound site found that these polar teeth were indeed most affected in six out of six cases. They proposed that the differences in the occurrence of enamel defects between morphologically similar teeth with overlapping developmental schedules might be related to genetic canalisation, as teeth under a greater genetic control are more strongly canalised and therefore less able to alter their size in response to environmental disturbances; (Goodman and Armelagos 1985a; Goodman and Rose 1990). In other words, Goodman and colleagues suggested that non-polar teeth are less genetically controlled and thus more buffered against environmental disturbances.

A detailed literature review concerning genetic control and tooth size is provided by Kieser (1990). He argued that the size of a single tooth as specified by genetic control may be too narrow a concept for the understanding of ontogenetic and phylogenetic processes and that it is likely that genetic control acts upon tooth groups (anterior versus posterior teeth, for example), which function as a unit within the dental arcade (Kieser 1990).

Differences in susceptibility explained as related to crown height, enamel secretion rates and enamel thickness are based on the concept of the lifespan of ameloblasts. More specifically, a longer period of activity of ameloblasts, might provide a larger "window of opportunity" for enamel to be affected by environmental, biological and social stresses known to affect amelogenesis and for these effects to be recorded as dental growth disturbances in both humans and primates (Condon and Rose 1992; Goodman and Rose 1990; Guatelli-Steinberg and Skinner 2000; Guatelli-Steinberg 2001; Moggi-Cecchi and Crovella 1991; Newell *et al*. 2006; Suckling *et al*. 1988; Witzel *et al*. 2006).

In terms of the effect of **crown height**, Goodman and Rose (1990) argued that larger teeth, such as those from gorillas as opposed to smaller species such as monkeys, are more susceptible to growth disturbances because ameloblasts forming larger teeth function over a longer period of crown formation and ageing ameloblasts are more sensitive to disruptions.

Guatelli-Steinberg and Skinner (2000) assessed the relationship between crown height and linear enamel hypoplasia, by comparing the number of defects (as estimated by the

number of matched defects on antimeres) between 66 specimens (a subset of 97 specimens of sympatric monkeys and apes from East Malaysia) with minimally worn paired canines and found a statistically significant higher rate (1.377) of defects in larger canines (df = 1, standard error = 0.0494, X^2 = 41.9, p = 0.001). However, when orangutans were excluded from the analysis, the relationship between crown height and number of defects became statistically insignificant. An earlier study focusing on gibbons by Guatelli-Steinberg (2000) supported this lack of association. Similarly, Reid and Dean (2000) have shown that in humans, no relation exists between tooth crown height and enamel formation time.

Guatelli-Steinberg and Skinner (2000) also assessed the intra-taxon variation in crown height and its relation to the number of defects, by studying both West African chimpanzees and gorillas and found no statistically significant association between crown height and number of defects in either taxon. From their large-scale study, they concluded that great apes show a higher frequency of enamel defects than gibbons and monkeys in West Africa and Malaysia, but they suggested that a taxonomic attribute other than high-crowned teeth might cause the variation in enamel hypoplasia frequencies. They argued that one such taxonomic attribute could be the **enamel secretion rate**, which may be slower or faster in gorillas as opposed to certain monkeys.

Studying the inter-tooth variability in defect occurrence in humans, Condon and Rose (1992) compared mandibular canines and first premolars from 30 individuals from the prehistoric Libben site in Northern Ohio. They found a high correspondence between furrow-form enamel hypoplasia on both tooth types. However, whereas all defects on the premolar could be matched in the canine, not all defects on the canine, (especially those located in the mid-crown region) could be matched with defects on the premolar. Based on these results, Condon and Rose (1992) proposed that the greater number of defects on canine crowns in relation to the first premolars is linked to the difference in the rate of enamel deposition between those two tooth types.

As described in Chapter 3, the distance between adjacent cross-striations provides a measure of daily secretion rates and this has been shown to be around 4.5μm per day for permanent human teeth (Hillson 1996; Massler and Schour 1946a; Smith 2008). However, this daily secretion rate is not constant across the crown of a single tooth, as it changes according to its position on the crown, with differences between rates within the inner versus outer enamel and cervical versus cuspal enamel (Smith 2008). As such, it is

necessary to assess the extent of the influence of daily secretion rates on the occurrence of enamel hypoplasia within one tooth type before any inter-tooth conclusions are drawn.

Condon and Rose (1992) and others have also regarded **enamel thickness** as an important variable related to the life span of ameloblasts, with thicker enamel implying a longer ameloblast life span and should therefore be more susceptible to insults in comparison with the thinner enamel (Condon and Rose 1992; Guatelli-Steinberg 2001; Suckling and Thurley 1984; Suckling *et al*. 1988).

As stated in Chapter 3, enamel varies in thickness according to tooth type. However, differences in enamel thickness not only occur between tooth types (upper versus lower dentitions, for example), but also across the tooth crown, with thinner enamel at the cervical part the crown in comparison to the occlusal or middle parts (Condon and Rose 1992; Hillson and Bond 1997). Similarly to Condon and Rose (1992), Suckling and colleagues (Suckling and Thurley 1984; Suckling *et al*. 1988) argued that the thicker enamel in the occlusal part of the tooth crown should therefore be more susceptible to insults in comparison with the thinner cervical part. Any comparison of susceptibility of tooth types to defects should therefore also take into account the extent of the influence of enamel thickness on individual teeth.

The difference in appearance of defects between different parts of the crown might not only be related to enamel thickness and enamel extension rates, but it might also be related to defect identification issues (Guatelli-Steinberg 2000). More specifically, as the angles in which the striae of Retzius reach the enamel-dentine junction change across the height of the crown, perikymata also appear differently at the crown surface (see Chapter 3). Where angles are large, such as in the cervical region of the crown, perikymata are more compressed and deep, and where angles are small, such as in the occlusal region of the crown, perikymata are more widely spaced and shallower (Goodman and Rose 1990; Hillson 1996; Newell *et al*. 2006). As enamel defects are identified by the appearance (spacing and depth) of perikymata, defects in some regions (such as the shallower perikymata of the occlusal part of the crown) will be more difficult to detect than in other areas (King *et al*. 2005; Newell *et al*. 2006).

Ageing of growth disruptions

Dental age based on the developing dentition is often used as a proxy for chronological age in bioarchaeological studies (Goodman and Song 1999; Hillson 1996; Hoppa and

Fitzgerald 1999; Saunders *et al.* 1993; Smith 1991). This estimation of age is based on developmental standards summarising the formation of crown and roots and/or tooth eruption patterns (Hillson 1996; Smith 1991). In enamel hypoplasia studies, estimations of the timing of furrow-form enamel hypoplasia have most often been obtained macroscopically, using charts, measurements and regression methods. All three approaches are based upon published tooth development schedules.

One of the oldest **dental development charts** was produced by Berten (1895), but Magitot (1881) and Black (1908) also developed various pictoral diagrams, separating the tooth crowns into various zones based upon calcification patterns (Goodman and Song 1999; Smith 1991). Much of this early work was based on dissection after dental surgery or during autopsy (Smith 1991).

The most widely used standard of development was produced much later and was based on the discovery of an important biological landmark, the neonatal ring (Massler *et al.* 1941; Schour 1936; Schour and Massler 1940, 1941). Schour and Massler (1941) used the neonatal line, the accentuated incremental ring within enamel which is produced at birth (see Chapter 3), as an anchor point for the construction of chronological tables of tooth formation (Fig. 4.5).

Sarnat and Schour (1941, 1942) studied the appearance and timing of enamel hypoplasia on 60 individuals aged seven to 31 years from hospitals and dental clinics in the Chicago area. They noted the position of enamel defects on the crown and compared this with the tooth development standard provided by Massler and colleagues (1941; Fig.4.5). Most enamel hypoplasia studies using the DDE index (or a modified version) used this method to determine the age at which each enamel defect occurred (Corruccini *et al*. 1985; FDI Commission on Oral Health 1982; Hutchinson and Larsen 1988; Moggi-Cecchi *et al.* 1994; Obertová 2005; Paluckbaité *et al.* 2002; Schultz and McHenry 1975).

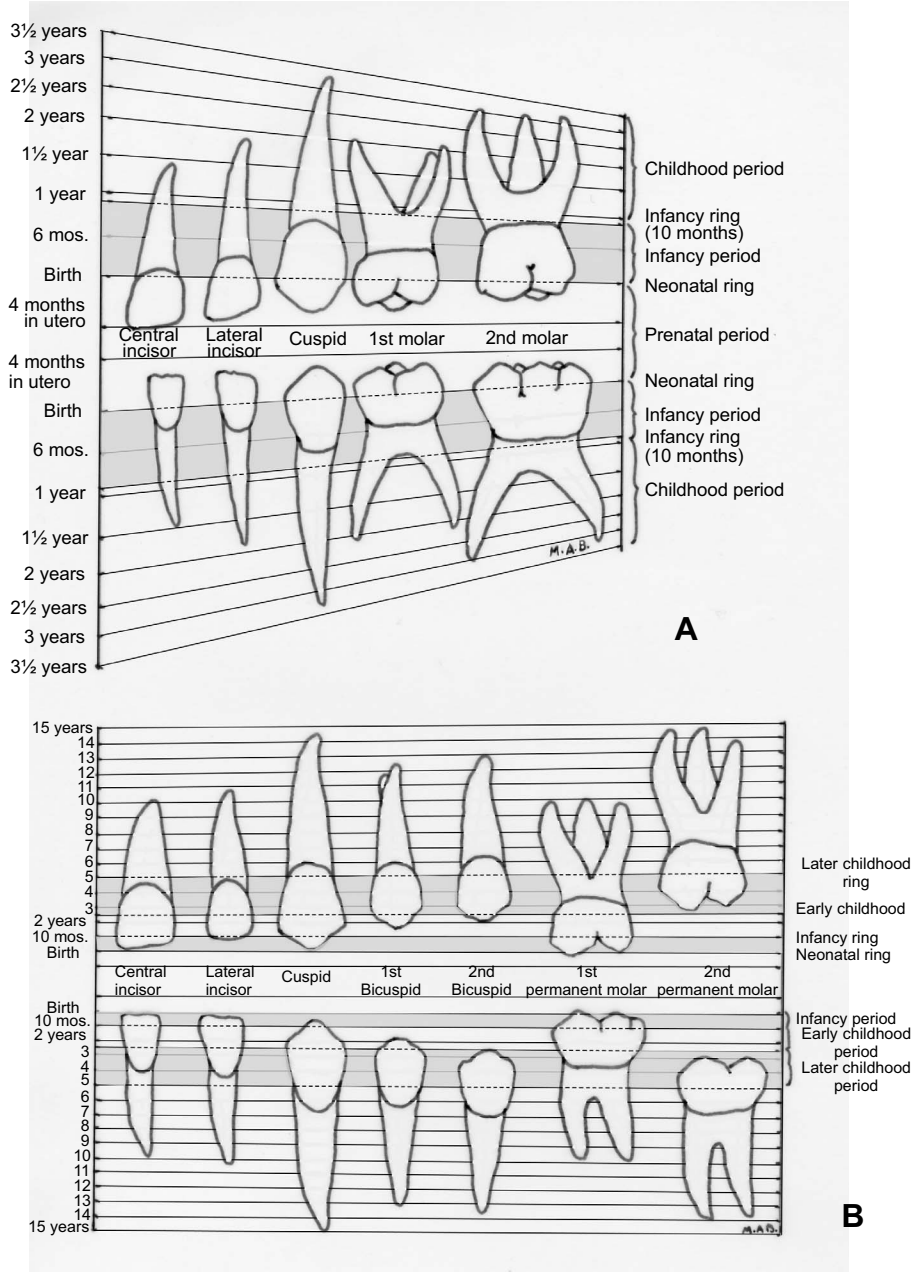

Figure 4.5: Chronology of tooth development (labial view) according to Massler et al. 1941 (Fig.7). Developmental lines and periods indicated on the right (A = deciduous teeth, B = permanent teeth)

Swärdstedt (1966) also based the timing of enamel defects on the Massler chart. He **measured the distance** of defects from the cemento-enamel junction and transferred these measured locations to time-intervals (so called half-year developmental zones) based upon the Massler chart. Similarly, Goodman and colleagues also used ages based upon the locations of defects relative to cement-enamel junction (Goodman *et al*. 1980; Goodman and Armelagos 1985b; Goodman 1989). Based on crown heights measurements by Swärdstedt (1966) and the Massler tooth development chart, they

formulated a series of **regression equations** in order to simplify the conversion of the enamel defect location into a dental age (Buikstra and Ubelaker 1994; Goodman and Rose 1990; Goodman and Song 1999; Rose *et al.* 1985).

There are various problems related to the use of dental development charts in order to obtain a chronology of enamel hypoplasia. Smith (1991) argued that even though the Massler chart is widely distributed in dental offices and classrooms today, it is similar to early pictoral diagrams, as it lacks documentation about the sources of the information used, both in terms of method and subject.

The Massler table was originally titled “Chronology of growth of human teeth”, and had a footnote crediting the table as “modified from Logan and Kronfeld 1933” (Smith 1991). For their proposed tooth development table, Logan and Kronfeld (1933) used histologic and radiographic techniques and published resources to study of jaws of children in order to obtain a chronology of tooth development from birth to 15 years. The initial sample included 25 children, 19 of which were under two years of age and six were older (2,5, 3, 4,5, 8, 11 and 15 years), but later studies included five additional subjects, including two newborns (Logan and Kronfeld 1933; Logan 1935; Smith 1991).

Whereas the subjects were useful for Kronfeld’s immediate purpose, to avoid damage to developing teeth during surgical repair of cleft palate, the sample is less than ideal in order to construct standards of normal human growth, not only because its limited number of individuals, but also because many of the children had died from diseases such as tuberculosis or enteritis (Goodman and Rose 1990; Goodman 1991; Goodman and Song 1999; Liversidge 1994; Smith 1991; also see Hillson 2005, 2014). The sample used in Logan and Kronfeld study was thus inherently biased as the eruption of successive teeth is influenced by disease and early tooth loss (Liversidge 2003). In addition, in general, reports on patterns of tooth development vary greatly and previously reported tables are limited by the inadequate age ranges, as not all teeth within the developing dentition have been assessed (AlQahtani *et al.* 2010; Goodman and Song 1999; Hillson 2005).

There are also inherent issues related to comparing deceased prehistoric children from different regions with healthy modern children from European origin, as there might be considerable intra-and inter-population variation in developmental timing (Lewis and Roberts 1997; Liversidge *et al.* 1998; Smith 1991).

One limitation of the measurement based methods used by Swärdstedt (1966) and Goodman and colleagues (1980; Goodman and Armelagos 1985b; Goodman 1989) is

that fact that they these not take into account the issue of “hidden” or “buried” cuspal enamel (Goodman and Song 1999; Hillson 1978; Hillson and Bond 1997; Ritzman *et al.* 2008). As described in Chapter 3, during crown formation, dome-like layers are laid down on the top of the crown (cuspal enamel) and sleeve-like layers are deposited towards the cervix of the crown (imbricational enamel). Depending on the duration of cuspal enamel formation, the enamel on the permanent teeth only becomes visible a certain time after the initiation of crown growth. For example, the enamel on anterior teeth is only visible after one year of age (Dean and Reid 2001; Reid and Dean 2006).

Without reference to cuspal formation times, the timing of enamel defects is likely to be underestimated (Ritzman *et al*. 2008). Histological studies have helped provide estimations as to the timing of this “hidden” cuspal enamel (Bromage and Dean 1985; Bullion 1987; Dean *et al*. 1986; Dean and Beynon 1991; Hillson and Bond 1997; Scott and Symons 1974). Based upon these advances in dental histology, some researchers have suggested the use of incremental structures as a basis for the timing of enamel defects (Goodman and Song 1999; Hillson and Bond 1997; Reid and Dean 2000).

In addition to the issue of hidden enamel, the use of equally spaced time zones in chart and regression methods is another cause of error in the estimation of timing of enamel defects. This division of the crown in equal zones implies that the variation in velocity of crown growth, proposed by various researchers (Gohdo 1982; Hillson and Bond 1997; Shellis 1984), is in fact negligible (Goodman and Rose 1990).

In their histological study of 115 anterior teeth, Reid and Dean (2000) demonstrated the non-linearity of crown formation, providing evidence for a slowing of growth towards the cervical part of the crown in all teeth. Taking into account this non-linearity, as well as cuspal enamel formation and crown initiation times, they proposed a new model for the timing of furrow-form enamel hypoplasia, based on the average ages derived from individual estimates of all teeth within the mouth (Reid and Dean 2000). A second histological study took into account the variation between populations (medieval Danish, North American, North European and South African) and found very similar cuspal formation times for anterior teeth, but some differences in posterior teeth, with shorter first molar cusp formation times in the South African sample (Reid and Dean 2006).

Based on the data and model provided by Reid and Dean’s analyses (2000, 2006), the timing of enamel hypoplasia can be estimated by assigning each defect to a decile of crown height (Fig. 4.6). The age of occurrence of each defect can then be calculated by

adding the number of days necessary for the formation of the assigned decile to the cuspal enamel formation and crown initiation times (Reid and Dean 2000; Ritzman *et al.* 2008; Temple *et al*. 2013).

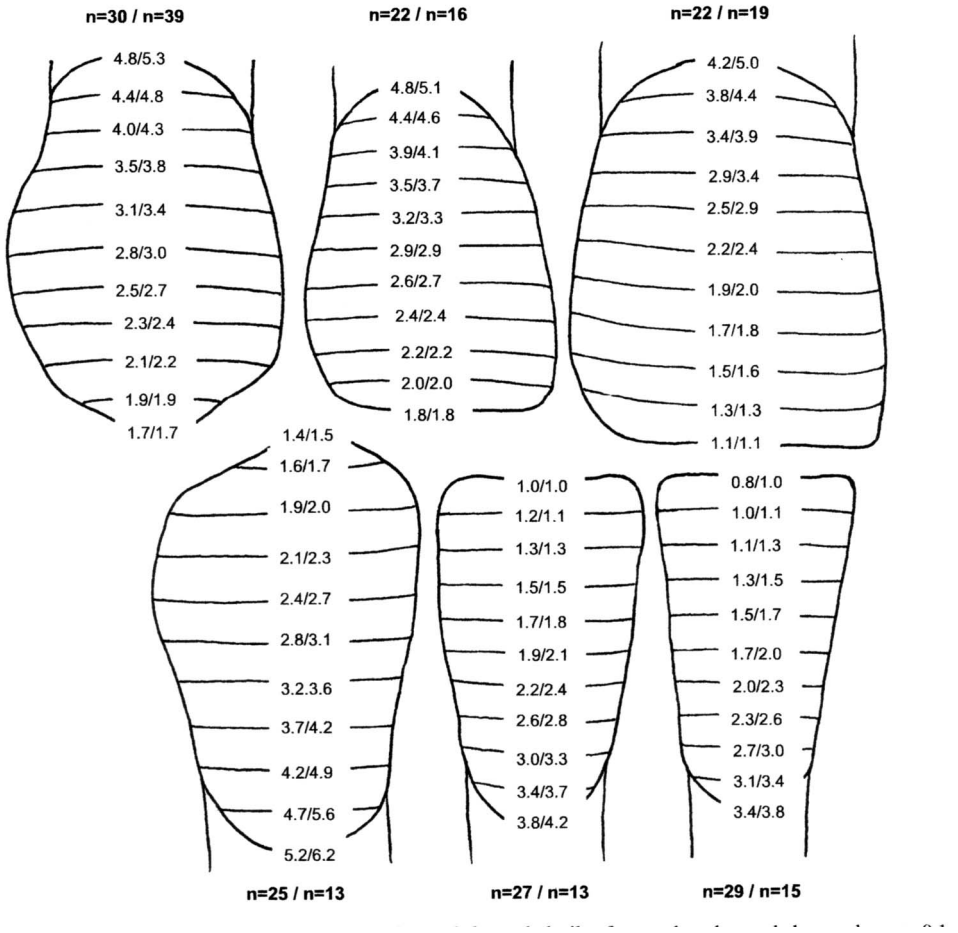

Figure 4.6: Chronology of tooth development according to Reid and Dean 2006 (Fig. 3). Mean estimates in anterior teeth for each decile of crown length for African and European samples

Hillson and colleagues took a different approach to Read and Dean (2000, 2006) and linked furrow-form enamel defects directly to perikymata, the incremental structures visible on the crown surface (Hillson and Bond 1997; King *et al.* 2002, 2005). This approach involves the microscopic identification of defects using the SEM and/or a measuring microscope. The age of matched defects is then determined by counting the number of perikymata from the cusp tip to the beginning of the first defect on each tooth and converting this into days by a set periodicity (the estimated number of days between adjacent perikymata, see Chapter 3). This number is then added to the average cuspal enamel formation and crown initiation times for that tooth (King *et al*. 2002, 2005).

The timing of enamel hypoplasia using the incremental structure approach is considered more accurate than the chart or regression methods, as it takes into account the underlying geometry of the crown (Reid and Dean 2000; Hillson and Bond 1997). However, the timing is still dependent on inferences related to the periodicity of long period lines (striae of Retzius). As described in Chapter 3, striae periodicity is uniform within a tooth and between teeth from a single individual, but varies between individuals and populations (Dean 1989; Fitzgerald 1998; Newman and Poole 1974; Reid and Dean 2006; Reid and Ferrell 2006; Risnes 1998; Smith *et al*. 2003, 2012).

The variation in periodicity leaves some level of assumption in the calculation of developmental schedules and the establishment of the chronology of enamel defects in different populations (Temple *et al*. 2012). Alternatively, estimations regarding initiation of tooth mineralisation, cuspal enamel formation times and periodicities can be minimised by calibrating the developmental schedules across the dentition using clear matches between one or two defects on different tooth types with overlapping developmental schedules (Smith *et al*. 2007b). King and colleagues (2002, 2005) used this approach, by counting perikymata between defects and aligning teeth based on a matching between these arrays.

Deducing health from archaeological samples

In their much-debated paper on the “osteological paradox”, Wood and colleagues (1992) discussed the inherent problems in bioarchaeology, both in terms of inferences about demography and health. They argued that there are three fundamental problems in the inference of health status from archaeological samples, namely demographic non-stationarity, selective mortality and heterogeneity in the risk of disease and death.

The concept of non-stationarity refers to the issue that, unless a population remains of a constant size, the age distribution is more an indicator of fertility levels than mortality patterns (Wright and Yoder 2003). This issue specifically relates to demographic reconstructions and will therefore not be covered in this study (for a more detailed discussion on this, see Wright and Yoder 2003 and references therein). The issue of heterogeneity in risk of disease has been discussed above (p. 111).

In terms of selective mortality, Wood and colleagues (1992) argued that archaeological skeletal samples are not only biased due to preservation issues, but that they are

inherently unrepresentative of any living population because they represent a death assemblage. They wrote that "*We never have a sample of all the individuals who were at risk of disease or death at a given age, but only of those who did in fact die at that age* (Wood *et al*. 1992, 344)". As a result, the observed frequency of any pathological condition is expected to overestimate the actual prevalence of this condition in the living population.

In terms of furrow-form enamel hypoplasia, the problem of selective mortality is in some ways circumvented, as a dentition is a cumulative (or longitudinal) record of an individual's growth through time, not one single snapshot at the time of an individual's death. As such, detailed studies of enamel hypoplasia, in comparison to other (osteological) types of pathology such as cribra orbitalia or porotic hyperostosis, do enable comparisons between individuals who were at risk of disease or death at a given age, as growth disturbances can be related to a detailed chronology of dental development. For example, individuals with completely developed crowns can be divided into age-specific groups (1.99-2.99; 2.99-3.99 etc.) based on perikymata counts. As such, comparisons of enamel defect frequencies between age-specific groups presents a "*modest solution to the problem of mortality selection* (Goodman and Rose 1990, 87)."

Despite being a cumulative record of growth, the comparison of dental growth profiles between groups is still problematic, as there is still an issue with group comparisons. This is especially the case with individuals who died before tooth crowns were fully formed. These individuals may have experienced more disruptions, but their dental growth profile is not complete and thus not included within the study sample (King *et al*. 2005).

The concept of stress

In the 1980s, as a reaction to the increasing separation of bioanthropological subfields and their methodological approaches, which were perceived to be threatening the connectedness of the discipline in terms of shared concepts and perspectives, Goodman and colleagues (1988) proposed the use of a shared concept, **stress**, as a methodological tool within the anthropological research world. As such, "stress" has been central to the attempts to reconstruct adaptive responses to environmental (or social) constraints using palaeopathological and palaeodemographic approaches (Goodman *et al.* 1988).

The overarching concept of stress, first applied by physical anthropologists to the origins of agriculture, has been widely applied in a diverse range of other contexts (Klaus and Tam 2009; Ribot and Roberts 1996; Šlaus *et al.* 2002; Temple 2007, 2010). In this section, I will outline two main problems with applying the idea of stress to prehistoric populations, one relates to the definition of stress and the other to the idea of resilience.

Definition of stress

The basis for the current use of the concept of stress as a medical idea can be traced back to Claude Bernard (1865) who identified the ability of all living creatures to maintain the constancy of their internal environment. Walter Cannon (1932) established the term *homeostasis* (the way in which the body maintains itself in a steady state) and put forward the idea of a bodily response to maintain homeostasis when this is threatened (Goldstein and Kopin 2007; Hillson 2014; Little 1995). However, the main influence on the bioarchaeological use of stress comes from the work of Selye (see Hillson 2014; Little 1995).

Based on experimental work with mice and their response to a variety of stimuli, Selye (1936, 1950, 1955, 1956, 1976) defined stress as "*the non-specific response of the body to any demand*" and stressors as "*agents that produce stress at any time* (Selye 1976, 53)". He proposed the idea of the General Adaptation Syndrome (GAS), as "*the chronologic response to stressors when their action is prolonged* (Selye 1976, 53)". GAS consists of three stages, including: 1) an initial alarm, 2) resistance, 3) adaptation or exhaustion and involves three elements: the thymus, lymph nodes and spleen (Selye 1976, 53).

Rice (2000) described the three GAS stages as follows: in normal, day-to-day situations, the human body functions with a level of normal resistance (homeostasis). When a stressor (the stimulus provoking a response) is encountered that exceeds the normal adaptive resistance, an alarm is initiated. The resistance stage involves the establishment of full resistance to the stressor, as an attempt is made to maintain and increase the level of a body's functioning, in order to facilitate the coexistence of a stressor and the organism. The exhaustion stage occurs when an organism is not able to return to its normal level of resistance (homeostasis) and permanent damage to the system is likely to occur. However, Rice (2000) argued that little has been written about Selye's third stage, as few studies have been carried out to study the details of this final stage of adaptation.

The bioarchaeological approach has used a slightly modified concept of Selyean "stress", in which the focus is upon the (permanent) damage to the system (Selye's third stage). This is visible as physiological change rather than "stress" as a three-stage response to stimuli and the stressor is a "deforming" force rather than a positive or negative stimulus provoking a response (Goodman *et al*. 1980; Little 1995).

Within this bioarchaeological modification, the emphasis is usually placed on physical, rather than physiological influences on health (Bush 1991, but see Hillson 1991). The study of the health (or stress) of past populations is also constrained due to the fact that individuals' mental state and the many diseases affecting internal organs are impossible to detect in the archaeological record (Waldron 2008).

There is currently no experimental evidence linking episodes where stressors trigger a stress response causing enamel defects and Hillson (2014) argued that it is difficult to isolate Selyean stress responses from other potential factors causing enamel hypoplasia. There is, however evidence that enamel defects are caused by disruptions to growth (enamel development). Therefore, rather than using a **stress** framework to construct a population model in which "health" is an output, this study will aim to construct a detailed record of **growth** based on examinations of the detailed developmental sequences of individuals.

4.2. Skeletal growth

4.2.1. Historical perspective

One of the first references to juvenile anatomy can be found in Leonardo Da Vinci's drawings, which are based on dissections of a seven month old fetus and stillborn full-term infants (Bogin 1999). Such Renaissance drawings were in the spirit of Pythagorean philosophy and concerned with the relative proportions of different body parts in order to search for the ideal artistic representation of the body rather than based on actual measurements (Tanner 1981). Similarly, during the seventeenth and eighteenth centuries, remarkably detailed non-metric observations were made from gross dissections, mainly focusing on fetal skeletons rather than individuals who survived into childhood (Albinus 1737; Kerckring 1717; for a review see Noback 1943, Fig. 4.7).

Quantitative approaches to the study of postnatal human growth date to the mid-eighteenth century, when George LeClerc, Comte de Buffon, and his collaborators

started measuring aborted fetuses, newborns and infants (Benzaquén 2004; Tanner 1981). The first longitudinal study of growth was carried out by one such collaborator, Comte de Montbeillard (1720-1785), who measured his son from his birth to this 18th birthday (Tanner 1981; Ulijaszek *et al.* 1998).

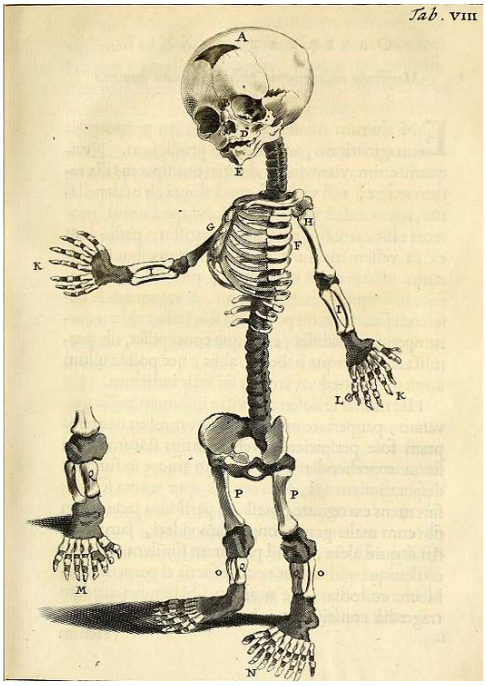

Figure 4.7: Drawing of fetal skeleton by Kerckring (1717)

Anthropometry or the practice of measuring human variation evolved as a consequence of military developments in the eighteenth century, as recruits were measured in order to assess if they fitted the military's height requirements (Harris 1997; Tanner 1981). For example, the Marine Society of the United Kingdom's Records show that from around 1786, young boys from the age of about 12 years were measured upon recruitment, possibly as a means of identification, to avoid admitting runaway apprentices (Tanner 1981). Such recruitment measurements were also implicitly based on the link between body size, health and productivity (Ulijaszek and Komlos 2010).

The crossover between anthropometry and health was investigated further from the nineteenth century onwards, as physical growth data was increasingly used to assess human welfare (Tanner 1981; Ulijaszek and Komlos 2010). For example, Quetelet, a Belgian mathematician (1796-1874) heavily influenced by Villermé (1782-1863), the founder of public health in France, argued that children's heights oscillate around a greater or lesser mean and that these oscillations were determined by climate, differences in nutrition and greater or lesser amounts of labour (Tanner 1981).

Quetelet carried out the first cross-sectional population survey of childhood growth. In two surveys (1831-32), he measured the height and weight of children from the Foundling Hospital and boarding houses in Brabant, Belgium. Quetelet was the first person to fit a curve to the succession of means of physical growth data, thereby applying the theory of the Normal Curve, discovered by Gauss and Laplace, to practice and initiating the continuous search to find the ideal mathematical growth curve (Klein 1997; Tanner 1981; Ulijaszek *et al*. 1998).

A major contribution to growth theory came from d'Arcy Thompson's work. Thompson (1917) combined classical approaches to natural philosophy and geometry with modern biology and mathemathics to understand form and growth of humans, animals and plants. He considered the form of all multicellular animals to be the result of the same general biological process which could be described mathematically using transformational grids (Thompson 1917; also see Bogin 1999 and Tanner 1981 for a detailed description of Thompson's work). Thompson showed that different patterns of growth of cranial (e.g. the mandible) and postcranial elements (e.g. the femur) are required to produce adult differences in body shape. In this way, differences between chimpanzees and humans were considered the result of unequal rates of growth in skeletal and muscular elements (Thompson 1917).

Around the same time as Thompson's theoretical approach was being formed, the methodologies behind physical growth data collection practices were being further developed through the influence of Franz Boas. His pioneering longitudinal study of growth among schoolchildren, begun in 1890, led to the production of national standards of height and weight of North American schoolchildren (Tanner 1981). Boas (1912;1932) used measurements of individuals rather than age group means to calculate growth rates and introduced the concept of the "tempo of growth" in order to understand the difference between early and late maturing individuals (also see Bogin 1999 and Tanner 1981 for a detailed description of Boas' work).

During the 1930s, a wealth of longitudinal growth studies was initiated, mainly to study the effect of the Great Depression on childhood health (Sherwood and Duren 2013). Large studies were carried out in metropolitan areas (for example the Denver growth study) and were also conducted in more rural areas such as Yellow Springs, Ohio (the Fels longitudinal growth study, described in Roche 1992).

Much of the data on physical growth comes from longitudinal radiological surveys carried out between the 1930s and 1960s and include mostly white middle class children (Oxford

Child Health Survey: Hewitt *et al.* 1955; University of Colorado longitudinal growth study: Maresh 1970; Harpenden growth study: Tanner *et al.* 1976; Brush Inquiry, Cleveland, Ohio: Nelson *et al.* 2000). As health concerns regarding radiation arose, such studies have been consigned to the past. However, new methods such are magnetic resonance imaging (MRI) continue to be developed, creatingnew data collection opportunities. Similar longitudinal growth studies continue today, such as the South African Birth to twenty study (Hawley *et al*. 2012; Sheppard *et al*. 2009), the Born in Bradford birth cohort study (Fairley *et al.* 2013; Johnson *et al.* 2013) and the Avon longitudinal study of children and parents (ALSPAC; Golding *et al*. 2001).

The most common anthropometrical approach for assessing health is to study the relation between weight and stature in terms of body mass, the Body Mass Index or BMI (Sherwood and Duren 2013). In addition to BMI for age, length and weight, height for age can also be used to follow and assess the growth trajectories of individual children (de Onis *et al.* 2006a). These measured parameters can then be compared to modern standards and charts in order to assess both the health and nutritional status of individual children and the general well-being of their communities (de Onis *et al*. 2006b). For example, when results indicate that a child is too lean for its current length (stature), they are interpreted as indicators of malnutrition or other growth disturbances (Sherwood and Duren 2013).

Johnston (1961, 1962) presented the first study of skeletal growth and maturation in a past population. He evaluated long bone growth in a prehistoric American population (Indian Knoll, Kentucky, Archaic period) and compared the relative increases in size of this skeletal sample to modern data (serial X-rays of white children collected by Maresh in 1955). Johnston found a smaller skeletal size for age (based on dental and osseous criteria) in the Indian Knoll sample in comparison to the modern sample, especially after two years of age and attributed this difference to both environmental and genetic factors (Johnston 1962).

In bioarchaeological studies such as Johnston’s, information on growth is necessarily cross-sectional and mostly derived from dry bone measurements (Saunders 2000; Scheuer and Black 2000a). In contrast to longitudinal growth studies of living children, cross-sectional studies of skeletal growth are based on deceased individuals who never reached maturity and as such, these individuals are only measured at the age of death. This type of study cannot examine individual variability in growth rates and data derived

from this approach does not represent the same velocity or “tempo of growth” curves as growth researchers such as Boas or d’Arcy Thompson described them (Hoppa and Fitzgerald 1999; Lewis 2007; Saunders 2000). Nevertheless, since Johnston’s first study of skeletal growth in past populations a multitude of publications has appeared, providing different approaches to the presentation and interpretation of skeletal development (Lewis 2007; Saunders 2000). These include assessments of either growth in height (skeletal measurements) or skeletal maturity (epiphyseal fusion).

4.2.2. Types of skeletal development data

Skeletal measurements

Linear measurements of long bones, and in particular the length of the diaphyses (the main shaft of long bones) are the most common employed variables for assessing skeletal growth in bioarchaeology (Lewis 2002). In most of these studies maximum lengths are measured using osteometric boards or sliding calipers following standard osteometric protocols (Bass 1966; Buikstra and Ubelaker 1994; Cardoso and Garcia 2009; Cook 1984; Fazekas and Kosa 1978; Hoppa 1992; Hummert and Van Gerven 1983; Jantz and Owsley 1984; Johnston and Zimmer 1989; Lovejoy *et al.* 1990; Mays *et al.* 2008, 2009; Merchant and Ubelaker 1977; Molleson 1993; Pinhasi *et al*. 2005; Saunders *et al*. 1993; Steyn and Henneberg 1996). However, diaphyseal measurements can only be taken on complete (non-broken) bones and prior to the union with the proximal or distal epiphyses (the mostly rounded end of long bones) which starts around 11 to 12 years of age and ends in the early 20s (see Chapter 3).

Both breakage and the age limit for diaphyseal measurements greatly reduce possible sample sizes. In order to increase sample size, some studies also use total long bone measurements, mathematically correcting for the size of the epiphyses in cases in which fusion has occurred (Humphrey 1998; Okazaki 2004; Ruff 2007). Another approach is to assess the width of long bone metaphyses (the widest portion of the long bone shaft, at the joint between the shaft and the epiphysis), which are less susceptible to breakage than long bone shafts and are also good indicators of environmental influences on growth (Hoppa 1992; Pinhasi *et al*. 2005).

The breadth of femoral metaphyses and epiphyses can also be used as indicators of body mass. Recently, Ruff (2007) proposed the use of prediction equations from distal femoral

metaphyseal breadths and femoral head breaths to estimate juvenile body mass. Using this method, Ruff and colleagues (2013) compared the body mass of individuals from the protohistoric Arikara site (South Dakota) with the Neolithic Çatalhöyük site (Turkey). In this study, the lower body mass values observed in early childhood in the Arikara sample compared to those of the Çatalhöyük sample were interpreted as reflecting environmental differences between the two groups, in this case, poorer health conditions for the Arikara sample (Ruff *et al.* 2013).

The proportion of endosteal (the thin layer lining internal cavities of bone) to periosteal (external surface of bone is covered by a fibrocollagenous membrane covering the external surface of bone) dimensions of the long bone diaphysis, referred to as cortical thickness or area, has also been assessed in growth studies, with excessive endosteal resorption interpreted as an indicator of malnutrition (Cook 1984; Garn *et al.* 1969; Himes *et al*. 1975; Hummert 1983; Mays *et al.* 2009; Kennedy 1985). However, recently, it has been shown that differences in cortical thickness might be more strongly related to increased activity levels (mechanical loading) than developmental disturbances (Gosman *et al*. 2013; Ruff 2000; Ruff *et al.* 1994, 2006b).

The inclusion of skeletal variables that represent different functional regions (cranium, mandible and postcranial bones) and grow at different rates, allows differences in growth to be recorded during these different developmental schedules (Humphrey 1998). As such, quantitative assessments of the shoulder, hip, hand and foot bones as well as the craniofacial complex, offer the possibility to explore growth trajectories in more detail (Hoppa and Fitzgerald 1999; Merchant and Ubelaker 1977; Miles and Bulman 1995; Saunders *et al.* 1993).

Skeletal maturity

Skeletal maturation is achieved through the completion of bone length as well as by the union of the epiphyses to the main shaft of the long bones. As such, the assessment of skeletal maturation can be carried out by analyses of the epipyseal fusion patterns of the limb bones (Cardoso 2005; Scheuer and Black 2000a). Epiphyseal union occurs during the teenage years and can be assessed by dividing the maturational continuum into three discrete stages which can then be scored and compared between individuals of the same (dental) age: no union; partial union, and complete union (Cardoso 2005; Johnston 1961; Johnston and Zimmer 1989).

Cardoso (2005), in his study of a known sex and age at death sample, calculated the discrepancy between skeletal age and actual chronological age. Skeletal age was estimated by the modal age when intervals for the epiphyseal union of long bones overlapped (taking into account sex differences) and these were compared to modern standards provided by Scheuer and Black (2000a). Positive scores indicated advancement of chronological age; negative scores indicated a lagging behind actual age. Cardoso (2005) found a significant difference between his sample and the modern data, indicating delayed maturation times for the sample under study. He also found that, compared to the growth in height (skeletal measurements), skeletal maturation was less affected by environmental factors, confirming the theory that insults have the greatest effect during the early childhood years of rapid growth as opposed to the slower period of skeletal maturation (Frisancho *et al*. 1970b; Martorell *et al.* 1979).

4.2.3. Interpreting skeletal growth

In order to construct skeletal growth patterns based on skeletal measurements, the latter need to be compared in the context of an independent “clock” (Cardoso 2005; Hoppa and Fitzgerald 1999; Maresh 1943). However, for most archaeological assemblages, except for those for which historical information such as coffin plates and parish register data exists, exact chronological age cannot be determined. Most often, age assessments are then based on the developing teeth, as dental age is currently the most accurate physiological indicator of chronological age (Saunders *et al.* 1993; Smith 1991).

Dental remains preserve well archaeologically and as dental development fits in with other aspects of life history such as body and brain weight (Smith 1989) and are thus a good means of measuring the timing and rate of development (Krovitz *et al*. 2003; Scheuer and Black 2000a). The growth of the deciduous and permanent dentition covers the entire range of juvenile development, starting from the embryonic period and completing in the late adolescent period, and the relative position of an individual’s development along the dental developmental continuum can be used as a proxy for chronological age, even though these rarely match exact chronological age (Jantz and Owsley 1984; Krovitz *et al*. 2003; Lampl and Johnston 1996; Scheuer and Black 2000a).

Estimations of age at death

Developing dentitions are generally assessed based on crown and root formation (Smith 1991, also see above p. 127). Additionally, tooth eruption, the gradual migration of teeth

through bone and soft tissue, follows a general pattern and has also been used as an indicator of dental age in the past (Armelagos *et al*. 1972; y'Edynak 1976). However, as tooth eruption is limited to the time during which teeth emerge through the gingivae, whereas root and crown formation patterns can trace the continuous development of teeth through childhood, the latter is often preferred as an indicator of physiological age (Jelliffe and Jelliffe 1973; Konigsberg and Holman 1999; Saunders 2000; Saunders *et al.* 1993; Scheuer and Black 2000a; Smith 1991).

A completely formed tooth is the end result of two periods of growth, the formation of the organic matrix and the subsequent calcification or mineralisation (Smith 1991). Calcification patterns can be studied radiographically or by dissection and are often used as a guide to the development of the dentition (Smith 1991). Both tooth emergence and tooth formation occur in developmental clusters. For example, permanent first molars, and incisors form within the 1st year and appear between 6-8 years, cheek teeth form between 2-4 years and appear between 10-12 years (Smith 1991).

These clusters have often been visualised in pictoral dental development charts, separating the tooth crowns into various zones based upon calcification patterns (Berten 1895; Black 1908; Magitot 1881, also see above p. 127). Much of this early work was based on dissection after dental surgery or during autopsy (Smith 1991). The most widely used standard of development, Massler's chronological table of tooth formation (1941), also uses a pictoral chart to represent clusters in eruption and tooth formation patterns and is often used as a dental age indicator in skeletal growth studies (Johnston 1962; Mays 1999; Merchant and Ubelaker 1977; Molleson 1993, for a critique of this method, see above p. 129).

In the 1950s up to the mid-1970s, a multitude of dental ageing techniques were developed, focusing on tooth formation patterns and based on large samples of radiographic data derived from cross-sectional or longitudinal growth studies of living children (Anderson *et al*. 1976; Demirjan *et al.* 1973; Fanning 1961; Fanning and Brown 1971; Fanning and Moorrees 1969; Haavikko 1970; Moorrees *et al*. 1963a, b). The different dental ageing methods varied in the number of stages provided, but they all contained at least three stages of tooth formation: initiation of calcification; crown completion and root completion (Smith 1991).

The Demirjan (1973) and Anderson (1976) stages have been used in child growth studies (Hoppa 1992; Mays *et al*. 2008), but the development stages for deciduous and

permanent teeth defined by Moorrees, Fanning and Hunt stages (1963a, b) are the most commonly used and recommended tooth formation standard (Bennike *et al*. 2005; Buikstra and Ubelaker 1994; Hillson 1996; Hoppa 1992; Jantz and Owsley 1984; Lewis 2002; Mays *et al*. 2008; Merchant and Ubelaker 1977; Pfeiffer and Harrington 2011; Pinhasi *et al*. 2005; Saunders *et al.* 1993). Smith (1991) reworked the Moorrees, Fanning and Hunt data (1963a, b) in order to predict dental age for permanent teeth (lower incisors, canines, premolars and molars) with values representing the midpoint between the age of appearance of a specific stage and the next. This method has been tested by Liversidge on a known age sample (1994) and has been shown to produce results that are closer to true age than the original Moorrees, Fanning and Hunt method.

The overall success of this age prediction method can be further enhanced by pooling assessments from multiple teeth rather than using single teeth, as this multi-tooth approach accounts for the variability within an individual (Hoppa 1992). As such, for each individual, every available tooth is assessed independently (based on tooth development scores) and the mean age is assigned as the dental age (Hoppa 1992; Smith 1991).

As sex cannot easily be determined for juvenile remains, values tend to be calculated based on the averages of male and females for each tooth, which, according to Smith (1991), introduces little extra error in the resulting ages. However, another limitation with the mean ages approach is the lack of established means for all tooth types (Smith 1991). For example, the tested method provided by Smith (1991) only provided values for the permanent lower dentition and the commonly used charts by Moorrees and colleagues (1963b) only included the lower deciduous canine and premolars.

An alternative is to use the length of the developing tooth as an age predictor. This length shows a linear relationship with age during fetal and postnatal growth and age can therefore be predicted using measurements of developing permanent and deciduous teeth (Deutsch *et al.* 1981; Deutsch *et al* 1983; Deutsch *et al* 1985; Liversidge *et al.* 1993; Liversidge and Molleson 1999). As this method is suitable for isolated teeth or radiographs of unerupted teeth, it has been employed in recent growth studies (Cardoso and Garcia 2009; Ruff *et al*. 2013).

Cardoso (2007) has tested this method on permanent teeth from a known age at death sample from Portugal and found this to be a relatively accurate estimator of age: when several teeth are used, estimated ages for this sample are within 0.17 years with a 95%

confidence interval. However, when using this method, he found it overestimated of the age at death of children younger than 6 years and warns that possible population differences might bias the age estimations (Cardoso 2007).

Age groups

Once individual dental ages are estimated, the skeletal information can be placed into groups of individuals which are similar in terms of dental development (Saunders *et al.* 1993). In theory, this should allow the comparison of individual children with the group standard (often represented as the mean of an age group) as well as the assessment of inter-population differences. However, while some studies note the confidence interval for individual bone measurements in each cohort, the range of variation in skeletal size within age groups is often not acknowledged (Hoppa 1992).

A second problem is the lack of methodological consistency in published reports (Saunders *et al.* 1993). One type of age grouping is based on a continuous scale, for example by dividing the data into growth phases, including Infants I (birth to 7 years), Infants II (7-14 years) and Juvenile, which marks the period just before the closure of the spheno-occipital synchondrosis around 22 years (Knussman 1988). Measurements can also be sorted according to age groups ranging from fetal, newborn to 0.5 years and one-year intervals for older children (Johnston 1962; Merchant and Ubelaker 1977) or even broader age categories (Bennike *et al*. 2005). Often, age categories are based on one year age groups (Hoppa 1992; Jantz and Owsley 1984; Lovejoy *et al*. 1990; Lewis 2002, Mays *et al*. 2008). However, the classification of these continuous growth phases differs according to the country where the research was conducted, leading to confusion when attempts are made to compare studies (Scheuer and Black 2000a).

A second type of age grouping is based on an ordinal scale and is achieved by seriating the data (Lovejoy *et al*. 1990; Saunders *et al*. 1993). However, this can create artificial subgroups of individuals who “do not quite fit” other categories, preventing future comparisons (Saunders *et al.* 1993).

Growth models

Skeletal growth comparisons can be carried out using either simple scatter plots or cross-sectional growth curves as a methodological basis (Mays *et al.* 2009; Saunders *et al*. 1993). Such visual approaches can then demonstrate whether children are smaller or

larger than children from comparable age groups and whether there is a trend for skeletal sizes to be larger or smaller in different samples (Humphrey 2000a).

Skeletal size at certain developmental stages can be expressed in various ways. Maresh (1943) presented the range of measurements for each age group in terms of percentile rankings. By plotting the percentile values for each age group and joining the corresponding percentiles by continuous lines, one is able to depict the zone distributions of values for bone length throughout the entire age range under consideration.

Percentiles are of limited use in archaeological assemblages, as samples sizes for individual age groups are often small and the midpoints for each group are therefore unlikely to be representative of the population average (Humphrey 2000a). As such, for archaeological assemblages, averages of bone measurements per age group are more suitable than growth percentiles (Humphrey 2000a). Means, standard deviations and ranges of measurements of the maximum diaphyseal length of long bones as well as percentages of relative increases in bone length have often been calculated for each developmental age group (Armelagos *et al*. 1972; Bennike *et al*. 2005; Hummert and Van Gerven 1983; Johnston 1962; Lewis 2002; Molleson 1993; Steyn and Henneberg 1996).

Most development studies compare data between different groups or populations, therefore an adequate control of population factors, in terms of age estimation, and mathematical descriptions of growth are both needed (Saunders 2000). For example, in order to correct for population-level differences in long bone size, subadult long bone lengths can be represented as percentages of the corresponding adult long bone lengths. In this way, the end point of growth is standardised (Humphrey 2000a, b; Lovejoy *et al*. 1990). In archaeological assemblages, this end point of growth (i.e. the adult long bone length) is always hypothetical and in such cases, the mean value of mature individuals within the same sample under study can be used as an estimate of final growth attainment (Humphrey 2003). Percentages of mean adult stature have also been calculated (Hoppa 1992), but the use of percentages attained from corresponding mean adult bone lengths are recommended, as these take into account variation in limb proportions (Hoppa 1992; Mays *et al*. 2008).

Visual inspection of graphs plotting skeletal size against dental age shows that these growth plots are curvilinear in form (Fig. 4.8). Additionally, longitudinal growth studies have shown that growth velocity is substantially greater in the first two years of life,

reflected in a steeper incline in the curvilinear plot during these early years (Eckhardt *et al.* 2005b; Maresh 1955; Martorell *et al.* 1995; Fig. 4.8). The mathematically modeling of these curvilinear plots is a commonly used approach to report the normal progress of growth in terms of describing, summarising and quantifying features and patterns (Himes 2004). Single growth curves, obtained by conventional general linear regression equations, are most often used (Cook 1984; Hoppa 1992; Hummert and Van Gerven 1983; Jantz and Owsley 1984; Lovejoy *et al*. 1990; Mays *et al*. 2008). Another approach is to use mixed effect regressions, which incorporate individual growth characteristics whilst simultaneously estimating a sample average curve (Johnson *et al*. 2013).

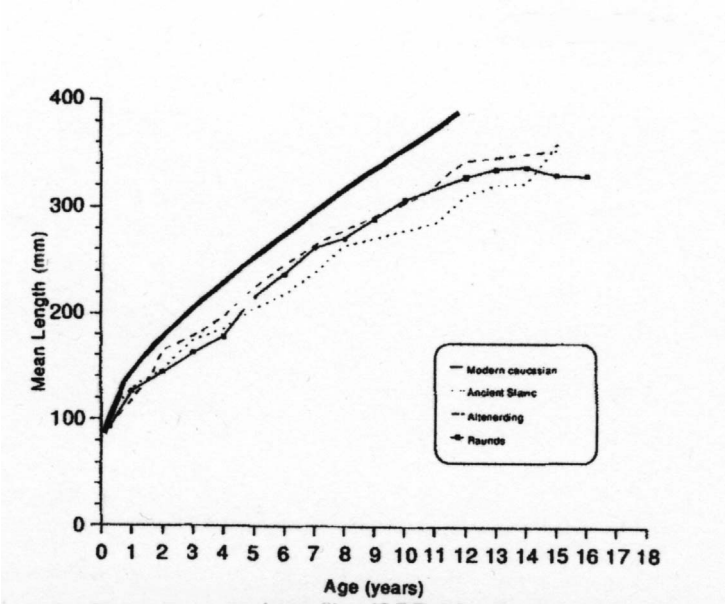

Figure 4.8: Example of skeletal growth profile based on femur (Hoppa 1992, 280)

Other mathematical models include polynomial regressions to fit curves onto the measurement means for each age category, which allows the analysis of the standardised residuals from this curve (Cardoso and Garcia 2009; Healy 1989; Humphrey 2000a; Mays *et al.* 2009). However, polynomial equations can bias results, particularly in the case of small sample sizes. As variation in long bone lengths increases with age, high residuals may be produced for older ages in cases where the sample includes fewer individuals from this age category (Cardoso 2005; Humphrey 2000a). Nevertheless, polynomial curve fitting procedures have been shown to work well when using a comprehensive sample such as the modern Denver reference sample (Humphrey 2000a).

As an alternative to polynomial curve fitting, a Z-score approach to the skeletal growth data can also be used and allows the mean bone size to be standardised across all ages (Cardoso 2005). For example Cardoso (2005; Cardoso and Garcia 2009), calculated Z-scores for femora by subtracting mean lengths of a reference sample from every observed length and dividing this by the standard deviation.

4.2.4. Limitations of skeletal growth studies

Cross-sectional studies of skeletal growth are based on deceased individuals who never reached maturity. The issue of biological mortality bias is therefore an important methodological problem in childhood growth studies (Humphrey 2003; Jantz and Owsley 1984; Johnston 1962; Johnston and Zimmer 1989; Lewis 2002; Scheuer and Black 2000a). The children examined in such studies are non-survivors who failed to adapt to environmental pressures and as such, do not represent the health of living children (Lewis 2002).

Practical difficulties associated with the study of growth patterns in the past, such as poor or biased preservation and recovery and small sample sizes also represent methodological limitations (Hoppa 1992; Hummert and Van Gerven 1983; Humphrey 2000a; Humphrey 2003; Jantz and Owsley 1984; Johnston and Zimmer 1989; Lewis 2002; Mays *et al*. 2009; Saunders 2000; Saunders *et al.* 1993; Scheuer and Black 2000a). The exclusion of neonate and infant remains from cemeteries or main adult burial sites, for cultural, religious or economic reasons might explain these differences in recovery (Saunders 2000; Scheuer and Black 2000a, b).

In terms of preservation, it has been suggested that preservation declines more rapidly with decreasing pH in juvenile bones than adult bones (Gordon and Buikstra 1981; Henderson 1987). While this might be the case for some immature bones, such as the fragile calvaria and facial bones, other skeletal elements (base of the skull, parts of vertebrae and most of the long bones) survive as well as their adult counterparts (Scheuer and Black 2000a; Sundick 1978). In effect, the largest bias in subadult bone preservation might be related to a limited ability to recognise subadult bones rather than different physicochemical properties (Saunders 2000; Scheuer and Black 2000a; Sundick 1978).

Another bias relates to how representative the sample is of the living population in terms of ages, as differences in susceptibility to illness and disease occur at specific ages. For

example, during the postnatal period, which includes children from birth to five years of age, growth is significantly more sensitive to developmental disruptions than during the post-infant period (Beaton *et al.* 1990; Eveleth and Tanner 1990; Hoppa 1992; Lovejoy *et al*. 1990; Saunders *et al.* 1993).

Different methodological approaches to ageing can also introduce a bias in growth assessments (Humphrey 2003; Merchant and Ubelaker 1977). If age is underestimated, the size of skeletal elements will be underestimated and as such, growth trajectory differences between groups might arise, not as a physiological indicator of more or less stressed individuals, but as a result of methodological differences in the technical approaches to age assignments (Humphrey 2003).

Finally, a major problem in the analysis of immature skeletal remains is the difficulty of reliably sexing juveniles (Scheuer and Black 2000a). Knowledge about sex differences in the growth rates of boys and girls is well established in the literature and these differences are also found in skeletal growth (Humphrey 1998; Maresh 1943; Saunders 2000). As males and females exhibit different rates of growth, age categories obtained by the assessment of skeletal growth are necessarily wider than they would be if sex had been known (Scheuer and Black 2000a).

4.2.5. Skeletal growth and “stress indicators”

The potential of combining the study of skeletal growth and assessments of non-specific stress indicators has been previously explored, with varying results (Flores-Mir *et al*. 2005). Evidence of enamel hypoplasia has been used as such an indicator (see above) as well as the presence of Harris lines, which are long growth arrest lines representing areas of increase bone density during insults to the growing long bones (Bennike *et al*. 2005; Mays 1985; Mays 1995; Molleson 1993; Ribot and Roberts 1996). This section will focus on the association between enamel hypoplasia and skeletal growth patterns.

Bennike and colleagues (2005) compared skeletal growth and enamel hypoplasia patterns between two Danish Medieval assemblages (Næstved, a leprosarium and Æbelholt, a “privileged” community). They found that both sites showed similar growth patterns up to the 10.6-14.5 age category, in which the mean diaphyseal lengths of the femur and tibia from the leprosarium sample were significantly ($P<0.05$; Wilcoxon rank

sum test) shorter in comparison to the “privileged” sample. They also found a significantly higher percentage of individuals affected by enamel hypoplasia in the leprosarium sample in comparison to the “priviliged” sample.

Lewis (2002) compared long bone growth patterns with frequencies of dental enamel hypoplasia from four Medieval and Postmedieval English sites (Raunds Furnells, Northamptonshire, St. Helen-on-the-Walls and Wharram Percy in Yorkshire and Christ Church Spitalfields in London). She found that the Spitalfields individuals were significantly shorter than those from St Helen-on-the-Walls. In contrast, a higher percentage of individuals was affected by enamel hypoplasia in St Helen-on-the-Walls in comparison to the Spitalfields sample, but this difference was not significant.

Finally, Ribot and Roberts (1996), in their assessment of two Medieval samples (Raunds and Chichester) found that non-specific stress indicators, including enamel hypoplasia, did not correlate with the growth of long bone lengths, as “very stressed” and “less stressed” individuals did not systematically show different skeletal growth patterns.

One explanation for the contrasting results from published studies is the fact that these studies only looked at the length of long bones. Various researchers have argued that the growth of the length of long bones adapts to stress at the expense of other skeletal variables such as cortical width (Himes *et al*. 1975; Huss-Ashmore *et al*. 1982; Mays 1995; Ribot and Roberts 1996). As such, the inclusion of skeletal variables other than long bone diaphyseal lengths, such as diaphyseal and metaphyseal widths in combination with enamel hypoplasia/skeletal growth studies should provide more information regarding the relationship between skeletal and dental growth in past populations.

Another explanation for the lack of association between the appearance of enamel hypoplasia and skeletal growth patterns might be the effect of catch up growth (Mays 1995). It is possible that the skeletal growth of some children who survived stress episodes (as identified by enamel defects) returned to its original trajectory. As such, catch-up growth, the return to the original growth curve achieved by an accelerated re-initiation of growth after a physiological disturbance, makes it impossible to detect delayed growth in some individuals.

A final potential reason for the contrasting results of the skeletal and dental comparisons is related to the identification of delayed skeletal growth and enamel hypoplasia. For

example, the studies by Ribot and Roberts (1996), Lewis (2002) and Bennike and colleagues (2005) identified enamel defects macroscopically and used calculations of the percentage of individuals affected in their comparisons. These methodological approaches have various shortcomings and are discussed above (p. 121). A more detailed analysis of dental growth, including statistical assessments of various hypoplasia parameters (number of defects, interval, duration, age at occurrence, etc.) should provide more conclusive results for the assessment of combined dental and skeletal growth of subadults.

Chapter 5. Methodology

The aim of this chapter is to provide a methodological basis for the construction of detailed records of growth based on detailed developmental sequences of individuals (see Chapter 4). The methods used to answer the methodological and archaeological research questions set out at the beginning of this thesis (see Chapter 1) are described in detail and include a new three-dimensional technique for the analysis of systemic growth disruptions using incremental microstructures of enamel (section 5.1) and the use of cranial and postcranial skeletal variables for a detailed assessment of skeletal growth (section 5.2).

5.1. Furow-form enamel hypoplasia

A wide variety of methods, both micro and macro, have been developed with which to study furrow formed enamel hypoplasia (see Chapter 4). Goodman and Rose (1990), Dobney (1991) and Hillson and colleagues (Hillson and Bond 1997; King *et al*. 2002, 2005 set out various fundamental issues to be addressed in terms of enamel hypoplasia studies, including:

a. The need for permanent records to be created in the form of photographs and casts as a routine procedure

b. The importance of preparation and recording methods being standardised

c. The need to take into account the geometry of crown growth when recording and identifying furrow-form enamel defects, as different parts of the crown present the same defect differently. This can be achieved by linking enamel defects to incremental structures in the enamel surface (perikymata).

Taking into account these recommendations, a new three-dimensional technique (Alicona 3D Infinite Focus imaging microscope and software) is used to study developmental features in the enamel of human incisors. The technique, using high-resolution casts of tooth crowns, allows for a direct on-screen comparison to be made between measurements and images, and both records can also be exported for later use with different software. Using this new technique, perikymata are measured down the crown, perikyma spacing profiles constructed and anomalies within these profiles detected.

This section section on enamel hypoplasia (5.1) consists of three parts: the first part introduces the methods employed in order to obtain surface records of each tooth, including cleaning, casting, imaging and recording. The second part is a case study assessing two mathematical approaches (Z-scores and curve fitting) applied to the identification of anomalies in the perikyma spacing profiles. The results of these comparative case studies serve as a basis for the subsequent analysis of the entire dataset. Finally, the third part of this section describes the methodology for the interpretation of identified defects, including the matching of defects across the dentition of one individual and the comparison of defects between individuals.

5.1.1. Data collection procedures

Cleaning, casting and imaging

As the imaging of the crown surface is influenced by the cleanliness of the teeth (Russ 2007), all tooth crowns were cleaned using acetone-impregnated cotton wool prior to imaging. The teeth could not be exported from Çatalhöyük, so impressions of the crown surfaces were taken on site and positive casts were made at UCL. Similar tooth replication techniques are often used in palaeontology and anthropology, as many original specimens are too valuable to be studied directly (Galbany *et al*. 2004).

For this study, Coltène President's Jet Light Body Plus (polyvinylsiloxane), was used to make crown surface impressions. This is a widely used high-resolution dental impression material, as it is easily released from delicate archaeological specimens and cures rapidly at room temperature (Hillson 1992). It is also a highly accurate technique for replicating small features from the surface of a tooth such as enamel prisms (Beynon (1987, Galbany *et al.* 2004).

The Light Body polyvinylsiloxane was applied to the whole crown surface with a spatula. Impressions were gently released from the teeth and kept in plastic bags to protect them from dust. Back in London, positive casts of the entire crown surface were made using Epotek 301 epoxy resin. The resin and hardener were mixed at a 1:4 ratio and carefully poured in the impressions using a pipette in order to eliminate possible air bubbles and left to dry for at least 48 hours. These types of casts have been show to preserve high resolution of the surface detail at less than 1μm (Beynon 1987; Hillson 1992).

The high reflectivity and translucency of tooth enamel makes it extremely difficult to capture complete 3D Alicona images of crowns (Bello *et al.* 2011). The resin casts were

also glossy and translucent, but gold sputter-coating resolved this issue and allowed clear images to be made (see Hillson, 1992; King *et al.* 2002, 2005).

The Alicona InfiniteFocus was used to capture and study images of the casts. It is a three-dimensional measuring microscope. It is fitted with a motorised stage which moves from side to side (X axis), forwards and backwards (Y axis) and vertically (Z axis). The replicas were positioned on the stage with the labial side upwards (Fig. 5.1). The light source is provided through a beam splitter to a series of objectives contained in a six-place nosepiece and the specimen's reflected light is returned through the same objective and projected through the beam splitter onto a digital sensor. The magnification and therefore the resolution with which features can be seen can be selected through changing the power of the objective. As in a conventional light microscope, the depth of focus decreases with the increasing power of the objective chosen but, in general, is relatively small. The focus depth is also smaller with slow scan speeds and larger with fast scan speeds. Highest resolution is therefore achieved by slow scans using a high power objective. These lenses, however, also have the smallest field of view. There is therefore a trade-off between resolution, the time taken to scan each separate image, and the number of images required to cover the full height of the tooth crown.

Figure 5.1: Image of the Alicona InfiniteFocus instrument

Through experimentation with the screen image, the highest and lowest Z axis settings of the microscope stage are chosen to include the full range of crown surface features required. Once this range is defined, the instrument moves the stage gradually from lowest to highest, to scan a series of image planes. Software is used to construct a detailed three-dimensional model of the surface from this stack of images, calculating x, y, and z coordinates for any point within the resolution of the scan (Fig. 5.2).

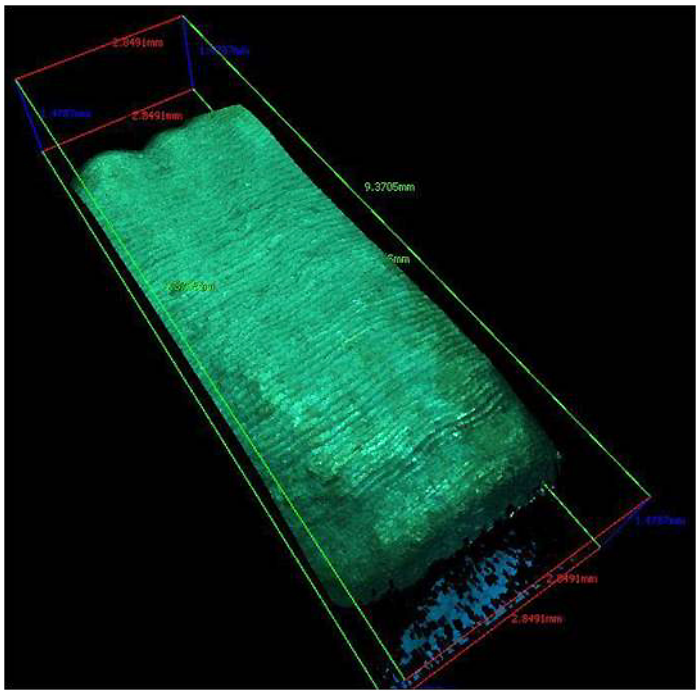

Figure 5.2: Three-dimensional model of lower central incisor crown, labial surface

Higher magnifications involve longer scanning times (Table 5.1) and it was found that higher magnifications also resulted in longer experimentation times with exposure and contrast settings (Elhechmi *et al*. 2013). For example, four hours were needed to scan one crown surface with a 10x objective, whereas for a 20x objective, an additional hour was necessary to obtain clear images. Images taken at a higher magnification also needed to be stitched together, potentially introducing a bias in the measurements.

A compromise between scanning times and the resolution of the images was achieved by scanning coated replicas of tooth crowns using a 5x objective lens, which produced acceptable images in which perikymata could be clearly identified and measured (Fig. 5.2, 5.3). In effect, this fits previous experience, in which it was found that objective lenses required for practical imaging of perikymata have a depth of focus of around 7μm (Bocaege *et al.* 2010). Images of the tooth crowns were captured from the cusp tips to the

cemento-enamel junction, along the mid-sagittal line of the labial surface of the anterior teeth using a vertical resolution of 8μm and a lateral resolution of 1.75 x 1.75μm. This allowed the capture of the entire tooth crown in one scan and thus avoided any bias introduced by overlapping fields of view.

Table 5.1: Technical specifications: objective details of Alicona InfiniteFocus (based on Lexa 2008)

Objectives	**2.5x**	**5x**	**10x**	**20x**	**50x**	**100x**
Lateral resolution	5.6μm	2.2μm	1.1μm	0.8μm	0.6μm	0.4μm
Vertical resolution (low speed)	2.3μm	0.4μm	0.1μm	0.05μm	0.02μm	0.01μm
Vertical resolution (high speed)	47.1μm	8.2μm	2μm	1μm	0.4μm	0.2μm
Scan speed (low)	112μm/s	20μm/s	5μm/s	2.5μm/s	1μm/s	0.5μm/s
Scan speed (high)	2300μm/s	400μm/s	100μm/s	50μm/s	20μm/s	10μm/s

Recording

The Alicona software renders images of the three dimensional surface model in different orientations and with the relief outlined by different directions of illumination and shadow. Through experimentation, it was possible to select image parameters that outlined the perikymata clearly, with the most cuspal at the top and the most cervical at the bottom.

A profile line was drawn down the image and this appeared as a graph underneath, with the horizontal axis recording the distance along the profile and the vertical axis the relative height of the surface. The vertical relief of the perikymata was found to be very small indeed – fractions of a micrometre – so they were not always recognisable in the profile. Instead, the image was used to identify the positions of the perikyma grooves along the profile line. A cursor matched these positions on the profile graph and it was possible to read off the horizontal and vertical coordinates of each one. One of the limitations of the Alicona software for this application is that these cannot be directly exported, so they were all noted and entered separately into an Excel spreadsheet. With a profile line drawn down the vertical axis of the tooth crown, this process was repeated from the first visible perikyma near the cusps/central mamelon to the cemento-enamel junction at the cervical base of the crown (Fig. 5.3). The spacing between pairs of perikyma grooves was calculated in the spreadsheet by simple application of the Pythagoras formula. In addition, cumulative spacing was calculated by continuously adding the pair-by-pair spacing, from cuspal to cervical. The rendered image of the crown surface model was exported as a JPEG file and each recorded perikyma groove was labelled on this exported image (using Microsoft Paint), so that it could be compared directly with graphs of the measured spacings.

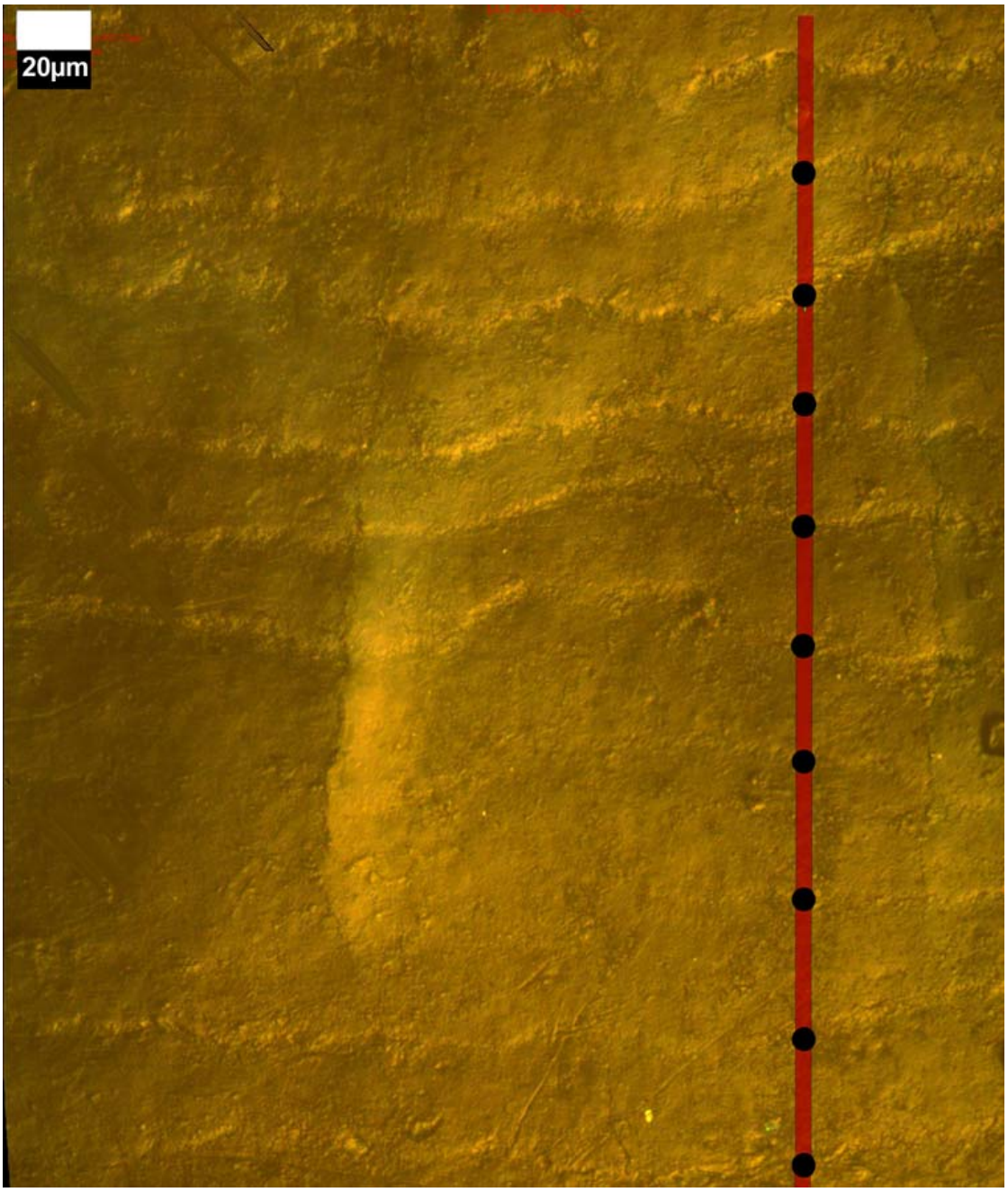

Figure 5.3: Labelled image of part of the crown of a lower central incisor

Nature of the dataset

Most recent enamel hypoplasia studies are based on the pioneering work of Hillson and colleagues, in which wider than expected spacings between consecutive pairs of external incremental growth markers (perikymata) were used as indicators of furrow-form enamel hypoplasia (Guatelli-Steinberg *et al*. 2004; Hassett 2011; Hillson and Jones 1989; Hillson

1992; Hillson and Bond 1997; King *et al*. 2002, 2005; Temple *et al*. 2012, 2013; Witzel *et al* 2008).

In order to obtain information about the density of perikymata, the latter can be counted over a particular distance (for example, per decile of crown height). These counts can then be used to estimate the average perikyma spacing within that region of the crown (Dean and Reid 2001; Guatelli-Steinberg *et al*. 2005, 2007a, b; Ramirez Rozzi and Bermudez de Castro 2004; Reid and Dean 2000). Using coordinates to calculate direct spacings, rather than perikyma counts, has the added advantage of allowing a comparison between the actual perikyma spacing and the underlying trend of a progressive decrease in spacing along the crown surface (Bocaege *et al*. 2010).

Perikyma spacing profiles can be presented either: as a direct plot of the horizontal and vertical coordinates for each perikyma groove; as a plot with the count of perikymata along the horizontal axis and the spacing (or cumulative spacing) along the vertical axis (Fig. 5.4: in blue), or as a plot with the count of perikymata along the horizontal and axis and the vertical coordinates along the vertical axis (Fig. 5.4: in green) or a combination of these. Most studies have used a relatively standard optical microscope to measure the vertical coordinates (Hillson and Jones 1989; Hillson 1992; King *et al*. 2002; Temple *et al*. 2012, 2013).

Graphs representing the vertical coordinates typically appear slightly bulging (Fig. 5.4), following the labial bulge of the incisor or canine crown side. Furrow-form defects of enamel hypoplasia are characterised by depressions in the enamel surface, and as such, enamel defects can be identified as major troughs within such surface graphs (Fig. 5.4). These surface depressions can also be associated with irregular changes in a plot of perikyma groove spacing (Hillson and Jones 1989; King *et al*. 2002; Temple *et al*. 2012, 2013) and this is the approach used here.

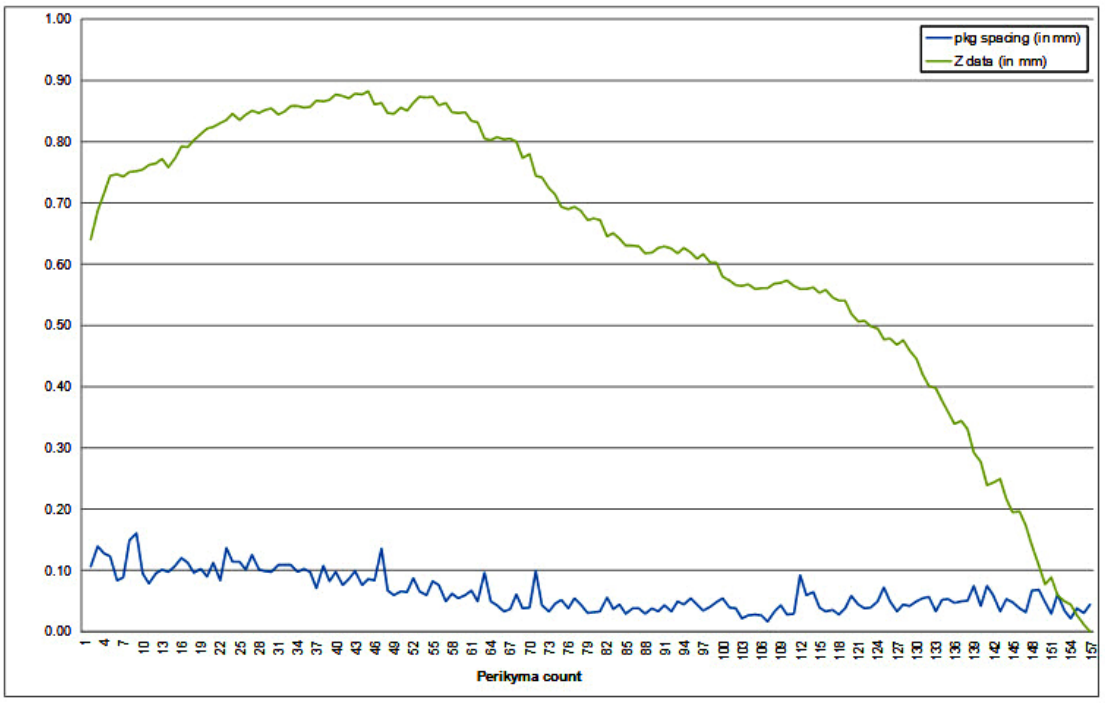

Figure 5.4: Enamel surface (green) and perikyma spacing (blue) profile for lower left lateral incisor

Perikyma spacing profiles show a marked decrease in spacing down the crown. For example, in Figure 5.4, the perikyma spacing ranges from 161μm (around the 8th perikyma) to 17μm (around the 106th perikyma), with averages of around 100μm for the first 50 perikymata pairs and around 50μm further down the crown. Wider spacings in the occlusal/cuspal part of the crown are caused by shallow angles of striae of Retzius with the surface, the closer spacing towards the cervix is caused by the sharper angles of striae of Retzius in the mid-crown and cervical parts of the tooth (see Chapter 3).

The detection of anomalies in this overall perikyma spacing trend is not a simple process, due to the variation in spacing between different parts of the crown. There is a general decrease in spacing down the crown and around the circumference of the crown. For example, a recent study compared the spacing between equivalent pairs of perikymata across the crown of a lower central incisor and found that the perikyma spacing varied in a particularly striking way between various locations across the crown, from a 5μm spacing in the middle part of the crown to a 40μm spacing in the corresponding mesial and distal parts (Bocaege *et al.* 2010).

If an analogy is made with signal processing, the variation in perikyma spacing can be referred to as noise. This so-called noise in the perikyma spacing profile needs to be

reduced in order to isolate the spacing trend down the crown. A fundamental problem in the signal processing literature involves the distinction between noise and signal, the signal being the measurement of interest and the noise the standard deviation from this measurement (O'Haver 2013). The noise can be estimated by looking at visible short-term fluctuations within the dataset, which are superimposed over a smoother signal. The reduction of noise in a dataset can be achieved by smoothing processes. Various algorithms can be used to smooth a dataset; including digital filters such as spline-wavelet filters and Fourier transform (Jiang *et al*. 2007).

In time series analysis, where data points are measured at successive point in time at regular intervals such as annual rainfall, a moving average is often used in order to highlight long-term trends (Longobardi and Villani 2010). Similarly, Hassett (2011) used local sets of neighbouring perikymata rather than separate distance values in order to capture the gradual trend of perikymata spacing down the crown. As such, instead of using one mean and standard deviation for the entire dataset, a moving mean and standard deviation can be used in order to identify anomalies in the spacing pattern.

A second approach is to express perikyma spacing in terms of distance from the first identified perikyma groove (Hillson 2014). That is, the distance to each successive perikyma groove is added on to the sum of all previous distances. This means that distances between perikyma grooves are not assessed individually, but considered as part of a cumulative process producing the final crown height of each tooth. As such, attempts can be made to describe the overall cumulative growth, bypassing the issue of noise because minor spacing variations down and around the circumference of the crown are minimised across the vertical (occlusal to cervical) sequence. When these cumulative perikymata measurements are plotted against time (in terms of perikymata), a longitudinal growth curve is constructed, to which a range of mathematically defined curves can be fitted in order to capture the underlying, normal trend of tooth growth (Fig. 5.5).

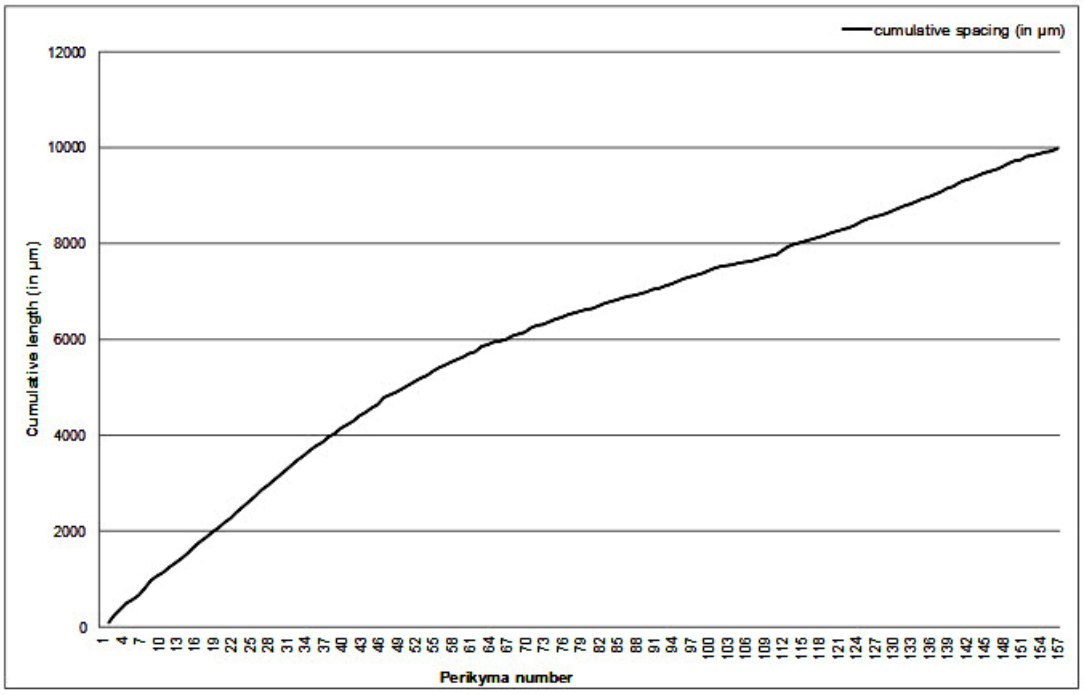

Figure 5.5: Cumulative spacing plot on perikyma counts for lower left lateral incisor

A preliminary study was carried out using two noise reduction methods and these results were used to identify the best method for assessing the data for this project:

1. Separate perikyma spacings, smoothed by moving averages
2. Cumulative perikyma spacings to which a curve is fitted.

Anomalies were identified using moving averages by calculating modified Z-scores and for the cumulative measurements, residuals were assessed from the fitted curves. The following section describes these approaches in detail and compares their ability to isolate the perikyma spacing trend down the crown and as such, to detect spacing anomalies. However, before embarking on this preliminary study, an error study was carried out in order to compare measurements between replicas and original teeth and to assess observer reliability.

Measurement error

The teeth could not be exported, so it was impossible to carry out a large scale comparison between measurements taken from original teeth and those from casts. A small study, however, was undertaken on the material housed at UCL, which compared measurements taken using the Alicona InfiniteFocus at the same points on the tooth

crown of a replica and an original of the same tooth (upper left central incisor of individual CH EVI7k40). The same number of perikymata was identified on both specimens and a visual examination of the measured perikyma spacings revealed no major differences, with both cumulative spacing plots showing an almost identical shape (Fig. 5.6).

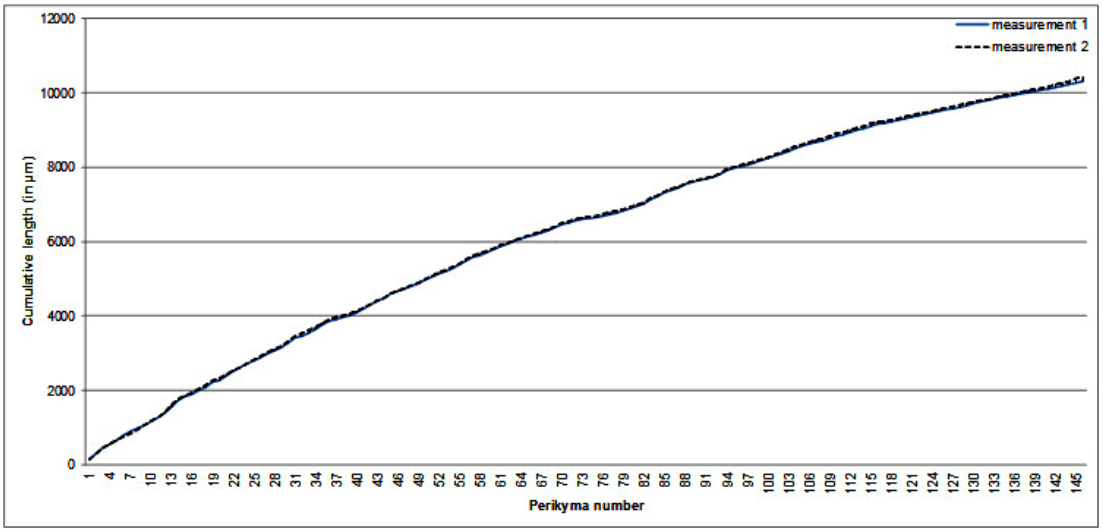

Figure 5.6: Cumulative spacing of measurements taken on upper left central incisor crown and replica (dotted line = replica, straight line = original)

In order to compare observer reliability with previous studies, an error study for perikyma counts was carried out based on the method outlined by Guatelli-Steinberg (2003). A profile line equivalent to 1mm was drawn along the vertical axis of the tooth from the occlusal extremity of the crown towards the cervical base of the crown. Perikymata were counted down this line for 20 cases (two teeth per randomly chosen individual) on two separate occasions. Similarly to Guatelli-Steinberg (2003), percent error was calculated using Calcagno's method (1989, 13), where the difference in measurement pairs is expressed as a proportion of the first measurement. The total of these values was then divided by the number of cases (20) and multiplied by 100 to give the percent error.

In this error study, the sum of values amounts to 0.39, corresponding to a percent error of 1.96% (Table 5.2) As such, the results from this quantitative analysis indicate an intra-observer error of less than 2% for perikymata counts, which is much lower than the previously reported error rates of 5% and 2.4% (Dean *et al*. 2001; Guatelli-Steinberg 2003).

Table 5.2: Percent error calculations (based on Calcagno 1989; Guatelli-Steinberg 2003)			
Specimen	**Perikyma count 1**	**Perikyma count 2**	**Calcagno proportion**
CH 7k40 URI1	8	8	0.00
CH 7k40 LLI2	8	8	0.00
CH 7k40(3) LLI1	7	8	0.14
CH 7k40(3) LRI2	8	8	0.00
CH 6682 LLI2	8	8	0.00
CH 6682 ULI1	7	7	0.00
CH 12876 ULI1	7	7	0.00
CH 12876 URI1	6	6	0.00
CH 6681 LRI1	10	9	0.10
CH 6681 ULI2	7	7	0.00
CH 1913 LLI1	8	8	0.00
CH 1913 LLI2	8	8	0.00
CH 1933 LRI2	6	6	0.00
CH 1923 URI1	6	6	0.00
CH 1925 LRI2	7	8	0.14
CH 1925 ULI1	7	7	0.00
CH 2119 LLI2	8	8	0.00
CH 2119 ULI1	8	8	0.00
CH 12935 LLI1	7	7	0.00
CH 12935 ULI2	6	6	0.00
		TOTAL	**0.39**

5.1.2. Identification of defects

Microscopic images (captured by the Alicona InfiniteFocus) of tooth crowns from one individual with antimeric teeth present were visually assessed for clear and well-delineated defects (CH 6682) and the visually identified defects were confirmed by assessing enamel surface profiles and perikyma spacing profiles (see Fig. 5.4). More specifically, a total of four clearly delineated and visually identified defects were evaluated with each method (Z-scores and curve-fitting procedures) for individual teeth. The outcomes were then compared between antimeres.

Z-scores

The use of Z-scores is a way to standardise outcomes in a continuous distribution (Madrigal 2000). Z-scores are standard deviation scores, which are calculated by dividing the difference from the mean by the standard deviation:

$$Z = \frac{x - \mu}{\sigma}$$

Where x is the value to be standardised, μ is the mean and σ the standard deviation. In this case, the individual spacings between immediately adjacent perikymata are plotted on the vertical axis against the count of perikymata on the horizontal axis. The x values are the individual spacings at given perikymata. The mean, therefore, cannot be the overall mean of spacings down the tooth crown, because these decrease systematically. In order to remove this effect, Hassett (2011) calculated a separate mean and standard deviation for each x value in the profile from the distances of a group of nearby perikymata. The size of this group remained constant down the profile. This was, in effect, a moving average smoothing of the distance curve. The smoothing effect increased with the number of neighbouring perikymata included.

Hassett (2011) recommended using 11 neighbouring measurements to calculate moving averages and standard deviations, but in this study, various other sets of measurements (5, 7, 9 and 13) were also assessed. In effect, the Z scores show the deviation from the smoothed curve for each perikyma spacing, standardised by the overall variability in that region of the curve. In theory, this should highlight those spacings which diverge markedly and therefore represent a defect. The size of the moving average group has an effect on this divergence, with larger groups giving stronger smoothing to the profile and thus making minor divergences less prominent.

An arithmetic mean is strongly affected by outlying values and an inspection of the profiles shows that there is wide variation above and below the smoothed line. A median is a more robust measure of central tendency in these circumstances because it is less affected by outlying values. This leads to a more robust way of calculating the Z score, as in the WHO Global Database on Child Growth and Malnutrition (de Onis and Blössner 1997), using the median and the median absolute deviation (MAD) as follows:

$$Z = \frac{value - median}{MAD}$$

Where the median absolute deviation is calculated by taking the median of the absolute deviations from the median:

Median($|X_1\text{-MED}|$, $|X_2\text{-MED}|$, ... , $|X_n\text{-MED}|$).

As for the approach using the arithmetic means (see above), sets of adjacent perikymata distances (5, 7, 9, 11 and 13 sets of measurements) were used to calculate the median and MAD.

It was necessary to define rules for the recognition of anomalous perikyma spacings that might confirm or indicate the presence of a defect. Two approaches, setting an arbitrary threshold value, were tested here. The first approach was to set the threshold for both types of Z scores (based on means and medians) at 2 standard deviations (following de Onis and Blössner 1997 and Hassett 2011).

The second approach was to use percentile ranks based on both calculated Z-scores (Madrigal 2000). Z-scores and percentiles can be converted to each other, but the commonly used threshold values are not at comparable levels. The commonly reported statistical boundary of 2 standard deviations for the Z-scores, for example, corresponds to the 97.7th percentile (Madrigal 2000; Wang and Chen 2012). One of the aim of this study was to trial more sensitive indicators of defect presence in comparison to the Z-scores and as such, the use of two arbitrary percentile threshold rankings was tested. One threshold ranking was set at the 75th percentile (equivalent to Z-scores of 0.68 and above) and a second threshold ranking was set at the 90th percentile (equivalent to Z-scores of 1.29 and above).

Curve fitting

The second approach tested here was to plot cumulative perikymata measurements on the vertical axis against the count of perikymata on the horizontal axis. Tests with parametric curves (least squares, cubic, polynomial) showed poor fits, particularly at the start and end of the series. Locally weighted scatter plot smoothing (LOWESS) proved to be a more flexible method and has a previous history of success in modelling primate growth and hominoid canine extension rates (Leigh 1992, 1996; Schwartz and Dean 2001).

LOWESS is a non-parametric method which fits parametric functions to localised subsets of the independent variables using weighted least squares in a moving fashion, similar to the way a time series is smoothed by moving averages (Cleveland and Devlin 1988; Cleveland and Grosse 1991; Jacoby 2000; Kohler *et al*. 2008).

Using non-parametric approaches such as LOWESS fitting, linearity is assumed over short, local sets of data (Moses *et al*. 1992). LOWESS is essentially a method for fitting a regression relationship to noisy data (Cleveland and Grosse 1991; Jacoby 2000; Kohler *et al*. 2008). As the LOWESS method requires fairly large and densely sampled datasets

in order to produce good models, cumulative perikyma spacing curves were deemed a good application of this method (Guthrie 2012). Finally, this procedure is relatively "resistant" to outlying values than other smoothing functions (Moses *et al*. 1992) so it effectively addressed the problems outlined above.

For LOWESS, the smoothness of the fit depends on α, a specific neighbourhood parameter and the definition of λ, the degree of the local loess polynomial (Cleveland and Grosse 1991; Jacoby 2000). The neighbourhood parameter α represents the number of points included, so larger values produce the smoothest functions, whereas fewer points in an analysis (smaller α) emphasise fluctuations in the data. Typically, α is set between 0.25 and 0.50 (Peltier 2009). However, many exceptions to this generalisation exist and in practice, α values are almost always determined using an iterative process using the residuals from the LOWESS fit as a diagnostic tool to assess goodness of fit (Cleveland and Grosse 1991; Jacoby 2000).

In relation to lambda, the local polynomials are typically of the first or second degree. Locally linear fitting (λ=1) applies to monotone data patterns, where values either gradually increase or decrease, whereas locally quadratic equations (λ=2) are used to assess non-monotone data patterns which exhibit local minima and maxima (Jacoby 2000).

Visual inspection of the cumulative scatterplot shows that the values gradually increase and as no local maxima can be discerned, locally linear fitting (λ=1) was considered sufficient to produce a curve that follows the data accurately. In order to select the most appropriate α value, the LOWESS fitting procedure was carried out using groups of 60, 45, 30 and 15 neighbouring points, corresponding to α values of 0.4, 0.3, 0.2 and 0.1 respectively. Residuals for the resulting curves were plotted against the count of perikymata (Fig. 5.7).

For α = 0.4, 0.3 and 0.2 it is still possible to make out the underlying trend, caused by larger perikyma spacings in the occlusal to mid-crown part of the tooth and small spacings in the cervical part. This trend was eliminated only in the plotted residuals of the fitted curve for α = 0.1 with values evenly distributed above and below the zero line (Fig. 5.7). Removal of the underlying trend was the central purpose of the procedure, so this low α value, corresponding to 15 neighbouring points, was chosen in order to identify departures from the trend more effectively.

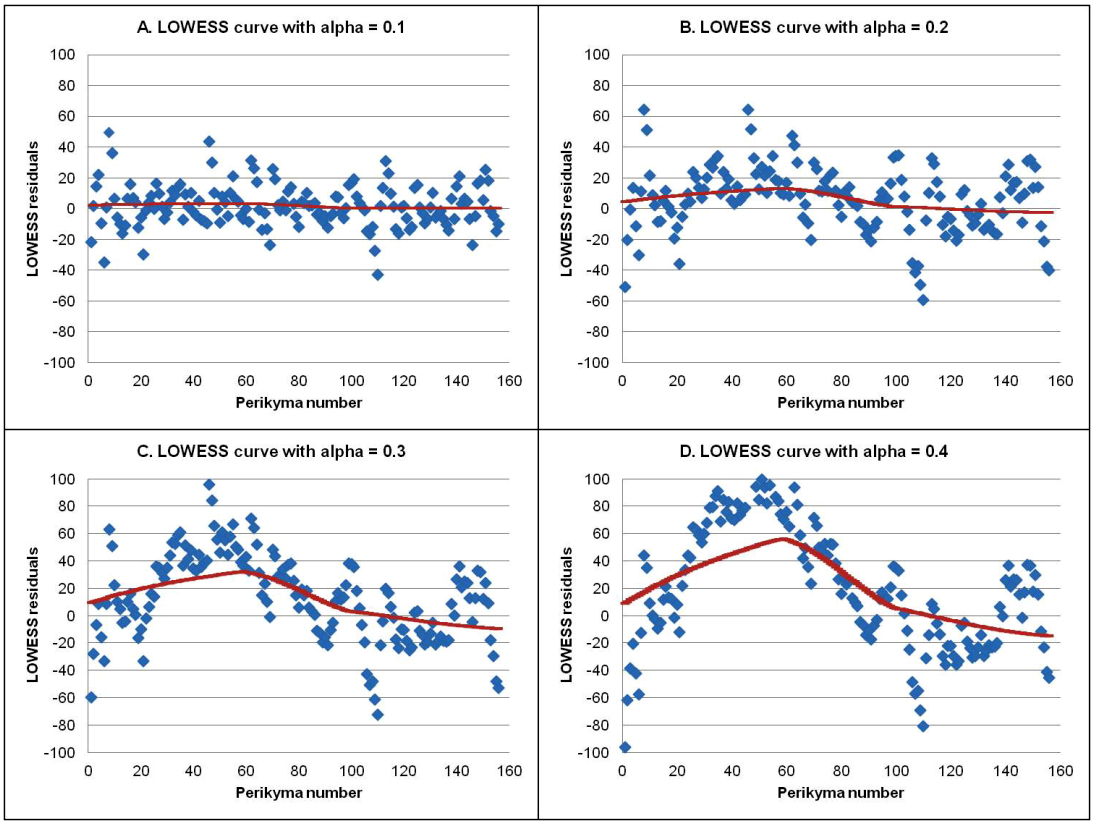

Figure 5.7: Effect of the alpha parameter on the LOWESS residuals. Residual plots from LOWESS curve fitted to cumulative perikyma spacings using alpha values of 0.1, 0.2, 0.3 and 0.4 corresponding to 15, 30, 45, 60 neighbouring points. Solid red line is LOWESS curve fitted to the residuals using an alpha value of 0.75 (method based on Jacoby 2000)

After fitting the curve using this value, residuals were calculated for each point in the curve as the ratio of the observed value to the predicted value given by the LOWESS curve for that point. Anomalies should stand out because of their high residual value (Moses *et al*. 1992). Percentiles were determined for the combined residual values. As measured values at or above the 90th percentile are commonly defined as threshold criteria in the medical literature (Messiah *et al*. 2010), perikymata spacings producing residuals greater than the 90th percentile were regarded as anomalous.

Case study

Figure 5.8 combines three plots against the perikyma count along the horizontal axis for the **lower left lateral incisor** of CH 6682. In green is the vertical coordinate from the Alicona InfiniteFocus profile for each perikyma groove, which is called here the *enamel surface profile*. In blue is the spacing between each perikyma groove and its cervical

neighbour, ranging between 0.16 and 0.02mm. In red is the curve of perikyma groove spacings, smoothed by a running median using a group of 13 neighbouring perikymata.

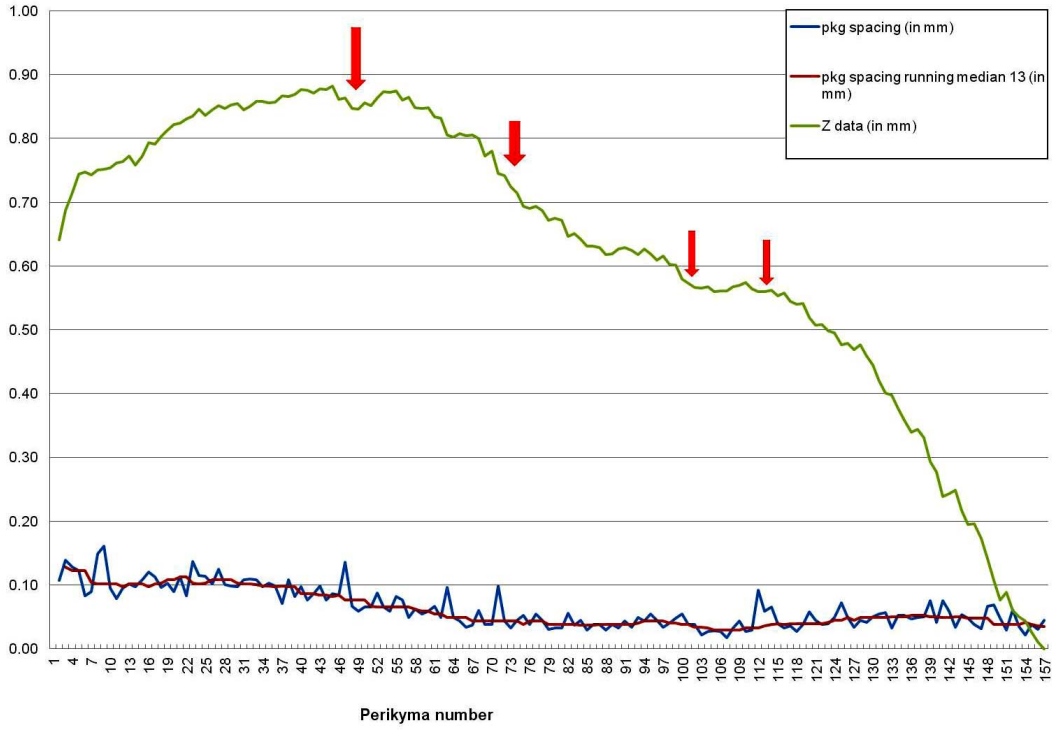

Figure 5.8: Enamel surface (green) and perikyma spacing (blue) profile for lower left lateral incisor (CH 6682), smoothed using a group of 13 neighbouring perikymata (red). Red arrows indicate visually identified defects corresponding to those listed in Table 5.3

The image of this tooth crown shows there were four clearly defined furrow-form defects which could be matched exactly to those on the image of the right lateral incisor (Table 5.3, Fig. 5.9, 5.12). These defects were also detected in the green enamel surface profiles for both teeth, in which each of these defects appeared as a sharp depression in the line (Fig. 5.8). The blue line representing the perikyma spacing matched the enamel surface profile with peaks for defects A, B and D, but the peak for defect C is less clear (Fig. 5.8). In addition, peaks were also observed in the perikyma spacings which had not been associated with a defect noted during visual examination of the image alone. The pattern of irregularities is the same in both antimeres of the lower lateral incisor.

Table 5.3: Visually identified, clearly delineated defects on lower lateral incisors (CH 6682)	
Defect	Perikyma numbers (pkg)
A	45-51
B	68-75
C	96-103
D	111-114

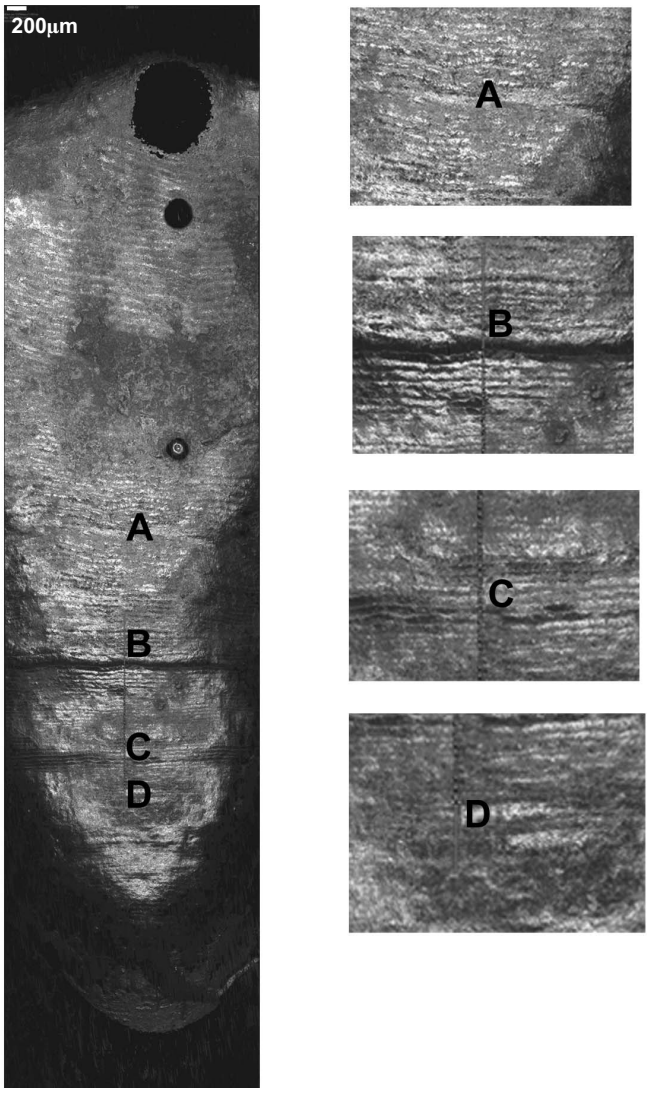

Figure 5.9: Image of the lower right lateral incisor (CH 6682). Letters correspond to visually identified and metrically verified defects (see Table 5.3)

Figure 5.10 shows Z-scores of the perikyma spacing profile from Figure 5.8, calculated using the two methods described above. In blue are the Z-scores calculated using a moving mean and standard deviation based on groups of 13 neighbouring perikymata. The values vary from -1.9 to 2.9. None of the values fall below -2 but for six perikyma pairs the value is +2 or more. As explained above, this is the threshold value. Defects A, B and D are all matched by a Z-score of more than +2, whereas defect C is not. In addition to these visually identified defects, there are three perikyma pairs with scores of +2 or more. In red are the Z-scores calculated using a running median and MAD based also on groups of 13 neighbouring perikymata. This shows a pattern of peaks and troughs which is in many ways similar to the Z-scores calculated using a moving mean and standard deviation based on groups of 13 neighbouring perikymata (highlighted in blue), but the

peaks are much more marked. In particular, there are very clear peaks matching defects A, B and D. The peak for defect C does not rise any higher than other peaks in the graph based on moving means and in fact there are 16 other peaks which rise to the same level or higher.

In terms of the metric approaches, it was found that defects were very difficult to detect using Z-scores determined by moving means, running medians and standard deviations of neighbouring sets of measurements lower than nine (four preceding and succeeding measurements), as these did not sufficiently smooth the dataset. Similarly, the use of the 75th percentile from Z-scores based on moving means and running medians was also rejected, as this metric approach proved to be too sensitive to fluctuations in the dataset and did not sufficiently remove noise from the spacing profile (also see Fig. 5.10).

As expected, Z-scores based on running medians are more robust than those based on moving means in the detection of perikyma spacing irregularities. For example, on the lower left lateral incisor, all four defects could be confirmed using Z-scores based on running medians and standard deviations of 13 neigbouring sets of measurements, whereas Z-scores of moving means and standard deviations of 13 local sets of perikymata failed to detect defect C (Fig. 5.10).

When converted to percentiles, Z-scores of both moving means and running medians could detect all four defects based on 9, 11 and 13 neighbouring sets of measurements, as these were grouped above the set threshold of the 90th percentile. For example, Figure 5.10 shows the percentiles calculated from the Z-scores based on the moving mean of 13 sets of neighbouring data, with defects A, B and D clearly visible as outliers. In this graph, defect C does not appear as a clear outlier, but its values still fall above the set threshold of the 90th percentile.

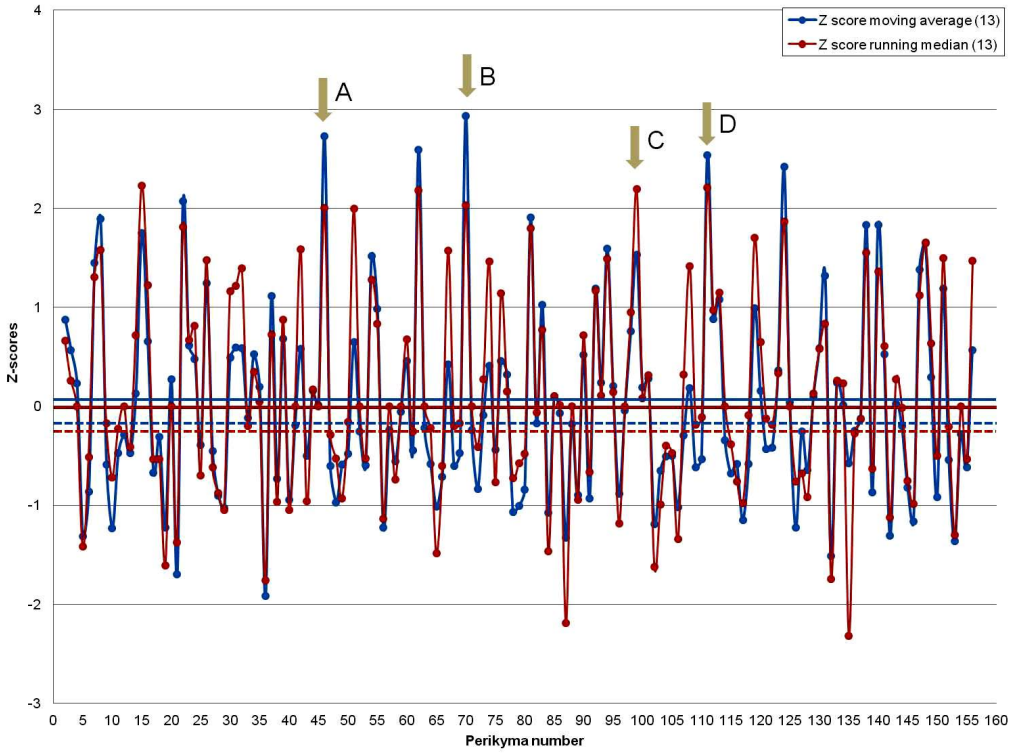

Figure 5.10: Z-scores for lower left lateral incisor (CH 6682). Based on moving means and running medians of 13 sets of neighbouring data, Z-scores of 2 or greater show where observed spacings are significantly greater than the local average (Z-score = 0). Grey arrows indicate visually identified defects corresponding to those listed in Table 5.3. Red and blue lines refer to percentile threshold values: straight blue line = moving means 90th percentile, dotted blue line = moving means 75th percentile; straight red line = moving medians 90th percentile, dotted red line = moving medians 75th percentile

In Figure 5.11, the perikymata count is plotted against the residual values calculated from the fitted LOWESS curve (obtained as described above, i.e. using 15 moving points, corresponding to an alpha value of 0.1) for the lower left lateral incisor. The values vary from -43.1 to 49.3. The residual plot shows a pattern of peaks and troughs, with nine very clear peaks, of which four correspond to the visually identified defects A, B, C and D. When converted to percentiles, defects A, B and D clearly stand out as outliers. Again, in this graph, defect C does not appear as clearly as an outlier, but its residual value still falls above the set threshold of the 90th percentile (Fig. 5.11).

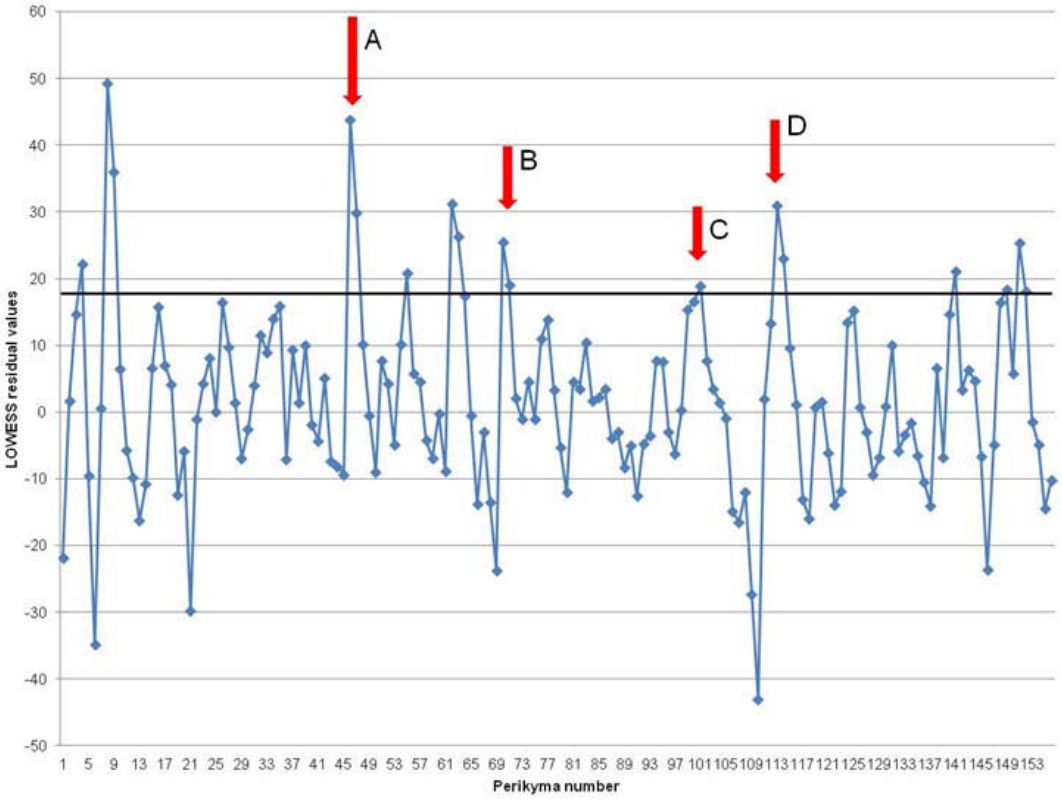

Figure 5.11: Plotted residuals of the LOWESS fitting procedure using cumulative perikyma spacings measured on the lower left lateral incisor (CH 6682). Red arrows indicate corresponding defects in Table 5.3. The dark straight line corresponds to the values for the 90th percentile

Interestingly, in addition to the visually identified defects, other spacing anomalies also stood out in the LOWESS residual plots (Fig. 5.11; Table 5.4). In order to ascertain that we are not identifying false positives using this metric approach, both images and surface profiles were re-examined. Upon visual examination, it emerges that the perikymata in question appear very prominent in the images of the lower left lateral incisor (Fig. 5.12). Similarly, irregular spacing changes indicating possible defects a, c, d and e can be seen as clear depressions in the enamel surface profile (Fig. 5.8). Possible defect b seems less extreme in the enamel surface graph, but nevertheless corresponds to more prominent perikymata (Fig. 5.8, 5.12).

Table 5.4: Metrically identified possible defects on lower left lateral incisor (CH 6682)	
Possible defect	pkg
a	8
b	54-55
c	62-63
d	140-141
e	148-149

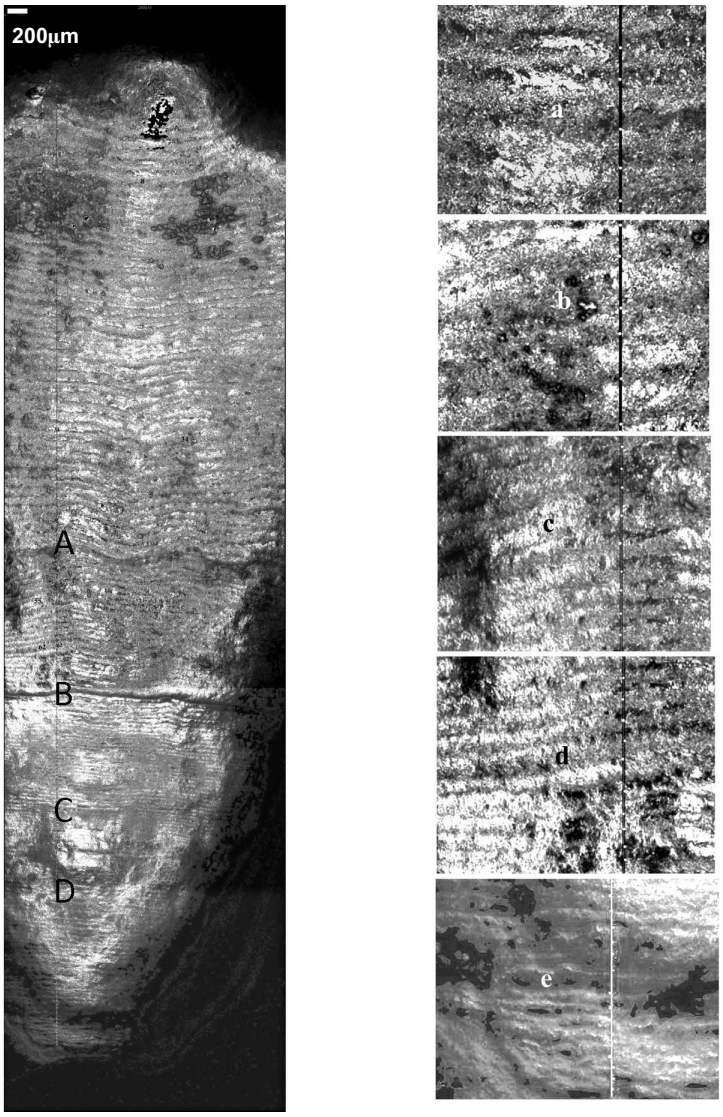

Figure 5.12: Image of the lower left lateral incisor (CH 6682). In-set are prominent perikymata identified using the LOWESS fitting procedure. Letters correspond to defects in Table 5.3 and 5.4

In order to eliminate the effects of regional differences on these residuals, residual values were compared according to their location on the crown. From the occlusal, mid-crown and cervical box-plots, we can see the defects around the 8th (possible defect a), 46th (defect A) and 62nd (possible defect c) perikymata clearly standing out as outliers (Fig. 5.13). Other extreme values in these separate datasets are limited to defects B, C and D and the irregularities around the 55th (possible defect b), the 140-141th (possible defect d) and 148th perikymata (possible defect e).

As these metrically identified defects are apparent both when analysing the entire tooth crown and when dividing the crown into different regions, we can conclude that the

detection of defects using the LOWESS procedure is not affected by the gradual change in perikyma spacing from the occlusal to the cervical end of the crown.

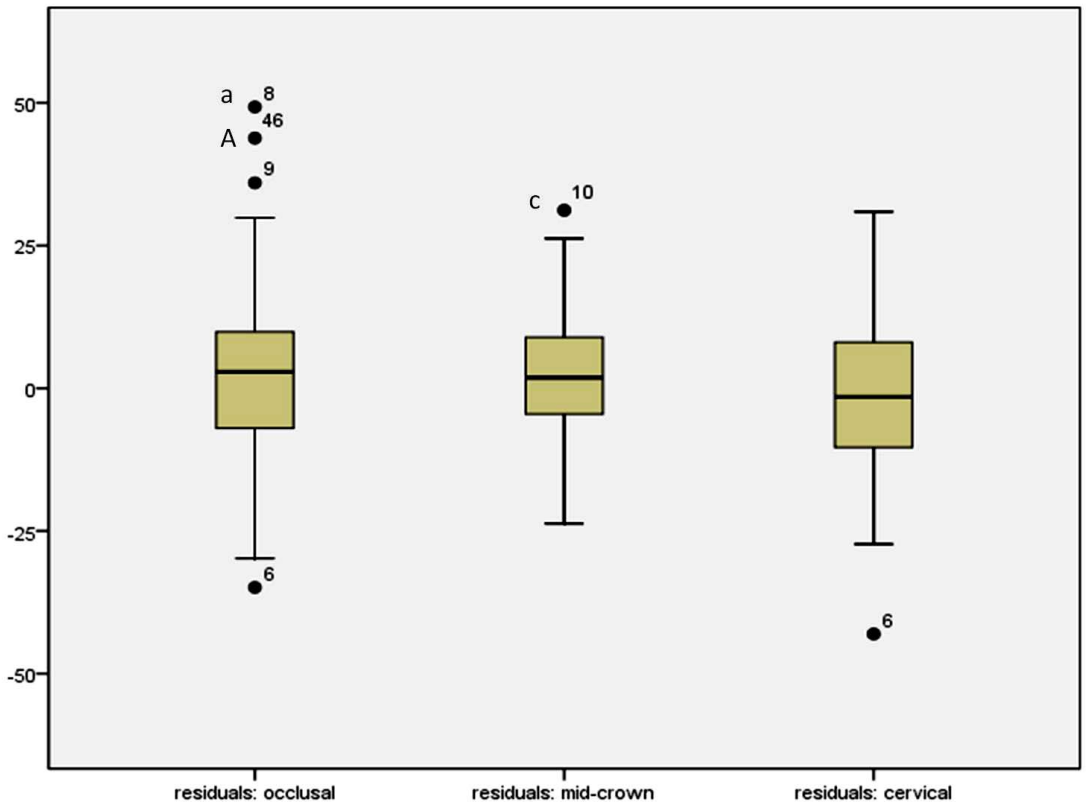

Figure 5.13: Box-plot of residual values for occlusal, mid-crown and cervical regions for the lower left lateral incisor (CH 6682). Letters indicate corresponding defects in Table 5.3 and Table 5.4

A final step in this first case study was to double-check the newly identified defects with the other metric approaches. In Figure 5.10, the Z-scores calculated using a moving mean and standard deviation based on groups of 13 neighbouring perikymata (in blue) show six perikyma pairs with scores of +2 or more. One of these peaks corresponds to a possible defects identified by the LOWESS method (defect c). In addition to this peak, there are two perikyma pairs with scores of +2 or more that are not matched by a prominent defect seen on the image (Fig. 5.10). In addition to this, visually confirmed defects a, b, d and e could not be confirmed using this method. In red are the Z-scores calculated using a running median and MAD based also on groups of 13 neighbouring perikymata. In these red Z-scores the pattern of peaks and troughs shows the four visually identified, clearly delineated defects (A, B, C and D) and two metrically identified defects b and c as peaks rising to the same level or higher as a Z-score of +2 (Fig. 5.10). In addition to these six peaks, there is one perikyma pair with a score of +2. As this could not

be matched by a prominent defect seen on the image or in the enamel surface graph, this can be classified as a false positive.

Due to the false positives appearing in both Z-score methods, it is difficult to identify subtle defects, as both methods are very sensitive to fluctuations in the dataset. This problem is even more apparent in the percentile approach, where an even greater number of perikyma pairs (14 for the values calculated from the moving means and 25 for the values calculated from the running median) appear as peaks rising above the threshold of the 90th percentile (Fig. 5.10).

In terms of the antimere comparison, all four clearly delineated defects which were visually identified on the lower left lateral incisors could also be matched on images and surface graphs of the **lower right lateral incisor** (Fig. 5.9). However, the outcomes of the metric approach differ between the two teeth. For example, Figure 5.14 shows Z-scores of the perikyma spacing profile from the lower right lateral incisor. In blue are the Z-scores calculated using a moving mean and standard deviation based on groups of 9 neighbouring perikymata. The values vary from -1.9 to 2.3: none of the values fall below -2 but four perikyma pairs show a value of +2 or more. Defects B and D are matched by a Z-score of more than +2, whereas defects A and C are not. In contrast, using the same method for the lower left lateral incisor, defects A, B and D are all matched by a Z-score of more than +2.

Figure 5.14 also shows the Z-scores calculated using a running median and MAD based on groups of 9 neighbouring perikymata (in red). The pattern of peaks and troughs is similar to the Z-scores calculated using a moving mean, but the peaks are much more marked. There are fifteen peaks which match a Z-score of more than +2, including those matching defects A, B and D. The peak for defect C does not rise any higher than the other peaks in the graph (Fig. 5.14). This is similar to the outcome of the metric method applied to the lower left lateral incisor and shows that Z-scores based on running medians are more robust than those based on moving means in the detection of perikyma spacing irregularities.

When converted to percentiles, Z-scores of both moving means and running medians could detect all four defects based on 9, 11 and 13 neighbouring sets of measurements, as these were grouped above the set threshold of the 90th percentile. For example, Figure 5.14 shows the percentiles calculated from the Z-scores based on the moving

mean of 9 sets of neighbouring data, with defects A, B and D clearly visible as outliers. In this graph, defect C does not appear as clearly as an outlier, but its values still fall above the set threshold of the 90th percentile.

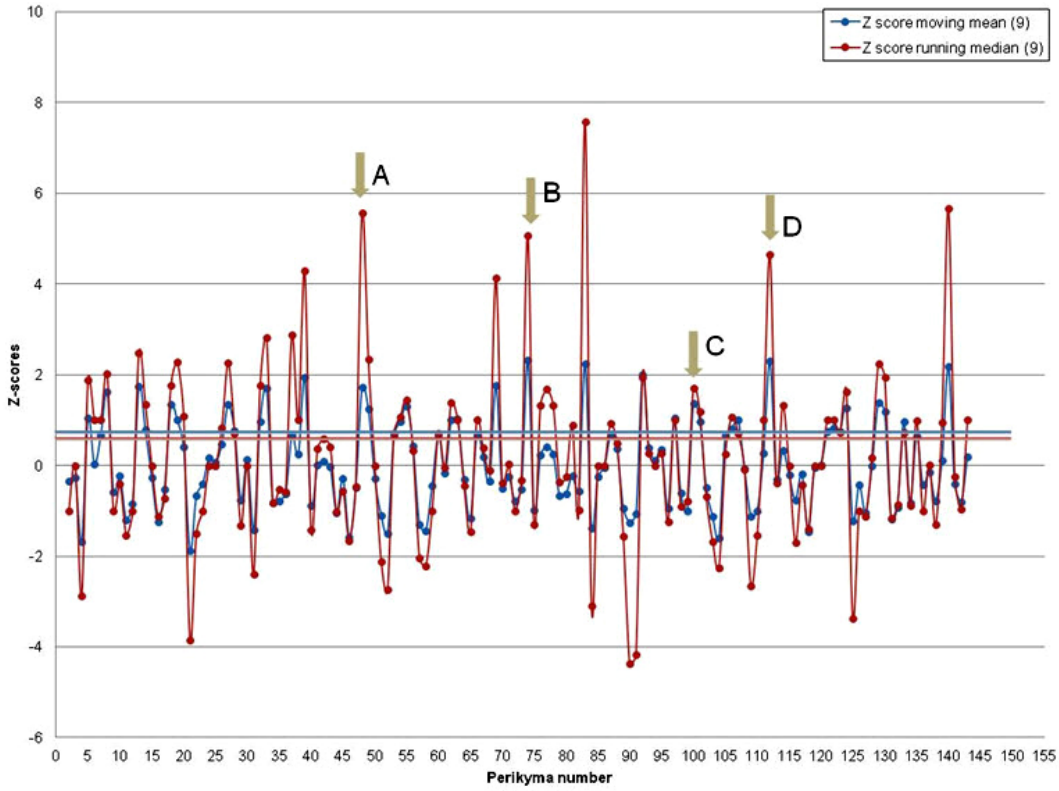

Figure 5.14: Z-scores for lower right lateral incisor (CH 6682). Based on moving means and running medians of 9 sets of neighbouring data, Z-scores of 2 or greater show where observed spacings are significantly greater than the local average (Z-score = 0). Grey arrows indicate visually identified defects corresponding to those listed in Table 5.3. Red and blue lines refer to percentile threshold values: straight blue line = moving means 90th percentile, straight red line = moving medians 90th percentile

In Figure 5.15, the perikymata count is plotted against the residual values calculated from the fitted LOWESS curve (obtained as described above, i.e. using 15 moving points, corresponding to an alpha value of 0.1) for the lower right lateral incisor. The values vary from -41.8 to 29.1. The residual plot shows a pattern of peaks and troughs, of which four peaks correspond to the visually identified defects A, B, C and D. When converted to percentiles, defects A, B and C clearly stand out as outliers. Defect D does not appear as clearly as an outlier, but its residual value still falls above the set threshold of the 90th percentile (Fig. 5.15).

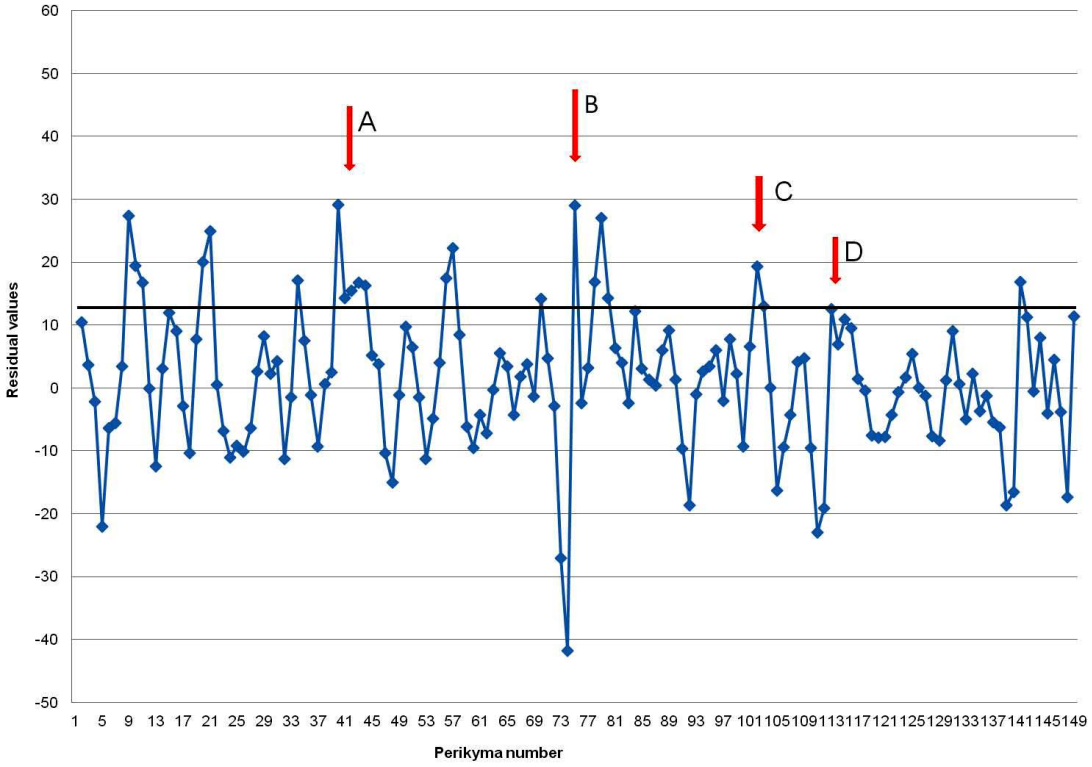

Figure 5.15: Plotted residuals of the LOWESS fitting procedure using cumulative perikyma spacings measured on the lower right lateral incisor (CH 6682). Red arrows indicate corresponding defects in Table 5.3. Dark straight line corresponds to the values for the 90th percentile

In addition to the four visually identified defects, six other spacing anomalies also stand out in the LOWESS residual plots (Fig. 5.15; Table 5.5). Some of these perikymata in question are very prominent in the images of the lower left lateral incisor (Fig. 5.12). In Figure 5.14, the Z-scores calculated using a moving mean and standard deviation based on groups of 9 neighbouring perikymata (in blue) show five perikyma pairs with scores of +2 or more. Three of these peaks correspond to visually identified defects (defects B, D and f), whereas the remaining perikyma pairs with scores of +2 cannot be matched by a prominent defect seen on the image. In red are the Z-scores calculated using a running median and MAD based also on groups of 9 neighbouring perikymata. Of the fifteen peaks which match a Z-score of more than +2, seven peaks correspond to visually identified defects (A, B, D, a, b, d and f). The remaining eight perikyma pairs with scores of +2 cannot be matched by a prominent defect seen on the image and are therefore classified as false positives.

Similarly to the results of metric method applied to the lower left lateral incisor, this problem of false positives is also more apparent in the percentile approach for the lower right lateral incisor, where a greater number of perikyma pairs (16 for the values calculated from the moving means and 21 for the values calculated from the running median) appear as peaks rising above the threshold of the 90th percentile (Fig. 5.14).

Table 5.5: Metrically identified possible defects on lower right lateral incisor (CH 6682)	
Possible defect	pkg
a	8
b	19-20
c	33
d	54-55
e	77-79
f	140-141

To confirm that the occurrences of furrow-form enamel hypoplasia were caused by a systemic physiological disturbance rather than localised trauma, enamel defects identified on an individual tooth needed to have an antimeric pair. Table 5.6 summarises the outcome of the matching procedure using all visually and metrically identified defects. A total of seven defects can be matched between the antimeres, confirming their systemic origin. All of these could be confirmed using the LOWESS and percentile approach. Only two of these could be confirmed using the Z-score moving average on both teeth (using 9, 11 and 13 neighbouring perikymata) and a maximum of 3 defects could be confirmed using the Z-score running median method (using sets of 9 and 11 neighbouring perikymata).

Table 5.6: Comparison of outcomes for the detection of clear and subtle defects based on Z-scores (MM= moving mean; RM = running median), associated percentiles and LOWESS fitting on lower left and right lateral incisors (CH 6682)

Defect	pkg	Z MM 9	Z MM 11	Z MM 13	Z MM 9 perc	Z MM 11 perc	Z MM 13 perc	Z RM 9	Z RM 11	Z RM 13	Z RM 9 perc	Z RM 11 perc	Z RM 13 perc	LOW-ESS
A	45-51	no	no	no	x	x	x	x	x	no	x	x	x	x
B	68-75	x	x	x	x	x	x	x	x	x	x	x	x	x
C	96-103	no	no	no	x	x	x	no	no	no	x	x	x	x
D	111-114	x	x	x	x	x	x	x	x	x	x	x	x	x
8	8	no	no	no	x	x	x	x	x	x	x	x	x	x
54-55	54-55	no	no	no	x	x	x	no	no	no	x	x	x	x
140-141	140-141	no	no	no	x	x	x	x	x	x	x	x	x	x

Summary

Perikyma spacing profiles were constructed for antimeres of a lower lateral incisor representing one individual in order to assess how a mathematical approach can be used

to reconstruct growth patterns in human dental remains and to remove some of the subjectivity associated with the visual identification of defect presence across dentitions.

On the antimeres of individual CH 6682, four clearly delineated defects were identified visually and confirmed using the enamel surface and perikyma spacing profiles. From the comparison between the visual and metric identification of these defects, it emerges that Z-scores based on running medians, moving averages and standard deviations of 9, 11 and 13 sets of neighbouring measurements are more robust smoothing methods than sets of measurements lower than nine. In addition, Z-scores based on running medians rather than moving means are also more consistent in detecting defects. Percentiles from Z-scores based on moving means and running medians (using neighbouring sets of 9, 11 and 13) and residuals calculated from the LOWESS fitting procedure were the most consistent metric methods in eliminating noisy data and identifying these clearly delineated four defects.

In addition to four clearly delineated defects, three more subtle spacing irregularities were detected using the LOWESS method, confirmed visually and matched between the antimeres. These defects were also confirmed using a percentile approach based on Z-scores of running medians and moving means (using 9, 11 and 13 sets of neighbouring measurements). The Z-score approach was less effective in detecting these defects, as only two (for moving means) or three (for running medians) of these defects could be confirmed using this metric approach.

From this case study, it emerges that the LOWESS fitting procedure is very successful in smoothing the dataset without removing interesting outliers. In contrast, the use of direct spacings (Z-scores) introduces a number of false positives, which makes it more difficult to identify subtle defects. Therefore, the LOWESS approach, in combination with visual inspection, seems to be the most appropriate technique for standardising the identification of defects.

Conclusion

Based on the results of this case study, a combined visual - metric approach using LOWESS residuals is recommended for the identification of enamel defects. This technique, which is based on images of the tooth crown as well as recorded measurements, has the potential to reduce the level of subjectivity in the analysis of crown surface characteristics. On the basis of this method, identified defects can then be

matched across the dentition and interpreted based upon comparisons between dentitions from individuals buried in different contexts.

5.1.3. Interpretation of defects

Matching across the dentition

To confirm that the occurrences of furrow-form enamel hypoplasia were caused by a systemic disturbance rather than localised trauma, defects were matched for all individuals where at least two teeth with overlapping developmental schedules where present (see also Hassett 2011; Hillson and Bond 1997; King *et al*. 2002, 2005; Reid and Dean 2000).

When matching one visually identified defect between multiple teeth within one dentition, it was found that a small number of such visually identified defects corresponded to high residuals, but not always within the 90th percentile threshold for all teeth. Not accepting these visually identified defects would bias calculations of average intervals between defects and as such, the defect identification protocol for the entire dataset was established as:

1. Visual identifications have to be confirmed metrically, with LOWESS residual values at or above the threshold of the 90th percentile FOR AT LEAST ONE of the visually identified defects within a matching sequence. Other visually identified defects within this sequence should also have high (at or above the 80th percentile) residual values.

2. Metrically detected defects using the above mentioned LOWESS method have to be confirmed visually.

Four tooth types were examined in this study (upper central and lateral incisors and lower central and lateral incisors). Within these tooth types, the first perikymata appear on the lower incisors at around 1 year of age and the last visible perikymata appear on the upper incisors at around 5 years of age (Reid and Dean 2000). In all cases, it was possible to use prominent defects to calibrate developmental schedules across the dentition, which minimised estimations regarding initiation of tooth mineralisation and cuspal enamel formation times (as per Smith *et al*. 2007b).

Comparisons between individuals

The pattern of furrow-form enamel defects was established for each individual. Following King and colleagues (2005), four parameters were looked at in detail: the frequency of

defects; the interval between defects; the duration of defects and the percentage of enamel formation time taken up by growth disturbances.

The ages of occurrence of the defects were estimated following King and colleagues (2002, 2005) for each individual. Perikymata were counted between the cusp tip and the recorded defects and converted into days using a periodicity of 9 days, which is in line with information from previous publications (King *et al*. 2002; Reid and Ferrell 2006; Smith *et al*. 2007b, 2010). Published averages of mineralisation and cuspal enamel formation times (Reid and Dean 2006) were added to this count to provide a total of days which was then converted into years by dividing by 365.

The frequency of defects was calculated for each individual using the total number of matched defects in each dentition. The percentage of growth (or enamel formation) affected by enamel hypoplasia was expressed as the percentage of affected perikymata out of the total number of perikymata recorded per individual. The average interval between defects was assessed using the number of perikymata between the beginning of one defect to the start of the next defect, whereas the average duration of defects was expressed as the mean number of affected perikymata in defects in each dentition.

Furrow-form enamel hypoplasia can involve defects of a short duration separated by short intervals, defects of a long duration, separated by short intervals, defects of a short duration with long intervals and defects with a long duration separated by long intervals. As the calculation of average intervals and duration does not distinguish between these types of furrow-form enamel hypoplasia, graphs were also constructed in order to take into account all defects (in terms of duration and interval) rather than average duration and interval calculations per individual.

Once the four parameters were obtained for each individual, non-parametric significance tests (Mann-Whitney) were carried out to investigate whether there were consistent differences in the occurrence of furrow-form enamel hypoplasia within the assemblage in terms of place (history houses versus non-history houses) and time (Peak versus Post-Peak contexts) of burial.

Hillson (2001) highlighted the problem of post-mortem tooth loss with regards to the recording of caries and suggested that statistics should be kept separate per tooth type in order to minimise the bias related to this post-mortem loss. The same rationale should be

applied to furrow-form enamel hypoplasia. This would also avoid or at least minimise the bias introduced by a possible differential sensitivity between tooth types. As such, in addition to a statistical analysis of the various parameters on the individual level, an analysis on individual tooth type level is therefore also included in this study.

5.2. Skeletal growth

Analyses of growth are particularly affected by the techniques they use for the estimation of chronological age and this is especially important in comparative analyses between populations (Cardoso 2007; Pfeiffer and Harrington 2011; Hoppa and Fitzgerald 1999). For this reason, a conscious decision was made to limit the skeletal growth analysis to an intra-population assessment, comparing the growth of individuals in terms of place and time of burial within one archaeological site, Çatalhöyük.

The aim of the following section is to describe the methodological basis for the analysis of skeletal growth within the Çatalhöyük sample. This section on skeletal growth (5.2) consists of three parts. The first introduces the data collection procedures, including bone measurements and dental age assessments. The second part assesses the nature of the dataset, including sources of variation between dental age assessment techniques and skeletal size variation within age cohorts. The third part describes the methodology for the analysis of skeletal growth patterns within the sample, including the comparison between individuals buried in different contexts. A detailed description of methodology for the comparison between skeletal and dental growth patterns is given in the fourth and final part.

5.2.1. Data collection procedures

Skeletal measurements

Most bioarchaeological studies have focused on linear measurements of long bones, in particular the diaphyseal length of the femur (Lewis 2002). Quantitative assessments of other areas of growth, including other postcranial elements such as the shoulder, hip, hand and foot bones and the craniofacial complex, offer the possibility to explore growth trajectories in more detail. The inclusion of skeletal variables representing different functional regions (cranium, mandible and postcranial bones) which grow at different rates, aims to capture differences occurring during these different developmental schedules (Humphrey 1998).

This study builds on the work of Hillson and Boz (in press) who investigated childhood growth at Çatalhöyük based on the maximum lengths of long bone diaphyses (clavicle, humerus, ulna, radius, femur, tibia, and fibula) and on the basilar portion of the occipital bone by extending the analysis to a total of 13 cranial (on basilar occipital, lateral occipital, mandible, orbit, petrous and zygomatic regions) and 59 postcranial variables, measured on disarticulated bones (Table 5.7).

As statistical analyses were carried out in order to investigate whether place (history houses versus non-history houses) and time (Peak versus Post-Peak contexts) of burial predicts variation in skeletal size within the sample of individuals examined, each skeletal variable was measured for at least 10 juveniles per assessed archaeological context (place and time of burial).

Table 5.7: List of skeletal variables (anatomical locations, epiphyses and metaphyses) and measurements

Element	Measurement	Element	Measurement	Element	Measure-ment
Occipital	Basilar length (sagittal and maxi-mum) /width Lateralis length (maximum) /width (maximum) Maximum basilar length	**Zygomatic**	Length/width	Frontal	Orbit breadth
Mandible	Chin height Mandibular ramus height Min. ramus breadth condylar to coronoid process	**Temporal**	Petrous length		
Clavicle	Diaphysis length/max width/min width Lateral width Sternal width	**Metacar-pal**	Length	Talus	Length/ width
Scapula	Scapula height/ breadth Glenoid width/height	**Pelvis**	Ilium breadth/ height Pubis length/ height Ischium length/ height	Calca-neus	Length/ width

Humerus	Diaphysis length/ antero-posterior width/ medio-lateral width Proximal metaphysis width Distal metaphysis width Proximal epiphysis diameter	**Femur**	Diaphysis length/antero-posterior width/medio-lateral width Proximal metaphysis width Distal metaphysis width Proximal epiphysis diameter Distal epiphysis width	Axis	Dens width/ height Axis length
Radius	Diaphysis length Proximal metaphysis width Distal metaphysis width	**Tibia**	Diaphysis length/antero-posterior width/medio-lateral width Proximal metaphysis width Distal metaphysis width Proximal epiphysis width Distal epiphysis width	Atlas	Length
Ulna	Diaphysis length Proximal metaphysis width Distal metaphysis width	**Fibula**	Diaphysis length Proximal metaphysis width Distal metaphysis width Distal epiphysis width	Sternum	Manubrium breadth/ length
Rib 1	Length	**Metatarsal**	Length		

Measurements were taken on the left side where possible and on the right side when the left side was absent or poorly preserved. An osteometric board or sliding callipers were used to measure the various skeletal elements, to the nearest tenth of a millimeter using digital sliding calipers, or to the nearest millimeter using a standard osteometric board. For the long bones, only the maximum length of the diaphyses (the main shaft of the bone) was included in the measurement of length, the epiphyses were measured separately. Individuals where the epiphyses had started to fuse to the shaft were excluded from the study. Measurements were taken following standard osteometric protocols (Bass 1966; Buikstra and Ubelaker 1994; Fazekas and Kosa 1978; Howells 1973).

Age assessments

The skeletal growth rate for the children from Çatalhöyük included in this study, was estimated by comparing the bone measurements with an independent assessment of age-at-death (Hoppa and Fitzgerald 1999). As stated in Chapter 4, exact chronological age in years after birth cannot be determined for most archaeological assemblages, where the age is not known from coffin plates or parish records (as it is for example at Spitalfields in London). This is inevitably the case in a Neolithic assemblage such as Çatalhöyük, so it is not possible to estimate growth rate as such. Instead, age was calculated from the dental age.

It must, however, be remembered that a dental age estimate is in reality a measure of the stage of development rather than a true estimate of chronological age. So, for example, if an archaeological jaw fits the six year stage of the Moorrees, Fanning and Hunt standard (Fig. 5.16), it does not mean that the child was necessarily 6 years old when it died. What it means is that the child had reached a state of dental development equivalent to the stage a modern child might be expected to reach at 6 years. That is a very different thing. Dental age estimates therefore are only useful as a way of summarising several different aspects of dental development – for example development of multiple teeth – in order to make a convenient single variable against which another system of development such as bone growth can be compared. That is how dental ages are used here.

Firstly, the **height of the developing tooth** was measured on both deciduous and permanent teeth to the nearest 0.1mm using a sliding calliper (Liversidge *et al*. 1993; Liversidge and Molleson 1999). Crown height measurements of ten developing teeth for each tooth type were repeated to assess the reliability of the measurements. Figure 5.17

is a plot of the first measurement (x-axis) against the second measurement (y-axis) and shows that the sets of measurements repeated on the same specimens are highly correlated.

Based upon the height measurements, ages were estimated using regression equations for permanent and deciduous teeth. Then, for each individual, an overall mean age estimate was calculated as the arithmetic mean of the ages obtained from all available teeth (as per Liversidge *et al.* 1993; Liversidge and Molleson 1999).

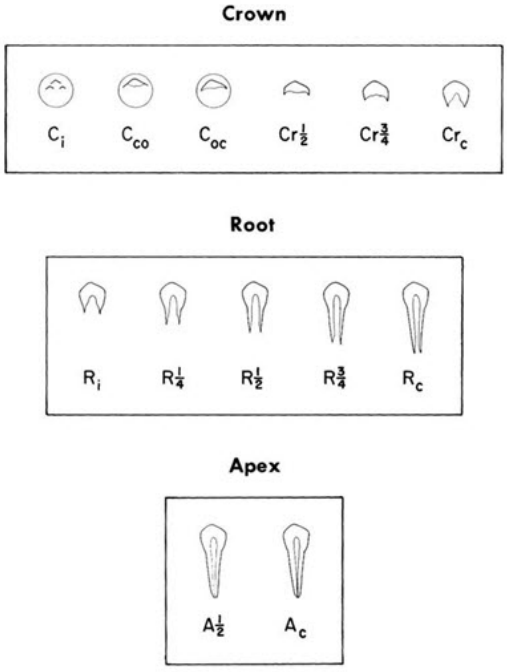

Coded symbols	Stage
C_i	Initial cusp formation
C_{co}	Coalescence of cusps
C_{oc}	Cusp outline complete
$Cr_{1/2}$	Crown ½ complete
$Cr_{3/4}$	Crown ¾ complete
Cr_c	Crown complete
R_i	Initial root formation
$R_{1/4}$	Root length ¼
$R_{1/2}$	Root length ½
$R_{3/4}$	Root length ¾
R_c	Root length complete
$A_{1/2}$	Apex ½ closed
A_c	Apex closure complete

Figure 5.16: Moorrees Fanning and Hunt formation stages for (single-rooted) permanent teeth (from Moorrees *et al.* 1963a, 1493)

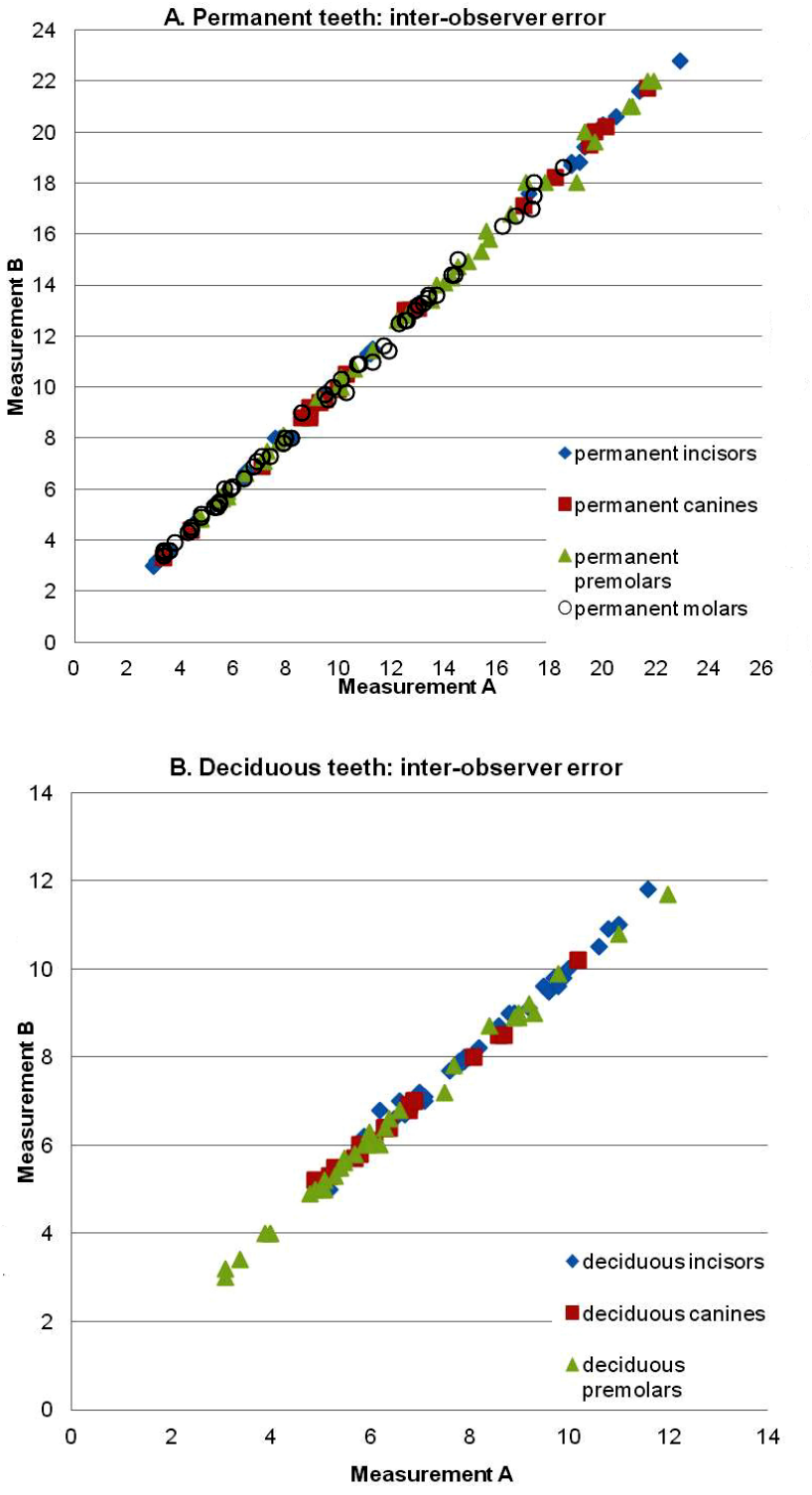

Figure 5.17: Plots comparing the first measurement (x-axis) against the second measurement (y-axis) of permanent (A) and deciduous (B) teeth

Secondly, the dental ages for this skeletal growth study were estimated from the **tooth development scores** for deciduous and permanent teeth, using the stages defined by

Moorrees, Fanning and Hunt (1963a, b), which is the most commonly used and recommended tooth formation standard in bioarchaeology (Buikstra and Ubelaker 1994; Hillson 1996; Saunders *et al.* 1993). Each tooth was scored separately and scores were only recorded if the tooth was loose or visible in the crypt, so that the formation of both roots and crowns could be assessed (Fig. 5.16).

Hoppa (1992) suggested that the overall success of age prediction can be enhanced by pooling assessments from multiple teeth rather than using single teeth, as this multi-tooth approach accounts for the variability within an individual. For all individuals, an age was therefore estimated independently for each available tooth from the development scores and a mean of these ages calculated in cases where more than one tooth was present to provide an overall dental developmental age (Hoppa 1992; Smith 1991, see Table 5.8).

The values for predicting age from the Moorrees stages for permanent teeth (lower incisors, canines, premolars and molars) were based on the work of Smith (1991) which used the original data of Moorrees and colleagues (1963a, b) to represent the midpoint between the age of appearance of one stage and the next rather than presenting the age of attainment of each dental stage, as interpolated from the Moorrees *et al.* chart. This method was tested by Liversidge (1994) on a known age sample which showed that the results were closer to true age than using values based on the original Moorrees, Fanning and Hunt graphs. As the sex of the Çatalhöyük children could not be established, values were calculated based on the averages of male and female values for each tooth, which, according to Smith (1991), introduces little extra error in the resulting ages. As Smith did not extend her study to deciduous teeth, mean ages for this tooth type were estimated based on Moorrees *et al*. (1963b). Using these values, individual-specific mean dental development ages and standard deviations were calculated and the latter were used to construct age cohorts (as per Hoppa 1992, see Table 5.8).

One limitation with the mean age approach is the lack of established mean ages for all tooth types (Smith 1991). For example, the method provided by Smith (1991) only gives values for the permanent lower dentition and the commonly used charts by Moorrees and colleagues (1963b) only include the lower deciduous canine and premolars.

It was deemed advantageous for this study to include all available teeth in the dental development age estimation and ages for each individual were therefore also calculated using the London atlas of tooth development and eruption, which uses the Moorrees,

Fanning and Hunt (1963a, b) standards as a basis (AlQahtani 2008; AlQahtani *et al*. 2010). This atlas is based on developing teeth from 72 prenatal and 104 postnatal skeletal remains of known age-at-death (held at the Royal College of Surgeons of England and the Natural History Museum, London, UK) and on data collected from archived dental radiographs of living individuals (M 264, F 264). Intra-examiner reproducibility for this atlas was 0.85 calculated using Kappa on 755 teeth (65 individuals). Using electronic interactive software (the dental age calculator), it is possible to enter data for tooth development, based on the Moorrees, Fanning and Hunt stages (1963a, b) and estimate the median stage for tooth development for all age categories (Table 5.8).

Table 5.8: Example of calculations for individual-specific means and standard deviations (*numbers mark the end of the age cohort, as per Hoppa 1992)

(**median dental developmental ages calculated using London atlas method, from AlQahtani 2008)

(***mean dental developmental ages for permanent teeth based on Smith (1991), ages for deciduous teeth based on Moorrees *et al*. (1963b)

Specimen nr	Age cohort*	Median**	Mean***	sd	I1	C	P1	M1	Ic	Ip3	Ip4
11973	0.3	0.1	0.2	0.1					0.3	0.1	0.1
10450	0.5	0.4	0.3	0.1					0.5	0.3	0.3
16641	6	6.0	5.6	0.6	5.5	5.1	6.3	5.5			

5.2.2. Variation in dental ageing

The analysis of skeletal growth patterns from archaeological assemblages is greatly influenced by the methodology used to estimate chronological age at death (see Chapter 4, Hoppa 1992; Saunders *et al*. 1993). Moreover, in archaeology, the accuracy of different dental age estimates can most often not be assessed because the chronological ages of the samples are rarely known (Saunders *et al.* 1993).

Saunders and colleagues' (1993) study of the subadults of St Thomas' cemetery (Belleville, Ontario) examined the variation between results for different dental ageing techniques (Anderson, Thompson and Popovich 1976 standards and Moorrees, Fanning and Hunt 1963a and b standards and combinations of these) by calculating the absolute differences in age estimation between the two methods for 17 individuals with documented ages between zero and nine years. They found that the Moorrees *et al.* standards were the most accurate dental estimates of age. A similar measure of variation was attempted with the Çatalhöyük sample in order to assess the differences between

the three ageing techniques used (regressions on tooth height, means based on dental stages and medians based on dental stages) even though, of course, it was not possible to make a similar comparison with independently known age.

The estimated dental developmental ages of 152 individuals between zero and 20 years were compared using simple subtractions between means based on dental stages ("*Hoppa method*") and means based on tooth height regressions ("*Liversidge method*") and between medians based on dental stages ("*London atlas method*") and means based on tooth height regressions("*Liversidge method*"). These were plotted against the mean of all age estimates (Fig. 5.18). Negative scores represent an overestimation of the tooth height regression or underestimation of the dental development methods, whereas positive scores represent an underestimation of the tooth height regression or overestimation of the dental development methods.

Two clear patterns emerge. Firstly, the variation in dental developmental age estimates increases with the increasing age of the individuals. In Figure 5.18a, where the differences between the medians of dental development stages (*London atlas method*) and tooth height regressions (*Liversidge method*) are shown, this increasing variation appears from around 12 years of age. These increasing differences can be explained by the lack of available teeth with low ageing variability in this specific age category. Only third molars were measured for these individuals which are known to be the most variable forming teeth within the dentition (Hillson 1996). Similarly, in a study of a known age population, Cardoso (2007) found that using third molars gave the largest difference between estimated and chronological age.

In Figure 5.18b, where the difference between the means from dental development stages (*Hoppa method*) and the results of the tooth height regressions (*Liversidge method*) are shown, this increasing variation is visible from around five years of age. This might be related to the number of teeth employed in the calculation of the means from dental development stages. As the mean dental stages method is limited to mandibular teeth, this method is less flexible and takes into account less overall variation than the tooth height method, which provides regressions for all teeth within the dentition.

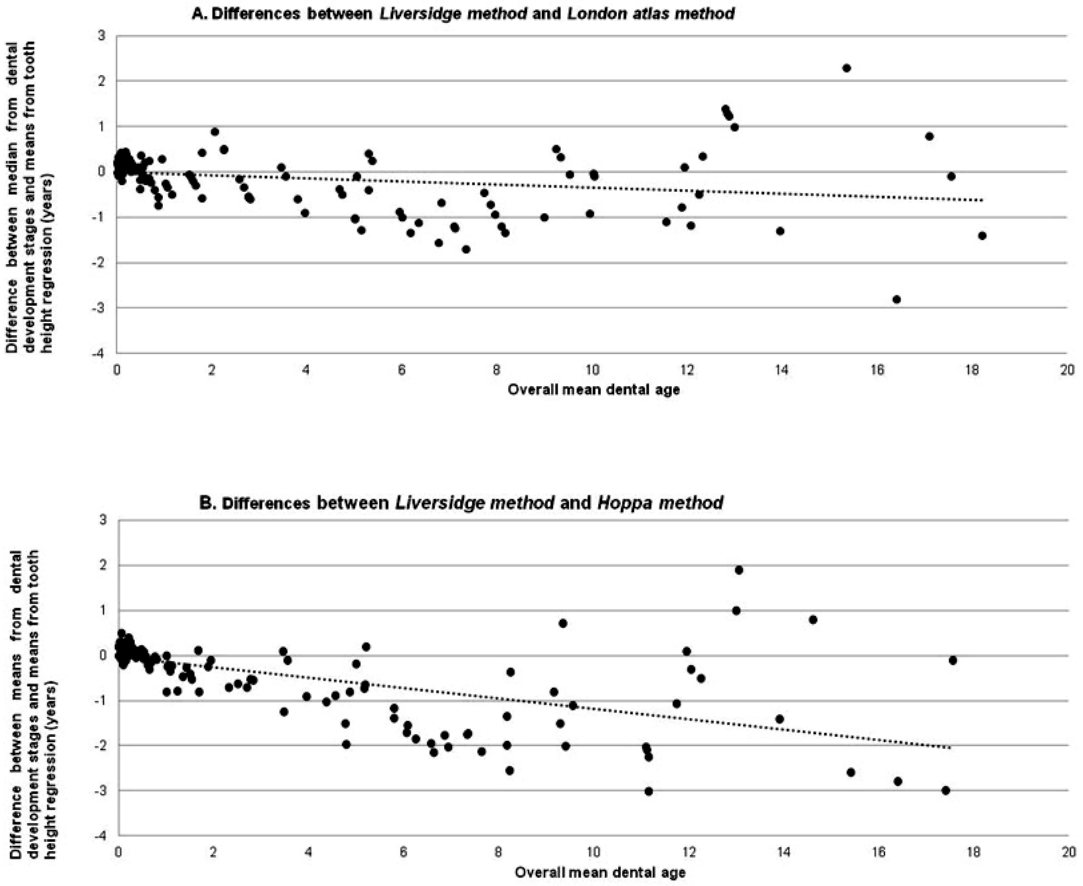

Figure 5.18: Scatterplot of the differences between dental age estimates based on means and medians from dental development stages (*London atlas* method: A) and means from dental development stages (*Hoppa method*: B) and dental age estimates based on tooth measurements (*Liversidge method*) plotted against the overall mean age

A second pattern which can be deducted from Figure 5.18a and b, is the possible overestimation of dental age by the tooth height method or the underestimation of the dental age by development stages method, indicated by the dashed linear trend line. In two separate accuracy tests of tooth height regressions on 20th century Portuguese (Lisbon identified skeletal collection, N = 88) and Spanish assemblages (Granada osteological collection, N = 140) of known age, overestimations of subadult ages using the tooth regression method were detected for individuals below 6 years of age in both (Cardoso 2009, Irurita Olivares *et al.* 2014). In contrast, the tooth height regression method underestimated ages for a group of healthy modern patients attending London hospitals aged between 8 and 12 years (Liversidge *et al.* 2003).

Cardoso (2009) explained this discrepancy between known and estimated ages as the result of different environmental conditions influencing the growth of children in the

reference sample and the sample under study, for example reflecting the worse environmental conditions of the 20th century Portuguese sample in comparison to Liversidge's Spitalfields sample and the better conditions of the modern children in comparison. Additionally, Irurita Oliveras and colleagues (2014) stressed the influence of the small size of the tooth height regression reference sample (63 individuals for the deciduous tooth regressions, and 76 individuals for the permanent tooth regressions).

The comparison between tooth height regression formulae and means and medians from dental stages shows that there is considerable variation between the three dental age estimation methods. The *Hoppa method*, which used overall means from dental development stages, is problematic because not all available teeth can be used to calculate the arithmetic mean and standard deviation for each individual. The *London atlas* method uses all available teeth from each individual to calculate medians and is based on a considerably larger reference sample than the *Liversidge* (tooth height regression) method.

An alternative is to use raw tooth height measurements to represent dental development, without converting these into dental developmental ages and as such, avoiding any mismatch between the reference sample and the assemblage under study. Tooth height measurements are strongly correlated within the deciduous dentition, particularly between the anterior teeth (Hillson 2014; Hillson and Boz in press; Fig. 5.19, Table 5.9).

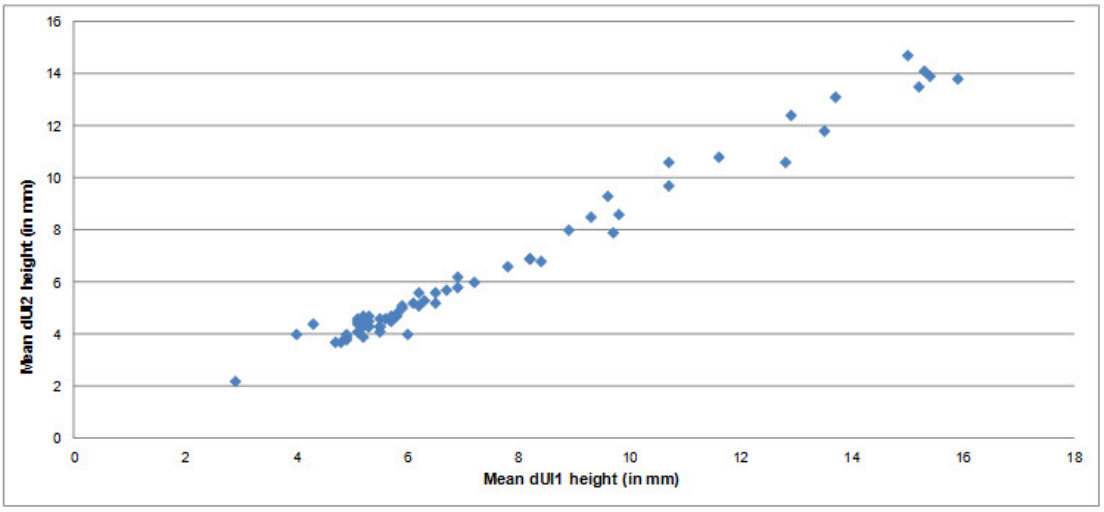

Figure 5.19: Tooth height of deciduous upper first incisor plotted against tooth height of deciduous upper second incisor (in mm, means of left and right sides)

The Çatalhöyük dental assemblage is characterised by a high number of deciduous teeth and a low number of comparable permanent teeth. Despite this low number, strong correlations of crown heights can be found between the deciduous and permanent anterior teeth, with the strongest correlation between the deciduous teeth and the permanent lower central incisor and between the deciduous teeth and the permanent lower canine (Table 5.9).

Table 5.9: Correlations of deciduous and permanent tooth height measurements (in mm)

(*mean of left and right sides)

(**Correlation is significant at the 0.01 level (2-tailed)

		Mean* dUI1 height	Mean* dUI2 height	Mean* dUC height	Mean* dLI1 height	Mean* dLI2 height	Mean* dLC height	Mean* LI1 height	Mean* LI2 height	Mean* LC height	Mean* UI1 height	Mean* UI2 height	Mean* UC height
mean dUI1 height	Pearson Correlation	1	.990**	.985**	.988**	.989**	.981**	.953**	.711**	.956**	.908**	.464**	.758
	Sig. (2-tailed)		.000	.000	.000	.000	.000	.003	.289	.003	.002	.354	.242
	N	71	60	45	54	57	48	6	4	6	8	6	4
mean dUI2 height	Pearson Correlation	.990**	1	.991**	.987**	.993**	.988**	.975**	.661**	.977**	.927**	.575**	.887**
	Sig. (2-tailed)	.000		.000	.000	.000	.000	.000	.339	.001	.000	.136	.045
	N	60	70	45	57	56	49	8	4	6	11	8	5
mean dUC height	Pearson Correlation	.985**	.991**	1	.981**	.993**	.997**	.993**	.934**	.995**	.964**	.654**	.961**
	Sig. (2-tailed)	.000	.000		.000	.000	.000	.000	.002	.000	.000	.029	.001
	N	45	45	56	40	42	43	9	7	8	14	11	7
mean dLI1 height	Pearson Correlation	.988**	.987**	.981**	1	.981**	.979**	.919**	.915**	.882**	.946**	.294**	.687**
	Sig. (2-tailed)	.000	.000	.000		.000	.000	.010	.265	.048	.000	.571	.313
	N	54	57	40	71	60	54	6	3	5	9	6	4
mean dLI2 height	Pearson Correlation	.989**	.993**	.993**	.981**	1	.989**	.985**	.683**	.973**	.932**	.611**	.819**
	Sig. (2-tailed)	.000	.000	.000	.000		.000	.000	.317	.005	.000	.145	.181
	N	57	56	42	60	74	54	7	4	5	9	7	4
mean dLC height	Pearson Correlation	.981**	.988**	.997**	.979**	.989**	1**	.989**	.961**	.984**	.969**	.703**	.948**
	Sig. (2-tailed)	.000	.000	.000	.000	.000		.000	.001	.000	.000	.023	.004
	N	48	49	43	54	54	66	8	7	6	10	10	6
mean LI1 height	Pearson Correlation	.953**	.975**	.993**	.919**	.985**	.989**	1*	.976**	.986**	.978**	.960**	.973**
	Sig. (2-tailed)	.003	.000	.000	.010	.000	.000		.000	.000	.000	.000	.000
	N	6	8	9	6	7	8	23	14	18	16	15	11
mean LI2 height	Pearson Correlation	.711	.661	.934**	.915	.683	.961**	.976	1*	.947**	.991	.959**	.951
	Sig. (2-tailed)	.289	.339	.002	.265	.317	.001	.000		.000	.000	.000	.000
	N	4	4	7	3	4	7	14	24	16	17	16	11
mean LC height	Pearson Correlation	.956**	.977**	.995**	.882*	.973**	.984**	.986	.947**	1**	.925**	.970**	.993**
	Sig. (2-tailed)	.003	.001	.000	.048	.005	.000	.000	.000		.000	.000	.000

	N	6	6	8	5	5	6	18	16	34	20	18	19
mean UI1 height	Pearson Correla-tion	.908**	.927**	.964**	.946**	.932**	.969**	.978*	.991**	.925**	1**	.973**	.944**
	Sig. (2-tailed)	.002	.000	.000	.000	.000	.000	.000	.000	.000		.000	.000
	N	8	11	14	9	9	10	16	17	20	34	20	14
mean UI2 height	Pearson Correla-tion	.464	.575	.654*	.294	.611	.703**	.960	.959**	.970**	.973**	1**	.970
	Sig. (2-tailed)	.354	.136	.029	.571	.145	.023	.000	.000	.000	.000		.000
	N	6	8	11	6	7	10	15	16	18	20	26	16
mean UC height	Pearson Correla-tion	.758	.887*	.961**	.687	.819	.948**	.973	.951*	.993**	.944*	.970**	1
	Sig. (2-tailed)	.242	.045	.001	.313	.181	.004	.000	.000	.000	.000	.000	
	N	4	5	7	4	4	6	11	11	19	14	16	25

The deciduous upper first incisor is the most commonly recovered developing tooth at Çatalhöyük, with teeth preserved on at least one side of the dentition for 73 individuals out of the 159 individuals for which bone measurements were available. As height measurements for developing deciduous teeth are highly correlated with one another (Table 5.9), it was possible to estimate deciduous upper first incisor height measurements for an additional 27 individuals lacking these teeth (referred to as predicted mean dUI1 height), based on a simple linear regression model (as per Hillson and Boz, in press).

5.2.3. Analysis of skeletal growth

Skeletal growth profiles were constructed by plotting the bone measurements against the predicted mean dUI1 heights and the estimated (median) dental development ages. That is, the predicted mean dUI1 heights or dental development ages (the independent variable) were plotted along the x axis of the graphs and the bone measurements (the dependent variable) along the y axis.

Polynomial expressions (of the type $y = b0 + b1x + b2x^2 + b3x^3 + b4x^4 + b5x^5$) are useful models in growth studies and have been used in the past to describe the relationship between growth and (dental) age (Mays *et al*. 2009; Temple *et al*. 2014). In the current context, this approach is used as a tool to evaluate trends in skeletal growth patterns in a comparative perspective, taking into account that these fitted lines do not represent true growth curves (as per Temple *et al.* 2014). Regressions describing the relationship between bone measurements and (median) dental development age were used as the basis for the analysis and fitted lines describing the relationship between bone measurements and predicted mean dUI1 heights were used as a check of this approach.

In order to fit a regression line that best described the relationship between the two variables, forward selection procedures were used in which different powers of the x variable were added to the equation. Using the same reasoning as Mays and colleagues (2009), the final choice of acceptance of x terms into the equation was based on their significant improvement of the prediction of y values. This was achieved by testing the increase in the r-squared values using the F-statistic (at $P < 0.05$).

For example, for the assessment of the relationship between the diaphyseal length of the radius (dependent variable y) and the predicted mean dUI1 height (independent variable x), a quadratic regression equation most adequately summarised the relationship with dental age (Fig. 5.20). First a linear regression was done, fitting an equation of the form $y = b0 + b1x$ to the data (dashed black line). Then an equation of the form: $y = b0 + b1x + b2x^2$, was fit to the data (straight black line). Next, an equation of the form: $y = b0 + b1x + b2x^2 + b3x^3$, was fit (dashed red line). All three regressions are significant ($p > 0.05$). The r^2 always increases when adding a higher-order term, but in forward selection procedures, the question is whether the increase in r^2 is significantly greater than expected due to chance (McDonald 2009). In this case, the increase in r^2 is tested and found to be significant for the quadratic regression ($p = 0.003$), but not for the cubic regression ($p = 0.435$).

When the regression procedures were found to optimally describe the relationship between each skeletal variable and dental development age and predicted mean dUI1 heights, raw residuals from this procedure could be calculated. In a similar approach to Temple and colleagues (2014), these values were then standardised based on Z-score transformations of the data:

$$Z = \frac{x - \mu}{\sigma}$$

Where x is the value to be standardised (the raw residual for each individual), μ is the mean and σ the standard deviation of the residuals for each skeletal parameter.

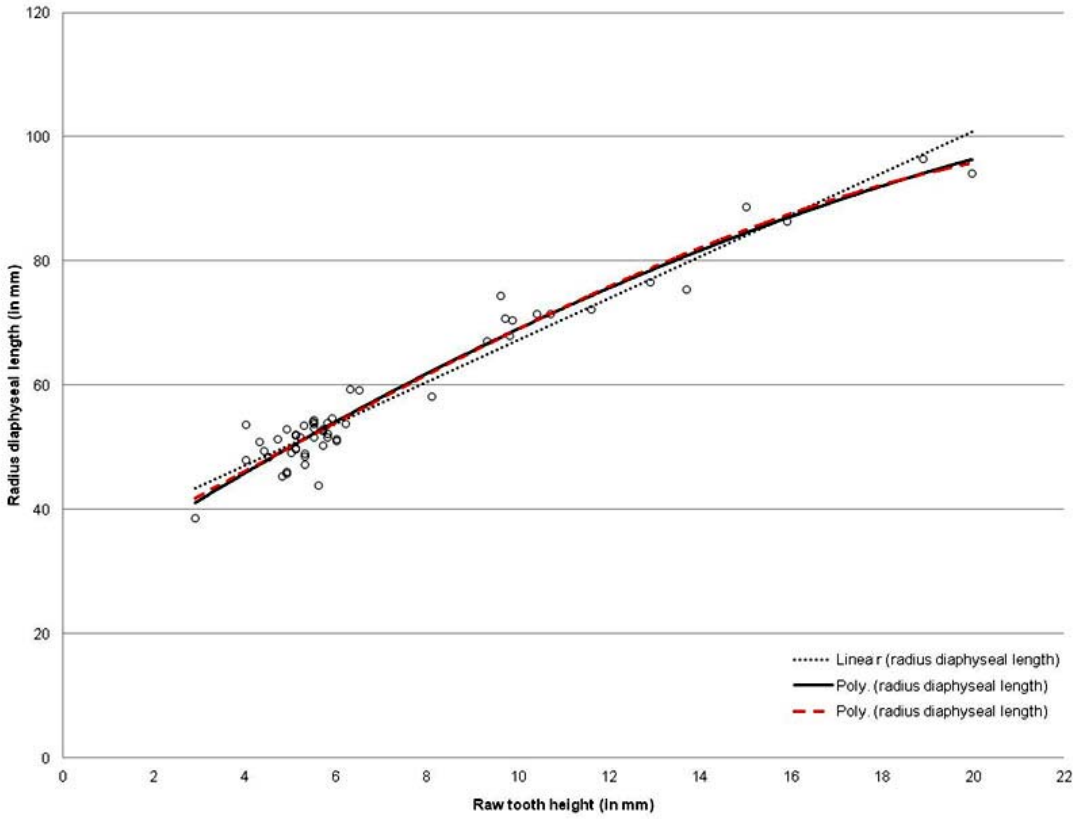

Figure 5.20: Plot of radius diaphyseal length against predicted mean dUI1 height with linear (dashed black line), quadratic (straight black line) and cubic (dashed red line) regression lines

One problem with such a curve fitting approach is the influence of age distribution on the magnitude of residuals, particularly for older children, which tend to have higher residuals, giving a false representation of bone dimension changes with age. Therefore, prior to the analysis of the standardised residuals, their distribution was assessed to ensure they are evenly distributed across all ages (Fig. 5.21). If the residual values clustered about a straight line, t-tests were conducted in order to establish whether there are significant differences between place and time of burial. As there were not enough individuals found in the pre-Peak period in order to assess their growth, only differences between Peak and Post-Peak periods were compared.

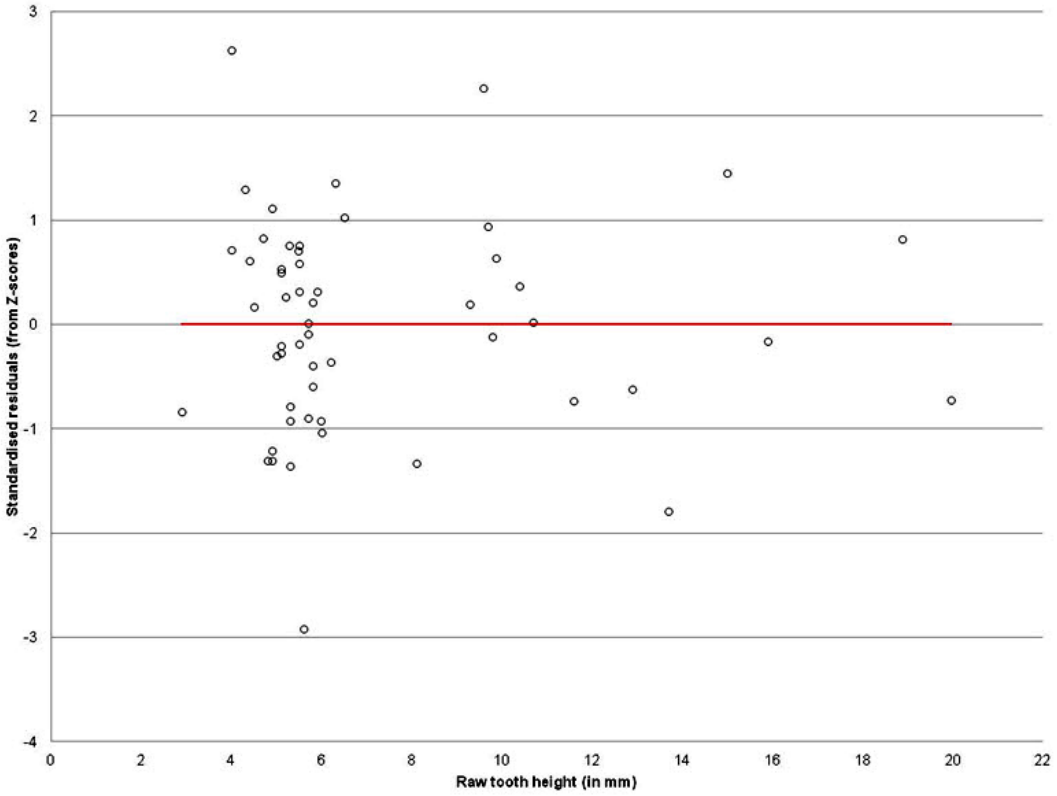

Figure 5.21: Distribution of residuals (standardised using Z-scores) from a quadratic regression mathematically describing the relationship between the diaphyseal length of the radius and predicted mean dUI1 heights

The null hypothesis for this study is that skeletal measurements do not differ between those buried in history house and non-history houses and do not differ between those buried in the Peak period and in the Post-Peak period. A statistically significant difference in regression residuals between the two different time and places will reject this null hypothesis.

5.2.4. Comparison of dental and skeletal growth patterns

A final analysis assesses the correlation between skeletal and dental growth patterns. It is expected that individuals with a greater proportion of crown development disrupted by defects will have smaller skeletal sizes for a given dental age than those with a lesser proportion disrupted. In order to address this question, residual values for skeletal growth parameters with the largest sample sizes (N =21 for the upper metaphyseal width of the ulna, N = 19 for the width of the scapular glenoid, N = 18 for the metatarsal length and N

=14 for basilar length) were compared to the number of matched defects per quarter (defect positions expressed as proportions of the perikymata count) and the number of affected perikymata per quarter.

For this comparison, three groups were differentiated, including individuals with a low degree of dental growth disruption per zone, individuals with a medium degree of disruption per zone and individuals with a high degree of disruption per zone, using the mean number of defects and mean number of affected perikymata per quarter as a cut-off point. As there were not enough individuals with matched skeletal and dental parameters to conduct a significance test between the groups, box plots comparing the residual values for each group were constructed and assessed visually.

Chapter 6. Materials

6.1. History of bioarchaeology at Çatalhöyük

During the four extensive excavations carried out at Çatalhöyük by Mellaart in the 1960s, a large sample of human remains was uncovered (Düring 2003; Mellaart 1964, 1966, 1998). However, the excavation took place without screening the removed deposits and with limited recording (Hodder 2010). In addition, no physical anthropologists were present during the excavations and therefore no aging, sexing or assessments of minimum numbers of individuals took place while the remains were *in situ* (Düring 2003). Mellaart did not publish a table of the number of burials discovered within each building and in his preliminary reports and burials were only occasionally mentioned and not quantified (Düring 2001).

It is known that the human remains recovered from the site were cleaned, “restorated” and numbered by a local physician from Çumra (Düring 2003). Like most of the finds recovered from the 1960s excavations, the human remains were taken to Ankara. Later, various analyses of the human remains were carried out at the university of Ankara, in which Angel, then based at the Smithsonian Institute in Washington (1965, 1971), mainly focused on pathology and Ferembach from the Institut de Paléontologie Humaine in Paris (1972, 1982), concentrated on demography (Düring 2003; Molleson *et al.* 2004).

Whilst working on the material in Konya (Central Anatolia, Turkey) and in the laboratories of the University of Ankara (Turkey), Ferembach estimated that around 462 individuals had been recovered from the site (Düring 2003). However, reports on minimum numbers of individuals differ considerably, possibly caused by different approaches to the reconstruction of skeletal elements by Angel and Ferembach, errors in writing, reading and copying labels, the loss of material and lack of access to further material in later years (Düring 2001, 2003).

The dental remains from this period of study are now housed at University College London. In 2009, the postcranial remains were moved to the site’s bioarchaeology laboratory in Çumra, but difficulties with record keeping and curation resulted in the loss of many (especially juvenile) remains, preventing a complete and detailed re-assessment using new methods (Hamilton 1996).

The more recent archaeological investigations at Çatalhöyük began in 1993, with the first two seasons concentrating on surface survey and surface scraping. In 1995 excavations started in the North Area and full scale excavation was carried out from 1996 onwards. Andrews and Molleson directed the study of the human remains at the site between 1995 and 1999 and during this period, a total of 94 inhumations were recovered from 49 graves, amounting to an estimated 94 individuals (Andrews *et al.* 2005).

From 2000 to 2009, under the Hillson and Larsen team, more burials were excavated and the minimum number of individuals recovered from the East Mound has increased to around 400 individuals, of which about two thirds are children (Hager and Boz in press). All of these remains were housed on site. The data for this study was collected during 2008-2009 field seasons and include all measurable skeletal and dental juvenile remains excavated between 1993 and 2008 as well as some dental remains from the Mellaart excavations.

6.2. Preservation and taphonomy

Whilst recalling the 1960s field seasons at Çatalhöyük, Mellaart (1998) wrote that the site is unique in its preservation of many types of remains, including brains, textiles and wood. Similarly, Hodder (2007a) stressed the good preservation of carbonised plants and phytoliths at Çatalhöyük.

Despite the excellent preservation of materials at Çatalhöyük some of the archaeological material appears to have been eroded. Matthews (1996, also see Roberts et al. 2007), for example, mentioned that at the beginning of the Hodder excavations, around 0.5 to 1m of the archaeological deposits had probably eroded from the northern eminence of the Eastern mound. The KOPAL study indicated that post-Neolithic lowering of this area amounts to around 2.5m (Hodder 2007a).

In terms of taphonomy, Andrews and colleagues (2005) stated that the main preservation issue was the drying out of bones, as remains have dried out over the years after Mellaart's excavations due to a lack of surface cover and because the water table dropped, causing moisture to decrease from the tell. Similarly, Hager and Boz (in press) wrote that 10% of the total number of individuals in the sample was found near the surface eroding from the topsoils (Fig. 6.1). In addition, disturbance to burials as a result of burial

practices (see Chapter 2) and animal burrowing is also common (Hager and Boz in press). Both the fragmentary nature and the movement of bones are main concerns when determining the minimum number of individuals in these burial contexts. The dry burial conditions also have an impact on the surface preservation of skeletal material (bone become much more fragile), which in turns affects the assessment of pathological changes in bone. The breakage of bones due to erosion also means that some skeletal measurements cannot be taken.

Figure 6.1: Neonatal skeleton (14818) found eroding out of North wall of Building 53 (South area, Space 272, Feature 4076)

6.3. Labelling and provenience

During Mellaart's excavations, various trenches were opened and material from these was labelled with the letters A to F (Farid 2007a; Molleson *et al*. 2004). Mellaart divided the occupation layers into different levels, indicated by Roman numerals. Material from identified buildings was indicated with Arabic numerals (Düring 2003; Farid 2007a; Mellaart 1963a; Molleson *et al.* 2004). So, for example, a label marked E VI 8 stands for Excavation area E, level VI, Building 8. Within the Mellaart assemblages, there are also remains marked with "no label". For these remains, provenance is unknown and they have been excluded from this study.

In the Hodder excavations, each excavated individual received a unique skeleton number, which was associated with a feature number (indicating ovens, walls, burials), space number (indicating platforms or rooms) and/or building number. For example, CH 4394 is the unique skeleton number of an individual associated with feature 460 (a burial), located in space 163 of Building 6. Each unit had at least one sample of up to 30l of sediment sent for flotation (with heavy residues collected using a 0.5mm mesh) and screening. All other sediment from a unit was scanned during excavation and dry-sieved through a 4mm mesh (Farid 2007c). This allowed for the recovery of micro-artefacts such as beads, but also plant residues and small human and animal bone fragments.

Bioarchaeologists were present on-site during Hodder's excavations and undertook the excavation and illustration of the human remains as well as an initial analysis. More detailed analysis took place in the human remains laboratory. After analysis using standard osteological and dental methods to estimate age and sex (Bass 1966; Buikstra and Ubelaker 1994; White and Folkens 2005) and verification by multiple researchers, skeletal and dental data was entered in the human remains database developed by Hillson which was linked to the site's relational database.

One particular problem related to provenance data occurred during the construction of two shelters covering the south and 4040 area in 2002 and 2007. Multiple foundation trenches with connecting beam slots were excavated around the footprints of the shelter and whilst some of these trenches lay over buildings defined in earlier excavation seasons and during surface scraping, others were part of sequences that have yet to be assessed or were outside the limits of the investigations (Farid 2007c, Fig. 6.2). In some

cases, this situation made it very difficult to reconstruct the chronology and the remains' relationship to buildings (Pilloud 2009). Specimens from this context were only included in this current study when a clear relationship to buildings and/or chronological context could be established.

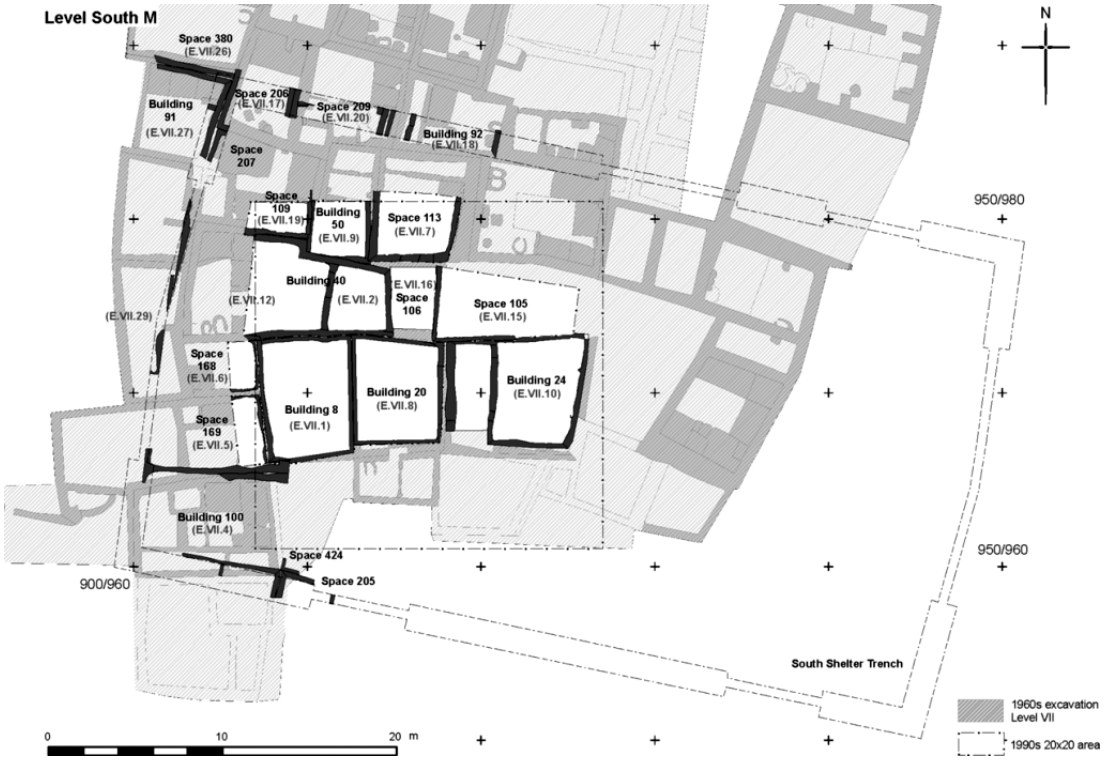

Figure 6.2: Footprint of permanent shelter in the South area; Settlement plan from Mellaart's Level VII (Hodder Level South M), Plan courtesy of the Çatalhöyük Research Project (From Love 2012, 147)

Finally, in addition to the complexity of the stratigraphy in Near Eastern sites in general and Çatalhöyük in particular, the temporal and spatial analysis should also be considered as biased by the skewing of the living population and the Neolithic cultural practice of frequent re-deposition of human remains, as described in Chapter two (Düring 2012; Molleson *et al.* 2005).

6.4. Specimen selection

6.4.1. Dental study

Tooth wear is likely to affect any enamel hypoplasia study using adult teeth. More specifically, as wear causes the disappearance of perikymata, it introduces error to the

identification of the number and spacing of these incremental structures (Guatelli-Steinberg *et al.* 2004; King *et al*. 2002). In order to deal with this issue, Guatelli-Steinberg and colleagues (2007a) restricted their study to teeth which were estimated to have 80% or more of their crown heights intact. Although crown heights were reconstructed in a scientifically rigorous way, this still meant that teeth missing up to 20% of their crown were included in the study and for these teeth, perikymata on the first two deciles (10% of crown height) were estimated rather than counted (Guatelli-Steinberg *et al*. 2007a).

Although these estimations were based upon the fact that the first two deciles have very low standard deviations, there seems to be a need for further comparative studies with larger sample sizes of unworn teeth in order to confirm this pattern. Similarly, estimations of perikymata numbers for single deciles containing indistinct perikymata based upon adjacent deciles also seem likely to introduce error in comparative studies of perikymata counts and spacing (Dean and Reid 2001; Guatelli-Steinberg *et al*. 2007a). An alternative is to limit these detailed studies to the relatively unworn dentitions of immature individuals (Hillson 1992). As such, a sample of 54 children and adolescents with relatively unworn (i.e. with visible perikymata) matching permanent teeth are included in the detailed dental growth study (Table 6.1).

The sample was limited to incisors in order to avoid biases introduced by comparisons of different tooth types, as differences in susceptibility and in the geometry of tooth crowns might affect the distribution of perikymata (and related defects) between tooth classes (Goodman and Rose 1990; Hillson and Bond 1997; Newell *et al.* 2006).

Table 6.1: Context information and teeth available for each individual included in the dental study

specimen nr	teeth available	place of burial	period
CH 1425	ULI1, ULI2	history house	Peak
CH 1484	LLI1, LRI2	history house	Peak
CH 1495	LLI1, URI2	history house	Peak
CH 1884	LRI1, URI1, LLI2, URI2	non-history house	Peak
CH 1885	LLI1, URI1	non-history house	Peak
CH 1913	LLI1, LLI2, ULI2, URI2, ULI1	history house	Peak
CH 1923	LRI2, URI1	history house	Peak
CH 1925	LRI2, ULI1	history house	Peak
CH 1938	LRI1, LRI2	history house	Peak
CH 1922	ULI1, URI2, LLI2	history house	Peak
CH 1959	LRI1, LRI2, ULI1	history house	Peak
CH 1960	LLI2, URI1	history house	Peak
CH 1995	URI1, URI2	history house	Peak
CH 2033	LRI1, LRI2, ULI1	non-history house	Peak

CH 2119	LLI2, LRI1, ULI1, ULI2	history house	Peak
CH 3529	ULI1, ULI2	non-history house	Peak
CH 4394	LRI2, URI2	history house	pre-Peak
CH 5608	ULI1, ULI2	non-history house	as yet unas-signed
CH 5795	LLI1, ULI2	non-history house	as yet unas-signed
CH 6681	LRI1, LRI2, ULI2	non-history house	Peak
CH 6682	LLI1, LLI2, LRI2, ULI1, ULI2	non-history house	Peak
CH 7541	LRI1, ULI2	non-history house	as yet unas-signed
CH 7576	LRI1, URI1	non-history house	as yet unas-signed
CH 7579	LLI1, LRI1	non-history house	as yet unas-signed
CH 8113	LLI1, LLI2	non-history house	Peak
CH 8114	ULI1, URI2	non-history house	Peak
CH 8423	LLI1, LLI2, ULI2, URI1	non-history house	Peak
CH 8425	ULI1, ULI2	non-history house	Peak
CH 8729	LLI2, LRI2	non-history house	as yet unas-signed
CH 8841	LLI2, LRI1	non-history house	as yet unas-signed
CH 10529	LRI1, LRI2, ULI1, ULI2	non-history house	pre-Peak
CH 11608.10	ULI2, URI2	history house	Post-Peak
CH 11982	ULI2, URI2	non-history house	Post-Peak
CH 12528	ULI1, ULI2	non-history house	Post-Peak
CH 12875	URI1, ULI2	history house	Post-Peak
CH 12876	ULI1, URI1	history house	Post-Peak
CH 12935	LLI1, LRI2, ULI2	history house	Post-Peak
CH 13125	LLI1, LLI2	history house	Post-Peak
CH 14020	LLI1, URI1	history house	Post-Peak
CH 14108	ULI1, URI1	non-history house	as yet unas-signed
CH 15467	ULI2, URI2	non-history house	Peak?
CH 15748	LRI1, LRI2, ULI2, URI1, URI2	history house	Post-Peak
CH 16125	LLI1, LRI2	non-history house	Peak?
CH 16168	ULI1, URI2	non-history house	Peak?
CH 16196	LLI1, LLI2, ULI1, ULI2	non-history house	Peak?
CH 16601	LLI2, URI2	non-history house	Peak
CH 16638	LRI1, URI2	non-history house	Peak
CH 16641	LLI1, URI1	non-history house	Peak
CH 16698	LRI1, LRI2, URI1, URI2	non-history house	Peak
CH 19022	URI1, ULI2	history house?	Peak
CH 19039	LLI2, ULI2	history house?	Peak
Mell 7k40	LLI2, LRI2, URI1, URI2	history house	Peak
Mell 7k40(3)	LLI1, LRI2	history house	Peak
Mell 8 (7l)	ULI1, URI1	history house	Peak

Of the 54 immature individuals included in the detailed dental growth part of the study, three originate from the Mellaart excavations housed at University College London. According to their label (labeled EVI 8 (7l), EVI 7k40(3) and EVI 7k40), it is possible to assign these individuals to what is currently called a “middle period” or “Peak context” (Mellaart 1963a). As such, in terms of chronological horizon, the total number of individuals from “Peak” contexts amounts to 31 individuals (ranging from Mellaart level VI, North G, South M, Bach G and 4040 G) compared to three individuals from early contexts (South L and South H) and 11 children were found in an early (Pre-Peak; N=2) or late (Post-Peak, N=9) period context (4040 H, South O, South Q, South R and South S).

Based upon their labels, all three Mellaart individuals seem to have come from complex E and were buried in very elaborate houses. Two individuals were recovered from the so-called shrine 7 (Mellaart 1963a). The third child was also found in a shrine (8; with horn cores, hand and honeycomb paintings) with the head, thorax and arms covered in ochre (Mellaart 1963a, 95; Fig. 6.3). On this basis, all three individuals from the Mellaart excavations are considered to have originated from a “special” context. Twenty-two additional individuals were also buried in history houses (Building 1, Building 6, Building 44, Building 56, Building 60, Building 65 and Building 77), which amounts to a total of 25 individuals who were found in a “special” context, as opposed to 29 individuals found in a “non-history house” context.

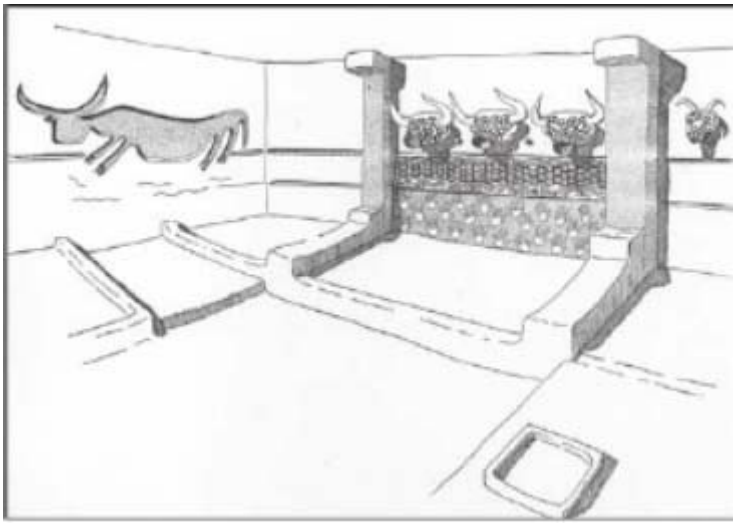

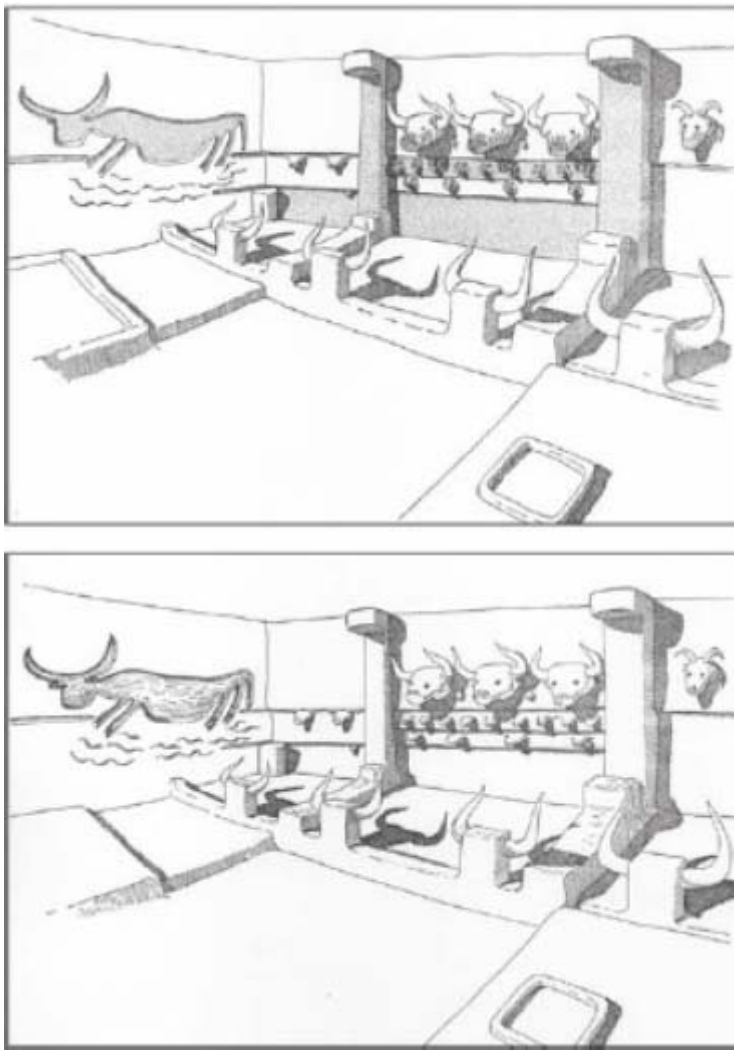

Figure 6.3: Shrine 8, Mellaart level EVI: Reconstruction of different phases of decoration on the east wall (after Mellaart 1963b; from Asouti 1995, 81)

6.4.2. Skeletal study

Cranial and postcranial measurements were taken from a total of 159 juveniles aged between birth and 18 years of age with associated dentitions (Table 6.2). As the Mellaart material housed at UCL only included dental remains, no postcranial measurements from the earlier excavations were included in this analysis.

In terms of the chronological horizon, fifteen individuals were recovered from an early context (2 in South K, 1 in South H, 9 in South L, 3 in South J), 62 juveniles originated from a middle or “Peak” context (28 from North G, 11 from South M, 10 from BACH G and 13

from 4040 G) and 61 juveniles were found in a late or “Post-Peak” context (1 from South P, 1 from South T, 21 from South Q, 6 from South R, 1 from South S, 2 from South O and 29 from 4040 H).

With regards to spatial differences within the site, of a total of 159 juveniles, fifty-five individuals come from special context “history houses”, more specifically from Building 1, Building 6, Building 18, Building 23, Building 17, Building 44, Building 56, Building 60, Building 65 and Building 77.

Table 6.2: Context information for each individual included in the skeletal study

specimen nr	place of burial	period	area	Hodder level	bldng
1425.1	history house	Peak	north	?G	1
1448.3	history house	Peak	north	?G	1
1450.1	history house	Peak	north	?G	1
1484.1	history house	Peak	north	?G	1
1495.1	history house	Peak	north	?G	1
1498.1	history house	Peak	north	?G	1
1884.1	non-history house	Peak	south	?M	50
1885.1	non-history house	Peak	south	?M	50
1912.1	history house	Peak	north	?G	1
1913.1	history house	Peak	north	?G	1
1916.1	history house	Peak	north	?G	1
1923.1	history house	Peak	north	?G	1
1925.1	history house	Peak	north	?G	1
1926.1	history house	Peak	north	?G	1
1935.1	history house	Peak	north	?G	1
1938.1	history house	Peak	north	?G	1
1950.1	history house	Peak	north	?G	1
1959.1	history house	Peak	north	?G	1
1960.1	history house	Peak	north	?G	1
1992.1	history house	Peak	north	?G	1
2033.1	non-history house	Peak	south	?M	50
2105.1	history house	Peak	north	?G	1
2119.1	history house	Peak	north	?G	1
2141.1	history house	Peak	north	?G	1
2197.1	history house	Peak	north	?G	1
2199.1	history house	Peak	north	?G	1
2362.1	non-history house	Peak	south	?M	50
2510.1	history house	Peak	north	?G	1
2515.1	history house	Peak	north	?G	1
2532.1	history house	Peak	north	?G	1
2728.1	non-history house	Peak	south	?M	50
2772.1	non-history house	Peak	south	?M	
2779.1	non-history house	Peak	south	?M	50
2842.1	non-history house	Peak	south	?M	50

4328.1	history house	Pre-Peak	south	L	6
4394	history house	Pre-Peak	south	L	6
4424.1	history house	Pre-Peak	south	L	6
4427.1	history house	Pre-Peak	south	L	6
4438.1	history house	Pre-Peak	south	L	6
4458.1	history house	Pre-Peak	south	L	6
4555.1	history house	Pre-Peak	south	J	18
4828.1	non-history house	Pre-Peak	south	H	
4853.1	history house	Pre-Peak	south	J	23
4861.1	history house	Pre-Peak	south	J	23
4927.1	history house	Pre-Peak	south	L	6
5177.1	history house	Pre-Peak	south	K	17
5357.1	history house	Pre-Peak	south	K	17
5608.1	non-history house	unassigned	north		
5617.1	non-history house	unassigned	south	?L - O ?	
5659.1	non-history house	Peak	south	?M	92
5726.1	non-history house	Post-Peak	south	?T	
5745.1	non-history house	Peak	south	?M	91
5747.1	non-history house	Peak	south	?M	91
5795.1	non-history house	unassigned	south		
6237.1	non-history house	Peak	Bach	?G	3
6681.1	non-history house	Peak	Bach	?G	3
6682.1	non-history house	Peak	Bach	?G	3
7541.1	non-history house	unassigned	4040		
7576.1	non-history house	unassigned	4040	Unstrat Neo	
7579.1	non-history house	unassigned	4040	Unstrat Neo	
8113.1	non-history house	Peak	Bach	?G	3
8114.1	non-history house	Peak	Bach	G	3
8184.1	non-history house	Peak	Bach	?G	3
8409.1	non-history house	Peak	Bach	?G	
8423.1	non-history house	Peak	Bach	?G	
8494.1	non-history house	Peak	Bach	?G	
8729.1	non-history house	unassigned	4040	Unstrat Neo	
10112.1	non-history house	Post-Peak	4040	H	45
10148.1	non-history house	Post-Peak	4040	H	
10267.1	non-history house	Post-Peak	4040	H	58
10333.1	non-history house	unassigned	4040		
10335.1	non-history house	Post-Peak	4040	H	57
10360.1	non-history house	Post-Peak	4040	H	58
10361.1	non-history house	Post-Peak	4040	H	58
10366.1	non-history house	Post-Peak	4040	H	58
10368.1	non-history house	Post-Peak	4040	H	58
10370.1	non-history house	Post-Peak	4040	H	58
10388.1	non-history house	Post-Peak	4040	H	
10389.1	non-history house	Post-Peak	4040	H	58
10390.1	non-history house	Post-Peak	4040	H	58
10391.1	non-history house	Post-Peak	4040	H	58
10400.1	non-history house	Post-Peak	south	Q	53

10450.1	non-history house	Post-Peak	south	R	42
10476.1	non-history house	Post-Peak	south	R	42
10495.1	non-history house	Post-Peak	south	R	42
10498.1	non-history house	Post-Peak	south	R	42
10527.1	non-history house	Pre-Peak	south	L	43
10529.1	non-history house	Pre-Peak	south	L	43
11254.2	history house	Post-Peak	south	S	44
11913.1	non-history house	Peak	4040	G	52
11957.1	non-history house	Post-Peak	4040	H	54
11971.1	non-history house	Post-Peak	4040	H	54
11972.1	non-history house	Post-Peak	4040	H	54
11973.1	non-history house	Post-Peak	4040	H	54
11975.1	non-history house	Post-Peak	4040	H	54
11979.1	non-history house	Post-Peak	4040	H	54
11982.1	non-history house	Post-Peak	4040	H	54
12506.1	non-history house	Post-Peak	south	Q	53
12528.1	non-history house	Post-Peak	south	Q	53
12542.1	non-history house	Post-Peak	south	Q	53
12570.1	non-history house	Post-Peak	south	Q	53
12875.1	history house	Post-Peak	south	R	56
12935.1	history house	Post-Peak	4040	H	60
13100.1	history house	Post-Peak	4040	H	60
13163.1	history house	Post-Peak	4040	H	60
13395.1	history house	Post-Peak	south	Q	56
14005.1	non-history house	Post-Peak	south	Q	
14010.1	history house	Post-Peak	south	Q	65
14020.1	history house	Post-Peak	south	Q	65
14101.1	non-history house	unassigned	4040		
14107.1	non-history house	unassigned	4040		
14108.1	non-history house	unassigned	4040		
14109.1	non-history house	unassigned	4040		
14138.1	non-history house	Post-Peak	4040	H	88
14146.1	non-history house	Post-Peak	4040	H	88
14148.1	non-history house	Post-Peak	4040	H	88
14150.1	non-history house	Post-Peak	4040	H	88
14162.1	non-history house	Post-Peak	4040	H	88
14165.1	non-history house	Post-Peak	4040	H	88
14536.1	history house	Post-Peak	south	Q	65
14818.1	non-history house	Post-Peak	south	Q	53
15467.1	non-history house	unassigned	4040		
15482.1	non-history house	unassigned	4040	unassigned Neo	
15739.1	non-history house	Post-Peak	south	Q	
15748.1	history house	Post-Peak	south	Q	65
15796.1	non-history house	Post-Peak	south	Q	
15799.1	non-history house	Post-Peak	south	Q	
16067.1	non-history house	unassigned	4040	unstratified Neo	
16125.1	non-history house	unassigned	4040	unstratified Neo	
16131.1	non-history house	unassigned	4040	unassigned Neo	

16168.1	non-history house	unassigned	4040	unassigned Neo	
16196.1	non-history house	unassigned	4040		
16203.1	history house	Post-Peak	south	Q	65
16204.1	history house	Post-Peak	south	Q	65
16207.1	non-history house	Post-Peak	south	Q	
16210.1	non-history house	Post-Peak	south	Q	
16213.1	non-history house	Post-Peak	south	Q	
16216.1	non-history house	Post-Peak	south	Q	
16601.1	non-history house	Peak	4040	G	49
16627.1	non-history house	Peak	4040	G	49
16638.1	non-history house	Peak	4040	G	49
16641.1	non-history house	Peak	4040	G	49
16660.1	non-history house	Peak	4040	G	49
16698.1	non-history house	Peak	4040	G	49
16712.1	non-history house	Peak	4040	G	52
16723.1	non-history house	Peak	4040	G	52
17063.1	non-history house	Post-Peak	south	P	75
17457.1	non-history house	Peak	4040	G	49
17546.1	non-history house	unassigned	4040	unstratified Neo	
17549.1	non-history house	unassigned	4040	unstratified Neo	
17939.1	non-history house	Peak	4040	G	49
18447.1	non-history house	Post-Peak	south	O	76
18464.1	non-history house	Post-Peak	south	O	76
19022.1	history house	Peak	4040		77
19039.1	history house	Peak	4040		77
12876.1	history house	Post-Peak	south	R	56
1939.1	history house	Peak	north	?G	1
2125.1	history house	Peak	north	?G	1
8425.1	non-history house	Peak	Bach	?G	

Chapter 7. Results

The aim of this chapter is to address the research questions set out at the beginning of this thesis, using the methods outlined in the previous chapter. The research questions are as follows:

1. Can enamel defects be assessed objectively?
2. Is there a correlation between delayed skeletal growth and patterns of furrow-form enamel hypoplasia?
3. Did human growth patterns vary in terms of place of residence at Çatalhöyük?
4. Did changes in community size and density affect human growth at Çatalhöyük?

The first part of this chapter presents the results of the study of furrow-form enamel hypoplasia. In this section, the metrically and visually identified defects are quantified and the parameters are compared in terms of place and time of burial. First, the procedure behind the matching of defects is discussed (Research Question 1). After this follows a description of the results of the comparison of defect appearance and characteristics between individuals, which is based upon the parameters outlined in the methods chapter, including the number of and interval between defects; the duration of defects and the percentage of enamel formation time taken up by growth disturbances. Using these parameters, this section investigates whether patterns of furrow-form enamel hypoplasia vary consistently in terms of place (history houses versus non-history houses) and/or time (Peak versus Post-Peak contexts) within the assemblage of individuals examined (Research Questions 3 and 4).

The second part of this chapter provides the results of the skeletal growth study. In order to address Questions 3 and 4 above, comparisons are made between history and non-history houses, and peak versus non-peak contexts.

The final section of the results chapter examines the relationship between dental developmental disturbances and skeletal growth, using the definitions of defects generated by the newly developed microscopic method (Research Question 2).

7.1. Furrow-form enamel hypoplasia

7.1.1. Matching of defects

Perikymata counts and periodicity

In permanent tooth crown development, perikymata appear first on the lower incisors. The perikyma grooves on the mamelons are formed between 9 months and 1 year of age in the central incisor and around one year of age in the lateral incisor (Reid and Dean 2000). The crown surface of the central incisor takes between 2.4 and 3 years to form and in this study, the mean count of perikyma grooves from mamelons to the lowest part of the cervical margin was established as 127 for this tooth type (Table 7.1). In lateral incisors, Reid and Dean (2000) found that the crown surface took around three years to form, give or take two months, and the present study found a mean perikyma groove count of 134.

Table 7.1: Mean, median, standard deviation, interquartile range and range of perikymata counts for permanent incisors in the Çatalhöyük collection

Tooth type	N of teeth	Mean pkg count per tooth	Standard deviation pkg count per tooth	Median pkg count per tooth	Interquartile range pkg count per tooth	Range of pkg counts per tooth
UI1	32	131	19	132	21	95-176
UI2	33	122	14	121	21	93-143
LI1	27	127	16	126	17	101-165
LI2	27	134	18	134	22	94-169

Perikymata start to form next in the upper central incisor, where the first grooves appear around the age of one year and one month (Reid and Dean 2000). This taller crown surface takes between three and four years to be completed and a mean count of 131 perikymata was determined for this tooth type. For the upper lateral incisor, on which the first forming perikymata appear at around the age of one year and nine months and the crown is also completed over three to four years, a mean perikyma count of 122 was determined (Reid and Dean 2000).

The range of perikymata counts in each tooth type for the Çatalhöyük teeth is inside the lower range of values recorded for modern populations (Guatelli-Steinberg *et al*. 2005). Only the mean perikymata counts recorded for South African populations are lower than the Çatalhöyük mean perikymata counts (Fig. 7.1).

Based on cross-striation counts, Guatelli-Steinberg and colleagues (2005) calculated mean periodicities of 9.097 (with a standard deviation of 1.207) and 8.748 (with a standard deviation of 1.042) for the South African and Newcastle samples respectively, with a modal periodicity of nine for both samples. This is similar to the modal periodicity found in a large sample of modern humans (Dean and Reid 2001; Fitzgerald 1998). This periodicity also falls within the range of periodicities (6-12, with 8 and 9 day periodicities most commonly found) found in more recent studies by Smith and colleagues (2007a, 2010) using a sample of 365 recent modern human (European, North American and African) physically-sectioned teeth and Reid and Ferrell (2006), using a smaller sample of 49 medieval Danish teeth (see Chapter 3). The similarity between the mean perikyma counts for the Çatalhöyük sample and these modern human samples supports the use of a 9 day periodicity in this study.

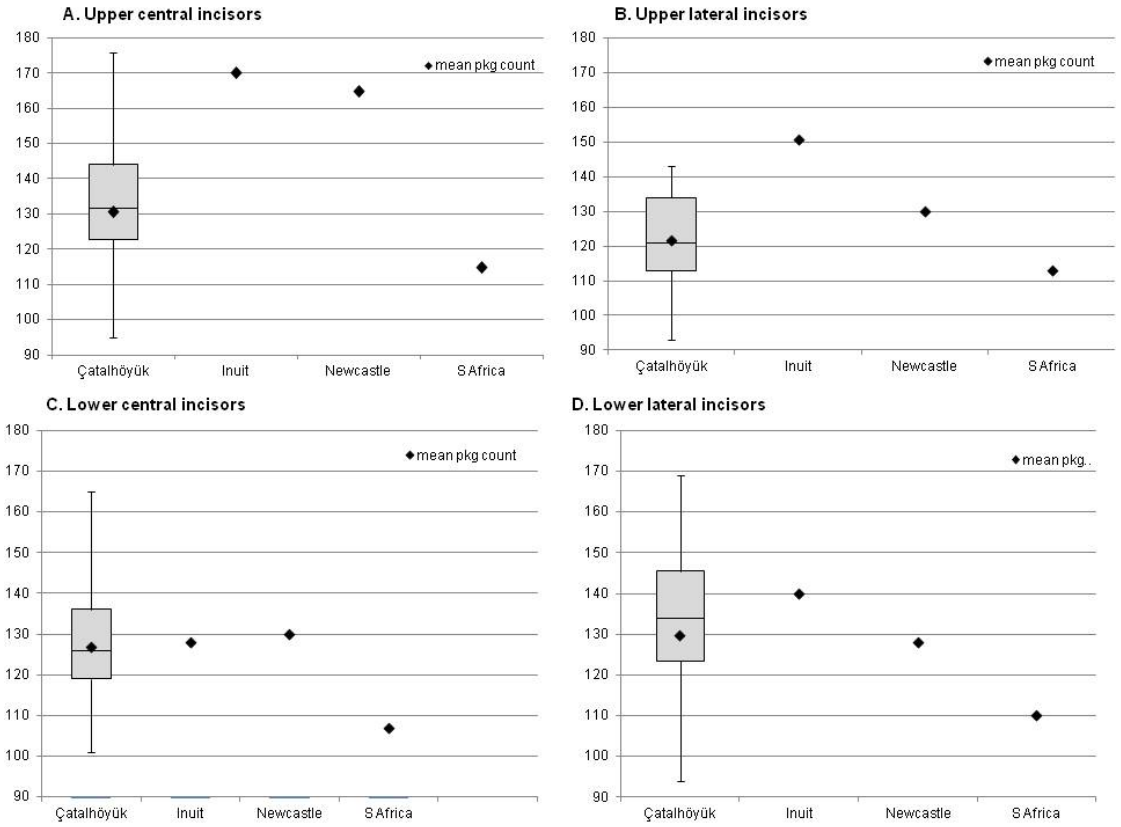

Figure 7.1: Box and whisker charts of Çatalhöyük permanent incisors and comparison of mean perikyma counts (black diamonds) per tooth type for Çatalhöyük, Inuit, Newcastle and South African data (based on Guatelli-Steinberg *et al*. 2005, 14199)

Registering defects across the dentition

A total of 134 teeth (upper central and lateral incisors and lower central and lateral incisors) from 54 individuals were recorded in this study. All individuals within the sample displayed furrow-form defects or enamel hypoplasia. In all cases, it was possible to use prominent defects to calibrate developmental schedules across the dentition (as per Smith *et al*. 2007b).

Figure 7.2 shows the developmental defects matched across the dentition of CH 1913. The blue arrow indicates a particularly prominent defect which was detected metrically (using the method outlined in Chapter 5) as well as visually on the lower central (Pkg 35-36), lower lateral (Pkg 35-37) and upper central incisor (Pkg 29-33). This defect (blue arrow) was chosen as an anchor point for the matching of other identified defects (green arrows).

Table 7.2 shows the details of the matching procedure for CH 1913. Of four prominent defects detected for this individual, two defects could not be detected using a 90th percentile threshold across the entire dentition (highlighted in grey). The values of the perikymata spacing in these areas of the upper central incisor are high (85th and 82nd percentiles), so that these were nevertheless accepted as defects. Details of the matching procedure, including the rationale for the choice of which prominent defect was chosen as an anchor point and the percentiles associated with each identified defect, are provided for all individuals and can be found in the appendix (see Appendix 1).

Table 7.2: Example of four matched defects observed on CH 1913

LLI1	**LLI2**	**ULI1**
Pkg 35-36 Matched: 90th percentile	Pkg 35-37 Matched: 90th percentile	Pkg 29-33 Matched: 90th percentile
Pkg 61-65 Matched: 90th percentile	Pkg 67-69 Matched: 90th percentile	Pkg 58-59 Matched: 85th percentile
Pkg 78-81 Matched: 90th percentile	Pkg 76-79 Matched: 90th percentile	Pkg 64-69 Matched: 90th percentile
Pkg 94-97 Matched: 90th percentile	Pkg 98-99 Matched: 90th percentile	Pkg 83-91 Matched: 82nd percentile

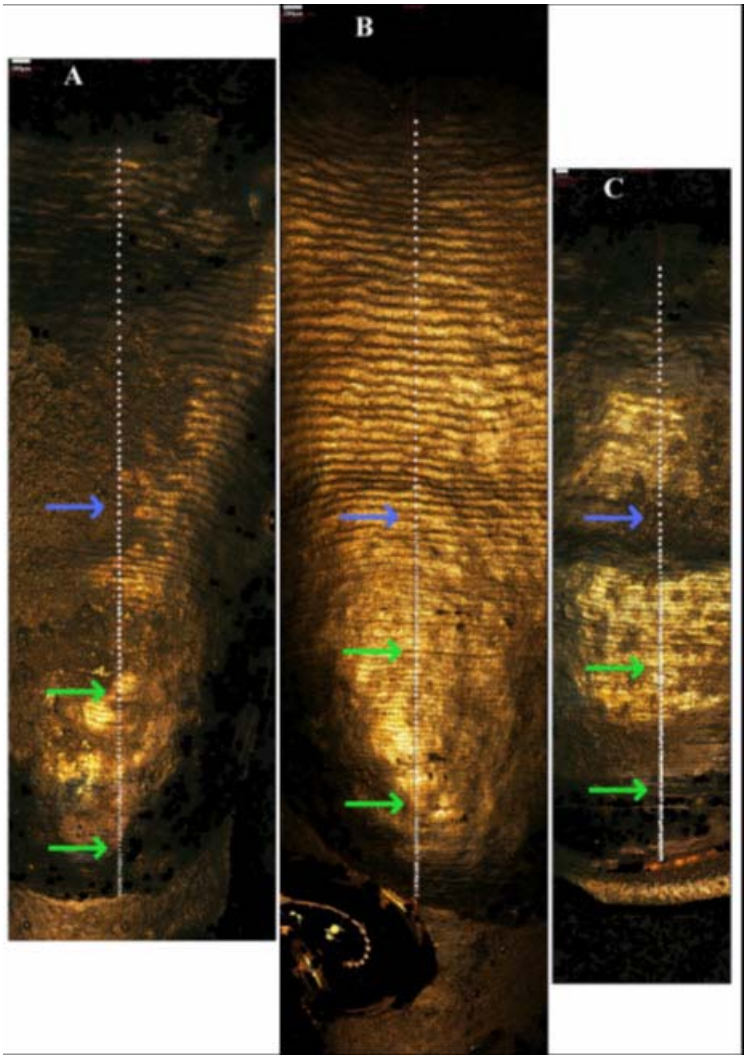

Figure 7.2: Example of tooth crown with prominent defect and matched defects based upon this prominent defect (CH1913)

Of the 54 individuals assessed for evidence of furrow-form enamel hypoplasia, a total of 378 visually and metrically detected defects could be matched between multiple teeth within one dentition. Per tooth type, this amounts to 200 matched defects for lower central incisors, 208 for lower lateral incisors, 223 for upper central incisors and 199 matched defects for upper lateral incisors. Of these, only a small number could be not be detected using a 90th percentile threshold on all tooth types (Table 7.3).

Table 7.3: Overview of metrically detected defects per tooth type			
Tooth type	Total number of detected defects	% defects detected above 90th percentile threshold	% defects visually detected with high residuals (between 80th and 90th per-centile threshold)
Lower central incisor	200	88.5% (N=177)	11.5% (N = 23)
Lower lateral incisor	208	92.3% (N=192)	7.7% (N = 16)
Upper central incisor	223	89.7% (N = 200)	10.3% (N = 23)
Upper lateral incisor	199	89.9% (N = 179)	10.1% (N = 20)

7.1.2. Comparison between individuals

Number and age distribution of defects

As the presence of furrow-form enamel hypoplasia indicates that an individual experienced some form of growth disturbance during his or her life, the prevalence of enamel defects is often used as a an indicator of the level of disturbances experienced during a child's life, with high defect frequencies associated with high levels of growth disturbances (for an overview and discussion: see Chapter 4). This commonly used parameter can be calculated based on the number of affected individuals (i.e. number of individuals with one or more matched defects as a proportion of the total number of individuals) or by the number of affected teeth per individual (Guatelli-Steinberg *et al*. 2004). As all individuals and teeth within the study sample displayed some form of furrow-form enamel hypoplasia as defined here, an alternative frequency parameter was employed in this study, based upon the number of matched defects per individual.

First, the **maximum number of matched defects per individual** was calculated as the total number of matched defects, taking into account all available teeth. This ranges from three (CH 4394, CH 14108) to 16 (CH 2119) defects, with an average of seven defects for the entire sample. As the maximum number of matched defects is expected to be affected by the number of teeth available in the analysis, the **mean number of matched defects per individual** was also calculated by counting and averaging the number of matched defects identified on each tooth (as per King *et al*. 2002, 2005). This mean number of defects per individual ranges from three (CH 4394, CH 14108) to thirteen (CH 12876) defects, with a mean of six defects for the entire sample.

The positions of defects within the dental development sequence were assessed as proportions of the total perikymata count. Perikymata sequences for all teeth within each

dentition were aligned for all individuals, constructing a full individual sequence from the first perikyma on the lower central incisor to the last perikyma on the upper lateral incisor. This sequence was then divided into quarters and the **number of matched defects per quarter** (referred to as zone 1, 2, 3 and 4) was counted for each individual.

The number of defects ranges from zero to five defects in zone 1, one to six defects in zone 2, zero to four defects in zone 3 and zero to three defects in zone 4. Figure 7.3 shows the mean (solid line), maximum and minimum number of defects (dashed lines) in all zones for the entire sample. Zone 2 has the highest number of defects across the entire dataset, with a maximum of six defects and a minimum of one defect. There is little variation between the individuals buried in history (triangles) and non-history houses (stars). The lowest number of defects is found in individuals buried in a post-peak context for all zones, but especially for zone 2 (squares).

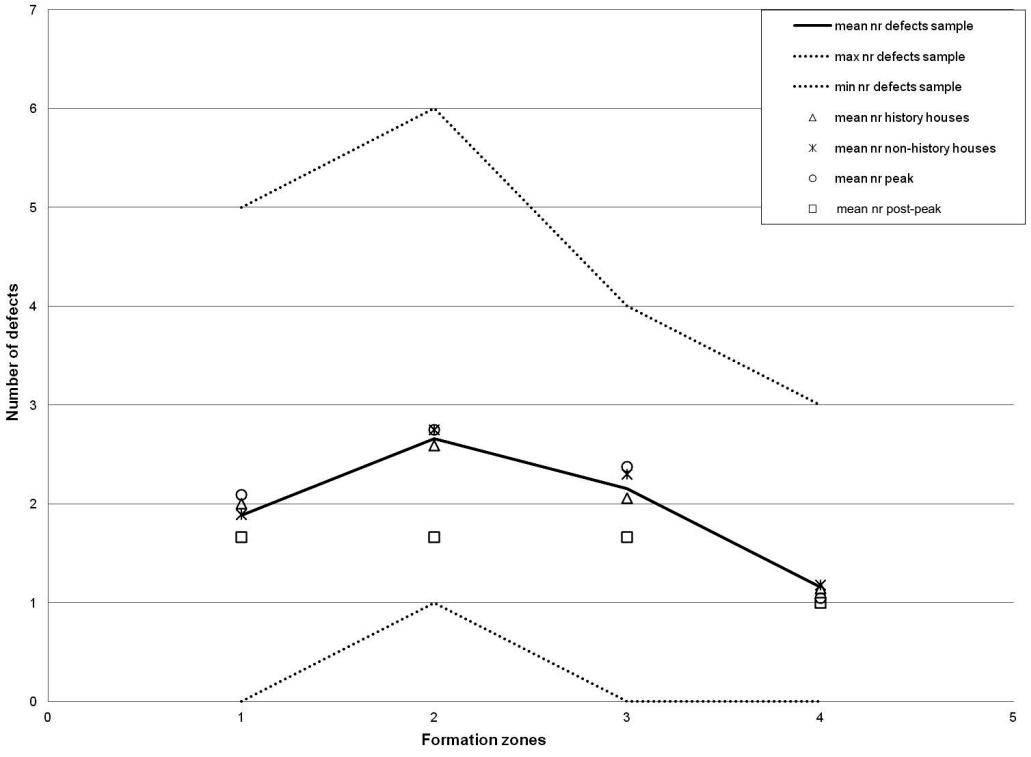

Figure 7.3: Frequency distribution of enamel defects matched across the incisors per zone. Solid line = mean number of defects entire sample, dashed line = maximum and minimum number of defects entire sample, triangles = individuals buried in history, stars = individuals buried in non-history houses, circles = individuals buried in a peak context, squares = individuals buried in a post-peak context

The age of the enamel defects was estimated by counting the number of perikymata from the tip of the mamelon to the onset of the prominent defect and converting this into days, using a nine-day periodicity (for the rationale behind this, see Chapter 5) and taking into account the average age at which perikymata start to appear on the enamel surface. The number of days can then converted into years by dividing the total by 365.

In terms of the **age distribution** of these matched defects, the highest mean numbers are found between two and four years of age (Table 7.4). This peak frequency is observed in individuals buried in history and non-history houses and from Peak and Post-Peak periods.

Table 7.4: Age profile of enamel defects in total samples and subsets based on place and time of burial (based upon mean number of defects)

		Age range in years			
	Sample size (N of individuals)	1.0-1.99	2.0-2.99	3.0-3.99	4.0-4.99
Total sample	54	1.6	2.6	2.1	0.7
History houses	23	1.5	2.6	1.8	0.6
Non-history house	29	1.2	2.4	2.1	0.8
Peak period	31	1.4	2.6	2.1	0.6
Post-Peak period	9	1.2	2.6	1.9	0.7

A non-parametric significance test (Mann-Whitney test) was carried out in order to investigate whether place or time of burial predicted variation in the frequency of enamel defects, with the frequency calculated as the maximum and mean number of defects per individual. Pre-Peak period individuals were not included in the “time of burial” analysis, as the sample size (N=2) was too low to provide meaningful results.

There are no significant differences in the maximum or mean number of defects in relation to place of burial or time of burial (Table 7.5). As expected from the visual examination of figure three, there is no significant variation between the defect frequencies of individuals buried in history and non-history houses for any of the four enamel formation zones. In addition, the lower number of defects in Post-Peak individuals for all enamel formation zones shown in Figure 7.3 is not significantly different to the defect frequency calculated for Peak individuals. Finally, when analysing the average number of defects per age group, there is no statistically significant difference in defect frequency in terms of time or place of burial (Table 7.5).

Table 7.5: Non-parametric significance test (Mann-Whitney) of enamel frequency based on individuals		
Parameter	Significance	
	Place of burial (History vs non-History houses)	Time of burial (Peak vs Post-Peak)
Max N defects	Z = -0.577 (p=0.564)	Z = -0.524 (p=0.600)
Mean N defects	Z= -0.411 (p=0.681)	Z= -0459 (p=0.646)
Mean N defects zone 1	Z = -0.125 (p=0.900)	Z = -0.039 (p=0.969)
Mean N defects zone 2	Z = -0.800 (p=0.424)	Z = -0.624 (p=0.532)
Mean N defects zone 3	Z = -0.565 (p=0.572)	Z = -0.404 (p=0.686)
Mean N defects zone 4	Z = -0.794 (p=0.427)	Z = -0.882 (p=0.378)
Mean N defects 1-1.99 years	Z = -0.790 (p=0.430)	Z = -1.030 (p=0.303)
Mean N defects 2-2.99 years	Z = -0.079 (p=0.937)	Z = -0.328 (p=0.743)
Mean N defects 3-3.99 years	Z = -0.693 (p=0.489)	Z = -1.007 (p=0.314)
Mean N defects 4-4.99 years	Z = -0.794 (p=0.427)	Z = -0.882 (p=0.378)

In order to minimise the bias related to the number of teeth available for matching defects, a separate analysis was also carried out **per tooth type**. For each of the tooth types, the number of defects was compared in relation to place and time of burial. In addition to this, the perikymata count for each tooth was divided into quarters. Defects were assigned to each quarter, the number of defects per quarter of each tooth type counted and compared in terms of place and time of burial. Finally, the mean number of defects per age range was also compared in terms of place and time of burial for each tooth type.

The mean number of defects ranges between 1.6 and 2.1 in the four zones of all tooth types, with the exception of the upper lateral incisor, for which mean number of defects of 1.3 defects was calculated in zone 4. The highest variation in numbers of defects can be found in zone 1 of the upper central incisors, where the number of defects ranges from zero to six. This is due to the high frequency of defects for one outlier (CH 12876).

Figure 7.4 shows the average (solid line), maximum and minimum number of defects (dashed lines) in all zones for each tooth type. There is little variation between the individuals buried in history (triangles) and non-history houses (stars) for all zones in each tooth type. There are some differences in the number of defects between peak and post-peak individuals. For the lower central and upper lateral incisors, defect numbers appear lower in post-peak individuals in zone 3 of the lower central incisors and zone 2 of the lower central and upper lateral incisors. In contrast, average defects numbers on post-peak individuals appear high in zone 1 of the upper central incisors, but this high number is likely to be caused by the outlier CH 12876. After removing this outlier, the average number of defects in post-peak individuals amounts to two, indicating little variation in average defect numbers for this tooth type.

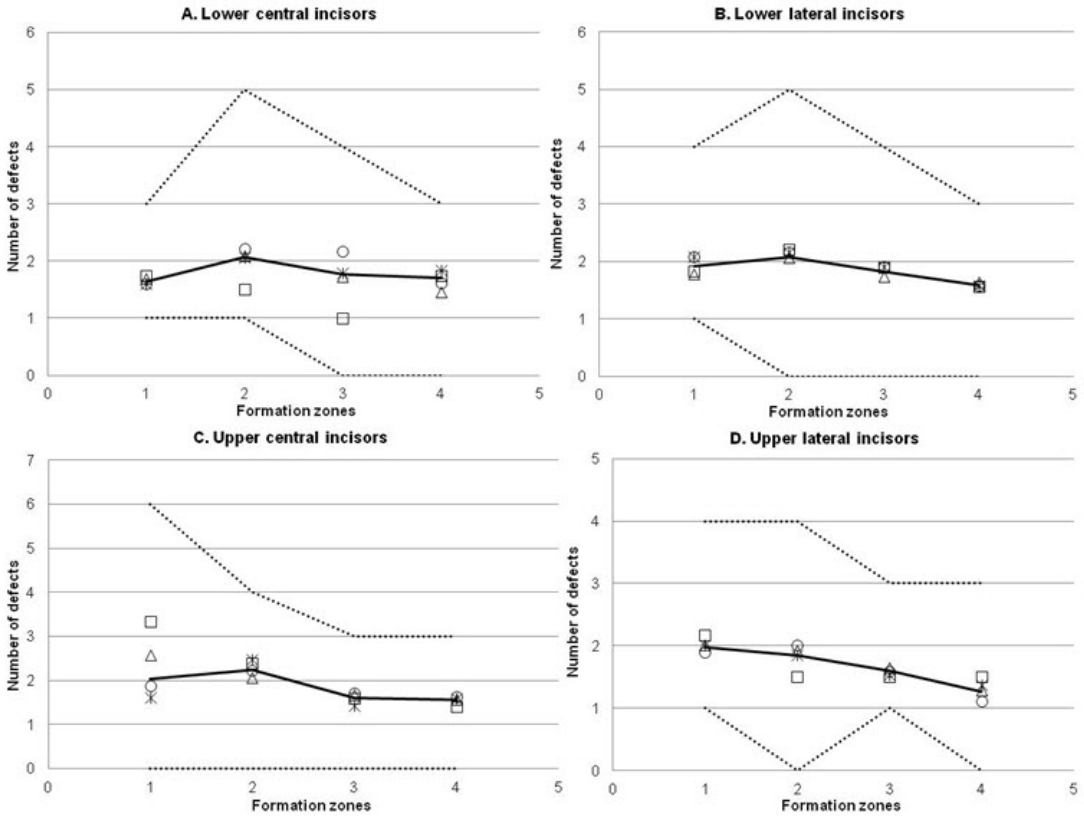

Figure 7.4: Frequency distribution of matched enamel defects per tooth type divided into zones. Solid line = mean number of defects entire sample, dashed line = maximum and minimum number of defects entire sample, triangles = mean number defects for individuals buried in history, stars = mean number of defects for individuals buried in non-history houses, circles = mean number of defects for individuals buried in a Peak context, squares = mean number of defects for individuals buried in a Post-Peak context

Similarly to the analysis based on individuals, the non-parametric significance test based on the separate tooth types shows no significant differences in the number of defects in terms of place of burial or time of burial (Table 7.6). When divided into zones or age groups, no clear significant differences are apparent. The differences between peak and post-peak individuals for zone 3 of the lower central incisors which are apparent in Figure 7.4 seem to be approaching significance (Table 7.6, highlighted in grey). On average, this zone includes perikymata 63 to 96. Using a nine day periodicity, this zone roughly corresponds to the 2-2.99 group, for which the differences between peak and post-peak individuals are not significant for any of the tooth types (Table 7.6).

Table 7.6: Non-parametric significance test (Mann-Whitney) of enamel frequency based on tooth types		
Parameter	Significance	
LOWER CENTRAL INCISOR	Place of burial (History vs non-History houses)	Time of burial (Peak vs Post-Peak)
N defects zone 1	Z = -0.275 (p=0.783)	Z = -0.662 (p=0.508)
N defects zone 2	Z = -0.158 (p=0.879)	Z = -1.294 (p=0.196)
N defects zone 3	Z = -0.023 (p=0.982)	**Z = -1.737 (p=0.082)**
N defects zone 4	Z = -0.956 (p=0.339)	Z = -0.319 (p=0.750)
N defects 1-1.99 years	Z = -0.047 (p=0.962)	Z = -0.239 (p=0.811)
N defects 2-2.99 years	Z = -0.686 (p=0.493)	Z = -1.356 (p=0.175)
N defects 3-3.99 years	Z = -0.683 (p=0.494)	Z = -0.095 (p=0.924)
N defects 4-4.99 years	Z = -0.510 (p=0.610)	Z = -1.046 (p=0.295)
N defects	Z = -0.762 (p=0.446)	Z = -0.862 (p=0.388)
LOWER LATERAL INCISOR		
N defects zone 1	Z = -0.604 (p=0.546)	Z = -0.491 (p=0.624)
N defects zone 2	Z = -0.127 (p=0.899)	Z = -0.602 (p=0.547)
N defects zone 3	Z = -0.133 (p=0.894)	Z = -0.755 (p=0.450)
N defects zone 4	Z = 0.107 (p=0.915)	Z = -0.741 (p=0.459)
N defects 1-1.99 years	Z = -0.835 (p=0.404)	Z = 0.000 (p=1.000)
N defects 2-2.99 years	Z = -0.807 (p=0.420)	Z = -0.337 (p=0.736)
N defects 3-3.99 years	Z = -0.791 (p=0.429)	Z = -0.429 (p=0.668)
N defects 4-4.99 years	Z = -0.725 (p=0.452)	Z = -0.059 (p=0.953)
N defects	Z = -0.719 (p=0.472)	Z = -0.862 (p=0.388)
UPPER CENTRAL INCISOR		
N defects zone 1	Z = -1.488 (p=0.137)	Z = -1.371 (p=0.170)
N defects zone 2	Z = -1.107 (p=0.268)	Z = -0.551 (p=0.581)
N defects zone 3	Z = -0.671 (p=0.502)	Z = -0.446 (p=0.655)
N defects zone 4	Z = -0.048 (p=0.961)	Z = -0.765 (p=0.445)
N defects 1-1.99 years	Z = -1.501 (p=0.133)	Z = -0.451 (p=0.652)
N defects 2-2.99 years	Z = -0.656 (p=0.512)	Z = -1.009 (p=0.313)
N defects 3-3.99 years	Z = -0.100 (p=0.921)	Z = -0.988 (p=0.323)
N defects 4-4.99 years	Z = -0.103 (p=0.918)	Z = -0.555 (p=0.579)
N defects	Z = -0.306 (p=0.760)	Z = -0.095 (p=0.924)
UPPER LATERAL INCISOR		
N defects zone 1	Z = -0.157 (p=0.875)	Z = -1.135 (p=0.256)
N defects zone 2	Z = -0.148 (p=0.882)	Z = -0.991 (p=0.319)
N defects zone 3	Z = -0.530 (p=0.596)	Z = -0.499 (p=0.618)
N defects zone 4	Z = -0.301 (p=0.764)	Z = -0.552 (p=0.581)
N defects 1-1.99 years	Z = -1.214 (p=0.225)	Z = -1.202 (p=0.230)
N defects 2-2.99 years	Z = -0.437 (p=0.662)	Z = 0.000 (p=1.000)
N defects 3-3.99 years	Z = -0.217 (p=0.828)	Z = -1.191 (p=0.234)
N defects 4-4.99 years	Z = -0.915 (p=0.360)	Z = -0.976 (p=0.329)
N defects	Z = -0.641 (p=0.521)	Z = -0.131 (p=0.896)

Number of affected perikymata

The assessment of enamel defect prevalence can be problematic as each defect is assumed to represent a similar disturbance, whereas some defects can affect enamel growth to a greater degree than others (Temple *et al.* 2013). An alternative way to quantify the presence of defects is to consider the cumulative record of perikymata affected by hypoplastic defects from the start to the end of enamel formation (as per King *et al.* 2005). Individuals with a high number of affected perikymata are thus considered to have more of their growth affected by physiological disturbances than individuals with few affected perikymata.

The **maximum number of perikymata affected** by growth disruptions was recorded and compared between individuals. As this number might be influenced by the variation in total perikyma counts, the **percentage of enamel formation affected** by growth disturbances was also calculated. This was the maximum number of affected perikymata expressed as the percentage of the maximum number of perikymata recorded per individual.

The total number of disrupted perikymata for each individual ranged between 16 and 50, with a mean of 29 affected perikymata for the entire assemblage. The percentage of enamel formation affected ranges from 12.7% to 39.1%, with a mean of 21.2% of the enamel affected for the entire group. Figure 7.5 shows the calculated minima, maxima, quartiles, means and medians for the percentage of growth affected by defects for individuals buried in each context (history and non-history house, Peak and Post-Peak period). Apart from the marginally lower mean and median values for the Post-Peak individuals, there are no apparent differences between individuals buried in different contexts (Fig. 7.5). There is a very high maximum number of affected perikymata for individuals from the Peak period, However, this high maximum value is likely to be caused by the outlier CH 16698 (39.1%).

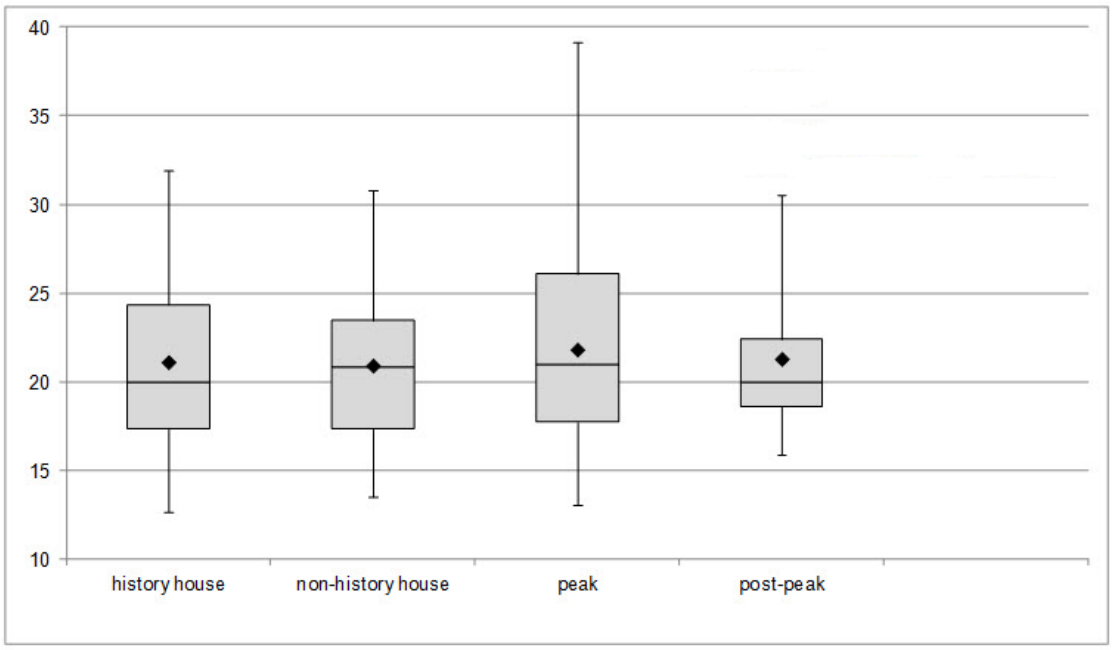

Figure 7.5: Box and whisker charts of the percentage of growth affected by defects for individuals buried in history and non-history houses and in Peak and Post-Peak periods. Central line = median percentage affected, Black diamond = mean percentage affected, Top box = upper quartiles, Bottom box = lower quartiles, Whiskers = maximum and minimum

Table 7.7 shows the results of the statistical analysis of the maximum counts of disrupted perikymata and the percentage of dental formation affected by hypoplastic defects. As expected from the visual inspection of Figure 7.5, there are no statistically significant differences between individuals buried in different contexts (history versus non-history houses and Peak versus Post-Peak contexts).

Table 7.7: Non-parametric significance test (Mann-Whitney) of affected perikymata numbers based on individuals

Parameter	Significance	
	Place of burial (History vs non-History houses)	Time of burial (Peak vs Post-Peak)
Max N disrupted pkg	Z = 0.000 (p=1.000)	Z = -0.373 (p=0.709)
Percentage formation affected by defects	Z = -0.313 (p=0.754)	Z= -0.097 (p=0.923)

Figure 7.6 shows the comparison of the percentages of formation affected by defects for each tooth type. The upper lateral incisors have the lowest percent of enamel formation affected by defects, with a mean of 19.6% compared to a mean of 22.9% for the lower central incisors, 22.0% for the lower lateral incisors and 21.6% for the upper central incisors. There is little variation in the percentage of enamel formation affected by growth

disruptions. A slightly lower percentage of enamel formation seems to be affected for all tooth types of individuals from Post-Peak contexts in comparison to the individuals from peak contexts but this trend is not statistically significant (Table 7.8).

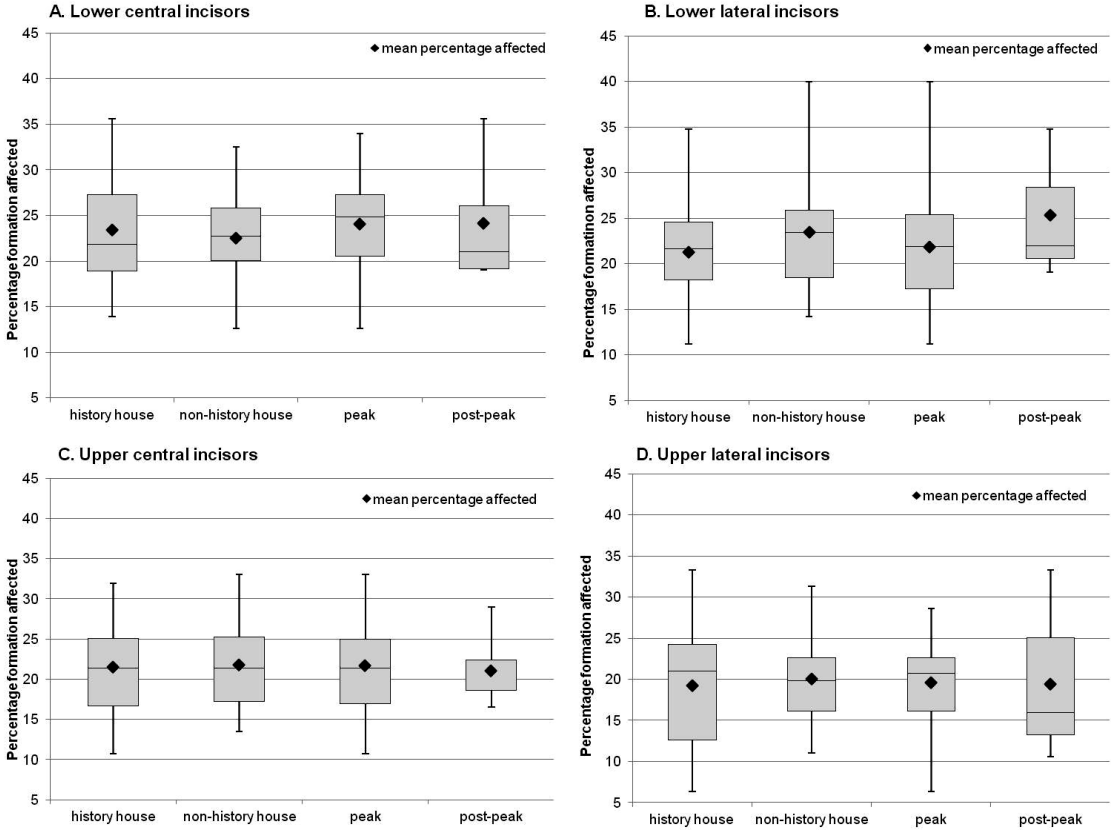

Figure 7.6: Box and whisker charts of the percentage of growth affected by defects per tooth type for individuals buried in history and non-history houses and in Peak and Post-Peak periods. Central line = median percentage formation affected, Black diamond = mean percentage growth affected, Top box = upper quartiles, Bottom box = lower quartiles, Whiskers = maximum and minimum

Table 7.8: Non-parametric significance test (Mann-Whitney) of percentage enamel formation affected by defects based on tooth types		
Parameter	Significance	
	Place of burial (History vs non-History houses)	Time of burial (Peak vs Post-Peak)
LI1 Percentage formation affected	Z = -0.022 (p=0.982)	Z = -1.048 (p=0.296)
LI2 Percentage formation affected	Z = -0.829 (p=0.407)	Z = -0.639 (p=0.523)
UI1 Percentage formation	Z = -0.151 (p=0.880)	Z = -0.125 (p=0.901)
UI2 Percentage formation	Z = -0.284 (p=0.776)	Z = -0.509 (p=0.611)

Duration of and interval between defects

Different enamel defect episodes may represent episodes of different durations. In order to take into account these differences, the number of perikymata within each defect can be used to represent the duration of each episode (Guatelli-Steinberg *et al.* 2004; Hillson and Bond 1997; King *et al.* 2002, 2005; Temple *et al.* 2012, 2013). Assuming that the duration of a defect represents the time needed for an individual to recover from a physiological disturbance, longer defect durations can be interpreted as reflecting more severe disruptions in comparison to shorter durations (King *et al.* 2005). Similarly, the duration of the intervals between defects can also be calculated, with shorter intervals reflecting more frequently occurring disruptions than longer intervals.

The **mean duration of defects** was calculated as the mean duration of all matched defects taking into account all available teeth. The duration of defects, in terms of these mean perikymata counts, ranges from three to six perikymata, with an average duration of four perikymata. When converted to days using a nine-day periodicity, the duration of defects ranges from 21 days to 54 days, with an average of 36 days.

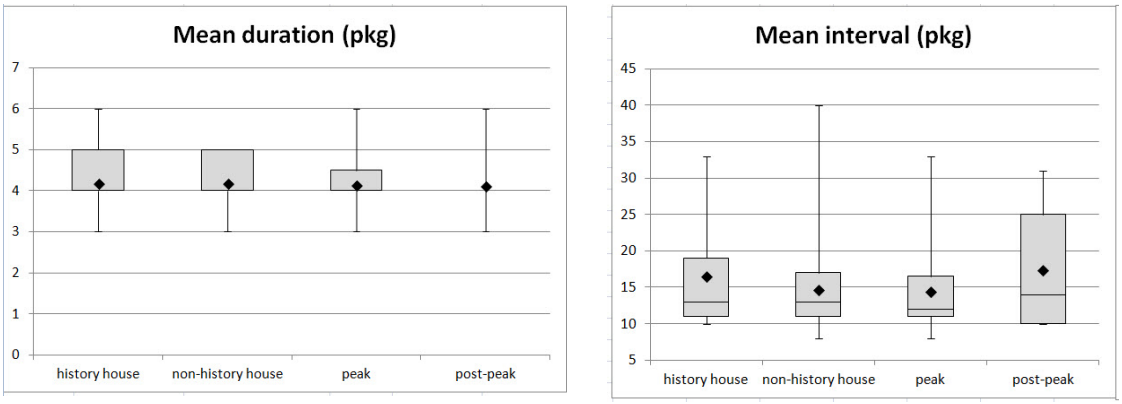

Figure 7.7: Box and whisker charts of the mean duration of and interval between defects for individuals buried in history and non-history houses and in Peak and Post-Peak periods. Central line = median duration, Black diamond = mean duration, Top box = upper quartiles, Bottom box = lower quartiles, Whiskers = maximum and minimum

The **mean interval between defects per individual** was calculated as the mean interval of all matched defects taking into account all available teeth. This ranges from 8 to 40, with an average interval of 16 perikymata between matched defects for the entire sample. When converted to days using a nine-day periodicity, intervals between matched defects range from 72 to 360 days, with an average of 140 days.

No clear differences were observed between history and non-history houses or Peak and Post-Peak individuals in terms of mean duration. In relation to the interval between

defects, the Post-Peak group of individuals has a slightly higher mean value than Peak individuals, but this trend is not statistically significant (Fig. 7.7; Table 7.9).

Using a similar methodology to the assessment of the number of defects per quarter (see above, p. 217), the **average duration per quarter** (zone 1, 2, 3 and 4) was also counted for each individual. Figure 7.8 shows the average (solid line), maximum and minimum duration of defects (dashed lines) in all zones. There is some variation apparent within this dataset, with individuals buried in history houses (triangles) showing substantially shorter durations in zone 3 in comparison to non-history houses (stars). However, this trend is not statistically significant (Table 7.9).

In addition to the lower number of defects in zone 2 and 3, the duration of defects in these zones is also shorter for post-peak individuals (squares) compared to Peak individuals (circles). A contrasting trend is visible for zones 1 and 4, where Post-Peak individuals appear to have longer durations in comparison to peak individuals (Fig. 7.8). For zone 4, this trend is approaching significance (Table 7.9, highlighted in grey).

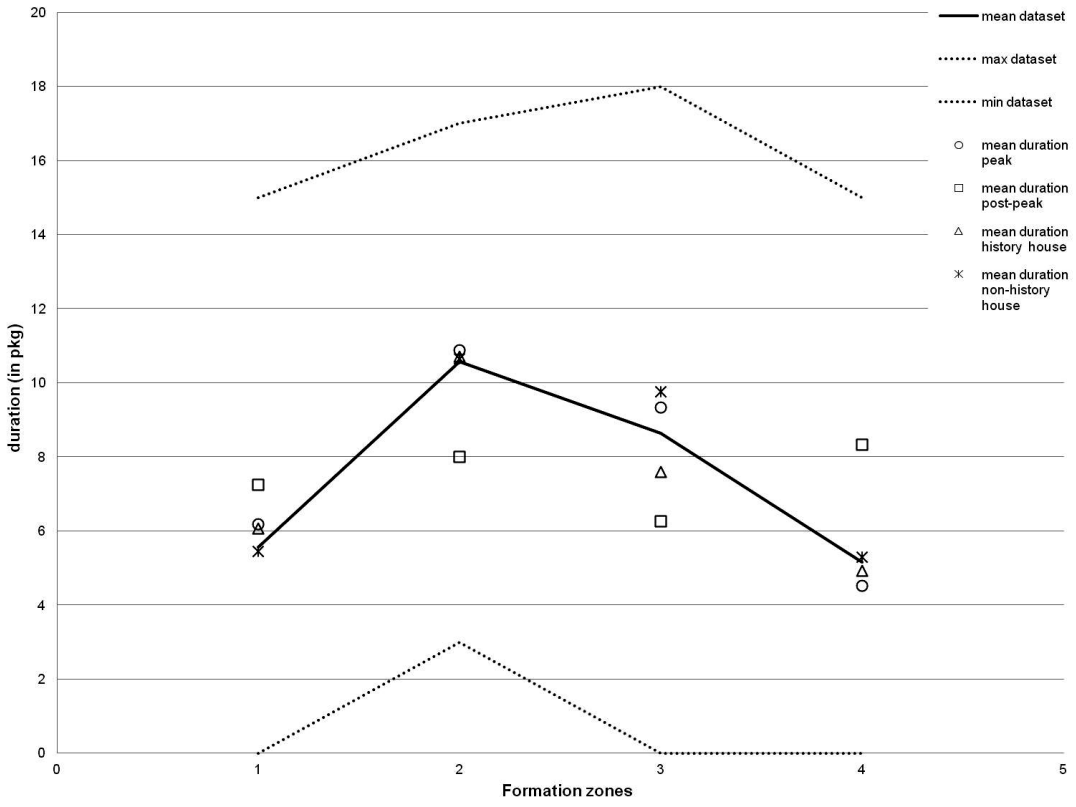

Figure 7.8: Duration of defects per zone of enamel formation. Solid line = mean duration of defects for entire sample, dashed line = maximum and minimum duration of defects for entire sample, triangles = mean duration of defects for individuals buried in history, stars = mean duration of defects for individuals buried in non-history houses, circles = mean duration of defects for

individuals buried in a Peak context, squares = mean duration of defects for individuals buried in a Post-Peak context

Table 7.9: Non-parametric significance test (Mann-Whitney) of duration and intervals between defects based on individuals		
Parameter	Significance	
	Place of burial (History vs non-History houses)	Time of burial (Peak vs Post-Peak)
Mean Duration defects (pkg)	Z = -0.226 (p=0.822)	Z = -0.272 (p=0.786)
Mean Interval defects (pkg)	Z = -0.463 (p=0.643)	Z = -0.783 (p=0.434)
Mean duration (pkg) zone 1	Z = -0.348 (p=0.728)	Z = -0.784 (p=0.433)
Mean duration (pkg) zone 2	Z = -0.153 (p=0.878)	Z = -1.583 (p=0.113)
Mean duration (pkg) zone 3	Z = -1.225 (p=0.225)	Z = -1.253 (p=0.210)
Mean duration (pkg) zone 4	Z = -0.081 (p=0.936)	**Z = -1.908 (p=0.056)**

For the individual tooth type analysis, both the mean duration of and interval between hypoplastic defects was calculated. The mean duration ranges from 3 to 7 perikymata on the upper and lower central incisors, from 2 to 8 perikymata for the lower lateral incisors and from 2 to 5 perikymata for the upper lateral incisors, with an average of 4 perikymata affected for all four tooth types. The mean interval ranges from 8 to 35 perikymata with an average interval of 15 perikymata on the lower central incisor. For the lower lateral incisor, the mean interval ranges from 7 to 29 perikymata, with a mean value of 14 perikymata. A similar mean value is found on the upper central incisors, for which the mean interval ranges from 7 to 40 perikymata, and on the upper lateral incisors, for which the mean interval ranges from 8 to 33 perikymata.

No clear differences stand out between history and non-history houses in terms of mean duration. Regarding the interval between defects, some differences can be distinguished. For the lower central and lateral incisors, the mean interval values are slightly higher in history house individuals in comparison with non-history house individuals (Fig. 7.9; Table 7.10).

For time of burial, no clear mean duration differences can be distinguished between Peak and Post-Peak individuals in any of the tooth types. In contrast, Post-Peak individuals have slightly higher (non-statistically significant) mean and median interval values than Peak individuals in the lower central incisors and the upper lateral incisors (Table 7.10).

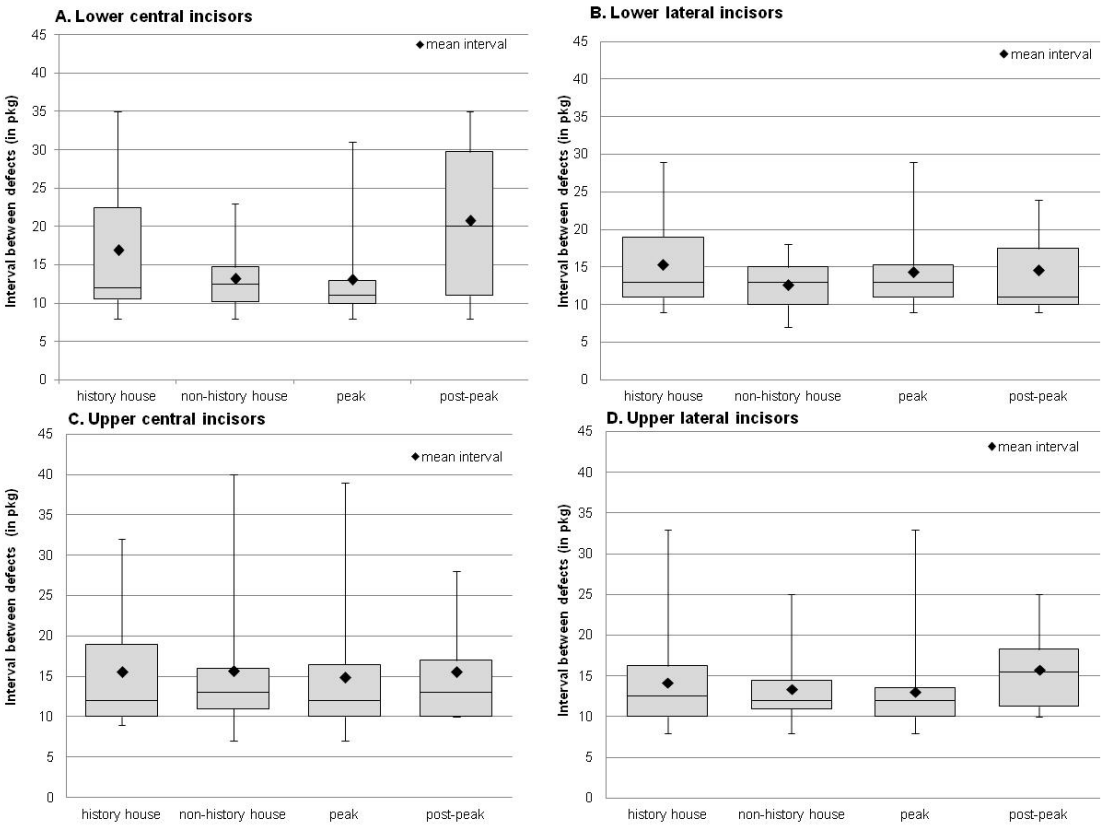

Figure 7.9: Box and whisker charts of the mean interval between defects per tooth type for individuals buried in history and non-history houses and in Peak and Post-Peak periods. Central line = median interval, Black diamond = mean interval, Top box = upper quartiles, Bottom box = lower quartiles, Whiskers = maximum and minimum

Table 7.10: Non-parametric significance test (Mann-Whitney) of duration of and interval between defects based on tooth types		
Parameter	Significance	
LOWER CENTRAL INCISOR	Place of burial (History vs non-History houses)	Time of burial (Peak vs Post-Peak)
Mean Duration defects (pkg)	Z = -0.096 (p= 0.924)	Z= -0.767 (p=0.443)
Mean Interval defects (pkg)	Z = -0.317 (p=0.751)	Z = -0.905 (p=0.365)
LOWER LATERAL INCISOR		
Mean Duration defects (pkg)	Z = -0.723 (p=0.470)	Z = -0.099 (p=0.921)
Mean Interval defects (pkg)	Z = -0.925 (p=0.355)	Z = -0.480 (p=0.631)
UPPER CENTRAL INCISOR		
Mean Duration defects (pkg)	Z = -0.282 (p=0.778)	Z = -0.200 (p=0.841)
Mean Interval defects (pkg)	Z= -0.171 (p=0.864)	Z = -0.218 (p=0.827)
UPPER LATERAL INCISOR		
Mean Duration defects (pkg)	Z = -0.433 (p=0.665)	Z = -0.112 (p=0.911)
Mean Interval defects (pkg)	Z = -0.325 (p=0.746)	Z = -0.096 (p=0.924)

The mean duration and interval per individual or tooth type do not show any significant differences between time and place of burial (Table 7.10). King and colleagues (2005) argued that the mean duration and interval parameters may not be truly meaningful as separate entities, as the latter do not distinguish between individuals who experienced long duration defects and short intervals (indicating a greater degree of physiological disturbances affecting dental growth) and individuals who experienced short duration defects and long intervals (indicating a lesser degree of physiological disturbances affecting dental growth).

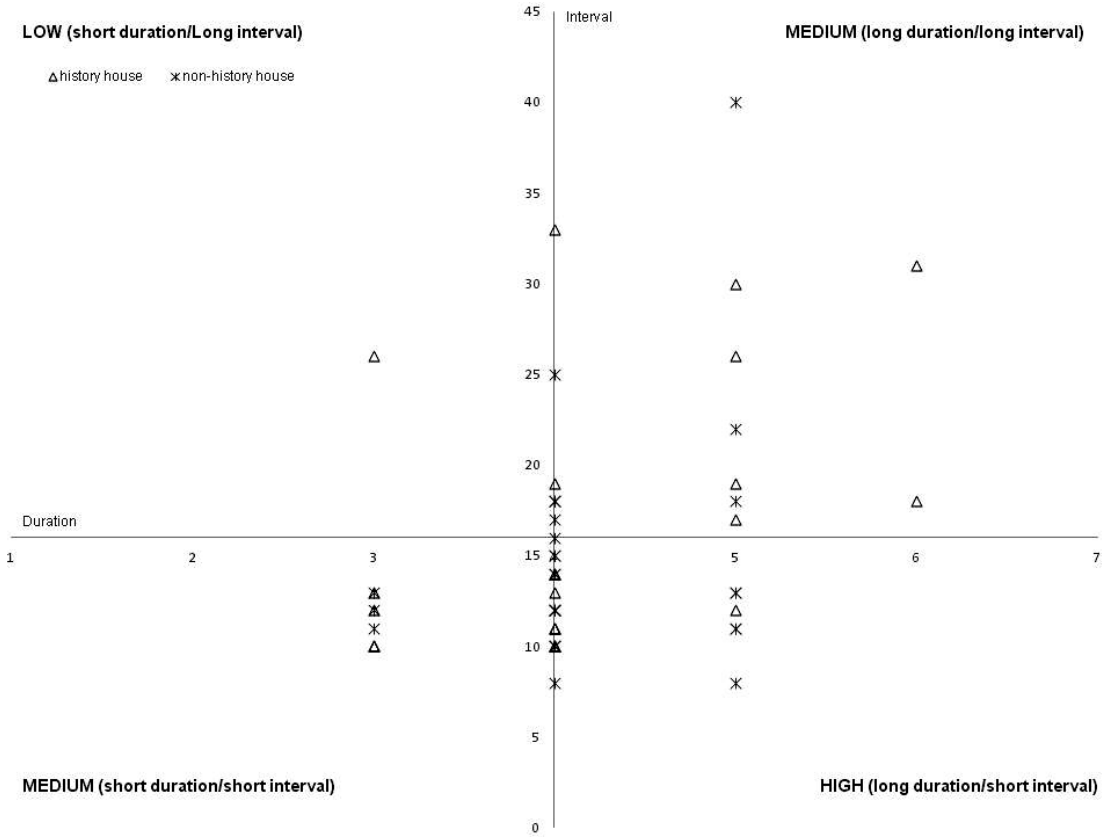

Figure 7.10: Combined mean intervals and durations compared in terms of place of burial, divided into a low degree of disruption (short durations combined with long intervals), a medium degree of disruption (short durations combined with short intervals and long durations combined with long intervals) and a high degree of disruption (long durations combined with short intervals). Triangles = individuals buried in history, stars = individuals buried in non-history houses

In an attempt to quantify the link between durations and intervals, graphs were constructed comparing the duration and interval parameters in terms of place of burial, including history (triangles) versus non-history houses (stars) and time of burial, including peak (circles) versus non-peak (squares) contexts (Fig. 7.10, 7.11). The X-axis on these

graphs represents the mean duration of defects in terms of perikymata numbers for each individual, the Y-axis represents the mean interval between defects for each individual, also in terms of perikymata numbers. The axes cross at the calculated average interval and duration for the entire dataset.

For these graphs, three parameters were differentiated, including a low degree of disruption (short durations combined with long intervals), a medium degree of disruption (short durations combined with short intervals and long durations combined with long intervals) and a high degree of disruption (long durations combined with short intervals). From figures 11 and 12, no clear differences between time and place of burial appear, with most individuals displaying values indicating a medium degree of disruption (Fig. 7.10, 7.11).

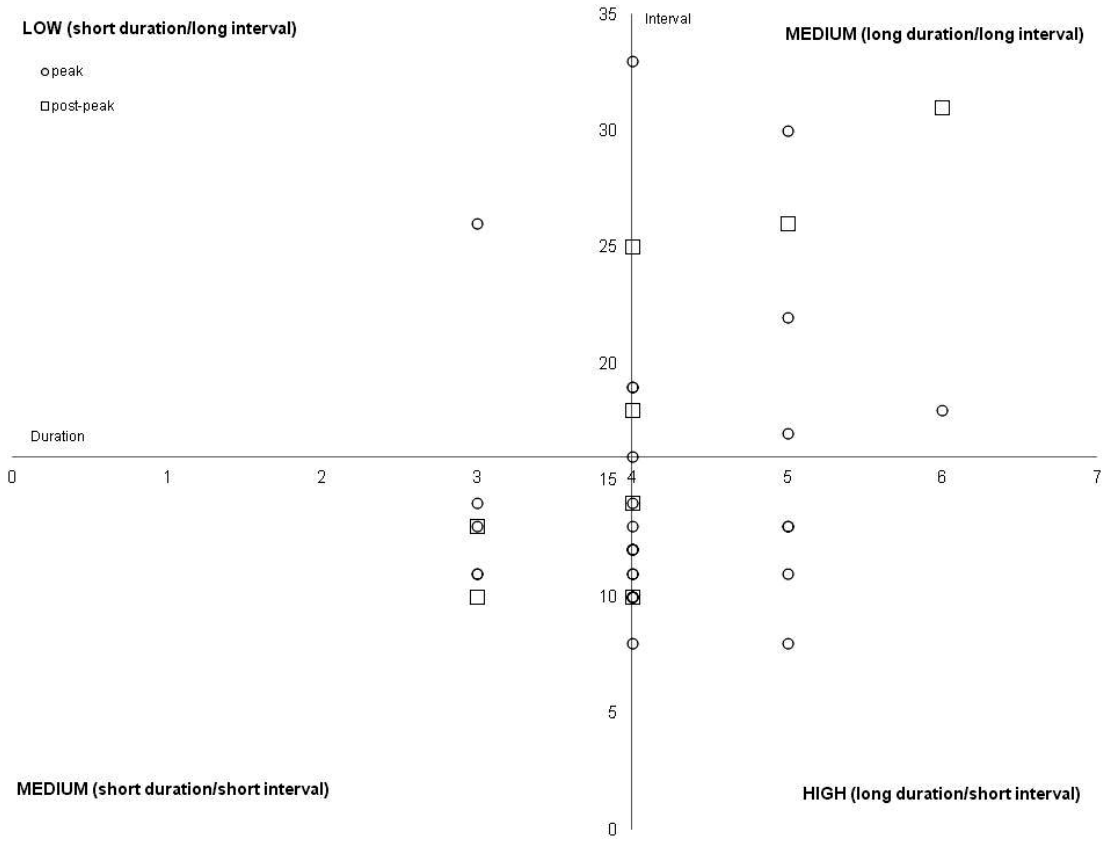

Figure 7.11: Combined mean intervals and durations compared in terms of place of burial, divided into a low degree of disruption (short durations combined with long intervals), a medium degree of disruption (short durations combined with short intervals and long durations combined with long intervals) and a high degree of disruption (long durations combined with short intervals). Circles = individuals buried in a Peak context, squares = individuals buried in a Post-Peak context

7.2. Skeletal growth

In this section, the methodological basis for the construction of site-specific skeletal growth patterns is discussed in terms of the age distribution, variation in bone size and curve fitting results for the Çatalhöyük sample. After this, the growth patterns are assessed and compared in terms of time and place of burial.

7.2.1. Dental age distribution

The skeletal growth assemblage consists of 159 juveniles with dental ages between birth and 18 years (Table 7.11). There is a clear heterogeneity in number of individuals per dental development cohort. Cohort sizes are small and unevenly distributed for individuals with dental ages older than one year, with only 1 individual in the 11 and 13 dental age categories, compared to 12 individuals in the 2-year dental age cohort. The largest proportion (52.8%) of the sample has a dental age of less than one year age (Table 7.11). The large number of very young individuals, often with recovered middle ear ossicles, shows that despite erosion and the drying out of bones, there is a good preservation and excellent recovery at the site.

Table 7.11: Dental development age distribution of the skeletal growth assemblage (*marks end age cohort)

Dental age group (in years)*	Number	Percentage of total number
0.3	56	35.2
0.5	13	8.2
1	19	11.9
2	6	3.8
3	8	5.0
4	4	2.5
5	7	4.4
6	7	4.4
7	4	2.5
8	5	3.1
9	1	0.6
10	6	3.8
11	1	0.6
12	6	3.8
13	0	0.0
14	5	3.1
15	2	1.3
16+	9	5.7
TOTAL	159	100

7.2.2. Variation in bone size

Summary statistics for the diaphyseal length data of the long bones (radius, humerus, ulna, tibia, clavicle, femur and fibula) have been grouped into age cohorts and are shown in Table 7.12. Sample sizes range from 64 individuals for the radius to 38 for the fibula. Summaries for other skeletal parameters are listed in the Appendix (2). For long bone widths (diaphysis, epiphysis and metaphysis), numbers of measurable specimens range from 114 for the upper metaphysis width of the ulna to 23 for the lower epiphysis width of the tibia. For the hand and foot bones, the numbers range from 92 individuals for metatarsal length to 55 for calcaneus width. For the pectoral girdle, they range from 98 specimens for the width of the scapular glenoid to 25 for scapular height. With the exception of the 0.3 to 1 year age cohorts, there are relatively few specimens for each age group when the assemblage is divided in this way. Individual measurements were therefore used in the analysis, rather than the cohort means or medians.

Table 7.12a: Summary statistics for maximum diaphyseal lengths of upper and lower limb bones grouped by age category (*number marks end dental developmental age cohort)

Radius length				**Humerus length**			**Ulna length**			**Tibia length**		
Dental age group (in years)*	N	mean	sd	N	mean	sd	N	mean	sd	N	mean	sd
0.3	34	50.6	3.6	37	62.9	3.9	26	58.1	3.8	35	61.5	4.7
0.5	5	53.5	5.4	4	70.3	3.3	5	62.0	4.6	3	70.5	6.9
1	10	70.1	5.0	8	91.0	7.8	8	77.2	8.6	6	93.7	8.2
2	3	83.6	7.1	4	111.0	8.6	3	94.6	7.5	2	122.5	2.5
3	3	95.4	1.2	2	120.1	14.8	3	98.3	13.3	3	134.1	4.1
4	2	105.0	9.6	2	142.5	9.6	2	118.5	9.4	1	141.8	
5	1	115.5		2	145.2	7.4	4	121.5	6.0	1	155.5	
6	0			1	158.5		0			1	184.0	
7	0			1	175.0		0			0		
8	2	129.2	0.7	1	165.5		2	142.8	5.8	0		
9	0			0			0			0		
10	1	150.5		1	200.3		3	179.3	27.8	1	236.0	
11	0			0			0			0		
12	2	162.9	14.3	1	207.2		2	180.6	17.6	0		
13	0			0			0			0		
14	0			0			0			0		
15	0			0			0			0		
16+	0			0			0			1	308.5	
TOTAL	64			64			58			54		

Table 7.12b: Summary statistics for maximum diaphyseal lengths of upper and lower limb bones grouped by age category (*number marks end dental developmental age cohort)

Clavicle length				**Femur length**			**Fibula length**					
Dental age group (in years)*	N	mean	sd	N	mean	sd	N	mean	sd			
0.3	19	42.0	3.2	28	70.8	5.9	24	59.6	4.4			
0.5	1	46.7		2	81.3	13.2	3	69.6	8.0			
1	8	54.0	5.1	3	114.9	13.8	6	88.9	7.0			
2	3	65.1	3.2	2	147.9	5.9	1	123.5				
3	1	61,4		1	177,0		1	133,7				
4	1	78.4		1	179.1		0					
5	3	78.6	1.1	1	205.1		2	148.8	9.1			
6	3	76.5	11.9	0			1	182.0				
7	0			0			0					
8	1	93.4		1	229.3		0					
9	0			0			0					
10	1	94.3		1	300.0		0					
11	0			0			0					
12	4	104.6	6.5	0			0					
13	0			0			0					
14	1	108.0		0			0					
15	0			0			0					
16+	1	140.0		0			0					
TOTAL	47			40			38					

7.2.3. Curve fitting

In Figure 7.12a, b, c and d, median dental development ages are plotted against the skeletal measurements for each individual (open circles) and polynomial curves are fitted to describe the growth pattern of the length of the radius (quartic), width of the upper metaphysis of the ulna (cubic), metatarsal length (quadratic) and the width of the scapular glenoid (quartic). The regression equations for all sets of measurements, together with the total sample sizes for each parameter are given in Table 7.13.

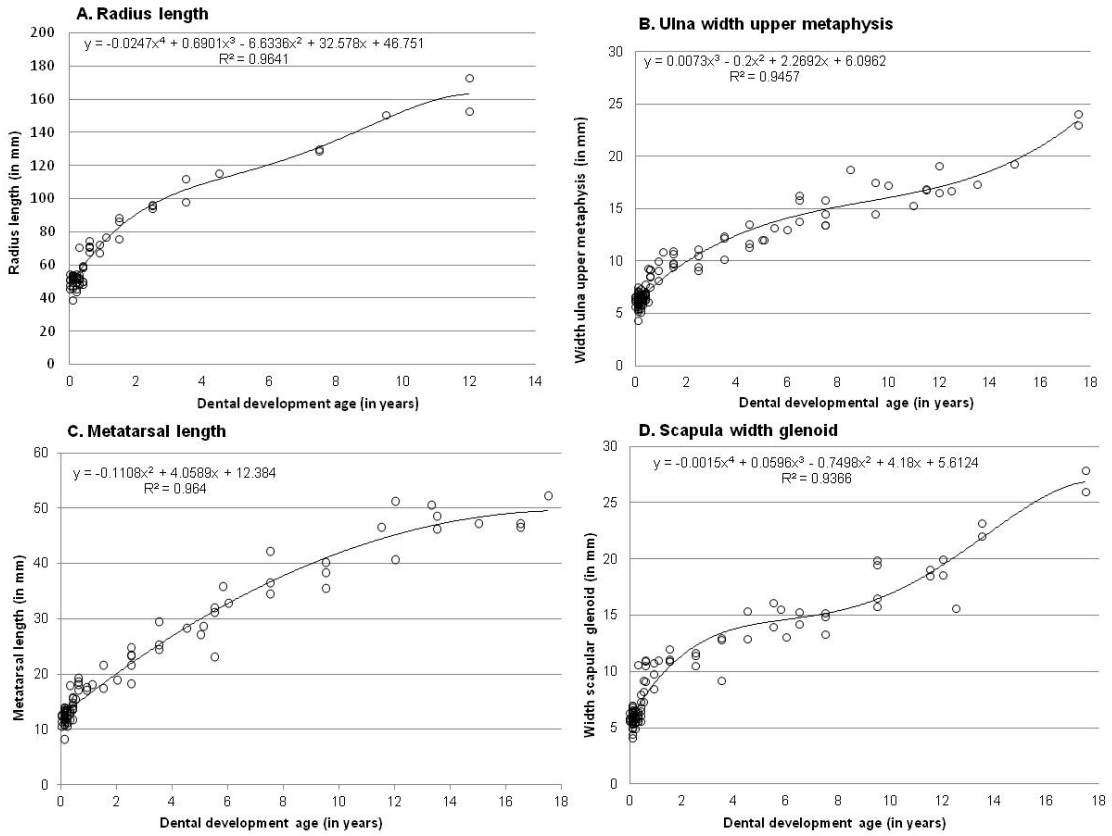

Figure 7.12: Polynomial regression curves showing relation of dental development age to the lengths of the radius (A), width of the upper metaphysis of the ulna (B), length of metatarsal (C) and width of the scapular glenoid (D)

On the regression curves shown in Figure 7.12, steep curves represent periods of rapid skeletal growth and the flattening of the curves represents slower skeletal growth. All four plots show a steep increase during early childhood (up to three years of dental developmental age). Longitudinal growth studies have shown that body size growth velocity is substantially greater in the first two years of life (see Chapter 4; Eckhardt *et al.* 2005a; Maresh 1955; Schroeder *et al.* 1995). The plots therefore imply that limb bone dimensions, which are correlated with stature, reflect this early rapid growth. It would not in any case be expected that an adolescent growth spurt could be distinguished. This is a cross sectional dataset, in which the fast growth rate of some individuals would be averaged out by the slower growth rate in other individuals due to differences in age at onset of the adolescent growth spurt between individuals and between males and females (Tanner *et al.* 1966).

Table 7.13: Polynomial regression equations for the fitted curves. Formula: $y = b0 + b1x + b2x^2 + b3x^3 + b4x^4 + b5x^5$ where y = bone measurement and x = dental development age

Parameter	N	b0	b1	b2	b3	b4	b5
LONG BONE LENGTH							
Humerus length	64	57.194	48.429	-10.778	1.1959	-0.0456	
Radius length	63	46.751	32.578	-6.6336	0.6901	-0.0247	
Ulna length	58	54.848	27.069	-0.5842	-1.2459	0.2077	-0.0091
Tibia length	54	55.549	50.123	-9.5753	0.9414	-0.0292	
Clavicle length	47	39.348	25.392	-7.535	1.178	-0.0729	0.0017
Femur length	40	62.321	70.394	-12.398	0.8028		
Fibula length	38	53.974	41.342	5.9018	-4.7139	0.5284	
LONG BONE WIDTH							
Ulna upper metaphysis width	113	6.09662	2.2692	-0.200032	0.0073		
Radius upper metaphysis width	105	5.335138	-0.000509	0,023595	-0,354922	2,537861	
Humerus lower metaphysis width	104	15.102139	-0.006705	0.190182	-1.848979	8.738789	
Femur upper metaphysis width	97	10.80413	-0.096058	2.898288			
Clavicle width (lateral)	90	7.58	1.1387	-0.0157			
Fibula lower metaphysis width	86	5.721746	-0.000775	0.035066	-0.533934	3.761659	
Radius lower metaphysis width	85	8.197283	0.000529	0.025453	-0.414378	3.301641	
Clavicle width (sternal)	84	7.770045	-0.008573	0.858624			
Ulna lower metaphysis width	79	6.273185	-0.024543	0.983301			
Humerus upper metaphysis width	66	10.130066	-0.001336	0.049368	-0.580217	3.589868	
Humerus ante-ro-posterior width	62	4.632932	-0.004615	0.127024	-1.168002	4.584191	
Humerus medio-lateral width	62	4.853371	0.030335	-0.608189	3.77437		

Tibia upper metaphysis width	61	13.311797	-0.002355	0.104665	-1.500359	10.391288	
Tibia lower metaphysis width	61	9.598263	-0.002249	0.082555	-1.003269	6.17905	
Femur lower metaphysis width	59	17.192785	-0.002281	0.106716	-1.640641	11.489565	
Tibia medio-lateral width	53	5.225402	-0.002758	0.087366	-0.84506	3.618147	
Tibia antero-posterior width	53	5.760607	-0.002166	0.07113	-0.72662	3.885479	
Clavicle max width	48	3.883403	-0.017268	0.569636			
Clavicle min width	48	3.026631	0.317581				
Fibula upper metaphysis width	45	4.627833	-0.001044	0.041689	-0.541827	3.495725	
Femur antero-posterior width	40	5.594056	0.00984	-0.144041	0.387476	2.329398	
Femur medio-lateral width	40	6.075731	0.008532	-0.089494	-0.162825	3.459011	
Femur upper epiphysis diameter	39	8.043326	3.251655	-0.092481			
Humerus upper epiphysis diameter	39	7.100707	-0.047127	2.588585			
Femur lower epiphysis width	31	11.984634	-0.208419	6.799508			
Tibia upper epiphysis width	29	12.333787	-0.014133	0.275706	2.566246		
Fibula lower epiphysis width	27	5.470613	0.003364	-0.136935	2.298216		
Tibia lower epiphysis width	23	10.925301	2.241129				
THORAX							
Scapula width Glenoid	98	5.6124	4.18	-0.7498	0.0596	-0.0015	
Dens width	92	4.852857	-0.000286	0.015674	-0.285179	1.959185	
Dens height	90	5.318145	0.003297	-0.118271	1.264334	-1.753836	
Scapula height Glenoid	86	11.09103	-0.003112	0.109667	-1.30433	7.346333	
Pelvis ilium breadth	74	31.643251	0.057237	-1.621805	16.342106		
Atlas length HC	73	13.001597	-0.067217	1.069183	-5.887098	14.962975	
Axis length	73	15.721034	0.314076	-1.456607	-1.571929	12.119853	
Pelvis ischium length	73	16.24532	-0.00511	0.186039	-2.247091	12.704052	

Atlas length FK	71	13.534793	-0.555528	7.046325			
Pelvis ilium height	65	26.95649	-0.008117	0.281459	-3.362002	19.412619	
Pelvis ischium height	63	10.000158	-0.020707	0.487268	-3.620026	11.957869	
Manubrium breadth	48	11.522074	2.185775				
Manubrium length	42	9.925079	1.923038				
Pelvic pubic length	42	12.48124	-0.019195	0.521443	-4.462766	15.566425	
Pelvis pubic height	39	5.397791	-0.066113	1.2392	-7.12466	16.656037	
First rib length	35	22.964907	0.048435	-1.129403	9.515451		
Scapula breadth	28	29.795669	3.760158				
Scapula height	25	33.723235	-0.256873	10.662553			
HAND/FOOT							
Metatarsal length	91	12.384	4.0589	-0.1108			
Metacarpal length	90	8.682867	-0.000416	0.021466	-0.383194	3.988614	
Talus length	77	9.586126	0.004319	-0.239986	5.343869		
Talus width	71	6.851921	-0.088519	3.421133			
Calcaneus length	63	10.085	8.0061	-0.4479	0.0099		
Calcaneus width	55	7.5377	4.0385	-0.182	0.0044		
CRANIAL							
Basilar length	92	11.978	1.7752	-0.0837			
Maximum basilar length	84	14.182	10.346	-5.5199	1.2099	-0.0845	
Basilar width	75	13.921	8.5415	-2.2403	0.2089		
Mandibular ramus height	70	13.686	6.5153	-0.725	0.0366	-0.006	
Zygomatic width	70	17.899	8.5491	-1.6042	0.1187	-0.003	
Orbit breadth	64	20.277	7.483	-1.7396	0.1497	-0.0042	
Minimum ramus breadth	63	13.415	5.0378	-0.5826	0.0316	-0.0006	
Lateralis length	55	22.093	17.284	-6.0415	0.7197		
Lateralis width	53	15.535	19.15	-6.5946	0.724		
Chin height	49	10.736	-1.6403	8.2822			
Zygomatic length	48	20.688	12.277	-2.8056	0.2685	-0.009	
Condylar to coronoid process	29	16.912	4.9459	-0.3772	0.0094		

7.2.4. Analysis of long bones

Diaphyseal length and dental development age

Once the curves had been fitted, residual were calculated and plotted for the radius, ulna, humerus, clavicle, femur, tibia and fibula diahyseal lengths. Residuals values were compared between individuals from history/non-history houses and Peak/Post-Peak contexts.

Figure 7.13 shows box and whisker plots for the standardised residuals from curves fitted to measurements of the diaphyseal length of long bones with the largest sample sizes, the radius (N=63), humerus (N=64), ulna (N=58) and tibia (N=54). Negative residuals indicate a lower size attainment for dental developmental age, relative to the fitted curve, whereas positive residuals indicate a higher size attainment for dental developmental age. For the radius, humerus and tibia, residual means and medians for Post-Peak individuals are visibly lower than the residual means and medians for Peak individuals (Fig. 7.13).

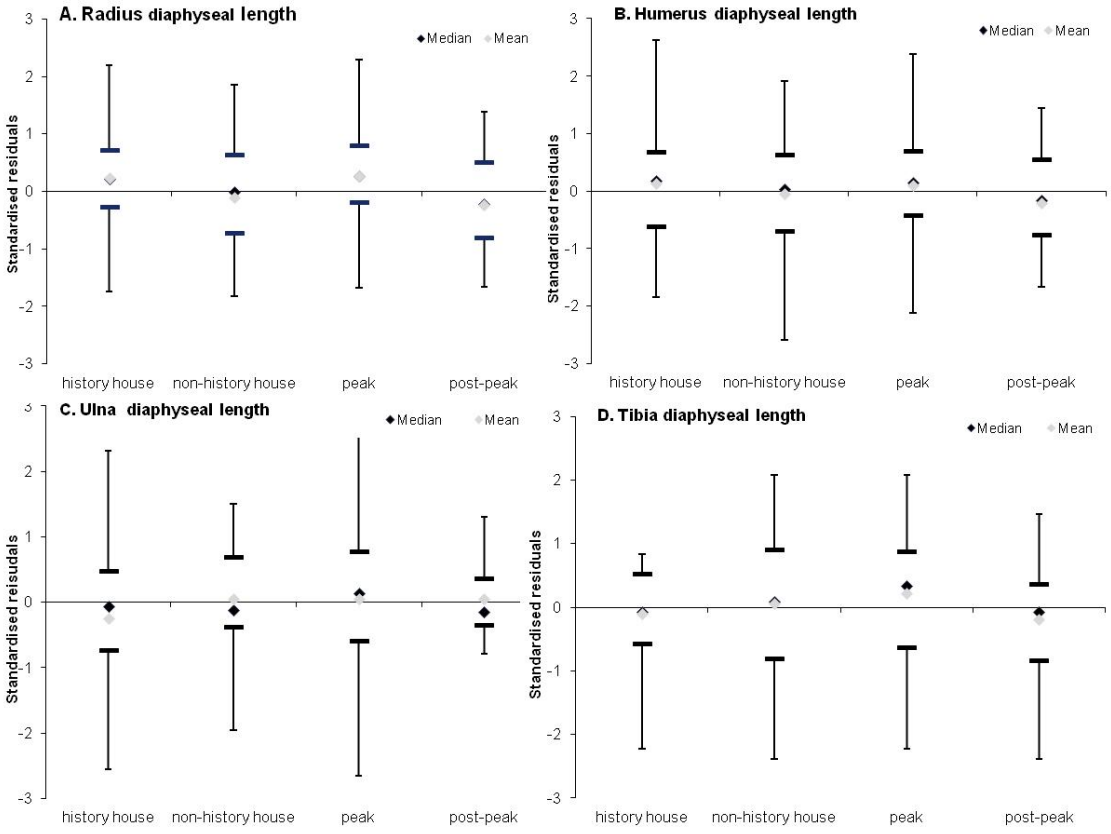

Figure 7.13: Box and whisker plots of residual from curves fitted to measurements of diaphyseal lengths of the radius (A), humerus (B), ulna (C) and tibia (D) based on dental development age. Grey diamond = mean, Black diamond = median, Black horizontal lines = first and third quartiles

Table 7.14 shows the mean standardised residuals from fitted curves describing the relationship between dental development age and measurements of the diaphyseal lengths of long bones in terms of time of burial. Mean residual values are lower for post-peak individuals compared to peak individuals for all parameters, except for the ulna, where the means in Peak and Post-Peak individuals are equal. A series of paired samples t-tests comparing the overall sample residual means for all the measured long bone diaphyses shows that this trend of lower residual means in Post-Peak individuals approaches significance for the residuals from curves fitted to the measurements of the fibula diaphyseal length (Table 7.14).

Table 7.14: Diaphyseal length long bones against median dental development age:
Summary statistics for standardised regression residuals by time of burial

	Peak			Post-Peak				
Skeletal variable	N	mean	sd	N	mean	sd	t	P
Radius length	24	0.26	1.16	28	-0.23	0.89	1.75	0.087
Humerus length	25	0.10	1.18	29	-0.15	0.88	0.86	0.393
Ulna length	24	0.05	1.27	22	0.05	0.56	-0.01	0.993
Tibia length	18	0.22	1.18	27	-0.19	0.97	1.29	0.204
Clavicle length	22	0.02	0.85	16	-0.03	0.64	0.20	0.842
Femur length	12	0.08	1.11	18	-0.20	1.09	0.68	0.501
Fibula length	14	0.43	1.15	17	-0.30	0.85	2.02	0.053

Figure 7.13 shows that there is little variation between the mean and median residuals of individuals buried in history and non-history houses in terms of diaphyseal length of the radius, humerus, ulna and tibia. The t-tests comparing residuals from the fitted curves for the radius, humerus, ulna, tibia, clavicle and fibula diaphyseal lengths (based on dental development age) show no statistically significant differences (Table 7.15).

Table 7.15: Diaphyseal length long bones against median dental development:
Summary statistics for standardised regression residuals by place of burial

	non-History house			History house				
Skeletal variable	N	mean	sd	N	mean	sd	t	P
Radius length	44	-0.10	0.94	19	0.23	1.15	1.19	0.239
Humerus length	46	-0.05	0.99	18	0.12	1.06	1.10	0.275
Ulna length	38	0.04	0.87	20	-0.08	1.25	-0.45	0.653
Tibia length	36	0.05	1.11	18	-0.10	0.80	-0.52	0.605
Clavicle length	32	-0.09	0.86	15	-0.19	1.30	0.88	0.384
Fibula length	22	0.03	0.98	16	-0.04	1.10	-0.13	0.895

Diaphyseal length and predicted mean dUI1 heights

In addition to skeletal growth profiles based on dental developmental ages as independent variables, profiles were also constructed using predicted mean dUI1 heights (estimated using a simple linear regression model described in Chapter 5). As these

profiles are solely based on deciduous teeth, samples are slightly smaller, and so this analysis was only carried out using the skeletal variables with the largest sample sizes, using 54 out of 63 individuals for profiles based on radius diaphyseal lengths and 56 out of 64 individuals for profiles based on humerus diaphyseal lengths.

The subsets based upon the fitted curves describing the relationship between the predicted mean dUI1 heights and radius and humerus diaphyseal length measurements show a (non-significant) trend of lower residual values for Post-Peak individuals compared to Peak individuals (Fig. 7.14; Table 7.16). Results of the subset analysis based upon the predicted mean dUI1 heights and its relationship to radius and humerus diaphyseal length measurements show a trend of lower residual values for individuals buried in non-history houses in comparison to individuals buried in history houses, but this trend is not significant (Fig. 7.14; Table 7.17).

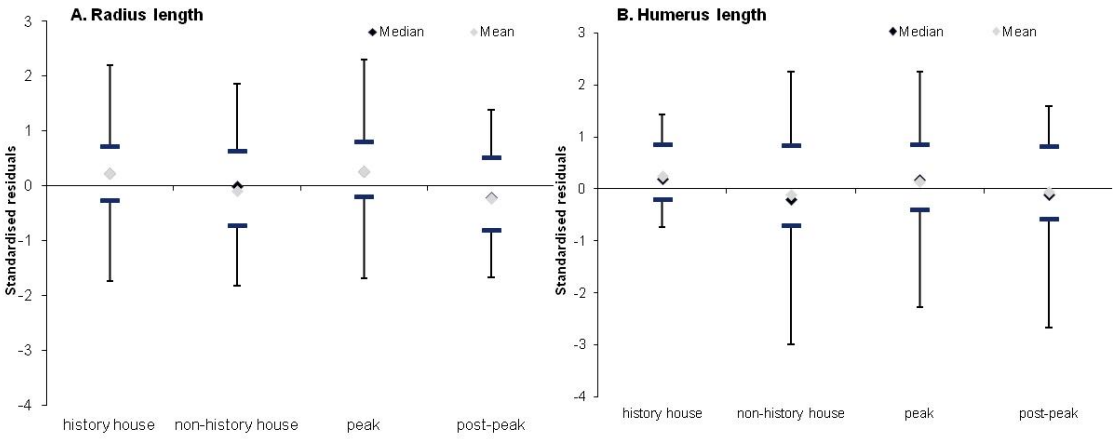

Figure 7.14: Box and whisker plots of residual from curves fitted to measurements of diaphyseal lengths of the radius (A), humerus (B) based on predicted mean dUI1 heights. Grey diamond = mean, Black diamond = median, Black horizontal lines = first and third quartiles

Table 7.16: Diaphyseal length long bones against deciduous tooth height measurements: Summary statistics for standardised regression residuals by time of burial

	Peak			Post-Peak				
Skeletal variable	N	mean	sd	N	mean	sd	t	P
Radius length	18	0.20	1.17	27	-0.19	0.98	1.24	0.223
Humerus length	20	0.15	1.05	29	-0.06	1.03	0.68	0.500

Table 7.17: Diaphyseal length long bones against deciduous tooth height measurements: Summary statistics for standardised regression residuals by place of burial

	Non-History house			History house				
Skeletal variable	N	mean	sd	N	mean	sd	t	P
Radius length	37	-0.09	1.08	17	0.21	0.83	1.02	0.312
Humerus length	40	-0.10	1.10	16	0.25	0.70	1.20	0.236

Long bone widths (diaphysis, epiphysis, metaphysis) and dental development age

Sample sizes for diaphyseal lengths are relatively small in the Çatalhöyük assemblage. Larger groups exist for measurements of the long bone widths, such as metaphyseal, diaphyseal and epiphyseal widths and these parameters can also be used to assess differences in skeletal growth patterns between groups (see Chapter 4).

Figure 7.15 shows the residual plots from curves fitted to measurements of long bone widths with the largest sample sizes, the upper metaphysis of the ulna (N=113), radius (N =105) and femur (N=97) and the lower metaphysis of the humerus (N=104). Similarly to the residual plots of the diaphyseal lengths, negative residuals indicate a lower size attainment for dental developmental age relative to the fitted curve, whereas positive residuals represent a higher size attainment for dental developmental age.

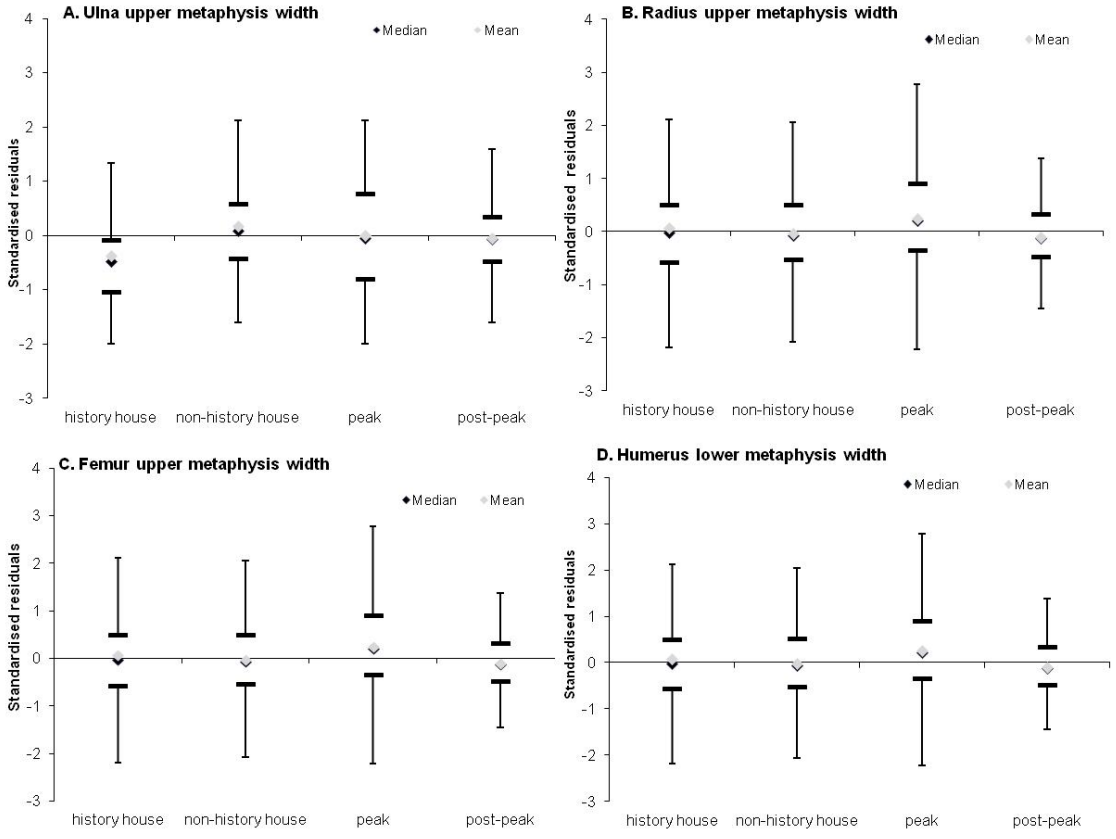

Figure 7.15: Box and whisker plots of residuals from curves fitted to measurements of widths of upper metaphysis of the ulna (A), radius (B) and femur (C) and the lower metaphysis of the humerus (D) based on dental development age. Grey diamond = mean, Black diamond = median, Black horizontal lines = first and third quartiles

Similarly to the results for diaphyseal length measurements, mean and median residuals of Post-Peak period individuals tend to be lower than mean and median residuals of Peak period individuals in the box and whisker plots of the upper metaphysis of the radius and femur and the lower metaphysis of the humerus, but not for the upper metaphysis of the ulna (Fig. 7.15).

The Post-Peak residual means for the width of the lateral end of the clavicle, the width of the upper metaphysis of the humerus and the antero-posterior diaphyseal width of the humerus are notably lower than the residual means for Peak individuals and this difference approaches significance for the lower metaphysis width of the humerus (Table 7.18).

Sample sizes are smaller for the remaining long bone widths, but a clear (non-statistically significant) trend of lower residuals means for Post-Peak individuals can be distinguished for the maximum width of the clavicle, the antero-posterior diaphyseal width of the femur and the antero-posterior and medio-lateral diaphyseal width of the tibia, the width of the upper metaphyses of the fibula and tibia and of the lower metaphysis for the femur and tibia (Table 7.18). Only two parameters show a contrasting trend: the minimum width of the clavicle and the mediolateral width of the femoral diaphysis, but the differences between the marginally lower residual means for Peak individuals in comparison to Post-Peak individuals are not statistically significant for these variables (Table 7.18).

When divided into Peak and Post-Peak groups, sample sizes are too small for statistical comparison in six parameters (the upper and lower epiphyses of the femur and tibia, the lower epiphysis of the fibula and the upper epiphysis of the humerus) and these are not included in Table 7.18.

Table 7.18: Widths of long bones against median dental development age: Summary statistics for standardised regression residuals by time of burial

	Peak			Post-Peak				
Skeletal variable	N	mean	sd	N	mean	sd	t	P
Ulna Upper metaphysis width	44	0.00	1.10	47	-0.054	0.74	-0.4	0.774
Radius Upper metaphysis width	40	0.11	1.20	44	-0.17	0.56	1.38	0.171
Humerus Lower metaphysis width	41	0.25	1.19	45	-0.11	0.65	1.78	0.079
Femur Upper metaphysis width	39	0.24	1.13	39	0.00	0.63	1.13	0.261
Clavicle width (lateral end)	35	0.42	1.00	37	-0.33	0.71	3.66	0.0005
Fibula lower metaphysis width	39	0.08	1.24	29	-0.14	0.46	-0.26	0.382

Radius lower metaphysis width	34	0.19	1.14	35	-0.11	0.58	1.38	0.171
Clavicle width (sternal end)	36	0.05	1.15	31	0.04	0.91	0.04	0.965
Ulna lower metaphysis width	37	0.20	1.00	25	0.00	0.62	0.86	0.392
Humerus upper metaphysis width	28	0.32	1.23	26	-0.23	0.58	2.08	0.042
Humerus antero-posterior width	24	0.42	1.07	29	-0.24	0.66	2.76	0.008
Humerus medio-lateral width	24	0.30	1.18	29	-0.16	0.74	1.73	0.089
Tibia upper metaphysis width	21	0.15	1.39	30	-0.10	0.69	0.82	0.415
Tibia lower metaphysis width	20	0.19	1.28	29	0.03	0.61	0.59	0.557
Femur lower metaphysis width	18	0.37	1.19	27	-0.02	0.59	1.46	0.151
Tibia medio-lateral width	18	1.07	1.04	26	0.67	0.82	1.30	0.200
Tibia antero-posterior width	18	0.32	1.25	26	-0.08	0.81	1.29	0.204
Clavicle width (max)	23	0.16	1.06	16	-0.24	0.60	1.38	0.177
Clavicle width (min)	23	-0.02	1.05	16	0.16	0.66	-0.59	0.562
Fibula upper metaphysis width	12	0.16	1.17	23	-0.13	0.90	0.81	0.422
Femur antero-posterior width	12	0.21	1.12	18	0.08	0.92	0.34	0.735
Femur medio-lateral width	12	0.06	1.01	18	0.08	0.94	-0.04	0.966

In terms of the comparison between individuals buried in history house and non-history houses, Figure 7.15 shows higher mean and median residuals for the upper metaphysis of the ulna for individuals buried in non-history houses in comparison to individuals buried in history houses, but this trend cannot be distinguished for the upper metaphysis of the radius and femur and the lower metaphysis of the humerus (Fig. 7.15).

Of a total of 25 observed skeletal variables, 17 appear to have higher residual means for non-history house individuals than history house individuals and this trend is statistically significant for the residuals from fitted curves to measurements of the width of the upper metaphysis of the ulna and the width of the lateral end of the clavicle (Table 7.19). In contrast, eight skeletal variables have (non-statistically significant) lower residual means for non-history house individuals in comparison to history house individuals (Table 7.19). Sample sizes for history house groups are too small for statistical comparison in three skeletal variables (the antero-posterior and medio-lateral diaphyseal width of the femur and the width of the lower epiphysis of the tibia) and are therefore not included in Table 7.19.

Table 7.19: Width of long bones (diaphysis, epiphysis and metaphysis) against median dental development age:
Summary statistics for standardised regression residuals by place of burial

	non-History house			History house				
Skeletal variable	N	mean	sd	N	mean	sd	t	P
Ulna upper metaphysis width	77	0.18	0.96	36	-0.37	10.99	-2.81	0.006
Radius upper metaphysis width	74	-0.03	0.98	31	0.06	1.07	0.43	0.671

Humerus Lower metaphysis width	73	-0.03	0.87	31	0.07	1.28	0.49	0.627
Femur upper metaphysis width	69	0.09	1.00	28	-0.22	1.00	-1.37	0.174
Clavicle width (lateral end)	63	0.15	1.09	27	-0.36	0.64	-2.28	0.025
Fibula lower metaphysis width	56	0.02	1.04	30	-0.04	0.95	-0.26	0.799
Radius lower metaphysis width	61	-0.09	0.93	24	0.23	1.16	1.33	0.187
Clavicle width (sternal end)	58	0.02	0.94	26	-0.04	1.15	-0.21	0.829
Ulna lower metaphysis width	53	0.00	1.03	26	0.01	0.97	0.04	0.966
Humerus upper metaphysis width	49	-0.07	0.88	17	0.20	1.31	0.96	0.339
Humerus antero-posterior width	45	-0.09	0.89	17	0.24	1.27	1.16	0.249
Humerus medio-lateral width	45	-0.01	1.00	17	0.04	1.05	0.18	0.859
Tibia upper metaphysis width	42	0.13	1.03	19	-0.29	0.93	-1.55	0.127
Tibia lower metaphysis width	41	0.14	0.96	20	-0.30	1.06	-1.62	0.111
Femur lower metaphysis width	44	0.13	1.07	15	-0.38	0.70	-1.72	0.090
Tibia medio-lateral width	36	0.09	0.94	17	-0.20	1.14	-0.99	0.326
Tibia antero-posterior width	36	0.10	1.01	17	-0.20	1.01	-1.01	0.319
Clavicle width (max)	33	0.02	1.00	15	-0.05	1.06	0.21	0.832
Clavicle width (min)	33	0.04	1.03	15	-0.10	1.00	-0.44	0.659
Fibula upper metaphysis width	30	-0.03	1.00	15	0.05	1.08	0.24	0.811
Femur upper epiphysis diameter	29	0.08	1.05	10	-0.23	0.92	-0.82	0.416
Humerus upper epiphysis diameter	28	0.10	1.04	11	-0.26	0.93	-0.99	0.331
Femur lower epiphysis width	21	0.20	0.97	10	-0.41	1.03	-1.59	0.123
Tibia upper epiphysis width	17	0.01	1.16	12	-0.02	0.82	-0.08	0.939
Fibula lower epiphysis width	17	0.14	1.02	10	-0.24	1.02	-0.95	0.350

Long bone widths and predicted mean dUI1 heights

The subsets based upon the fitted curves describing the relationship between the predicted mean dUI1 heights and measurements of the width of the upper metaphysis of the radius (N=80 out of 105 individuals) show a (non-significant) trend of lower residual values for Post-Peak individuals compared to Peak individuals (Fig. 7.16; Table 7.20). In contrast, for the width of the upper metaphysis of the ulna (N=82 out of 113 individuals), the mean residual value of the Peak individuals is (non-significantly) lower than the mean residual of the Post-Peak individual (Fig. 7.16; Table 7.20).

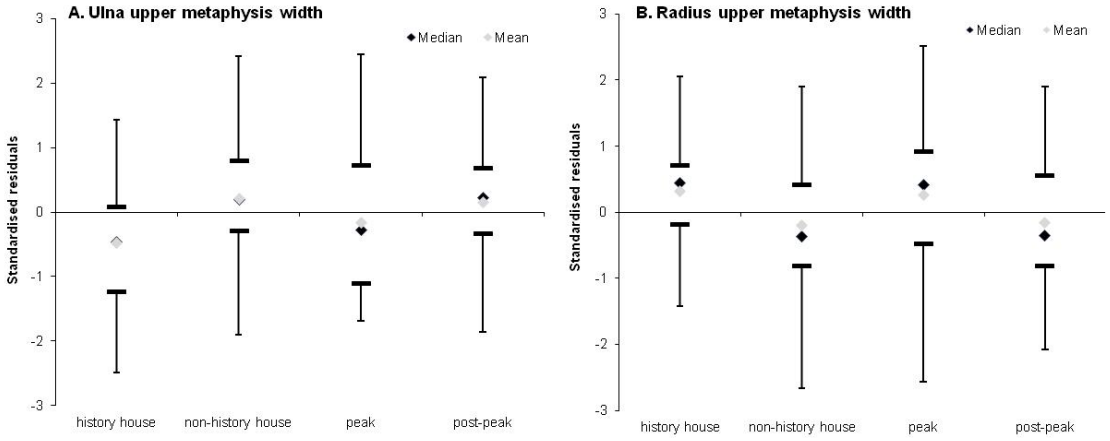

Figure 7.16: Box and whisker plots of residual from curves fitted to measurements of the width of the upper metaphysis of the ulna (A) and radius (B) based on predicted mean dUI1 heights. Grey diamond = mean, Black diamond = median, Black horizontal lines = first and third quartiles

Table 7.20: Width of long bones against deciduous tooth height measurements:
Summary statistics for standardised regression residuals by time of burial

	Peak			Post-Peak				
Skeletal variable	N	mean	sd	N	mean	sd	t	P
Ulna Upper metaphysis width	25	-0.16	1.17	43	0.16	0.91	-1.23	0.221
Radius Upper metaphysis width	24	0.27	1.15	42	-0.16	0.95	1.62	0.111

For the subset analysis based on predicted mean dUI1 heights (Fig. 7.16; Table 7.21) statistically significantly higher residual means were observed for non-history house individuals in comparison to history house individuals for the upper metaphysis of the ulna. In addition, statistically significant lower residual means were found for non-history house individuals in comparison to history house individuals for the upper metaphysis of the radius. (Fig. 7.16; Table 7.21).

Table 7.21: Width of long bones against deciduous tooth height measurements:
Summary statistics for standardised regression residuals by place of burial

	Non-History house			History house				
Skeletal variable	N	mean	sd	N	mean	sd	t	P
Ulna upper metaphysis width	56	0.22	0.96	26	-0.47	0.96	-3.01	0.004
Radius upper metaphysis width	55	-0.20	1.02	25	0.32	0.90	2.19	0.032

7.2.5. Thorax, pectoral and pelvic girdles

Thorax, pectoral and pelvic girdles and dental development age

Figure 7.17 shows the residual plots from curves fitted to measurements of skeletal elements from the thorax, pectoral and pelvic girdles with the largest sample sizes, the width (N=98) and height (N=86) of the scapular glenoid (N=86) and the width (N=92) and height (N=90) of the dens. Similarly to the residual plots of the long bone lengths and widths, mean and median residuals of these scapular and vertebral parameters are lower in Post-Peak individuals compared to the mean and median residuals in Peak individuals (Fig. 7.17). This trend towards lower residual means in Post-Peak individuals approaches significance for the width of the scapular glenoid, but is not statistically significant for the height of the scapular glenoid or the width and height of the dens (Table 7.22).

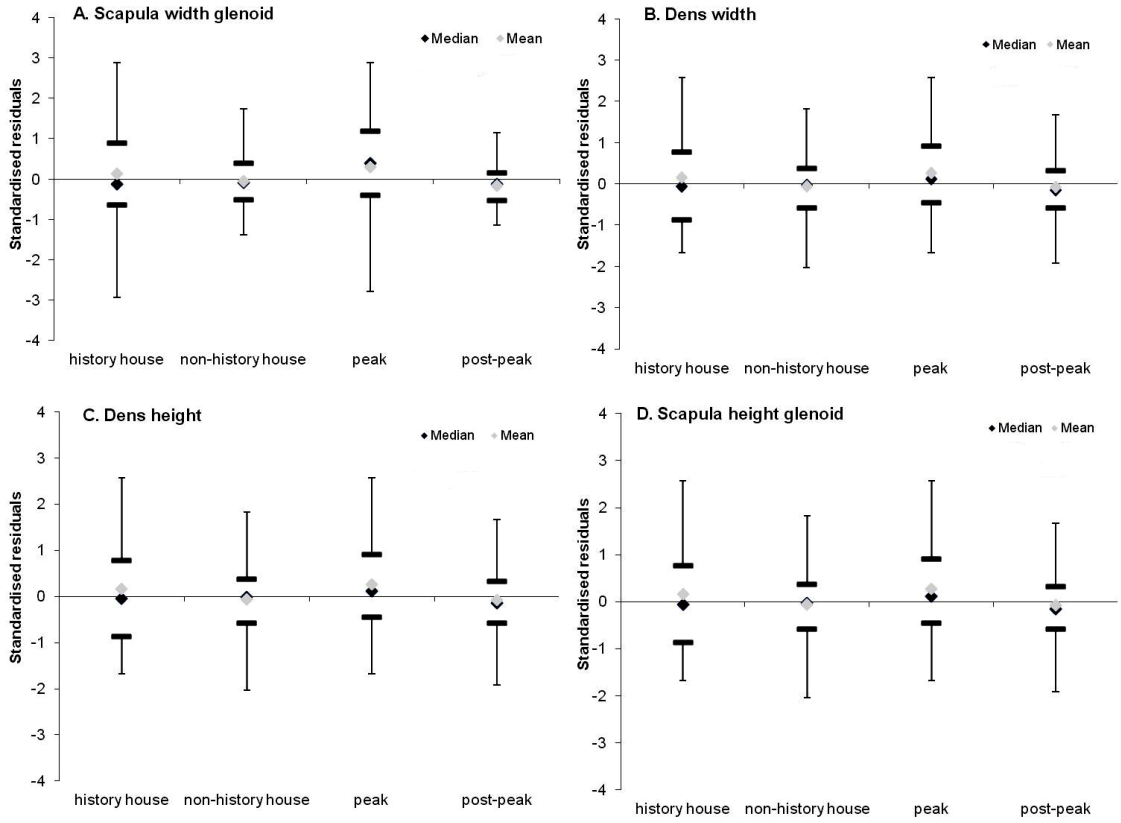

Figure 7.17: Box and whisker plots of residuals from curves fitted to measurements of the height and width of the scapular glenoid (D and A) and the height and width of the vertebral dens (C and B) based on dental development age. Grey diamond = mean, Black diamond = median, Black horizontal lines = first and third quartiles

For the remaining parameters of the thoracic, pectoral and pelvic girdle, a clear (non-statistically significant) trend of lower overall means for post-peak individuals could be distinguished for all skeletal variables (Table 7.22). Sample sizes for each group (Peak and Post-Peak) are too small for statistical comparison in terms of scapular height and are therefore not included in Table 7.22.

Table 7.22: Thorax, pectoral and pelvic girdle against median dental development age:
Summary statistics for standardised regression residuals by time of burial

	Peak			Post-Peak				
Skeletal variable	N	mean	sd	N	mean	sd	t	P
Scapula width glenoid	38	0.30	1.40	38	-0.16	0.50	1.94	0.056
Dens width	40	0.10	1.14	32	-0.14	0.72	1.06	0.294
Dens height	39	0.15	1.32	30	-0.08	0.38	0.92	0.361
Scapula height glenoid	31	0.20	1.34	35	-0.12	0.53	1.33	0.189
Pelvis Ilium breadth	28	0.27	1.08	32	-0.08	0.79	1.13	0.158
Atlas length (HC)	22	0.07	1.46	36	0.04	0.63	0.11	0.913
Axis length	24	0.22	1.17	35	-0.11	0.77	1.31	0.196
Pelvis Ischium length	27	0.19	1.26	32	0.02	0.66	0.68	0.498
Atlas length (FK)	21	0.13	1.43	36	0.04	0.52	0.36	0.724
Pelvis Ilium height	24	0.28	1.22	28	-0.05	0.65	1.23	0.224
Pelvis Ischium height	21	0.38	1.17	30	-0.08	0.72	1.74	0.088
Manubrium breadth	20	0.12	1.11	16	0.02	1.05	0.26	0.800
Manubrium length	18	0.19	1.20	14	-0.09	0.72	0.79	0.435
Pelvis Pubis length	11	0.43	1.24	20	-0.07	0.70	1.45	0.159
Pubic height	12	0.46	1.44	19	-0.07	0.68	1.39	0.175
First rib length	13	0.27	1.44	16	-0.04	0.61	0.77	0.449
Scapula breadth	12	0.15	1.22	11	-0.28	0.66	1.05	0.305

Regarding the comparison based on the place of burial (history and non-history houses), Figure 7.17 shows marginally lower mean residuals for the width and height of the scapular glenoid and the width and height of the dens, but this trend is not statistically significant (Table 7.23).

Of a total of 17 observed skeletal variables, seven appear to have higher residual means for non-history house individuals than history house individuals, but this trend is not statistically significant for any of the observed parameters (Table 7.23). In contrast, nine variables have (non-statistically significant) lower residual means for non-history house individuals in comparison to history house individuals (Table 7.23). The residual means for the length of the manubrium are equal for individuals buried in history and non-history houses. Sample size for history house groups are too small for statistical comparison in terms of the length of the first rib (N=9) and this skeletal variable was therefore not included in the Table 7.23.

Table 7.23: Thorax, pectoral and pelvic girdle against median dental development age:
Summary statistics for standardised regression residuals by place of burial

	non-History house			History house				
Skeletal variable	N	mean	sd	N	mean	sd	t	P
Scapula width glenoid	68	-0.06	0.68	30	0.13	1.51	0.86	0.393
Dens width	57	-0.06	0.89	35	0.09	1.18	0.68	0.495
Dens height	55	0.02	0.95	35	-0.03	1.10	-0.24	0.815
Scapula height glenoid	60	-0.07	0.79	26	0.15	1.39	0.92	0.359
Pelvis Ilium breadth	52	-0.07	0.93	22	0.15	1.18	0.86	0.395
Atlas length (HC)	47	0.05	0.79	26	-0.10	1.32	-0.62	0.535
Axis length	44	-0.03	1.02	29	0.04	1.00	0.30	0.768
Pelvis Ischium length	54	-0.04	0.93	19	0.11	1.22	0.54	0.592
Atlas length (FK)	48	0.03	0.73	23	-0.06	1.45	-0.33	0.744
Pelvis Ilium height	48	-0.00	1.00	17	0.01	1.07	0.03	0.975
Pelvis Ischium height	46	0.03	0.87	17	-0.08	1.34	-0.38	0.703
Manubrium breadth	31	0.01	0.92	17	-0.03	1.19	-0.13	0.900
Manubrium length	27	0.00	1.02	15	0.00	1.00	0.00	0.999
Pelvis Pubis length	29	0.08	1.00	13	-0.17	1.06	-0.72	0.479
Pelvis Pubis height	26	0.01	0.95	13	-0.02	1.17	-0.07	0.945
Scapula breadth	18	-0.04	1.01	10	0.08	1.09	0.30	0.769
Scapula height	14	-0.21	0.78	11	0.27	1.25	1.17	0.248

Thorax, pectoral and pelvic girdles and predicted mean dUI1 heights

In comparison to the analysis based on the median dental age, the subset based upon the fitted curve describing the relationship between the predicted mean dUI1 heights and the width of the scapular glenoid (N=72 out of 98 individuals) shows a similar (non-statistically significant) trend of lower residuals for post-peak individuals compared to peak individuals (Fig. 7.18; Table 7.24).

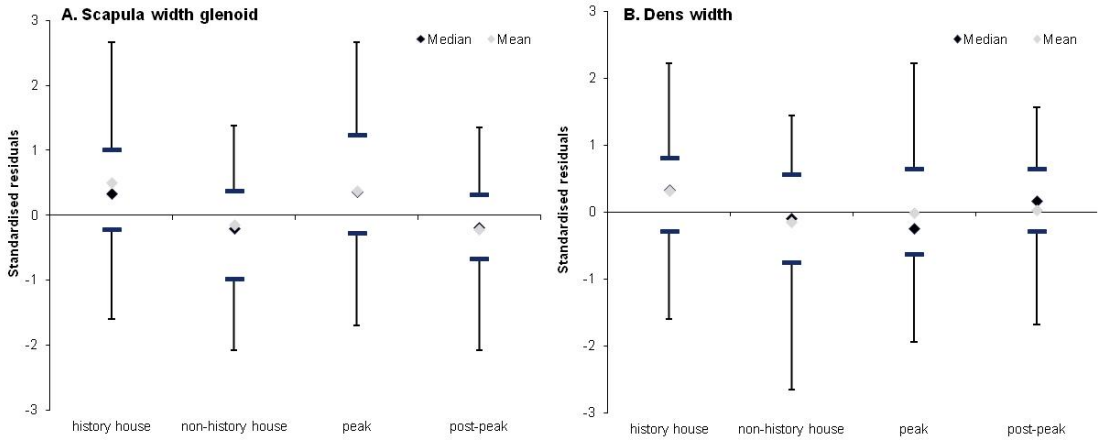

Figure 7.18: Box and whisker plots of residuals from curves fitted to measurements of the width of the scapular glenoid (A) and the width of the vertebral dens (B) based on predicted mean dUI1 heights. Grey diamond = mean, Black diamond = median, Black horizontal lines = first and third quartiles

In contrast, the subset based upon the polynomial regression describing the relationship between the predicted mean dUI1 heights and the width of the dens (N=67 out of 92 individuals) shows marginally (non-statistically significant) higher residual values for Post-Peak individuals in comparison to Peak individuals (Fig. 7.18; Table 7.24).

Table 7.24: Thorax, pectoral and pelvic girdle against deciduous tooth height measurements:
Summary statistics for standardised regression residuals by time of burial

	Peak			Post-Peak				
Skeletal variable	N	mean	sd	N	mean	sd	t	P
Scapula width glenoid	22	0.38	1.20	35	-0.11	0.87	1.78	0.080
Dens width	24	-0.01	1.01	30	0.05	1.10	-0.21	0.835

The subset analysis based on predicted mean dUI1 heights and the width of the dens and of the scapular glenoid shows similar results to the analysis based on the dental development age: for both skeletal variables, residual values are lower in non-history house individuals in comparison to history house individuals and this difference between residual values is significant for the width of the scapular glenoid (Fig. 7.18; Table 7.25).

Table 7.25: Thorax, pectoral and pelvic girdle against deciduous tooth height measurements:
Summary statistics for standardised regression residuals by place of burial

	Non-History house			History house				
Skeletal variable	N of individuals	mean	sd	N	mean	sd	t	P
Scapula width glenoid	51	-0.19	1.06	21	0.46	0.93	2.57	0.012
Dens width	42	-0.14	1.04	25	0.27	0.91	1.63	0.108

7.2.6. Hand and foot bones

Hand and foot bones and dental development age

In terms of hand and foot bones, the metatarsal (N=91) and metacarpal (N=90) lengths and the talus length (N=77) and width (N = 71) were the skeletal variables with the largest sample sizes and are represented in Figure 7.19. From this figure, a pattern of lower mean and median residuals for Post-Peak individuals in comparison to Peak individuals can be detected for these four skeletal variables. This is also reflected in the statistically significant results of the paired t-test for the residuals of the metacarpal length (Table 7.26).

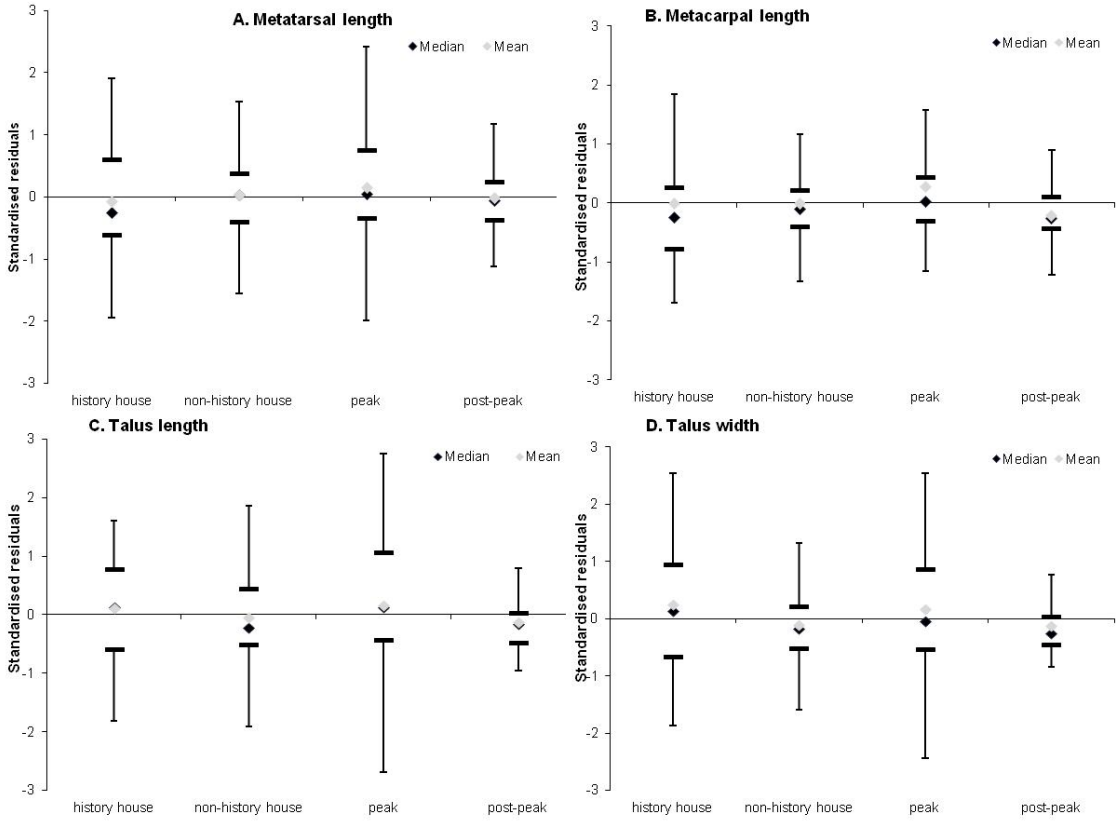

Figure 7.19: Box and whisker plots of residuals from curves fitted to measurements of the length of the metarsal (A), metacarpal (B) and the length and width of the talus (C and D) based on dental development age. Grey diamond = mean, Black diamond = median, Black horizontal lines = first and third quartiles

The skeletal variables with the smallest sample size for foot and hand bones (calcaneus length and width) show contrasting trends, with lower calcaneus length residuals in post-peak individuals in comparison to peak individuals and marginally higher calcaneus width residuals in post-peak individuals in comparison to peak individuals. Both trends are not statistically significant (Table 7.26).

Table 7.26: Hand and foot bones against median dental development age: Summary statistics for standardised regression residuals by time of burial

	Peak			Post-Peak				
Skeletal variable	N	mean	sd	N	mean	sd	t	P
Metatarsal length	37	0.15	1.19	38	0.00	0.62	0.70	0.4
Metacarpal length	36	0.28	1.21	36	-0.21	0.54	2.24	0.028
Talus length	35	0.17	1.21	29	-0.12	0.50	1.20	0.234
Talus width	30	0.17	1.20	28	-0.12	0.48	1.19	0.238
Calcaneus length	26	0.10	1.21	23	0.01	0.56	0.33	0.745
Calcaneus width	21	0.09	1.08	22	0.15	0.79	-0.20	0.845

From the residual plots in Figure 7.19, no clear trend can be detected in terms of place of burial. For the metatarsal lengths, mean and median residuals are lower in history house individuals in comparison to non-history house individuals, but for the length and the width of the talus, this trend is inverted, with higher mean and median residuals for history house individuals in comparison to non-history house individuals (Fig. 7.19). The results of the t-tests for these hand and foot bone variables show no statistically significant differences in terms of place of burial (Table 7.27).

The variables with the smallest sample size for foot and hand bones (calcaneus length and width) show a similar trend to the metatarsal length residuals, with lower calcaneus length and width residuals in history house individuals in comparison to non-history house individuals and this difference is statistically significant in terms of calcaneus width (Table 7.27).

Table 7.27: Hand and foot bones against median dental development age: Summary statistics for standardised regression residuals by place of burial

	Non-History house			History house				
Skeletal variable	N	mean	sd	N	mean	sd	t	P
Metatarsal length	60	0.04	1.04	31	-0.07	0.95	-0.50	0.615
Metacarpal length	62	0.00	0.98	28	0.00	1.08	-0.01	0.989
Talus length	54	-0.05	1.04	23	0.11	0.94	0.63	0.533
Talus width	50	-0.10	0.93	21	0.25	1.15	1.34	0.184
Calcaneus length	41	0.14	1.04	22	-0.27	0.90	-1.55	0.126
Calcaneus width	35	0.29	0.86	20	-0.51	1.08	-3.02	0.004

Hand and foot bones and predicted mean dUI1 heights

In comparison to the analysis based on the median dental age, the subset based upon the fitted curves describing the relationship between the predicted mean dUI1 heights and the metatarsal (N=64 out of 91 individuals) and metacarpal length (N= 60 out of 90 individuals) show a similar (non-statistically significant) trend of lower residuals for Post-Peak individuals compared to Peak individuals (Fig. 7.20; Table 7.28).

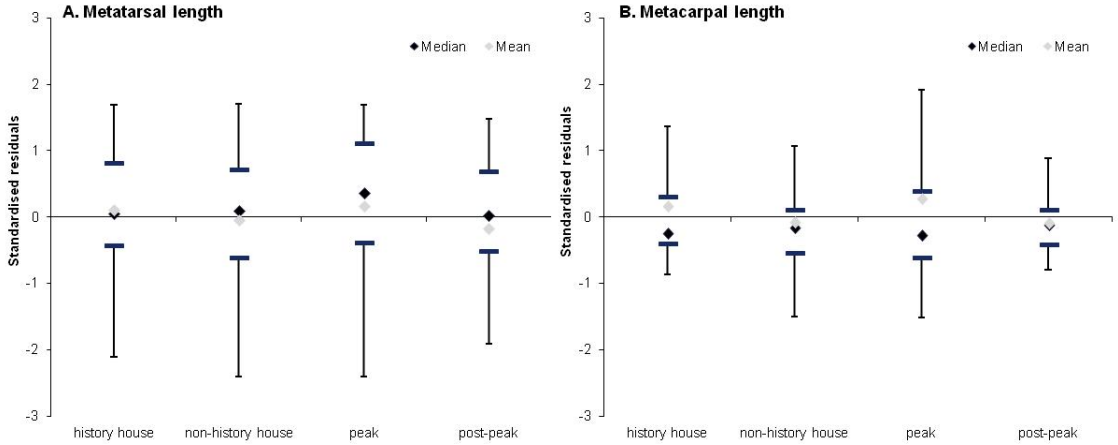

Figure 7.20: Box and whisker plots of residuals from curves fitted to measurements of the length of the metarsal (A) and metacarpal (B) based on predicted mean dUI1 heights. Grey diamond = mean, Black diamond = median, Black horizontal lines = first and third quartiles

Table 7.28: Hand and foot bones against deciduous tooth height measurements:
Summary statistics for standardised regression residuals by time of burial

	Peak			Post-Peak				
Skeletal variable	N	mean	sd	N	mean	sd	t	P
Metatarsal length	19	0.17	1.22	34	-0.02	0.84	0.65	0.517
Metacarpal length	19	0.28	1.60	31	-0.07	0.56	1.13	0.264

In contrast to the analysis based on the median dental age, the subset based upon the fitted curves describing the relationship between the predicted mean dUI1 heights and the metatarsal and metacarpal length show a (non-statistically significant) trend of lower residuals for non-history house individuals compared to history house individuals (Fig. 7.20; Table 7.29).

Table 7.29: Hand and foot bones against deciduous tooth height measurements:
Summary statistics for standardised regression residuals by place of burial

	non-History house			History house				
Skeletal variable	N	mean	sd	N	mean	sd	t	P
Metatarsal length	40	-0.04	1.00	24	0.07	1.04	0.41	0.687
Metacarpal length	34	-0.09	0.96	19	0.16	1.08	1.15	0.255

7.2.7. Cranial variables

Cranial variables and dental development age

The cranial variables with the largest sample size are the basilar length (N= 92) and width (N= 75), the maximum basilar length (N= 84) and the mandibular ramus height (N= 70)

and these are represented in Figure 7.21. From this figure, a clear pattern of lower mean and median residuals for Post-Peak individuals in comparison to Peak individuals can be detected for all four cranial variables. This is also reflected in results of the paired t-test for the residuals of the basilar length, for which the difference in residuals approaches significance (Table 7.30).

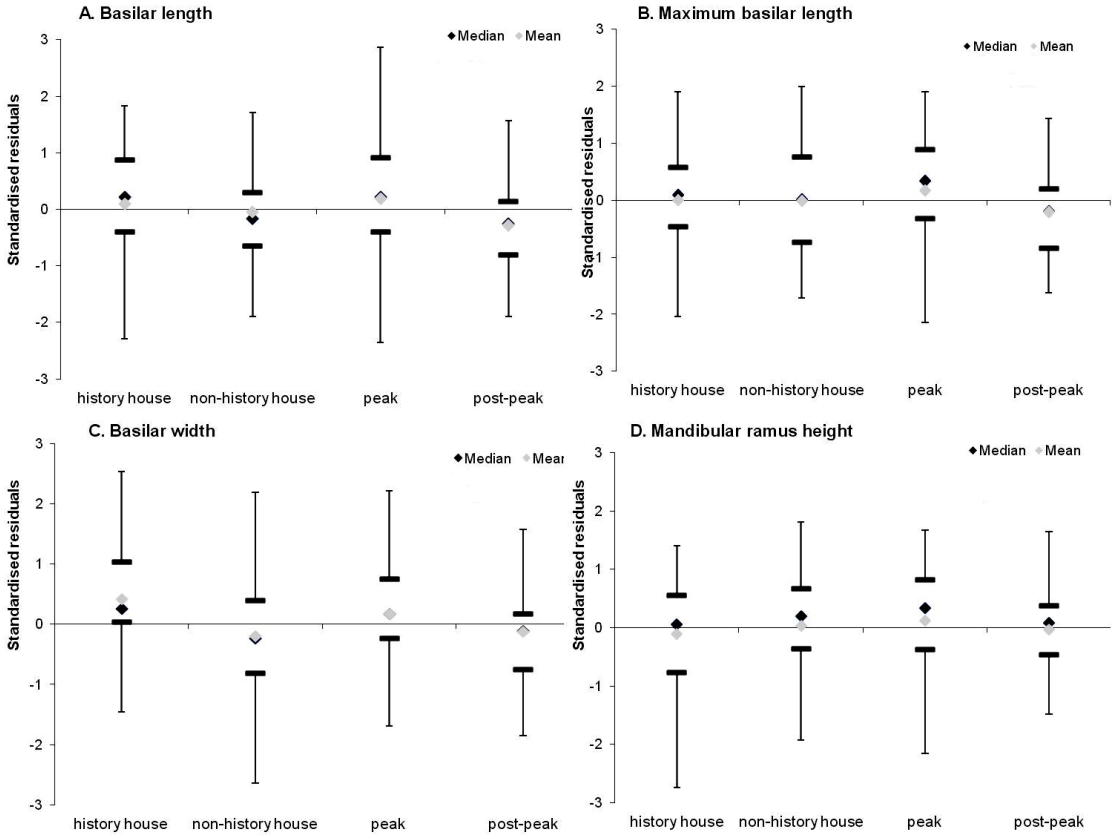

Figure 7.21: Box and whisker plots of residuals from curves fitted to measurements of the basilar length (A), the maximum basilar length (B), basilar width (C) and the mandibular ramus height (D) based on dental development age. Grey diamond = mean, Black diamond = median, Black horizontal lines = first and third quartiles

Cranial variables with lower sample sizes, including the zygomatic width and length, orbit breadth, minimum ramus breadth and the lateralis length and width also show a pattern of lower mean residuals for Post-Peak individuals in comparison to Peak individuals and this difference approaches significance for the zygomatic width measurements (Table 7.30). The chin height and condylar to coronoid measurements do not have a large enough sample sizes for each archaeological group (Peak or Post-Peak) and are therefore not included in the statistical analysis.

Table 7.30: Cranial parameters against median dental development age: Summary statistics for standardised regression residuals by time of burial								
	Peak			Post-Peak				
Skeletal variable	N	mean	sd	N	mean	sd	t	P
Basilar length	37	0.19	1.20	35	-0.29	0.81	1.97	0.053
Maximum basilar length	33	0.18	1.16	34	-0.21	0.77	1.60	0.114
Basilar width	29	0.17	1.07	33	-0.13	0.82	1.25	0.216
Mandibular ramus height	29	0.19	1.08	27	-0.03	0.82	0.59	0.554
Zygomatic width	26	0.34	0.99	31	-0.14	0.90	1.90	0.063
Orbit breadth	28	0.04	0.97	27	-0.01	1.01	0.18	0.862
Minimum ramus breadth	29	0.19	1.01	19	0.13	0.88	0.20	0.844
Lateralis length	17	0.20	1.04	26	-0.03	0.88	0.77	0.448
Lateralis width	17	0.05	1.11	27	0.01	0.88	0.13	0.894
Zygomatic length	15	0.08	1.04	26	0.02	1.10	0.16	0.875

Figure 7.21 shows no clear pattern of residual distribution in terms of place of burial. Means and median residuals are higher for individuals buried in history houses when looking at the basilar length and width and this difference is statistically significant in terms of basilar width (Table 7.31). In contrast, mean and median residual values are virtually equal between individuals buried in history and non-history houses in terms of maximum basilar length and on the mandibular ramus height plot, mean and median residuals are lower in individuals buried in history house in comparison to individuals buried in non-history houses (Fig. 7.21).

In contrast to the mean residual values of the basilar length and width, most other cranial variables (orbit breadth, minimum ramus breadth, lateralis length and width, chin height, zygomatic length and the space between the condylar and coronoid processes) show higher mean residuals for non-history house individuals in comparison to history house individuals but this trend is not statistically significant in any of the variables (Table 7.31).

Table 7.31: Cranial parameters against median dental development age: Summary statistics for standardised regression residuals by place of burial								
	non-History house			History house				
Skeletal variable	N	mean	sd	N	mean	sd	t	P
Basilar length	63	-0.04	0.95	29	0.10	1.12	0.63	0.533
Maximum basilar length	55	0.00	0.96	29	0.01	1.11	0.04	0.971
Basilar width	51	-0.20	0.98	24	0.42	0.95	2.59	0.012
Mandibular ramus height	50	0.04	0.99	20	-0.10	1.07	-0.55	0.586
Zygomatic width	49	0.00	0.95	21	0.00	1.15	-0.01	0.992
Orbit breadth	49	0.03	0.99	15	-0.09	1.10	-0.38	0.704
Minimum ramus breadth	40	0.10	0.95	22	-0.15	1.13	-0.92	0.361
Lateralis length	39	0.06	0.97	16	-0.15	1.12	-0.71	0.480
Lateralis width	40	0.13	1.03	13	-0.39	0.88	-1.65	0.105
Chin height	37	0.14	0.98	12	-0.42	1.03	-1.68	0.099
Zygomatic length	37	0.04	0.98	11	-0.13	1.16	-0.47	0.642
Condylar to coronoid	17	0.04	0.93	12	-0.16	1.16	-0.53	0.598

Cranial variables and predicted mean dUI1 heights

In comparison to the analysis based on the median dental age, the subset analysis based upon the fitted curves describing the relationship between the predicted mean dUI1 heights and the basilar (N= 72 out of 92 individuals) and maximum basilar length (N=73 out of 84 individuals) show a similar trend of lower residuals for Post-Peak individuals compared to Peak individuals, which is statistically significant for the basilar length (Fig. 7.22; Table 7.32).

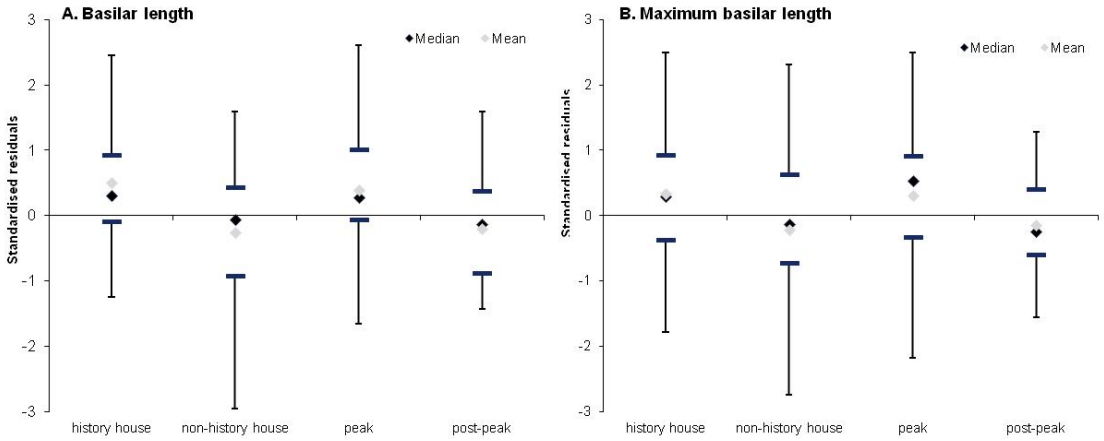

Figure 7.22: Box and whisker plots of residuals from curves fitted to measurements of the basilar length (A) and the maximum basilar length (B), based on predicted mean dUI1 heights. Grey diamond = mean, Black diamond = median, Black horizontal lines = first and third quartiles

Table 7.32: Cranial bones against deciduous tooth height measurements: Summary statistics for standardised regression residuals by time of burial

	Peak			Post-Peak				
Skeletal variable	Nr of individuals	mean	sd	Nr	mean	sd	t	P
Basilar length	25	0.40	1.04	31	-0.20	0.78	2.46	0.017
Maximum basilar length	25	0.30	1.24	32	-0.15	0.74	1.70	0.094

Similar to the analysis based on the median dental age, the subset based upon the fitted curves describing the relationship between the predicted mean dUI1 heights and the basilar and maximum basilar length show a trend of lower residuals for non-history house individuals compared to history house individuals; this difference between residual values is statistically significant for the basilar length and approaches significance for the maximum basilar length (Fig. 7.22; Table 7.33).

Table 7.33: Cranial bones against deciduous tooth height measurements: Summary statistics for standardised regression residuals by place of burial								
	Non-History house			History house				
Skeletal variable	N	mean	sd	N	mean	sd	t	P
Basilar length	49	-0.23	0.96	23	0.49	0.95	2.97	0.004
Maximum basilar length	48	-0.16	0.99	25	0.31	0.99	1.96	0.054

To summarise, **the results of the skeletal growth analysis show a trend towards lower mean residual values for Post-Peak individuals in comparison to Peak individuals** and this is the case for the analysis based on dental development age and diaphyseal long bone lengths and widths (apart from the diaphyseal length of the ulna, the minimum clavicle width and the medio-lateral width of the femur), skeletal elements of the thorax, pectoral and pelvic girdle, the hand and foot bones (but not for the calcaneus width) and the cranial variables. This trend is also visible on the analysis based on tooth height measurements and the radius and humerus diaphyseal lengths, the width of the upper metaphysis of the radius (but not for the width of the upper metaphysis of the ulna), the width of the scapular glenoid (but not for the width of the dens), the length of the metarcarpals and metatarsals and the length and maximum length of the basilar occipital.

This trend of lower mean residual values in post-peak individuals is statistically significant for the analysis based on dental development and the width of the lateral end of the clavicle, the width of the upper metaphysis of the humerus and the antero-posterior diaphyseal width of the humerus and the length of the metacarpal. It is also statistically significant for the analysis based on deciduous tooth height measurements and the length of the basilar occipital.

There are no consistent differences in terms of the growth profile comparison between individuals buried in history houses and individuals buried on non-history houses, Some skeletal variables indicate lower residual values for individuals buried in history houses and others indicate lower residual values for individuals buried in non-history houses.

There are statistically significant differences for the analysis based on dental development include lower residuals for individuals buried in history houses in terms of the width of the upper metaphysis of the ulna and the width of the calcaneus and higher residuals for individuals buried in history houses for the width of the basilar occipital.

Statistically significant differences for the analysis based on deciduous tooth height measurements include lower residuals for individuals buried in history houses in terms of

the width of the upper metaphysis of the ulna and higher residuals for individuals buried in history houses in terms of the width of the upper metaphysis of the radius, the width of the scapular glenoid and the length of the basilar occipital.

7.3. Comparisons of skeletal and dental development

7.3.1. Number of matched defects per zone

Standardised residuals from curves fitted to measurements of the skeletal growth parameters with the largest sample sizes (the width of the upper metaphysis of the ulna, the length of the metatarsal, the width of the scapular glenoid and the length of the basilar occipital) were compared between individuals with a low degree of dental growth disruption, individuals with a medium degree of disruption and individuals with a high degree of disruption (for a description of this procedure, see Chapter 5).

Comparisons between the three groups were based upon the number of matched defects and the number of affected perikymata per dental developmental zone. The approach based on dental developmental zones was considered the most sensitive parameter for detecting differences between groups, as both the number of matched defects and the number of affected perikymata identified the greatest (N=2) number of (significant and approaching significance) differences between groups in this study. In the box and whisker plots of the residuals constructed for each group, negative residuals indicate a lower size attainment for dental developmental age, whereas positive residuals indicate a higher size attainment for dental developmental age.

Sample sizes are very small for each of the skeletal variables (Table 7.34), but when plotting the residual values for each group, some trends can be detected visually. **In terms of the comparison between groups with a low and medium degree of dental growth disruptions**, mean and median residual values tend to be higher for individuals with a low degree of dental growth disruptions in comparison to individuals with a medium degree of dental growth disruptions. This is the case for dental development zone 1 when comparing residuals from fitted curves to the measurements of the width of the upper metaphysis of the ulna, the metatarsal length (Fig. 7.23) and the width of the scapular glenoid (Fig. 7.24). This trend can also be detected in zone 2 when looking at residuals

based on measurements of the width of the upper metaphysis of the ulna, the metatarsal length, the width of the scapular glenoid and the basilar length, in zone 3 for the residuals based on the basilar length, the width of the upper metaphysis of the ulna and the metatarsal length and in zone 4 for residuals based on the width of the upper metaphysis of the ulna and the metatarsal length (Fig. 7.23).

For dental development zone 1, no clear differences can be detected in the residual values of the basilar length for groups with a low and medium degree of disruptions. In addition to this, there is a contrasting trend of lower residual values for individuals with a low degree of dental growth disruptions in comparison to individuals with a medium degree of dental growth disruptions in dental development zone 3 when comparing residuals from fitted curves to the measurements of the scapular glenoid width and in zone 4 for residuals based on scapular glenoid width and basilar length (Fig. 7.24).

Table 7.34:
Sample sizes for matched skeletal and dental growth profiles (N = number of individuals included in comparison dental growth and skeletal variables)

	N Ulna upper metaphysis	N Metatarsal length	N Scapula width glenoid	N Basilar length
Zone 1: low	6	5	7	4
Zone 1: medium	6	4	5	4
Zone 1: high	6	5	8	3
Zone 2: low	8	5	3	5
Zone 2: medium	10	9	8	10
Zone 2: high	3	3	3	4
Zone 3: low	4	3	4	3
Zone 3: medium	5	3	2	4
Zone 3: high	12	11	13	7
Zone 4: low	5	3	4	2
Zone 4: medium	6	6	6	4
Zone 4: high	6	4	6	6

In terms of the comparison between groups with a low and high degree of dental growth disruptions, no clear trend can be distinguished. Mean and median residuals are higher for individuals with a low degree of dental growth disruptions in comparison to individuals with a high degree of dental growth disruptions in dental development zone 1 for the width of the upper metaphysis of the ulna, the width of the scapular glenoid and the metatarsal length, but a contrasting trend of lower means and median residuals for individuals with a low degree of dental growth disruptions in comparison to individuals

with a high degree of dental growth disruptions is visible in this zone in the analysis based on basilar length.

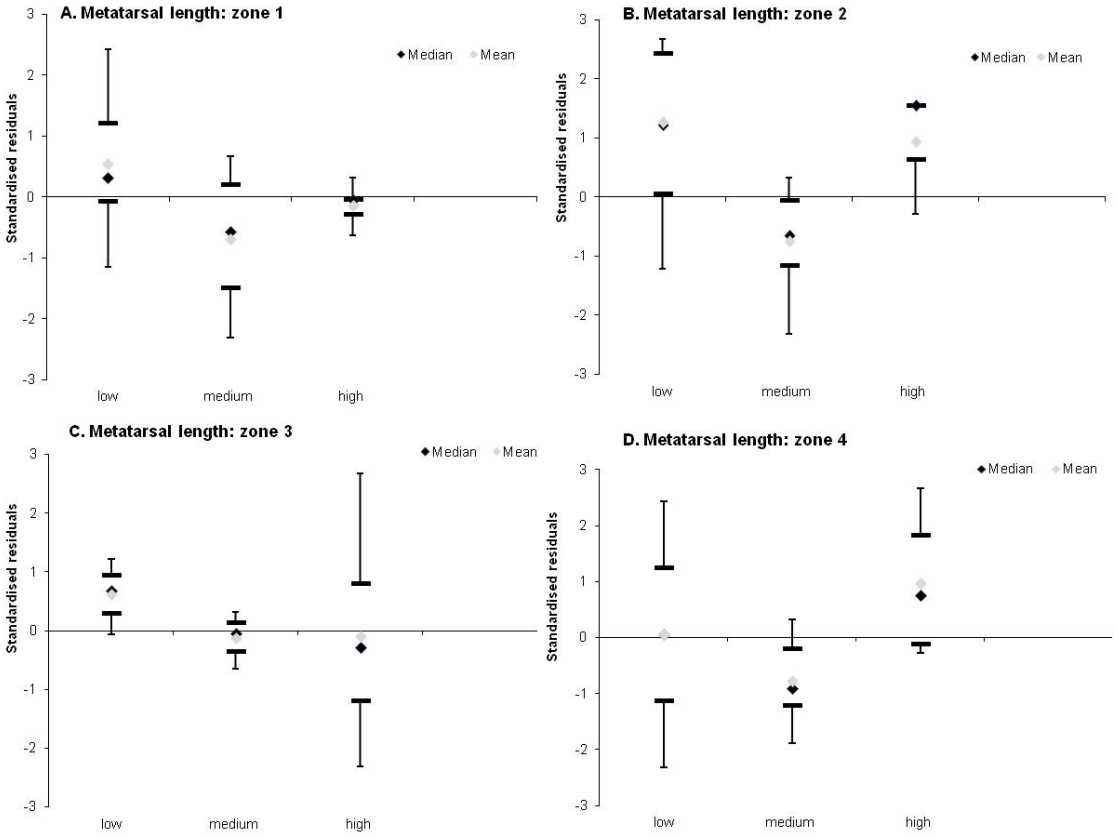

Figure 7.23: Box and whisker plots of residuals from curves fitted to measurements of the metatarsal length, presented per zone of enamel formation. Grey diamond = mean residuals, Black diamond = median residuals, Black horizontal lines = first and third quartiles, Low = group of individuals with low degree of dental growth disruptions in terms of matched defects per zone, Medium= group of individuals with medium degree of dental growth disruptions in terms of matched defects per zone, High= group of individuals with high degree of dental growth disruptions in terms of matched defects per zone

No clear differences between the groups can be distinguished for dental development zone 2 for residuals based on the width of the scapular glenoid. and the metatarsal length. The mean residuals are lower for individuals with a low degree of dental growth disruptions in comparison to individuals with a high degree of dental growth disruptions based on the width of the upper metaphysis of the ulna and the basilar length. In contrast, mean residuals are higher for individuals with a low degree of dental growth disruptions in comparison to individuals with a high degree of dental growth disruptions based on the metatarsal length (Fig. 7.23).

In dental development zone 3, means and median residuals are higher for individuals with a low degree of dental growth disruptions in comparison to individuals with a high degree of dental growth disruptions. This is the case for residuals based on the basilar length, the width of the upper metaphysis of the ulna and the metatarsal length, but not for the scapular glenoid, where mean and median residuals are lower for individuals with a low degree of dental growth disruptions in comparison to individuals with a high degree of dental growth disruptions.

Finally, in dental development zone 4, means and median residuals are lower for individuals with a low degree of dental growth disruptions in comparison to individuals with a high degree of dental growth disruptions for the basilar length, the ulna upper metaphysis width, the metatarsal length and the width of the scapular glenoid (Fig. 7.24).

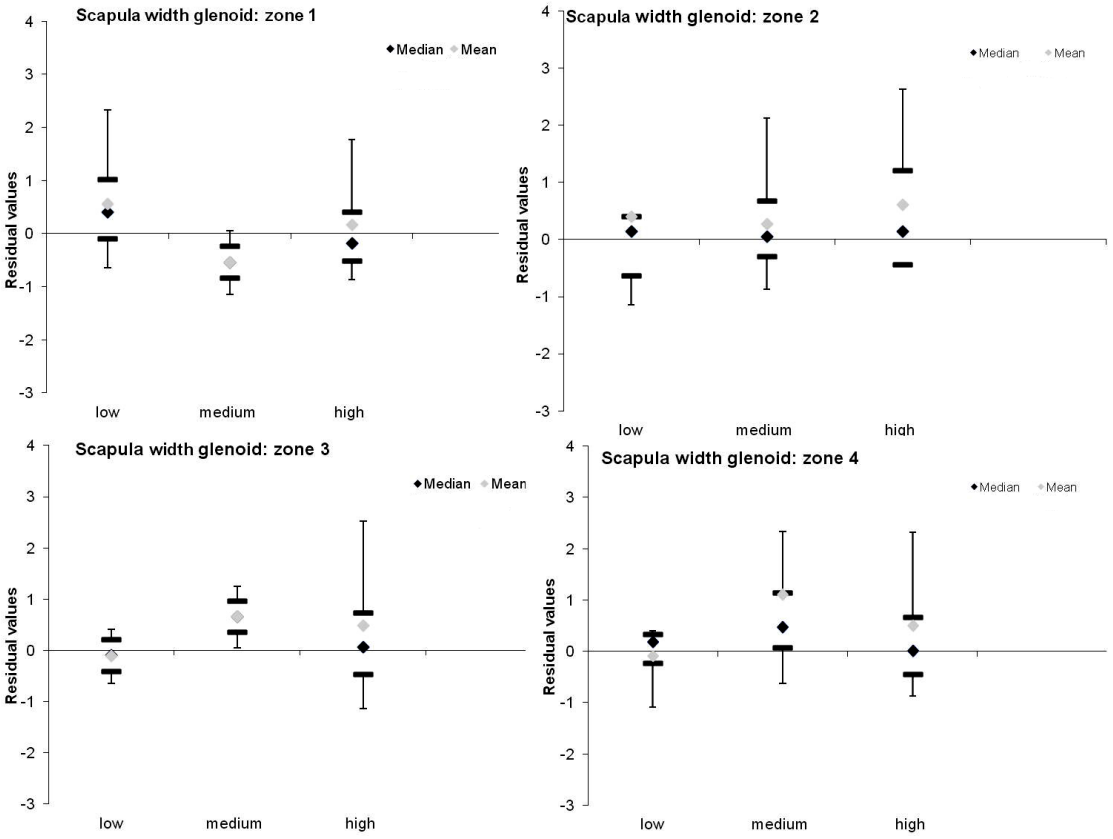

Figure 7.24: Box and whisker plots of residuals from curves fitted to measurements of the width of the scapular glenoid, presented per zone of enamel formation. Grey diamond = mean residuals, Black diamond = median residuals, Black horizontal lines = first and third quartiles, Low = group of individuals with low degree of dental growth disruptions in terms of matched defects per zone, Medium= group of individuals with medium degree of dental growth disruptions in terms of matched defects per zone, High= group of individuals with high degree of dental growth disruptions in terms of matched defects per zone

In terms of the comparison between groups with a medium and high degree of dental growth disruptions, means and median residuals tend to be lower for individuals with a medium degree of dental growth disruptions. This is the case in dental development zones 1 and 2 for all skeletal parameters and in zone 3 for residuals based on basilar length. However, in dental development zone 3, no clear differences can be detected in the residuals based on the width of the scapular glenoid and a contrasting trend of higher mean residuals for individuals with a medium degree of dental growth disruptions in comparison to individuals with a high degree of dental growth disruptions is visible from residuals based on of the upper metaphysis of the ulna and the metatarsal length.

In dental development zone 4, mean and median residuals tend to be lower for individuals with a medium degree of dental growth disruptions in comparison to individuals with a high degree of dental growth disruptions. This is the case for residuals based on the width of the upper metaphysis of the ulna, the metatarsal length and the basilar length, but not for residuals based the width of the scapular glenoid, which have higher mean residuals for individuals with a medium degree of dental growth disruptions in comparison to individuals with a high degree of dental growth disruptions in this dental development zone (Fig. 7.24).

7.3.2. Number of affected perikymata per quarter

In addition to the comparison between standardised residuals and the number of defects per dental developmental zones, the three groups (individuals with a low degree of dental growth disruption, individuals with a medium degree of disruption and individuals with a high degree of disruption), were also compared based on the number of affected perikymata per dental developmental zone. Similar to the comparison above (p. 257), negative residuals indicate a lower size attainment for dental developmental age, whereas positive residuals indicate a higher size attainment for dental developmental age.

No clear trend can be distinguished in terms of the comparison between groups with a low and medium degree of dental growth disruptions. No consistent differences can be detected between the groups when considering dental development zone 1. For the width of the upper metaphysis of the ulna and the width of the scapular

glenoid, mean and median residual values tend to be higher for individuals with a low degree of dental growth disruptions in comparison to individuals with a medium degree of dental growth disruptions (Fig. 7.25). However, there is a contrasting trend of lower mean residuals for individuals with a low degree of dental growth disruptions in comparison to individuals with a medium degree of dental growth disruptions in the analyses based on the residuals from the basilar length and metatarsal length in this zone.

Similarly to dental development zone 1, no consistent differences can be detected between the groups when considering dental development zone 2. Mean and median residual values are higher for individuals with a low degree of dental growth disruptions in comparison to individuals with a medium degree of dental growth disruptions when looking at residuals from the width of the upper metaphysis of the ulna and the width of the scapular glenoid, but an opposite trend of lower residual values for individuals with a low degree of dental disruptions is visible in the residuals from the metatarsal length and no clear differences can be detected between the residuals from the basilar length.

In dental development zone 3, mean and median residual values tend to be higher for individuals with a low degree of dental growth disruptions in comparison to individuals with a medium degree of dental growth disruptions when looking at residuals from the metatarsal length, but no clear trend can be detected between the residuals from the width of the upper metaphysis of the ulna and the width of the scapular glenoid.

Based upon the residuals from the width of the upper metaphysis of the ulna and the width of the scapular glenoid, mean and median residual values are higher for individuals with a low degree of dental growth disruptions in comparison to individuals with a medium degree of dental growth disruptions in dental development zone 4 (Fig. 7.25). However, when looking at residuals from the basilar length, a contrasting trend of lower mean residuals for individuals with a low degree of dental growth disruptions in comparison to individuals with a medium degree of dental growth disruptions can be detected. In addition, no clear differences can be detected between residuals based on the metatarsal length in developmental zone 4.

No clear trend can be distinguished in terms of the comparison between groups with a low and high degree of dental growth disruptions, In zone 1, mean and median residuals are higher for individuals with a low degree of dental growth disruptions in comparison to individuals with a high degree of dental growth disruptions when

considering residuals from the upper metaphysis width of the ulna, the metatarsal length and the width of the scapular glenoid, but an opposite trend of lower residuals individuals with a low degree of dental growth disruptions can be detected based on the residuals from the basilar length. In contrast to zone 1, dental development zone 2 shows a clear trend of higher mean and median residuals for individuals with a low degree of dental growth disruptions in comparison to individuals with a high degree of dental growth disruptions in all skeletal parameters.

Similarly to dental development zone 2, in zone 3, higher mean and median residuals for individuals with a low degree of dental growth disruptions in comparison to individuals with a high degree of dental growth disruptions are visible in the plots based on basilar length. However, in this zone, no clear differences can be detected between the residuals from the metatarsal length and a contrasting trend of lower mean residuals for individuals with a low degree of dental growth disruptions in comparison to individuals with a high degree of dental growth disruptions is visible in the plots based on the residuals from width of the scapular glenoid and the width of the upper metaphysis of the ulna (Fig. 7.25).

In dental development zone 4, lower mean residuals for individuals with a low degree of dental growth disruptions in comparison to individuals with a high degree of dental growth disruptions can be detected when looking at residuals from the width of the upper metaphysis of the ulna, the metatarsal length and the basilar length. This is not the case for the residuals from the width of the scapular glenoid, where residuals are higher for individuals with a low degree of dental growth disruptions in comparison to individuals with a high degree of dental growth disruptions.

No clear trend can be distinguished in terms of the comparison between groups with a medium and high degree of dental growth disruptions. In zone 1, means and median residuals tend to be lower for individuals with a medium degree of dental growth disruptions in comparison to individuals with a high degree of dental growth disruptions when looking residuals from the basilar length, but higher for individuals with a medium degree of dental growth disruptions in comparison to individuals with a high degree of dental growth disruptions when considering residuals from the metatarsal length and the width of the scapular glenoid.

No clear differences can be detected between residuals from the width of the upper metaphysis of the ulna in dental development zones 1 or 2 (Fig. 7.25). In the latter, higher

mean residuals for individuals with a medium degree of dental growth disruptions in comparison to individuals with a high degree of dental growth disruptions are visible in the plots based on residuals from the metatarsal length and the basilar length, but lower mean residuals for individuals with a medium degree of dental growth disruptions can be detected when looking at residuals from the width of the scapular glenoid.

In dental development zone 3, lower mean residuals for individuals with a medium degree of dental growth disruptions can also be detected when looking at residuals from the width of the upper metaphysis of the ulna, the metatarsal length and the width of the scapular glenoid and this is also the case for all skeletal parameters in dental development zone 4.

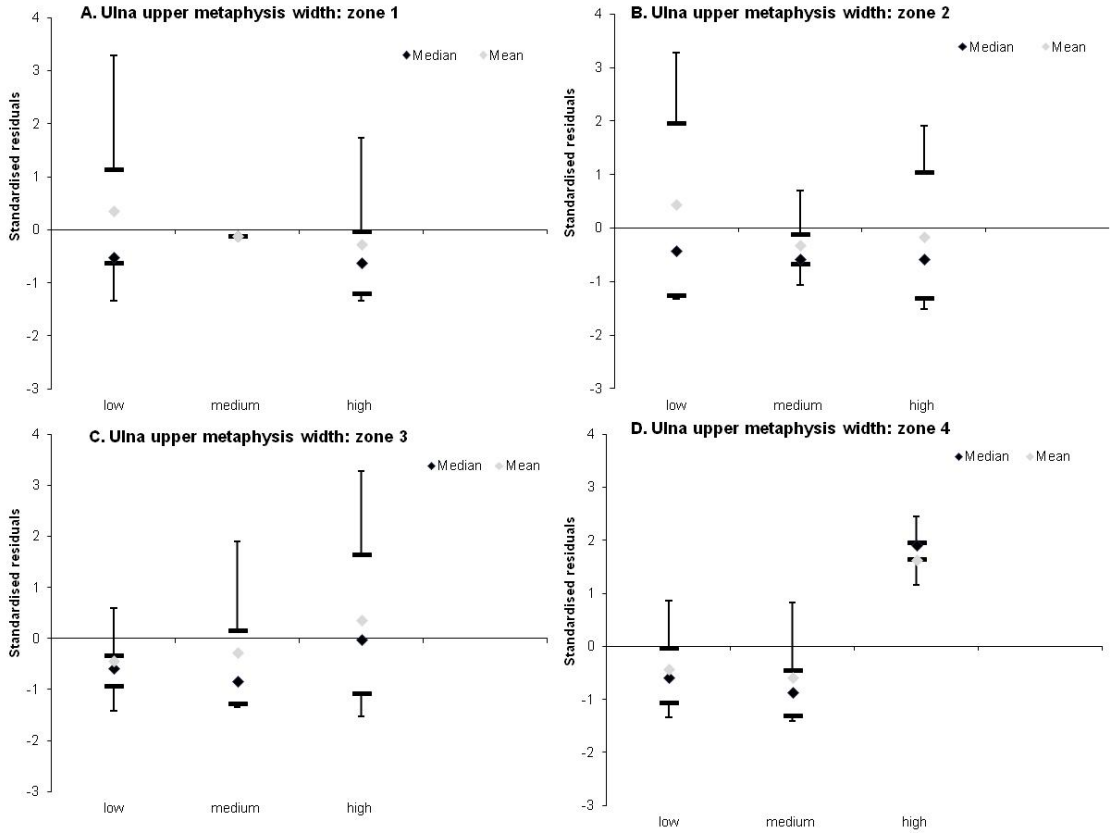

Figure 7.25: Box and whisker plots of residuals from curves fitted to measurements of the width of the upper metaphysis of the ulna, presented per zone of enamel formation. Grey diamond = mean, Black diamond = median, Black horizontal lines = first and third quartiles, Low = group of individuals with low degree of dental growth disruptions in terms of matched defects per zone, Medium= group of individuals with medium degree of dental growth disruptions in terms of matched defects per zone, High= group of individuals with high degree of dental growth disruptions in terms of matched defects per zone

Chapter 8. Discussion

Four main research questions were proposed in Chapter 1, of which two were related to methodological issues and a further two were related to the interpretation of health at the Neolithic site of Çatalhöyük. The two archaeological research questions were accompanied by hypotheses outlined in Chapter 2. Using the methodology and results outlined in Chapters 5 and 7, each of these four key questions can now be addressed.

8.1. Can enamel defects be assessed objectively?

As described in Chapter 4, the term “enamel hypoplasia” refers to an underdevelopment or incomplete development of the enamel covering the tooth crown. Enamel defects are a permanent record of a disturbance to the formation of the crown occurring during amelogenesis. Three types of enamel defects can be differentiated on permanent teeth, pit-form, plane-form and furrow-form (Berten 1895; Hillson 1996; Hillson and Bond 1997; Hillson 2014). Furrow-form enamel hypoplasia, which is the focus of this study, is produced by the premature cessation of matrix secretion of a larger than usual band of ameloblasts and can be identified microscopically by a wider than expected spacing between consecutive pairs of perikymata for that particular area of the crown (Hillson 1996; Hillson and Bond 1997; Witzel *et al.* 2008).

As outlined in Chapters 1 and 5, the standardisation of furrow-form defect identification is of crucial importance in order to reduce a currently substantial bias in the bioarchaeological assessment of health and growth in the past. This study’s aim was to enhance an objective, microscopic identification of such defects in human dentitions by creating permanent records and working towards the standardisation of recording methods.

In this study, a new three-dimensional technique (Alicona 3D Infinite Focus imaging microscope and software) was used to assess developmental features in the enamel (perikymata) of permanent human incisors. In terms of **imaging**, the technique constitutes a substantial advancement to the engineer’s microscope method (as described in Chapter 4; Hassett 2011; Hillson and Jones 1989; King *et al*. 2002, 2005; Temple *et al.* 2012, 2013), as the Infinite Focus imaging microscope allows the on-screen

visualisation of perikymata morphology which enhances the subsequent identification of perikymata grooves. It also allows for a direct on-screen comparison to be made between measurements and images and the export of high resolution images for future use (with different software if required).

A current limitation of the Alicona software for the perikyma spacing profile application is that the horizontal and vertical coordinates of each perikyma groove could not be directly exported, so that these had to be entered separately into an Excel spreadsheet. A second limitation to the application of three-dimensional imaging techniques is that these require specialist and expensive software and instruments, which are not yet readily available in most archaeological laboratories.

As with other imaging techniques, the acquisition of digital images of the tooth crown is heavily dependent on the preservation of the tooth crown and calculus, dirt and cracks can make the observation of perikymata extremely difficult. Added to this, during an individual's life, dental wear can cause the disappearance of perikymata and the loss of crown height, introducing error to the identification of the number and spacing of these incremental structures (Guatelli-Steinberg *et al.* 2005; King *et al.* 2002; Newell *et al.* 2006).

The dental sample used in this study is extremely well preserved and any dirt could be removed using acetone-impregnated cotton wool before the replication of the tooth crowns and subsequent scanning and analysis. A decision was also made to limit this study to relatively unworn dentitions of immature individuals. Any future application of this and other three-dimensional imaging techniques will have to take into account these sample size limitations caused by the dental preservation status and even though it is possible to find some adult individuals with a limited amount of calculus and dental wear, it is unlikely that many accurate spacing profiles can be constructed using large adult samples, especially for individuals over 40 years (King *et al.* 2005).

The three-dimensional imaging technique addresses one of the fundamental issues outlined by Goodman and Rose (1990), Dobney (1991) and Hillson and colleagues (Hillson and Bond 1997; King *et al*. 2002, 2005), as permanent records can be created in the form of A) photomicrographs and B) high-resolution epoxy resin casts of tooth crowns. Two further critical issues were addressed in the **quantitative analysis** employed in this study.

First, using enamel microstructures as a basis for the identification of defects, the geometry of crown growth is taken into account. Based upon recent advances in dental anthropology which have made it possible to construct spacing patterns of perikymata, such spacing profiles are compared to the underlying trend along the crown surface. Using this method, irregularities (wider than expected spacings) in the perikymata spacing can be detected and used to identify the occurrence of furrow-form enamel hypoplasia. To check this identification, these are cross-matched between teeth with overlapping developmental schedules (Guatelli-Steinberg 2004; Hassett 2011; Hillson and Bond 1997; King *et al*. 2002, 2005; Newell *et al*. 2006; Temple *et al.* 2012, 2013; Witzel *et al*. 2008).

Building upon this first issue, the present study aimed at the standardisation of the detection of anomalies in the perikyma spacing pattern by proposing a mathematical approach. This detection of irregularities is complicated by the variation in spacing down the crown and around the circumference of the crown. This 'normal' variation (called 'noise' in signal processing literature) in the perikyma spacing profile needs to be reduced in order to isolate the underlying spacing trend down the crown.

This study assessed two noise reduction methods; separate perikyma spacings, smoothed by moving averages (as per Hassett 2011) and cumulative perikyma spacings to which a curve is fitted (Hillson 2014). The first application used a Z-score approach, whereas the second used locally weighted scatter plot smoothing (LOWESS). The results of a methodological case study showed that the cumulative spacing/LOWESS method successfully detected four clearly delineated and three more subtle spacing irregularities, which could be confirmed visually and matched between antimeres. The Z-score approach was less effective in detecting these defects as the use of direct spacings introduced a number of false positives, making it difficult to identify subtle defects.

In terms of the **interpretation of enamel defects**, as all individuals and teeth within the study sample displayed some form of furrow-form defect, traditional enamel prevalence approaches based on the proportion of individuals affected or the proportion of affected teeth per individual would not be meaningful. Additionally, as the mean numbers of defects can only be comparable between individuals if they all have a full set of crowns covering the phases of development being compared, a range of alternative parameters were also employed in this study, based upon the number of matched defects per

individual (mean and maximum number of defects and the number of matched defects per formation zone or per age group per individual), the number of affected perikymata (maximum number and percentage of perikymata affected per individual) and the duration and interval between matched defects.

The analysis based onformation zones in terms of the number of matched defects, number of affected perikymata and mean duration and interval per zone were the most sensitive parameter for detecting differences between groups of individuals within the Çatalhöyük sample. These variables showed clearly distinguishable trends and the greatest number of differences approaching significance between the separate groups of individuals.

Summary

Although a subjective element remains in the identification of the exact location of perikymata grooves, the mathematical and microscopic approach in this study provides a more thorough understanding of dental growth disturbances in archaeological populations than previous microscopic and macroscopic approaches. It enables researchers to assess (on-screen and exported) high-resolution three-dimensional digital images, to construct dental growth profiles using coordinates calculated from a detailed three-dimensional model of the crown surface and to use a set threshold value for a more objective definition and identification of furrow-form enamel defects. Once enamel defects have been identified, the analysis based on formation zones was considered the most sensitive parameter for comparisons of patterns of furrow-form defects between individuals.

8.2. Is there a correlation between delayed skeletal growth and patterns of furrow-form enamel hypoplasia?

Human growth is defined by patterns of size changes related to age and variation in human growth patterns occurs through the interaction of biological, cultural and environmental conditions (Ribot and Roberts 1996). As growing individuals are the most sensitive to changes in these conditions, the analysis of human growth patterns is an important tool to reconstruct the living conditions of past populations (Ribot and Roberts 1996). Skeletal and dental growth patterns are influenced by environmental factors in different ways, so the combination of these two bioarchaeological approaches could potentially provide a more holistic insight into the living conditions of past populations.

As described in Chapter 4, the combined skeletal/dental growth approach has been used previously with only limited success. Based upon the large sample of subadults at Çatalhöyük, and the detailed microscopic analysis of dental growth, the aim of the second methodological research question was therefore to study the possible relationship between dental growth disruptions and delayed growth in the skeleton.

In this study, it was expected that individuals with a greater proportion of crown development disrupted by defects would have smaller dimensions for growing parts of the their skeleton for a given dental age than those with a smaller proportion disrupted. Patterns of furrow-form enamel hypoplasia and skeletal growth (width of the upper metaphysis of the ulna, the length of the metatarsal, the width of the scapular glenoid fossa and the length of the basilar occipital) were compared in terms of the number of matched defects and the number of affected perikymata per quarter of crown formation zones. For this comparison, three groups were differentiated, including individuals with a low degree of dental growth disruption per zone, individuals with a medium degree of disruption per zone and individuals with a high degree of disruption per zone, using the mean number of defects and mean number of affected perikymata per quarter as a cut-off point.

The results showed no systematic relationship between enamel disruption and age-related changes in the width of the scapular glenoid. However, for the remaining skeletal parameters, individuals with a medium and high degree of dental growth disruption in tooth crown development zone 3 appeared to have consistently smaller bone dimensions for a given dental age than individuals with a low degree of dental disruptions. For zones 1, 2 and 4, no systematic differences between the groups could be detected, apart from the smaller dimensions (for the length of the metatarsal and the width of the upper metaphysis of the ulna) for a given dental age for individuals with a medium degree of dental growth disruption.

In contrast to the analysis based on the number of defects per formation zone, the results of the analysis based on the number of perikymata affected per formation zone showed no systematic differences between dental growth and age-related changes in the width of the scapular glenoid, the width of the upper metaphysis of the ulna, the length of the metatarsal, or the length of the basilar.

One of the principal weaknesses in this correlation study is the small sample size available for the direct comparison between enamel defects and skeletal growth

parameters. However, small sample size is unlikely to be the only reason for this lack of a strong relationship as the control of development in dentition and skeleton is highly complex. Cardoso (2005) also found low correlations between dental (expressed as growth in tooth length and attainment of tooth formation stages) and skeletal development (expressed as long bone length) and argued that these are indications that skeletal and dental growth patterns are relatively independent processes.

Studies on living populations also show the difference between dental growth and other maturing body systems. For example, a cross-sectional study comparing growth stunting (expressed as height-for-age, according to the World Health Organisation standards) and dental development (expressed as the dental development of the left mandibular canine) in 280 living Peruvian schoolchildren aged 9.5 to 16.5 years showed that growth stunting was not associated with delayed dental development (Flores-Mir *et al.* 2005). A large cross-sectional study of living children from Sudan (aged 2-22 years, N=2115) shows similar results, with similar ($p>0.05$) mean ages at entry and within tooth stages between groups affected by severe malnutrition and normal children (Elamin and Liversidge 2013).

As described in Chapter 4, comparable studies assessing the relationship between skeletal development and detailed studies of enamel hypoplasia using microstructures are currently not available. Less detailed comparative studies using enamel hypoplasia exist, but are problematic due to the non-standardised identification of furrow-form enamel defects. Nevertheless, the results of these comparative analyses indicate a clear trend. For example, in a recent cross-sectional study of modern Australian Aborigines, Floyd and Littleton (2006) compared the onset and number of defects (scored based on the DDE index using dental casts) with height-for-age Z-scores. They found that the adolescent height for age was significantly ($N=60$, $p=0.019$) negatively correlated with the number of defects appearing earlier than two years of age (Floyd and Littleton 2006).

Further comparative studies are limited to cross-sectional bioarchaeological studies, which show similar results to the current study. Lewis (2002) compared long bone growth patterns with prevalence of dental enamel hypoplasia from four Medieval and Postmedieval English sites found that sites with significantly shorter individuals had a (non-significantly) higher percentage of individuals affected by enamel hypoplasia. Conversely, Ribot and Roberts (1996), in their assessment of two Medieval samples (Raunds and Chichester) found that patterns of enamel hypoplasia, did not correlate with the growth of long bone lengths.

Previous explanations for the contrasting results in published studies focused on the fact that such studies were limited to assessments of long bone lengths, whereas the increase in long bone length may be adapted to growth disruptions at the expense of other skeletal variables such as cortical width (Himes *et al*. 1975, Huss-Ashmore *et al*. 1982, Mays 1995, Ribot and Roberts 1996). However, this study has shown that the inclusion of metaphyseal long bone widths, foot bones and cranial parameters in combined enamel hypoplasia/skeletal growth studies shows similar non-or negative correlations.

The lack of a strong relationship between patterns of postcranial growth and furrow-form enamel defects might be related to **the timing of the enamel defects**. As described in Chapter 3, cranial parameters are indicators of early childhood growth patterns, with the fastest growing skeletal variables measured on the cranial vault. Similarly, the permanent teeth also develop during early childhood, with perikymata appearing on the enamel surface between from around 1 year of age (Hillson 1996). In contrast, diaphyseal lengths and widths of long bones and pelvic and scapular dimensions are indicators of intermediate to late skeletal growth patterns (Humphrey 1998).

Whereas the postcranial skeletal variables can be considered as giving complementary growth information to enamel and cranial growth parameters, they can not necessarily be linked to patterns of disruptions to dental development. Such disruptions represent single episodes whereas development of, for example, a long bone diaphysis is a continuous process and the measurement at death must be the result of an accumulation of periods of slower and faster growth. It is likely that an episode of growth disruption would be followed by a period of **catch up growth**, particularly by middle or late childhood. The term ‘catch up growth’ refers to the regaining of the normal/natural growth curve trajectory after a physiological disturbance. This is achieved by an accelerated growth after such disturbances, making it impossible to detect delayed growth in some individuals (Mays 1995).

It is also important to note that there is no detailed information on the quality (i.e. **sensitivity and specificity**) **of dental enamel hypoplasia** as a marker of disruptions to childhood growth (Boldsen 1998; Hillson 2014). For example, growth disturbances causing furrow-form enamel defects of short durations during early childhood might well have been too brief to produce any effect on the skeletal growth pattern. A detailed comparison of enamel hypoplasia patterns, based on dental microstructures, and the skeletal growth pattern of a sample with a greater proportion of enamel affected by

defects than the Çatalhöyük sample, might show stronger relationships between skeletal and dental growth patterns.

Summary

This study did not detect a consistent relationship between delayed skeletal growth and patterns of furrow-form enamel hypoplasia. This lack of a systematic association between enamel defect proportions and skeletal growth parameters might be related to the timing of the enamel defects and the difference in sensitivity to disruptions in dental and skeletal growth.

As there is a lack of association between skeletal and dental growth patterns, the interpretation of the growth disruptions in terms of place (individuals buried in history house and non-history house contexts) and time of burial (individuals buried in Peak and Post-Peak contexts) is difficult. In order to take into account the potential effect of the timing of defects, the discussions on the group comparisons are divided into sections based on early and late childhood growth parameters.

8.3. Did human growth patterns vary in terms of place of residence at Çatalhöyük?

In Çatalhöyük, some houses were rebuilt over more generations than other houses and more symbolic manifestations such as wild bull horns, relief sculptures and wall paintings have been found in these “special houses” in comparison to other locations (Hodder 2005a, b; Hodder 2006). These structures, called ‘history houses’ by Hodder (2005a, 2006, Hodder and Pels 2010) were also preferred burial locations.

In this study, the subadult remains were analysed with these specific characteristics of the Çatalhöyük buildings in mind and variation in dental and skeletal growth patterns was assessed in terms of spatial differences. More specifically, it was expected that children buried in “special houses” (history houses) would be advantaged in comparison to children buried in other houses. These children would therefore have a smaller proportion of enamel affected by growth disturbances would also show evidence of an earlier achievement of skeletal growth states relative to children buried in other contexts.

In terms of the **enamel hypoplasia analysis**, no statistically significant differences have been detected in terms of number and age distribution of defects, number of affected

perikymata or the duration of and interval between furrow-form defects. Some (non-statistically significant) trends were however noted, including shorter durations of defects in history house individuals in comparison to non-history house individuals (for formation zone 3) and longer intervals between defects in history house individuals compared to non-history house individuals (for the separate tooth analysis). This might be interpreted as evidence of lesser growth disruption in the children who were ultimately buried in the history houses. Similarly, for the cranial development measurements, the residual values for the basilar width also indicate a lower degree of skeletal growth disruption for individuals buried in history houses in comparison to individuals buried in non-history houses. This finding confirms the initial hypothesis outlined at the start of this thesis, proposing that children buried in ”special houses” would have a lesser proportion of enamel affected by growth disturbances relative to children buried in other contexts and that these children would also show less evidence of delayed bone growth.

However, the results of the analyses of **postcranial skeletal development measurements** which later childhood growth show a contrasting trend, with significantly lower mean residual values for the upper metaphysis of the ulna, the width of the lateral end of the clavicle and the width of the calcaneus for individuals buried in history houses in comparison to individuals buried in non-history houses, indicating a delayed bone growth pattern for individuals buried in “special contexts”.

One possible interpretation of this contrast between early and late growth parameters that there was a transition in the level of growth disruptions from less to more during the development of the children buried in the history houses. Mays and colleagues (2008) found a similar pattern of shorter long bone dimensions for age from a 19th century urban sample (St Martin’s Churchyard Birmingham) in comparison with a contemporary rural assemblage (Wharram Percy) for younger age cohorts and tentatively ascribed this difference to the effect of prolonged breastfeeding in the Wharram Percy children, based upon the known health benefits of breastmilk. Similarly, evidence from nitrogen and carbon isotope data suggests that the end of exclusive breastfeeding (ie the start of the introduction of supplementary foods, also called the start of the weaning period) continued until around 1 year at Çatalhöyük (Richards et al. 2003; Pearson et al. 2010). Pearson and colleagues (2010) suggested that differences in the duration of this weaning period may have been caused by household or kin responses to immediate socio-economic demands.

An alternative interpretation of the contrasting results between early and late growth parameters is that a comparison based on ‘history houses’ or ‘non-history houses’ might not be an appropriate level of analysis. Another approach would be to assess individuals buried in different neighourhoods or clusters of domestic buildings. Düring (2007) estimated that the site consisted of between 27 and 53 such clusters (See Chapter 2). Hodder (2006; 2012; Hodder and Pels 2010) referred to these as clusters as composed of large groups of houses (10-30) bounded by refuse areas or alleyways, but note that due to the nature of the site, it is extremely difficult to accurately assign particular houses (and therefore individuals buried in these houses) to these neighbourhoods.

The face-to-face interactions between members of the same neighbourhood, which probably occurred on a daily basis across the rooftops might have formed a basis of particular social networks in which members mutually supported each other in times of difficulty (Düring 2007; Hodder 2012). In a large-scale study on dental metrics and morphology, Pilloud (2009), argued that people buried together in houses were not be biologically related and that membership of ‘moieties or descent groups’ might have been fluid and not completely based on relatedness (Pilloud 2009). Similarly, Hodder (2012) put forward that individual houses had complex and multiple relationships that its inhabitants could draw upon in times of hardship (Hodder 2012). As such, the contrasting trends of the history versus non-history house growth analyses might be reflective of a cultural resiliency based on group choices and individual agency, defined by Salisbury and Bácsmegi (2013, 145) as “*the ability of a society to maintain and develop identity, knowledge and ways of making a living, despite challenges and disturbances, by resisting damage and recovering quickly*.”

Summary

This study indicates that children buried in ”special houses” (history houses) do not have a statistically significant smaller proportion of enamel affected by growth disturbances relative to children buried in non-history houses. Added to this, children buried in non-history houses do not show evidence of delayed growth during early childhood. However, the null hypothesis suggesting that no differences would be found between children buried in history houses and non-history houses cannot be rejected, as skeletal parameters marking later childhood growth show evidence of delayed bone growth in history house individuals in comparison to non-history house individuals.

These contrasting results could indicate that growth status differs from infancy to late childhood in the history and non-history houses or that place of burial (‘history houses’ or

'non-history houses') might not be an appropriate level of analysis, as other social networks such as neighbourhoods in which members mutually supported each other blur the boundaries between individual houses.

8.4. Did health decline with changes in community size and density at Çatalhöyük?

Because of its long-lasting habitation sequence (spanning over 1400 years), Çatalhöyük is an optimal site for the study of diachronic change (see Chapter 2). Previous archaeological research at has revealed an increase in size and occupation density of the site at about 6500 BC and additional archaeological analyses have indicated changes in symbolism, consumption practices and herding practices occurring around this time (see Chapter 2).

In this study, the subadult remains were divided into three broad temporal categories: early (”Pre-Peak”), middle (”Peak”) and late (”Post-Peak”) periods. In the hypothesis outlined at the start of the thesis it was expected that children buried in ”Post-Peak” burials would have a higher proportion of enamel affected by growth disturbances than children buried in ”Peak” contexts and that these “Post-Peak” children would also show evidence of delayed bone growth relative to “Peak” children.

In the study of **enamel hypoplasia**, no statistically significant differences were detected for number and age distribution of defects, number of affected perikymata or the duration of and interval between furrow-form defects. However, some differences between Peak and Post-Peak individuals approached significance. For example, the number of defects was lower for all four crown formation zones in Post-Peak individuals in comparison with Peak individuals and this trend approached significance for zone 3 of the lower central incisor. The longer mean duration for Post-Peak individuals in comparison to Peak individuals approached significance in one of the crown formation zones (zone 4). Thus, individuals buried in both Peak and Post-Peak showed a pattern of a long duration of defects and a long interval between defects.

In contrast, the bone development measurements showed lower mean residual values for Post-Peak individuals in comparison with Peak individuals. This trend approached significance in terms of early childhood skeletal parameters (basilar occipital length and

zygomatic width) and was statistically significant in terms of later childhood skeletal parameters, including the diaphyseal length of the radius, the width of the lateral end of the clavicle, the width of upper metaphysis of the humerus, the antero-posterior diaphyseal width of the humerus and the length of the metacarpal.

These findings in part confirm the hypothesis outlined above. The trend affected all subadults, both during early and late childhood. This could be explained by the marked reduction in house number and density described in Chapter 2, as a smaller population would imply a smaller support group provided by the multiple relationships within the neighbourhoods.

Summary

This study indicates that children from Post-Peak contexts did not have a higher proportion of enamel affected by growth disturbances than children buried in Peak contexts, but bone development measurements marking both early and later childhood growth showed evidence of delayed bone growth in individuals buried in Post-Peak contexts in comparison with individuals buried in Peak contexts.

Chapter 9. Conclusion

The new method for measuring the perikyma spacing on anterior teeth used in this study, combined with availability of a large collection of juvenile remains made it possible to study patterns of childhood growth in detail at this site, taking into account detailed archaeological evidence of place (history and non-history houses) and time of burial (Peak and Post-Peak periods). Sample sizes were large enough, at least in some cases, to consider the variability of enamel hypoplasia and skeletal growth patterns within this site.

This new method for recording perikyma spacing provides a detailed micrographic record of dental growth. The intra-observer error for identifying perikymata is lower than previously reported error rates and the method is therefore a powerful tool for assessing dental growth patterns of modern human populations and fossil specimens. The three-dimensional approach also provides a solid basis for the quantitative analysis of furrow-form enamel defects, which can be detected using irregularities in the perikymata spacing. Suggested further investigations include a quantitative comparison between original tooth crowns and casts and the assessment of the limits to which perikymata can be observed on worn teeth. A current limitation is of the method is the cost of the Alicona instrument and software used for the acquisition and interpretation of the three-dimensional models. Possibilities for future research include comparisons between the assessment of three-dimensional models using available analytical freeware and the Alicona software as well as comparisons with other 3D imaging techniques such as SEM (Alicona MeX) and Polynomial Texture Mapping (PTM) domes.

Using the new 3D approach, this study aimed at the standardisation of the detection of anomalies in the perikyma spacing pattern (furrow-form enamel hypoplasia) by proposing a mathematical approach. A methodological case study showed that using locally weighted scatter plot smoothing (LOWESS) both clearly delineated and more subtle spacing irregularities could successfully be detected, confirmed visually and matched between antimeres. This study was limited to recording enamel defects on incisors, but the method could be easily adapted to detect anomalies in the perikyma spacing of other tooth types.

In terms of the interpretation of enamel defects, different parameters were investigated in this study, including traditional enamel defect frequency approaches (the number of

individuals displaying furrow-form enamel hypoplasia and the mean number of defects per individual) and a range of alternative parameters. This study found that the most sensitive parameter for comparisons of patterns of furrow-form defects between subgroups was the approach based on dental development zones in terms of number of matched defects and number of affected perikymata.

The relationship between skeletal and dental growth disruptions has been highlighted by this study, but requires further investigation, using larger sample sizes in order to confirm the lack of a consistent correlation between delayed skeletal growth and patterns of furrow-form enamel hypoplasia. Nevertheless, a combination of dental and skeletal approaches to growth is suggested in order to provide a more comprehensive insight into level of disturbances affecting past populations.

In contrast to previous comparative studies of bioarchaeological assemblages from Near Eastern Neolithic sites, the goal of this research project was to undertake a detailed case study of one large Neolithic sample, with the detailed archaeological evidence of settlement, lifestyle, diet, and living conditions at Çatalhöyük providing an excellent contextual framework for an assessment of local variation in childhood growth patterns.

The first archaeological research question addressed the issue of history houses, which were rebuilt over more generations than other houses and and which contained more symbolic manifestations such as wild bull horns, relief sculptures and wall paintings than other houses. Using evidence of skeletal and dental growth disruptions, the conditions that allowed some buildings to exist for longer whilst others did not were explored in terms of biological variation (i.e. differences in growth profiles). If children buried in the “dominant history houses” were advantaged or disadvantaged in comparison to children buried in other houses, it was expected that there will evidence of systematic differences in the level of growth disruptions affecting children buried in these two types of houses.

The results of this study indicated that children buried in history houses and other houses do not have significantly different proportions of enamel affected by growth disturbances. In contrast, some, but not all, skeletal parameters (width of the upper metaphysis of the ulna, the lateral end of the clavicle and the calcaneus) show evidence of significantly smaller skeletal sizes for age in history house individuals in comparison to non-history house individuals. As these skeletal parameters are characteristic of the late childhood period, these results could indicate that growth status differed from infancy to late

childhood in the history and non-history houses or that “house type” (history and non-history house) might not be an appropriate level of analysis, as social networks in which members mutually supported each other caused the boundaries between individual houses to be blurred. A potential area for future research could be the exploration of difference between “neighbourhoods”, which have recently been identified by Hodder (2012) as different radial zones with different types of symbolic manifestations within the site.

The second archaeological research question involved the assessment of potential diachronic changes within the sample. The long-lasting habitation sequence at Çatalhöyük allows an intra-population comparison based upon archaeological evidence of an increase and decrease in size and occupation density of the site. Therefore, in this study, the subadult remains were analysed in terms of temporal differences, consisting of three categories: early (“Pre-Peak” population size and density), middle (“Peak” population size and density) and late (“Post-Peak” population size and density) periods.

Individuals buried in both Peak and Post-Peak periods were affected by a medium degree of disruption during enamel growth. In contrast, statistically significant difference between both groups could be detected using skeletal parameters, with individuals buried in the Post-Peak period has smaller skeletal sizes for their ages than individuals buried in the Peak period. It seems reasonable to suppose that this difference occurred as a consequence of smaller population sizes with smaller support groups provided by the multiple relationships within the site and therefore less buffering against growth disruptions. It is hoped that future research will include greater sample sizes for Peak, Post-Peak and Pre-Peak period to assess this possible explanation.

Bibliography

Adams, R.L., 2005. Ethnoarchaeology in Indonesia illuminating the ancient past at Çatalhöyük? *American Antiquity* 70/1, 181-188

Al-abassi, E. and Sarie, S.,1997. Prevalence of dental hypoplasia in the Neolithic site of Wadi Shu'eib in Jordan. *Dental Anthropology* 11, 1-4

Albinus, B.S., 1737. *Icones ossium foetus humani*. Leiden: Verbeek

AlQahtani, S.J., 2008. *Atlas of tooth development and eruption*. Barts and the London School of Medicine and Dentistry. London: Queen Mary University of London. MclinDent

AlQahtani, S.J., Hector, M.P. and Liversidge, H.M., 2010. Brief communication: The London atlas of human tooth development and eruption. *American Journal of Physical Anthropology* 142/3, 481-490

Alvear, J., Artaza, L., Vial, M., Guerrero, S. and Muzzo, J., 1986. Physical growth and bone age of survivors of protein energy malnutrition*. Archives of Disease in Childhood* 61, 257-262

Anderson, D.L., Thompson, G.W. and Popovich, F., 1976. Age of attainment of mineralisation stages of the permanent dentition. *Journal of Forensic Sciences* 21, 191-200

Andreasen, J.O. and Ravn, J.J., 1971. The effect of traumatic injuries to primary teeth on their permanent successors II. A clinical and radiographic follow-up study of 213 teeth. *Scandinavian Journal of Dental Research* 79, 284-294

Andreasen, J.O. and Ravn, J.J., 1973. Enamel changes in permanent teeth after trauma to their primary predecessors. *Scandinavian Journal of Dental Research* 81, 203 – 209

Andreasen, J.O., Sundstrom, B. and Ravn J.J., 1971. The effect of traumatic injuries to primary teeth on their permanent successors: A clinical and histological study of 117 injured permanent teeth*. Scandinavian Journal of Dental Research* 79, 219 – 283

Andrews, P., Molleson, T. and Boz, B., 2005. The human burials at Çatalhöyük. In: I. Hodder (Ed.), *Inhabiting Çatalhöyük: reports from the 1995-1999 seasons.* (McDonald Institute Monographs). Cambridge: McDonald Institute for Archaeological Research; London: British Institute of Archaeology at Ankara, 261-278

Angel, J.L., 1965. *Unpublished analysis notes and observations on skeletal remains excavated by James Mellaart, Çatalhöyük, Turkey*. Washington, DC: National Anthropological Archives, Smithsonian Institution

Angel, J.L., 1966. Porotic hyperostosis, anemias, malarias, and marshes in the prehistoric eastern Mediterranean. *Science* 153 /3737, 760-763

Angel, J.L., 1971. Early Neolithic skeletons from Catal Hüyük: demography and pathology. *Anatolian Studies* 21, 77-98

Angel, J.L., 1984. Health as a crucial factor in the changes from hunting to developed farming in the Eastern Mediterranean. In: M.N. Cohen and G.J. Armelagos (Eds.), *Paleopathology at the origins of agriculture*. New York: Academic Press, 51-69

Antoine, D.M., 2000. Evaluating the periodicity of incremental structures in dental enamel as a means of studying growth in children from past human populations. Unpublished Ph.D. thesis, Institute of Archaeology, UCL

Antoine, D.M., Dean, M.C. and Hillson, S.W., 1999. The periodicity of incremental structures in dental enamel based on the developing dentition of post-medieval known-age children. In: J.T. Mayhall and T. Heikkinen (Eds.), *Dental Morphology 1998*. Oulu: Oulu University Press, 48-55

Antoine, D.M., Hillson, S.W. and Dean, C.M., 2009a. The developmental clock of dental enamel: a test for the periodicity of prism cross-striations in modern humans and an evaluation of the most likely sources of error in histological studies of this kind. Journal of Anatomy 214, 45-55

Antoine, D.M., Hillson, S.W., Keene, D., Dean, M.C. and Milne, G., 2005. Using growth structures in teeth from victims of the Black Death to investigate the effects of the Great Famine (AD 1315-1317). *American Journal of Physical Anthropology* 40, 65

Antoine, D.M., Hillson, S.W., Keene, D., Milne, G., Waldron, A. and White, W., 2009b. A study of human growth in London over the past 1000 years using tooth histology to determine a precise age-at-death. *American Journal of Physical Anthropology* Supplement 45, 108-109

Armelagos, G.J., Mielke, J.H., Owen, K.H., Van Gerven, D.P., Dewey, J.R. and Mahler, P.E., 1972. Bone growth and development in prehistoric populations from Sudanese Nubia. *Journal of Human Evolution* 1/1, 89–118

Asouti, E., 1995. Group identity and the politics of dwelling at Neolithic Çatalhöyük. In: I. Hodder (Ed.), *Çatalhöyük perspectives: themes from the 1995-1999 seasons* (McDonald

Institute Monographs). Cambridge McDonald Institute for Archaeological Research; London: British Institute of Archaeology at Ankara, 75-91

Asouti, E. and Hather, J., 2001. Charcoal analysis and the reconstruction of ancient woodland vegetation in the Konya basin, south-central Anatolia, Turkey: results from the Neolithic site of Çatalhöyük East. *Vegetation History and Archaeobotany* 10, 23-34

Asper, H., 1916. Über die Braune Retziussche Paralell streifung im Schmelz der menschlichen Zähne. *Schweiz Vierteljahresschrift für Zahnheilkunde* 26, 275-314

Atalay, S. and Hastorf, C., 2006. Food, meals, and daily activities: The habitus of food practices at Neolithic Çatalhöyük. *American Antiquity* 71/2, 283-319

Augustin, G., Antabak, A. and Davila, S., 2007. The periosteum Part 1: anatomy, histology and molecular biology. *Injury* 38, 1115-1130

Bäckman, B. and Holm, A., 1986. Amelogenesis Imperfecta: prevalence and incidence in a Northern Swedish County. *Community Dentistry and Oral Epidemiology* 14, 43-47

Bacon, A.M., 1989. Estimation de l'âge à la mort des enfants actuels et fossiles à partir des stries d'accroissement de l'émail dentaire. *Bulletins et Mémoires de la Société d'Anthropologie de Paris* 1/1-2, 3-11

Baird, D., 2002. Early Holocene settlement in central Anatolia: problems and prospects as seen from the Konya plain. In: F. Gerard and L. Thissen (Eds.), *The Neolithic of Anatolia*. Istanbul: Ege Yayinlari, 139-152

Baird, D., 2005. The history of settlement and social landscapes in the early Holocene in the Çatalhöyük area. In: I. Hodder (Ed.*), Çatalhöyük perspectives: themes from the 1995-1999 seasons*. (McDonald Institute Monographs). Cambridge McDonald Institute for Archaeological Research; London: British Institute of Archaeology at Ankara, 55-74

Baird, D., 2006. The Boncuklu project: the origins of sedentism, cultivation and herding in central Anatolia. *Anatolian Archaeology* 13, 14-17

Baird, D., 2008. The Boncuklu project: the origins of sedentism, cultivation and herding in central Anatolia. *Anatolian Archaeology* 14, 11-12

Baird, D., 2010. Was Çatalhöyük a centre? The implications of a late aceramic Neolithic assemblage from the neighbourhood of Çatalhöyük. In: D. Bolger and L.C. Maguire (Eds.), *Development of pre-state communities in the Near East*. Oxford: Oxbow, 207–216

Baird, D., Carruthers, D., Fairbairn, A. and Pearson, J., 2011. Ritual in the landscape evidence from Pınarbaşı in the seventh-millenium cal bc, Konya Plain. *Antiquity* 85, 380-394

Bass, W.M., 1966. *Human osteology: A laboratory and field manual*. Springfield: Missouri Archaeological Society

Bastir, M., O'Higgins, P. and Rosas, A., 2007. Facial ontogeny in Neanderthals and modern humans. *Proceedings of the Royal Society B-Biological Sciences* 274, 1125-1132

Bayliss, A. and Farid, S., 2008. Re-assessment of the existing dating of the East Mound – a progress report. *Çatalhöyük 2008 Archive Report*. http://www.catalhoyuk.com/downloads/Archive_Report_2008.pdf (retrieved on14/05/14)

Bayliss, A. and Farid, S., 2010. Modelling chronology. *Çatalhöyük 2010 Archive Report.* http://www.catalhoyuk.com/downloads/Archive_Report_2010.pdf. (retrieved on 14/05/14)

Bayliss, A. and Farid, S., 2012. Modelling chronology. *Çatalhöyük 2012 Archive Report.* http://www.catalhoyuk.com/downloads/Archive_Report_2012.pdf (retrieved on 14/05/14)

Bayliss, A., Farid, S. and Higham, T., in press. Time will tell: practicing Bayesian chronological modeling on the East Mound. In: I. Hodder (Ed.), *Çatalhöyük excavations: the 2000–2008 seasons* (Monographs of the Cotsen Institute of Archaeology). Los Angeles: University of California at Los Angeles, Los Angeles

Baysal, A. and Wright, K.I., 2005. Cooking, crafts and curation: the ground stone artefacts from Çatalhöyük, 1995-1999. In: I. Hodder (Ed.), Changing materialities at Çatalhöyük: reports from the 1995-1999 seasons. (McDonald Institute Monographs). Cambridge: McDonald Institute for Archaeological Research; London: British Institute of Archaeology at Ankara, 307-324

Beaton, G., Kelly, A., Kevany, J., Martorell, R. and Mason, J., 1990. *Appropriate uses of anthropometric indices in children. A report based on an ACC/SCN workshop*. ACC/SCN State-of-the-art series; Nutrition Policy discussion paper 7. Geneva: World Health Organisation

Bello, S.M., Verveniotou, E., Cornish, L. and Parfitt, S.A., 2011. 3-Dimensional microscope analysis of bone tooth surface modifications: comparison of fossil specimens and replicas. *Scanning* 33, 1-9

Bennike, P., Lewis, M.E., Schutkowski, H. and Valentin, F., 2005. Comparison of child morbidity in two contrasting Medieval cemeteries from Denmark. *American Journal of Physical Anthropology* 128, 734-746

Benzaquén, A.J., 2004. Childhood, identity and human science in the Enlightenment. *History Workshop Journal* 57/1, 34-57

Berbesque, J. and Doran, G., 2008. Brief communication: physiological stress in the Florida archaic - enamel hypoplasia and patterns of developmental insult in Early North American hunter-gatherers. *American Journal of Physical Anthropology* 136/3, 351-356

Berkovitz, B.K.B., Holland, G.R. and Moxham, B.J., 2009. *Oral anatomy, histology and embryology*. (Fourth edition). London: Elsevier

Bernard, C., 1865. *Introduction à l'étude de la médecine expérimentale*. Paris: JB Baillière et fils

Berten, J., 1895. Hypoplasie des Schmelzes (Congenitale Schmelzdefekte; Erosionen). *Deutsche Monatsschrift für Zahnheilkunde* 13, 425–439, 483–498, 533–548, 587–600

Bertini, L.C., 2011. *Changes in suid and caprine husbandry practices through Dynastic Egypt using linear enamel hypoplasia*. Unpublished Ph.D. thesis, University of Durham

Beynon, A.D., 1987. Replication technique for studying microstructure in fossil enamel. *Scanning Microscopy* 1, 663-669

Beynon, D., Clayton, C.B., Ramirez-Rozzi, F.V. and Reid, D.J., 1998. Radiographic and histological methodologies in estimating the chronology of crown development in modern humans and great apes: a review, with some applications for studies on juvenile hominids. *Journal of Human Evolution* 35, 351-370

Birch, W., 2005. A possible case of shortness of breath at Çatalhöyük - black lungs. In: I. Hodder (Ed.), *Inhabiting Çatalhöyük: reports from the 1995-1999 seasons* (McDonald Institute Monographs). Cambridge: McDonald Institute for Archaeological Research; London: British Institute of Archaeology at Ankara, 593-596

Black, G.V., 1908. *Operative dentistry*. Chicago: Medico-Dental Publishing Company

Black, G.V. and McKay, F.S., 1916. Mottled teeth. An endemic developmental imperfection of the enamel of the teeh heretofore unknown in the literature of dentistry. *Dental Cosmos* 58, 132-156

Black, S. and Scheuer, L., 1996. Age changes in the clavicle: from the early neonatal period to skeletal maturity. *International Journal of Osteoarchaeology* 6, 425–434

Black, T., 1979*. The biological and social analysis of a Mississippian cemetery from S.E. Missouri, The Turner Site, 23 Bu 21A*. Ann Arbor, Michigan: Anthropological Papers of the Museum of Anthropology 68

Blakey, M.L., Leslie, T.E. and Reidy, J.P., 1994. Frequency and chronological distribution of dental enamel hypoplasia in enslaved African Americans: A test of the weaning hypothesis*. American Journal of Physical Anthropology* 95, 371-383

Bloch, M., 2010. Is there religion in Çatalhöyük... or just houses? In: I. Hodder (Ed.), *Religion in the emergence of civilization: Çatalhöyük as a case study*. Cambridge: Cambridge University Press, 146-163

Boas, F., 1912. Changes in the bodily form of descendants of immigrants. American Anthropologist 14, 530-562

Boas, F., 1932. Studies in growth. Human Biology 4/3, 307-350

Bocaege, E., Humphrey, L.T. and Hillson, S.W., 2010. Technical note: a new three-dimensional technique for high resolution quantitative recording of perikymata. *American Journal of Physical Anthropology* 141, 498-503

Bocquet-Appel, J.P., 2002. Paleoanthropological traces of a Neolithic demographic transition. *Current Anthropology* 43/4, 637-650

Bodecker, C.F., 1930. Concerning defects in the enamel of teeth of ancient American Indians. *Journal of Dental Research* 10, 313

Bogaard, A. and Charles, M., 2007. Macro botanical remains. *Çatalhöyük 2007 Archive Report.*
http://www.catalhoyuk.com/downloads/Archive_Report_2007.pdf (retrieved on 14/05/14)

Bogaard, A., Charles, M., Twiss, K., Fairbairn, A., Yalman, N., Filipovic, D., Demirergi, G., Ertug, F., Russell, N. and Henecke, J., 2009. Private pantries and celebrated surplus: storing and sharing food at Neolithic Çatalhöyük, Central Anatolia. *Antiquity* 83, 649-668

Bogaard, A., Charles, M. and Twiss, K.C., 2011. Food storage and sharing at Çatalhöyük: the botanical and faunal evidence. In: M. Benz (Ed.), *The principle of sharing: segregation and construction of social identities at the transition from foraging to farming*. Studies in

Early Near Eastern production, subsistence and environment 14. Berlin: Ex Oriente, 313–330

Bogaard, A., Henton, E., Evans, J.A., Twiss, K.C., Charles, M.P., Vaiglova, P. and Russell, N., 2013. Locating land use at Neolithic Çatalhöyük, Turkey: the implications of $^{87}Sr/^{86}Sr$ signatures in plants and sheep tooth sequences. *Archaeometry* doi:10.1111/arcm.12049 (retrieved on 15/07/14)

Bogaard, A., Charles, M., Livarda, A., Ergun, M., Filipovic, D. and Jones, G., in press. The archaeobotany of mid-later Neolithic occupation levels at Çatalhöyük In: I. Hodder (ed.) *Humans and landscapes of Çatalhöyük: Reports from the 2000-2008 seasons*. (Monographs of the Cotsen Institute of Archaeology). Los Angeles: University of California at Los Angeles

Bogin, B., 1999. *Patterns of human growth*. Cambridge: Cambridge University Press

Bogin, B., Smith, P., Orden, A.B., Varela Silva, M.I. and Loucky, J., 2002. Rapid change in height and body proportions of Maya American children. *American Journal of Human Biology* 14, 753-761

Boldsen, J., 1998. Body proportions in a medieval village population: effects of early childhood episodes of ill health. *Annals of Human Biology* 25, 309-317

Boskey, A.L., 1989. Non-collagenous matrix proteins and their role in mineralization. *Bone and Mineral* 6, 111-123

Boskey, A.L., 2007. Mineralization of bones and teeth. *Elements* 3, 387-393

Bourdieu, P., 1979. *La distinction, critique sociale du jugement*. Pars: Minuit

Boyde, A., 1963. Estimation of age at death of young human skeletal remains from incremental lines in dental enamel. *Third International Meeting in Forensic Immunology, Medicine, Pathology and Toxicology*, 36-46

Boyde, A., 1970. The surface of the enamel in human hypoplastic teeth. *Archives of Oral Biology* 15, 897–898

Boyde, A., 1979. Carbonate concentration, crystal centers, core dissolution, caries, cross striations, circadian rhythms, and compositional contrast in the SEM. *Journal of Dental Research* 58, 981-983

Boyde, A., 1989. Enamel. In: A. Oksche and L. Volrath (Eds.), *Teeth. Handbook of microscopic anatomy, volume 6.* Berlin: Springer Verlag, 309-473

Boyde, A., 1990. Developmental interpretations of dental microstructure. In: C.J. DeRouseau (Ed.), *Primate life history and evolution*. Chichester: Wiley-Liss, 229-267

Boyde, A. and Jones, S.J., 1998. Aspects of anatomy and development of bone. The nm, μm and mm hierarchy. In: M. Zaidi (Ed.), *Advances in organ biology, volume 5A*. Greenwich, Connecticut: JAI press, 3-44

Boyer, P., Roberts, N. and Baird, D., 2006. Holocene environment and settlement on the Çarşamba alluvial fan, south-central Turkey: Integrating geoarchaeology and archaeological field survey. *Geoarchaeology* 21/7, 675-698

Boz, B., 2005. The oral health of Çatalhöyük Neolithic people. In: I. Hodder (Ed.), *Inhabiting Çatalhöyük: reports from the 1995-1999 seasons* (McDonald Institute Monographs). Cambridge: McDonald Institute for Archaeological Research; London: British Institute of Archaeology at Ankara, 587-592

Boz, B., Pilloud, M.A. and Hillson, S., 2013. The prevalence of dental caries in Neolithic Anatolia. *Paleopathology association 40th annual North American meeting*, Knoxville, Tennesse, April 2013 (abstract)

Braveman, P.A., Cubbin, C., Egerter, S., Chideya, S., Marchi, K.S., Metzler, M. and Posner, S., 2005. Socioeconomic status in health research: one size does not fit all. *Journal of the American Medical Association* 294/22, 2879-2888

Bromage, T.G and Dean, M.C., 1985. Re-evaluation of the age at death of immature fossil hominids. *Nature* 317, 525–527

Bromage, T.G., 1991. Enamel incremental periodicity in the pig-tailed macaque: a polychrome fluorescent labelling study of dental hard tissues. *American Journal of Physical Anthropology* 86, 205-214

Bromage, T., Lacruz, R., Perez-Ochoa, A. and Boyde, A., 2007. Portable confocal scanning optical microscopy of Australopithecus africanus enamel structure. In: S. Bailey and J-J. Hublin (Eds.), *Dental perspectives on human evolution*. Dordrecht: The Netherlands: Springer, 193-209

Brook, A.H., Fearne, J.M. and Smith, J.M., 1997. Environmental causes of enamel defects. In: J. Chadwick and G. Cardew (Eds.), *Ciba Foundation Symposium 205 - Dental enamel*. Chichester, UK: John Wiley and Sons, 212-225

Brook, A.H. and Smith, J.M., 2006. Hypoplastic enamel defects and environmental stress in a homogeneous Romano–British population. *European Journal of Oral Sciences* 114(S1), 370-374

Brothwell, D.R., 1959. Teeth in earlier human populations. *Proceedings of the Nutrition Society* 18/1, 59-65

Brothwell, D.R., 1963*. Dental anthropology*. Oxford: Pergamon Press

Buikstra, J.E. and Ubelaker, D.H., 1994. *Standards for data collection from human skeletal remains*. Arkansas, Fayetteville: Archaeological Survey Research Series No 44

Bullion, S.K., 1987. *Incremental structures of enamel and their application to archaeology*. Unpublished Ph.D. thesis, University of Lancaster

Bunon, R.M., 1743. *Essay sur les maladies des dents, ou l'on propose les moyens de leur procurer une bonne conformation dès la plus tendre enfance, et d'en assurer la conservation pendant tout le cours de la vie avec une lettre où l'on discute quelques opinions particulieres de l'auteur de l'orthopédie*. Paris: Chez Briasson

Bush, H., 1991. Concepts of health and stress. In: H. Bush and M. Zvelebil (Eds.), *Health in past societies: biocultural interpretation of human skeletal remains in archaeological contexts*. Oxford: BAR international series, 11-21

Byerly, R.M., 2007. Palaeopathology in late Pleistocene and early Holocene Central Plains bison: dental enamel hypoplasia, fluoride toxicosis and the archaeological record. *Journal of Archaeological Science* 34/11, 1847-1858

Calcagno, J.M., 1989. *Mechanisms of dental reduction: a case study from post-Pleistocene Nubia*. Lawrence: University of Kansas

Cannon, W.B., 1932. *The wisdom of the body*. New York: WW Norton

Canti, M.G., 1999. The production and preservation of faecal spherulites: animals, environment and taphonomy. *Journal of Archaeological Science* 26/3, 251-258

Cardoso, H.F.V., 2005*. Patterns of growth and development of the human skeleton and dentition in relation to environmental quality: a biocultural analysis of a sample of 20th century Portuguese subadult documented skeletons*. Unpublished Ph.D. thesis. McMaster University, Hamilton

Cardoso, H.F.V., 2007. A test of the differential accuracy of the maxillary versus the mandibular dentition in age estimations of immature skeletal remains based on developing tooth length. *Journal of Forensic Sciences* 52/2, 434-437

Cardoso, H.F.V., 2009. Accuracy of developing tooth length as an estimate of age in human skeletal remains: the permanent dentition. *American Journal of Forensic Medical Pathology* 30/2, 127-133

Cardoso, H.F.V. and Garcia, S., 2009. The not-so Dark Ages: ecology for human growth in Medieval and Early Twentieth century Portugal as inferred from skeletal growth profiles. *American Journal of Physical Anthropology* 138/2, 136-147

Carleton, W.C., Connolly, J. and Collard, M., 2013. Corporate kin-groups, social memory, and “history houses”? A quantitative test of recent reconstructions of social organization and building function at Çatalhöyük during the PPNB. *Journal of Archaeological Science* 40/4, 1816–1822

Carruthers, D., 2004. Hunting and herding in Central Anatolian prehistory: the 9th and 7th millennium BC site at Pınarbası. In: H. Buitenhuis, A.M. Choyke, L. Martin, L. Bartosiewicz and M. Mashkour (Eds.), *Archaeozoology of the Near East VI. Proceedings of the sixth international symposium on the zooarchaeology of southwestern Asia and adjacent areas*. Groningen, Netherlands: ARC Publicities, 85-95

Carsten, J. and Hugh-Jones, S., 1995. Introduction. In: J. Carsten J and S. Hugh-Jones (Eds.), *About the house.* Cambridge: Cambridge University Press, 1-47

Carter, T., 2011. A true gift of mother earth: the use and significant of obsidian at Çatalhöyük. *Anatolian Studies* 61, 1-19

Cattaneo, C., 2007. The skeletal remains of a child, victim of organized crime: the study of post-mortem interval, personal identification and cause and manner of death. In: M.B. Brickley and R. Ferllini (Eds.), *Forensic anthropology: case studies from Europe*. Springfield, Illinois: Thomas Books, 137-150

Cendekiawan, T., Wong, R.W.K. and Rabie, A.B.R., 2010. Relationships between cranial base synchondroses and craniofacial development: a review. *Open Anatomy Journal* 2, 67-75

Cessford, C., 2005. Estimating the Neolithic population of Çatalhöyük. In: I. Hodder (Ed.), *Inhabiting Çatalhöyük: reports from the 1995-1999 seasons* (McDonald Institute Monographs). Cambridge: McDonald Institute for Archaeological Research; London: British Institute of Archaeology at Ankara, 323-328

Cessford, C. and Carter, T., 2005. Quantifying the consumption of obsidian at Neolithic Çatalhöyük, Turkey. *Journal of Field Archaeology* 30/3, 305-15

Cessford, C., Newton, M., Kuniholm, P., Manning, S., Özbakan, M., Özer, A.M., Akoglu, K.G., Higham, T. and Blumbach, P., 2005. Absolute dating at Çatalhöyük. In I. Hodder (Ed.), *Changing materialities at Çatalhöyük: reports from the 1995-1999 seasons.*

(McDonald Institute Monographs). Cambridge: McDonald Institute for Archaeological Research; London: British Institute of Archaeology at Ankara, 65–100

Cessford, C. and Near, J., 2005. Fire, burning and pyrotechnology at Çatalhöyük. In: I. Hodder (Ed.*), Çatalhöyük perspectives: themes from the 1995-1999 seasons*. (McDonald Institute Monographs). Cambridge McDonald Institute for Archaeological Research; London: British Institute of Archaeology at Ankara, 171-183

Charles, M., Doherty, C., Asouti, E., Bogaard, A., Henton, E., Larson, C., Ruff, C., Ryan, P., Sadvari, J. and Twiss, K., 2014, in press. Landscape and taskscape at Çatalhöyük: an integrated perspective. In: I. Hodder (Ed.), Integrating Çatalhöyük: themes from the 2000-2008 seasons. (BIAA Monograph) London: British Institute of Archaeology at Ankara

Chollet, M.B. and Teaford, M.F., 2008. Ecological stress and linear enamel hypoplasia in Cebus. American Journal of Physical Anthropology 46, 78-79

Clarke, B., 2008. Normal bone anatomy and physiology. *Clinical Journal of the American Society of Nephrology* 3(S3), 131-139

Clarkson, J. and O'Mullane, D., 1989. A modified DDE Index for use in epidemiological studies of enamel defects. *Journal of Dental Research* 68/3, 445-450

Cleveland, W.S. and Devlin, S.J., 1988. Locally weighted regression: an approach to regression analysis by local fitting. *Journal of the American Statistical Association* 83/403, 596-610

Cleveland, W.S. and Grosse, E., 1991. Computational methods for local regression. *Statistics and Computing* 1, 47-62

Cohen, H.R. 1970. The palaeoecology of south central Anatolia at the end of the Pleistocene and the beginning of the Holocene. *Anatolian Studies* 20, 119-137

Colombo, A., Coqueugniot, H., Dutailly, B., Desbarats, P. and Tillier, A.M., 2013. Nouvelles données sur l'édification des molaires et l'estimation de l'âge dentaire des enfants par imagerie médicale et 3D: apports et perspectives. *Bulletins et mémoires de la Société d'Anthropologie de Paris* 25/3-4, 127-146

Colyer, F., 1936. *Variation and diseases of the teeth of animals*. London: Bale & Danielsson

Colyer, F., 1947. Dental disease in animals. *British Dental Journal* 82, 4-10

Condon, K., 1981. *Correspondence of developmental enamel defects between the mandibular canine and first premolar*. Unpublished MA thesis, University of Arkansas

Condon, K. and Rose, J.C., 1992. Intertooth and intratooth variability in the occurence of developmental enamel defects. In: A.H. Goodman and L.L. Capasso (Eds.), *Recent contributions of the study of enamel developmental defects*. Journal of Paleopathology monograph series 2. Chieti, Italy: Associazione Anthropologica Abruzzese, 61-79

Connolly, J., 1999. Technical strategies and technical change at Neolithic Çatalhöyük, Turkey. *Antiquity* 73, 791-800

Cook, D.C., 1980. Hereditary enamel hypoplasia in a prehistoric Indian child. *Journal of Dental Research* 59/9, 1522

Cook, D.C., 1981. Mortality, age-structure, and status in interpretation of stress indicators in prehistoric skeletons: a dental sample from the lower Illinois valley. In: R. Chapman, I. Kinnes and K. Randsborg (Eds.), *The archaeology of death*. Cambridge: Cambridge University Press, 133-155

Cook, D.C., 1984. Subsistence and health in the lower Illinois Valley: osteological evidence. In: M.N. Cohen and G.J. Armelagos (Eds.), *Paleopathology at the origins of agriculture.* Orlando: Academic Press, 237–270

Copley, M., Clark, K. and Evershed, R., 2005. Organic residue analysis of pottery vessels and clay balls. In: I. Hodder (Ed.), *Changing materialities at Çatalhöyük: reports from the 1995-1999 seasons*. (McDonald Institute Monographs). Cambridge: McDonald Institute for Archaeological Research; London: British Institute of Archaeology at Ankara, 169-174

Coqueugniot, H., 1999. Identification de caractères diagnosiques sur la tête osseuse chez les enfants néandertaliens: nouvelle approche. *Bulletins et Mémoires de la Société d'Anthropologie de Paris* 11/3-4, 486-487

Coqueugniot, H., 2005. Les hétérochronies du développement: intérêts et limites pour l'étude de l'évolution humaine. In: O. Dutour, J-J. Hublin and B. Vandermeersch (Eds.), *Origine et evolution des populations humaines*. Paris: Comité des Travaux Historiques et Scientifiques, 373-376

Coqueugniot, H. and Minugh-Purvis, N., 2003. Ontogenetic patterning and phylogenetic significance of mental foramen number and position in the evolution of Upper Pleistocene Homo sapiens. In: J.L. Thompson, G.E. Krovitz and A.J. Nelson (Eds.), *Patterns of growth and development in the genus Homo*. Cambridge: Cambridge University Press, 343-360

Coqueugniot, H., Hublin, J-J., Veillon, F., Houët, F. and Jacob, T., 2004. Early brain growth in Homo erectus and implications for cognitive ability. *Nature* 431, 299-302

Corruccini, R.S., Handler, J.S. and Jacobi, K.P., 1985. Chronological distribution of enamel hypoplasias and weaning in a Caribbean slave population. *Human Biology* 57/4, 699-711

Craig, E.F. and Buckberry, J.L., 2010. Investigating social status using evidence of biological status: a case study from Raunds Furnells. In: J.L. Buckberry and A.K. Cherryson (Eds.), Burial *in Later Anglo-Saxon England, c. 650–1100 AD*. Oxford: Oxbow, 128-142

Cucina, A., 2002. Brief communication: diachronic investigation of linear enamel hypoplasia in prehistoric skeletal samples from Trentino, Italy. *American Journal of Physical Anthropology* 119/3, 283-287

Currey, J.D., 2002*. Bones: structure and mechanics*. Princeton: Princeton University Press

Cutting, M., 2005. The architecture of Çatalhöyük: continuity, household and settlement. In: I. Hodder (Ed*.), Çatalhöyük perspectives: themes from the 1995-1999 seasons*. (McDonald Institute Monographs). Cambridge McDonald Institute for Archaeological Research; London: British Institute of Archaeology at Ankara, 151-171

D'arcy, W. Thompson, 1917. *On growth and form*. Cambridge: Cambridge University Press

Dabbs, G.R., 2011. Health status among prehistoric Eskimos from Point Hope, Alaska. *American Journal of Physical Anthropology* 146/1, 94-103

Danforth, M.E., Herndon, K.S. and Propst, K.B., 1993. A preliminary study of patterns of replication in scoring linear enamel hypoplasias. *International Journal of Osteoarchaeology* 3/4, 297-302

Dean, H.T., 1934. Classification of mottled enamel diagnosis. *Journal of the American Dental Association* 21, 1421-1426

Dean, M.C., 1987a. Growth layers and incremental markings in hard tissues: a review of the literature and some preliminary observations about enamel structure in Paranthropus boisei. *Journal of Human Evolution* 16, 157-172

Dean, M.C., 1987b. The dental developmental status of six East African juvenile fossil hominids. *Journal of Human Evolution* 16, 197-213

Dean, M.C., 1989. The developing dentition and tooth structure in hominoids. *Folia Primatologica* 53, 160-170

Dean, M.C., 1995. The nature and periodicity of incremental lines in primate dentine and their relationship to periradicular bands in OH16. In J. Moggi-Cecchi (Ed.), *Aspects of dental biology, palaeontology, anthropology and evolution*. Florence: International Institute for the Study of Man, 36-46

Dean, M.C., 2006. Tooth microstructure tracks the pace of human life-history evolution. *Proceedings of the Royal Society Series B* 273, 2799–2808

Dean, M.C., 2010. Retrieving chronological age from dental remains of early fossil hominins to reconstruct human growth in the past. *Philosophical Transactions of the Royal Society Series B* 365, 3397-3410

Dean, M.C. and Beynon, A.D., 1991. Histological reconstruction of crown formation times and initial root formation times in a modern human child. *American Journal of Physical Anthropology* 86, 215-228

Dean, M.C. and Cole, T.J., 2013. Human life history evolution explains dissociation between the timing of tooth eruption and peak rates of root growth. *PLoS ONE* 8/1, 1-14

Dean, M.C., Leakey, M.G., Reid, D., Schrenk, F., Schwartz, G., Stringer, C. and Walker, A., 2001. Growth processes in teeth distinguish modern humans from Homo erectus and earlier hominins. *Nature* 414, 628-631

Dean, M.C. and Reid, D.J., 2001. Perikymata spacing and distribution on hominid anterior teeth. *American Journal of Physical Anthropology* 116, 209-215

Dean, M.C. and Scandrett, A.E., 1996. The relation between long-period incremental markings in dentine and daily cross-striations in enamel in human teeth. *Archives of Oral Biology* 41/3, 233-241

Dean, M.C., Stringer, C.B. and Bromage, T.G., 1986. Age at death of the Neanderthal child from Devil's Tower, Gibraltar and the implications for studies of general growth and development in Neanderthals. *American Journal of Physical Anthropology* 70, 301-309

Demirergi, G.A., Filipovic, D. and Charles, M., 2008. Two sides of the same coin: archaeological and ethnographic perspectives on storing and sharing food at Çatalhöyük. Part II, Sharing. *Society for American Archaeology Meeting 73, Vancouver, Canada*

Demirjan, A., Goldstein, H. and Tanner, J.M., 1973. A new system of dental age assessment. *Human Biology* 45, 211-227

De Onis, M. and Blössner, M., 1997. *WHO Global Database on Child Growth and Malnutrition*. Geneva: World Health Organisation. http://www.who.int/nutgrowthdb/about/introduction/en/index4.html (retrieved on 13/11/13)

De Onis, M., Onyango, A.W., Borghi, E., Garza, C. and Yong, H., 2006b. Comparison of the World Health Organization (WHO) Child Growth Standards and the National Center for Health Statistics/WHO international growth reference: implications for child health programmes. *Public Health Nutrition* 9, 942-947

De Onis, M., WHO multicentre growth reference study group, 2006a. *WHO child growth standards, length/height-for-age, weight-for-age, weight-for-length, weight-for-height and body mass index-for-age: methods and development*. Geneva: World Health Organisation

Desbat, A., Rottier, S., Coqueugniot, H. and Thiol, S., 2012. Determining the age composition of the immature population in mass graves: a Neolithic example from the "Truie Pendue" site at Passy (Northern France). *Bulletins et Mémoires de la Société d'Anthropologie de Paris* 24, 152-166

Deutsch, D.E., Goultschin, J. and Anteby, S., 1981. Determination of human fetal age from the length of femur, mandible and maxillary incisor. *Growth* 45, 232–238

Deutsch, D.E., Pe'er, E. and Gedalia, I., 1983. Changes in size, morphology and weight of human anterior teeth during the fetal period. *Growth* 48/1, 74-85

Deutsch, D.E., Tam, O. and Stack, M.V., 1985. Postnatal changes in size, morphology and weight of developing postnatal deciduous anterior teeth. *Growth* 49, 202-217

Dirks, W., 1998. Histological reconstruction of dental development and age at death in a juvenile gibbon (Hylobates lar). *Journal of Human Evolution* 35/4-5, 411-425

Dobney, K., 1991. *A modern epidemiological study of enamel hypoplasia: a putative model for the study of physiological stress in past human populations*. Unpublished Ph.D. thesis, University of Bradford

Dobney, K., Ervynck, A., Albarella, U. and Rowley-Conwy, P., 2004. The chronology and frequency of a stress marker (linear enamel hypoplasia) in recent and archaeological populations of Sus scrofa in north-west Europe, and the effects of early domestication. *Journal of Zoology* 264, 197–208

Dobney, K., Ervynck, A., Albarella, U. and Rowley-Conwy, P., 2007. The transition from wild boar to domestic pig in Eurasia, illustrated by a tooth developmental defect and biometric data. In: U. Albarella, K. Dobney, A. Ervynck and P. Rowley-Conwy (Eds.), *Pigs and humans, 10 000 years of interaction*. Oxford: Oxford University Press, 57-83

Doherty, C., 2007. Clay sourcing- matching the materials and the landscape*. Çatalhöyük 2007 Archive Report*.
http://www.catalhoyuk.com/downloads/Archive_Report_2007.pdf (retrieved on 14/05/14)

Doherty, C., Charles, M. and Bogaard, A., 2007. Preliminary coring. *Çatalhöyük 2007 Archive Report*.
http://www.catalhoyuk.com/downloads/Archive_Report_2007.pdf (retrieved on 14/05/14)

Doherty, C., 2008. Clay sourcing*. Çatalhöyük 2008 Archive Report.*
http://www.catalhoyuk.com/downloads/Archive_Report_2008.pdf (retrieved on 14/05/14)

Duarte, C., Maurício, J., Pettitt, P.B., Souto, P., Trinkaus, E., van der Plicht, H. and Zilhão, J., 1999. The early Upper Paleolithic human skeleton from the Abrigo do Lagar Velho (Portugal) and modern human emergence in Iberia. *Proceedings of the National Academy of Sciences* 96, 7604-7609

Ducos, P., 1988. Archeozoologie quantitative: Les valeurs numeriques immediates a Catal Huyuk. (Cahiers du Quaternaire 12). Paris: Centre National de la Recherche Scientifique Centre regional de publication de Bordeaux

Duray, S.M., 1990. Deciduous enamel defects and caries susceptibility in a prehistoric Ohio population. *American Journal of Physical Anthropology* 81/1, 27-34

Duren, D.L., Seselj, M., Froehle, A.W., Nahha, K.W. and Sherwood, R.J., 2013. Skeletal growth and the changing genetic landscape during childhood and adulthood*. American Journal of Physical Anthropology* 150, 48-57

Düring, B.S., 2001. Social dimensions in the architecture of Neolithic Catalhöyuk*. Anatolian Studies* 51, 1-18

Düring, B.S., 2003. Burials in context: the 1960s inhumations of Çatalhöyük East. *Anatolian Studies* 53, 1-15

Düring, B.S., 2005. Building continuity in the Central Anatolian Neolithic: exploring the meaning of buildings at Asikli Höyük and Çatalhöyük. *Journal of Mediterranean Archaeology* 18, 3-29

Düring, B.S., 2006. *Constructing communities: clustered neighbourhood settlements of the Central Anatolian Neolithic ca. 8500-5500 cal*. Unpublished Ph.D. thesis, University of Leiden

Düring, B.S., 2007. Reconsidering the Çatalhöyük community: from households to settlement systems. *Journal of Mediterranean Archaeology* 20/2, 155-182

Düring, B.S., 2012. The trouble with stratigraphy: case studies from the Near East. In: C. Bakels and H. Kamermans (Eds*.), The end of our fifth decade*. Leiden: Analecta Praehistorica Leidensia, 325-333

Eckhardt, C.L., Suchindran, C., Gordon-Larsen, P. and Adair, L.S., 2005a. The association between diet and height in the postinfancy period: changes with age and socioeconomic status in Filipino Youths. *The Journal of Nutrition* 135, 2192-2198

Eckhardt, C.L., Gordon-Larsen, P. and Adair, L.S., 2005b. Growth patterns of Filipino children indicate potential compensatory growth. *Annals of Human Biology* 32/1, 3-14

Eddisford, D., 2006. Building 49. *Çatalhöyük 2006 Archive Report*. http://www.catalhoyuk.com/downloads/Archive_Report_2006.pdf (retrieved on 14/05/14)

Eddisford, D., Regan, R. and Taylor, J.S., 2009. The experimental firing of a Neolithic oven. *Çatalhöyük 2009 Archive Report*. http://www.catalhoyuk.com/downloads/Archive_Report_2009.pdf (retrieved on 14/05/14)

Elamin, F. and Liversidge, H.M., 2013. Malnutrition has no effect on the timing of human tooth formation. PloSone 8, e72274

Elgenmark, O., 1946. The normal development of the ossification centres during infancy and childhood: clinical, roentgenologic and statistical study. *Acta Pediatrica* 33/S1, 1-79

Elhechmi, I., 2010. *Instrumentation optique pour la mesure des périkymaties de la couronne dentaire.* Unpublished Ph.D. thesis, Université de Franche-Comté

Elhechmi, I., Braga, J., Dasgupta, G. and Gharbi, T., 2013. Accelerated measurement of perikymata by an optical instrument. *Biomedical Optics Express* 4/10, 2124-2137

Eli, I., Sarnat, H., Talmi, E. and Judes, H., 1986. The width of the neonatal line in primary enamel and its use as a possible diagnostic tool in developmental disturbances. *Journal of Dental Research* 65(s2), 754

El-Najjar, M., DeSanti, M. and Ozebel, L., 1978. Prevalence and possible etiology of dental enamel hypoplasia. *American Journal of Physical Anthropology* 48, 185-192

Eisenberg, M.J., 1938. A microscopical study of the surface enamel of human teeth. *The Anatomical Record* 71, 221-231

Eisenmann, D.R., 1994. Enamel structure. In: A.R. Ten Cate (Ed*.), Oral histology: development, structure and function*. London: Mosby, 239-257

Enlow, D.H., 1976. The prenatal and postnatal growth of the human basicranium. In J.F. Bosma (Ed.), *Symposium on the development of the basicranium*. Bethesda, Maryland: US department of health, 192-205

Enlow, D.H., 1990*. Facial growth*. London: WB Saunders

Ensor, B.E. and Irish, J.D., 1995. Hypoplastic area method for analyzing dental enamel hypoplasia*. American Journal of Physical Anthropology* 98/4, 507-517

Enwonu, C.O., 1973. Influence of socio-economic conditions on dental development in Nigerian children. *Archives of Oral Biology* 18, 95-107

Ervynck, A. and Dobney, K., 1999. Lining up on the M1: a tooth defect as a bio-indicator for environment and husbandry in ancient pigs. *Environmental Archaeology* 4, 1-8

Ervynck, A., Dobney, K., Hongo, H. and Meadow, R., 2001. Born free? New evidence for the status of ”Sus scrofa” at Neolithic Çayönü Tepesi (Southeastern Anatolia, Turkey). *Paléorient* 27/2, 47-73

Eveleth, P.B. and Tanner, J.M., 1976. *Worldwide variation in human growth*. Cambridge: Cambridge University Press

Eveleth, P.B. and Tanner, J.M., 1990. *Worldwide variation in human growth*. Cambridge: Cambridge University Press

Evershed, R., Payne, S., Sherratt, A., Copley, M., Urem-Kotsu, D., Kotsakis, K., Özdogan, M., Özdogan, A., Bailey, D., Nieuwenhuyse, O., Akkermans, P., Campbell, S., Farid, S., Hodder, I., Yalman, N., Özbarasan, M., Biçakci, E., Garfinkel, Y., Levy, T. and Burton, M., 2008. Earliest date for milk use in the Near East and Southeastern Europe linked to cattle herding*. Nature* 455, 528-531

Fairbairn, A., 2005. A history of agricultural production at Neolithic Çatalhöyük East, Turkey. *World Archaeology* 37/2, 197-210

Fairbairn, A., Near, J. and Martinoli, D., 2005. Macrobotanical investigation of the North, South and KOPAL area excavations at Çatalhöyük East. In: I. Hodder (Ed.), *Inhabiting*

Çatalhöyük: reports from the 1995-1999 seasons . (McDonald Institute Monographs). Cambridge: McDonald Institute for Archaeological Research; London: British Institute of Archaeology at Ankara, 137-201

Fairbairn, A., Martinoli, D., Butler, A. and Hillman, G., 2007. Wild plant seed storage at Neolithic Çatalhöyük East, Turkey. *Vegetation History and Archaeobotany* 16/6, 467-479

Fairley, L., Petherick, E.S., Howe, L.D., Tilling, K., Cameron, N., Lawlor, D.A., West, J. and Wright, J., 2013. Describing differences in weight and length growth trajectories between white and Pakistani infants in the UK: analysis of the Born in Bradford birth cohort study using multilevel linear spline models*. Archives of Disease in Childhood* 98/4, 274-279

Falin, L.I., 1961. Histological and histochemical studies of human teeth of the Bronze and Stone ages. *Archives of Oral Biology* 5, 5-13

Fanning, E.A., 1961. A longitudinal study of tooth formation and tooth resorption. *New Zealand Dental Journal* 57, 202-217

Fanning, E.A. and Brown, T., 1971. Primary and permanent tooth development*. Australian Dental Journal* 16/1, 41-43

Fanning, E.A. and Moorrees, C.F.A., 1969. A comparison of permanent mandibular molar formation in Australian Aborigines and Caucasoids. *Archives of Oral Biology* 14/9, 999-1006

Farid, S., 1999. Archive summary for the South Area*. Çatalhöyük 1999 Archive Report*. http://www.catalhoyuk.com/archive_reports/1999/ar99_03.html(retrieved on 15/05/14)

Farid, S., 2004. Excavations overview *Çatalhöyük 2004 Archive Report*. http://www.catalhoyuk.com/archive_reports/2004/index.html (retrieved on 14/05/14)

Farid, S., 2007a. Neolithic excavations in the South area, East mound, Çatalhöyük 1995-1999. In I. Hodder (Ed.), *Excavating Çatalhöyük: South, North and KOPAL area reports from the 1995-1999 seasons*. (McDonald Institute Monographs). Cambridge: McDonald Institute for Archaeological Research; London: British Institute at Ankara, 41-42

Farid, S., 2007b. Level VIII. In I. Hodder (Ed.), *Excavating Çatalhöyük: South, North and KOPAL area reports from the 1995-1999 seasons*. (McDonald Institute Monographs). Cambridge: McDonald Institute for Archaeological Research; London: British Institute at Ankara, 227-282

Farid, S., 2007c. Areas of excavation 2007. *Çatalhöyük 2007 Archive Report.* http://www.catalhoyuk.com/downloads/Archive_Report_2007.pdf (retrieved on 14/05/14)

Fauchard, P., 1746. *Le chirurgien dentiste, au traité des dents. Ou l'on enseigne les moyens de les entretenir propres et saines, de les embellir, d'en réparer la perte et de remedier à leurs maladies, à celles des geneives et aux accidens qui peuvent survenir aux autres parties voisines des dents. Avec observations et des reflexions sur plusieurs cas singuliers*. (second edition). Paris: Jean Mariette

Fazekas, I.G.Y. and Kósa, F., 1978. *Forensic fetal osteology*. Budapest: Akademiai Kaido

FDI Commission on Oral Health, 1982. An epidemiological index of developmental defects of dental enamel (DDE index). *International Dental Journal* 32, 159-167

Fearne, J.M., Elliott, J.C., Wong, F.S.L., Davis, G.R., Boyde, A. and Jones, S.J., 1994. Deciduous enamel defects in low-birth-weight children: correlated X-ray microtomographic and backscattered electron imaging study of hypoplasia and hypomineralization. *Anatomy and Embryology* 189/5, 375-381

Fejerskov, O., Thylstrup, A. and Larsen, M.J., 1977. Clinical and structural features and possible pathogenic mechanisms of dental fluorosis. *Scandinavian Journal of Dental Research* 85, 510–534

Ferembach, D., 1972. Les hommes du gisement neolithique de Catal Huyuk. In*: VII Turk Tarih Kongresi (1970), Ankara* (1970), 15-21

Ferembach, D., 1982. *Mesures et indices des squelettes humains neolithiques de Catal Huyuk (Turquie)*. Paris: CNRS

Ferrell, R.J., 2006. *Enamel defects, well-being and mortality in a Medieval Danish village.* Unpublished Ph.D. thesis, Pennsylvania State University

Fincham, A.G., Moradian-Oldak, J. and Simmer, J.P., 1999. The structural biology of the developing dental enamel matrix. *Journal of Structural Biology* 126, 270–299

FitzGerald, C.M., 1998. Do enamel microstructures have regular time dependency? Conclusions from the literature and a large-scale study. *Journal of Human Evolution* 35, 371–386

FitzGerald, C.M. and Rose, J., 2000. Reading between the lines: dental development and subadult age assessment using the microstructural growth markers of teeth. In: M.A.

Katzenberg and S.R. Saunders (Eds.), *Biological anthropology of the human skeleton*. London: Wiley-Liss, 163–186

Fitzgerald, C.M. and Saunders, S.R., 2005. Test of histological methods of determining chronology of accentuated Striae in deciduous teeth. *American Journal of Physical Anthropology* 127, 277–290

Fitzgerald, C.M., Saunders, S.R., Bondioli, L. and Macchiarelli, R., 2006. Health of infants in an Imperial Roman skeletal sample: Perspective from dental microstructure*. American Journal of Physical Anthropology* 130, 179–189

Flannery, K.V. (ed.), 1976*. The Early Mesoamerican village*. New York: Academic Press

Flores-Mir, C., Mauricio, F.R., Orellana, M.F. and Major, P.W., 2005. Association between growth stunting with dental development and skeletal maturation stage. *The Angle Orthodontist* 75/6, 935-940

Floyd, B. and Littleton, J., 2006. Linear enamel hypoplasia and growth in an Australian Aboriginal community: not so small, but not so healthy either. *Annals of Human Biology* 33/4, 424-443

Formicola, V., 1987. Neolithic transition and dental changes: the case of an Italian site. *Journal of Human Evolution* 16/2, 231-239

Frame, S., Russell, N. and Martin, L., 1999. Animal bone report*. Çatalhöyük 1999 Archive Report*.
http://www.catalhoyuk.com/archive_reports/1999/ar99_12.html (retrieved on 14/05/14)

Francis, G.C. and Werle, P.P., 1939. The appearance of centres of ossification from birth to 5 years*. American Journal of Physical Anthropology* 24, 273-286

Franz-Odendaal, T.A., 2004. Enamel hypoplasia provides insights into early systemic stress in wild and captive giraffes (Giraffa camelopardalis*). Journal of Zoology London* 263, 197–206

Franz-Odendaal, T.A., Chinsamy, A. and Lee-Thorp, J., 2004. High prevalence of enamel hypoplasia in an early Pliocene giraffid (Sivatherium hendeyi) from South Africa. *Journal of Vertebrate Paleontology* 24, 235–244

Franz-Odendaal, T.A., Hall, B.K. and Witten, P.E., 2006. Buried alive: how osteoblasts become osteocytes. *Developmental Dynamics* 235, 176-190

Franz-Odendaal, T.A., Lee-Thorp, J. and Chinsamy, A., 2003. Insights from stable light isotopes on enamel defects and weaning in Pliocene herbivores. *Journal of Bioscience* 28, 765–773

Fraser, D.R., 1988. Nutritional growth retardation: experimental studies with special reference to calcium. In: J.C. Waterlow (Ed.), *Linear growth retardation in less developed countries*. Nestlé nutrition workshop series 14. New York: Raven press, 127-141

Frisancho, A.R. and Baker, P.T., 1970. Altitude and growth: a study of the patterns of physical growth of a high altitude Peruvian Quechua population. *American Journal of Physical Anthropology* 32, 279-292

Frisancho, A.R., Garn, S.M. and Ascoli, W., 1970a. Childhood retardation resulting in reduction of adult body size due to lesser adolescent skeletal delay. *American Journal of Physical Anthropology* 33, 325–336

Frisancho, A.R., Garn, S.M. and Ascoli, W., 1970b. Subperiosteal and endosteal bone apposition during adolescence. *Human Biology* 42/4, 639-664

Galbany, J., Martínez, L.M. and Pérez-Pérez, A., 2004. Tooth replication techniques, SEM imaging and microwear analysis in primates: methodological obstacles. *Anthropologie* 42, 5-12

Garcin, V., Bruzek, J., Alduc-Le Bagousse, A., Sellier, P. and Velemínsky, P., 2010. La croissance des populations du passé: désillusions, espoirs et perspectives. *Bulletins et Mémoires de la Société d'Anthropologie de Paris* 22, 47-54

Garn, S.M., Guzmán, M.A. and Wagner, B., 1969. Subperiosteal gain and endosteal loss in protein–calorie malnutrition. *American Journal of Physical Anthropology* 30/1, 153-155

Garn, S.M. and Rohmann, C.G., 1960. Variability in the order of ossification of the bony centers of the hand and wrist. *American Journal of Physical Anthropology* 18, 219-230

Garn, S.M., Rohmann, C.G. and Blumenthal, T., 1966. Ossification sequence polymorphism and sexual dimorphism in skeletal development. *American Journal of Physical Anthropology* 24, 101-115

Garofalo, E.M., Larsen, C.S. and Ruff, C.B., 2011. Revisiting health in Neolithic Çatalhöyük: a study of growth and development. *American Journal of Physical Anthropology* 144(S52), 140

Gawlikowska-Sroka, A., Dąbrowski, P., Szczurowski, J., Staniowski, T., 2013. Analysis of interaction between nutritional and developmental instability in mediaeval population in Wrocław.*Anthropological Review* 76/1, 51-62

Glick, P.L. and Rowe, D.J., 1981. Effects of chronic protein deficiency on the formation of the rat incisor teeth. *Archives of Oral Biology* 26/6, 459-466

Gohdo, S., 1982. Different rates of enamel formation on human tooth surfaces deduced from the striae of Retzius. *Archives of Oral Biology* 27/4, 289-296

Golden, M.H.N., 1988. The role of individual nutrient deficiencies in growth retardation of children as exemplified by zinc and protein. In: J.C. Waterlow (Ed.), *Linear growth retardation in less developed countries*. Nestlé nutrition workshop series 14. New York: Raven Press, 143-163

Golding, J., Pembrey, M. and Jones, R., 2001. ALSPAC–The Avon longitudinal study of parents and children. *Paediatric and Perinatal Epidemiology* 15/1, 74–87

Goldstein, D.S. and Kopin, I.J., 2007. Evolution of concepts of stress. *Stress* 10/2, 109-120

Goodman, A.H., 1988. The chronology of enamel hypoplasias in an industrial population: a reappraisal of Sarnat and Shour (1941, 1942). *Human Biology* 60/5, 781-791

Goodman, A.H., 1989. Dental enamel hypoplasias in prehistoric populations. *Advances in Dental Research* 3/2, 265-271

Goodman, A.H., 1991. Variation in estimation of age at formation of a linear enamel hypoplasia due to choice of developmental standard. *American Journal of Physical Anthropology* S12, 80-81

Goodman, A.H., Allen, L.H., Hernandez, G.P., Amador, A., Arriola, L.V., Chávez, A. and Pelto, G.H., 1987. Prevalence and age at development of enamel hypoplasias in Mexican children. *American Journal of Physical Anthropology* 72, 7–19

Goodman, A.H., Armelagos, G.J. and Rose, J.C., 1980. Enamel hypoplasias as indicators of stress in three prehistoric populations from Illinois. *Human Biology* 52/3, 515-527

Goodman, A.H., Armelagos, G.J. and Rose, J.C., 1984a. The chronological distribution of enamel hypoplasias from prehistoric Dickson mounds populations. *American Journal of Physical Anthropology* 65, 259-266

Goodman, A.H. and Armelagos, G.J., 1985a. Factors affecting the distribution of enamel hypoplasias within the human permanent dentition. *American Journal of Physical Anthropology* 68, 479-493

Goodman, A.H. and Armelagos, G.J., 1985b. The chronological distribution of enamel hypoplasia in human permanent incisor and canine teeth. *Archives of Oral Biology* 30, 503-507

Goodman, A.H. and Armelagos , G.J., 1988. Childhood stress and decreased longevity in a prehistoric population. *American Anthropologist* 90/4, 936-944

Goodman, A.H., Lallo, J., Armelagos, G.J. and Rose, J.C., 1984b. Health changes at Dickson Mounds, Illinois (A.D. 950-1300). In: M.N. Cohen and G.J. Armelagos (Eds.), *Paleopathology at the origins of agriculture*. New York: Academic Press, 271-305

Goodman, A.H. and Leatherman, T.L., 1998. *Building a new biocultural synthesis: Political-economic perspectives on human biology*. Michigan: University of Michigan Press

Goodman, A.H., Martin, D.L., Perry, A., Martinez, C., Chavez, A. and Dobney, K., 1989. The effect of nutritional supplementation on permanent tooth development and morphology. *American Journal of Physical Anthropology* 78, 129-130

Goodman, A.H., Pelto, G.H., Allen, L.H. and Chavez, A., 1992. Socioeconomic and anthropometric correlates of linear enamel hypoplasia in children from Solis, Mexico. In A.H. Goodman and L.L. Capasso (Eds.), *Recent contributions of the study of enamel developmental defects*. Journal of Paleopathology monograph series 2. Chieti, Italy: Associazione Anthropologica Abruzzese, 373-380

Goodman, A.H. and Rose, J.C., 1990. Assessment of systemic physiological disturbances from dental enamel hypoplasia and associated histological structures. *Yearbook of Physical Anthropology* 33, 59-110

Goodman, A.H. and Song, R.J., 1999. Sources of variation in estimated ages at formation of linear enamel hypoplasias. In: R.D. Hoppa and C.M. Fitzgerald (Eds.), *Human growth in the past: studies from bones and teeth*. Cambridge: Cambridge University Press, 210-240

Goodman, A.H., Thomas, R., Swedlund, A. and Armelagos, G.J., 1988. Biocultural perspectives on stress in prehistoric, historical, and contemporary population research. *Yearbook of Physical Anthropology* 31, 169-202

Gordon, C.C. and Buikstra, J.E., 1981. Soil pH, bone preservation, and sampling bias at mortuary sites. *American Antiquity* 46/3, 566-571

Gosman, J.H., Hubbell, Z.R., Shaw, C.N. and Ryan, T.M., 2013. Development of cortical bone geometry in the human femoral and tibial diaphysis. *Anatomical Record* 296/5, 774-787

Gottlieb, B., 1920. Rachitis and enamel hypoplasia. *Dental Cosmos* 62, 1209-1221, 1316-1326

Griffin, R.C. and Donlon, D., 2009. Dental enamel hypoplasias and health changes in the Middle Bronze Age – Early Iron Age transition at Pella in Jordan. *HOMO—Journal of Comparative Human Biology* 58, 211–220

Grigson, C., 1989. Size and sex: evidence for the domestication of cattle in the Near East, in A. Milles, D. Williams and N. Gardner (Eds.), The beginnings of agriculture. Oxford: British Archaeological Reports, 77-109

Grimbert, L. and Pigeat, G., 1961. Examen des répliques de la surface de l'émail au moyen du microscope à contraste interferential: système nomarski. *Archives of Oral Biology* 6, 139-148

Guatelli-Steinberg, D., 2000. Linear enamel hypoplasia in gibbons (Hylobates lar carpenteri). *American Journal of Physical Anthropology* 112/3, 395-410

Guatelli-Steinberg, D., 2001. What can developmental defects of enamel reveal about physiological stress in non-human primates? *Evolutionary Anthropology* 10, 138-151

Guatelli-Steinberg, D., 2003. Macroscopic and microscopic analyses of linear enamel hypoplasia in Plio Pleistocene South African Hominins with respect to aspects of enamel development and morphology. *American Journal of Physical Anthropology* 120, 309-322

Guatelli-Steinberg, D., 2004. Analysis and significance of linear enamel hypoplasia in Plio-Pleistocene hominins. *American Journal of Physical Anthropology* 123/3, 199-215

Guatelli-Steinberg, D. and Benderlioglu, Z., 2006. Brief communication: linear enamel hypoplasia and the shift from irregular to regular provisioning in Cayo Santiago rhesus monkeys (Macaca mulatta). *American Journal of Physical Anthropology* 131/3, 416-419

Guatelli-Steinberg, D., Buzhilova, A.P. and Trinkaus, E., 2011. Developmental stress and survival among the Mid Upper Paleolithic Sunghir children: Dental enamel hypoplasias of Sunghir 2 and 3. *International Journal of Osteoarchaeology* 23/4, 421-431

Guatelli-Steinberg, D. and Lukacs, J., 1999. Interpreting sex differences in enamel hypoplasia in human and non-human primates: developmental, environmental and cultural considerations. *Yearbook of Physical Anthropology* 42, 73-126

Guatelli-Steinberg, D., Reid, D.J., Bishop, T.A. and Larsen, C.S., 2005. Anterior tooth growth periods in Neanderthals were comparable to those of modern humans. *Proceedings of the National Academy of Sciences* 102/40, 14197-14202

Guatelli-Steinberg, D., Reid, D.J. and Bishop, T.A., 2007a. Did the lateral enamel of Neanderthal anterior teeth grow differently from that of modern humans? *Journal of Human Evolution* 52, 72-84

Guatelli-Steinberg, D., Reid, D.J., Bishop, T.A. and Larsen, C.S., 2007b. Not so fast: A reply to Ramirez Rozzi and Sardi (2007). *Journal of Human Evolution* 53, 114-118

Guatelli-Steinberg, D. and Skinner, M., 2000. Prevalence and etiology of linear enamel hypoplasia (LEH) in monkeys and apes from Asia and Africa. *Folia Primatologica* 71, 115-132

Guatelli-Steinberg, D., Spencer-Larsen, C. and Hutchinson, D., 2004. Prevalence and duration of linear enamel hypoplasia: a comparative study of Neanderthals and Inuit foragers. *Journal of Human Evolution* 47, 65-84

Gunz, P., Neubauer, S., Golovanova, L., Doronichev, V., Maureille, B. and Hublin, J-J., 2012. A uniquely modern human pattern of endocranial development. Insights from a new cranial reconstruction of the Neanderthal newborn from Mezmaiskaya. *Journal of Human Evolution* 62/2, 300-315

Gustafson, A.G., 1959. A morphologic investigation of certain variations in the structure and mineralization of human dental enamel. *Odontologisk Tidskrift* 67, 361-472

Gustafson G. and Gustafson, A.G., 1967. Microanatomy and histochemistry of enamel. In: A.E.W. Miles (Ed.), *Structural and chemical organisation of teeth*. London: Academic Press, 135-162

Gustafson, G. and Koch, G., 1974. Age estimation up to 16 years of age based on dental development. *Odontologisk Revy* 25, 297-306

Guthrie, W., 2012. Process modeling. In *NIST Engineering Statistics Handbook.* http://www.itl.nist.gov/div898/handbook/pmd/section1/pmd144.htm (retrieved on 27/05/13)

Gysi, A., 1931. Metabolism in adult enamel. *Dental Digest* 37, 661-668

Haavikko, K., 1970. The formation and the alveolar and clinical eruption of the permanent teeth. *Proceedings of the Finnish Dental Society* 66, 103- 170

Hager, L. and Boz, B., in press. Burial treatment. In: I. Hodder (Ed.), *Humans and landscapes of Çatalhöyük: Reports from the 2000-2008 seasons.* (Monographs of the Cotsen Institute of Archaeology). Los Angeles: University of California at Los Angeles

Hall, R.K., 1989. The prevalence of developmental defects of tooth enamel (DDE) in a pediatric hospital department of dentistry population (Part I). *Advances in Dental Research* 3/2, 114-119

Hamilton, N., 1996. Figurines, clay balls, small finds and burials. In: I. Hodder (Ed.), On the surface: Çatalhöyük 1993-1995. (McDonald Institute Monographs). Cambridge: McDonald Institute for Archaeological Research; London: British Institute of Archaeology at Ankara, 215-263

Hamilton, N., 2005. Social aspects of burial. In: I. Hodder (Ed.), *Inhabiting Çatalhöyük: reports from the 1995-1999 seasons* (McDonald Institute Monographs). Cambridge: McDonald Institute for Archaeological Research; London: British Institute of Archaeology at Ankara, 301-307

Hannibal, D.L. and Guatelli-Steinberg, D., 2005. Linear enamel hypoplasia in the great apes: analysis by genus and locality. *American Journal of Physical Anthropology* 127, 13–25

Harrington, L. and Pfeiffer, S., 2008. Juvenile mortality in southern African archaeological contexts. *South African Archaeological Bulletin* 63, 95-101

Harris, B., 1997. Growing taller, living longer? Anthropometric history and the future of old age. *Ageing and Society* 17/5, 491-512

Harrison, K., 2009. Oven firing experiments. *Çatalhöyük 2009 Archive Report*. http://www.catalhoyuk.com/downloads/Archive_Report_2009.pdf (retrieved on 14/05/14)

Hartweg, R., 1945. Remarques sur la denture et statistiques sur la carie dentaire en France aux époques préhistorique et protohistorique. *Bulletins et Mémoires de la Société d'Anthropologie de Paris* 6/1, 71-113

Hassett, B.R., 2011. Evaluating sources of variation in the identification of linear hypoplastic defects of enamel: a new quantified method. *Journal of Archaeological Science* 39, 560-565

Hawley, N.L., Rousham, E.K., Johnson, W., Norris, S.A., Pettifor, J.M. and Cameron, N., 2012. Determinants of relative skeletal maturity in South African children. *Bone* 50, 259-264

Healy, M.J.R., 1989. Growth curves and growth standards-The state of the art. In: J.M. Tanner (Ed.), *Auxology 88. Perspectives in the science of growth and development*. London: Smith-Gordon, 13-21

Hémard, U., 1582. *Recherche de la vraye anathomie des dents, nature et propriété d'icelles. Le tout tiré des authorités d'Hippocras, Galien & Aristote confirmees des plus graues, anciens, & modernes*. Lyon: par Benoist Rigaud

Henderson, J., 1987. Factors determining the state of preservation of human remains. In: A. Boddington, A.N. Garland and R.C. Janaway (Eds.), *Death decay and reconstruction: approaches to archaeology and forensic science*. Manchester: Manchester University Press, 43-54

Henton, L., 2010. *Herd management and the social role of herding at Neolithic Çatalhöyük: an investigation using oxygen isotope and dental microwear evidence in sheep*. Unpublished Ph.D. thesis, University College London

Henton, L., 2012. The combined use of oxygen isotopes and microwear in sheep teeth to elucidate seasonal management of domestic herds: the case study of Çatalhöyük, central Anatolia. *Journal of Archaeological Science* 39, 3264-3276

Henton, L., Meier-Augenstein, W. and Kemp, H.F., 2010. The use of oxygen isotopes in sheep molars to investigate past herding practices at the Neolithic settlement of Çatalhöyük, Central Anatolia. *Archaeometry* 52/3, 429-449

Hershkovitz, I., Garfinkel, Y. and Arensburg, B., 1986. Neolithic skeletal remains at Yiftahel, area C(Israël). *Paléorient* 12/1, 43-81

Hewitt, D., Westropp, C.K. and Acheson, R.M., 1955. Oxford child health survey: effect of childish ailments on skeletal development. *British Journal of Preventive and Social Medicine* 9/4, 179-186

Hillson, S.W., 1978. *Human biological variation in the Nile valley in relation to environmental fractors*. Unpublished Ph.D. thesis, University of London

Hillson, S.W., 1991. Dental histology as an index of past community health. In: H. Bush and M. Zvelebil (Eds.), *Health in past societies: biocultural interpretation of human skeletal remains in archaeological contexts*. Oxford: BAR international series, 53-64

Hillson, S.W., 1992. Impression and replica methods for studying hypoplasia and perikymata on human tooth crown surfaces from archaeological sites. *International Journal of Osteoarchaeology* 2, 65-78

Hillson, S.W., 1996. *Dental anthropology*. Cambridge: Cambridge University Press

Hillson, S.W., 2001. Recording dental caries in archaeological human remains. *International Journal of Osteoarchaeology* 11/4, 249-289

Hillson, S.W., 2005. *Teeth*. (second edition). Cambridge: Cambridge University Press

Hillson, S.W., 2014. *Tooth development in human evolution and bioarchaeology*. Cambridge: Cambridge University Press

Hillson, S.W., Antoine, D. and Dean, C., 1999. A detailed developmental study of defects of dental enamel in a group of Post-Medieval children from London. In: J.T. Mayhall, T. Heikkinen (Eds.), *Dental Morphology 1998: Proceedings of the 11th International Symposium on Dental Morphology*. Oulu: Oulu University Press, 102-111

Hillson, S.W. and Bond, S., 1997. Relationship of enamel hypoplasia to the pattern of tooth crown growth: a discussion. *American Journal of Physical Anthropology* 104, 89-103

Hillson, S.W. and Boz, B., in press. Growth and development. In: I. Hodder (ed.), *Humans and landscapes of Çatalhöyük: Reports from the 2000-2008 seasons*. (Monographs of the Cotsen Institute of Archaeology). Los Angeles: University of California at Los Angeles

Hillson, S.W., Grigson, C. and Bond, S., 1998. Dental defects of congenital syphilis. *American Journal of Physical Anthropology* 107, 25-40

Hillson, S.W. and Jones, B.K., 1989. Instruments for measuring surface profiles: an application in the study of ancient human tooth crown surfaces, *Journal of Archaeological Science* 16, 95-105

Hillman, G.C.E., Makeyska, E. and Hather, J.G., 1989. Wild plant foods and diet of Late Palaeolithic Wadi Kubbaniya: the evidence from charred remains. In F. Wendorf, R. Schild and A. Close (Eds.), *The prehistory of Wadi Kubbaniya Vol. 2: stratigraphy, palaeoeconomy and environment*. Dallas: Southern Methodist University Press, 162-242

Himes, J.H., Martorell, R., Habicht, J., Yarbrough, C., Malina, R.M. and Klein, R.E., 1975. Patterns of cortical bone growth in moderately malnourished preschool children. *Human Biology* 47/3, 337-350

Himes, J.H., 2004. Why study child growth and maturation? In: R.C. Hauspie, N. Cameron and L. Molinari (Eds.), *Methods in human growth research*. Cambridge: Cambridge University Press, 3-26

Hodder, I., 1990. *The domestication of Europe: structure and contingency in Neolithic societies*. Oxford: Blackwell

Hodder, I., 1996. Introduction*. Çatalhöyük1996 Archive Report*. http://www.catalhoyuk.com/archive_reports/1996/ar96_01.html (retrieved on 15/05/14)

Hodder, I., 1998. The domus: Some problems reconsidered. In: M. Edmonds and C. Richards (Eds.), *Understanding the Neolithic of North- Western Europe*. Glasgow: Cruithne Press, 84-101

Hodder, I., 2005a. Peopling Çatalhöyük and its landscape. In: I. Hodder (Ed.), *Inhabiting Çatalhöyük: reports from the 1995-1999 seasons.* (McDonald Institute Monographs). Cambridge: McDonald Institute for Archaeological Research; London: British Institute of Archaeology at Ankara, 1-32

Hodder, I., 2005b. Socialization and feasting at Çatalhöyük: a response to Adams. *American Antiquity* 70, 189–191

Hodder, I., 2006. *The leopard's tale: revealing the mysteries of Çatalhöyük*. London: Thames and Hudson

Hodder, I., 2007a. Introduction and synthesis. In I. Hodder (Ed.), *Excavating Çatalhöyük: South, North and KOPAL area reports from the 1995-1999 seasons*. (McDonald Institute Monographs). Cambridge: McDonald Institute for Archaeological Research; London: British Institute at Ankara, 3-24

Hodder, I., 2007b. Çatalhöyük in the context of the Middle Eastern Mediterranean. *Annual Review of Anthropology* 36, 105-120

Hodder, I., 2009. Season review. *Çatalhöyük 2009 Archive Report*. http://www.catalhoyuk.com/downloads/Archive_Report_2009.pdf (retrieved on 14/05/14)

Hodder, I., 2010. Probing religion at Çatalhöyük: an interdisciplinary experiment. In: I. Hodder (Ed.), *Religion in the emergence of civilization: Çatalhöyük as a case study*. Cambridge: Cambridge University Press, 1-32

Hodder, I., 2011. (ed.). *The Çatalhöyük sequence*. Templeton lecture presented at Çatalhöyük excavation house, July 2011, Çatalhöyük, Turkey

Hodder, I., 2012*. Entangled : an archaeology of the relationships between humans and things*. Chichester: Wiley-Blackwell

Hodder, I. and Cessford, C., 2004. Daily practice and social memory at Çatalhöyük. *American Antiquity* 69, 17-40

Hodder, I. and Meskell, L., 2011. “A curious and sometimes a trifle macabre artistry”: Some aspects of symbolism in Neolithic Turkey. *Current Anthropology* 52, 235–263

Hodder, I. and Pels, P., 2010. History houses. In: I. Hodder (Ed.), *Religion in the emergence of civilization: Çatalhöyük as a case study*. Cambridge: Cambridge University Press, 163-186

Holden, C., 1993. Failing to cross the biology-culture gap. *Science* 262/5139, 1641–1642

Hoppa, R.D., 1992. Evaluating human skeletal growth: an Anglo-Saxon example. *International Journal of Osteoarchaeology* 2/4, 275-288

Hoppa, R.D. and FitzGerald, C.M., 1999. From head to toe: Integrating studies from bones and teeth in biological anthropology. In: R.D. Hoppa and C.M. FitzGerald (Eds.), *Human growth in the past: studies from bones and teeth*. Cambridge: Cambridge University Press, 1-31

Howells, W.W., 1973. Cranial variation in man. A study by multivariate analysis of pattern of difference among recent human populations. *Papers of the Peabody Museum of Archaeology and Ethnology* 67, 1-259

Hubbard, A., Guatelli-Steinberg, D. and Sciulli, P., 2008. Under restrictive conditions, can the widths of linear enamel hypoplasias be used as relative indicators of stress episode durations. *American Journal of Physical Anthropology* 138, 177-189

Huda, T.F.J. and Bowman, J.E., 1995. Age determination from dental microstructure in juveniles. *American Journal of Physical Anthropology* 97, 135-150

Hudson, M.J., Dougherty, S.P., Tsuneki, A. and Hydar, J., 2003. Neolithic human burials from Tell Ain el-Kerkh, northwest Syria. *Antiquity* 77/295, 1-6

Hummert, J.R., 1983. Cortical bone growth and dietary stress among subadults from Nubia’s Batn El Hajar. *American Journal of Physical Anthropology* 62/2, 167-176

Hummert, J.R. and van Gerven, D.P., 1983. Skeletal growth in a Medieval population from Sudanese Nubia. *American Journal of Physical Anthropology* 60, 471-476

Humphrey, L.T., 1998. Patterns of growth in the modern human skeleton. *American Journal of Physical Anthropology* 105, 57-72

Humphrey, L.T., 2000a. Growth studies of past populations: an overview and an example. In: M. Cox M and S. Mays (Eds.), *Human osteology in archaeology and forensic science*. Cambridge: Cambridge University Press, 23-38

Humphrey, L.T., 2000b. Interpretation of the growth of past populations. In: J. Sofaer Derevenski (Ed.), *Children and material culture*. London: Routledge, 193-205

Humphrey, L.T., 2003. Linear growth in the archaeological record. In: G.E. Krovitz, A.J. Nelson and J.L. Thompson (Eds.), *Patterns of growth and development in the genus Homo*. Cambridge: Cambridge University Press, 144-169

Huss-Ashmore, R., Goodman, A.H. and Armelagos, G.J., 1982. Nutritional inference from paleopathology. In: M. Schiffer (Ed.), *Advances in archaeological method and theory (Vol.5)*. New York: Academic Press, 395-474

Hutchinson, J., 1861. Heredito-Syphilitic struma and on the teeth as a means of diagnosis. *British Medical Journal* 1, 515-517

Hutchinson, D.L. and Larsen, C.S., 1988. Determination of stress episode from linear enamel hypoplasias: a case study from St.Catherine's Island, Georgia. *Human Biology* 60, 93–110

Infante, P.F. and Gillespie, G.M., 1974. An epidemiologic study of linear enamel hypoplasia of deciduous anterior teeth in Guatemalan children. *Archives of Oral Biology* 19, 1055-1061

Infante, P.F. and Gillespie, G.M., 1977. Enamel hypoplasia in relation to caries in Guatemalan children. *Journal of Dental Research* 56/5, 493-498

Irurita Olivares, J., Alemán, I., Badal, J., Luca, S. and Botella, M., 2014. Evaluation of the maximum length of deciduous teeth for estimation of the age of infants and young children: proposal of new regression formulas. *International Journal of Legal Medicine* 128/5, 345-352

Jackes, M., 2011. Representativeness and bias in archaeological skeletal samples. In: S.C. Agarwal and B.A. Glencross (Eds.), *Social bioarchaeology*. Oxford: Blackwell, 107-146

Jackes, M. and Meiklejohn, C., 2008. The paleodemography of Central Portugal and the Mesolithic-Neolithic transition. In: J.P. Bocquet-Appel (Ed.), *Recent advances in paleodemography: data, techniques, patterns*. Springer: Netherlands, 209-258

Jackson, D., 1961. A clinical study of non – endemic mottling of enamel. *Archives of Oral Biology* 5, 212 – 223

Jacobi, K.P., Cook, D.C., Corruccini, R.S. and Handler, J.S., 1992. Congenital syphilis in the past: slaves at Newton Plantation, Barbados, West Indies. *American Journal of Physical Anthropology* 89/2, 145-158

Jacoby, W.G., 2000. Loess: a nonparametric, graphical tool for depicting relationships between variables. *Electoral Studies* 19, 577-613

Jantz, R.L. and Owsley, D.W., 1984. Long bone growth variation among Arikira skeletal populations. *American Journal of Physical Anthropology* 63, 13-20

Jeffery, N. and Spoor, F., 2004. Ossification and midline shape changes of the human fetal cranial base. *American Journal of Physical Anthropology* 123, 78-90

Jelliffe, P.E.F. and Jelliffe, D.B., 1973. Deciduous dental eruption, nutrition and age assessment. *Journal of Tropical Pediatrics and Environmental Child Health* 19, 193-248

Jenkins, E.L., 2000. Microfauna. *Çatalhöyük 2000 Archive Report*. http://www.catalhoyuk.com/archive_reports/2000/ar00_11.html (retrieved on 14/05/14)

Jenkins, E.L., 2005. Çatalhöyük microfauna: preliminary results and interpretations. In: I. Hodder (Ed.), *Inhabiting Çatalhöyük: reports from the 1995-1999 seasons* (McDonald Institute Monographs). Cambridge: McDonald Institute for Archaeological Research; London: British Institute of Archaeology at Ankara, 111-117

Jenkins, E.L., 2009. *Unwanted inhabitants? The microfauna from Çatalhöyük and Pınarbaşı*. Saarbrücken, Germany: VDM-Verlag

Jenkins, E.L., 2012. Mice, scats and burials: unusual concentrations of microfauna found in human burials at the Neolithic site of Çatalhöyük, Central Anatolia. *Journal of Social Archaeology* 12/3, 380-403

Jennings, J., 2010. *Stress along the Medieval Anglo-Scottish border? Skeletal indicators of conflict-zone health.* Unpublished Ph.D. thesis, Durham University

Jiang, X., Scott, P.J., Whitehouse, D.J. and Blunt, L., 2007. Paradigm shifts in surface metrology. Part II. The current shift. *Proceedings of the Royal Society A: Mathematical, Physical and Engineering Science* 463/2085, 2071-2099

Johnston, F.E., 1961. Sequence of epiphyseal union in a prehistoric Kentucky population from Indian Knoll. *Human Biology* 23, 66-81

Johnston, F.E., 1962. Growth of the long bones of infants and young children at Indian Knoll. *American Journal of Physical Anthropology* 20/3, 249-254

Johnston, F.E., 1968. Growth of the skeleton in earlier peoples. In: D.R. Brothwell (Ed.), *The skeletal biology of earlier human populations*. Oxford: Pergamon press, 57-66

Johnston, F.E., Newman, B., Cravioto, J., Delicardie, E. and Scholl, T., 1980. A factor analysis of correlates of nutritional status in Mexican children, birth to 3 years. In: L.S. Green and F.E. Johnston (Eds.), *Social and biological predictors of nutritional status, physical growth and neurological development.* New York: Academic Press, 291-307

Johnston, F.E. and Zimmer, L.O., 1989. Assessment of growth and age in the immature skeleton. In: M.Y. Iscan and K.A.R. Kennedy (Eds.), *Reconstructing life from the skeleton*. Alan R Riss: New York, 11-21

Johnson, W., Balakrishna, N. and Griffiths, P.L., 2013. Modeling physical growth using mixed effects models. *American Journal of Physical Anthropology* 150, 58–67

Kassowitz, K., 1924. Die Schmelzhypoplasie der Zähne als Index der Erkrankungen während der ersten Lebensjahre. *Zeitschrift für Kinderheilkunde* 1 38/3, 1 224-231

Kausmally, T., 2008. Dental pathology. In: N. Powers (Ed.), Human osteology method statement. London: Centre for human bioarchaeology. http://archive.museumoflondon.org.uk/NR/rdonlyres/3A7B0C25-FD36-4D43-863E-B2FDC5A86FB7/0/OsteologyMethodStatementrevised2012.pdf (retrieved on 10/05/14)

Keenleyside, A., 2008. Dental pathology and diet at Apollonia, a Greek colony on the Black Sea. *International Journal of Osteoarchaeology* 18/3, 262-279

Keller, W., 1988. The epidemiology of stunting. In: J.C. Waterlow (Ed.), *Linear growth retardation in less developed countries.* Nestlé nutrition workshop series 14. New York: Raven Press, 17-40

Kelley, J. and Bulicek, C., 2000. Identification of a birth cohort in the Miocene hominoid fossil record. *American Journal of Physical Anthropology* S30, 195

Kelley, J. and Schwartz, G.T., 2010. Dental development and life history in living African and Asian apes. *Proceedings of the National Academy of Sciences of the USA* 107, 1035-1040

Kennedy, G.E., 1985. Bone thickness in Homo erectus. *Journal of Human Evolution* 14/8, 699-708

Kerckring, T., 1717. *Opera omnia anatomica continentia specilegium anatomicum, osteogeniam foetuum nec non anthropogeniae ichnographiam, accuratissimis figuris aeri incisis illustrata*.(Second Edition. 2). Lugduni Batavorum (Leiden): Boutesteyn

Kierdorf, H. and Kierdorf, U., 1997. Disturbances of the secretory stage of amelogenesis in fluorosed deer teeth: a scanning electron-microscopic study. *Cell Tissue Research* 289, 125–135

Kierdorf, H., Kierdorf, U., Richards, A. and Josephsen, K., 2004. Fluoride-induced alterations of enamel structure: an experimental study in the miniature pig. *Anatomy and Embryology* 207, 463 – 474

Kieser, J.A., 1990. *Human adult odontometrics*. Cambridge: Cambridge University Press

King, T., Hillson, S.W. and Humphrey, L., 2002. A detailed study of enamel hypoplasia in a post-medieval adolescent of known age and sex. *Archives of Oral Biology* 47, 29-39

King, T., Humphrey, L. and Hillson, S.W., 2005. Linear enamel hypoplasias as indicators of systemic physiological stress: evidence from two known age-at-death and sex populations from Postmedieval London. *American Journal of Physical Anthropology* 128, 547-559

Klaus, H.D. and Tam, M.E., 2009. Contact in the Andes: bioarchaeology of systemic stress in colonial Mórrope, Peru. *American Journal of Physical Anthropology* .138/3, 356-68

Klein, J.L., 1997. *Statistical visions in time: a history of time series analysis*, 1662-1938. Cambridge: Cambridge University Press

Knussman, R., 1988. Somametrie. In: R. Knussmann, F. Schwidetzky, H.W. Jurgens and G. Ziegelmayer (eds.), *Anthropologie*. Stuttgart: Gustav Fischer Verlag, 232-285

Kohler, T.A., Glaud, M.P., Bocquet-Appel, J.P. and Kemp, B.M., 2008. The Neolithic demographic transition in the US Southwest. *American Antiquity* 73/4, 645-669

Konigsberg, L. and Holman, D., 1999. Estimation of age at death from dental emergence and implications for studies of prehistoric somatic growth. In: R.D. Hoppa and C. M. Fitzgerald (Eds.), *Human growth in the past: Studies from bones and teeth*. Cambridge: Cambridge University Press, 264-290

Kozak, J. and Krenz-Niedbała, M., 2002. The occurrence of cribra orbitalia and its association with enamel hypoplasia in a medieval population from Kołobrzeg, Poland. *Variability and Evolution* 10, 75-82

Kreshover, S.J., 1940. Histopathologic studies of abnormal enamel formation in human teeth. *American Journal of Orthodontics and Oral Surgery* 26, 1083-1101

Kreshover, S.J., 1960. Metabolic disturbances in tooth formation. *Annals of the New York Academy of Sciences* 85, 161-167

Kronfeld, R. and Schour, I., 1939. Neonatal dental hypoplasia. *Journal of the American Dental Association* 26, 18-32

Krovitz, G.E., Nelson, A.J. and Thompson, J.L., 2003. Introduction. In: J.L. Thompson, G.E. Krovitz and A.J. Nelson (Eds.), *Patterns of growth and development in the genus Homo*. Cambridge: Cambridge University Press, 1-14

Lacruz, R.S., Ramirez Rozzi, F. and Bromage, T.G., 2005. Dental enamel hypoplasia, age at death, and weaning in the Taung child: research letter. *South African Journal of Science* 101, 567

Lampl, M. and Johnston, F.E., 1996. Problems in the aging of skeletal juveniles: perspectives from maturation assessments of living children. *American Journal of Physical Anthropology* 101/3, 345-355

Lanphear, K.M., 1990. Frequency and distribution of enamel hypoplasias in a historic skeletal sample. *American Journal of Physical Anthropology* 81/1, 35-43

Larsen, C.S., 1995. Biological changes in human populations with agriculture. *Annual Review of Anthropology* 24, 185-213

Larsen, C.S., Garofalo, E.M. and Ruff, C.B., 2012. Development of bone strength and rigidity at Neolithic Çatalhöyük: adaptation and lifestyle in early Holocene farmers from south-central Anatolia. *American Journal of Physical Anthropology* 147(S54), 189

Last, J., 2005. Art. In: I. Hodder (Ed.*), Çatalhöyük perspectives: themes from the 1995-1999 seasons*. (McDonald Institute Monographs). Cambridge McDonald Institute for Archaeological Research; London: British Institute of Archaeology at Ankara, 197-209

Leigh, S.R., 1992. Patterns of variation in the ontogeny of primate body size dimorphism. *Journal of Human Evolution* 23, 27-50

Leigh, S.R., 1996. Evolution of human growth spurts. *American Journal of Physical Anthropology* 101/4, 455-474

Lévi-Strauss, C., 1979. Nobles sauvages. In: *Culture, science et développement. Contribution à une histoire de l'homme. Mélanges en l'honneur de Charles Morazé*. Toulouse: Privat, 41-55

Lewis, A.B. and Garn, S.M., 1960. The relationship between tooth formation and other maturational factors. *The Angle Orthodontist* 30/2, 70-77

Lewis, M.E., 2002. The impact of industrialisation: comparative study of child health in four sites from medieval and post-medieval England (850-1859). *American Journal of Physical Anthropology* 119/3, 211-223

Lewis, M.E., 2007. *The bioarchaeology of children. Current perspectives in biological and forensic anthropology.* Cambridge: Cambridge University Press

Lewis, M.E. and Roberts, C., 1997. Growing pain: the interpretation of stress indicators. *International Journal of Osteoarchaeology* 7, 581-586

Lexa, B., 2008. Alicona IFM measurement report: corrosion samples. http://www.edcc.com.cn/news/manage/upload/upfiles/200991611332.pdf (retrieved on 14/05/14)

Lieberman, D.E., 2000. Ontogeny, homology and phylogeny in the Hominid craniofacial skeleton: the problem of the browridge. In: P. O'Higgins and M. Cohn (Eds.), *Development, growth and evolution: implications for the study of hominid skeletal evolution*. London: Academic Press, 85-122

Lillie, M.C., 1996. Mesolithic and Neolithic populations of Ukraine: indications of diet from dental pathology. *Current Anthropology* 37/1, 135-142

Little, M.A., 1995. Adaptation, adaptability and multidisciplinary research. In: N.T. Boaz and L.D. Wolfe (Eds.), *Biological anthropology: the state of the science*. Bend: IIHER Publications, 121-147

Littleton, J., 2007. The production of local biologies: childhood development at Yuendumu to 1970. *Current Anthropology* 48/1, 135-145

Littleton, J. and Townsend, G.C., 2005. Linear enamel hypoplasia and historical change in a central Australian community. *Australian Dental Journal* 50/2, 101-107

Liversidge, H.M., 1994. Accuracy of age estimation from developing teeth of a population of known age (0–5.4 years). *International Journal of Osteoarchaeology* 4/1, 37-45

Liversidge, H.M., 2003. Variation in modern human dental development. In: J.L. Thompson, G.E. Krovitz and A.J. Nelson (Eds.), *Patterns of growth and development in genus Homo*. Cambridge: Cambridge University Press, 73-113

Liversidge, H.M., Dean, M.C. and Molleson, T.I., 1993. Increasing human tooth length between birth and 5.4 years. *American Journal of Physical Anthropology* 90, 307-313

Liversidge, H.M., Herdeg, B. and Rösing, F.W., 1998. Dental age estimation of non-adults. A review of methods and principles. In: K.W. Alt, F. W. Rösing and M. Teschler-Nicola (Eds.), *Dental anthropology*. Vienna: Springer, 419-442

Liversidge, H.M., Lyons, F. and Hector, M.P., 2003. The accuracy of three methods of age estimation using radiographic measurements of developing teeth. *Forensic Sciences International* 131, 22-29

Liversidge, H.M. and Molleson, T.I., 1999. Developing permanent tooth length as an estimate of age. *Journal of Forensic Sciences* 44/5, 917-920

Liversidge, H.M. and Molleson, T.I., 2004. Variation in crown and root formation and eruption of human deciduous teeth. *American Journal of Physical Anthropology* 123, 172–180

Lock, M. and Kaufert, P., 2001. Menopause, local biologies and cultures of ageing. *American Journal of Human Biology* 13/4, 494-504

Lock, M. and Nguyen, V.K., 2010. *An anthropology of biomedicine*. Chichester: Wiley-Blackwell

Logan, W.H.G., 1935. A histological study of the anatomic structures forming the oral cavity. *Journal of the American Dental Association* 22, 3-30

Logan, W.H.G. and Kronfeld, R., 1933. Development of the human jaws and surrounding structures from birth to the age of fifteen years. Journal of the American Dental Association 20, 379-427

Lomas, H., 2008. *A study of parasites in the archaeological record*. Unpublished MSc thesis, University College London

Longford, C., 2010. Field season. *Çatalhöyük 2010 Archive Report*. http://www.catalhoyuk.com/downloads/Archive_Report_2010.pdf (retrieved on 14:05/14)

Longobardi, A. and Villani, P., 2010. Trend analysis of annual and seasonal rainfall time series in the Mediterranean area. *International Journal of Climatology* 30/10, 1538-1546

Love, S., 2012. The geoarchaeology of mudbrick architecture: A methodological study from Çatalhöyük, Turkey. *Geoarchaeology* 27, 140-156

Lovejoy, C.O., Russell, K.F. and Harrison, M.L., 1990. Long bone growth velocity in the Libben population. *American Journal of Human Biology* 2, 533-541

Lovell, N.C. and Dawson, L., 2003 Intra-and inter-tooth analysis of hypoplastic and hypocalcified enamel defects. *Journal of Human Ecology* 14/4, 241-248

Lukacs, J.R., 2001. Enamel hypoplasia in the deciduous teeth of great apes: variation in prevalence and timing of defects. *American Journal of Physical Anthropology* 116/3, 199-208

Macho, G., Reid, D.J., Leakey, M.G., Jablonski, N. and Beynon, A.D., 1996. Climatic effects on dental development of Theropithecus oswaldi from Koobi Fora and Olorgesailie. *Journal of Human Evolution* 30, 57–70

Macho, G., 2008. The fossil evidence of seasonality and environmental change. In H. Schutkowski (Ed.), *Between*

biology and culture. Cambridge: Cambridge University Press, 129-141

Macchiarelli, R., Bondioli, L., Debenath, A., Mazurier, A., Tournepiche, J.F., Birch, W. and Dean, C.M., 2006. How Neanderthal molar teeth grew. *Nature* 444, 748-751

Madrigal, L., 2000. *Statistics for anthropology*. Cambridge: Cambridge University Press

Magitot, E., 1881. *Sur l'érosion des dents considérée comme signe retrospectif de reclampsie infantile,VII*. London: International Medical Congress

Mahoney, P., 2011. Human deciduous mandibular molar incremental enamel development. *American Journal of Physical Anthropology* 144, 204-214

Mahoney, P., 2012. Incremental enamel development in modern human deciduous anterior teeth. *American Journal of Physical Anthropology* 147, 637-651

Malville, N.J., 1997. Enamel hypoplasia in ancestral Puebloan populations from southwestern Colorado: I. Permanent dentition. *American Journal of Physical Anthropology* 102/3, 351-367

Maresh, M., 1943. Growth of major long bones in healthy children. *American Journal of Diseases in Children* 66, 227-254

Maresh, M., 1955. Linear growth of long bones of extremities from infancy through adolescence: continuing studies. *Archives of Pediatrics and Adolescent Medicine* 89/6, 725-742

Maresh, M., 1970. Measurements from roentgenograms: Heart size, long bone lengths, bone, muscle and fat widths, skeletal maturation. In: R.W. McCammon (Ed.), *Human growth and development*. Springfield: Charles C Thomas, 155-200

Marks, S.C. and Schroeder, H.E., 1996. Tooth eruption: theories and facts. *The Anatomical Record* 245, 374–393

Marshall, J.A., 1936. Dental hypoplasia: its occurrence, histology, pathology and etiology. *Journal of the American Dental Association* 23, 2074-2082

Marshall, J.A., 1939. Dental caries. *Physiological Reviews* 19/3, 389-414

Martin, L., Russell, N. and Carruthers, D., 2002. Animal remains from the central Anatolian Neolithic. In: F. Gérard and L. Thissen (Eds.), *The Neolithic of Central Anatolia: internal developments and external relations during the 9th to 6th millenia cal BC. Proceedings of the CANeW Table Ronde*, Istanbul 23-24 November 2001. Istanbul: Ege publishing, 193-205

Martorell, R., 1980. Interrelationships between diet, infectious disease, and nutritional status. In: L.S. Green and F.E. Johnston (Eds.), *Social and biological predictors of nutritional status, physical growth and neurological development*. New York: Academic Press, 81-106

Martorell, R., Schroeder, D.G., Rivera, J.A. and Kaplowitz, H.J., 1995. Patterns of linear growth in rural Guatemalan adolescents and children. *The Journal of Nutrition* 125/4, 1060-1067

Martorell, R., Yarbrough, C., Klein, R.E. and Lechtig, A., 1979. Malnutrition, body size and skeletal maturation: interrelationships and implications for catch-up growth. *Human Biology* 51/3, 371-389

Massler, M. and Schour, I., 1946a. The appositional life span of the enamel and dentin-forming cells. I. Human deciduous teeth and first permanent molars. *Journal of Dental Research* 25, 145-150

Massler, M. and Schour, I., 1946b. Growth of the child and the calcification pattern of the teeth. *American Journal of Orthodontics and Oral Surgery* 32/9, 495-517

Massler, M., Schour, I. and Poncher, H.G., 1941. Developmental pattern of the child as reflected in the calcification pattern of the teeth. *American Journal of Diseases of Children* 62, 33-67

Matthews, R., 1996. Surface scraping and planning. In: I. Hodder (Ed.), On the surface: Çatalhöyük 1993-1995. (McDonald Institute Monographs). Cambridge: McDonald Institute for Archaeological Research; London: British Institute of Archaeology at Ankara, 79-100

Matthews, W., 2005a. Micromorphological and microstratigraphic traces of uses and concepts of space. In: I. Hodder (Ed.), *Inhabiting Çatalhöyük: reports from the 1995-1999 seasons* (McDonald Institute Monographs). Cambridge: McDonald Institute for Archaeological Research; London: British Institute of Archaeology at Ankara, 355-398

Matthews, W., 2005b. Life-cycle and life-course of buildings. In: I. Hodder (Ed.), *Çatalhöyük perspectives: themes from the 1995-1999 seasons* (McDonald Institute Monographs). Cambridge McDonald Institute for Archaeological Research; London: British Institute of Archaeology at Ankara,125-149

May, R.L., Goodman, A.H. and Meindl, R.S., 1993. Response of bone and enamel formation to nutritional supplementation and morbidity among malnourished Guatemalan children. *American Journal of Physical Anthropology* 92/1, 37-51

Mayes, A.T. and Barber, S.B., 2008. Osteobiography of a high-status burial from the lower Río Verde Valley of Oaxaca, Mexico. *International Journal of Osteoarchaeology* 18/6, 573-588

Mays, S., 1985. The relationship between Harris line formation and bone growth and development. *Journal of Archaeological Science* 12, 207-220

Mays, S., 1995. The relationship between Harris lines and other aspects of skeletal development in adults and juveniles. *Journal Archaeological Science* 12, 207-220

Mays, S., 1999. Linear and appositional long bone growth in earlier human populations: a case study from Mediaeval England. In: R.D. Hoppa and C.M. FitzGerald (Eds.), *Human growth in the past: studies from bones and teeth*. Cambridge: Cambridge University Press, 290-313

Mays, S., Brickley, M. and Ives, R., 2008. Growth in an English population from the Industrial Revolution. *American Journal of Physical Anthropology* 136, 85-92

Mays, S., Ives, R. and Brickley, M., 2009. The effect of socioeconomic status on endochondral and appositional bone growth in children from 19th century Birmingham, England. *American Journal of Physical Anthropology* 140, 410-416

McCarty, S.M. and Ogden, J.A., 1982a. Radiology of postnatal development V distal humerus. *Skeletal Radiology* 7, 239-249

McCarthy, S.M. and Ogden, J.A., 1982b. Radiology of postnatal skeletal development VI Elbow joint, proximal radius and ulna. *Skeletal Radiology* 9, 17-26

McDonald, J.H., 2009. *Handbook of biological statistics*. (second edition). Baltimore, Maryland: Sparky house Publishing

McGregor, I.A., Billewicz, W.Z. and Thomson, A.M., 1961. Growth and mortality in children in an African village. *British Medical Journal* 2/5268, 1661-1666

Mead, A.J., 1999. Enamel hypoplasia in Miocene rhinoceroses (Teleoceras) from Nebraska: evidence of severe physiological stress. *Journal of Vertebrate Paleontology* 19, 391–397

Meiklejohn, C. and Zvelebil, M., 1991. Health status of European populations of the agricultural transition and the implication for the adoption of farming. In: H. Bush and M. Zvelebil (Eds*.), Health in past societies: biocultural interpretations of human skeletal remains in archaeological contexts*. Oxford: BAR international series 567, 129-145

Mellaart, J., 1963a. Excavations at Çatal Hüyük, 1962: second preliminary report. *Anatolian Studies* 13: 43-103

Mellaart, J., 1963b. Deities and shrines of Neolithic Anatolia. Excavations at Çatal Hüyük 1962 *Archaeology* 16/1, 29-38

Mellaart, J., 1964. Excavations at Çatal Hüyük, 1963: third preliminary report. *Anatolian Studies* 14, 39-119

Mellaart, J., 1965. Çatal Hüyük: A Neolithic city in Anatolia*. Proceedings of the British Academy* 51, 201-213

Mellaart, J., 1966. Excavations at Çatal Hüyük, 1965, Fourth Preliminary Report. *Anatolian Studies* 16, 165-191

Mellaart, J., 1975. *The Neolithic of the near east*. London: Thames and Hudson

Mellaart, J., 1998. Çatal Hüyük: the 1960's seasons. In: R. Matthews (Ed.), *Ancient Anatolia: fifty years work by the British Institute of Archaeology at Ankara*. London: British Institute at Ankara, 35–41

Mellanby, M., 1927. The structure of human teeth. *British Dental Journal* 48, 737-751

Mellanby, M., 1929. *Diet and the teeth: an experimental study part 1, dental structure in dogs*. London: His Majesty's Stationery Office

Mellanby, M., 1930. *Diet and the teeth: an experimental study part 2.* Medical research council special reports 153. London: His Majesty's Stationery Office

Mellanby, M., 1941. Effect of maternal dietary deficiency of vitamin A on dental tissues in rats. *Journal of Dental Research* 20, 489-509

Menninger, M., 2008. *Die schnurkeramischen bestattungen von Lauda-Königshofen*. Unpublished Ph.D. thesis, Eberhard-Karls university, Tübingen

Merchant, V.L. and Ubelaker, D.H., 1977. Skeletal growth of the protohistoric Arikara. *American Journal of Physical Anthropology* 46/1, 61-72

Messiah, S.E., Arheart, K.L., Lipshultz, S.E. and Miller, T.L., 2010. Prevalence of the metabolic syndrome in US Youth. In: D. Bagchi (Ed.), *Global perspectives on childhood obesity: current status, consequences and prevention*. London: Academic Press, 107-119

Miles, E.A.W. and Bulman, J.S., 1995. Growth curves of immature bones from a Scottish island population of sixteenth to mid-nineteenth century: Shoulder girdle, ilium, pubis and ischium. *International Journal of Osteoarchaeology* 5/1, 15-27

Mitchell, P.D., 2006. Child health in the crusader period inhabitants of Tel Jezreel, Israel. *Levant* 38/1, 37-44

Mittler, D.M., Van Gerven, D.P., Sheridan, S.G. and Beck, R., 1992. The epidemiology of enamel hypoplasia, cribra orbitalia and subadult mortality in an ancient Nubian population. In: A.H. Goodman and L.L. Capasso (Eds.), *Recent contributions of the study of enamel developmental defects*. Journal of Paleopathology monograph series 2. Chieti, Italy: Associazione Anthropologica Abruzzese, 143-151

Miszkiewicz, J.J., 2012. Linear enamel hypoplasia and age-at-death at Medieval (11th–16th Centuries) St. Gregory's priory and cemetery, Canterbury, UK. *International Journal of Osteoarchaeology* (early view)

Moggi-Cecchi, J. and Crovella, S. 1991. Occurence of enamel hypoplasia in the dentitions of simian primates. *Folia Primatologica* 57, 106-110

Moggi-Cecchi, J., Pacciani, E. and Pinto-Cisternas, J., 1994. Enamel hypoplasia and age at weaning in 19th-century Florence, Italy. *American Journal of Physical Anthropology* 93/3, 299-306

Molleson, T.I., 1993. The human bones. In: E. Farwell and T.I. Molleson (Eds.), *Excavations at Poundbury 1966*-80 Volume II: the cemeteries. Dorchester: Dorset Natural History and Archaeological Society.

Molleson, T.I., 2007. Times of stress at Çatal. In: M. Faerman, L.K. Horwitz, T. Kahana and U. Zilberman (Eds.), *Faces from the past. Faces from the past: diachronic patterns* in the biology of human populations from the eastern Mediterranean : papers in honour of Patricia Smith. Oxford: Archaeopress, 140-150

Molleson, T.I., Andrews, P. and Boz, B., 1999. Report on human remains recovered from the South Area, together with a summary of material from the BACH area and the KOPAL trench. Çatalhöyük 1999 Archive Report.
http://www.catalhoyuk.com/archive_reports/1999/ar99_14.html (retrieved on 14/05/14)

Molleson, T.I., Andrews, P. and Boz, B., 2005. Reconstruction of the Neolithic people at Çatalhöyük. In: I. Hodder (Ed.), *Inhabiting Çatalhöyük: reports from the 1995-1999 seasons.* (McDonald Institute Monographs). Cambridge: McDonald Institute for Archaeological Research; London: British Institute of Archaeology at Ankara, 279-301

Molleson, T.I., Ottevanger, J. and Compton, T., 2004. Variation in Neolithic teeth from Çatalhöyük (1961-1964). Anatolian Studies 54, 1-26

Molnar, S., Przybeck, T.R., Gantt, D.G., Elizondo, R. and Wilkerson, J.E., 1981. Dentin apposition rates as markers of primate growth. *American Journal of Physical Anthropology* 55, 443 -453

Molnar, S. and Ward, S.C., 1975. Mineral metabolism and microstructural defects in primate teeth. *American Journal of Physical Anthropology* 43, 3-18

Moorrees, C.F.A., Fanning, E.A. and Hunt, E.E., 1963a. Age variation of formation stages for ten permanent teeth. *Journal of Dental Research* 42/6, 1490-1502

Moorrees, C.F.A., Fanning, E.A. and Hunt, E.E., 1963b. Formation and resorption of three deciduous teeth in children. *American Journal of Physical Anthropology* 21/2, 205-213

Moses, L.E., Gale, L.C. and Altmann, J., 1992. Methods for analysis of unbalanced, longitudinal growth data. *American Journal of Primatology* 28, 49-59

Neiburger, E.J., 1990. Enamel hypoplasia: Poor indicators of dietary stress. *American Journal of Physical Anthropology* 82, 231–232

Nelson, S., Hans, M.G., Broadbent, B.H. and Dean, D., 2000. The brush inquiry: An opportunity to investigate health outcomes in a well-characterized cohort. *American Journal of Human Biology* 12, 1–9

Newell, E.A., Guatelli-Steinberg, D., Field, M., Cooke, C. and Feeney, R.N., 2006. Life history, enamel formation, and linear enamel hypoplasia in the Ceboidea. *American Journal of Physical Anthropology* 131/2, 252-260

Newman, H. and Poole, D., 1974. Observations with scanning and transmission electron microscopy on the structure of human surface enamel. *Archives of Oral Biology* 19, 1135-1143

Nikiforuk, G. and Fraser, D., 1981. The etiology of enamel hypoplasia: a unifying concept. *Journal of Pediatrics* 98/6, 888-893

Niven, L.B., Egeland, C.P. and Todd, L.C., 2004. An inter-site comparison of enamel hypoplasia in bison implications for paleoecology and modeling Late Plains Archaic subsistence. *Journal of Archaeological Science* 31, 1783–1794

Noback, C.R., 1943. Some gross structural and quantitative aspects of the developmental anatomy of the human embryonic, fetal and circumnatal skeleton. *The Anatomical Record* 87/1, 29-51

Obertová, Z., 2005. Environmental stress in the early mediaeval Slavic population at Borovce (Slovakia). *HOMO-Journal of Comparative Human Biology* 55/3, 283-291

Ogden, J.A., 1984a. Radiology of postnatal skeletal development IX. Proximal tibia and fibula. *Skeletal Radiology* 11, 169-177

Ogden, J.A., 1984b. Radiology of postnatal skeletal development X. Patella and tibial tuberosity. *Skeletal Radiology* 11, 246-257

Ogden, J.A., Conlogue, G.J. and Jensen, R.T.P., 1978. Radiology of postnatal skeletal development: the proximal humerus. *Skeletal Radiology* 2/3, 153-160

Ogden, J.A. and McCarty, S.M., 1983. Radiology of postnatal skeletal development VIII Distal tibia and fibula. *Skeletal Radiology* 10, 209-220

Ogden, J.A., Murphy, M.J., Southwick, W.O. and Ogden, D.A., 1986. Radiology of postnatal skeletal development XII1. C1-C2 interrelationships. *Skeletal Radiology* 15/6, 433-438

Ogden, J.A. and Phillips, S.B., 1983. Radiology of postnatal skeletal development VII Scapula. *Skeletal Radiology* 9, 157-169

Ogilvie, M.D., Curran, B. and Trinkaus, E., 1989. Incidence and patterning of dental enamel hypoplasia among the Neandertals. *American Journal of Physical Anthropology* 79, 25–41

Ogilvie, M.D. and Trinkaus, E., 1990. Reply to Neiburger. *American Journal of Physical Anthropology* 82/2, 232-233

O'Haver, T., 2013. A pragmatic introduction to signal processing with applications in chemical analysis.
http://terpconnect.umd.edu/~toh/spectrum/TOC.html (retrieved on 24/05/14)

Okazaki, K., 2004. A morphological study of the growth patterns of ancient people in the northern Kyushu-Yamaguchi region, Japan. *Anthropological Science* 112, 219-234

O'Rahilly, R., Müller, F., Carpenter, S. and Swenson, R., 2004. Basic human anatomy: a regional study of human structures. Online version developed at Darthmouth medical school
https://www.dartmouth.edu/~anatomy/Lowerextremity/leg-knee/radiology/APknee-child.htm(retrieved on 15/05/14)

Orban, B.J., 1957. *Oral histology and embryology*. (fourth edition). St Louis: C V Mosby & Co

Orenuga, O.O. and Odukoya, O.O., 2010. An epidemiological study of developmental defects of enamel in a group of Nigerian children. *Pesquisa Brasileira em Odontopediatria e Clínica Integrada* 10/3, 385-391

Owen, R., 1840-1845. *Odontography: or a treatise on the comparative anatomy of the teeth : their physiological relations, mode of development, and microscopic structure, in the vertebrate animals*. London : H. Baillière

Oyamada, J., Igawa, K., Kitagawa, Y., Manabe, Y., Kato, K., Matsushita, T. and Rokutanda, A., 2008. Pathology of deciduous teeth in the samurai and commoner children of early modern Japan. *Anthropological Science* 116/1, 9-15

Oyamada, J., Igawa, K., Manabe, Y., Kato, K., Matsushita, T., Rokutanda, A. and Kitagawa, Y., 2010. Preliminary analysis of regional differences in dental pathology of early modern commoners in Japan. *Anthropological Science* 118(1), 1-8

Oyamada, J., Kato, K., Matsushita, T., Tsurumoto, T. and Manabe, Y., 2012. Sex differences in linear enamel hypoplasia (LEH) in early modern Japan. *Anthropological Science* 120/2, 97-101

Palubeckaité, Z., Jankauskas, R. and Boldsen, J., 2002. Enamel hypoplasia in Danish and Lithuanian late Medieval/early modern samples: a possible reflection of child morbidity and mortality patterns. *International Journal of Osteoarchaeology* 12, 189-201

Parfitt, A.M., 1994. Osteonal and hemi-osteonal remodeling: the spatial and temporal framework for signal traffic in adult human bone. *Journal of Cell Biochemistry* 55, 273-286

Parfitt, A.M., Travers, R., Rauch, F. and Glorieux, F.H., 2000. Structural and cellular changes during bone growth in healthy children. *Bone* 27/4, 487-494

Parker Pearson, M., 2003. Food, culture and identity: an introduction and overview. In: M. Parker Pearson (Ed.), *Food, culture and identity in the Neolithic and Early Bronze Age*. Oxford: Archaeopress, 1-30

Pawłowska, K., 2007 Microscopic study of bone structure: preliminary report. *Çatalhöyük 2007 Archive Report*
http://www.catalhoyuk.com/downloads/Archive_Report_2007.pdf (retrieved on 14/05/14)

Paynter, K.J. and Grainger, R.M., 1956. The relation of nutrition to the morphology and size of the rat molar teeth. *Journal of the Canadian Dental Association* 22, 519-531

Pearson, J.A., Buitenhuis, H., Hedges, R.E.M., Martin, L., Russell, N. and Twiss, K.C., 2007. New light on early caprine herding strategies from isotope analysis: A case study from Neolithic Anatolia. *Journal of Archaeological Science* 34/12, 2170-2179

Pearson, J.A., Hedges, R.E.M., Molleson, T.I. and Özbek, M., 2010. Exploring the relationship between weaning and infant mortality: An isotope case study from Aşıklı Höyük and Çayönü Tepesi. American Journal of Physical Anthropology 143, 448–457

Peltier, J., 2009. LOESS smoothing in excel.
http://peltiertech.com/WordPress/loess-smoothing-in-excel/ (retrieved on 27/05/13)

Perkins, D., 1969. Fauna of Çatal Hüyük: evidence for early cattle domestication in Anatolia. *Science* 164, 177-79

Pfeiffer, S., Crowder, C., Harrington, L. and Brown, M., 2006. Secondary osteon and Haversian canal dimensions as behavioural indicators. *American Journal of Physical Anthropology* 131, 460-468

Pfeiffer, S. and Harrington, L., 2011. Bioarchaeological evidence for the basis of small adult stature in southern Africa. *Current Anthropology* 52/3, 449-461

Pickerill, H.P., 1913. The structure of enamel. *Dental Cosmos* 55/10, 969-988

Pickerill, H.P., 1914. *The prevention of dental caries and oral sepsis*. London: Baillère, Tindall and Cox

Pilloud, M.A., 2009. *Community structure at Neolithic Çatalhöyük: Biological distance analysis of household, neighborhood, and settlement*. Unpublished Ph.D. thesis, Ohio university

Pilloud, M.A. and Larsen, C., 2011. ”Official” and ”practical” kin: Inferring social and community structure from dental phenotype at Neolithic Çatalhöyük, Turkey. *American Journal of Physical Anthropology* 145/4, 519-530

Pindborg, J.J., 1970. *Pathology of the dental hard tissues*. Copenhagen: Munksgaard

Pindborg, J.J., 1982. Aetiology of developmental enamel defects not related to fluorosis. *International Dental Journal* 32, 123-134

Pinhasi, R., Shaw, R., White, B. and Ogden, D., 2006. Morbidity, rickets and long bone growth in post-medieval Britain: a cross-population analysis. *Annals of Human Biology* 33, 372-389

Pinhasi, R., Teschler-Nicola, M., Knaus, A. and Shaw, P., 2005. A cross-population analysis of the growth of long bones and the os coxae of three Early Medieval Austrian populations. *American Journal of Human Biology* 17, 470-488

Plog, S., 1990. Agriculture, sedentism and environment in the evolution of political systems. In: S. Upham (Ed.), *The evolution of political systems: sociopolitics in small-scale sedentary societies*. Cambridge: Cambridge University Press, 177-199

Ponce de León, M.S. and Zollikofer, C.P.E., 2001. Neanderthal cranial ontogeny and its implications for late hominid diversity. *Nature* 412, 534-538

Popkin, P., in press. Prehistoric Anatolian subsistence practices: Zooarchaeological evidence. I: C. Wawruschka (Ed.), *Prehistoric economies of Anatolia: subsistence strategies and exchange*. Vienna: Austrian Academy of Sciences

Poulsen, S., Gjørup, H., Haubek, D., Haukali, G., Hintze, H., Løvschall, H. and Errboe, M., 2008. Amelogenesis imperfecta- a systemic literature review of associated dental and oro-facial abnormalities and their impact on patients. *Acta Odontologica* 66/4, 193-199

Rajendran, R., 2009. *Shafer’s oral pathology*. India: Elsevier

Ramirez-Rozzi, F. and Bermudez de Castro, J., 2004. Surprisingly rapid growth in Neanderthals. *Nature* 428, 935-939

Ramirez-Rozzi, F. and Sardi, M., 2007. Crown formation times in Neanderthal anterior teeth revisited. *Journal of Human Evolution* 53, 108-113

Rauch, F., 2005. Bone growth and length and width: the Yin and Yang of bone stability. *Journal of Musculoskeletal and Neuronal Interactions* 5/3, 194-201

Reese, D.S., 2005. The Çatalhöyük shells. In: I. Hodder (Ed.), *Inhabiting Çatalhöyük: reports from the 1995-1999 seasons.* (McDonald Institute Monographs). Cambridge: McDonald Institute for Archaeological Research; London: British Institute of Archaeology at Ankara, 123-129

Reid, D.J., Beynon, A.D. and Ramirez Rozzi, F.V., 1998. Histological reconstruction of dental development in four individuals from a medieval site in Picardie, France. *Journal of Human Evolution* 35, 463-477

Reid, D.J. and Dean, M.C., 2000. Brief communication: the timing of linear enamel hypoplasias on human anterior teeth. *American Journal of Physical Anthropology* 113, 135-139

Reid, D.J. and Dean, M.C., 2006. Variation in modern human enamel formation times. *Journal of Human Evolution* 50, 329-346

Reid, D.J. and Ferrell, R.J., 2006. The relationship between number of striae of Retzius and their periodicity in imbricational enamel formation. *Journal of Human Evolution* 50, 195-202

Renz, H. and Radlanski, R.J., 2006. Incremental lines in root cementum of human teeth: a reliable age marker? *Homo – Journal of Comparative Human Biology* 57/1, 29-50

Retzius, A., 1837. Bemerkungen über den inneren Bau der Zähne, mit besonderer Rücksicht auf den im Zahnknochen vorkommende Röhrenbau. *Arkiv für Anatomie, Physiologie und Wissenschaftliche Medecin*, 486-566

Ribot, I. and Roberts, C., 1996. A study of non-specific stress indicators and skeletal growth in two Mediaeval subadult populations. *Journal of Archaeological Science* 23, 67–79

Rice, V.H., 2000. Theories of stress and relationship to health. In: V.H. Rice (Ed.), *Handbook of stress, coping and health: Implications for nursing, research, theory and practice*. Detroit: Sage Publications, 27-42

Richards, M.P., Pearson, J.A., Molleson, T.I., Russell, N. and Martin, L., 2003. Stable isotope evidence of diet at Neolithic Çatalhöyük, Turkey. *Journal of Archaeological Science* 30, 67-76

Richards, M.P. and Pearson, J.A., 2005. Stable-isotope evidence of diet at Çatalhöyük. In: I. Hodder (Ed.), *Inhabiting Çatalhöyük: reports from the 1995-1999 seasons.* (McDonald Institute Monographs). Cambridge: McDonald Institute for Archaeological Research; London: British Institute of Archaeology at Ankara, 313-322

Risnes, S., 1990. Structural characteristics of staircase-type Retzius lines in human dental enamel analyzed by Scanning Electron Microscopy. *Anatomical Record* 226, 135-146

Risnes, S., 1998. Growth tracks in dental enamel. *Journal of Human Evolution* 35, 331–350

Ritchey, T., 1996. Note on the building complexity. In: I Hodder (Ed.), On the surface: Çatalhöyük 1993-1995. (McDonald Institute Monographs). Cambridge: McDonald Institute for Archaeological Research; London: British Institute of Archaeology at Ankara, 7-18

Ritzman, T.B., Baker, B.J. and Schwartz, G.T., 2008. A fine line: a comparison of methods for estimating ages of linear enamel hypoplasia formation. *American Journal of Physical Anthropology* 135/3, 348-361

Robb, J., Bigazzi, R., Lazzarini, L., Scarsini, C. and Sonego, F., 2001. Social “status” and biological “status”: a comparison of grave goods and skeletal indicators from Pontecagnano. *American Journal of Physical Anthropology* 115, 213-222

Roberts, C.A. and Connell, B., 2004. Guidance on recording palaeopathology. In: *Guidelines to the standards for recording human remains*. Southamption; Reading: British association for biological anthropology and osteoarchaeology and Institute of field archaeology, 34-39

Roberts, N., Black, S., Boyer, P., Eastwood, W.J., Griffiths, H.I., Lamb, H.F., Leng, M.J., Parish, R., Reed, J.M., Twigg, D. and Yigitbasioglu, H., 1999. Chronology and stratigraphy of Late Quaternary sediments in the Konya Basin, Turkey: Results from the KOPAL Project. *Quaternary Science Reviews* 18/4-5, 611-630

Roberts, N., Boyer, P. and Parish, R., 1996. Preliminary results of geoarchaeological investigations at Çatalhöyük. In: I. Hodder (Ed.), On the surface: Çatalhöyük 1993-1995. (McDonald Institute Monographs). Cambridge: McDonald Institute for Archaeological Research; London: British Institute of Archaeology at Ankara, 19-40

Roberts, N., Boyer, P. and Merrick, J., 2007. The KOPAL On-site and off-site excavations and sampling. In I. Hodder (Ed.), *Excavating Çatalhöyük: South, North and KOPAL area*

reports from the 1995-1999 seasons. (McDonald Institute Monographs). Cambridge: McDonald Institute for Archaeological Research; London: British Institute at Ankara, 553-572

Roberts, N., Reed, J.M., Leng, M.J., Kuzucuoglu, C., Fontugne, M., Bertaux, J., Woldring, H., Bottema, S., Black, S., Hunt, E. and Karabiyikoglu, M., 2001. The tempo of Holocene climatic change in the eastern Mediterranean region: new high-resolution crater-lake sediment data from central Turkey. *The Holocene* 11, 721-736

Roberts, N. and Rosen, A., 2009. Diversity and complexity in early farming communities of Southwest Asia: new insights into the economic and environmental basis of Neolithic Çatalhöyük. Current Anthropology 50/3, 393-402

Roche, A.F., 1992. *Growth, maturation, and body composition: the Fels longitudinal study 1929-1991*. Cambridge: Cambridge University Press

Rose, J.C., 1977. Defective enamel histology of prehistoric teeth from Illinois. *American Journal of Physical Anthropology* 46, 439-446

Rose, J.C., 1979. Morphological variations of enamel prisms within abnormal striae of Retzius. *Human Biology* 51/2, 139-151

Rose, J.C., Armelagos, G.J. and Lallo, J.W., 1978. Histological enamel indicator of childhood stress in prehistoric skeletal samples. *American Journal of Physical Anthropology* 49, 511-516

Rose, J.C., Condon, K.W. and Goodman, A.H., 1985. Diet and dentition: developmental disturbances. In: R.I. Gilbert and J.H. Mielke (Eds.), *The analysis of prehistoric diets*. London: Academic Press, 281-305

Rudney, J.D., 1983. The age-related distribution of dental indicators of growth disturbance in ancient lower Nubia: an etiological model from the ethnographic record. *Journal of Human Evolution* 12/6, 535-543

Ruff, C.B., 2000. Biomechanical analysis of archaeological human skeletons. In: M.A. Katzenberg and S.R. Saunders (Eds.), *Biological anthropology of the human skeleton*. New York: Wiley Liss, 71-102

Ruff, C.B., 2007. Body size prediction from juvenile skeletal remains. *American Journal of Physical Anthropology* 133/1, 698-716

Ruff, C.B., Garofalo, E. and Holmes, M.A., 2013. Interpreting skeletal growth in the past from a functional and physiological perspective. *American Journal of Physical Anthropology* 150, 29-37

Ruff, C.B., Larsen, C.S., Cowgill, L.W. and Hager, L.D., 2006a. Life in a Neolithic community: body size and activity levels at Çatalhöyük, Turkey. American Journal of Physical Anthropology 129/S42, 155–156

Ruff, C.B., Holt, B. and Trinkaus, E., 2006b. Who's afraid of the big bad Wolff?:"Wolff's law" and bone functional adaptation. *American Journal of Physical Anthropology* 129/4, 484-498

Ruff, C.B., Walker, A. and Trinkaus, E., 1994. Postcranial robusticity in Homo. III: ontogeny. *American Journal of Physical Anthropology* 93(1), 35-54

Rushton, M.A., 1933. Fine contour lines of enamel milk teeth. *Dental Research* 53, 170

Russ, J., 2007. *The image processing handbook*. London: CRC Press

Russell, N., 1998. Bone tools. *Çatalhöyük 1998 Archive Report*. http://www.catalhoyuk.com/archive_reports/1998/ar98_13.html (retrieved on 14/05/14)

Russell, N., 1999. Bone tools. *Çatalhöyük 1999 Archive Report*. http://www.catalhoyuk.com/archive_reports/1999/ar99_13.html (retrieved on 14/05/14)

Russell, N., 2001. The social life of bone: A preliminary assessment of bone tool manufacture and discard at Çatalhöyük. In: A.M. Choyke and L. Bartosiewicz (Eds.), *Crafting bone: skeletal technologies through time and space*. Oxford: Bar International Series, 241-249

Russel, N., 2012. Hunting sacrifice at Neolithic Çatalhöyük. In: A. Porter and G.M. Schwartz (Eds.), *Sacred killing: the archaeology of sacrifice in the Ancient Near East*. Warsaw, IN: Eisenbrauns, 79-95

Russell, N. and Martin, L., 2005. The Çatalhöyük mammal remains. In: I. Hodder (Ed.), *Inhabiting Çatalhöyük: reports from the 1995-1999 seasons.* (McDonald Institute Monographs). Cambridge: McDonald Institute for Archaeological Research; London: British Institute of Archaeology at Ankara, 33-98

Russell, N. and Martin L., 2012. Cooking meat and bones at Neolithic Çatalhöyük, Turkey. In: S.R. Graff and E. Rodríguez-Alegría (Eds.), *The menial art of cooking: Archaeological studies of cooking and food preparation*. Boulder: University Press of Colorado, 87-97

Russell, N., Martin, L. and Buitenhuis, H., 2005. Cattle domestication at Çatalhöyük revisited. *Current Anthropology* 46/5, 101-108

Russell, N., Martin, L. and Twiss, K.C., 2009. Building memories: commemorative deposits at Çatalhöyük. In: B.S. Arbuckle, C.A. Makarewicz and A.L. Atici (Eds.), *Zooarchaeology and the reconstruction of cultural systems: case studies from the Old World*. Anthropozoologica 1. Paris: L'Homme et l'Animal, Société de Recherche Interdisciplinaire, 103-128

Russell, N. and McGowan, K.J., 2000. Bird bones. *Çatalhöyük 2000 Archive Report*. http://www.catalhoyuk.com/archive_reports/2000/ar00_11.html (retrieved on 14/05/14)

Russell, N. and McGowan, K.J., 2003. Dance of the cranes: Crane symbolism at Çatalhöyük and beyond*. Antiquity* 77, 445-455

Russell, N. and McGowan, K.J., 2005. The Çatalhöyük bird bones. In: I. Hodder (Ed.), *Inhabiting Çatalhöyük: reports from the 1995-1999 seasons.* (McDonald Institute Monographs). Cambridge: McDonald Institute for Archaeological Research; London: British Institute of Archaeology at Ankara, 99-111

Russell, N. and Meece, S., 2005. Animal representations and animal remains at Çatalhöyük. In: I. Hodder (Ed*.), Çatalhöyük perspectives: themes from the 1995-1999 seasons*. (McDonald Institute Monographs). Cambridge McDonald Institute for Archaeological Research; London: British Institute of Archaeology at Ankara, 209-231

Russell, N., Twiss, K., Orton, D. and Demirergi, A., in press. Changing Neolithic animal use at Çatalhöyük. In: B. De Cupere and V. Linseele (Eds.), *Archaeozoology of the Near East 10*. Leuven: Peeters

Sabel, N., Johansson, C., Kühnisch, J., Robertson, A., Steiniger, F., Norén, J.G., Klingberg, G. and Nietzsch, S., 2008. Neonatal lines in the enamel of primary teeth—A morphological and scanning electron microscopic investigation. *Archives of Oral Biology* 53, 954-963

Sadvari, J. and Larsen, C., in press. Femoral midshaft index and mobility. In: I. Hodder (ed.), *Humans and landscapes of Çatalhöyük: Reports from the 2000-2008 seasons*. (Monographs of the Cotsen Institute of Archaeology). Los Angeles: University of California at Los Angeles

Salisbury, R.B. and Bácsmegi, G., 2013. Resilience in the Neolithic: how people may have mitigated environmental change in prehistory. *Anthropologie* 2, 143-155

Sarnat, H. and Moss, S.J., 1985. Diagnosis of enamel defects*. NewYork State Dental Journal* 51, 103–106

Sarnat, B.G. and Schour, I., 1941. Enamel hypoplasia (chronological enamel hypoplasia) in relation to systemic disease: a chronologic, morphologic and etiologic classification. *Journal of the American Dental Association* 28, 1989-2000

Sarnat, B.G. and Schour, I., 1942. Enamel hypoplasia (chronological enamel hypoplasia) in relation to systemic disease: a chronologic, morphologic and etiologic classification. *Journal of the American Dental Association* 29, 397-418

Saunders, S.R., 2000. Subadult skeletons and growth-related studies. In: A.M. Katzenberg and S.R. Saunders (Eds.), *Biological anthropology of the human skeleton*. New York: Wiley-Liss, 135-163

Saunders, S.R., Hoppa, R. and Southern, R., 1993. Diaphyseal growth in a nineteenth century skeletal sample of subadults from St Thomas' church, Belleville, Ontario. *International Journal of Osteoarchaeology* 3/4, 265-281

Saunders, S.R. and Keenleyside, A., 1999. Enamel hypoplasia in a Canadian historic sample. *American Journal of Human Biology* 11, 513–524

Schaefer, S.C., Black, S. and Scheuer, L., 2009. *Juvenile osteology: A laboratory and field manual*. San Diego: Academic Press

Scheuer, L. and Black, S., 2000a. *Developmental juvenile osteology*. London: Academic Press

Scheuer, L. and Black, S., 2000b. Development and ageing of the juvenile skeleton. In: M. Cox and S. Mays (Eds.), *Human osteology in archaeology and forensic science*. Cambridge: Cambridge University Press, 9-22

Scheuer, L. and Black, S., 2004. *The juvenile skeleton*. London: Elsevier

Schour, I., 1936. Neonatal line in enamel and dentine of human deciduous teeth and first permanent molar. *Journal of the American Dental Association* 23, 1946-1955

Schour, I. and Hoffmann, M.M., 1939a. Studies in tooth development. I. The 16 microns calcification rhythm in the enamel and dentin from fish to man. *Journal of Dental Research* 18, 91-102

Schour, I. and Hoffmann, M.M., 1939b. Studies in tooth development. II. The rate of apposition of enamel and dentin in man and other animals. *Journal of Dental Research* 18, 161-175

Schour, I. and Kronfeld, R., 1938. Tooth ring analysis: IV. Neonatal dental hypoplasia analysis of the teeth of an infant with injury of the brain at birth. *Archives of Pathology* 26, 471-490

Schour, I. and Massler, M., 1937. Rate and gradient of growth in the human deciduous teeth, with special reference to neonatal ring. In: *International association for dental research, proceedings of the 15th general meeting, Baltimore, Maryland March 13-14, 1937*, 349

Schour, I. and Massler, M., 1940. Studies in tooth development: the growth pattern of human teeth. *Journal of the American Dental Association* 27, 1778-1792, 1918-1931

Schour, I. and Massler, M., 1941. The development of the human dentition. *Journal of the American Dental Association* 28, 1153-1160

Schour, I. and Poncher, H.G., 1937. Rate of apposition of enamel and dentin, measured by the effect of acute fluorosis. *American Journal of Diseases of Children* 54, 757-776

Schroeder, D.G., Martorell, R., Rivera, J.A., Ruel, M.T. and Habicht, J.P., 1995. The INCAP follow-up study: Age differences in the impact of nutritional supplementation on growth. *Journal of Nutrition* 125/4, 1051-1059

Schultz, P.D. and McHenry, H.M., 1975. Age distribution of enamel hypoplasia in prehistoric California Indians. *Journal of Dental Research* 54, 913

Schwartz, G.T. and Dean, C.M., 2001. Ontogeny of canine dimorphism in extant hominoids. *American Journal of Physical Anthropology* 115, 269-283

Schwartz, G.T., Reid, D.J., Dean, C.M. and Zihlman, A.L., 2006. A faithful record of stressful life events preserved in the dental development record of a juvenile gorilla. *International Journal of Primatology* 27/4, 1201-1219

Sciulli, P.W., 1977. A descriptive and comparative study of the deciduous dentition of prehistoric Ohio Valley Amerindians. *American Journal of Physical Anthropology* 47, 71–80

Sciulli, P.W., 2007. Relative dental maturity and associated skeletal maturity in prehistoric Native Americans of the Ohio Valley area. *American Journal of Physical Anthropology* 132, 545-557

Scott, D.B., 1952. Microscopic studies of dental tissues. I. Electron microscopy of tooth structure. *Oral Surgery, Oral Medicine, Oral Pathology* 5/5, 527-535

Scott, D.B. and Wyckopf, R.W.G., 1946. Shadowed replicas of tooth surfaces. *Public Health Report* 61, 697-700

Scott, D.B. and Wyckopf, R.W.G., 1949. Studies of tooth surface structure by optical and electron microscopy. *Journal of the American Dental Association* 39, 275-282

Scott, J.H. and Symons, N.B.B., 1974. *Introduction to dental anatomy*. (seventh edition). Edinburgh: Churchill Livingstone

Selye, H., 1936. A syndrome produced by diverse nocuous agents. *Nature* 138/3479, 32

Selye, H., 1950. Stress and the general adaptation syndrome. *British Medical Journal* 1/4667, 1383-1392

Selye, H., 1955. Stress and disease. *The Laryngoscope* 65/7, 500-514

Selye, H., 1956. *The stress of life*. New York: McGraw-Hill

Selye, H., 1976. Forty years of stress research: principal remaining problems and misconceptions. *Canadian Medical Association Journal* 115, 53-56

Seow, K.W., 1997. Clinical diagnosis of enamel defects: Pitfalls and practical guidelines *International Dental Journal* 47, 173-182

Seow, K.W., 1992. Dental enamel defects in low birthweight children. In: A.H. Goodman and L.L. Capasso (Eds.), *Recent contributions of the study of enamel developmental defects*. Journal of Paleopathology monograph series 2. Chieti, Italy: Associazione Anthropologica Abruzzese, 321-330

Shellis, R.P., 1984. Variations in growth of the enamel crown in human teeth and a possible relationship between growth and enamel structure. *Archives Oral Biology* 29/9, 697-705

Shellis, R.P., 1998. Utilisation of periodic markers in enamel to obtain information on tooth growth. *Journal of Human Evolution* 35, 387-400

Sheppard, Z.A., Norris, S.A., Pettifor, J.M., Cameron, N. and Griffiths, P.L., 2009. Approaches for assessing the role of household socioeconomic status on child anthropometric measures in urban South Africa. *American Journal of Human Biology* 21/1, 48-54

Sherwood, R.J. and Duren, D.L., 2013. Growth of a species, an association, a science: 80 years of growth and development research. *American Journal of Physical Anthropology* 150/1, 1-4

Shillito, L.M., Matthews, W., Almond, M.J. and Bull, I.D., 2011a. The microstratigraphy of middens: capturing daily routing in rubbish at Neolithic Çatalhöyük, Turkey. *Antiquity* 85/329, 1024-1038

Shillito, L.M., Bull, I.D., Matthews, W., Almond, M.J., Williams, J.M. and Evershed, R., 2011b. Biomolecular and micromorphological analysis of suspected faecal deposits at Neolithic Çatalhöyük, Turkey. *Journal of Archaeological Science* 38/8, 1869-1877

Sidell, J. and Scudder, C., 2005. The eggshell from Çatalhöyük: a pilot study. In: I. Hodder (Ed.), *Inhabiting Çatalhöyük: reports from the 1995-1999 seasons.* (McDonald Institute Monographs). Cambridge: McDonald Institute for Archaeological Research; London: British Institute of Archaeology at Ankara, 117-123

Simmer, J.P., Papagerakis, P., Smith, C.E., Fisher, D.C., Rountrey, A.N., Zheng, L. and Hu, J.C.C., 2010. Regulation of dental enamel shape and hardness. *Journal of Dental Research* 89/10, 1024-1038

Simpson, S., 1999. Reconstructing patterns of growth disruptions from enamel microstructure. In: R.D. Hoppa and C.M. Fitzgerald (Eds.), *Human growth in the past: Studies from bones and teeth*. Cambridge: Cambridge University Press, 241-264

Skinner, M.F., 1986. Enamel hypoplasia in sympatric chimpanzee and gorilla. *Human Evolution* 1/4, 289-312

Skinner, M.F., 1996. Developmental stress in immature hominines from Late Pleistocene Eurasia: evidence from enamel hypoplasia*. Journal of Archaeological Science* 23/6, 833-852

Skinner, M.F., 2000. Periodicity of repetitive linear enamel hypoplasia in Asian and African apes. *American Journal of Physical Anthropology* S30, 283

Skinner, M.F. and Dupras, T.L., 1993. Variation in birth timing and location of the neonatal line in human enamel. *Journal of Forensic Sciences* 38, 1383-1390

Skinner, M.F., Dupras, T.L. and Moya-Sola, S., 1995. Periodicity of enamel hypoplasia among Miocene Dryopithecus from Spain. *Journal of Paleopathology* 7, 197–222

Skinner, M.F. and Hopwood, D., 2004. Hypothesis for the causes and periodicity of repetitive linear enamel hypoplasia in large, wild African (Pan troglodytes and Gorilla gorilla) and Asian (Pongo pygmaeus) apes. *American Journal of Physical Anthropology* 123, 216-235

Skinner, M.F. and Hung, J.T.W., 1989. Social and biological correlates of localized enamel hypoplasia of the human deciduous canine tooth. *American Journal of Physical Anthropology* 79, 159-175

Skinner, M.F. and Pruetz, J.D., 2012. Reconstruction of periodicity of repetitive linear enamel hypoplasia from perikymata counts on imbricational enamel among dry-adapted chimpanzees (Pan troglodytes verus) from Fongoli, Senegal. *American Journal of Physical Anthropology* 149, 468–482

Skinner, M.F., Skinner, M.M. and Boesch, C., 2012. Developmental defects of the dental crown in chimpanzees from the Taï National Park, Côte D'Ivoire: Coronal waisting. *American Journal of Physical Anthropology* 149, 272–282

Smith, B.H., 1989. Dental development as a measure of life history in primates. *Evolution* 43/3, 683-688

Smith, B.H., 1991. Standards of human tooth formation and dental age assessment. In: M.A. Kelley and C.S. Larsen (Eds.), *Advances in dental anthropology*. New York: Wiley-Liss, 143-168

Smith, P., Bar-Yosef, O. and Sillen, A., 1984. Archaeological and skeletal evidence for dietary change during the late Pleistocene/early Holocene in the Levant. In: M.N. Cohen and G.J. Armelagos (Eds.), *Palaeopathology at the origins of agriculture*. New York: Academic Press, 101-136

Smith, P. and Horwitz, L., 2007. Ancestors and inheritors: a bioanthropological perspective on the transition to agropastoralism in the Southern Levant. In: M.N. Cohen and G. Crane-Kramer (Eds.), *Ancient health: skeletal indicators of agricultural and economic intensification*. Gainesville: University Press of Florida, 207-223

Smith, T.M., 2006. Experimental determination of the periodicity of incremental features in enamel. *Journal of Anatomy* 208, 99–113

Smith, T.M., 2008. Incremental dental development: Methods and applications in hominoid evolutionary studies. *Journal of Human Evolution* 54, 205-224

Smith, T.M., Martin, L.B. and Leakey, M.G., 2003. Enamel thickness, microstructure and development in Afropithecus turkanensis. *Journal of Human Evolution* 44, 283–306

Smith, T.M., Olejniczak, A.J., Zermeno, J.P., Tafforeau, P., Skinner, M.M., Hoffmann, A., Radovčić, J., Toussaint, M., Kruszynski, R., Menter, C., Moggi-Cecchi, J., Glasmacher,

U.A., Kullmer, O., Schrenk, F., Stringer, C. and Hublin, J-J., 2012. Variation in enamel thickness within the genus Homo. Journal of Human Evolution 62/3, 395-411

Smith, T.M., Reid, D.J., Dean, M.C., Olejniczak, A.J., Ferrell, R.J. and Martin, L.B., 2007a. New perspectives on chimpanzee and human molar crown development. In: S.E. Bailey and J-J. Hublin (Eds.), *Dental perspectives on human evolution. State-of-the-art research in dental palaeoanthropology*. Dordrecht: Springer, 177-192

Smith, T.M. and Tafforeau, P., 2008. New visions of dental tissue research: Tooth development, chemistry, and structure. *Evolutionary Anthropology* 17, 213-226

Smith, T.M., Tafforeau, P., Reid, D.J., Pouech, J., Lazzai, V., Zermeno, J.P., Guatelli-Steinberg, D., Olejniczak, A.J., Hoffman, A., Radov, J., Makaremi, M., Toussaint, M., Stringer, C. and Hublin, J-J., 2010. Dental evidence for ontogenetic differences between modern humans and Neanderthals. *Proceedings of the National Academy of Sciences* 107/49, 20923–20928

Smith, T.M., Toussaint, M., Reid, D.J., Olejniczak, J. and Hublin, J-J., 2007b. Rapid dental development in a middle Palaeolithic Belgian Neanderthal. *Proceedings of the National Academy of Sciences* 104/51, 20220-20225

Soggnaes, R.F., 1949. The organic elements of the enamel III. The pattern of the organic framework in the region of the neonatal and other incremental lines of the enamel. *Journal Dental Research* 18/6, 558-564

Soggnaes, R.F., 1955. Post-mortem microscopic defects in the teeth of ancient man. *Archives of Pathology* 59, 559-570

Soggnaes, R.F., 1956. Histological evidence of developmental lesions in teeth originating from Paleolithic, prehistoric and ancient man. *American Journal of Pathology* 32, 547-577

Standring, S., 2008. Head and neck. In: S. Standring (Ed.), Gray's anatomy. (40th edition). London: Elsevier, 395-699

Starling, A. and Stock, J.T., 2007. Dental indicators of heath and stress in early Egyptian and Nubian agriculturalists: Difficult transition and gradual recovery. *American Journal of Physical Anthropology* 134/4, 520-528

Steckel, R.H., 2005. Young adult mortality following severe physiological stress in childhood: Skeletal evidence. *Economics and Human biology* 3, 314–328

Steckel, R.H., Larsen, C.S., Sciulli, P.W. and Walker, P.L., 2006. Data collection codebook. In: R.H. Steckel, C.S. Larsen, P.W. Sciulli and P.L. Walker (Eds.), *The global history of health project.*
http://global.sbs.ohio-state.edu/new_docs/Codebook_08_25_05.pdf (retrieved on 10/05/14)

Steyn, M. and Henneberg, M., 1996. Skeletal growth of children from the Iron Age site at K 2 (South Africa). *American Journal of Physical Anthropology* 100/3, 389-396

Stephens, C.V. and Herring, D.A., 2011. Collecting, collections, and practice in the anthropologies of health and disease. *Reviews in Anthropology* 40/3, 232-260

Suckling, G.W., 1989. Developmental defects of enamel - historical and present-day perspectives of their pathogenesis. *Advanced Dental Research* 3, 87-94

Suckling, G.W. and Cutress, T., 1977. Traumatically induced defects of enamel in permanent teeth in sheep. *Journal of Dental Research* 56/11, 14-29

Suckling, G.W., Elliott, D.C. and Thurley, D.C., 1983. The production of developmental defects of enamel in the incisor teeth of penned sheep resulting from induced parasitism. *Archives of Oral Biology* 28, 393-399

Suckling, G.W., Elliott, D.C. and Thurley, D.C., 1986. The macroscopic appearance and associated histological changes in the enamel organ of hypoplastic lesions of sheep incisor teeth resulting from induced parasitism. *Archives of Oral Biology*, 31, 427–439

Suckling, G.W. and Purdell-Lewis, D.J., 1982. The pattern of mineralization of traumatically-induced developmental defects of sheep enamel assessed by microhardness and microradiography. *Journal of Dental Research* 61/10, 1211-1216

Suckling, G.W. and Thurley, D.C., 1984. Histological, macroscopic and microhardness observations of fluoride-induced changes in the enamel organ and enamel of sheep incisor teeth. *Archives of Oral Biology*, 29, 165–177

Suckling, G.W., Thurley, D.C. and Nelson, D.G.A., 1988. The macroscopic and scanning electron-microscopic appearance and microhardness of the enamel, and the related histological changes in the enamel organ of erupting sheep incisors resulting from a prolonged low daily dose of fluoride*. Archives of Oral Biology* , 33, 361–373

Sundel, S. and Valentin, J., 1986. Hereditary aspects and classification of hereditary amelogenesis imperfecta. *Community Dentistry and Oral Epidemiology* 14, 211–216

Sundick, R.I., 1978. Human skeletal growth and age determination. *Homo (Gottingen)* 29/4, 228-249

Susanne, C., 1980. Socioeconomic differences in growth patterns. In: F.E. Johnston, A.F. Roche and C. Susanne (Eds.), *Human physical growth and maturation: methodologies and factors*. NATO Advanced study Institute series 30. London: Plenum Press, 329-338

Sutphen, J.L., 1985. Growth as a measure of nutrition. *Journal of Pediatric Gastroenterology and Nutrition* 4, 164-181

Swärdstedt, T., 1966. *Odontological aspects of a Medieval population in the province of Jamtland/Mid-Sweden*. Stockholm: Tiden–Barnänken

Sweeney, E.A., Cabrera, J., Urritia, J. and Mata, L., 1969. Factors associated with linear hypoplasia of human deciduous incisors. *Journal of Dental Research* 48, 1275-1279

Sweeney, E.A., Saffir, A.J. and DeLeon, R., 1971. Linear hypoplasia of deciduous incisor teeth in malnourished children. *American Journal of Clinical Nutrition* 24, 29-31

Šešelj, M., 2013. The relationship between dental development and skeletal growth in modern humans and its implications for the interpretation of fossil hominins. *American Journal of Physical Anthropology* 150, 38-47

Šlaus, M., 2008. Osteological and dental markers of health in the transition from the Late Antique to the Early Medieval period in Croatia. *American Journal of Physical Anthropology* 136/4, 455-469

Šlaus, M., Kollmann, D., Novak, S.A. and Novak, M., 2002. Temporal trends in demographic profiles and stress levels in medieval (6th-13th century) population samples from continental Croatia. *Croatian Medical Journal* 43 /5, 598-605

Tanner, J.M., 1981. *A history of the study of human growth*. Cambridge: Cambridge University Press

Tanner, J.M., 1989. *Fetus into man: physical growth from conception to maturity*. Harvard: Harvard University Press

Tanner, J.M., Whitehouse, R.H. and Takaishi, M., 1966. Standards from birth to maturity for height, weight, height velocity and weight velocity: British children, 1965. *Archives of Disease in Childhood* 41, 454-471

Tanner, J.M., Whitehouse, R.H., Marubini, E. and Resele, L.F., 1976. The adolescent growth spurt of boys and girls of the Harpenden Growth Study. *Annals of Human Biology* 3/2, 109-126

Temple, D.H., 2007. Dietary variation and stress among prehistoric Jomon foragers from Japan. *American Journal of Physical Anthropology* 133/4, 1035-1046

Temple, D.H., 2008. What can variation in stature reveal about environmental differences between prehistoric Jomon foragers? Understanding the impact of systemic stress on developmental stability. *American Journal of Human Biology* 20, 431-439

Temple, D.H., 2010. Patterns of systemic stress during the agricultural transition in prehistoric Japan. *American Journal of Physical Anthropology* 142, 112-124

Temple, D.H., Bazaliiski, V.I., Goriunova, O.I. and Weber, A.W., 2014. Skeletal growth in early and late Neolithic foragers from the Cis-Baikal region of Eastern Siberia. *American Journal of Physical Anthropology* 153/3, 377-386

Temple, D.H., Nakatsukasa, M. and Mcgroarty, J.N., 2012 Reconstructing patterns of systemic stress in a Jomon period subadult using incremental microstructures of enamel *Journal of Archaeological Science* 39/5, 1634-1641

Temple, D.H., McGroarty, J.N., Guatelli-Steinberg, D., Nakatsukasa, M. and Matsumura, H., 2013. A comparative study of stress episode prevalence and duration among Jomon period foragers from Hokkaido. *American Journal of Physical Anthropology* 152/2, 230-238

Ten Cate, A.R., 1994. Hard tissue formation and destruction. In: A.R. Ten Cate (Ed.), *Oral histology: development, structure and function*. London: Mosby, 111-120

Tomczyk, J., Tomczyk-Gruca, M. and Zalewska, M., 2012. Frequency and chronological distribution of linear enamel hypoplasia (LEH) in the Late Neolithic and Early Bronze Age population from Šerniki Górne (Poland)–preliminary report. *Anthropological Review* 75/1, 61-73

Tomes, C.S., 1882. *A manual of dental anatomy: human and comparative*. London: J & A Churchill

Turner, J.G., 1912. Two cases of hypoplasia of enamel. *Proceedings of the Royal Society of Medicine* 5 (odontological section), 73-76

Twiss, K.C., 2008. Transformations in an early agricultural society: Feasting in the Southern Levantine Pre-Pottery Neolithic. *Journal of Anthropological Archaeology* 27, 418-442

Twiss, K.C., 2012. The complexities of home cooking: public feasts and private meals inside the Çatalhöyük house. In: S. Pollock (Ed.), Commensality, social relations and

ritual: Between feasts and daily meals. *Journal of Ancient Studies*. Special volume 2, 53-73

Twiss, K.C., Bogaard, A., Bogdan, D., Carter, T., Charles, M.P., Farid, S., Russell, N., Stevanovic, M., Yalman, E.N. and Yeomans, L., 2008. Arson or accident? The burning of a Neolithic house at Çatalhöyük. *Journal of Field Archaeology* 33, 44-57

Twiss, K.C., Bogaard, A., Charles, M.P., Henecke, J., Russell, N., Martin, L. and Jones, G., 2009. Plants and animals together: Interpreting organic remains from Building 52 at Çatalhöyük. *Current Anthropology* 50/6, 885-895

Ubelaker, D.H., 1978. *Human skeletal remains: excavation, analysis, interpretation*. Chicago: Aldine

Ubelaker, D.H., 1984. Prehistoric human biology of Ecuador: Possible temporal trends and cultural correlations. In: M.N. Cohen and G.J. Armelagos (Eds.), *Palaeopathology at the origins of agriculture*. New York: Academic Press, 491-513

Ulijaszek, S.J., Johnston, F.E. and Preece, M.A., 1998. *The Cambridge encyclopedia of human growth and development.* Cambridge: Cambridge University Press

Ulijaszek, SJ. and Komlos, J., 2010. From a history of anthropometry to anthropometric history. In: C.G.N. Mascie-Taylor and S.J. Ulijaszek (Eds.), *Human variation: From the laboratory to the field*. Boca Raton: CRC Press, 183-197

Upex, B., 2009. *Enamel hypoplasia in modern and archaeological caprine populations: The development and application of a new methodological approach*. Unpublished Ph.D. thesis, Durham University

van de Locht, R. and Hardy, K., 2009. Starch. Çatalhöyük 2009 Archive Report. http://www.catalhoyuk.com/downloads/Archive_Report_2009.pdf (retrieved on 14/05/14)

Van Lerberghe, W., 1989. Growth, infection and mortality: is growth monitoring an efficient screening instrument? In: J.M. Tanner (Ed.), *Auxology '88: Perspectives in the science of growth and development*. London: Smith Gordon, 101-110

Waldron, T., 2008. *Palaeopathology*. Cambridge: Cambridge University Press

Walker, P.L., Bathurst, R.R., Richman, R., Gierdrum, T. and Andrushko, V.A., 2009. The causes of porotic hyperostosis and cribra orbitalia: a reappraisal of the iron-deficiency-anemia hypothesis. *American Journal of Physical Anthropology* 139/2, 109-125

Walker, R., Gurven, M., Hill, K., Migliano, A.B., Chagnon, N., Souza, R.D., Djurovic, G., Hames, R., Hurtado, A.M., Kaplan, H., Kramer, K., Oliver, W.J., Valeggia, C. and Yamauchi, T., 2006. Growth rates and life histories in twenty-two small-scale societies. *American Journal of Human Biology* 18, 295-311

Walkhoff, O., 1894. *Mikrophotographischer Atlas der normalen Histologie menschlicher Zähne*. Hagen: Risel

Wang, Y. and Chen, H.J., 2012. The use of percentiles and Z-scores in anthropometry. In: V.R. Preedy (Ed.), *Handbook of anthropometry: physical measures of human form in health and disease*. New York: Springer, 29-48

Waterlow, J.C., 1988. Observations on the natural history of stunting. In: J.C. Waterlow (Ed.), *Linear growth retardation in less developed countries*. Nestlé nutrition workshop series 14. New York: Raven Press, 1-16

Weber, D.F. and Eisenmann, D.R., 1971. Microscopy of the neonatal line in developing human enamel. *American Journal of Anatomy* 132, 375-392

Weinmann, J., Svoboda, J. and Woods, R., 1945. Hereditary disturbances of enamel formation and calcification. *Journal of the American Dental Association* 32, 397 – 418

Wendrich, W., 2005. Çatalhöyük basketry. In: I. Hodder (Ed.), *Changing materialities at Çatalhöyük: reports from the 1995-1999 seasons*. (McDonald Institute Monographs). Cambridge: McDonald Institute for Archaeological Research; London: British Institute of Archaeology at Ankara, 333-338

White, T.D. and Folkens, P.A., 2005. *The human bone manual*. London: Elsevier

Whittaker, D.K. and Richards, D., 1978. Scanning electron microscopy of the neonatal line in human enamel. *Archives of Oral Biology* 23, 45 – 50

Wigley, C., 2008. Cells, tissues and systems. In: S. Standring (Ed.), *Gray's anatomy*. (40th edition). London: Elsevier, 1-145

Wilson, D. and Shroff, F., 1970.The nature of the striae of Retzius as seen with the optical microscope. *Australian Dental Journal* 15/3, 162-171

Willson, R.M.H. and Cleaton-Jones, P., 1978. Enamel mottling and infectious exanthemata in a rural community. *Journal of Dentistry* 6/2, 161-165

Witkop, C.J.J., 1989. Amelogenesis imperfecta, dentinogenesis imperfecta and dentin dysplasia revisited, problems in classification. *Journal of Oral Pathology* 17, 547–553

Witzel, C., Kierdorf, U., Dobney, K., Ervynck, A., Vanpoucke, S. and Kierdorf, H., 2006. Reconstructing impairment of secretory ameloblasts function in porcine teeth by analysis of morphological alterations in dental enamel. *Journal of Anatomy* 209, 93–110

Witzel, C., Kierdorf, U., Schultz, M. and Kierdorf, H., 2008. Insights from the inside: histological analysis of abnormal enamel microstructure associated with hypoplastic enamel defects in human teeth. American *Journal of Physical Anthropology* 136/4, 400-414

Wollstonecroft, M. and Erkal, A., 1999. Summary of plant processing experiments at Çatalhöyük, August 1999. *Çatalhöyük 1999 Archive Report.* http://www.catalhoyuk.com/archive_reports/1999/index.html (retrieved on 14/05/14)

Wood, J.W., Milner, G.R., Harpending, H.C. and Weiss, K.A., 1992. The osteological paradox: problems of inference of prehistoric health from skeletal samples. *Current Anthropology* 33/4, 343-370

Wright, K.I., 2014. Domestication and inequality? Households, corporate groups and food processing tools at Neolithic Çatalhöyük. *Journal of Anthropological Archaeology* 33, 1-33

Wright, L.E., 1990. Stresses of conquest: A study of Wilson Bands and enamel hypoplasias in the Maya of Lamanai, Belize. *American Journal of Human Biology* 2, 25-35

Wright, L.E. and Yoder, C.J., 2003. Recent progress in bioarchaeology: approaches to the osteological paradox. *Journal of Archaeological Research* 11/1, 43-70

y'Edynak, G., 1976. Long bone growth in western Eskimo and Aleut skeletons. *American Journal of Physical Anthropology* 45/3, 569-574

Yeomans, L., 2008. External areas and the stratigraphic sequence. *Çatalhöyük 2008 Archive Report*. http://www.catalhoyuk.com/downloads/Archive_Report_2008.pdf (retrieved on 15/05/14)

Young, M.F., 2003. Bone matrix proteins: their function, regulation and relationship to osteoporosis. Osteoporosis International 14/S3, 35-42

Zhou, L. and Corruccini, R.S., 1998. Enamel hypoplasias related to famine stress in living Chinese. *American Journal of Human Biology* 10, 723-733

Zsygmondi, O., 1893. Beitrage zur kentniss der enstehungsursache der hypoplastischen emaildefecte. In: A.W. Harlan and L. Offoty (Eds.), *Transactions of the World's Columbian dental congress, Chicago, August 14, 15, 16, 17, 18 and 19*. Chicago: Knight, Leonard, 48-67

APPENDIX 1: Defect matching procedure

CH 1425

1. Visually identified defects

1.1 Visually identified defects ULI1		1.2 Visually identified defects ULI2	
defect	pkg	defect	pkg
A	3-7	A	9-10
B	27-32	B	15-17
C	43-49	C	47-50
D	61-69	D	99
E	91-92		
F	124-129		
G	138-140		

2. Metric approach

2.1 Metrically identified defects ULI1		2.2 Metrically identified defects ULI2	
defect	pkg	defect	pkg
A	3-7	A	9-10
B	27-32	B	15-17
C	43-49 (83^{rd} percentile)	C	47-50
D	61-69	D	99
E	No	a	29-32
F	124-129 (80^{th} percentile)	b	110 (88^{th} percentile)
G	138-140	c	115
		d	137
Defect E could not be confirmed metrically (79^{th} percentile)			

3. Matching

defect	ULI1	ULI2
1	C	B
2	D	a
3	F	D
4	G	b

Based upon visually matched clear defects B (ULI2) and C (ULI1) as anchor point

CH 1484

1. Visually identified defects

1.1 Visually identified defects LLI1		1.2 Visually identified defects LRI2	
defect	pkg	defect	pkg
A	56-59	A	41-53
B	96-100	B	95-103
C	103-104		

2. Metric approach

2.1 Metrically identified defects LLI1		2.2 Metrically identified defects LRI2	
defect	pkg	defect	pkg
A	56-59	A	41-48
B	96-100	B	95-103
C	103-104	a	11-12
a	7-12	b	16-19
b	26-33	c	53-55
c	41-45		
d	133-137		

3. Matching

defect	LLI1	LRI2
1	a	a
2	c	A
3	A	c
4	B	B

Based upon visually matched clear defect B (LLI1 and LLI2) as anchor point

CH 1495

1. Visually identified defects

1.1 Visually identified defects LLI1		1.2 Visually identified defects URI2	
defect	pkg	defect	pkg
A	36-41	A	14-16
B	45-46	B	37-38
C	56-60	C	42-47
D	63-65	D	51-54
E	71-72		
F	89-91		

2. Metric approach

2.1 Metrically identified defects LLI1		2.2 Metrically identified defects URI2	
defect	pkg	defect	pkg
A	36-41	A	14-16
B	45-46 (81st percentile)	B	37-38
C	56-60	C	42-47
D	63-65	D	51-54 (82nd percentile)
E	71-72	a	20-24
F	89-91	b	31-34
a	18-23	c	58-61
b	113-119	d	80-84
		e	90-93

3. Matching

defect	LLI1	URI2
1	B	A
2	C	a

3	D	b
4	E	B
5	F	c
6	b	d

Based upon visually matched clear defect on URI2 (defect a) and LLI1 (defect C) as anchor point

CH 1884

1. Visually identified defects

1.1 Visually identified defects LLI2		1.2 Visually identified defects URI2	
defect	pkg	defect	pkg
A	52-58	A	34-35
B	102-108	B	40
C	117-121	C	65-71
		D	103-108

1.3 Visually identified defects LRI1		1.4 Visually identified defects URI1	
defect	pkg	defect	pkg
A	53-58	A	36-44
B	102-107	B	79-83
C	112-116	C	108-116

2. Metric approach

2.1 Metrically identified defects LLI2		2.2 Metrically identified defects URI2	
defect	pkg	defect	pkg
A	52-58	A	34-35 (88th percentile)
B	102-108	B	40 (85th percentile)
C	117-121	C	65-71
a	17-18	D	103-108
b	34-35	a	17-21
c	61-64	b	45-46
d	84-85	c	56-58
e	96-97	d	74-77
		e	126-130

2.3 Metrically identified defects LRI1		2.4 Metrically identified defects URI1	
defect	pkg	defect	pkg
A	53-58	A	36-44
B	no	B	no
C	112-116	C	108-116
a	6-8	a	20-22
b	27-30	b	31-33
c	33-34		
d	85-88		
Defect B could not be confirmed metrically (53rd percentile)		Defect B could not be confirmed metrically (73rd percentile)	

3. Matching

defect	LLI2	LRI1	URI1	URI2
1	b	c	a	/
2	A	A	A	a
3	d	d	/	b
4	e	/	/	c
5	B	/	/	C
6	C	C	C	d

Based upon visually matched clear defects A (LRI1, LLI2, URI1) and defect a (URI2) as anchor point

CH 1885

1. Visually identified defects

1.1 Visually identified defects LLI1		1.2 Visually identified defects URI1	
defect	pkg	defect	pkg
A	17-19	A	7-8
B	37-40	B	24-26
C	59-65	C	37-41
D	97-102	D	91-98
E	117-121	E	106-109

2. Metric approach

2.1 Metrically identified defects LLI1		2.2 Metrically identified defects URI1	
defect	pkg	defect	pkg
A	17-19	A	7-8
B	37-40	B	24-26
C	59-65	C	37-41
D	97-102	D	no
E	117-121	E	106-109
a	45-49	a	48-56
b	81-86	b	74-75
		c	86-88
		D could not be identified metrically (79th percentile). Two additional defects were identified and confirmed visually and on the surface graph (defect a and b).	

3. Matching

defect	LLI1	URI1
1	A	A
2	B	B
3	a	C
4	C	a
5	b	b
6	D	c
7	E	E

Based upon visually matched clear defect B (LLI1, URI1) as anchor point

CH 1913

1. Visually identified defects

1.1 Visually identified defects LLI1		1.2 Visually identified defects LLI2	
defect	pkg	defect	pkg
A	61-65	A	35-37
		B	67-69
		C	121-122

1.3 Visually identified defects ULI2		1.4 Visually identified defects URI2	
defect	pkg	defect	pkg
A	25-29	A	22-29
B	48-51	B	49-53
		C	82-85

1.5 Visually identified defects ULI1	
defect	pkg
A	29-33
B	83-91

2. Metric approach

2.1 Metrically identified defects LLI1		2.2 Metrically identified defects LLI2	
defect	pkg	defect	pkg
A	61-65	A	35-37
a	18	B	67-69
b	25-26	C	122-124
c	35-36	a	4
d	47-49	b	23
e	78-81	c	27
f	94-97	d	31
g	101-104	e	49-50
		f	76-79
		g	98-99
		h	107-109

2.3 Metrically identified defects ULI2		2.4 Metrically identified defects URI2	
defect	pkg	defect	pkg
A	25-29	A	22-29
B	48-51 (86^{th} percentile)	B	no
a	10	C	82-85
b	40-43	a	9-10
c	60-61	b	40-42
d	65-70	c	59-61
e	82-85 (89^{th} percentile)	d	68-69
f	99-102	e	72-75

		f	95
		Defect B could not be confirmed metrically (41st percentile)	

2.5 Metrically identified defects ULI1	
defect	pkg
A	29-33
B	83-91 (82nd percentile)
a	17-18
b	42
c	58-59 (85th percentile)
d	64-69
e	96-100

3. Matching

defect	ULI2	URI2	LLI1	LLI2	ULI1
1	/	/	/	b	a
2	/	/	b	c	/
3	/	/	c	A	A
4	a	a	d	e	b
5	A	A	A	B	c
6	b	b	e	f	d
7	c	c	f	g	B
8	d	d	g	h	e
9	e	C	/	C	/

Based upon visually matched clear defects A (ULI2, URI2, LLI1) and defects c (LLI1)A(LLI2/ULI1) as anchor points

CH 1923

1. Visually identified defects

1.1 Visually identified defects LRI2		1.2 Visually identified defects URI1	
defect	pkg	defect	pkg
A	26-29	A	19-22
B	87-92	B	58-65
C	96-99	C	94-97
D	103-105	D	102-107
E	129-132		

2. Metric approach

2.1 Metrically identified defects LRI2		2.2 Metrically identified defects URI1	
defect	pkg	defect	pkg
A	26-29	A	19-22
B	87-92	B	58-65
C	96-99	C	94-97
D	103-105	D	102-107 (81st percentile)
E	129-132	a	4
a	8-10	b	8
b	32-33	c	27-30

c	39-46	d	33-35
d	68-76	e	70-75
		f	115-116
		g	137-138

3. Matching

defect	LRI2	URI1
1	a	a
2	A	A
3	b	c
4	c	d
5	d	B
6	D	C

Based upon visually matched clear defects A (LRI2/URI1) as anchor point

CH 1925

1. Visually identified defects

1.1 Visually identified defects LRI2		1.2 Visually identified defects ULI1	
defect	pkg	defect	pkg
A	48-49	A	5-6
B	66-70	B	22-24
C	81	C	43-49
		D	58-65
		E	123-128

2. Metric approach

2.1 Metrically identified defects LRI2		2.2 Metrically identified defects ULI1	
defect	pkg	defect	pkg
A	48-49	A	5-6
B	66-70	B	22-24
C	81	C	43-49
a	6-8	D	58-65
b	23	E	123-128
c	37-41	a	33-35
d	54	b	72-78
e	60-62	c	89-90 (88^{th} percentile)
f	93-96	d	109-113
g	111-117		
h	128-130		

3. Matching

defect	LRI2	ULI1
1	a	A
2	b	B
3	c	a
4	A	C
5	B	D
6	C	b

7	f	c
8	g	d
9	h	E

Based upon visually matched clear defect on LRI2 (defect c) and ULI1 (defect a) as anchor point

CH 1938

1. Visually identified defects

1.1 Visually identified defects LRI1		1.2 Visually identified defects LRI2	
defect	pkg	defect	pkg
A	60-63	A	74-77
B	43-47		

2. Metric approach

2.1 Metrically identified defects LRI1		2.2 Metrically identified defects LRI2	
defect	pkg	defect	pkg
A	60-63	A	74-77
B	43-47	a	9-11
a	12-13	b	29-30
b	29-30	c	45-49
c	51-55	d	59-61
d	74-76		

Four additional defects were detected metrically and confirmed visually and using the surface graph.

3. Matching

defect	LRI1	LRI2
1	a	a
2	b	b
3	B	c
4	A	d
5	d	A

Based upon visually matched clear defect on LRI1 (defect A) and LRI2 (defect d) as anchor point

CH 1939-1922

1. Visually identified defects

1.1 Visually identified defects ULI1		1.2 Visually identified defects URI2	
defect	pkg	defect	pkg
A	40-43	A	27-30
B	64-68	B	82-83
C	91-94		

1.3 Visually identified defects LLI2	
defect	pkg
A	58-64

2. Metric approach

2.1 Metrically identified defects ULI1		2.2 Metrically identified defects URI2	
defect	pkg	defect	pkg
A	40-43	A	27-30
B	64-68	B	82-83
C	91-94	a	5-7
a	11-14	b	12-14
b	23-24	c	41-45
c	32-34	d	56-60
d	51-55 (80^{th} percentile)	e	65-68
e	80-83 (81^{st} percentile)	f	73-74 (88^{th} percentile)
f	98-101	g	93
g	110-112	h	130-133

2.3 Metrically identified defects LLI2	
defect	pkg
A	58-64
a	9-13
b	22-27
c	45-49
d	76-78 (80^{th} percentile)
e	89-91 (87^{th} percentile)
f	108-111
g	116-117

3. Matching

defect	LLI2	URI2	ULI1
1	b	/	a
2	/	a	c
3	c	b	A
4	A	A	d
5	d	c	B
6	e	d	e
7	/	e	C
8	f	f	f
9	g	B	g

Based upon visually matched clear defect A (LLI2 and URI2) and defect c(URI2)/B(ULI1) as anchor points

CH 1959

1. Visually identified defects

1.1 Visually identified defects LRI1		1.2 Visually identified defects LRI2	
defect	pkg	defect	pkg
A	65-67	A	48-50

B	80-83	B	67-73
C	89-95	C	76-79

1.3 Visually identified defects ULI1	
defect	pkg
A	89-90
B	132-136
C	142-145
D	152-154

2. Metric approach

2.1 Metrically identified defects LRI1		2.2 Metrically identified defects LRI2	
defect	pkg	defect	pkg
A	65-67	A	47-50
B	80-83	B	67-73
C	89-95	C	76-79
a	8-10	a	27-28
b	17-18	b	31 (88^{th} percentile)
c	31	c	34
d	40-43	d	97-98
e	98-100	e	108-109
f	105-108 (82^{nd} percentile)	f	120-124
g	119-120 (86^{th} percentile)	g	132-134
h	140-142	h	137-138
i	150-152	i	151-152

2.3 Metrically identified defects ULI1	
defect	pkg
A	89-90
B	132-136
C	142-145
D	no
a	7
b	14
c	20-21
d	26-28
e	31-35
f	59-62
g	70-73
h	79-82
i	112-113
Defect D could not be confirmed metrically (78^{th} percentile)	

3. Matching

defect	LRI1	LRI2	ULI1
1	a	/	a
2	b	/	b
3	/	a	c
4	c	c	d

5	d	A	e
6	A	B	f
7	B	C	g
8	C	/	h
9	e	d	A
10	f	e	/
11	g	f	i
12	h	h	B
13	i	i	C

Based upon visually matched clear defect on LRI1 (A), LRI2 (B) and ULI1 (f) as anchor point

CH 1960

1. Visually identified defects

1.1 Visually identified defects LLI2		1.2 Visually identified defects URI1	
defect	pkg	defect	pkg
A	56-63	A	64-71
B	66-70	B	86-90
C	97-100	C	94-97

2. Metric approach

2.1 Metrically identified defects LLI2		2.2 Metrically identified defects URI1	
defect	pkg	defect	pkg
A	56-63	A	64-71
B	66-70	B	86-90
C	97-100	C	94-97
a	21-22	a	7
b	25	b	13
c	32-33	c	19-21
d	43	d	37-39
e	50-52	e	48-50
f	74-76	f	79-80
g	83-85	g	102-105
h	105-109		
i	118-122		
j	130-131		

3. Matching

defect	LLI2	URI1
1	a	b
2	b	c
3	d	d
4	A	e
5	B	A
6	g	f
7	C	C
8	h	g

Based upon visually matched clear defect on LLI2 (B) and ULI1 (A) as anchor point

CH 1995

1. Visually identified defects

1.1 Visually identified defects URI1		1.2 Visually identified defects URI2	
defect	pkg	defect	pkg
A	42-46	A	16-17
B	62-64	B	19-21
C	90-91	C	56-59
D	96-97	D	98-104

2. Metric approach

2.1 Metrically identified defects URI1		2.2 Metrically identified defects URI2	
defect	pkg	defect	pkg
A	42-46	A	16-17
B	62-64	B	19-21
C	90-91 (88^{th} percentile)	C	56-59
D	96-97	D	98-104
a	3-7	a	8-10
b	27	b	32-35
c	31	c	75-80
d	103	d	107
e	108-110	e	111-113

3. Matching

defect	URI1	URI2
1	A	A
2	B	b
3	C	C
4	e	c

Based upon visually matched clear defect on URI1 (A) and URI2 (b) as anchor point,

CH 2033

1. Visually identified defects

1.1 Visually identified defects LRI1		1.2 Visually identified defects LRI2	
defect	pkg	defect	pkg
A	7-11	No defects detected	

1.3 Visually identified defects ULI1	
defect	pkg
A	57-60
B	65-69
C	76-77

2. Metric approach

2.1 Metrically identified defects LRI1		2.2 Metrically identified defects LRI2	
defect	pkg	defect	pkg
A	7-11	a	5-7
a	25-27	b	32-33
b	38-40	c	42
c	44-45	d	51-54
d	57-58		
e	66-69		

2.3 Metrically identified defects ULI1	
defect	pkg
A	57-60
B	No
C	76-77
a	6-10
b	21-23
c	28-29
d	33-36
e	40-41
f	89-92
g	99-103
Defect B could not be detected metrically (79^{th} percentile).	

3. Matching

defect	LRI1	LRI2	ULI1
1	A	a	a
2	a	/	b
3	/	b	c
4	b	/	d
5	c	c	e
6	d	d	/
7	e	/	A

Based upon visually matched clear defect on LRI1 (defect A), LRI2 (defect a) and ULI1 (defect a) as anchor point

CH 2119

1. Visually identified defects

1.1 Visually identified defects LRI1		1.2 Visually identified defects LLI2	
defect	pkg	defect	pkg
A	18-21	A	46-48
B	45-46	B	84-88
C	87-92	C	147-150
D	131-139		

1.3 Visually identified defects ULI1		1.4 Visually identified defects ULI2	
defect	pkg	defect	pkg
A	25-28	A	31-35

B	85-89	B	51-55
C	117-119	C	72-73
D	125-129	D	96-97

2. Metric approach

2.1 Metrically identified defects LRI1		2.2 Metrically identified defects LLI2	
defect	pkg	defect	pkg
A	18-21	A	46-48
B	45-46	B	84-88
C	87-92	C	147-150
D	131-139	a	8-10
a	7-11	b	27-29
b	31-32	c	32-34
c	56-59	d	43-44
d	61-63	e	58-60 (89th percentile)
e	66-68 (88th percentile)	f	63
f	74-75 (85th percentile)	g	71-75
g	101-104 (84th percentile)	h	93
h	121-126	i	96-99
		j	112-113
		k	121-124
		l	136-137

2.3 Metrically identified defects ULI1		2.4 Metrically identified defects ULI2	
defect	pkg	defect	pkg
A	25-28	A	31-35
B	85-89 (87th percentile)	B	51-55
C	117-119	C	no
D	125-129	D	96-97
a	15-18	a	8
b	41-45	b	13-16
c	53-54 (89th percentile)	c	19-23
d	73-75	d	40-41
e	132-137	e	44-49
f	155-158	f	61-62 (86th percentile)
		g	65-67
		h	83-84
		i	107-108
		j	116-117
		k	123-125
		l	128
		Defect C could not be detected metrically (51st percentile).	

3. Matching

defect	LLI1	LRI2	ULI1	ULI2
1	a	a	/	/
2	A	/	a	/
3	b	b	A	/
4	B	d	b	a
5	/	A	/	b
6	c	/	c	c
7	d	e	/	/

8	e	f	/	A
9	f	g	d	d
10	C	B	B	B
11	/	h	/	f
12	g	i	/	g
13	h	k	C	h
14	D	l	e	D
15	/	C	/	i
16	/	/	f	j

Based upon visually matched clear defect on LRI1 (defect D) LLI2 (defect l) and ULI1 (defect e) and visually matched clear defect on LLI2 (defect B) and ULI2 (defect B) as anchor points

CH 3529

1. Visually identified defects

1.1 Visually identified defects ULI1		1.2 Visually identified defects ULI2	
defect	pkg	defect	pkg
A	24-29	A	24-27
B	43-45	B	87-92
C	63-67		

2. Metric approach

2.1 Metrically identified defects ULI1		2.2 Metrically identified defects ULI2	
defect	pkg	defect	pkg
A	24-29	A	24-27
B	43-45	B	87-92
C	63-67	a	13-15 (85^{th} percentile)
a	12-14	b	18-20
b	36-40	c	33-39
c	88-91	d	62-64
d	114-117	e	82-83
e	136-138	f	106-109

3. Matching

defect	ULI1	ULI2
1	b	a
2	B	b
3	C	c
4	c	d
5	d	B
6	e	f

Based upon visually matched clear defects B (ULI1) and defect b (ULI2) as anchor point

CH 4394

1. Visually identified defects

1.1 Visually identified defects LRI2		1.2 Visually identified defects URI2	
defect	pkg	defect	pkg
A	71-79	A	45-47
B	81-82	B	56-66
C	89	C	92-95

2. Metric approach

2.1 Metrically identified defects LRI2		2.2 Metrically identified defects URI2	
defect	pkg	defect	pkg
A	71-79	A	45-47
B	81-82	B	56-66
C	no	C	92-99
a	17-19	a	13-16
b	32-34	b	25-26
c	55-56	c	71-72
d	96-97	d	103-107
		e	109-113
Defect C could not be confirmed metrically (75^{th} percentile). Four additional defects were detected and confirmed visually and on the surface graph.			

3. Matching

defect	LRI2	URI2
1	c	b
2	A	A
3	d	B

Based upon visually matched clear defect on LRI2 (defect A) and URI2 (defect A) as anchor point

CH 5608

1. Visually identified defects

1.1 Visually identified defects ULI1		1.2 Visually identified defects ULI2	
defect	pkg	defect	pkg
A	9	A	70-71
B	25-28	B	91-92
C	53-57		
D	61-66		
E	119-122		

2. Metric approach

2.1 Metrically identified defects ULI1		2.2 Metrically identified defects ULI2	
defect	pkg	defect	pkg
A	No	A	70-71
B	25-28	B	91-92
C	53-57	a	8-10
D	61-66	b	16-22
E	119-122	c	34-37
a	12-13	d	51-52
b	31-32	e	57-60 (86^{th} percentile)
c	43-46	f	96-100
d	69-70	g	107-108 (88^{th} percentile)
e	80-83 (85^{th} percentile)		
f	94-98		
g	125-127		
Defect A could not be confirmed metrically (28^{th} percentile).			

3. Matching

defect	ULI1	ULI2
1	b	a
2	c	b
3	C	c
4	f	A
5	E	f
6	g	g

Based upon visually matched clear defect on ULI1 (defect B) and ULI2 (defect a) as anchor point

CH 5795

1. Visually identified defects

1.1 Visually identified defects LLI1		1.2 Visually identified defects ULI2	
defect	pkg	defect	pkg
A	24-29	A	19-20
B	33-34	B	73-74
C	58-64		
D	98-105		

2. Metric approach

2.1 Metrically identified defects LLI1		2.2 Metrically identified defects ULI2	
defect	pkg	defect	pkg
A	24-29	A	19-20
B	33-34 (87^{th} percentile)	B	73-74
C	58-64	a	8-13
D	98-105	b	31-34
a	10-11	c	39-41
b	37-39	d	112-116
c	48-50		
d	124		

3. Matching

defect	LLI1	ULI2
1	b	a
2	c	A
3	C	b
4	D	B

Based upon visually matched clear defect on LLI1 (defect b) and ULI2 (defect a) as anchor point

CH 6681

1. Visually identified defects

1.1 Visually identified defects LRI1		1.2 Visually identified defects LRI2	
defect	pkg	defect	pkg
A	3-4	A	13-16
B	20-24	B	61-69
C	58-60	C	72-74
D	69-74		
E	78-83		
F	91-94		

1.3 Visually identified defects ULI2	
defect	pkg
A	45-47
B	53-57
C	73-77

2. Metric approach

2.1 Metrically identified defects LRI1		2.2 Metrically identified defects LRI2	
defect	pkg	defect	pkg
A	no	A	13-16
B	20-24	B	61-69
C	58-60	C	72-74
D	69-74 (85th percentile)	a	29-31
E	78-83	b	41-43 (83rd percentile)
F	91-94	c	49-50
a	33-35 (88th percentile)	d	78-79
b	41-46	e	88-91 (83rd percentile)
c	51-52	f	97-98
d	64-65		
Defects A could not be confirmed metrically (51st percentile).			

Three additional spacing irregularities were identified and confirmed visually and using the surface graph.

2.3 Metrically identified defects ULI2	
defect	pkg
A	45-47 (84th percentile)
B	53-57
C	73-77 (86th percentile)
a	12-16

b	24-30
c	60-64
d	93-98

3. Matching

defect	LRI1	LRI2	ULI2
1	B	A	/
2	a	a	/
3	b	b	/
4	c	c	a
5	D	B	b
6	E	d	A
7	F	e	B
8	/	f	c

Based upon visually matched clear defect on LRI1 (defect E), LRI2 (defect d) and ULI2 (defect A) as anchor point

CH 6682

1. Visually identified defects

1.1 Visually identified defects LLI1		1.2 Visually identified defects LLI2	
defect	pkg	defect	pkg
A	51-55	A	45-51
B	73-75	B	68-75
C	128-132	C	96-103
D	141-145	D	111-114
E	157-158		

1.3 Visually identified defects ULI1		1.4 Visually identified defects ULI2	
defect	pkg	defect	pkg
A	51-53	A	30-32
B	72-77	B	98-100
C	84-87		
D	134-137		

2. Metric approach

2.1 Metrically identified defects LLI1		2.2 Metrically identified defects LLI2	
defect	pkg	defect	pkg
A	51-55	A	45-51
B	no	B	68-75
C	128-132	C	96-103
D	141-145	D	111-114
E	157-158	a	8
a	4-7	b	19-20
b	13	c	34-35
c	23-25	d	54-55
d	36-38	e	62-63
e	66-69	f	77-79
f	82-84	g	140-141
g	93-96	h	148-149
h	100-103 (89^{th} percentile)		

i	116-118 (89th percentile)		
j	160-161		
Defect B could not be confirmed metrically (46th percentile). Eight additional defects were detected metrically and confirmed visually and using the surface graph.			

(all possible defects combined for procedure: see method chapter)

2.3 Metrically identified defects ULI1		2.4 Metrically identified defects ULI2	
defect	pkg	defect	pkg
A	51-53	A	30-32
B	72-77	B	98-100
C	84-87	a	5-8
D	134-137	b	40
a	13-15	c	52-55
b	41-44	d	69-74
c	62-65	e	86-88
d	92-94 (80th percentile)	f	109-110
e	102-105		
f	124-126		
g	146-149		
Five additional spacing irregularities were identified and confirmed visually and on the surface graph.		Four additional defects could be confirmed visually and on the surface graph.	

3. Matching

defect	LLI1	LI2	ULI1	ULI2
1	b	a	/	/
2	c	b	a	/
3	d	c	/	/
4	A	A	b	a
5	/	d	A	/
6	e	e	c	/
7	/	B	/	A
8	f	f	B	b
9	g	/	C	c
10	h	C	d	/
11	i	D	e	d
12	C	/	f	e
13	D	g	D	B
14	E	h	g	f

Based upon visually matched clear defects A (LLI1/LI2) and B (LI2, ULI1) as anchor points

CH 7541

1. Visually identified defects

1.1 Visually identified defects LRI1		1.2 Visually identified defects ULI2	
defect	pkg	defect	pkg
A	14-17	A	94-98

2. Metric approach

2.1 Metrically identified defects LRI1		2.2 Metrically identified defects ULI2	
defect	pkg	defect	pkg
A	14-17	A	94-98
a	29-31	a	11-14
b	39-44	b	21-25
c	55-56	c	39-42
d	64-67	d	58-61
e	81-82	e	69-72
f	86-87	f	83-84
g	100	g	114-119
h	111-114		
i	124-125 (83rd percentile)		

3. Matching

defect	Duration (nr pkg)	Interval (nr pkg)	chronology	LRI1	URI2
1	3-6	/	1.9-2.2	b	a
2	2-5	7-11	2.2-2.5	c	b
3	4	8-14	2.5-2.9	d	c
4	2-4	16-19	3.0-3.3	f	d
5	1-4	8-13	3.4-3.6	g	e
6	2-4	11	3.6-3.9	h	f
7	2-5	10	3.9-4.3	i	A

Based upon visually matched clear defects c (LRI1) and defect b (ULI2) as anchor point

CH 7576

1. Visually identified defects

1.1 Visually identified defects LRI1		1.2 Visually identified defects URI1	
defect	pkg	defect	pkg
A	10-12	A	68-72
B	39-42		
C	68-74		
D	81-84		
E	89-91		

2. Metric approach

2.1 Metrically identified defects LRI1		2.2 Metrically identified defects URI1	
defect	pkg	defect	pkg
A	10-12	A	68-72
B	39-42	a	7-8

C	68-74	b	22-24
D	81-84 (84th percentile)	c	48-51
E	89-91 (84th percentile)	d	53-56
a	20-22	e	97-102
b	59-63 (88th percentile)	f	107-110
c	114-118	g	112-114

3. Matching

defect	LRI1	URI1
1	a	a
2	B	b
3	b	c
4	C	d
5	D	A
6	c	e

Based upon visually matched clear defects b (LRI1) and c (URI1) as anchor point

CH 7579

1. Visually identified defects

1.1 Visually identified defects LLI1		1.2 Visually identified defects LRI1	
defect	pkg	defect	pkg
A	50-53	A	6
B	119-123	B	27-29
		C	65-67
		D	77-78

2. Metric approach

2.1 Metrically identified defects LLI		2.2 Metrically identified defects LRI	
defect	pkg	defect	pkg
A	50-53	A	6
B	119-123	B	27-29
a	7-9	C	65-67
b	24-26	D	77-78
c	33-34	a	39-43
d	39-40	b	53-57
e	59-63	c	104-107
f	70-72		
g	79-86		
h	103-105 (85th percentile)		
i	126-128		

3. Matching

defect	LRI1	LLI1
1	A	a
2	B	b
3	a	d
4	b	A
5	C	e
6	D	g
7	c	h

Based upon visually matched clear defects as A (LRI1) and a (LLI1) anchor points

CH 8113

1. Visually identified defects

1.1 Visually identified defects LLI1		1.2 Visually identified defects LLI2	
defect	pkg	defect	pkg
A	24-25	A	21-26
B	72-78	B	77-84
		C	93-95

2. Metric approach

2.1 Metrically identified defects LLI		2.2 Metrically identified defects LLI2	
defect	pkg	defect	pkg
A	24-25	A	21-26
B	72-78	B	77-84 (83rd percentile)
a	14-16	C	93-95
b	29-32	a	10-14
c	34-35	b	48-51
d	52-56	c	65-68 (84th percentile)
e	67-68	d	102-103
f	97-100		
g	106-107		

3. Matching

defect	LLI1	LLI2
1	a	a
2	A	A
3	d	b
4	e	c
5	B	B
6	f	C
7	g	d

Based upon visually matched clear defects A (LLI1, LLI2) as anchor point

CH 8114

1. Visually identified defects

1.1 Visually identified defects ULI1		1.2 Visually identified defects URI2	
defect	pkg	defect	pkg
A	7-10	A	87
B	30-36	B	105-106
C	102-107		

2. Metric approach

2.1 Metrically identified defects ULI1		2.2 Metrically identified defects URI2	
defect	pkg	defect	pkg
A	7-10	A	87
B	30-36	B	105-106
C	102-107	a	6-9

a	39-40	b	17-18
b	47-48	c	22-25
c	59-62	d	37-40
d	97	e	58-65
		f	73-75

3. Matching

defect	ULI1	URI2
1	B	a
2	a	b
3	b	c
4	c	d
5	d	f
6	C	A

Based upon visually matched clear defect B (ULI1) and defect a (URI2) as anchor point

CH 8423

1. Visually identified defects

1.1 Visually identified defects LLI1		1.2 Visually identified defects LLI2	
defect	pkg	defect	pkg
A	107-114	A	90-95

1.3 Visually identified defects ULI2		1.4 Visually identified defects URI1	
defect	pkg	defect	pkg
A	35-38	A	92-97
B	100-103		

2. Metric approach

2.1 Metrically identified defects LLI1		2.2 Metrically identified defects LLI2	
defect	pkg	defect	pkg
A	107-114	A	90-95 (82nd percentile)
a	9	a	6-7
b	16-19	b	13-15
c	31-35	c	22-23
d	42-45	d	26-27
e	54-56 (88th percentile)	e	29
f	61-62 (83rd percentile)	f	43-45
g	86-88	g	65-67
h	91-93	h	115-117

2.3 Metrically identified defects ULI2		2.4 Metrically identified defects URI1	
defect	pkg	defect	pkg
A	35-38	A	92-97
B	100-103	a	19-22
a	7-12	b	33-36
b	17-19	c	45-46
c	25-29	d	65-67
d	57-59	e	82-87
e	73-76	f	126-130
f	133	g	137-138

3. Matching

defect	LLI1	LLI2	URI1	ULI2
1	a	a	/	/
2	b	b	/	/
3	c	e	a	/
4	d	f	b	a
5	e	/	c	b
6	f	g	/	c
7	/	/	d	A
8	h	A	e	d
9	A	h	A	e
10	/	/	f	B

Based upon visually matched clear defect A (LLI1/ULI1)/defect h (LLI2) and defect h (LLI1)/defect e (URI1) and defect f (URI1)/defect B (ULI2) as anchor points

CH 8425

1. Visually identified defects

1.1 Visually identified defects ULI1		1.2 Visually identified defects ULI2	
defect	pkg	defect	pkg
A	65-69	A	82-88
		B	107-108

2. Metric approach

2.1 Metrically identified defects ULI		2.2 Metrically identified defects ULI2	
defect	pkg	defect	pkg
A	no	A	82-88
a	28-31	B	107-108
b	34-37 (88^{th} percentile)	a	8-9
c	48-53	b	24-28
d	70-73	c	37-39
e	79-83	d	48-52
f	89-92	e	63-66
		f	96-98
		g	100-101
Defect A could not be confirmed metrically (53^{rd} percentile).			

3. Matching

defect	ULI1	ULI2
1	b	a
2	c	b
3	d	c
4	e	d
5	f	e

Based upon visually matched clear defects d (ULI1) and defect c (ULI2) as anchor point

CH 8729

1. Visually identified defects

1.1 Visually identified defects LLI2		1.2 Visually identified defects LRI2	
defect	pkg	defect	pkg
A	47-50	A	4-6
B	55-60	B	15-17
		C	36-38
		D	44-46

2. Metric approach

2.1 Metrically identified defects LLI2		2.2 Metrically identified defects LRI2	
defect	pkg	defect	pkg
A	47-50	A	4-6
B	no	B	15-17
a	8-13	C	36-38
b	21-24	D	44-46
c	32-34	a	30-31
d	42-43	b	50-53
e	90-92	c	64-67
		d	92-97
Defect B could not be confirmed metrically (43th percentile).			

3. Matching

defect	LLI2	LRI2
1	a	B
2	c	C
3	d	D
4	A	b
5	e	d

Based upon visually matched clear defects a (LLI2) and defect B (LRI2) as anchor point

CH 8841

1. Visually identified defects

1.1 Visually identified defects LLI2		1.2 Visually identified defects LRI1	
defect	pkg	defect	pkg
A	42-46	A	12-13
B	87-89	B	82-85
C	96-107	C	88-89
		D	95-98
		E	103-110
		F	116-117

2. Metric approach

2.1 Metrically identified defects LLI2		2.2 Metrically identified defects LRI1	
defect	pkg	defect	pkg
A	42-46	A	no

B	87-89	B	82-85
C	96-107	C	no
a	10	D	no
b	15	E	103-110
c	20-22	F	116-117
d	36-37	a	9
e	50-52	b	24-25
f	114-117	c	38-45
g	122	d	121-122
		Defects A , C and D could not be confirmed metrically (23rd, 76th and 75th percentiles respectively).	

3. Matching

defect	LRI1	LLI2
1	a	a
2	b	c
3	c	A
4	B	B
5	E	C
6	F	f
7	d	g

Based upon visually matched clear defects a (LRI1) and defect A (LLI2) as anchor point

CH 10529

1. Visually identified defects

1.1 Visually identified defects LRI1		1.2 Visually identified defects LRI2	
defect	pkg	defect	pkg
A	52-53	A	7-9
B	58-61	B	52-55
C	72-77	C	74-77
		D	94-98
		E	104-106
		F	108-111
		G	139-142

1.3 Visually identified defects ULI1		1.4 Visually identified defects ULI2	
defect	pkg	defect	pkg
A	7-10	A	50-55
B	62-66		
C	77-82		
D	110-116		

2. Metric approach

2.1 Metrically identified defects LRI1		2.2 Metrically identified defects LRI2	
defect	pkg	defect	pkg
A	52-53	A	7-9
B	58-61	B	52-55
C	72-77	C	74-77

a	9-11	D	94-98
b	15-16 (87th percentile)	E	104-106
c	24	F	108-111
d	30-33	G	139-142
e	36-39	a	13-14
f	104-105 (81st percentile)	b	23-25
		c	34-35
		d	60
		e	79-82
		f	116-118 (87th percentile)

2.3 Metrically identified defects ULI1		2.4 Metrically identified defects ULI2	
defect	pkg	defect	pkg
A	7-10	A	50-55
B	62-66	a	5-6
C	77-82	b	20-23
D	110-116	c	39-41 (89th percentile)
a	18-22	d	59-61 (83rd percentile)
b	39-44	e	69-71 (89th percentile)
c	94-96	f	86-89
		g	98-100
		h	128-129

3. Matching

defect	LRI1	LRI2	ULI1	ULI2
1	a	A	/	/
2	b	a	A	/
3	c	b	a	/
4	e	c	/	a
5	B	B	b	b
6	C	C	B	c
7	/	e	C	A
8	/	D	/	d
9	f	E	c	e
10	/	f	D	f

Based upon visually matched clear defect C (LRI1, LRI2)/defect B (URI1) and defect a (ULI2/LRI2) as anchor points

CH 11608.10

1. Visually identified defects

1.1 Visually identified defects ULI2		1.2 Visually identified defects URI2	
defect	pkg	defect	pkg
A	15-18	A	9-12
B	31-35	B	32-35
C	48-50	C	37-38
D	58-60	D	54
E	91-94	E	107-111

2. Metric approach

2.1 Metrically identified defects ULI2		2.2 Metrically identified defects URI2	
defect	pkg	defect	pkg
A	15-18	A	9-12
B	31-35	B	32-35
C	48-50	C	37-38
D	58-60 (86th percentile)	D	54
E	91-94 (86th percentile)	E	107-111
a	9-12	a	15-16
b	73-77	b	47-48
c	81-82	c	62-68
d	84-85	d	73-77
e	98-99	e	81-87
		f	95-99
		g	116-118

3. Matching

defect	ULI2	URI2
1	a	A
2	A	a
3	B	B
4	C	b
5	D	c
6	b	d
7	c	e
8	e	f

Based upon visually matched clear defect a (ULI2)/defect A (URI2) as anchor points

CH 11982

1. Visually identified defects

1.1 Visually identified defects ULI2		1.2 Visually identified defects URI2	
defect	pkg	defect	pkg
A	18-21	A	9
B	62-65	B	30-34
C	71-79	C	74-81
D	88-95		

2. Metric approach

2.1 Metrically identified defects ULI2		2.2 Metrically identified defects URI2	
defect	pkg	defect	pkg
A	18-21	A	9
B	62-65	B	no
C	no	C	74-81 (89th percentile)
D	88-95 (86th percentile)	a	15-18
a	9-10	b	59-61
		c	65-68 (88th percentile)
		d	90-94
Defects C and D could not be confirmed metrically (77th percentile)		Defect B could not be confirmed metrically (67th percentile)	

3. Matching

defect	ULI2	URI2
1	a	A
2	A	a
3	B	b
4	D	d

Based upon visually matched clear defect a (ULI2)/defect A (URI2) as anchor points

CH 12528

1. Visually identified defects

1.1 Visually identified defects ULI1		1.2 Visually identified defects ULI2	
defect	pkg	defect	pkg
A	53-58	A	37-40
B	76-82	B	48-50
C	106-110	C	89
D	137-140		

2. Metric approach

2.1 Metrically identified defects ULI1		2.2 Metrically identified defects ULI2	
defect	pkg	defect	pkg
A	53-58	A	37-40
B	76-82	B	48-50
C	106-110	C	89 (88^{th} percentile)
D	137-140	a	7-11
a	7-9	b	23-27
b	35-37 (86^{th} percentile)	c	30-33
c	61 (89^{th} percentile)	d	115-118
d	123-126	e	123-128

3. Matching

defect	ULI1	ULI2
1	b	a
2	A	c
3	c	A
4	B	B
5	C	C
6	D	d

Based upon visually matched clear defect A (ULI1) and defect c (ULI2) as anchor point,

CH 12875

1. Visually identified defects

1.1 Visually identified defects URI1		1.2 Visually identified defects ULI2	
defect	pkg	defect	pkg
A	22-27	A	44-47
B	34-38	B	58-63
C	48-51	C	80-84
D	72-78		

2. Metric approach

2.1 Metrically identified defects URI1		2.2 Metrically identified defects ULI2	
defect	pkg	defect	pkg
A	22-27	A	44-47
B	34-38	B	58-63
C	48-51	C	80-84
D	72-78 (88th percentile)	a	7-9
a	17-19	b	22
b	85-87		

3. Matching

defect	URI1	ULI2
1	B	a
2	C	b
3	D	A
4	b	B

Based upon visually matched clear defect on URI1 (A) and ULI2 (a) as anchor point

CH 12876

1. Visually identified defects

1.1 Visually identified defects URI1		1.2 Visually identified defects ULI1	
defect	pkg	defect	pkg
A	29-33	A	29-33
B	48-54	B	48-54

2. Metric approach

2.1 Metrically identified defects URI1		2.2 Metrically identified defects ULI1	
defect	pkg	defect	pkg
A	29-33	A	29-33
B	48-54	B	48-54
a	4-6	a	6-8
b	14	b	13-15
c	16	c	16-18
d	20-24	d	20-21
e	34-35	e	34-36
f	42-43	f	42
g	63-64	g	60-63
h	74-77	h	103
i	80-82	i	114-116
j	91-95	j	124-127
k	102-106	k	153-154
l	110		
m	122-125		
n	136-142		
o	152		

3. Matching

defect	ULI1	URI1
1	a	a
2	b	b
3	c	c
4	d	d
5	A	A
6	e	e
7	f	f
8	B	B
9	g	g
10	h	k
11	i	l
12	j	m
13	k	o

Based upon visually matched clear defects A and B as anchor points

CH 12935

1. Visually identified defects

1.1 Visually identified defects LLI1		1.2 Visually identified defects LRI2	
defect	pkg	defect	pkg
A	7-8	A	72-75
B	80-85	B	92-96

1.3 Visually identified defects ULI2	
defect	pkg
A	6-7
B	77-79
C	100-103
D	130-135

2. Metric approach

2.1 Metrically identified defects LLI1		2.2 Metrically identified defects LRI2	
defect	pkg	defect	pkg
A	7-8	A	72-75
B	80-85	B	92-96
a	12-14	a	15-18
b	21-22	b	22-25
c	28-31	c	37-39
d	51-52	d	46-48
e	87-90	e	61-62
f	100-101	f	80-81
g	105-107 (86^{th} percentile)	g	99-100
		h	102
		i	114-116
		j	120

2.3 Metrically identified defects ULI2	
defect	pkg
A	6-7

B	77-79
C	100-103
D	130-135
a	21-23
b	34-35
c	61-64
d	91-93

3. Matching

defect	LLI1	LRI2	ULI2
1	b	a	/
2	c	b	/
3	d	d	a
4	/	e	b
5	B	A	/
6	e	f	/
7	f	B	c
8	g	h	B
9	/	j	d

Based upon visually matched clear defect B (LLI1)/defect A (LRI2) and defect e (LLI1/LRI2)/defect d (ULI2) as anchor points

CH 13125

1. Visually identified defects

1.1 Visually identified defects LLI1		1.2 Visually identified defects LLI2	
defect	pkg	defect	pkg
A	36-41	A	83-89
B	50-55		

2. Metric approach

2.1 Metrically identified defects LLI1		2.2 Metrically identified defects LLI2	
defect	pkg	defect	pkg
A	36-41	A	83-89 (86^{th} percentile)
B	50-55	a	15-17
a	9-13	b	21-24
b	25-27	c	47-50 (89^{th} percentile)
c	90-96	d	52-54 (85^{th} percentile)

3. Matching

defect	LLI1	LLI2
1	a	a
2	b	b
3	B	c
4	c	A

Based upon visually matched clear defects a (LLI1/LLI2) and b (LLI1/LLI2) as anchor points

CH 14020

1. Visually identified defects

1.1 Visually identified defects LLI1		1.2 Visually identified defects ULI1	
defect	pkg	defect	pkg
A	6-13	A	88-91
B	43-47	B	102-110
C	89-94		
D	107-114		

2. Metric approach

2.1 Metrically identified defects LLI1		2.2 Metrically identified defects ULI1	
defect	pkg	defect	pkg
A	6-13	A	88-91 (86^{th} percentile)
B	43-47	B	102-110
C	89-94	a	10-11
D	107-114	b	18-19
a	52-55	c	28-34
b	62-68	d	69-74
		e	78-81

3. Matching

defect	LLI1	ULI1
1	A	a
2	B	c
3	C	A
4	D	B

Based upon visually matched clear defect on LLI1 (A) and ULI1 (a) as anchor point

CH 14108

1. Visually identified defects

1.1 Visually identified defects ULI1		1.2 Visually identified defects URI1	
defect	pkg	defect	pkg
A	55-58	A	17-18
B	95-98	B	97-99
C	114-116	C	105-110

2. Metric approach

2.1 Metrically identified defects ULI1		2.2 Metrically identified defects URI1	
defect	pkg	defect	pkg
A	55-58	A	17-18
B	95-98	B	97-99
C	114-116	C	105-110
a	5-15	a	11-14
b	49-50	b	42
c	89-90	c	47-51

3. Matching

defect	ULI1	URI1
1	a	a
2	b	c
3	B	B

CH 15467

1. Visually identified defects

1.1 Visually identified defects ULI2		1.2 Visually identified defects URI2	
defect	pkg	defect	pkg
A	97-100	A	59-63
		B	87-90
		C	97-99
		D	109-111

2. Metric approach

2.1 Metrically identified defects ULI2		2.2 Metrically identified defects URI2	
defect	pkg	defect	pkg
A	97-100	A	59-63 (86^{th} percentile)
a	10-11	B	87-90
b	13	C	97-99 (88^{th} percentile)
c	27-29	D	no
d	33-35	a	26-28
e	43-45	b	31-33
f	75-78	c	35-37
g	87-90 (85^{th} percentile)	d	48-53
h	107-109	e	75-76
		f	118-119
		Defect D could not be confirmed metrically (68^{th} percentile)	

3. Matching

defect	ULI2	URI2
1	c	a
2	d	b
3	e	d
4	f	e
5	g	B
6	A	C

Based upon visually matched clear defect on ULI2 (c) and URI2 (a) as anchor point

CH 15748

1. Visually identified defects

1.1 Visually identified defects LRI2		1.2 Visually identified defects ULI2	
defect	pkg	defect	pkg
A	45-48	A	40-46

B	69-73	B	74-79
C	93-96	C	86-90
D	108-113	D	105-108

1.3 Visually identified defects URI1		1.4 Visually identified defects URI2	
defect	pkg	defect	pkg
A	34-37	A	24-28
B	95-101	B	30-31
C	118-123	C	69-73
		D	97-101

1.5 Visually identified defects LRI1	
defect	pkg
A	49-56
B	87-89
C	93-95

2. Metric approach

2.1 Metrically identified defects LRI2		2.2 Metrically identified defects ULI2	
defect	pkg	defect	pkg
A	45-48	A	40-46
B	69-73	B	74-79
C	93-96	C	86-90
D	108-113	D	105-108
a	7-10	a	5-8
b	25-28	b	14-16
c	31-36	c	54-59
d	57-58	d	94-97
e	59-63		

2.3 Metrically identified defects URI1		2.4 Metrically identified defects URI2	
defect	pkg	defect	pkg
A	34-37	A	24-28
B	95-101	B	30-31
C	118-123	C	69-73
a	13-14	D	97-101
b	18-20	a	9
c	42-45	b	12-13
d	54-58	c	14-15
e	62-64 (88^{th} percentile)	d	36-39
f	70-73 (85^{th} percentile)	e	46-48
		f	56-58
		g	108-113

2.5 Metrically identified defects LRI1	
defect	pkg
A	49-56
B	87-89
C	93-95
a	10-15
b	20-24
c	32-34

d	39-40
e	60-62
f	68-72
g	100-101

3. Matching

defect	LRI1	LRI2	URI1	ULI2	URI2
1	a	a	a	/	/
2	b	/	b	/	/
3	c	b	/	/	/
4	d	c	A	a	a
5	A	A	c	b	c
6	e	d	d	/	A
7	f	e	e	/	d
8	/	B	f	A	e
9	B	/	/	c	f
10	g	C	B	B	C
11	/	D	/	C	/
12	/	/	C	d	D
13	/	/	/	D	g

Based upon visually matched clear defects a (LRI1, LRI2, ULI1) and defect f (LRI1)/defect B (ULI1)/defect C (LRI2) and defect A(ULI1)/defect a (URI2, ULI2) as anchor points

CH 16125

1. Visually identified defects

1.1 Visually identified defects LLI1		1.2 Visually identified defects LRI2	
defect	pkg	defect	pkg
A	76-84	A	72-76
B	88-95	B	102-112
C	112-118	C	133-140
D	133-134		

2. Metric approach

2.1 Metrically identified defects LLI1		2.2 Metrically identified defects LRI2	
defect	pkg	defect	pkg
A	76-84	A	72-76
B	88-95	B	102-112
C	112-118	C	133-140
D	133-134 (82^{nd} percentile)	a	10-13
a	4-5	b	17-18 (83^{rd} percentile)
b	21-25	c	44-46
c	39-40	d	52-53
d	52-54	e	122-125 (89^{th} percentile)
e	121-123		
f	125-127		

3. Matching

defect	LLI1	LRI2
1	b	b

2	d	c
3	A	A
4	C	B
5	f	e
6	D	C

Based upon visually matched clear defects b (LLI1) and b (LRI2) as anchor point

CH 16168

1. Visually identified defects

1.1 Visually identified defects ULI1		1.2 Visually identified defects URI2	
defect	pkg	defect	pkg
A	37-41	A	19-23
B	51-54	B	26-31
		C	54-60
		D	72-75
		E	115-116

2. Metric approach

2.1 Metrically identified defects ULI1		2.2 Metrically identified defects URI2	
defect	pkg	defect	pkg
A	37-41	A	19-23
B	51-54	B	26-31
a	6-8	C	54-60
b	20-23	D	72-75
c	29-32	E	115-116
d	62-65	a	8-12
e	96-99	b	36-40
f	114-117	c	92-96
g	122-126	d	102-104
h	132-136	e	106-110

3. Matching

defect	ULI1	URI2
1	A	a
2	B	B
3	d	b
4	e	D
5	f	c
6	g	d
7	h	e

Based upon visually matched clear defect B (ULI1, URI2) as anchor point

CH 16196

1. Visually identified defects

1.1 Visually identified defects LLI1		1.2 Visually identified defects LLI2	
defect	pkg	defect	pkg
A	47-54	A	41-43
B	85-89	B	77-80
C	115-120	C	92-99

1.3 Visually identified defects ULI1		1.4 Visually identified defects ULI2	
defect	pkg	defect	pkg
A	55-56	A	47-53
B	58-65	B	74-77
C	92-99	C	90-96
D	109-113	D	116-122
E	127-133		

2. Metric approach

2.1 Metrically identified defects LLI1		2.2 Metrically identified defects LLI2	
defect	pkg	defect	pkg
A	47-54	A	41-43
B	85-89	B	77-80
C	115-120	C	92-99
a	19-21	a	7-8
b	72-73	b	15-17
c	101-104 (81st percentile)	c	21
d	124-126	d	32-35
		e	47-48
		f	50-54
		g	56-59
		h	67-70
		i	107-109
		j	120-123 (89th percentile)
		k	136-138

2.3 Metrically identified defects ULI1		2.4 Metrically identified defects ULI2	
defect	pkg	defect	pkg
A	55-56 (88th percentile)	A	47-53 (88th percentile)
B	58-65	B	74-77
C	92-99 (82nd percentile)	C	90-96
D	109-113	D	116-122
E	127-133	a	5-12
a	7-10	b	24-26 (83rd percentile)
b	15-16	c	39-43
c	25-27	d	80-82
d	33-36	e	106-110
e	48-51		

3. Matching

defect	LLI1	LLI2	ULI1	ULI2
1	/	a	a	/
2	a	b	b	/
3	/	d	c	a
4	A	f	e	b
5	/	g	A	/
6	b	h	B	c
7	B	B	/	A
8	c	C	C	B
9	C	i	D	d
10	d	j	/	C
11	/	k	E	e

Based upon visually matched clear defects A (LLI1)/defect c (LLI2), defect C (LLI1)/defect D (ULI1) and defect b (ULI1)/defect a (ULI2) as anchor point

CH 16601

1. Visually identified defects

1.1 Visually identified defects LLI2		1.2 Visually identified defects URI2	
defect	pkg	defect	pkg
A	68-70	A	81-88
B	87-93	B	98-103
		C	112-114

2. Metric approach

2.1 Metrically identified defects LLI2		2.2 Metrically identified defects URI2	
defect	pkg	defect	pkg
A	68-70	A	81-88
B	87-93	B	98-103
a	4-6	C	112-114
b	15-17	a	15-19
c	44-45	b	33-34
d	57-61 (85^{th} percentile)	c	38-39
e	99-106	d	44-46
f	126-131	e	55-57
g	134-137	f	65-67 (84^{th} percentile)
h	145-150	g	108-109

3. Matching

defect	LLI2	URI2
1	d	a
2	A	b
3	B	e
4	e	f
5	f	A
6	g	B
7	h	g

Based upon visually matched clear defects e (LLI2) and defect A (URI2) as anchor point

CH 16638

1. Visually identified defects

1.1 Visually identified defects LRI1		1.2 Visually identified defects URI2	
defect	pkg	defect	pkg
A	75-80	A	97-102
B	96-100		

2. Metric approach

2.1 Metrically identified defects LRI1		2.2 Metrically identified defects URI2	
defect	pkg	defect	pkg
A	75-80	A	97-102

B	96-100	a	7-10
a	14-15	b	17-18
b	17-19	c	24-25
c	37-40	d	31-33 (89th percentile)
d	56-60	e	39-42 (89th percentile)
e	64-67	f	54-57 (88th percentile)
f	104-105	g	69-71
		h	81-83
		i	86-91

3. Matching

defect	LRI1	URI2
1	c	a
2	d	c
3	e	d
4	A	e
5	B	f
6	f	g

Based upon visually matched clear defects c (LRI1) and defect a (URI2) as anchor point

CH 16641

1. Visually identified defects

1.1 Visually identified defects LLI1		1.2 Visually identified defects URI1	
defect	pkg	defect	pkg
A	8-12	A	26-32
B	66-69	B	53-56
C	101-107	C	61-66
		D	74-76
		E	99-103

2. Metric approach

2.1 Metrically identified defects LLI1		2.2 Metrically identified defects URI1	
defect	pkg	defect	pkg
A	8-12	A	26-32
B	66-69	B	53-56
C	101-107	C	61-66
a	22-26	D	74-76
b	36-38 (88th percentile)	E	99-103
c	59-61	a	13-15
d	81-83	b	24-25
e	91-93	c	44-45
f	112-115	d	82-83
		e	109-113
		f	133-135
		g	142-143

3. Matching

defect	LLI1	URI1
1	a	a
2	b	A

3	c	B
4	B	C
5	d	D
6	e	d
7	C	E
8	f	e

Based upon visually matched clear defects c (LLI1) and defect B (URI1) as anchor point

CH 16698

1. Visually identified defects

1.1 Visually identified defects LRI1		1.2 Visually identified defects LRI2	
defect	pkg	defect	pkg
A	10-16	A	45-50
B	112-116	B	78-83
		C	101-108

1.3 Visually identified defects URI1		1.4 Visually identified defects URI2	
defect	pkg	defect	pkg
A	21-24	A	6-10
B	71-80	B	40-43
C	85-88	C	70-79
		D	99-101

2. Metric approach

2.1 Metrically identified defects LRI1		2.2 Metrically identified defects LRI2	
defect	pkg	defect	pkg
A	10-16	A	45-50
B	112-116	B	78-83
a	22-26	C	101-108
b	33-36	a	9-14
c	45-49	b	21-25
d	59-60 (85^{th} percentile)	c	30-34
e	67-70	d	58-61
f	74-77	e	64-66
g	88-90	f	85-89 (86^{th} percentile)
		g	93-94

2.3 Metrically identified defects URI1		2.4 Metrically identified defects URI2	
defect	pkg	defect	pkg
A	21-24	A	6-10
B	71-80	B	40-43
C	85-88	C	70-79
a	27-30	D	99-101
b	37-40	a	18-21
c	45-51	b	32-33
d	53-58	c	46-50
e	94-96	d	88-93

3. Matching

defect	LRI1	LRI2	URI1	URI2
1	A	a	/	/
2	a	b	/	/
3	b	c	A	/
4	c	A	b	A
5	d	d	c	a
6	e	e	d	b
7	f	B	/	B
8	g	f	B	c
9	/	g	C	/
10	B	C	e	C

Based upon visually matched clear defects A (LRI1)/defect a (LRI2) and defect e (LRI1)/defect B (LRI2, URI1 and URI2) as anchor points

CH 19022

1. Visually identified defects

1.1 Visually identified defects URI1		1.2 Visually identified defects ULI2	
defect	pkg	defect	pkg
A	59-65	A	25-31
B	71-73	B	46-50
C	107-112	C	68-71
		D	85-86
		E	94-95

2. Metric approach

2.1 Metrically identified defects URI1		2.2 Metrically identified defects ULI2	
defect	pkg	defect	pkg
A	59-65 (80th percentile)	A	25-31
B	71-73 (86th percentile)	B	46-50
C	107-112	C	68-71
a	7-11	D	85-86
b	26-29	E	94-95
c	46-49	a	6-8
d	81-83 (83rd percentile)	b	60-63
e	91-96 (84th percentile)	c	104-106

3. Matching

defect	URI1	ULI2
1	b	a
2	c	A
3	B	B
4	d	b
5	e	C
6	C	D

Based upon visually matched clear defect C (URI1) and defect D (ULI2) as anchor point

CH 19039

1. Visually identified defects

1.1 Visually identified defects LLI2		1.2 Visually identified defects ULI2	
defect	pkg	defect	pkg
A	68-72	A	20-25
B	112-117	B	50-53
C	124-125	C	65-69
		D	78-82
		E	94

2. Metric approach

2.1 Metrically identified defects LLI2		2.2 Metrically identified defects ULI2	
defect	pkg	defect	pkg
A	68-72	A	20-25
B	112-117	B	50-53
C	no	C	65-69
a	19-22	D	78-82 (85^{th} percentile)
b	43-45	E	94
c	77-80	a	9-11
		b	15-17
		c	36-38
		d	102-109
Defect C could not be confirmed metrically (78^{th} percentile)			

3. Matching

defect	LLI2	ULI2
1	b	b
2	A	c
3	c	B
4	B	D

Based upon visually matched clear defect c (LLI2) and defect B (ULI2) as anchor point

Mell 7k40

1. Visually identified defects

1.1 Visually identified defects LLI1		1.2 Visually identified defects URI1	
defect	pkg	defect	pkg
A	54-64	A	5-7
B	81-86	B	54-60
C	97-107	C	62-69
		D	72-76
		E	91-99

1.3 Visually identified defects URI2	
defect	pkg
A	10-15
B	47-50

2. Metric approach

2.1 Metrically identified defects LLI1		2.2 Metrically identified defects URI1	
defect	pkg	defect	pkg
A	54-64	A	5-7
B	81-86	B	54-60
C	97-107	C	62-69
a	13-17	D	72-76
b	45-49	E	91-99
		a	14-16
		b	35-39

2.3 Metrically identified defects URI2	
defect	pkg
A	10-15
B	47-50
a	30-36
b	64-67
c	73-75

3. Matching

defect	LI2	URI1	URI2
1	a	A	/
2	b	b	A
3	A	B	a
4	B	D	B
5	C	E	b

Based upon visually matched clear defects A (LI2) and defect B (URI1)/defect D (URI1) and defect B (LI2 and URI2) as anchor points

Mell 7k40 (3)

1. Visually identified defects

1.1 Visually identified defects LLI1		1.2 Visually identified defects LRI2	
defect	pkg	defect	pkg
A	46-54	A	41-45
B	62-64	B	118-123

2. Metric approach

2.1 Metrically identified defects LLI1		2.2 Metrically identified defects LRI2	
defect	pkg	defect	pkg
A	46-54	A	41-45
B	62-64	B	118-123
a	5-8	a	4-5
b	36-40	b	25-28
c	68-76 (88^{th} percentile)	c	52-54
d	78-80	d	57-60
		e	65-68
		f	139-145
		g	155-157

3. Matching

defect	LLI1	LRI2
1	a	a
2	b	b
3	A	A
4	B	d
5	c	e

Based upon visually matched clear defect A (LLI1 and LRI2) as anchor point

Mell 8 (7l)

1. Visually identified defects

1.1 Visually identified defects ULI1		1.2 Visually identified defects URI1	
defect	pkg	defect	pkg
A	10-14	A	21-23
B	102-105	B	96-98
		C	105-107

2. Metric approach

2.1 Metrically identified defects ULI1		2.2 Metrically identified defects URI1	
defect	pkg	defect	pkg
A	10-14	A	21-23
B	No	B	No
a	21-24	C	No
b	32-35	a	5-6
c	67	b	36-38
d	113-117	c	64-67 (83rd percentile)
		d	119-121
Defect B could not be confirmed metrically (56th percentile)		Defects B and C could not be confirmed metrically (87th and 80th percentiles respectively)	

3. Matching

defect	ULI1	URI1
1	A	a
2	a	A
3	b	b
4	c	c
5	d	d

Based upon visually matched clear defect A (ULI1) and a (URI) as anchor point

APPENDIX 2: Summary statistics

LONG BONE LENGTH

Radius length			
age cohort (nr marks end cohort)	Nr	mean	sd
0.3	34	50.6	3.6
0.5	5	53.5	5.4
1	10	70.1	5.0
2	3	83.6	7.1
3	3	95.4	12
4	2	105.0	9.6
5	1	115.5	
6	0		
7	0		
8	2	129.2	0.7
9	0		
10	1	150.5	
11	0		
12	2	162.9	14.3
13	0		
14	0		
15	0		
16+	1	230.5	
TOTAL	**64**		**5.84**

Humerus length			
age cohort (nr marks end cohort)	Nr	mean	sd
0.3	37	62.9	3.9
0.5	4	70.3	3.3
1	8	91.0	7.8
2	4	111.0	8.6
3	2	120.1	14.8
4	2	142.5	9.6
5	2	145.2	7.4
6	1	158.5	
7	1	175.0	
8	1	165.5	
9	0		
10	1	200.3	
11	0		
12	1	207.2	
13	0		
14	0		
15	0		
16+	0		
TOTAL	**64**		**7.9**

Ulna length			
age cohort (nr marks end cohort)	Nr	mean	sd
0.3	26	58.1	3.8
0.5	5	62.0	4.6
1	8	77.2	8.6
2	3	94.6	7.5
3	3	98.3	13.3
4	2	118.5	9.4
5	4	121.5	6.0
6	0		
7	0		
8	2	142.8	5.8
9	0		
10	3	179.3	27.8
11	0		
12	2	180.6	17.6
13	0		
14	0		
15	0		
16+	0		
TOTAL	**58**		**10.45**

Tibia length			
age cohort (nr marks end cohort)	nr	mean	sd
0.3	35	61.5	4.7
0.5	3	70.5	6.9
1	6	93.7	8.2
2	2	122.5	2.5
3	3	134.1	4.1
4	1	141.8	
5	1	155.5	
6	1	184.0	
7	0		
8	0		
9	0		
10	1	236.0	
11	0		
12	0		
13	0		
14	0		
15	0		
16+	1	308.5	
TOTAL	**54**		**5.3**

Clavicle length			
age cohort (nr marks end cohort)	nr	mean	sd
0.3	19	42.0	3.2
0.5	1	46.7	
1	8	54.0	5.1
2	3	65.1	3.2
3	1	61.4	
4	1	78.4	
5	3	78.6	1.1
6	3	76.5	11.9
7	0		
8	1	93.4	
9	0		
10	1	94.3	
11	0		
12	4	104.6	6.5
13	0		
14	1	108.0	
15	0		
16+	1	140.0	
TOTAL	**47**		**5.2**

Femur length			
age cohort (nr marks end cohort)	Nr	mean	sd
0.3	28	70.8	5.9
0.5	2	81.3	13.2
1	3	114.9	13.8
2	2	147.9	5.9
3	1	177.0	
4	1	179.1	
5	1	205	
6	0		
7	0		
8	1	229.3	
9	0		
10	1	300.0	
11	0		
12	0		
13	0		
14	0		
15	0		
16+	0		
TOTAL	**40**		**9.7**

Fibula length			
age cohort (nr marks end cohort)	nr	mean	sd
0.3	24	59.6	4.4
0.5	3	69.6	8.0
1	6	88.9	7.0
2	1	123.5	
3	1	133.7	
4	0		
5	2	148.8	9.1
6	1	182.0	
7	0		
8	0		
9	0		
10	0		
11	0		
12	0		
13	0		
14	0		
15	0		
16+	0		
TOTAL	**38**		**7.1**

LONG BONE WIDTH (diaphyses, epiphyses and metaphyses)

Ulna UM width			
age cohort (nr marks end cohort)	nr	mean	sd
0.3	50	6.2	0.7
0.5	11	6.8	0.4
1	12	8.6	1.4
2	5	10.1	0.7
3	4	10.1	0.9
4	3	11.6	1.2
5	5	12.1	0.8
6	2	13.1	0.1
7	3	15.3	1.3
8	4	14.3	1.1
9	1	18.7	
10	3	16.4	1.7
11	1	15.3	
12	5	17.2	1.1
13	0		
14	1	17.3	
15	1	19.3	
16+	2	23.5	0.7
TOTAL	**113**		

Radius UM width			
age cohort (nr marks end cohort)	nr	mean	sd
0.3	48	5.4	0.5
0.5	12	6.3	0.8
1	13	8.0	0.8
2	4	8.9	0.9
3	4	9.2	0.5
4	2	10.6	0.6
5	3	11.0	1.6
6	2	11.8	0.4
7	2	12.6	0.1
8	4	12.2	2.0
9	1	17.3	
10	3	13.2	0.9
11	0		
12	4	15.0	1.3
13	0		
14	1	16.2	
15	0		
16+	2	20.1	0.9
TOTAL	**105**		

Humerus LM width			
age cohort (nr marks end cohort)	Nr	mean	sd
0.3	53	15.8	1.6
0.5	9	17.8	1.6
1	11	22.9	2.1
2	4	25.3	1.3
3	4	25.6	1.6
4	2	29.6	1.3
5	4	31.4	1.6
6	3	33.1	2.5
7	2	35.6	1.9
8	3	35.9	4.7
9	0		
10	4	39.9	2.7
11	0		
12	4	42.4	3.6
13	0		
14	1	44.2	
15	0		
16+	0		
TOTAL	**104**		

Femur UM width			
age cohort (nr marks end cohort)	Nr	mean	sd
0.3	41	10.8	1.2
0.5	9	12.0	1.1
1	10	14.2	1.3
2	3	16.5	2.1
3	6	17.6	2.5
4	2	22.0	1.4
5	3	22.7	2.1
6	3	23.2	2.7
7	2	24.0	3.5
8	4	26.8	4.1
9	0		
10	4	28.7	1.3
11	0		
12	6	32.2	2.8
13	0		
14	2	33.4	3.7
15	0		
16+	2	32.3	1.6
TOTAL	**97**		

Clavicle width (lateral)			
age cohort (nr marks end cohort)	Nr	mean	sd
0.3	34	7.1	1.1
0.5	5	8.0	0.7
1	16	9.4	1.4
2	6	10.2	0.7
3	5	10.5	1.1
4	2	12.9	0.0
5	4	13.6	1.8
6	4	12.4	1.0
7	2	15.5	0.6
8	3	13.6	3.3
9	0		
10	3	15.5	1.9
11	0		
12	3	20.5	3.6
13	0		
14	2	19.1	5.2
15	0		
16+	2	24.3	1.3
TOTAL	**91**		

Fibula LM width			
age cohort (nr marks end cohort)	Nr	mean	sd
0.3	34	6.1	0.8
0.5	6	7.0	1.2
1	10	8.7	1.0
2	4	10.4	2.4
3	2	12.2	0.7
4	3	12.7	0.4
5	5	14.5	1.4
6	4	15.7	2.9
7	1	16.5	
8	4	17.4	2.4
9	0		
10	4	16.4	0.9
11	0		
12	4	18.5	3.2
13	0		
14	1	18.9	
15	0		
16+	4	23.5	2.3
TOTAL	**86**		

Radius LM width			
age cohort (nr marks end cohort)	Nr	mean	sd
0.3	37	8.3	1.0
0.5	6	9.0	1.0
1	11	11.7	1.2
2	4	12.9	0.7
3	5	13.6	0.7
4	2	14.9	0.7
5	2	16.5	1.3
6	2	16.9	0.9
7	2	18.3	0.6
8	3	18.4	2.0
9	1	23.5	
10	1	19.4	
11	0		
12	5	20.6	1.8
13	0		
14	2	23.0	0.1
15	0		
16+	2	26.2	0.9
TOTAL	**85**		

Clavicle width (sternal)			
age cohort (nr marks end cohort)	Nr	mean	sd
0.3	29	7.6	1.0
0.5	4	7.9	0.5
1	13	8.7	1.3
2	4	10.5	0.9
3	3	10.1	0.6
4	3	11.2	1.9
5	4	11.6	1.7
6	4	12.7	2.3
7	1	14.0	
8	2	13.4	0.5
9	0		
10	2	12.9	0.4
11	1	16.2	
12	5	16.6	1.6
13	0		
14	2	19.0	2.1
15	2	17.4	2.2
16+	5	21.5	3.0
TOTAL	**84**		

Ulna LM width			
age cohort (nr marks end cohort)	nr	mean	sd
0.3	28	6.0	0.8
0.5	5	6.9	1.1
1	10	7.6	1.0
2	3	9.0	0.7
3	5	8.5	0.6
4	2	9.8	0.8
5	4	10.5	1.2
6	3	11.6	1.3
7	3	10.9	0.8
8	4	11.9	1.6
9	1	16.3	
10	3	13.0	2.0
11	1	14.7	
12	3	13.7	1.4
13	0		
14	1	14.8	
15	1	14.4	
16+	2	16.7	1.0
TOTAL	**79**		

Humerus UM width			
age cohort (nr marks end cohort)	nr	mean	sd
0.3	28	10.2	1.0
0.5	2	11.1	0.0
1	10	13.8	1.4
2	4	15.1	1.6
3	3	14.7	0.8
4	2	16.5	2.1
5	2	19.6	0.4
6	3	18.7	2.4
7	1	22.3	
8	2	20.6	1.1
9	0		
10	3	23.6	2.2
11	0		
12	3	27.8	3.2
13	0		
14	1	27.5	
15	0		
16+	2	34.7	2.4
TOTAL	**66**		

Humerus width (AP)			
age cohort (nr marks end cohort)	nr	mean	sd
0.3	36	5.1	0.5
0.5	4	6.1	0.3
1	7	8.5	1.3
2	4	9.7	0.8
3	2	9.0	2.1
4	2	10.5	1.3
5	2	12.9	1.9
6	1	11.0	
7	1	12.3	
8	1	11.1	
9	0		
10	1	14.5	
11	0		
12	1	15.2	
13	0		
14	0		
15	0		
16+	0		
TOTAL	**62**		

Humerus width (ML)			
age cohort (nr marks end cohort)	nr	mean	sd
0.3	36	5.2	0.4
0.5	4	6.0	0.4
1	7	8.1	1.2
2	4	9.7	0.5
3	2	9.8	0.4
4	2	11.7	0.3
5	2	12.8	1.6
6	1	12.0	
7	1	12.5	
8	1	10.0	
9	0		
10	1	13.3	
11	0		
12	1	14.6	
13	0		
14	0		
15	0		
16+	0		
TOTAL	**62**		

Tibia LM width			
age cohort (nr marks end cohort)	nr	mean	sd
0.3	33	10.3	1.3
0.5	5	12.3	0.5
1	5	14.1	0.9
2	2	20.7	1.3
3	4	18.9	3.1
4	1	21.3	
5	3	23.7	2.0
6	1	26.0	
7	0		
8	2	26.7	0.5
9	0		
10	1	31.0	
11	0		
12	2	36.7	2.2
13	0		
14	1	35.0	
15	0		
16+	1	42.4	
TOTAL	**61**		

Tibia UM width			
age cohort (nr marks end cohort)	nr	mean	sd
0.3	36	14.5	1.5
0.5	3	16.3	1.9
1	4	22.4	2.3
2	3	28.6	4.7
3	2	29.9	4.2
4	1	34.9	
5	4	38.0	2.7
6	3	40.3	2.8
7	1	43.5	
8	0		
9	0		
10	1	49.6	
11	0		
12	2	54.4	2.5
13	0		
14	0		
15	0		
16+	1	73.2	
TOTAL	**61**		

Femur LM width			
age cohort (nr marks end cohort)	nr	mean	sd
0.3	38	18.4	2.0
0.5	3	21.4	2.8
1	4	26.2	2.9
2	2	39.4	0.9
3	2	33.0	3.1
4	1	42.2	
5	2	47.8	5.1
6	1	36.0	
7	0		
8	1	48.2	
9	0		
10	0		
11	0		
12	1	56.4	
13	0		
14	1	65.3	
15	0		
16+	3	72.7	4.3
TOTAL	**59**		

Tibia width (ML)			
age cohort (nr marks end cohort)	nr	mean	sd
0.3	34	5.7	0.6
0.5	3	6.3	0.2
1	6	7.8	0.8
2	2	9.4	0.4
3	3	10.4	2.0
4	1	11.0	
5	1	10.7	
6	1	11.9	
7	0		
8	0		
9	0		
10	1	15.8	
11	0		
12	0		
13	0		
14	0		
15	0		
16+	1	19.3	
TOTAL	**53**		

Tibia width (AP)			
age cohort (nr marks end cohort)	nr	mean	sd
0.3	34	6.2	0.7
0.5	3	6.8	0.4
1	6	9.2	0.6
2	2	11.4	0.6
3	3	10.8	1.5
4	1	14.7	
5	1	13.2	
6	1	16.2	
7	0		
8	0		
9	0		
10	1	20.3	
11	0		
12	0		
13	0		
14	0		
15	0		
16+	1	29.3	
TOTAL	**53**		

Clavicle width (max)			
age cohort (nr marks end cohort)	nr	mean	sd
0.3	19	3.6	0.5
0.5	1	4.1	
1	8	4.9	0.5
2	3	5.7	0.6
3	1	5.8	
4	1	5.2	
5	3	6.6	0.5
6	3	5.8	0.8
7	0		
8	2	6.8	0.5
9	0		
10	1	7.3	
11	0		
12	4	8.6	1.9
13	0		
14	1	7.8	
15	0		
16+	1	8.9	
TOTAL	**48**		

Clavicle width (min)			
age cohort (nr marks end cohort)	nr	mean	sd
0.3	19	2.8	0.4
0.5	1	3.4	
1	8	3.8	0.4
2	3	3.5	0.2
3	1	4.0	
4	1	4.8	
5	3	4.8	0.8
6	3	4.2	0.5
7	0		
8	2	5.7	1.1
9	0		
10	1	5.5	
11	0		
12	4	6.9	1.2
13	0		
14	1	7.2	
15	0		
16+	1	8.6	
TOTAL	**48**		

Fibula UM width			
age cohort (nr marks end cohort)	nr	mean	sd
0.3	25	5.0	0.6
0.5	4	6.1	1.6
1	6	7.4	0.8
2	1	8.7	
3	1	9.9	
4	0		
5	4	12.9	1.2
6	2	13.9	0.2
7	0		
8	0		
9	0		
10	1	16.2	
11	0		
12	0		
13	0		
14	0		
15	0		
16+	1	24.3	
TOTAL	**45**		

Femur width (AP)			
age cohort (nr marks end cohort)	nr	mean	sd
0.3	28	5.9	0.8
0.5	2	6.6	0.6
1	3	7.6	1.5
2	2	10.4	0.3
3	1	10.7	
4	1	13.0	
5	1	15.9	
6	0		
7	0		
8	1	15.0	
9	0		
10	1	19.4	
11	0		
12	0		
13	0		
14	0		
15	0		
16+	0		
TOTAL	**40**		

Femur width (ML)			
age cohort (nr marks end cohort)	nr	mean	sd
0.3	28	6.5	0.8
0.5	2	7.9	0.4
1	3	9.3	0.8
2	2	11.4	0.4
3	1	10.8	
4	1	12.5	
5	1	15.4	
6	0		
7	0		
8	1	11.7	
9	0		
10	1	17.1	
11	0		
12	0		
13	0		
14	0		
15	0		
16+	0		
TOTAL	**40**		

Humerus UE diameter			
age cohort (nr marks end cohort)	nr	mean	sd
0.3	0		
0.5	0		
1	4	8.7	2.0
2	3	10.7	1.7
3	4	13.4	5.3
4	2	18.0	4.0
5	3	18.1	3.4
6	4	20.2	6.0
7	1	22.4	
8	3	22.5	3.1
9	0		
10	4	25.3	2.7
11	1	34.3	
12	4	30.5	4.2
13	0		
14	2	35.5	1.1
15	1	35.4	
16+	3	40.1	2.1
TOTAL	**39**		

Femur UE diameter			
age cohort (nr marks end cohort)	nr	mean	sd
0.3	1	7.5	
0.5	0		
1	2	12.3	1.8
2	2	12.3	2.1
3	2	13.8	3.1
4	3	19.3	2.5
5	5	20.8	2.3
6	4	23.7	5.3
7	1	28.5	
8	4	27.0	4.6
9	0		
10	4	29.5	1.3
11	1	35.2	
12	6	33.4	3.3
13	0		
14	1	38.2	
15	1	36.5	
16+	2	36.0	0.4
TOTAL	**39**		

Femur LE width			
age cohort (nr marks end cohort)	nr	mean	sd
0.3	0		
0.5	2	12.2	1.3
1	4	18.2	3.3
2	2	23.8	2.7
3	4	22.8	8.1
4	3	36.7	5.0
5	5	41.3	5.5
6	1	48.0	
7	1	53.6	
8	2	48.7	2.3
9	0		
10	1	51.5	
11	0		
12	2	61.2	4.7
13	0		
14	2	66.5	3.5
15	0		
16+	2	68.3	2.7
TOTAL	**31**		

Tibia UE width			
age cohort (nr marks end cohort)	nr	mean	sd
0.3	0		
0.5	1	11.0	
1	9	14.1	2.2
2	2	19.2	1.9
3	2	19.7	4.6
4	1	24.9	
5	5	29.7	2.5
6	3	32.0	8.8
7	0		
8	1	34.9	
9	0		
10	1	56.0	
11	0		
12	1	58.5	
13	0		
14	2	61.0	4.2
15	0		
16+	1	66.3	
TOTAL	**29**		

Fibula LE width			
age cohort (nr marks end cohort)	nr	mean	sd
0.3	0		
0.5	0		
1	2	7.3	2.1
2	0		
3	0		
4	0		
5	0		
6	2	15.8	0.4
7	1	15.8	
8	2	15.9	1.0
9	0		
10	5	17.2	1.4
11	1	17.5	
12	5	19.5	1.9
13	0		
14	4	20.8	1.2
15	1	20.2	
16+	4	21.5	2.6
TOTAL	**27**		

Tibia LE width			
age cohort (nr marks end cohort)	nr	mean	sd
0.3	1	7.0	
0.5	0		
1	0		
2	0		
3	1	15.5	
4	2	19.8	1.0
5	3	22.7	1.3
6	3	22.9	6.5
7	0		
8	1	25.6	
9	0		
10	3	36.7	4.4
11	0		
12	4	36.7	3.6
13	0		
14	2	40.0	1.4
15	0		
16+	3	48.9	5.0
TOTAL	**23**		

FOOT AND HAND BONES

Metatarsal length			
age cohort (nr marks end cohort)	Nr	mean	sd
0.3	39	12.2	1.3
0.5	7	14.2	1.4
1	10	17.3	1.6
2	3	19.4	2.1
3	5	22.4	2.5
4	3	26.5	2.7
5	3	28.0	0.8
6	5	31.0	4.8
7	0		
8	3	37.7	4.0
9	0		
10	3	38.1	2.4
11	0		
12	3	46.2	5.3
13	0		
14	3	48.5	2.2
15	1	47.2	
16+	3	48.7	3.1
TOTAL	**91**		

Metacarpal length			
age cohort (nr marks end cohort)	Nr	mean	sd
0.3	37	8.8	1.0
0.5	6	10.4	2.1
1	8	12.9	2.8
2	5	15.7	4.6
3	3	15.7	2.0
4	2	18.7	1.5
5	2	19.3	1.1
6	3	20.5	4.4
7	2	24.8	1.8
8	3	26.0	4.4
9	0		
10	4	27.0	1.3
11	1	27.4	
12	4	30.0	2.6
13	0		
14	3	30.5	1.4
15	2	37.3	1.5
16+	5	37.6	5.1
TOTAL	**90**		

Talus length			
age cohort (nr marks end cohort)	Nr	mean	sd
0.3	23	9.2	1.1
0.5	5	10.3	1.2
1	12	15.9	2.0
2	2	19.5	5.4
3	3	20.0	4.5
4	3	25.9	2.7
5	5	29.8	2.4
6	5	32.0	5.1
7	1	36.5	
8	3	39.9	5.0
9	0		
10	5	41.0	5.3
11	1	44.9	
12	4	46.4	7.2
13	0		
14	1	50.6	
15	0		
16+	4	54.5	4.9
TOTAL	**77**		

Talus width			
age cohort (nr marks end cohort)	Nr	mean	sd
0.3	23	6.6	0.8
0.5	5	7.4	0.8
1	11	11.1	1.6
2	2	13.9	3.3
3	3	13.8	3.3
4	3	18.5	1.7
5	5	20.6	2.1
6	5	21.2	3.7
7	1	31.0	
8	1	27.1	
9	0		
10	3	33.0	2.3
11	0		
12	4	35.7	3.4
13	0		
14	1	35.2	
15	0		
16+	4	38.8	2.2
TOTAL	**71**		

Calcaneus length			
age cohort (nr marks end cohort)	Nr	mean	sd
0.3	20	10.4	1.9
0.5	6	11.7	1.3
1	8	19.9	4.1
2	4	23.1	5.3
3	4	28.1	11.3
4	2	33.1	1.6
5	3	37.1	2.6
6	5	42.5	6.2
7	0		
8	2	54.1	9.1
9	0		
10	2	52.6	1.3
11	0		
12	3	58.4	6.1
13	0		
14	2	61.8	1.2
15	0		
16+	3	64.4	6.2
TOTAL	**64**		

Calcaneus width			
age cohort (nr marks end cohort)	Nr	mean	sd
0.3	20	7.7	1.2
0.5	5	8.6	1.0
1	6	11.9	2.2
2	4	14.1	1.2
3	3	14.3	1.9
4	2	19.3	0.9
5	3	23.4	2.7
6	3	26.9	1.3
7	0		
8	1	28.1	
9	0		
10	2	31.6	1.6
11	0		
12	2	36.0	1.6
13	0		
14	2	41.4	0.2
15	0		
16+	2	43.7	0.8
TOTAL	**55**		

THORAX (RIB, ILIUM, STERNUM, SCAPULA and VERTEBRAE)

Scapula width glenoid			
age cohort (nr marks end cohort)	nr	mean	sd
0.3	46	5.8	0.7
0.5	6	6.9	1.3
1	12	9.6	1.4
2	4	11.2	0.5
3	3	11.2	0.6
4	3	11.7	2.1
5	2	14.2	1.8
6	4	14.7	1.4
7	2	14.8	0.8
8	3	14.5	1.0
9	0		
10	4	17.9	2.1
11	0		
12	5	18.4	1.7
13	0		
14	2	22.6	0.8
15	0		
16+	2	27.0	1.3
TOTAL	**98**		

Dens W			
age cohort (nr marks end cohort)	Nr	mean	sd
0.3	35	4.8	0.5
0.5	10	5.6	0.8
1	16	6.7	0.7
2	2	7.4	0.8
3	4	7.8	0.5
4	2	7.6	0.8
5	4	9.4	0.9
6	3	9.1	0.8
7	1	9.8	
8	2	9.5	0.6
9	0		
10	3	8.8	1.1
11	1	9.4	
12	3	8.6	1.1
13	0		
14	1	8.5	
15	1	7.4	
16+	4	9.4	0.9
TOTAL	**92**		

Dens H			
age cohort (nr marks end cohort)	Nr	mean	sd
0.3	35	4.6	0.5
0.5	10	4.9	0.8
1	16	6.1	0.7
2	3	6.9	0.8
3	4	7.4	0.9
4	1	7.5	
5	3	9.6	1.1
6	3	14.9	5.4
7	2	23.6	1.1
8	3	27.1	5.3
9	0		
10	3	28.5	1.7
11	0		
12	3	29.1	3.2
13	0		
14	1	32.8	
15	1	29.5	
16+	2	37.6	3.7
TOTAL	**90**		

Scapula height glenoid			
age cohort (nr marks end cohort)	nr	mean	sd
0.3	44	11.6	1.1
0.5	6	12.7	1.6
1	12	17.8	2.1
2	4	20.9	1.4
3	2	20.5	0.8
4	2	20.2	4.7
5	1	28.8	
6	3	27.6	0.9
7	1	31.9	
8	2	27.8	3.9
9	0		
10	3	33.8	2.9
11	0		
12	4	34.5	3.1
13	0		
14	2	41.1	0.8
15	0		
16+	0		
TOTAL	**86**		

Ilium breadth			
age cohort (nr marks end cohort)	nr	mean	sd
0.3	36	32.3	2.8
0.5	5	39.1	6.5
1	9	49.0	5.3
2	3	56.7	4.7
3	3	64.3	2.3
4	2	73.5	9.0
5	5	74.8	3.4
6	1	63.3	
7	0		
8	3	87.8	7.2
9	0		
10	2	97.0	10.4
11	0		
12	2	96.1	5.0
13	0		
14	0		
15	0		
16+	3	118.5	18.6
TOTAL	**74**		

Axis L			
age cohort (nr marks end cohort)	Nr.	mean	sd
0.3	45	16.9	1.4
0.5	7	19.8	1.8
1	14	23.4	2.1
2	3	25.6	3.5
3	2	26.4	3.6
4	1	23.3	
5	1	34.5	
6	0		
7	0		
8	0		
9	0		
10	0		
11	0		
12	0		
13	0		
14	0		
15	0		
16+	0		
TOTAL	**73**		

Atlas L (HC)			
age cohort (nr marks end cohort)	nr	mean	sd
0.3	38	14.7	1.4
0.5	9	17.4	2.0
1	11	21.9	3.2
2	2	23.5	3.5
3	5	28.5	3.5
4	2	25.9	8.1
5	2	33.8	0.4
6	2	32.8	6.3
7	1	35.5	
8	1	32.3	
9	0		
10	0		
11	0		
12	0		
13	0		
14	0		
15	0		
16+	0		
TOTAL	**73**		

Ischium length			
age cohort (nr marks end cohort)	nr	mean	sd
0.3	35	17.1	1.6
0.5	7	20.8	3.2
1	10	27.0	4.5
2	5	31.8	4.4
3	4	33.4	4.1
4	2	42.5	2.1
5	2	43.3	0.1
6	2	43.4	9.4
7	0		
8	1	48.3	
9	0		
10	0		
11	1	59.8	
12	3	59.8	5.3
13	0		
14	0		
15	0		
16+	1	71.5	
TOTAL	**73**		

Atlas L (FK)			
age cohort (nr marks end cohort)	Nr	mean	sd
0.3	40	14.1	1.3
0.5	7	15.8	1.9
1	10	20.5	1.8
2	2	21.6	1.6
3	5	28.1	3.9
4	2	26.3	7.3
5	2	33.9	0.9
6	1	40.3	
7	1	38.1	
8	1	32.7	
9	0		
10	0		
11	0		
12	0		
13	0		
14	0		
15	0		
16+	0		
TOTAL	**71**		

Ilium height			
age cohort (nr marks end cohort)	nr	mean	sd
0.3	36	29.2	2.5
0.5	3	30.2	2.4
1	7	44.2	5.7
2	2	53.4	2.7
3	3	56.9	2.5
4	1	61.9	
5	3	68.3	3.4
6	2	70.9	19.0
7	0		
8	3	76.9	4.0
9	0		
10	2	87.3	3.5
11	0		
12	2	89.9	0.3
13	0		
14	0		
15	0		
16+	1	95.3	
TOTAL	**65**		

Ischium height			
age cohort (nr marks end cohort)	nr	mean	sd
0.3	35	11.2	1.1
0.5	7	13.4	1.8
1	9	17.8	2.2
2	4	23.0	2.6
3	3	21.5	3.5
4	1	27.5	
5	1	29.7	
6	1	26.3	
7	0		
8	1	36.2	
9	0		
10	0		
11	0		
12	1	40.0	
13	0		
14	0		
15	0		
16+	0		
TOTAL	**63**		

Manubrium breadth			
age cohort (nr marks end cohort)	nr	mean	sd
0.3	11	9.5	2.3
0.5	2	8.9	3.1
1	10	15.2	4.3
2	2	18.4	1.9
3	0		
4	2	23.9	7.8
5	3	18.0	4.6
6	3	30.2	2.8
7	1	27.1	
8	3	23.6	5.9
9	0		
10	2	33.4	1.3
11	1	32.9	
12	4	37	5.1
13	0		
14	2	41.3	4.0
15	0		
16+	2	50.4	0.1
TOTAL	**48**		

Manubrium length			
age cohort (nr marks end cohort)	Nr	mean	sd
0.3	10	8.3	1.9
0.5	3	9.0	1.7
1	8	13.3	4.2
2	1	20.8	
3	1	13.7	
4	1	16.5	
5	2	16.1	3.8
6	3	26.8	1.9
7	1	26.8	
8	3	20.7	6.0
9	0		
10	2	28.2	7.9
11	0		
12	4	30.7	2.2
13	0		
14	1	37.1	
15	0		
16+	2	45.3	5.2
TOTAL	**42**		

Pubic length			
age cohort (nr marks end cohort)	nr	mean	sd
0.3	20	14.1	2.0
0.5	5	17.4	3.0
1	7	23.1	2.9
2	2	28.3	4.5
3	1	22.5	
4	1	34.2	
5			
6	2	33.4	6.6
7	0		
8	0		
9	0		
10	1	46.9	
11	0		
12	2	59.9	5.9
13	0		
14	1	53.8	
15	0		
16+	0		
TOTAL	**42**		

Pubic height			
age cohort (nr marks end cohort)	nr	mean	sd
0.3	21	7.3	1.7
0.5	4	9.7	2.4
1	7	15.4	2.6
2	2	18.8	2.4
3	1	15.5	
4	1	21.7	
5	0		
6	1	26.9	
7	0		
8	0		
9	0		
10	2	44.6	6.8
11	0		
12	0		
13	0		
14	0		
15	0		
16+	0		
TOTAL	**39**		

First rib length			
age cohort (nr marks end cohort)	nr	mean	sd
0.3	19	23.1	2.4
0.5	1	27.3	
1	5	34.3	4.5
2	1	30.8	
3	0		
4	2	41.8	10.9
5	1	48.0	
6	0		
7	0		
8	1	50.1	
9	0		
10	1	56.5	
11	0		
12	4	57.9	4.2
13	0		
14	0		
15	0		
16+	0		
TOTAL	**35**		

Scapula breadth			
age cohort (nr marks end cohort)	nr	mean	sd
0.3	16	27.7	2.1
0.5	0		
1	6	38.3	2.5
2	0		
3	1	40.5	
4	0		
5	1	57.7	
6	1	54.2	
7	0		
8	0		
9	0		
10	1	65.3	
11	0		
12	1	69.9	
13	0		
14	0		
15	0		
16+	1	94.5	
TOTAL	**28**		

Scapula height			
age cohort (nr marks end cohort)	nr	mean	sd
0.3	16	33.5	2.7
0.5	0		
1	4	49.4	3.4
2	0		
3	1	58.4	
4	0		
5	1	78.4	
6	1	77.4	
7	1	93.6	
8	0		
9	0		
10	0		
11	0		
12	0		
13	0		
14	0		
15	0		
16+	1	142.0	
TOTAL	**25**		